NOVEL PLATFORM FOR ANTIGEN DELIVERY TO DENDRITIC CELLS FOR IMMUNOTHERAPY

EDITED BY: Alsya J. Affandi, Maud Plantinga and Irina Caminschi
PUBLISHED IN: Frontiers in Immunology

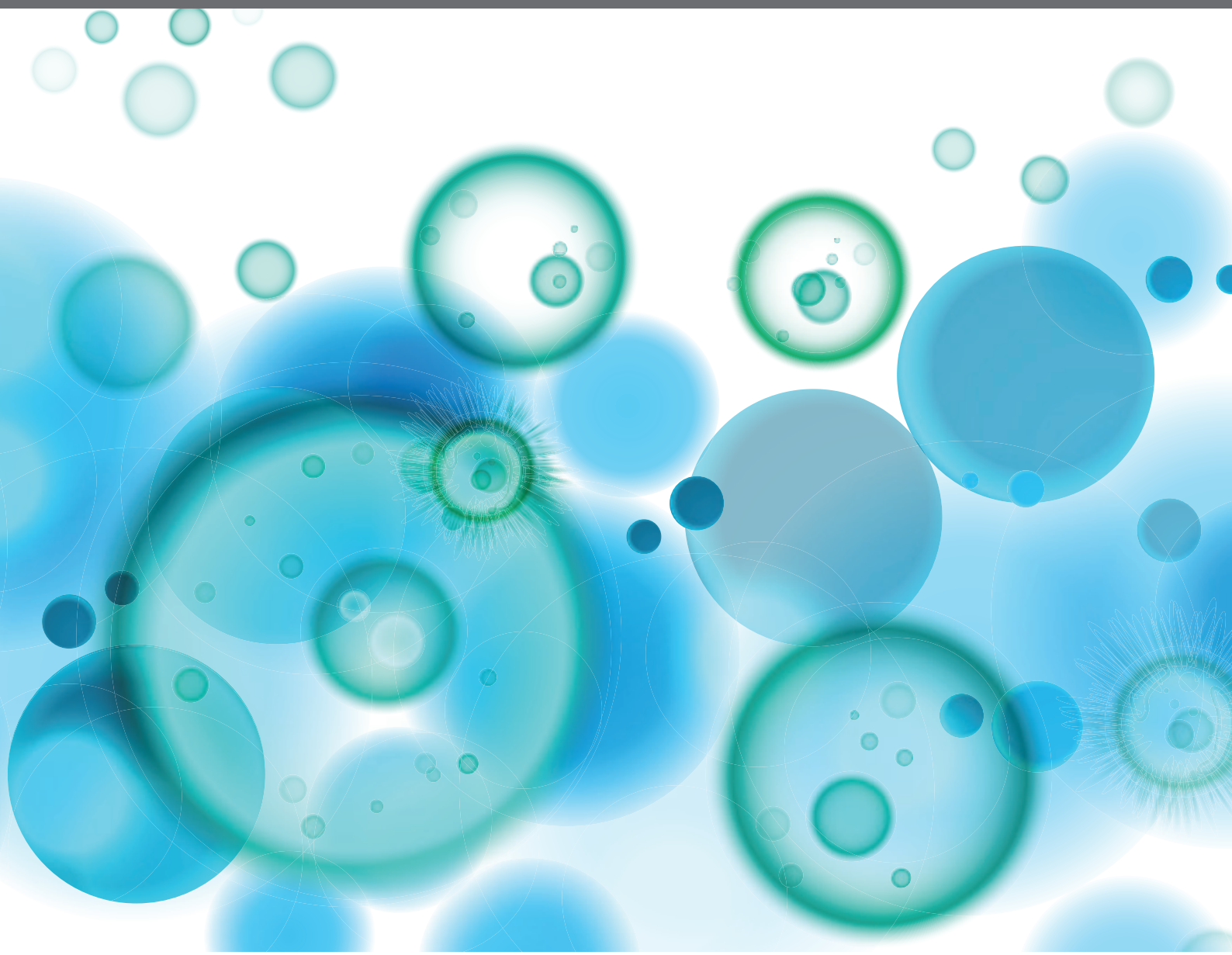

frontiers Research Topics

frontiers

ISSN 1664-8714
ISBN 978-2-88976-427-3
DOI 10.3389/978-2-88976-427-3

About Frontiers

Frontiers is more than just an open-access publisher of scholarly articles: it is a pioneering approach to the world of academia, radically improving the way scholarly research is managed. The grand vision of Frontiers is a world where all people have an equal opportunity to seek, share and generate knowledge. Frontiers provides immediate and permanent online open access to all its publications, but this alone is not enough to realize our grand goals.

Frontiers Journal Series

The Frontiers Journal Series is a multi-tier and interdisciplinary set of open-access, online journals, promising a paradigm shift from the current review, selection and dissemination processes in academic publishing. All Frontiers journals are driven by researchers for researchers; therefore, they constitute a service to the scholarly community. At the same time, the Frontiers Journal Series operates on a revolutionary invention, the tiered publishing system, initially addressing specific communities of scholars, and gradually climbing up to broader public understanding, thus serving the interests of the lay society, too.

Dedication to Quality

Each Frontiers article is a landmark of the highest quality, thanks to genuinely collaborative interactions between authors and review editors, who include some of the world's best academicians. Research must be certified by peers before entering a stream of knowledge that may eventually reach the public - and shape society; therefore, Frontiers only applies the most rigorous and unbiased reviews.
Frontiers revolutionizes research publishing by freely delivering the most outstanding research, evaluated with no bias from both the academic and social point of view. By applying the most advanced information technologies, Frontiers is catapulting scholarly publishing into a new generation.

What are Frontiers Research Topics?

Frontiers Research Topics are very popular trademarks of the Frontiers Journals Series: they are collections of at least ten articles, all centered on a particular subject. With their unique mix of varied contributions from Original Research to Review Articles, Frontiers Research Topics unify the most influential researchers, the latest key findings and historical advances in a hot research area! Find out more on how to host your own Frontiers Research Topic or contribute to one as an author by contacting the Frontiers Editorial Office: frontiersin.org/about/contact

NOVEL PLATFORM FOR ANTIGEN DELIVERY TO DENDRITIC CELLS FOR IMMUNOTHERAPY

Topic Editors:
Alsya J. Affandi, VU Medical Center, Netherlands
Maud Plantinga, University Medical Center Utrecht, Netherlands
Irina Caminschi, Monash University, Australia

Citation: Affandi, A. J., Plantinga, M., Caminschi, I., eds. (2022). Novel Platform for Antigen Delivery to Dendritic Cells for Immunotherapy.
Lausanne: Frontiers Media SA. doi: 10.3389/978-2-88976-427-3

Table of Contents

04 ***Editorial: Novel Platform for Antigen Delivery to Dendritic Cells for Immunotherapy***
Maud Plantinga and Alsya J. Affandi

07 ***Tolerogenic Immunotherapy: Targeting DC Surface Receptors to Induce Antigen-Specific Tolerance***
Charlotte Castenmiller, Brigitte-Carole Keumatio-Doungtsop, Ronald van Ree, Esther C. de Jong and Yvette van Kooyk

21 ***PLGA Nanoparticles Co-encapsulating NY-ESO-1 Peptides and IMM60 Induce Robust CD8 and CD4 T Cell and B Cell Responses***
Yusuf Dölen, Uzi Gileadi, Ji-Li Chen, Michael Valente, Jeroen H. A. Creemers, Eric A. W. Van Dinther, N. Koen van Riessen, Eliezer Jäger, Martin Hruby, Vincenzo Cerundolo, Mustafa Diken, Carl G. Figdor and I. Jolanda M. de Vries

36 ***Arrest in the Progression of Type 1 Diabetes at the Mid-Stage of Insulitic Autoimmunity Using an Autoantigen-Decorated All-*trans *Retinoic Acid and Transforming Growth Factor Beta-1 Single Microparticle Formulation***
Brett E. Phillips, Yesica Garciafigueroa, Carl Engman, Wen Liu, Yiwei Wang, Robert J. Lakomy, Wilson S. Meng, Massimo Trucco and Nick Giannoukakis

51 ***Pre-Existing Humoral Immunity Enhances Epicutaneously-Administered Allergen Capture by Skin DC and Their Migration to Local Lymph Nodes***
Pierre-Louis Hervé, Camille Plaquet, Noémie Assoun, Nathalie Oreal, Laetitia Gaulme, Audrey Perrin, Adeline Bouzereau, Véronique Dhelft, Jean-Louis Labernardière, Lucie Mondoulet and Hugh A. Sampson

61 ***Moving on From Sipuleucel-T: New Dendritic Cell Vaccine Strategies for Prostate Cancer***
Sarah I. M. Sutherland, Xinsheng Ju, L. G. Horvath and Georgina J. Clark

80 ***Quantitative Phosphoproteomic Analysis Reveals Dendritic Cell- Specific STAT Signaling After α2-3–Linked Sialic Acid Ligand Binding***
Rui-Jún Eveline Li, Aram de Haas, Ernesto Rodríguez, Hakan Kalay, Anouk Zaal, Connie R. Jimenez, Sander R. Piersma, Thang V. Pham, Alex A. Henneman, Richard R. de Goeij-de Haas, Sandra J. van Vliet and Yvette van Kooyk

94 ***Therapeutic Liposomal Vaccines for Dendritic Cell Activation or Tolerance***
Noémi Anna Nagy, Aram M. de Haas, Teunis B. H. Geijtenbeek, Ronald van Ree, Sander W. Tas, Yvette van Kooyk and Esther C. de Jong

110 ***CD169 Defines Activated CD14$^+$ Monocytes With Enhanced CD8$^+$ T Cell Activation Capacity***
Alsya J. Affandi, Katarzyna Olesek, Joanna Grabowska, Maarten K. Nijen Twilhaar, Ernesto Rodríguez, Anno Saris, Eline S. Zwart, Esther J. Nossent, Hakan Kalay, Michael de Kok, Geert Kazemier, Johannes Stöckl, Alfons J. M. van den Eertwegh, Tanja D. de Gruijl, Juan J. Garcia-Vallejo, Gert Storm, Yvette van Kooyk and Joke M. M. den Haan

125 ***Targeting Xcr1 on Dendritic Cells Rapidly Induce Th1-Associated Immune Responses That Contribute to Protection Against Influenza Infection***
Demo Yemane Tesfaye, Sonja Bobic, Anna Lysén, Peter Csaba Huszthy, Arnar Gudjonsson, Ranveig Braathen, Bjarne Bogen and Even Fossum

frontiers | Frontiers in Immunology

EDITORIAL
published: 30 May 2022
doi: 10.3389/fimmu.2022.915604

Editorial: Novel Platform for Antigen Delivery to Dendritic Cells for Immunotherapy

Maud Plantinga[1] *and Alsya J. Affandi*[2,3,4]*

[1] Center for Translational Immunology, divisie Laboratoria, Apotheek en Biomedische Genetica (dLAB), University Medical Center Utrecht, Utrecht, Netherlands, [2] Amsterdam University Medical Center (UMC) location Vrije Universiteit Amsterdam, Molecular Cell Biology and Immunology, Amsterdam, Netherlands, [3] Cancer Center Amsterdam, Cancer Biology and Immunology, Amsterdam, Netherlands, [4] Amsterdam institute for Infection and Immunity, Cancer Immunology, Amsterdam, Netherlands

Keywords: dendritic cells, vaccine, antigen, immunotherapy, cancer, infection, allergy, autoimmunity

OPEN ACCESS

Edited and reviewed by:
Florent Ginhoux,
*Singapore Immunology Network (A*STAR), Singapore*

***Correspondence:**
Alsya J. Affandi
a.affandi@amsterdamumc.nl

Specialty section:
This article was submitted to Antigen Presenting Cell Biology, a section of the journal Frontiers in Immunology

Received: *08 April 2022*
Accepted: *21 April 2022*
Published: *30 May 2022*

Citation:
Plantinga M and Affandi AJ (2022) Editorial: Novel Platform for Antigen Delivery to Dendritic Cells for Immunotherapy. Front. Immunol. 13:915604. doi: 10.3389/fimmu.2022.915604

Editorial on the Research Topic

Novel Platform for Antigen Delivery to Dendritic Cells for Immunotherapy

Dendritic cells (DCs) are a group of antigen-presenting cells (APCs) that link innate and adaptive immune systems. DCs are specialized in processing and presenting antigens to T cells and instructing the appropriate T cells responses (1). DCs express various pattern recognition receptors (PRRs) that are capable of distinguishing 'danger signals' from 'safe signals', to ensure the proper T cell responses are initiated. For example, toll-like receptors (TLRs) mediate DCs sensing of pathogenic bacteria or viruses, which initiates cascades of immune activation. Next to this, DCs also express receptors that recognize 'self' structure, such as the sialic acid binding immunoglobulin type lectins (Siglecs) receptors, that promote immune suppression. Additionally, DCs integrate signals from the surrounding tissue microenvironment to further tailor the required T cell responses. In a healthy situation, DCs play a crucial role in maintaining homeostasis, by activating T cells to eliminate infected or malignant cells, or by promoting regulatory T cells to prevent chronic inflammation. Impaired immunity may result in the development of cancer, and conversely, failure to dampen immune response can lead to allergic or autoimmune diseases. This profession of the DCs lends itself particularly well for therapeutic purposes (2, 3). In this Research Topic, 9 articles cover many emerging platforms that harness DCs' potential in re-directing T cell responses for therapeutic purposes, with a wide range of potential applications from cancer and autoimmunity, to infectious diseases (summarized in **Figure 1**).

DCs can be broadly categorized into plasmacytoid DCs (pDCs) and conventional DCs (cDCs). While pDCs' main function is to produce type I interferon (IFN-I), cDCs are the most potent in

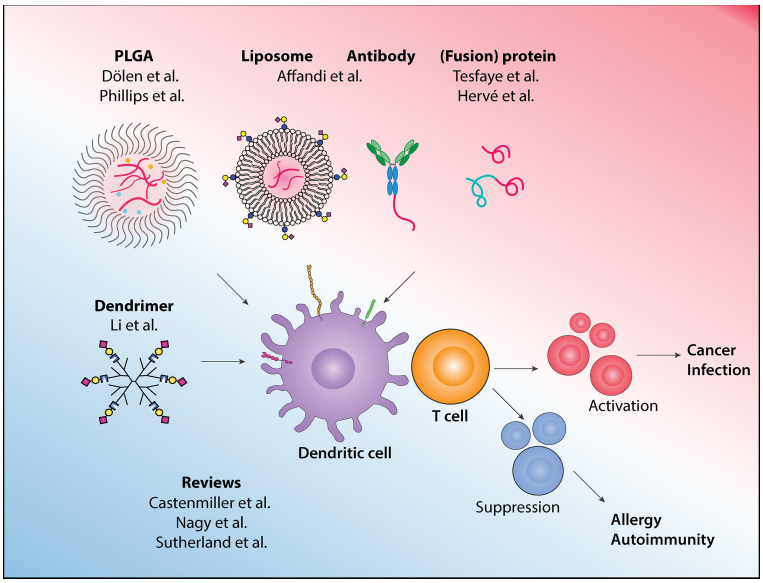

FIGURE 1 | In this Research Topic, various approaches to target antigens to dendritic cells for immunotherapy and to drive the appropriate immune responses are described, and the latest development and other emerging platforms in the field are reviewed.

antigen presentation and T cell activation. cDCs can be further subdivided into distinct subsets such as the DC1 and DC2, which primarily activates $CD8^+$ and $CD4^+$ T cells, respectively. Furthermore, recent single-cell technologies have allowed a deeper characterization of new DC subsets that includes DC3, with hybrid $CD14^+$ monocytes/DC2 phenotype, and pre-DC/AS DC (4, 5). In this collection, two reviews by Castenmiller et al. and Nagy et al. highlight recent discoveries of DC subsets, their ontogenies, and functions, as well as their potential for immunotherapies.

Due to the scarcity of DCs, initial development of DC-based therapies in cancer were prepared using enriched APCs or monocytes, which have shown promises albeit with limited clinical benefits. Focusing on prostate cancer, Sutherland et al. discuss these earlier methodologies while highlighting current advancement that allows direct isolation of blood-derived DCs, as well as *in situ* targeting technologies. Among these *in situ* targeting platforms, Dölen et al. have developed poly lactic-co-glycolic acid (PLGA)-based nanoparticles that encapsulate tumor-associated antigen NY-ESO-1 and IMM60, a novel α-GalCer analog. The inclusion of IMM60 activates invariant natural killer T (iNKT) cells, essentially serving as an adjuvant, leading to robust antigen-specific T cell and B cell responses.

To further improve antigen delivery towards DCs *in situ*, cell surface receptors that are exclusively expressed on DCs can be used as guiding molecules. In this vein, Tesfaye et al. further elaborate on their developed fusion vaccines using Xcl1 protein, a ligand for Xcr1, to deliver vaccines specifically towards DC1. This method stimulates high IgG2 production and the Xcl1-HA fusion vaccine confers protection in an influenza infection model. Affandi et al. focus on CD169, a receptor that is expressed on highly activated $CD14^+$ monocytes and a small proportion of DC3. This study uses two platforms, antibody-based and liposomal-based, to deliver tumor-associated antigens to CD169-expressing $CD14^+$ monocytes for effective stimulation of antigen-specific $CD8^+$ T cells. Focusing on the liposome platform, Nagy et al. review how liposomes can also be used for activating or tolerizing DCs, by adjusting the physiochemical properties and the incorporated adjuvant.

Next to immune activation, this special issue also describes how DC-based therapies can be directed to establish tolerance against allergy or to suppress autoimmune responses. Castenmiller et al. discuss the most promising cell surface receptors used as targets to induce tolerogenic DCs (tolDCs), as well as various methods to target these receptors, such as antibody- or carbohydrate-antigen conjugates. In this collection, Phillips et al. formulate PLGA-microparticles that contain retinoid acid (RA) and TGFβ1. Combined with insulin autoantigen, these microparticles can target DCs and prevent disease onset in a type 1 diabetes model.

While many of the PRRs expressed by DC contain immunoreceptor tyrosine-based activation motif (ITAM) to signals for immune activation, most members of the Siglec receptor family bear immunoreceptor tyrosine-based inhibition motif (ITIM) (6). In this light, Li et al. investigate the mechanisms of how sialic acid-containing dendrimers promote tolerance using phosphoprotemic approach. This study reveals that the sialic acid/Siglec axis alters the JAK-STAT pathway on DCs and thereby promotes the immune regulating phenotype of DCs.

Finally, the route of administration also determines the type of DCs targeted, antigen routing, and the resulting immune responses (7, 8). Work by Hervé et al. describes that in sensitized animals, pre-existing antibodies enhance allergen uptake by

migratory DCs upon epicutaneous application. This mainly involves IgG and IgG Fc receptors (FcγR) and this approach may also have the potential for a needle-free booster vaccination strategy.

Targeting DCs is a promising approach to harnessing a patient's immune system. However, only through the effective delivery of antigens and adjuvants directly to DCs, the goal will be reached of vaccines that can stimulate adequate T cell responses for the treatment of diseases including cancer, infection, allergy, or autoimmunity. The articles in this issue highlight emerging technologies and describe several novel platforms that can optimize DCs' potential for immunotherapy.

REFERENCES

1. Cabeza-Cabrerizo M, Cardoso A, Minutti CM, Pereira da Costa M, Reis e Sousa C. Dendritic Cells Revisited. *Annu Rev Immunol* (2021) 39:131–66. doi: 10.1146/annurev-immunol-061020-053707
2. Wculek SK, Cueto FJ, Mujal AM, Melero I, Krummel MF, Sancho D. Dendritic Cells in Cancer Immunology and Immunotherapy. *Nat Rev Immunol* (2020) 20:7–24. doi: 10.1038/s41577-019-0210-z
3. Phillips BE, Garciafigueroa Y, Trucco M, Giannoukakis N. Clinical Tolerogenic Dendritic Cells: Exploring Therapeutic Impact on Human Autoimmune Disease. *Front Immunol* (2017) 8:1279. doi: 10.3389/fimmu.2017.01279
4. Villani A-C, Satija R, Reynolds G, Sarkizova S, Shekhar K, Fletcher J, et al. Single-Cell RNA-Seq Reveals New Types of Human Blood Dendritic Cells, Monocytes, and Progenitors. *Sci (New York NY)* (2017) 356:eaah4573. doi: 10.1126/science.aah4573
5. See P, Dutertre C-A, Chen J, Günther P, McGovern N, Irac SE, et al. Mapping the Human DC Lineage Through the Integration of High-Dimensional Techniques. *Sci (New York NY)* (2017) 356(6342):eaag3009. doi: 10.1126/science.aag3009
6. Lübbers J, Rodríguez E, van Kooyk Y. Modulation of Immune Tolerance *via* Siglec-Sialic Acid Interactions. *Front Immunol* (2018) 9:2807. doi: 10.3389/fimmu.2018.02807
7. Kreutz M, Tacken PJ, Figdor CG. Targeting Dendritic Cells–Why Bother? *Blood* (2013) 121:2836–44. doi: 10.1182/blood-2012-09-452078
8. Richardson N, Wraith DC. Advancement of Antigen-Specific Immunotherapy: Knowledge Transfer Between Allergy and Autoimmunity. *Immunotherapy Adv* (2021) 1:ltab009. doi: 10.1093/immadv/ltab009

AUTHOR CONTRIBUTIONS

All authors listed have made a substantial, direct, and intellectual contribution to the work, and approved it for publication.

ACKNOWLEDGMENTS

We are grateful for editorial contributions from Dr. Irina Caminschi (University of Melbourne, Monash University, Australia) for this Research Topic.

Conflict of Interest: The authors declare that the research was conducted in the absence of any commercial or financial relationships that could be construed as a potential conflict of interest.

frontiers in Immunology

REVIEW
published: 19 February 2021
doi: 10.3389/fimmu.2021.643240

Tolerogenic Immunotherapy: Targeting DC Surface Receptors to Induce Antigen-Specific Tolerance

Charlotte Castenmiller[1†], *Brigitte-Carole Keumatio-Doungtsop*[2†], *Ronald van Ree*[1,3], *Esther C. de Jong*[1†] *and Yvette van Kooyk*[2*†]

[1] *Department of Experimental Immunology, Amsterdam University Medical Centers, Amsterdam Institute for Infection & Immunity, University of Amsterdam, Amsterdam, Netherlands,* [2] *Department of Molecular Cell Biology and Immunology, Amsterdam University Medical Centers, Amsterdam Institute for Infection & Immunity, Vrije Universiteit Amsterdam, Amsterdam, Netherlands,* [3] *Department of Otorhinolaryngology, Amsterdam University Medical Centers, University of Amsterdam, Amsterdam, Netherlands*

Dendritic cells (DCs) are well-established as major players in the regulation of immune responses. They either induce inflammatory or tolerogenic responses, depending on the DC-subtype and stimuli they receive from the local environment. This dual capacity of DCs has raised therapeutic interest for their use to modify immune-activation *via* the generation of tolerogenic DCs (tolDCs). Several compounds such as vitamin D3, retinoic acid, dexamethasone, or IL-10 and TGF-β have shown potency in the induction of tolDCs. However, an increasing interest exists in defining tolerance inducing receptors on DCs for new targeting strategies aimed to develop tolerance inducing immunotherapies, on which we focus particular in this review. Ligation of specific cell surface molecules on DCs can result in antigen presentation to T cells in the presence of inhibitory costimulatory molecules and tolerogenic cytokines, giving rise to regulatory T cells. The combination of factors such as antigen structure and conformation, delivery method, and receptor specificity is of paramount importance. During the last decades, research provided many tools that can specifically target various receptors on DCs to induce a tolerogenic phenotype. Based on advances in the knowledge of pathogen recognition receptor expression profiles in human DC subsets, the most promising cell surface receptors that are currently being explored as possible targets for the induction of tolerance in DCs will be discussed. We also review the different strategies that are being tested to target DC receptors such as antigen-carbohydrate conjugates, antibody-antigen fusion proteins and antigen-adjuvant conjugates.

Keywords: dendritic cell, tolerance, immunotherapy, surface receptors, C-type lectins, Siglecs, allergy, auto immune diseases

OPEN ACCESS

Edited by:
Irina Caminschi,
Monash University, Australia

Reviewed by:
Angel L. Corbi,
Consejo Superior de Investigaciones Científicas (CSIC), Spain
Laura Santambrogio,
Cornell University, United States

***Correspondence:**
Yvette van Kooyk
y.vankooyk@amsterdamumc.nl

[†] *These authors have contributed equally to this work*

Specialty section:
This article was submitted to Antigen Presenting Cell Biology, a section of the journal Frontiers in Immunology

Received: *17 December 2020*
Accepted: *02 February 2021*
Published: *19 February 2021*

Citation:
Castenmiller C, Keumatio-Doungtsop B-C, van Ree R, de Jong EC and van Kooyk Y (2021) Tolerogenic Immunotherapy: Targeting DC Surface Receptors to Induce Antigen-Specific Tolerance. Front. Immunol. 12:643240. doi: 10.3389/fimmu.2021.643240

INTRODUCTION

Dendritic cells (DCs) are important antigen presenting cells during the induction of immune responses and are essential in directing immune responses toward either immunity or tolerance. This decision is of great importance as undesired inflammatory responses could cause autoimmune or allergic diseases. In the periphery, DCs capture antigens and process them while migrating to the draining lymph nodes, where they present antigen-specific peptides to T lymphocytes. This migration process causes a dramatic transformation of the DC phenotype, called maturation.

Maturation is associated with increased MHC-II complex levels, costimulatory molecule expression, enhanced secretion of polarizing cytokines and molecules, and alterations in chemokine receptor expression, all resulting in an optimal microenvironment to direct T cell responses (1–3). Although various DC subsets have been shown to preferentially induce specific T cell responses in non-inflammatory conditions, the induction of T cell immunity is adapted to and dictated by the encounter with pathogens (4). The unique capacity of DCs to coordinate innate and adaptive immune responses has highlighted them as potential targets for immune activating or dampening therapies to combat undesired immune responses (3).

Immunomodulatory agents such as vitamin D3, retinoic acid, rapamycin, dexamethasone, corticosteroids, ligands of the aryl hydrocarbon receptor (AhR), or specific cytokines (IL-10, TGFβ) have been key in determining the existence and function of tolerogenic DCs (tolDCs) *ex vivo* (**Figure 1**) (5–7). These tolDCs can induce tolerance through various mechanisms, including the induction of Tregs, autoreactive T cell anergy and apoptosis, and could be used in tolerizing immunotherapies (6, 8, 9). *Ex vivo* tolDC immunotherapies are based on re-education of patient-derived DCs to a tolerizing phenotype and the subsequent reinfusion into the body, where they suppress inflammatory immune responses (**Figure 1**). The first clinical study utilizing tolerogenic DCs (tolDCs) for the treatment of autoimmune diseases was performed in 2011 in adult type I diabetes (T1D) patients. Since then, phase I and II clinical trials have been conducted for T1D, rheumatoid arthritis (RA), Crohn's disease, and multiple sclerosis (MS) (5), but also for kidney and liver transplant recipients (8–10). However, due to the personalized, laborious, and expensive nature of *ex vivo*-generated tolDCs, new approaches for inducing tolDCs *in vivo* are being developed.

The feasibility and potential of *in vivo* strategies lie in the ability of DCs to recognize and internalize antigens through surface receptors that not only route antigens to the antigen processing machinery of DCs for subsequent presentation to T cells but also transmit signals that direct anti-inflammatory immune responses. This allows direct modulation of specific DC subsets due to differential surface receptor expression profiles between them. *In vivo* DC-targeting has several advantages compared to *ex vivo* DC-targeting, including fewer hospital visits for the patient, less laborious production methods, and the possibility of large scale production, which is more cost-effective. Additionally, the induction of antigen-specific T cell responses with *in vivo* DC-targeting strategies reduces the risk of generalized immunosuppression, which is induced during the current *ex vivo* strategies using only immunosuppressive agents. The main strategies for *in vivo* tolDC generation take advantage of modalities binding to specific endocytic receptors on DC surfaces, ensuring the delivery of antigen of interest into the antigen-processing machinery (**Figure 1**) (11). Antigens could either be directly coupled to antibodies (11) or loaded on nanoparticles or in liposomes, reviewed elsewhere (12). Another strategy being explored in this regard involves chemically conjugating antigens with specific glycan structures which are ligands for DC surface receptors. In this review we discuss the different DC-subsets used for targeting, the receptors expressed on their surface that have potential to induce tolerogenic signals (but might not be inherently tolerogenic), and the current state of research in their use for the treatment of auto-immune or allergic diseases.

HUMAN DENDRITIC CELL SUBSETS AND THE INDUCTION OF TOLEROGENIC DENDRITIC CELLS

It is now recognized that DCs are a heterogeneous population of cells. The different subsets are defined by surface markers and transcriptome profiles, nicely reviewed by various colleagues (4, 13–16). DCs are generally classified into four major subsets, namely, $CD141^+$ conventional DCs (cDC1s), $CD1c^+$ conventional DCs (cDC2s), monocyte-derived DCs (moDCs), and plasmacytoid DCs (pDCs). The cDC1 subset is a relatively homogenous population that is specialized in cross-presentation of extracellular antigens and efficiently primes $CD8^+$ T cells (16). In contrast, the cDC2 subset is a heterogeneous population and could be further subdivided in separate lineages. For example, the cDC2A and cDC2B lineage are defined by distinct developmental pathways regulated by the transcription factors T- bet and RORγt, respectively (17). Both lineages are potent stimulators of $CD4^+$ naïve T cell, however, cDC2Bs have been shown to be more prone to secrete pro-inflammatory cytokine than cDC2As (13, 17). Additionally identified cDC2 lineages include monocyte-like DC2s, inducing Th1 responses, and DC3s, responsible for Th2, Th17 and Treg differentiation (15, 17). The moDC subset arises from monocytes and retains, like the DC3s, the monocyte marker CD14. They are recruited to inflamed tissue sites *in vivo* where they efficiently cross-present antigens to $CD8^+$ T cells in peripheral tissues (18). The last subset, pDCs, differs from the other subsets as they are marked by quick secretion of pro-inflammatory type I interferons (IFN) following viral infection. pDCs are defined as $CD123^+$ $CD303^+$ $CD304^+$ cells and were originally classified within the myeloid compartment. However, recent findings providing evidence for a lymphoid origin of the majority of pDCs challenges this hypothesis (4, 13, 19, 20). Finally, the tissues where DCs reside, such as lymph nodes, skin, lung, intestines and liver, offer the above mentioned DC subsets additional environmental factors to further adapt to their specific niche resulting in tissue specific DC subsets (8, 21, 22).

Although the immune system encounters many innocuous antigens, including self-antigens and allergens, the chance to develop autoimmune or allergic diseases is relatively small due to the phenomenon of "natural tolerance." Natural tolerance is achieved through the presence of tolerance-inducing DCs located both centrally and in the periphery. Central tolerance induction is mediated by thymic epithelial cells and thymic DCs, which regulate negative selection of autoreactive T cells and induction of natural Tregs (23, 24). Even though the specific role of each thymic DC subset in peripheral immune homeostasis remains elusive, thymic pDCs and the $Sirp\alpha^+$ cDC subset have been proposed to contribute to the prevention of allergic or commensal-specific autoimmune diseases, as they originate

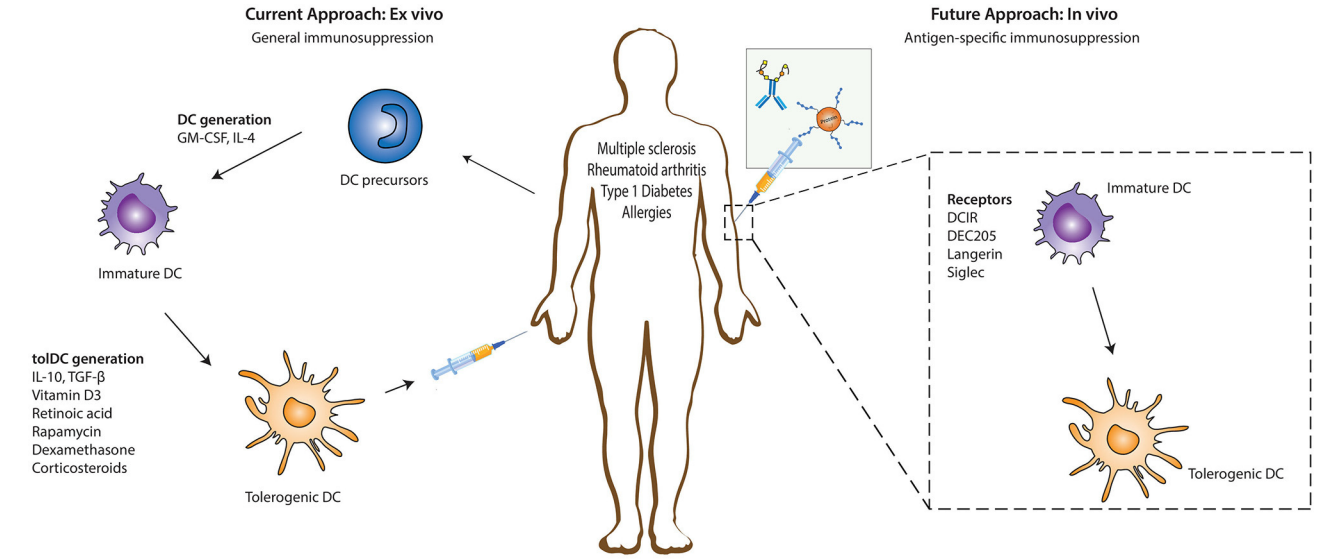

FIGURE 1 | *Ex vivo* and *in vivo* strategies for generation of tolerogenic DCs for DC-based therapies. The current DC-based immunotherapy strategy in the treatment of immunopathologies involves the isolation of DC precursors either from PBMCs or bone marrow-derived cells which could either be allogeneic or autologous. These DC precursors are then differentiated into immature DCs in the presence of GM-CSF and recombinant IL-4 which are subsequently differentiated into tolerogenic DCs (tolDCs) by the addition of pharmacologic agents or immunomodulatory cytokines. Administration of these tolDCs leads to the generation of a suppressive immune environment which dampens inflammation. Future strategies are focusing more on *in vivo* targeting of DCs, where specific antigen-based vaccine formulations targeting specific receptors on DCs in their natural environment are injected into the patient. The antigen is taken up by DCs through these receptors, resulting in the induction of a tolerogenic program in DCs that leads to the generation of antigen-specific immunosuppression. DC, dendritic cells; GM-CSF, Granulocyte-macrophage colony-stimulating factor; IL-4, Interleukin 4; IL-10, Interleukin-10; TGF-β, Transforming growth factor beta.

from the periphery where they encounter many innocuous antigens, followed by migration to the thymus (23–25). On the other hand, peripheral tolerance is mediated by peripheral DCs, preferentially located at the border between the body and the external environment, such as lung, intestine and skin. Steady state or immature DCs were the original identified peripheral tolDCs (26–28). They exhibit low expression of co-stimulatory (CD40, CD80/86) and MHC molecules due to lack of appropriate activation signals and are able to maintain tolerance *via* deletion of self-reactive T cells, induction of T cell anergy or differentiation of antigen-specific Tregs (2). These immature DCs have been reported to be the primary cell types involved in maintaining tolerance in the periphery and mainly carry self-antigens. However, recent identification of partial- or semi-mature DCs with tolerizing capacities, questions the dogma that only immature DCs induce tolerance (22, 27). Similar to immunogenic DCs, tolDCs may be defined by integration of all the signals they transmit to T cells, including maturation marker expression, as well as the presence of, in this case, anti-inflammatory-related tolerizing signals consisting of surface molecule expression (PD-L1, ILT3/4, ICOSL, CTLA-4), tolerogenic cytokine profiles (IL-10, TGFβ) and the presence of other tolerance-inducing metabolites (IDO, RA) (14, 22). Furthermore, the presence or absence of pro-inflammatory cytokines seems to be decisive in inducing either immunity or tolerance, respectively. Nevertheless, no standard tolDCs profile has been established yet, and may not exist due to the great diversity between those that have been described till date.

Besides the immature and semi-mature tolDCs, several tissue-specific DCs exhibit inherent tolerogenic properties, including those in the skin and intestines. In the skin, Langerhans cells (LCs), which are characterized by the expression of Langerin (CD207), CD1a, E-Cadherin, CD39, FcεRI, and Birbeck granules, are the sole tissue-resident DC population in the epidermis (29). LCs constantly migrate from the skin to draining lymph nodes, even in steady-state conditions, and have been implicated in both immunogenic as well as tolerogenic immune reactions (30–32). In contrast, $CD14^+(CD141^+)$ dermal DCs constitutively secrete the anti-inflammatory cytokine IL-10 and are prone to induce T cell anergy and Tregs that inhibit skin inflammation (33, 34). The ability to produce extensive levels of IL-10 is shared with $CD14^+CD16^+CD141^+CD163^+$ DCs isolated from peripheral blood, identified by Gregori and colleagues, which might correspond to the DC3 subset expressing the same surface markers (16, 35). The same group has shown that these cells express the surface receptors HLA-G, ILT2, ILT3, and ILT4 and have the potency to induce type 1 Tregs (Tr1) *in vitro* (36–38). In the intestines, the main subset involved in oral tolerance during steady state conditions are the $CD103^+$ DCs in the lamina propia and mesenteric lymph nodes. They are able to prime Tregs in gut lymphoid tissues through the production of TGF-β and RA (39–42). Additionally, $CD103^+$ DCs express high levels of RALDH2, converting vitamin A to RA which enhances Treg induction (29). These studies demonstrate that various tissues contain specific subsets of tolDCs, emphasizing the power of the immune system to adapt to specific environmental factors

functioning to maintain immune homeostasis during tissue-specific circumstances.

DENDRITIC CELL PATHOGEN RECOGNITION RECEPTORS MODULATING IMMUNE RESPONSES

Signals such as pathogen-associated molecular patterns (PAMPS) from pathogens, damage associated molecular patterns (DAMPS) from inflammation, and self-associated molecular patterns (SAMPS) can be recognized by pattern recognition receptors (PRRs) on the surface of DCs (21, 43). C-type lectins (CLRs) and Sialic-acid binding immunoglobulin-type lectins (Siglecs) are families of PRRs equipped with a carbohydrate recognition domain that specifically recognizes glycan moieties on host cells, pathogens, as well as innocuous antigens such as allergens (21, 43–46).

CLRs function both as adhesion molecules and endocytic receptors, but also have a function in directing immunity to various pathogens, cellular proteins and lipids (44, 47, 48). Induction of immune response through these receptors can alternate between inflammation and immune tolerance depending on several factors including the nature of the ligand (49). They recognize a large and diverse range of ligands and trigger immune responses by inducing signaling pathways *via* an immunoreceptor tyrosine-based activation motif (ITAM), ITAM-like motif, or immunoreceptor tyrosine-based inhibitory motif (ITIM) that signal through Syk or phosphatases (21, 44, 45, 49, 50), generating pro- or anti-inflammatory signals, respectively. Only a few CLRs, such as, DC immunoreceptor (DCIR), Clec12A and Clec12B, bear the ITIM motif (51). Moreover, an important number of CLRs do not signal through Syk or phosphatases but may bear ITAM/ITIM motifs which are important for endocytosis (45, 52). Examples include: dendritic cell-specific intercellular adhesion molecule-3-grabbing non-integrin (DC-SIGN), LSECtin, macrophage C-type lectin (MCL), Langerin, macrophage-galactose lectin (MGL), mannose receptor (MR) and DEC205 (11, 44, 48). These CLRs mediate antigen internalization, followed by processing and subsequent presentation *via* MHC-I or II molecules (53–56).

Next to CLRs, the Siglecs are also expressed on DCs and recognize self- and non-self-antigens (43, 46). Similar to CLRs, they could serve as adhesion molecules and endocytic receptors, and have been shown to be important instructors of T cell immunity (57, 58). Most members of the Siglec family signal through ITIM or ITIM-like motifs resulting in the generation of anti-inflammatory signals that modulate DC function (59). Overall, the ability of effective antigen uptake, processing, and presentation as well as the regulation of immunogenic and tolerogenic immune responses through the modulation of DC function positions DC receptors as promising candidates for novel DC-targeting immunotherapies. In the next sections, we explore current knowledge regarding the most promising DC-receptors being targeted for *in vivo* generation of tolDCs for the treatment of immune dysregulated pathologies.

ITAM- AND ITIM-INDEPENDENT RECEPTORS

DEC205

DEC205 (CD205) is an endocytic receptor highly expressed on cDC1s and belongs to the macrophage- mannose receptor family of CLRs (54). Although the natural ligand of DEC205 remains to be elucidated, some studies suggest apoptotic and necrotic material as well as CpG motifs as consecutive ligands (60). Upon antigen encounter, DEC205 internalizes and recycles very efficiently back to the surface (61). DEC205 was one of the first receptors used for *in vivo* antibody targeting of DCs (**Table 1**). Initial experiments using model antigens, such as hen egg lysozyme or ovalbumin (OVA), coupled to anti-DEC205 antibodies, demonstrated that these antigens were taken up by DCs (82–84). When OVA-anti-DEC205 fusion antibodies were administered to mice in the presence of maturation stimuli, strong immunogenic responses were induced (85). Conversely, when anti-DEC-antigens were injected into animals without adjuvants, DCs remained non-activated as their expression levels of costimulatory molecules was comparable to those obtained in DCs from control mice (83, 85). The analysis of antigen-specific T cell populations in injected mice revealed increased numbers of antigen-specific IL-10 producing $CD25^+Foxp3^+$ Tregs that were able to suppress proliferation of $CD4^+$ T cells *in vivo* (83) (**Figure 2**). Since then, DEC205 targeting has been tested in various autoimmune disease animal models. For instance, in experimental autoimmune encephalomyelitis (EAE), the murine model for MS (63, 66, 86), injection of the autoantigen, myelin oligodendrocyte glycoprotein (MOG) or proteolipid protein (PLP) fused to anti-DEC205-specific antibodies led to elicitation of IL-10-producing $CD4^+CD25^+Foxp3^+$ Tregs, the deletion of antigen-specific $CD4^+$ and $CD8^+$ T cells, reduced Th17 cell activity and significantly ameliorated disease symptoms and substantially delayed the disease onset (63, 64, 67) (**Figure 2**). In some studies, the conversion of some autoreactive T cells into Foxp3+ pTreg cells was reported. These findings were confirmed in non-obese diabetic (NOD), a mouse model of T1D, inflammatory bowel disease (IBD) (71), proteoglycan-arthritis (68), spontaneous experimental autoimmune uveoretinitis (EAU) (72), an animal model of ocular inflammation, as well as a model of graft-vs. host disease (65, 69, 70, 73). Because the use of DEC205 antibodies has proven to be more effective than the administration of free synthetic peptides, in these models of autoimmune diabetes, it is being considered as a possible, important therapeutic tool in the treatment of various autoimmune diseases (**Table 1**). In summary, these data establish DC targeting *via* DEC205 as an effective strategy to tolerize against autoantigens to protect against autoimmunity. However, this DC targeting strategy for the induction of tolerance is yet to be tested in human settings. Moreover, the future prospects of targeting DEC205 to induce tolerance in humans may be hampered by the varied expression pattern of this receptor on the different subsets of DCs (87). Although DEC-205 is predominantly expressed in mice $CD8^+$ DCs, dermal DCs and LCs, human DEC-205 is relatively high expressed on myeloid blood DCs and monocytes, at moderate levels on B cells, and

TABLE 1 | Summary of *in vivo* studies to induce tolDCs using either antigen-antibody fusion compounds or carbohydrate-modified antigens.

Receptor	Disease	Model	Antigen	Targeting strategy	Cellular response	Reference
Clec9A		Multiple mouse models	OVA	Anti-clec9A	$Foxp3^+$ T cells↑	(62)
DCIR2	MS	EAE mice	MOG	Anti-DCIR2	MOG-specific $Foxp3^+$ T cells	(63)
			PLP	Anti-DCIR2	$CD4^+Foxp3^+$ T cells↑, pathogenic T cells↓	(64)
	T1D	NOD mice	BDC2.5	Chimeric anti-DEC205 (33D1)	$CD4^+Foxp3^+$ T cells↑, T cell apoptosis	(65)
DEC205 (CD205)	MS	EAE mice	MOG	Anti-DEC205, single-chain fragment variables specific for DEC205	$CD4^+CD25^+Foxp3^+$ T cells↑	(63, 66)
			PLP	Chimeric anti-DEC205	$CD4^+Foxp3^+$ T cells↑, $CD4^+$ Th17 cells↓	(64, 67)
	RA	PGIA mice	PG	Anti-DEC205	$CD4^+Foxp3^+$ T cells↑, PG-specific $CD4^+$ cells↓	(68)
	T1D	INS-HA/TCR-HA transgenic mice	HA	Anti-DEC205	$CD4^+Foxp3^+$ T cells↑, $CD4^+CTLA4^+$ T cells↑	(69)
		NOD mice	BDC2.5, MimA2	Chimeric anti-DEC205	Antigen-specific $CD4^+$ and $CD8^+$ T cells↓	(65, 70)
	IBD	VILLIN-HA transgenic mice	HA	Anti-DEC205	HA-specific $CD4^+Foxp3^+$ T cells↑	(71)
	EAU	Spontaneous EAU mice	HEL	Anti-DEC205-HEL	$CD4^+CD25^+Foxp3^+$ T cells↑, $CD4^+$ cells↓	(72)
	GVHD	C57BL/6 mice	hNC16A	Anti-DEC205-hNC16A	$CD4^+$ and $CD8^+$ graft infiltration↓	(73)
Langerin (CD207)	MS	EAE mice	MOG	Anti-Langerin	$Foxp3^+$ T cells↑	(63)
MR, DC-SIGN, MGL	MS	EAE mice	PLP	Mannosylation	T cell proliferation↓	(74, 75)
	Grass pollen allergy	Human cells, BALB/c mice	Polymerized *P. pratense* allergens	Mannosylation	$CD4^+CD25^+Foxp3^+$ T cells↑	(76, 77)
	Birch pollen allergy	Human cells, BALB/c mice	Bet v 1	GalNAc-linking, mannosylation	T cell proliferation↑	(78)
Siglecs	MS	EAE mice, BALB/c mice	MOG, OVA	Chimeric anti-Siglec-H	$CD4^+$ T cell anergy	(79)
		C57BL/6 mice	OVA	Sialyation	$CD4^+Foxp3^+$ T cells↑	(80)
	Grass pollen allergy	BALC/c mice	Phl-p5a	Sialylation	$CD4^+Foxp3^+$ T cells↑, $CD4^+$ Th2 cells↓, eosinophilic airway inflammation↓	(81)
Treml4	MS	EAE mice	MOG	Anti-Treml4	MOG-specific $Foxp3^+$ T cells↑	(63)

EAE, experimental autoimmune encephalomyelitis; EAU, experimental autoimmune uveoretinitis; GVHD, graft versus host disease; HA, hemagglutinin; IBD, inflammatory bowel disease; MimA2, mimotype peptide; MOG, myelin oligodendrocyte glycoprotein; MS, multiple sclerosis; NOD, non-obese diabetic; OVA, ovalbumin; PG, proteoglycan; PLP, proteolipid protein; RA, rheumatoid arthritis.

at low levels on pDCs, T cells and natural killer cells (87, 88). This differential expression pattern of DEC205 in humans is problematic for the development of DEC205-targeted vaccines for humans due to potential offsite targeting and needs to be addressed carefully during the design of potential clinical studies.

DC-SIGN, MR, and MGL

DC-SIGN and MR are other members of the CLR family which recognize several mannose and fucose-containing structures, present on many antigens (49) and activate signaling pathways in CLR-expressing cells (44, 52, 60). These receptors are widely expressed on DCs and have been extensively exploited in several fields as potential targets for immunotherapy (89–91). Previously, antibody-mediated CLR targeting has been the most studied strategy for antigen delivery and activation of DCs *in vivo*, but in recent years glycan-based targeting approaches are gaining increasing attention (**Table 1**) (89, 90). Compared to antibody-mediated targeting, in glycan-based targeting, the spatial orientation of displayed carbohydrate CLR ligands can be varied more easily according to the distances between receptor binding sites thereby enhancing receptor-ligand binding and subsequent signaling (89). DC-SIGN is exclusively expressed on immature DCs and shows properties that are often, but not always, associated with Th2 polarization, suppression of inflammation and/or induction of regulatory immune response inhibiting pro-inflammatory Th1/Th17 immunity, especially when it recognizes helminth or allergen associated antigens (92–96). Interestingly, binding of the mycobacterial cell wall component Mannose-capped Lipoarabinomannan (ManLAM) to DC-SIGN inhibits DC maturation and induces IL-10 production (97). Also, the use of fucosylated ligands targeting DC-SIGN biases immune responses toward anti-Th1 responses, with an enhanced Th2 response, and has been shown to ameliorate different autoimmune conditions pre-clinically (92, 98). For instance, exposure of NOD mice to fucose-containing schistosome antigens inhibited the development of type 1 diabetes. This finding is in agreement with reports that have shown that such glycan-CLR signaling can induce a regulatory T cell phenotype having IL-10 and TGF-β production (99), which could explain the observed prevention of the development of autoimmunity in these mice (98, 100).

The MR recognizes terminal mannose, fucose and *N*-acetylglycosamine carbohydrates *via* its carbohydrate recognition domains. In humans, the MR has been identified in $CD1a^{high}$ and $CD1a^{low}$ dermal DCs, as well as *in vitro* monocyte-derived DCs and macrophages (101). In mice, the MR is mainly expressed by tissue and lymphoid-resident macrophages, but also in various endothelial cells and tracheal smooth muscle cells (101, 102). Additionally, MR expression can be detected in cultured murine moDCs, however the *in vivo* expression of MR on murine DCs remains unknown (61, 101). The MR has been reported to induce DC-mediated anti-inflammatory responses, including IL-10 production upon binding to some natural ligands that bind inside the MR binding sites (103). In contrast, when MR interacts with ligands that bind outside the carbohydrate recognition domains, there is no induction of IL-10 secretion, suggesting that, the efficacy of MR-targeted vaccines to induce tolerance will greatly depend on the appropriate selection of targeting vehicles and conditions (104). Notably, in a murine autoimmune model of collagen antibody-induced arthritis, treatment of mice with an epitope of *Leishmania* analog of the receptors for activated C kinase (LACK) from *Leishmania major,* inhibited joint inflammation and downregulated Th1 and Th17 cell responses through binding to the MR in $CD11c^{+}$ DCs (105). Similarly, mannosylated forms of the myelin peptide $PLP_{139-151}$ and MOG induced a state of tolerance in EAE mice (74, 75). Inhibition of EAE disease severity was suggested to be mediated by modulation of peripheral autoreactive T cells. This is in agreement with a study where treatment with mannosylated OVA peptides induced impaired Th1 effector functions and abrogated the activity of pre-existing effector T cells (106).

MGL is well-characterized for its specificity for terminal GalNAc (N-Acetylgalactosamine) residues, expressed by both mammalian cells and pathogens (49). In humans, MGL is expressed *in vivo* by human DCs of skin and lymph nodes and *in vitro* by macrophages and moDCs (107). In mice however, the homologs of human MGL, MGL1, and MGL2 are expressed by dermal DCs and alternatively activated macrophages. Upon ligand binding, the intracellular signaling pathways that are triggered vary extensively depending on the structure of the ligands. In this regard, it has recently been reported that, glycoconjugates from *Fasciola hepatica* potentiate the production of IL-10 by moDCs *via* engagement of MGL (94). Moreover, MGL-expressing DCs from mice infected with these glycoconjugates expanded IL-10-producing T cells and suppressed Th1 responses. Correspondingly, recent data has labeled the MGL as a negative regulator in autoimmune-induced neuroinflammation as MGL was shown to induce apoptosis of autoreactive T cells, the reduction of autoantibodies and the induction of IL-10 (108).

The use of glycan-based strategies has been substantially tested in pre-clinical and a few clinical settings for the treatment of allergies (**Table 1**). In these studies, carbohydrate-modified allergens were used to dampen allergic immune responses while installing antigen-specific T cell anergy both *in vivo* and *in vitro* (76, 77, 109–112). A notable mention is a study by Sirvent *et al* where they conjugated non-oxidized mannan from *Saccharomyces cerevisae* to polymerized grass pollen allergens (PM) and demonstrated that PM-treated human moDCs favor the induction of $CD4^{+}CD25^{high}CD127^{-}Foxp3^{+}$ Tregs over Th1 cells through PD-L1 signaling, subsequently causing an increase in the IL-10/IL-5 cytokine ratio produced by T cells (76) (**Figure 2**). PM was captured *via* the MR and DC-SIGN and proved to be hypoallergenic during *in vivo* skin prick tests and *ex vivo* basophil activation tests. The same group demonstrated that this strategy is equally effective in the treatment of canine atopic dermatitis (77). Interestingly, oxidation of mannan impaired the tolerogenic properties of PM shown in both human and mice, emphasizing the importance of the mannan structure for its functional properties (76, 109, 113). Also, Mathiesen et al. used the major birch pollen allergen, Bet v 1, coupled to defined carbohydrate structures and demonstrated that the prophylactic treatment of mice with GalNAc-coupled Bet v 1 significantly reduces IgE responses (78) (**Figure 2**). This finding suggests

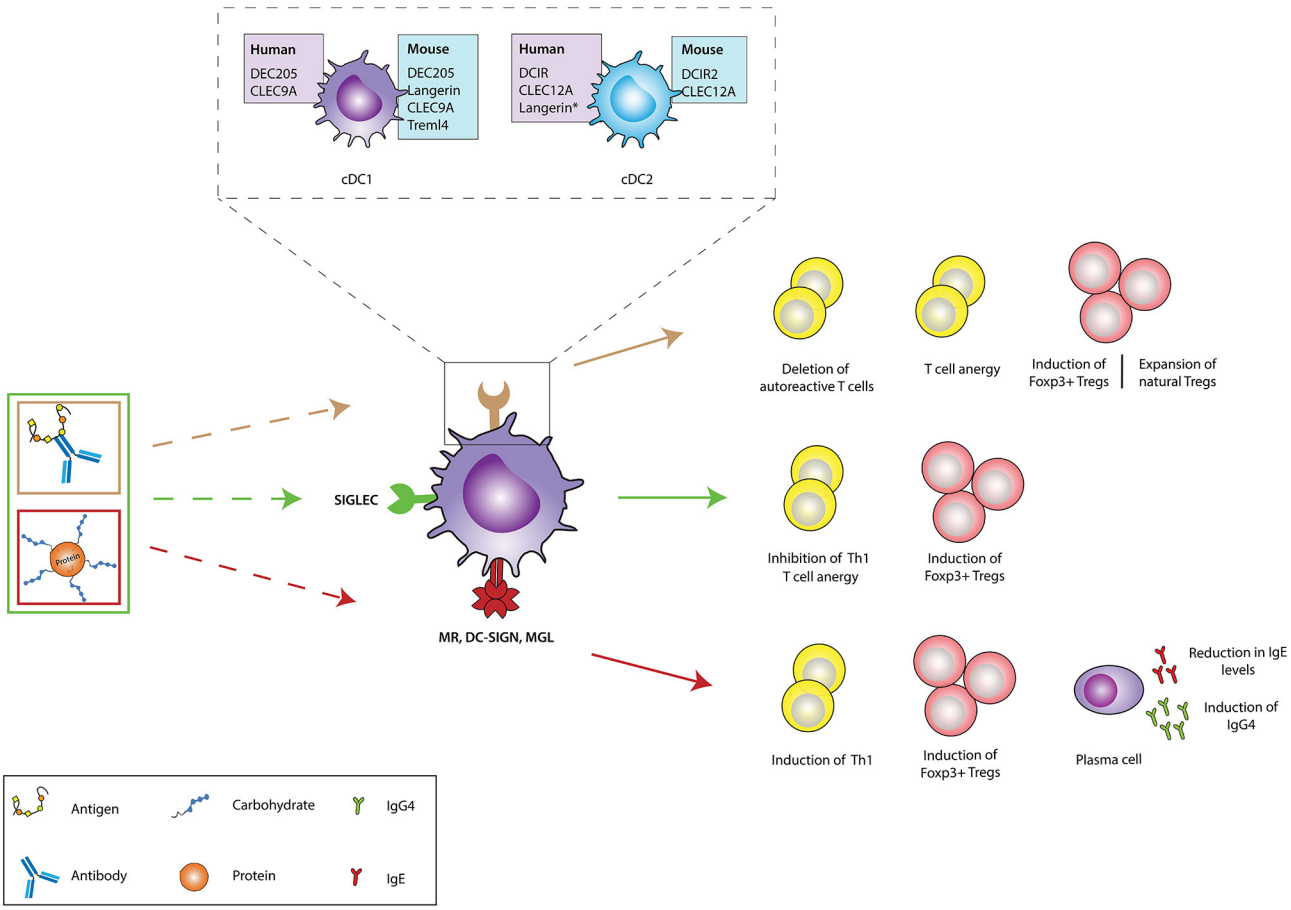

FIGURE 2 | *In vivo* targeting of receptors on DCs against immunopathologies. Different receptors on dendritic cells (DCs) could be targeted using either antigen-antibody fusion compounds or carbohydrate-modified antigens. Brown arrows: the cDC1 and cDC2 subsets express a variety of receptors in both humans (purple boxes) and mice (blue boxes), which recognize and internalize fusion antibodies coupled with antigens, specific for a DC receptor and mediate the deletion of autoreactive T cells, induction of T cell anergy, generation of antigen-specific Foxp3$^+$ Tregs and expansion of natural Tregs (These tolerogenic responses are abrogated if fusion antibodies are administered together with adjuvants like Poly:C). The generation of either antigen-specific Foxp3$^+$ Tregs or promotion of natural Tregs expansion depends of the receptor being targeted. Green arrows: Fusion antibodies against Siglecs, coupled with antigens or sialic acid-modified antigens bind to Siglec receptors on DCs and induce anti-inflammatory signals that result in the induction of Foxp3$^+$ T cells, T cell anergy and the inhibition of Th1 responses. Red arrows: Targeting the MR, DC-SIGN and MGL on DCs with antigens conjugated to specific glycan moieties, result in the polarization of Th2 responses in allergy to Th1 responses and the induction of Foxp3$^+$ T cells. Moreover, this interaction promotes the production of IgG4 blocking antibodies and mediates the reduction of IgE secretion. CLEC9A, C-type lectin domain family 9 member A; Treml4, The Triggering Receptor Expressed on Myeloid cells-like 4; DCIR, dendritic cell immunoreceptor; CLEC12A, C-type lectin domain family 12 member A; cDC1, Conventional type 1 dendritic cells; cDC2, Conventional type 2 dendritic cells; Siglec, Sialic acid-binding immunoglobulin-type lectins; MR, Mannose receptor; DC-SIGN, Dendritic Cell-Specific Intercellular adhesion molecule-3-Grabbing Non-integrin; MGL, macrophage galactose-type C-type lectin. Langerin*: Induced expression.

that MGL, which recognizes terminal α-and β-linked GalNAc structures, might be involved in the induction of the observed immune responses and may thus qualify as another potential candidate for specific antigen-delivery to DCs for induction of tolerance (114). Cumulatively, available data suggest that targeting DC-SIGN, MR and MGL for specific antigen delivery is a promising strategy to be further explored for the management of dysregulated immune pathologies (**Figure 2**).

Langerin

Langerin (CD207) is a transmembrane protein that functions as an endocytic receptor by binding various sugars, including mannose, *n*-acetylglucosamine, fucose, and sulfated sugars, and mediates efficient antigen presentation on MHC I and II products *in vivo* (115). Langerin is highly expressed on surfaces of human LCs, but also at low levels on cDC2s isolated from dermal, lung, liver and lymphoid tissue (116). Yet, langerin is not expressed on circulating cDC2s isolated from blood (116). In mice, langerin is expressed on LCs and CD8α$^+$DEC205$^+$ cDC1s of the spleen and skin draining, however, langerin has not been identified in the homologous human cDC1 subset, indicating that langerin targeting strategies could induce distinct outcomes between mice and human experiments due to differential expression of the targeting receptor in both species (44, 52). Nevertheless, the tolerogenic role of LCs under physiological conditions as well as their accessible location at the surface of the body, marked

langerin as a promising target for *in vivo* delivery of self-antigens to alter disease severity in autoimmune diseases (30, 31, 63). A notable mention is a report from Idoyaga *et al* that showed that, targeting MOG_{35-55} peptides to murine skin and lung langerin$^+$ migratory DCs *via* conjugation with anti-langerin antibodies lessens EAE symptom severity through the induction of Foxp3$^+$ Tregs (63) (**Figure 2**). The effect was comparable to the reduction of disease symptoms following administration of anti-DEC205-MOG fusion proteins. Interestingly, the langerin$^+$ DC population is known to co-express high levels of DEC205, suggesting that the DC subset that is targeted with anti-langerin is also a target for anti-DEC205 mediated induction of Foxp3$^+$ Tregs (117). However, in contrast to the above findings, co-administration of recombinant langerin-mAbs fused to antigen and maturation stimuli like anti-CD40 or polyI:C leads to efficient CD4$^+$ and CD8$^+$ T cell priming, proliferation, and differentiation (118). These results suggest that the strength of the activation signal targeted to langerin$^+$ DC is a very important factor that must be strictly controlled in order to exploit these subsets in autoimmune therapy. Nonetheless, the ability of langerin$^+$ DCs to induce antigen-specific Foxp3$^+$ Tregs in lungs, suggest that anti-langerin mAbs is an attractive candidate for the treatment of respiratory dysregulated immune responses like allergies (**Figure 2**).

Cell Death Receptors: Clec9A and Treml4

DCs are able to recognize and take up DAMPs through surface receptors such as Clec9A, a homodimeric type II transmembrane protein with a single extracellular C-type lectin-like domain expressed on cDC1s in both mice and human (119–121). The highly restricted expression of Clec9A on the human and mice cDC1 subset makes it an attractive receptor for targeting this specific subset of DCs (118). Clec9A ligation to its ligand F-actin either results in immunity or tolerance. As Clec9A promotes CD8$^+$ T cell cross-priming, several *in vitro* studies have been performed to explore Clec9A targeting to induce anti-tumor immune responses (121). To determine whether Clec9A is a promising receptor for DC targeting in the context of autoimmune diseases, mice were injected with anti-Clec9A-antigen conjugates. In steady-state conditions in the absence of adjuvants, these conjugates promoted the differentiation of Foxp3$^+$ Treg cells (62) (**Figure 2**). On the other hand, when anti-Clec9A was administered in combination with polyI:C, tolerance was prevented and instead promoted the development of potent antibody and Th1 or Th17 responses (62). Also, it has been reported that antigen delivery *via* Clec9A enhances the humoral response, even in the absence of adjuvant CpG. However, the immunoglobulin classes and resulting tolerogenic or immunogenic functions, were not explored in this study (122). Although targeting Clec9A can induce Tregs, extensive research is still needed to perfectly map out the optimal conditions that are necessary for tolerance induction.

Treml4 is another cell death receptor and binds to late apoptotic bodies necrotic cells (123). It is a member of the the triggering receptor expressed on myeloid cells (Trem)-family receptors which are primarily expressed on murine CD8$^+$ lymphoid resident DCs and CD103$^+$ lung DCs (63, 123). Treml4 has been investigated as a therapeutic target in a study by Idoyaga and colleagues. In this study, it was demonstrated that, intranasal inoculation of anti-Treml4-MOG peptide conjugates could induce MOG-specific Foxp3$^+$ T cells in mice, but this did not prevent the development or promote improvement of EAE symptoms in diseased mice (63). The molecular mechanisms underlying these observations were not explored but it seems like signaling through this receptor does not produce a strong enough signal necessary for DC-mediated polarization of T cells to Tregs or the suppressive capacity of induced Tregs may be impaired in some way. Mechanistic studies addressing these issues will be very valuable in further exploring the therapeutic potential of this receptor in human settings in the context of immune pathologies. It is also important to note that the expression of Treml4 on human DC is yet to be reported. Therefore, the use of cell death sensing receptors for tolerizing therapies remains elusive until additional studies shed light on their relevance for clinical applications.

ITIM-BEARING RECEPTORS

The Siglec-Family

Siglec receptors are a family of receptors expressed on a wide variety of immune cells, including DCs (43, 59). They recognize sialic acid, which is the last carbohydrate structure added during the process of glycosylation, positioning sialic acid groups on the distal end of sugar-moieties (124). These sialic acid groups are present in the glycocalyx of all mammalian cells and could be considered as SAMPs (43). Siglecs are divided into two groups: (1) Siglecs that are conserved throughout different species, namely Siglec-1 (sialoadhesin), Siglec-2 (CD22), Siglec-4 myelin associated glycoprotein (MAG) and Siglec-15, and (2) the CD33-related Siglecs that have rapidly expanded and have no clear orthologs in mammalian species viz; Siglec−3 (CD33), −5, −6, −7, −8, −9, −10, −11, −14 and −16. The expression of Siglecs on myeloid cells and their subsequent intracellular signaling pathways have been nicely reviewd by Lübbers et al. (59). In short, monocytes and monocyte-derived DCs express high levels of Siglec-3, −7 and −9, and low levels of Siglec-10. cDCs also express Siglec-3, −7, and −9, augmented with low expression levels of Siglec-2 and −15. On the other hand, pDCs only express Siglec-1, which is a non-signaling Siglec that internalizes upon ligand binding, and Siglec-5 (59). The binding affinity to sialic-acid-containing glycan varies between Siglecs. This is determined by the linkage of the sialic acid group to the underlying carbohydrate moiety (α2,3; α2,6 or α2,8 linkage). Another noteworthy feature of Siglecs is their ability to either bind their ligand *via* a *trans* interaction (on a different cell) or *via* a *cis* interaction (on the same cell). These *cis* interactions might contribute to sustain a tolerogenic phenotype, as surface proteins on tolerogenic DCs, immature DCs and Tregs are highly α2,6-sialylated, and could serve as a ligand for tolerogenic Siglecs (125). The conserved Siglec-2 and the CD33-related Siglec-3, and−5 till−11 contain an intracellular ITIM or ITIM-like motif that deliver negative signals *via* recruitment of SHP1 and SHP2 (43).

Interestingly, this immune modulating mechanism has been exploited by pathogen and cancer cells. For example, the protozoan parasite *Trypanosoma cruzi* enzymatically cleaves sialic acid moieties from the host and transfers them *via* α2,3-linkage to its own surface, subsequently downregulating pro-inflammatory IL-12 production and upregulating anti-inflammatory IL-10 production in murine DCs (126). Furthermore, various tumors upregulate α2,3; α2,6; and α2,8 sialic acid on their surface to evade anti-tumor T cell responses and to induce tumor-specific tolerance (59). Comparable to these natural Siglec-mediated immune modulation events, the tolerance inducing capacity of Siglecs could be used in therapeutic strategies to treat auto-immune and allergic diseases. So far, several *in vitro* and *in vivo* mouse studies have been performed to address this concept (**Table 1**). Targeting Siglec H on murine pDCs using anti-Siglec-H-antigen (OVA or MOG peptides) conjugates resulted in a decrease of $CD4^+$ T cell expansion and Th1/Th17 differentiation, which subsequently delayed the onset and reduced disease severity in EAE when using the anti-Siglec-H-MOG conjugate (79). Similarly, direct modification of OVA and MOG peptides with α2,3 or α2,6 sialyl-lactose targeted these antigens to Siglec E on DCs and dampened pro-inflammatory responses in the same EAE mouse model upon treatment with sialylated MOG peptides (80). Siglec E targeting resulted in the induction of $Foxp3^+$ $CD4^+$ Tregs and inhibition of inflammatory effector cells after stimulation with LPS, both *in vitro* and *in vivo* (80) (**Figure 2**). Finally, the potential of sialic acid modified antigens was tested in an experimental murine model for grass pollen allergy. Subcutaneous treatment with sialic acid modified grass pollen peptides induced significant numbers of antigen specific Tregs, inhibited antigen specific effect Th2 cells, and reduced the accumulation of eosinophils (81).

Overall, these studies demonstrate that targeting DC through Siglecs could be very promising for induction of tolerogenic immune responses as a treatment for autoimmune and allergic diseases (**Figure 2**). However, most studies have been performed in mice and are therefore not sufficient for translation to human settings. Consequently, it is important to elucidate their potential and consequences in the human immune system.

DCIR

DCIR is another member of the family of CLRs expressed on cDCs, moDCs and pDCs (44, 45, 127). The human DCIR-Fc protein has been reported to bind a variety of carbohydrate structures including $Lewis^b$, Man3 glycans, and bisecting GlcNAc residues (127). The mouse homolog of DCIR, DCIR2 is primarily expressed on $CD8^+$DCs. DCIR is important for the homeostasis of the immune system by, in part, regulating DC differentiation or polarization, as DCIR-deficient mice were prone to develop autoimmune encephalitis (128). As such, consistent with results obtained in mouse models (128, 129), polymorphisms of the DCIR gene are associated with the susceptibility to RA in humans (130). $DCIR2^+$ DCs have been shown to stimulate natural $Foxp3^+$ Tregs to mediate tolerance to self-antigens in the absence of immune stimuli (41). However, in the presence of a maturation stimulus, they induce T cell expansion and production of pro-inflammatory cytokines (41). Upon triggering with DCIR-specific mAbs, DCIR is internalized in both pDCs as well as human moDCs, resulting in efficient antigen presentation to T cells and downregulation of IFN-α production (131). Interestingly, using an anti-DCIR2-$PLP_{139-151}$ and MOG fusion antibody to target DCs resulted in the amelioration of EAE symptoms (63, 64). This effect was suggested to be mediated primarily through the depletion of autoreactive T cells or induction of anergy in pathogenic T cells (**Figure 2**). However, DCIR2-targeting did not induce *de novo* generation of Ag-specific Treg from naïve $CD4^+$ T cell precursors in the steady state due to lack of TGF-β expression by $CD4^+$ $CD11b^+$ DC but instead stimulated and expanded natural Tregs (64). Similarly, targeting β-Cell antigen using chimeric DCIR2 antibodies in NOD mice, elicited tolerogenic $CD4^+$ T cell responses and induced increased T cell apoptosis while delaying diabetes induction (65). Targeting DCs with anti-DCIR2-antigen has also shown some promise in the field of transplantation where, an anti-DCIR2-MHC I monomer successfully inhibited allorecognition and the production of IgG alloantibodies leading to long-term allograft survival (132). Unexpectedly, DCIR2 targeting of mice DCs augmented spontaneous EAU development, characterized by local reduction in Tregs (133). While DCIR2 may be a promising candidate for *in vivo* Ag delivery in mice, this may not be the case for humans because, even though DCIR2 is highly restricted to $CD11b^+$ DC subset in mice it is not detectable on the human $CD1a/b^+$ cDC subset, a proposed equivalent of mouse $CD11b^+$ DCs (130). Thus, there is need for identification of surface molecules that are specifically and similarly expressed by mouse and human DCs to allow exploration of clinical effectiveness of vaccines targeting these DC subsets.

Clec12A (MICL)

The human myeloid inhibitory C-type lectin receptor (MICL) or Clec12A is expressed on alveolar macrophages, cDC1s, cDC2s, and pDCs, while the mouse Clec12A is expressed on myeloid cells (45, 134). Clec12A selectively binds to dead cells that have lost their plasma membrane integrity (130). The endocytic capacity of Clec12A has led to its being exploited for DC-specific antigen targeting. In this regard, antibody-mediated targeting of OVA to Clec12A in mice was able to induce potent antibody responses but no tolerogenic responses (135). Such targeting of Clec12A with anti-Clec12A antibodies seems to be sufficient for antigen internalization, processing and presentation but not for activation of DCs as reported in targeting of DEC205 with mAbs (122, 135). These mAbs may therefore simply serve to deliver Ags to DCs. The study of Clec12A in the context of immunotherapy for dysregulated immune pathologies is still in its infancy and further research is warranted given that preliminary data and the biological properties of Clec12A portrays this receptor as a promising candidate in this field.

FUTURE PERSPECTIVES AND CONCLUSIONS

Due to the unique capacity of DCs to coordinate innate and adaptive immune responses, they have been extensively studied and have proven to be a very promising strategy for immunotherapy. In the past decades, our knowledge of the potential of DCs in cancer and autoimmune disease/allergy therapy has expanded remarkably, advancing from the current *ex vivo* generated DC-based vaccines to *in vivo* targeting of DCs *via* specific receptors (**Figure 1**). Various compounds, such as vitamin D3, retinoic acid, dexamethasone, or IL-10, and TGFβ have shown the potency of tolDCs as immunotherapy in autoimmune diseases. However, there has been an increasing interest in moving toward *in vivo* targeting strategies where the induction of tolerance is achieved by targeting different receptors on DCs in their natural environment with antigen-delivering antibodies and antigen-carbohydrate conjugates. This has proven to be very effective in the amelioration of disease processes in a range of mouse models including MS, diabetes and allergies. Nevertheless, there is still a need to expand our knowledge on the potential application of such *in vivo* targeting strategies in human settings because, despite the many important similarities that exist between human and mouse DCs, very crucial incompatibilities between both species still limits the capacity to translate findings from one species to the other. Nonetheless, the potential for future clinical translation and therapeutic application of *in vivo* antigen targeting to DCs is very promising, although additional research is necessary to decipher the specific molecular mechanisms involved in the anti-disease tolerance promoted by such DCs. During the development of potential vaccines for autoimmune and allergic diseases, multiple inevitable questions need to be addressed. For instance, receptors that are not inherently tolerogenic but are capable of inducing tolerance under certain conditions, such as DEC205, DC-SIGN, and langerin, the induced tolerogenic effect is abrogated in the presence of pro-inflammatory modulators. Therefore, the appropriate optimization of vaccine formulations to target such receptors will be of utmost importance. In contrast, Siglecs have the ability to induce tolerogenic immune responses even in the presence of the pro-inflammatory modulator LPS (80, 136) and the resulting responses are not particularly affected by the presence of adjuvants. Moreover, there is still uncertainty about the right antigen-antibody/glycan dosage necessary for induction of tolerance, the duration of the resulting tolerogenic response, the effect on other immune cells expressing similar receptors as those being targeted, the use of a vehicle, and the method of administration. Finally, it may also be important to further investigate the potential positive or negative effects that receptor-specific antigen targeting may have on other myeloid cells, such as macrophages that express some of the DC receptors that can be targeted. Although further investigation is warranted, the effects might be negligible giving the lower antigen presenting capacity of macrophages. Overall, it is clear that the generation of a tolerogenic immune response *via* DC receptor targeting depends on the receptor, the DC subset being targeted, and the specific micro-environmental factors.

AUTHOR CONTRIBUTIONS

CC and B-CKD performed the literature search, wrote the manuscript, and created all figures. EdJ and YvK critically read and carefully revised all versions of the manuscript providing valuable guidance and insight. RvR critically read the manuscript and provided valuable additions. All authors contributed to the article and approved the submitted version.

FUNDING

This work was supported by a grant from Health Holland (SIALLERGEN HH LSHM19073).

REFERENCES

1. Merad M, Sathe P, Helft J, Miller J, Mortha A. The dendritic cell lineage: ontogeny and function of dendritic cells and their subsets in the steady state and the inflamed setting. *Annu Rev Immunol.* (2013) 31:563–604. doi: 10.1146/annurev-immunol-020711-074950
2. Audiger C, Rahman MJ, Yun TJ, Tarbell KV, Lesage S. The importance of dendritic cells in maintaining immune tolerance. *J Immunol.* (2017) 198:2223–31. doi: 10.4049/jimmunol.1601629
3. Fucikova J, Palova-Jelinkova L, Bartunkova J, Spisek R. Induction of tolerance and immunity by dendritic cells: Mechanisms and clinical applications. *Front Immunol.* (2019) 10:2393. doi: 10.3389/fimmu.2019.02393
4. Collin M, Bigley V. Human dendritic cell subsets: an update. *Immunology.* (2018) 154:3–20. doi: 10.1111/imm.12888
5. Cauwels A, Tavernier J. Tolerizing strategies for the treatment of autoimmune diseases: from *ex vivo* to *in vivo* strategies. *Front Immunol.* (2020) 11: e674. doi: 10.3389/fimmu.2020.00674
6. Navarro-Barriuso J, Mansilla MJ, Naranjo-Gómez M, Sánchez-Pla A, Quirant-Sánchez B, Teniente-Serra A, et al. Comparative transcriptomic profile of tolerogenic dendritic cells differentiated with vitamin D3, dexamethasone and rapamycin. *Sci Rep.* (2018) 8:14985. doi: 10.1038/s41598-018-33248-7
7. Quintana FJ, Murugaiyan G, Farez MF, Mitsdoerffer M, Tukpah AM, Burns EJ, et al. An endogenous aryl hydrocarbon receptor ligand acts on dendritic cells and T cells to suppress experimental autoimmune encephalomyelitis. *Proc Natl Acad Sci USA.* (2010) 107:20768–73. doi: 10.1073/pnas.1009201107
8. Obregon C, Kumar R, Pascual MA, Vassalli G, Golshayan D. Update on dendritic cell-induced immunological and clinical tolerance. *Front Immunol.* (2017) 8:1514. doi: 10.3389/fimmu.2017.01514
9. Ten Brinke A, Martinez-Llordella M, Cools N, Hilkens CMU, Van Ham SM, Sawitzki B, et al. Ways forward for tolerance-inducing cellular therapies- An afactt perspective. *Front Immunol.* (2019) 10:181. doi: 10.3389/fimmu.2019.00181
10. Aragão-França LS, Rocha VCJ, Cronemberger-Andrade A, Costa FHB, Vasconcelos JF, Athanazio DA, et al. Tolerogenic dendritic cells reduce airway inflammation in a model of dust mite triggered allergic inflammation. *Allergy Asthma Immunol Res.* (2018) 10:406–19. doi: 10.4168/aair.2018.10.4.406
11. Lehmann CHK, Heger L, Heidkamp GF, Baranska A, Lühr JJ, Hoffmann A, et al. Direct delivery of antigens to dendritic cells *via* antibodies specific for

endocytic receptors as a promising strategy for future therapies. *Vaccines.* (2016) 4:8. doi: 10.3390/vaccines4020008
12. Schwendener RA. Liposomes as vaccine delivery systems: a review of the recent advances. *Ther Adv Vaccines.* (2014) 2:159–82. doi: 10.1177/2051013614541440
13. Rhodes JW, Tong O, Harman AN, Turville SG. Human dendritic cell subsets, ontogeny, and impact on HIV infection. *Front Immunol.* (2019) 10:1088. doi: 10.3389/fimmu.2019.01088
14. Lamendour L, Deluce-Kakwata-nkor N, Mouline C, Gouilleux-Gruart V, Velge-Roussel F. Tethering innate surface receptors on dendritic cells: a new avenue for immune tolerance induction? *Int J Mol Sci.* (2020) 21:1–15. doi: 10.3390/ijms21155259
15. Amon L, Lehmann CHK, Heger L, Heidkamp GF, Dudziak D. The ontogenetic path of human dendritic cells. *Mol Immunol.* (2020) 120:122–9. doi: 10.1016/j.molimm.2020.02.010
16. Villani AC, Satija R, Reynolds G, Sarkizova S, Shekhar K, Fletcher J, et al. Single-cell RNA-seq reveals new types of human blood dendritic cells, monocytes, and progenitors. *Science.* (2017) 356:eaah4573. doi: 10.1126/science.aah4573
17. Brown CC, Gudjonson H, Pritykin Y, Deep D, Lavallée VP, Mendoza A, et al. Transcriptional basis of mouse and human dendritic cell heterogeneity. *Cell.* (2019) 179:846–63.e24. doi: 10.1016/j.cell.2019.09.035
18. Schlitzer A, McGovern N, Ginhoux F. Dendritic cells and monocyte-derived cells: two complementary and integrated functional systems. *Semin Cell Dev Biol.* (2015) 41:9–22. doi: 10.1016/j.semcdb.2015.03.011
19. Rodrigues PF, Tussiwand R. Novel concepts in plasmacytoid dendritic cell (pDC) development and differentiation. *Mol Immunol.* (2020) 126:25–30. doi: 10.1016/j.molimm.2020.07.006
20. Swiecki M, Colonna M. The multifaceted biology of plasmacytoid dendritic cells. *Nat Rev Immunol.* (2015) 15:471–85. doi: 10.1038/nri3865
21. Busold S, Nagy NA, Tas SW, van Ree R, de Jong EC, Geijtenbeek TBH. Various tastes of sugar: the potential of glycosylation in targeting and modulating human immunity *via* C-type lectin receptors. *Front Immunol.* (2020) 11:1–12. doi: 10.3389/fimmu.2020.00134
22. Iberg CA, Hawiger D. Natural and induced tolerogenic dendritic cells. *J Immunol.* (2020) 204:733–44. doi: 10.4049/jimmunol.1901121
23. Oh J, Shin JS. The role of dendritic cells in central tolerance. Immune Netw. (2015) 15:111–20. doi: 10.4110/in.2015.15.3.111
24. Klein L, Hinterberger M, Wirnsberger G, Kyewski B. Antigen presentation in the thymus for positive selection and central tolerance induction. *Nat Rev Immunol.* (2009) 9:833–44. doi: 10.1038/nri2669
25. Proietto AI, Van Dommelen S, Zhou P, Rizzitelli A, D'Amico A, Steptoe RJ, et al. Dendritic cells in the thymus contribute to T-regulatory cell induction. *Proc Natl Acad Sci USA*. (2008) 105:19869–74. doi: 10.1073/pnas.0810268105
26. Steinman RM. Decisions about dendritic cells: past, present, and future. *Annu Rev Immunol.* (2012) 30:1–22. doi: 10.1146/annurev-immunol-100311-102839
27. Lutz MB, Schuler G. Immature, semi-mature and fully mature dendritic cells: which signals induce tolerance or immunity? *Trends Immunol.* (2002) 23:445–9. doi: 10.1016/S1471-4906(02)02281-0
28. Steinman RM, Hawiger D, Nussenzweig MC. Tolerogenic dendritic cells. *Annu Rev Immunol.* (2003) 21:685–711. doi: 10.1146/annurev.immunol.21.120601.141040
29. Adnan E, Matsumoto T, Ishizaki J, Onishi S, Suemori K, Yasukawa M, et al. Human tolerogenic dendritic cells generated with protein kinase C inhibitor are optimal for functional regulatory T cell induction—A comparative study. *Clin Immunol.* (2016) 173:96–108. doi: 10.1016/j.clim.2016.09.007
30. West HC, Bennett CL. Redefining the role of langerhans cells as immune regulators within the skin. *Front Immunol.* (2018) 8:1941. doi: 10.3389/fimmu.2017.01941
31. Azukizawa H, Döhler A, Kanazawa N, Nayak A, Lipp M, Malissen B, et al. Steady state migratory RelB+ langerin+ dermal dendritic cells mediate peripheral induction of antigen-specific CD4+CD25+Foxp3+ regulatory T cells. *Eur J Immunol.* (2011) 41:1420–34. doi: 10.1002/eji.201040930
32. Devi KSP, Anandasabapathy N. The origin of DCs and capacity for immunologic tolerance in central and peripheral tissues. *Semin Immunopathol.* (2017) 39:137–52. doi: 10.1007/s00281-016-0602-0
33. Chu CC, Ali N, Karagiannis P, Di Meglio P, Skowera A, Napolitano L, et al. Resident CD141 (BDCA3) + dendritic cells in human skin produce IL-10 and induce regulatory T cells that suppress skin inflammation. *J Exp Med.* (2012) 209:935–45. doi: 10.1084/jem.20112583
34. Klechevsky E, Morita R, Liu M, Cao Y, Coquery S, Thompson-Snipes LA, et al. Functional specializations of human epidermal langerhans cells and CD14+ dermal dendritic cells. *Immunity.* (2008) 29:497–510. doi: 10.1016/j.immuni.2008.07.013
35. Comi M, Avancini D, Santoni de Sio F, Villa M, Uyeda MJ, Floris M, et al. Coexpression of CD163 and CD141 identifies human circulating IL-10-producing dendritic cells (DC-10). *Cell Mol Immunol.* (2020) 17:95–107. doi: 10.1038/s41423-019-0218-0
36. Amodio G, Mugione A, Sanchez AM, Viganò P, Candiani M, Somigliana E, et al. HLA-G expressing DC-10 and CD4+ T cells accumulate in human decidua during pregnancy. *Hum Immunol.* (2013) 74:406–11. doi: 10.1016/j.humimm.2012.11.031
37. Comi M, Amodio G, Gregori S. Interleukin-10-producing DC-10 is a unique tool to promote tolerance *via* antigen-specific T regulatory type 1 cells. *Front Immunol.* (2018) 9:6. doi: 10.3389/fimmu.2018.00682
38. Gregori S, Tomasoni D, Pacciani V, Scirpoli M, Battaglia M, Magnani CF, et al. Differentiation of type 1 T regulatory cells (Tr1) by tolerogenic DC-10 requires the IL-10-dependent ILT4/HLA-G pathway. *Blood.* (2010) 116:935–44. doi: 10.1182/blood-2009-07-234872
39. Coombes JL, Siddiqui KRR, Arancibia-Cárcamo CV, Hall J, Sun CM, Belkaid Y, et al. A functionally specialized population of mucosal CD103+ DCs induces Foxp3+ regulatory T cells *via* a TGF-β -and retinoic acid-dependent mechanism. *J Exp Med.* (2007) 204:1757–64. doi: 10.1084/jem.20070590
40. Tordesillas L, Berin MC. Mechanisms of oral tolerance. *Clin Rev Allergy Immunol.* (2018) 55:107–17. doi: 10.1007/s12016-018-8680-5
41. Yamazaki S, Morita A. Dendritic cells in the periphery control antigen-specific natural and induced reulatory T cells. *Front Immunol.* (2013) 4:e151. doi: 10.3389/fimmu.2013.00151
42. Matteoli G, Mazzini E, Iliev ID, Mileti E, Fallarino F, Puccetti P, et al. Gut CD103+ dendritic cells express indoleamine 2,3-dioxygenase which influences T regulatory/T effector cell balance and oral tolerance induction. *Gut.* (2010) 59:595–604. doi: 10.1136/gut.2009.185108
43. Läubli H, Varki A. Sialic acid–binding immunoglobulin-like lectins (Siglecs) detect self-associated molecular patterns to regulate immune responses. *Cell Mol Life Sci.* (2020) 77:593–605. doi: 10.1007/s00018-019-03288-x
44. del Fresno C, Iborra S, Saz-Leal P, Martínez-López M, Sancho D. Flexible signaling of Myeloid C-type lectin receptors in immunity and inflammation. *Front Immunol.* (2018) 9:1. doi: 10.3389/fimmu.2018.00804
45. Geijtenbeek TBH, Gringhuis SI. Signalling through C-type lectin receptors: shaping immune responses. *Nat Rev Immunol.* (2009) 9:465–79. doi: 10.1038/nri2569
46. Duan S, Paulson JC. Siglecs as immune cell checkpoints in disease. *Annu Rev Immunol.* (2020) 38:365–95. doi: 10.1146/annurev-immunol-102419-035900
47. García-Vallejo JJ, Van Kooyk Y. Endogenous ligands for C-type lectin receptors: the true regulators of immune homeostasis. *Immunol Rev.* (2009) 230:22–37. doi: 10.1111/j.1600-065X.2009.00786.x
48. Iborra S, Sancho D. Signalling versatility following self and non-self sensing by myeloid C-type lectin receptors. *Immunobiology.* (2015) 220:175–84. doi: 10.1016/j.imbio.2014.09.013
49. Zizzari IG, Napoletano C, Battisti F, Rahimi H, Caponnetto S, Pierelli L, et al. MGL receptor and immunity: when the ligand can make the difference. *J Immunol Res.* (2015) 2015:450695. doi: 10.1155/2015/450695
50. Rapoport EM, Khaidukov SV, Gaponov AM, Pazynina GV, Tsygankova SV, Ryzhov IM, et al. Glycan recognition by human blood mononuclear cells with an emphasis on dendritic cells. *Glycoconj J.* (2018) 35:191–203. doi: 10.1007/s10719-017-9811-6
51. Redelinghuys P, Brown GD. Inhibitory C-type lectin receptors in myeloid cells. *Immunol Lett.* (2011) 136:1–12. doi: 10.1016/j.imlet.2010.10.005
52. Sancho D, Reis e Sousa C. Signaling by myeloid C-type lectin receptors in immunity and homeostasis. *Annu Rev Immunol.* (2012) 30:491–529. doi: 10.1146/annurev-immunol-031210-101352.Signaling
53. Fehres CM, Unger WWJ, Garcia-Vallejo JJ, van Kooyk Y. Understanding the biology of antigen cross-presentation for the design of vaccines against cancer. *Front Immunol.* (2014) 5:149. doi: 10.3389/fimmu.2014.00149

54. Streng-Ouwehand I, Ho NI, Litjens M, Kalay H, Boks MA, Cornelissen LAM, et al. Glycan modification of antigen alters its intracellular routing in dendritic cells, promoting priming of T cells. *Elife.* (2016) 5:11765. doi: 10.7554/eLife.11765
55. Nair P, Amsen D, Blander JM. Co-ordination of incoming and outgoing traffic in antigen-presenting cells by pattern recognition receptors and T Cells. *Traffic.* (2011) 12:1669–76. doi: 10.1111/j.1600-0854.2011.01251.x
56. McGreal EP, Miller JL, Gordon S. Ligand recognition by antigen-presenting cell C-type lectin receptors. *Curr Opin Immunol.* (2005) 17:18–24. doi: 10.1016/j.coi.2004.12.001
57. Pereira MS, Alves I, Vicente M, Campar A, Silva MC, Padrão NA, et al. Glycans as key checkpoints of T cell activity and function. *Front Immunol.* (2018) 9:2754. doi: 10.3389/fimmu.2018.02754
58. Crespo HJ, Lau JTY, Videira PA. Dendritic cells: a spot on sialic acid. *Front Immunol.* (2013) 4:491. doi: 10.3389/fimmu.2013.00491
59. Lübbers J, Rodríguez E, van Kooyk Y. Modulation of immune tolerance *via* siglec-sialic acid interactions. *Front Immunol.* (2018) 9:2807. doi: 10.3389/fimmu.2018.02807
60. Figdor CG, Van Kooyk Y, Adema GJ. C-type lectin receptors on dendritic cells and langerhans cells. *Nat Rev Immunol.* (2002) 2:77–84. doi: 10.1038/nri723
61. Mahnke K, Guo M, Lee S, Sepulveda H, Swain SL, Nussenzweig M, et al. The dendritic cell receptor for endocytosis, DEC-205, can recycle and enhance antigen presentation *via* major histocompatibility complex class II-positive lysosomal compartments. *J Cell Biol.* (2000) 151:673–83. doi: 10.1083/jcb.151.3.673
62. Joffre OP, Sancho D, Zelenay S, Keller AM, Reis E Sousa C. Efficient and versatile manipulation of the peripheral CD4+ T-cell compartment by antigen targeting to DNGR-1/CLEC9A. *Eur J Immunol.* (2010) 40:1255–65. doi: 10.1002/eji.201040419
63. Idoyaga J, Fiorese C, Zbytnuik L, Lubkin A, Miller J, Malissen B, et al. Specialized role of migratory dendritic cells in peripheral tolerance induction. *J Clin Invest.* (2013) 123:844–54. doi: 10.1172/JCI65260
64. Tabansky I, Keskin DB, Watts D, Petzold C, Funaro M, Sands W, et al. Targeting DEC-205-DCIR2+ dendritic cells promotes immunological tolerance in proteolipid protein-induced experimental autoimmune encephalomyelitis. *Mol Med.* (2018) 24:17. doi: 10.1186/s10020-018-0017-6
65. Price JD, Hotta-Iwamura C, Zhao Y, Beauchamp NM, Tarbell KV. DCIR2+ cDC2 DCs and Zbtb32 restore CD4+ T-cell tolerance and inhibit diabetes. *Diabetes.* (2015) 64:3521–31. doi: 10.2337/db14-1880
66. Ring S, Maas M, Nettelbeck DM, Enk AH, Mahnke K. Targeting of autoantigens to DEC205 + dendritic cells *in vivo* suppresses experimental allergic encephalomyelitis in mice. *J Immunol.* (2013) 191:2938–47. doi: 10.4049/jimmunol.1202592
67. Stern JNH, Keskin DB, Kato Z, Waldner H, Schallenberg S, Anderson A, et al. Promoting tolerance to proteolipid protein-induced experimental autoimmune encephalomyelitis through targeting dendritic cells. *Proc Natl Acad Sci USA.* (2010) 107:17280–5. doi: 10.1073/pnas.1010263107
68. Spiering R, Margry B, Keijzer C, Petzold C, Hoek A, Wagenaar-Hilbers J, et al. DEC205 + dendritic cell–targeted tolerogenic vaccination promotes immune tolerance in experimental autoimmune arthritis. *J Immunol.* (2015) 194:4804–13. doi: 10.4049/jimmunol.1400986
69. Bruder D, Westendorf AM, Hansen W, Prettin S, Gruber AD, Qian Y, et al. On the edge of autoimmunity: T-cell stimulation by steady-state dendritic cells prevents autoimmune diabetes. *Diabetes.* (2005) 54:3395–401. doi: 10.2337/diabetes.54.12.3395
70. Mukhopadhaya A, Hanafusa T, Jarchum I, Chen YG, Iwai Y, Serreze DV, et al. Selective delivery of β cell antigen to dendritic cells *in vivo* leads to deletion and tolerance of autoreactive CD8+ T cells in NOD mice. *Proc Natl Acad Sci USA.* (2008) 105:6374–9. doi: 10.1073/pnas.0802644105
71. Wadwa M, Klopfleisch R, Buer J, Westendorf AM. Targeting antigens to DEC-205 on dendritic cells induces immune protection in experimental colitis in mice. *Eur J Microbiol Immunol.* (2016) 6:1–8. doi: 10.1556/1886.2015.00048
72. Kamoi K, Martín-Granados C, Bobu C, Wikstrom M, Degli-Esposti M, Steinman R, et al. Anti-DEC205 mediated delivery of self-antigen to dendritic cell restores tolerance in spontaneous EAU. *Invest Ophthalmol Vis Sci.* (2012) 53:6233.
73. Ettinger M, Gratz IK, Gruber C, Hauser-Kronberger C, Johnson TS, Mahnke K, et al. Targeting of the hNC16A collagen domain to dendritic cells induces tolerance to human type XVII collagen. *Exp Dermatol.* (2012) 21:395–8. doi: 10.1111/j.1600-0625.2012.01474.x
74. Kel J, Oldenampsen J, Luca M, Drijfhout JW, Koning F, Nagelkerken L. Soluble mannosylated myelin peptide inhibits the encephalitogenicity of autoreactive T cells during experimental autoimmune encephalomyelitis. *Am J Pathol.* (2007) 170:272–80. doi: 10.2353/ajpath.2007.060335
75. Luca ME, Kel JM, Van Rijs W, Drijfhout JW, Koning F, Nagelkerken L. Mannosylated PLP139-151 induces peptide-specific tolerance to experimental autoimmune encephalomyelitis. *J Neuroimmunol.* (2005) 160:178–87. doi: 10.1016/j.jneuroim.2004.11.014
76. Sirvent S, Soria I, Cirauqui C, Cases B, Manzano AI, Diez-Rivero CM, et al. Novel vaccines targeting dendritic cells by coupling allergoids to nonoxidized mannan enhance allergen uptake and induce functional regulatory T cells through programmed death ligand 1. *J Allergy Clin Immunol.* (2016) 138:558–67.e11. doi: 10.1016/j.jaci.2016.02.029
77. Soria I, Alvarez J, Manzano AI, López-Relaño J, Cases B, Mas-Fontao A, et al. Mite allergoids coupled to nonoxidized mannan from *Saccharomyces cerevisae* efficiently target canine dendritic cells for novel allergy immunotherapy in veterinary medicine. *Vet Immunol Immunopathol.* (2017) 190:65–72. doi: 10.1016/j.vetimm.2017.07.004
78. Mathiesen CBK, Carlsson MC, Brand S, Möller SR, Idorn M, Thor Straten P, et al. Genetically engineered cell factories produce glycoengineered vaccines that target antigen-presenting cells and reduce antigen-specific T-cell reactivity. *J Allergy Clin Immunol.* (2018) 142:1983–7. doi: 10.1016/j.jaci.2018.07.030
79. Loschko J, Heink S, Hackl D, Dudziak D, Reindl W, Korn T, et al. Antigen targeting to plasmacytoid dendritic cells *via* siglec-h inhibits Th cell-dependent autoimmunity. *J Immunol.* (2011) 187:6346–56. doi: 10.4049/jimmunol.1102307
80. Perdicchio M, Ilarregui JM, Verstege MI, Cornelissen LAM, Schetters STT, Engels S, et al. Sialic acid-modified antigens impose tolerance *via* inhibition of T-cell proliferation and *de novo* induction of regulatory T cells. *Proc Natl Acad Sci USA.* (2016) 113:3329–34. doi: 10.1073/pnas.1507706113
81. Hesse L, Feenstra R, Ambrosini M, de Jager WA, Petersen A, Vietor H, et al. Subcutaneous immunotherapy using modified Phl p5a-derived peptides efficiently alleviates allergic asthma in mice. *Allergy Eur J Allergy Clin Immunol.* (2019) 74:2495–8. doi: 10.1111/all.13918
82. Mahnke K, Ring S, Enk AH. Antibody targeting of "steady-state" dendritic cells induces tolerance mediated by regulatory T cells. *Front Immunol.* (2016) 7:63. doi: 10.3389/fimmu.2016.00063
83. Mahnke K, Qian Y, Knop J, Enk AH. Induction of CD4+/CD25+ regulatory T cells by targeting of antigens to immature dendritic cells. *Blood.* (2003) 101:4862–9. doi: 10.1182/blood-2002-10-3229
84. Maksimow M, Miiluniemi M, Marttila-Ichihara F, Jalkanen S, Hänninen A. Antigen targeting to endosomal pathway in dendritic cell vaccination activates regulatory T cells and attenuates tumor immunity. *Blood.* (2006) 108:1298–305. doi: 10.1182/blood-2005-11-008615
85. Bonifaz L, Bonnyay D, Mahnke K, Rivera M, Nussenzweig MC, Steinman RM. Efficient targeting of protein antigen to the dendritic cell receptor DEC-205 in the steady state leads to antigen presentation on major histocompatibility complex class I products and peripheral CD8+ T cell tolerance. *J Exp Med.* (2002) 196:1627–38. doi: 10.1084/jem.20021598
86. Hawiger D, Masilamani RF, Bettelli E, Kuchroo VK, Nussenzweig MC. Immunological unresponsiveness characterized by increased expression of CD5 on peripheral T cells induced by dendritic cells *in vivo*. *Immunity.* (2004) 20:695–705. doi: 10.1016/j.immuni.2004.05.002
87. Inaba K, Swiggard WJ, Inaba M, Meltzer J, Miryza A, Sasagawa T, et al. Tissue distribution of the DEC-205 protein that is detected by the monoclonal antibody NLDC-145. I. Expression on dendritic cells and other subsets of mouse leukocytes. *Cell Immunol.* (1995) 163:148–56. doi: 10.1006/cimm.1995.1109
88. Kato M, McDonald KJ, Khan S, Ross IL, Vuckovic S, Chen K, et al. Expression of human DEC-205 (CD205) multilectin receptor on leukocytes. *Int Immunol.* (2006) 18:857–69. doi: 10.1093/intimm/dxl022

89. Lepenies B, Lee J, Sonkaria S. Targeting C-type lectin receptors with multivalent carbohydrate ligands. *Adv Drug Deliv Rev.* (2013) 65:1271–81. doi: 10.1016/j.addr.2013.05.007
90. Li RE, van Vliet SJ, van Kooyk Y. Using the glycan toolbox for pathogenic interventions and glycan immunotherapy. *Curr Opin Biotechnol.* (2018) 51:24–31. doi: 10.1016/j.copbio.2017.11.003
91. Johannssen T, Lepenies B. Glycan-based cell targeting to modulate immune responses. *Trends Biotechnol.* (2017) 35:334–46. doi: 10.1016/j.tibtech.2016.10.002
92. Marciani DJ. Effects of immunomodulators on the response induced by vaccines against autoimmune diseases. *Autoimmunity.* (2017) 50:393–402. doi: 10.1080/08916934.2017.1373766
93. Favoretto BC, Casabuono AAC, Portes-Junior JA, Jacysyn JF, Couto AS, Faquim-Mauro EL. High molecular weight components containing N-linked oligosaccharides of Ascaris suum extract inhibit the dendritic cells activation through DC-SIGN and MR. *Mol Immunol.* (2017) 87:33–46. doi: 10.1016/j.molimm.2017.03.015
94. Rodríguez E, Carasi P, Frigerio S, da Costa V, van Vliet S, Noya V, et al. Fasciola hepatica immune regulates CD11c+ cells by interacting with the macrophage gal/GalNAc lectin. *Front Immunol.* (2017) 8:264. doi: 10.3389/fimmu.2017.00264
95. Klaver EJ, Kuijk LM, Laan LC, Kringel H, van Vliet SJ, Bouma G, et al. Trichuris suis-induced modulation of human dendritic cell function is glycan-mediated. *Int J Parasitol.* (2013) 43:191–200. doi: 10.1016/j.ijpara.2012.10.021
96. Cvetkovic J, Ilic N, Gruden-Movsesijan A, Tomic S, Mitic N, Pinelli E, et al. DC-SIGN signalling induced by Trichinella spiralis products contributes to the tolerogenic signatures of human dendritic cells. *Sci Rep.* (2020) 10:20283. doi: 10.1038/s41598-020-77497-x
97. Gringhuis SI, den Dunnen J, Litjens M, van der Vlist M, Wevers B, Bruijns SCM, et al. Dectin-1 directs T helper cell differentiation by controlling noncanonical NF-κB activation through Raf-1 and Syk. *Nat Immunol.* (2009) 10:203–13. doi: 10.1038/ni.1692
98. Zaccone P, Burton O, Miller N, Jones FM, Dunne DW, Cooke A. Schistosoma mansoni egg antigens induce Treg that participate in diabetes prevention in NOD mice. *Eur J Immunol.* (2009) 39:1098–107. doi: 10.1002/eji.200838871
99. Maizels RM, Smits HH, McSorley HJ. Modulation of host immunity by helminths: the expanding repertoire of parasite effector molecules. *Immunity.* (2018) 49:801–18. doi: 10.1016/j.immuni.2018.10.016
100. Ruyssers NE, De Winter BY, De Man JG, Loukas A, Herman AG, Pelckmans PA, et al. Worms and the treatment of inflammatory bowel disease: are molecules the answer? *Clin Dev Immunol.* (2008) 2008:567314. doi: 10.1155/2008/567314
101. Taylor PR, Gordon S, Martinez-Pomares L. The mannose receptor: linking homeostasis and immunity through sugar recognition. *Trends Immunol.* (2005) 26:104–10. doi: 10.1016/j.it.2004.12.001
102. Linehan SA, Martínez-Pomares L, Stahl PD, Gordon S. Mannose receptor and its putative ligands in normal murine lymphoid and nonlymphoid organs: *in situ* expression of mannose receptor by selected macrophages, endothelial cells, perivascular microglia, and mesangial cells, but not dendritic cells. *J Exp Med.* (1999) 189:1961–72. doi: 10.1084/jem.189.12.1961
103. Chieppa M, Bianchi G, Doni A, Del Prete A, Sironi M, Laskarin G, et al. Cross-linking of the mannose receptor on monocyte-derived dendritic cells activates an anti-inflammatory immunosuppressive program. *J Immunol.* (2003) 171:4552–60. doi: 10.4049/jimmunol.171.9.4552
104. Keler T, Ramakrishna V, Fanger MW. Mannose receptor-targeted vaccines. *Expert Opin Biol Ther.* (2004) 4:1953–62. doi: 10.1517/14712598.4.12.1953
105. Yang F, Fan X, Huang H, Dang Q, Lei H, Li Y. A single microorganism epitope attenuates the development of murine autoimmune arthritis: regulation of dendritic cells *via* the mannose receptor. *Front Immunol.* (2018) 9:1528. doi: 10.3389/fimmu.2018.01528
106. Kel JM, De Geus ED, Van Stipdonk MJ, Drijfhout JW, Koning F, Nagelkerken L. Immunization with mannosylated peptide induces poor T cell effector functions despite enhanced antigen presentation. *Int Immunol.* (2008) 20:117–27. doi: 10.1093/intimm/dxm123
107. van Vliet SJ, Paessens LC, Broks-van den Berg VCM, Geijtenbeek TBH, van Kooyk Y. The C-type lectin macrophage galactose-type lectin impedes migration of immature APCs. *J Immunol.* (2008) 181:3148–55. doi: 10.4049/jimmunol.181.5.3148
108. Ilarregui JM, Rabinovich GA. Tolerogenic dendritic cells in the control of autoimmune neuroinflammation: an emerging role of protein-glycan interactions. *Neuroimmunomodulation.* (2010) 17:157–60. doi: 10.1159/000258712
109. Benito-Villalvilla C, Soria I, Subiza JL, Palomares O. Novel vaccines targeting dendritic cells by coupling allergoids to mannan. *Allergo J Int.* (2018) 27:256–62. doi: 10.1007/s40629-018-0069-8
110. Soria I, López-Relaño J, Viñuela M, Tudela JI, Angelina A, Benito-Villalvilla C, et al. Oral myeloid cells uptake allergoids coupled to mannan driving Th1/Treg responses upon sublingual delivery in mice. *Allergy Eur J Allergy Clin Immunol.* (2018) 73:875–84. doi: 10.1111/all.13396
111. Palomares F, Ramos-Soriano J, Gomez F, Mascaraque A, Bogas G, Perkins JR, et al. Pru p 3-glycodendropeptides based on mannoses promote changes in the immunological properties of dendritic and t-cells from LTP-allergic patients. *Mol Nutr Food Res.* (2019) 63:553. doi: 10.1002/mnfr.201900553
112. Manzano AI, Javier Cañada F, Cases B, Sirvent S, Soria I, Palomares O, et al. Structural studies of novel glycoconjugates from polymerized allergens (allergoids) and mannans as allergy vaccines. *Glycoconj J.* (2016) 33:93–101. doi: 10.1007/s10719-015-9640-4
113. Benito-Villalvilla C, Soria I, Pérez-Diego M, Fernández-Caldas E, Subiza JL, Palomares O. Alum impairs tolerogenic properties induced by allergoid-mannan conjugates inhibiting mTOR and metabolic reprogramming in human DCs. *Allergy Eur J Allergy Clin Immunol.* (2020) 75:648–59. doi: 10.1111/all.14036
114. van Vliet SJ, van Liempt E, Saeland E, Aarnoudse CA, Appelmelk B, Irimura T, et al. Carbohydrate profiling reveals a distinctive role for the C-type lectin MGL in the recognition of helminth parasites and tumor antigens by dendritic cells. *Int Immunol.* (2005) 17:661–9. doi: 10.1093/intimm/dxh246
115. Idoyaga J, Cheong C, Suda K, Suda N, Kim JY, Lee H, et al. Cutting edge: langerin/CD207 receptor on dendritic cells mediates efficient antigen presentation on MHC I and II products *in vivo*. *J Immunol.* (2008) 180:3647–50. doi: 10.4049/jimmunol.180.6.3647
116. Bigley V, McGovern N, Milne P, Dickinson R, Pagan S, Cookson S, et al. Langerin-expressing dendritic cells in human tissues are related to CD1c + dendritic cells and distinct from Langerhans cells and CD141 high XCR1 + dendritic cells. *J Leukoc Biol.* (2015) 97:627–34. doi: 10.1189/jlb.1hi0714-351r
117. Petzold C, Schallenberg S, Stern JNH, Kretschmer K. Targeted antigen delivery to DEC-205+ dendritic cells for tolerogenic vaccination. *Rev Diabet Stud.* (2012) 9:305–18. doi: 10.1900/RDS.2012.9.305
118. Flacher V, Tripp CH, Mairhofer DG, Steinman RM, Stoitzner P, Idoyaga J, et al. Murine langerin + dermal dendritic cells prime CD 8 + T cells while L angerhans cells induce cross-tolerance. *EMBO Mol Med.* (2014) 6:1191–204. doi: 10.15252/emmm.201303283
119. Schreibelt G, Klinkenberg LJJ, Cruz LJ, Tacken PJ, Tel J, Kreutz M, et al. The C-type lectin receptor CLEC9A mediates antigen uptake and (cross-)presentation by human blood BDCA3+ myeloid dendritic cells. *Blood.* (2012) 119:2284–92. doi: 10.1182/blood-2011-08-373944
120. Crozat K, Tamoutounour S, Vu Manh T-P, Fossum E, Luche H, Ardouin L, et al. Cutting edge: expression of XCR1 defines mouse lymphoid-tissue resident and migratory dendritic cells of the CD8α + type. *J Immunol.* (2011) 187:4411–5. doi: 10.4049/jimmunol.1101717
121. Huysamen C, Willment JA, Dennehy KM, Brown GD. CLEC9A is a novel activation C-type lectin-like receptor expressed on BDCA3+ dendritic cells and a subset of monocytes. *J Biol Chem.* (2008) 283:16693–701. doi: 10.1074/jbc.M709923200
122. Lahoud MH, Ahmet F, Kitsoulis S, Wan SS, Vremec D, Lee C-N, et al. Targeting antigen to mouse dendritic cells *via* Clec9A induces potent CD4 T cell responses biased toward a follicular helper phenotype. *J Immunol.* (2011) 187:842–50. doi: 10.4049/jimmunol.1101176
123. Hemmi H, Idoyaga J, Suda K, Suda N, Kennedy K, Noda M, et al. A new triggering receptor expressed on myeloid cells (trem) family member, trem-like 4, binds to dead cells and is a DNAX activation protein 12-linked marker for subsets of mouse macrophages and dendritic cells. *J Immunol.* (2009) 182:1278–86. doi: 10.4049/jimmunol.182.3.1278
124. Varki A. Glycan-based interactions involving vertebrate sialic-acid-recognizing proteins. *Nature.* (2007) 446:1023–9. doi: 10.1038/nature05816

125. Jenner J, Kerst G, Handgretinger R, Müller I. Increased α2,6-sialylation of surface proteins on tolerogenic, immature dendritic cells and regulatory T cells. *Exp Hematol.* (2006) 34:1211–7. doi: 10.1016/j.exphem.2006.04.016
126. Erdmann H, Steeg C, Koch-Nolte F, Fleischer B, Jacobs T. Sialylated ligands on pathogenic *Trypanosoma cruzi* interact with Siglec-E (sialic acid-binding Ig-like lectin-E). *Cell Microbiol.* (2009) 11:1600–11. doi: 10.1111/j.1462-5822.2009.01350.x
127. García-Vallejo JJ, Bloem K, Knippels LMJ, Garssen J, van Vliet SJ, van Kooyk Y. The consequences of multiple simultaneous C-type lectin-ligand interactions: DCIR alters the endo-lysosomal routing of DC-SIGN. *Front Immunol.* (2015) 6:87. doi: 10.3389/fimmu.2015.00087
128. Seno A, Maruhashi T, Kaifu T, Yabe R, Fujikado N, Ma G, et al. Exacerbation of experimental autoimmune encephalomyelitis in mice deficient for DCIR, an inhibitory C-type lectin receptor. *Exp Anim.* (2015) 64:109–19. doi: 10.1538/expanim.14-0079
129. Fujikado N, Saijo S, Yonezawa T, Shimamori K, Ishii A, Sugai S, et al. Dcir deficiency causes development of autoimmune diseases in mice due to excess expansion of dendritic cells. *Nat Med.* (2008) 14:176–80. doi: 10.1038/nm1697
130. Kaifu T, Iwakura Y. Dendritic cell immunoreceptor (DCIR): an ITIMharboring C-type lectin receptor. In: *C-Type Lectin Receptors in Immunity*. Springer Japan. (2016). p. 101–13. doi: 10.1007/978-4-431-56015-9_7
131. Meyer-Wentrup F, Cambi A, Joosten B, Looman MW, de Vries IJM, Figdor CG, et al. DCIR is endocytosed into human dendritic cells and inhibits TLR8-mediated cytokine production. *J Leukoc Biol.* (2009) 85:518–25. doi: 10.1189/jlb.0608352
132. Tanriver Y, Ratnasothy K, Bucy RP, Lombardi G, Lechler R. Targeting MHC class I monomers to dendritic cells inhibits the indirect pathway of allorecognition and the production of IgG alloantibodies leading to long-term allograft survival. *J Immunol.* (2010) 184:1757–64. doi: 10.4049/jimmunol.0902987
133. Iberg CA, Hawiger D. Advancing immunomodulation by *in vivo* antigen delivery to DEC-205 and other cell surface molecules using recombinant chimeric antibodies. *Int Immunopharmacol.* (2019) 73:575–80. doi: 10.1016/j.intimp.2019.05.037
134. Álvarez B, Nieto-Pelegrín E, Martínez de la Riva P, Toki D, Poderoso T, Revilla C, et al. Characterization of the porcine CLEC12A and analysis of its expression on blood dendritic cell subsets. *Front Immunol.* (2020) 11:863. doi: 10.3389/fimmu.2020.00863
135. Lahoud MH, Proietto AI, Ahmet F, Kitsoulis S, Eidsmo L, Wu L, et al. The C-type lectin Clec12A present on mouse and human dendritic cells can serve as a target for antigen delivery and enhancement of antibody responses. *J Immunol.* (2009) 182:7587–94. doi: 10.4049/jimmunol.0900464
136. Spence S, Greene MK, Fay F, Hams E, Saunders SP, Hamid U, et al. Targeting siglecs with a sialic acid-decorated nanoparticle abrogates inflammation. *Sci Transl Med.* (2015) 7:303ra140. doi: 10.1126/scitranslmed.aab3459

Conflict of Interest: The authors declare that the research was conducted in the absence of any commercial or financial relationships that could be construed as a potential conflict of interest.

frontiers in Immunology

ORIGINAL RESEARCH
published: 25 February 2021
doi: 10.3389/fimmu.2021.641703

PLGA Nanoparticles Co-encapsulating NY-ESO-1 Peptides and IMM60 Induce Robust CD8 and CD4 T Cell and B Cell Responses

*Yusuf Dölen[1,2†], Uzi Gileadi[3†], Ji-Li Chen[3], Michael Valente[1,4], Jeroen H. A. Creemers[1,2], Eric A. W. Van Dinther[1,2], N. Koen van Riessen[1], Eliezer Jäger[5], Martin Hruby[5], Vincenzo Cerundolo[3‡], Mustafa Diken[6], Carl G. Figdor[1,2] and I. Jolanda M. de Vries[1]**

[1] Department of Tumor Immunology, Radboud University Medical Center, Radboud Institute for Molecular Life Sciences, Nijmegen, Netherlands, [2] Oncode Institute, Nijmegen, Netherlands, [3] Medical Research Council Human Immunology Unit, Radcliffe Department of Medicine, Weatherall Institute of Molecular Medicine, University of Oxford, Oxford, United Kingdom, [4] Aix Marseille Univ, CNRS, INSERM, CIML, Centre d'Immunologie de Marseille-Luminy, Marseille, France, [5] Institute of Macromolecular Chemistry v. v. i., Academy of Sciences of the Czech Republic, Prague, Czechia, [6] TRON - Translational Oncology at the University Medical Center of the Johannes Gutenberg University Mainz gGmbH, Mainz, Germany

OPEN ACCESS

Edited by:
Maud Plantinga,
University Medical Center
Utrecht, Netherlands

Reviewed by:
Wenxue Ma,
University of California, San Diego,
United States
Joke M. M. Den Haan,
VU University Medical
Center, Netherlands

***Correspondence:**
I. Jolanda M. de Vries
Jolanda.devries@radboudumc.nl

†These authors have contributed equally to this work

‡Deceased on 7 January 2020

Specialty section:
This article was submitted to Antigen Presenting Cell Biology, a section of the journal Frontiers in Immunology

Received: 14 December 2020
Accepted: 28 January 2021
Published: 25 February 2021

Citation:
Dölen Y, Gileadi U, Chen J-L, Valente M, Creemers JHA, Van Dinther EAW, van Riessen NK, Jäger E, Hruby M, Cerundolo V, Diken M, Figdor CG and de Vries IJM (2021) PLGA Nanoparticles Co-encapsulating NY-ESO-1 Peptides and IMM60 Induce Robust CD8 and CD4 T Cell and B Cell Responses. Front. Immunol. 12:641703. doi: 10.3389/fimmu.2021.641703

Tumor-specific neoantigens can be highly immunogenic, but their identification for each patient and the production of personalized cancer vaccines can be time-consuming and prohibitively expensive. In contrast, tumor-associated antigens are widely expressed and suitable as an off the shelf immunotherapy. Here, we developed a PLGA-based nanoparticle vaccine that contains both the immunogenic cancer germline antigen NY-ESO-1 and an α-GalCer analog IMM60, as a novel iNKT cell agonist and dendritic cell transactivator. Three peptide sequences (85–111, 117–143, and 157–165) derived from immunodominant regions of NY-ESO-1 were selected. These peptides have a wide HLA coverage and were efficiently processed and presented by dendritic cells *via* various HLA subtypes. Co-delivery of IMM60 enhanced CD4 and CD8 T cell responses and antibody levels against NY-ESO-1 *in vivo*. Moreover, the nanoparticles have negligible systemic toxicity in high doses, and they could be produced according to GMP guidelines. Together, we demonstrated the feasibility of producing a PLGA-based nanovaccine containing immunogenic peptides and an iNKT cell agonist, that is activating DCs to induce antigen-specific T cell responses.

Keywords: NY-ESO-1, iNKT cell, B cell epitope, peptide vaccine, IMM60, PLGA nanoparticle, CD8 T cell, CD4 T cell

INTRODUCTION

Recent advancements in cancer immunotherapy such as checkpoint blockade therapy, CAR T cells, and neo-epitope-based RNA vaccines show that once activated, the adaptive immune system is capable of recognizing and eradicating tumor cells (1). This recognition is based on tumor antigens which are either normal proteins that are aberrantly or over-expressed in tumors [tumor-associated antigens (TAA)], or proteins that are mutated

during tumorigenesis (tumor-specific antigens or neoantigens). While neoantigens are patient-specific, TAAs are widely expressed in a majority of cancer patients with various types of tumors (1). One subset of TAAs is cancer germline antigens which are generally expressed in immune-privileged sites such as germ cells of the testes, in fetal ovaries, and on trophoblasts (1, 2). The immune system is thought not to be desensitized against cancer germline- and mutated-proteins and therefore, T cell responses can be induced against these antigens (3, 4).

Invariant Natural Killer T (iNKT) cells represent a specialized subset of immune cells characterized by the expression of a restricted αβ T cell antigen receptor (TCR) that specifically recognizes lipid antigens such as α-GalCer presented by CD1d molecules expressed by dendritic cells (DCs), macrophages and B cells (5). Upon activation, they rapidly secrete large amounts of cytokines and induce subsequent activation of different cell types, including DCs, NK cells, and T cells (6). Due to the production of cytokines (i.e., IFN-γ, IL-4) and DC activation through CD40-CD40L interaction, iNKT cells can act as a helper T cell to boost cytotoxic T cell (CTL) responses. Hence, α-galactosylceramide (α-GalCer) and its analogs are explored as vaccine adjuvants (7).

NY-ESO-1 antigen has been used in clinical vaccination studies, mainly because of its expression in a broad range of cancers with high incidence (one-third to one-fourth of melanoma, lung, breast, esophageal, liver, gastric, prostate, ovarian, and bladder cancer) (8–10). Vaccinations led to an enhancement of humoral and cellular immune responses and clinical improvements have been documented in some patients, supporting the role of NY-ESO-1 as an attractive antigen for therapeutic vaccination (3, 11, 12). Moreover, the development of potent vaccines with multiple shared tumor antigens including NY-ESO-1 in combination with checkpoint blockade therapy has recently been shown to enhance the clinical response rates of cancer patients (13).

Effective cancer vaccines should induce strong and long-lasting immune responses. Our previous preclinical data with nanoparticle-encapsulated iNKT cell agonists (α- GalCer and IMM60) and antigens (ovalbumin and HPV-E7) in mice demonstrated regression of tumors after a single injection of nanoparticles (14, 15). We observed that iNKT cell agonists have a high adjuvant effect at dosages that could be loaded within PLGA nanoparticles and therefore, has an advantage over TLR ligands that could not be sufficiently loaded (14). Additionally, activation of iNKT cells by PLGA nanoparticles led to activation and mobilization of multiple cell types such as NK cells, B cells, CD4, and CD8 T cells as well as alternative cognate licensing of DCs (15, 16). Moreover, we and others showed that antigen vaccinations, together with iNKT cell agonists, provide a strong immune response and long-lasting tumor regression if employed in combination with checkpoint blockade therapy (15, 17).

Here we describe the design of a PLGA-based nanoparticle, for co-delivery of NY-ESO-1 peptides with an iNKT cell agonist, as a cancer vaccine. We selected IMM60 as an iNKT cell agonist because of its enhanced ability to activate human iNKT-cells compared with α-GalCer, resulting in extended iNKT responses (18). Using NY-ESO-1-specific TCR mRNA transfection of healthy donor T cells, and patient-derived T cells, we confirmed previous observations that peptides are indeed more immunogenic than the whole protein (19) and that the selected peptides could be efficiently processed and presented by multiple HLA types either in solution or in nanoparticle-encapsulated form. Furthermore, we demonstrated enhanced *in vivo* immune responses with nanoparticles compared to soluble peptide injections and a further enhancement due to co-delivery of iNKT cell agonist IMM60 within the nanoparticles.

METHODS

Reagents

PLGA (Resomer RG 502 H, lactide/glycolide molar ratio 50:50) was purchased from Evonik Solvents. Dichloromethane was obtained from Merck. CryoSure-DMSO from WAK-Chemie. Polyvinyl alcohol 80% (PVA) from Sigma. Pure water from Braun. Isopropyl alcohol, ≥ 99.7% ACN, ≥ 99.9%, MeOH, ≥ 99.9%, and ($CHCl_3$, ≥ 99%) were obtained from Sigma-Aldrich. NY-ESO-1 derived peptides; 85–111 (SRLLEFYLAMPFATPMEAELARRSLAQ), 117–143 (PVPGVLLKEFTVSGNILTIRLTAADHR), and 157–165 (SLLMWITQC) were custom synthesized by Genscript and Pichem; 153–167 (LQQLSLLMWITQCFL), and 97–111 (ATPMEAELARRSLAQ) was produced by Genscript. All peptides had >95% purity and concentrations were based on net peptide weights determined by nitrogen analysis. IMM-60 was provided by Ian Walters of iOx Therapeutics. RPMI 1,640 medium was obtained from Life Technologies. Full-length NY-ESO-1 protein was produced in *Escherichia coli* by the Ludwig Institute for Cancer Research, New York branch. 0.5 mg NY-ESO-1 protein was dissolved in 1 ml water containing 240 mg urea, 3.75 mg glycine, 13.8 mg Sodium Dihydrogen Phosphate Monohydrate, and 8.5 mg Sodium Chloride.

Nanoparticle production

All PLGA nanoparticles (NPs) were prepared using a single emulsion and solvent evaporation–extraction method, as described previously (10). Briefly, 100 mg of PLGA was dissolved in 3 ml of dichloromethane containing 1 mg of each peptide (**Supplementary Table 3**) and 150 μg IMM60 dissolved in DMSO. This organic phase was added dropwise to 25 ml of aqueous phase containing 2.5% PVA and emulsified for 120 s using a digital probe sonicator (Branson Ultrasonics, Danbury, CT). The organic phase was evaporated overnight at RT while stirring, and nanoparticles were collected by centrifugation at 10,000 rpm (13304 RCF) for 35 min, washed three times with pure water, and lyophilized. Different peptide and IMM60 concentrations were examined and reported in the results section.

Nanoparticle Characterization

The size and polydispersity index of the nanoparticles was analyzed by dynamic light scattering using a Nanotrac Flex (Microtrac). The peptide content of the NPs was determined by HPLC analysis using a standard dilution of peptides based on net peptide content (15). All amounts of PLGA-NPs used in this study were calculated according to their net peptide contents

except for the particles containing full NY-ESO-1 protein which the content could not be determined due to high amounts of urea and glycine contamination. IMM60 content of the NPs was determined by a Corona Veo Charged Aerosol Detector (CAD) coupled to a DIONEX UltiMate 3000 HPLC system (Thermo Fischer Scientific). The NPs were dissolved in DMSO for a complete dissolution of the components and analyzed by CAD on an XSelect CSH C_{18} 2.5 µm 3.0 × 150 mm XP column (Waters) with VanGuard Cartridges (Waters) coupled to a column heater (65°C), eluents MeOH-Formic Acid-Triethylamine (99.0/0.05/0.05 vol. %) with isocratic gradient flow rate = 1.0 ml·min^{-1}. The quantity of IMM60 was calculated by interpolation of the standard calibration curves of IMM60 performed in the same way as for the NPs. The endotoxin content of the nanoparticles was analyzed using the gel-clot method by Eurofins PROXY laboratories, Leiden, The Netherlands, and found to be lower than 0.1 EU/mg particles.

In vitro Antigen Presentation With TCR mRNA Transfected T Cells

HLA typed leukapheresis products were obtained from the blood bank Sanquin, Nijmegen, and subjected to density gradient separation with Ficoll to obtain PBMCs. Monocytes were isolated from PBMCs *via* positive MACS separation with CD14 microbeads according to the manufacturer's protocol (Miltenyi Biotech). The remaining cells were subjected to the untouched separation of T cells with either the CD8 T Cell Isolation Kit or the CD4 T Cell Isolation Kit according to the manufacturer's protocol (Miltenyi Biotech). Monocytes, CD8, or CD4 T cells were frozen in FBS 10% DMSO solution and stored in liquid nitrogen until further use. Monocytes were thawed, and 10 × 10^6 cells were cultured at 37°C 5% CO_2 in 8 ml of full RPMI medium (supplemented with 10% FBS, 100 U/ml penicillin, 100 µg/ml streptomycin, 2 mM ultraglutamine) containing 300 U/ml IL-4 and 450 U/ml GM-CSF to generate DCs. On day 3, 3600 U IL-4 and 5400 U GM-CSF were added. On day 6, floating immature DCs were harvested, and 20 × 10^3 cells/well were plated in a 96 U-bottom plate. Peptides dissolved in DMSO (free form) or encapsulated within nanoparticles were prepared in different concentrations based on net peptide contents in full RPMI and added to the wells. DCs were cultured with antigens for 24 h at 37°C 5% CO_2. Autologous T cells isolated from the PBMCs were thawed, transferred to full RPMI medium containing 2 µg/ml DNase and incubated for 30 min at 37°C 5% CO_2. 10 ml of PBS was added, and the cell suspension was centrifuged (8 min, 300 g at room temperature). T cells were counted, 10 ml of serum-free *X-VIVO* 15 medium (Lonza) was added, and the cell suspension was centrifuged for 8 min, 300 g at room temperature. Cells were resuspended in serum-free *X-VIVO* 15 medium in a concentration of 40 × 10^6 cells/ml and transferred to 4 mm gap Gene Pulser/MicroPulser Electroporation Cuvettes (Bio-Rad). Ten Microgram of mRNA encoding α and β chains of TCR recognizing NY-ESO-1 was mixed with the cells and electroporated with a single square pulse of 500 V for 3 ms using a Gene Pulser Xcell Electroporation System (Bio-Rad). Electroporated cells were transferred to a tube containing 1 ml IVS medium (IMDM GlutaMAX + 5% human AB serum) and incubated for 2 h at 37°C 5% CO_2. 50 × 10^3 TCR transfected T cells were added to each well of DCs. LPS was added on the wells to a final concentration of 0.2 ug/ml. Supernatants were collected 72 h after the establishment of DC-T cell co-cultures and analyzed for IFN-γ by ELISA.

In vitro Antigen Presentation Assay With Patient-Derived PBMCs

Frozen PBMCs of two patients who participated in a clinical vaccination trial using NY-ESO-1 whole protein in ISCOMATRIX followed by a booster with recombinant fowlpox virus expressing NY-ESO-1 (20) were analyzed for a response to NY-ESO-1 derived peptides. These PBMCs were previously stimulated for 14 days *in vitro* with a pool of overlapping peptides covering the entire sequence of NY-ESO-1 protein. EBV-transformed B cells of the same patients were loaded with peptides dissolved in DMSO (free form) or nanoparticles for 18 h. These were then used as antigen-presenting cells in co-culture with autologous PBMCs. Separately, free form peptides and nanoparticles were incubated with PBMCs without being loaded to EBV transformed B cells. 5 h later, CD8 and CD4 T cells in the co-cultures were analyzed for intracellular IFN-γ by flow cytometry. For stimulation with NY-ESO-$1_{157-165}$, HLA-A*02:01 positive EBV-transformed B cells were loaded with the peptide and then co-cultured with a T-cell clone (4D8) which specifically recognizes this peptide. Intracellular IFN-γ production was assessed by flow cytometry.

Mice and Tissues

Wild-type C57BL/6J were obtained from Charles River, Germany. AAD mice [Immp2l$^{Tg(HLA-A/H2-D)2Enge}$] were obtained from Jackson, USA. HHD mice were bred in the animal facility of the University of Oxford. All mice were aged between 8 and 15 weeks at the start of experiments. 1G4-HHD mice are transgenic for a mouse-human hybrid TCR m1G4 (with the human variable domains of the human 1G4 TCR that is specific for NY-ESO-$1_{157-165}$ peptide/HLA-A2 complex). All mice were maintained under specific pathogen-free conditions at the Central Animal Laboratory of Radboudumc (Nijmegen, The Netherlands, or at the animal facility of the University of Oxford, UK). Drinking water and food were provided *ad libitum*. PLGA nanoparticles were dissolved in ice-cold PBS by vortexing for 30 s before injected *via* iv route at the tail vein. Blood was collected *via* tail vein puncture or retro-orbital puncture during terminal anesthesia. Spleens were isolated under sterile conditions and stored at 4°C in RPMI 1640 medium supplemented with 100 U/ml penicillin and 100 µg/ml streptomycin until processing for maximally 2 h. Spleens were meshed through a 100 µm cell strainer by using a syringe plunger. The cell suspension was spun at 400 × g for 5 min and resuspended in 3 ml of 1x ammonium chloride solution for the lysis of erythrocytes. After 5 min of incubation at room temperature, cells were washed with 10 ml of PBS. Cells were counted by a hemocytometer and cultured in full RPMI 1,640 medium supplemented with 50 µM 2-mercaptoethanol in 96 well plates.

In vivo Priming

F1 (HHD × C57BL/6J) mice were intravenously injected with 1.1 ug (0.6 nmol) peptide-3-LP (153–167, LQQLSLLMWITQCFL) either in solution or encapsulated within nanoparticles mixed with 50 ng IMM60 in solution. Twenty eight days later all mice were boosted with iv injection of 1.1 ug peptide-3-LP in a solution mixed with 50 ng IMM60. Eight days after the boost, mice were euthanized, splenocytes were processed and stained with fluorescent antibodies and tetrameric pMHC (HLA-A2/K^b NY-ESO-$1_{157-165}$) (21) to identify antigen-specific CD8 T cell frequencies. F1 (HHD × B6SJLCD45.1) mice were intravenously injected with nanoparticles containing 2,000 ng (1.1 nmol), 100 ng (55 pmol), or 10 ng (5.5 pmol) peptide-3-LP intravenously and 10 days later, mice were euthanized, splenocytes processed, and stained using fluorescent antibodies and tetrameric pMHC (HLA-A2/K^b NY-ESO-$1_{157-165}$). Cells were analyzed on a BD LSR Fortesa flow cytometer.

C57Bl/6 mice were intravenously injected with 1 mg NPs containing all three peptides (8.8 ug Peptide-1, 5.9 ug Peptide-2, and 12 ug Peptide-3 per mg NP) with 1.2 ug IMM60 per mg NP or (6.1 ug Peptide-1, 4.3 ug Peptide-2, and 11 ug Peptide-3 per mg NP) without IMM60 (last two rows of **Supplementary Table 3B**). Seven days later, splenocytes were isolated and frozen in FBS 10% DMSO. Once thawed, splenocytes were stimulated *ex vivo* with 10 uM peptides 1, 2, and 3 separately. Fourty eight hours later, IFN-γ levels in culture supernatants were determined by ELISA. Splenocytes were stimulated for 16 h at 37°C/5% CO_2 before the addition of BFA (Sigma) (10 μg/ml) and cultured for 4 h. Cells were washed and surface stained with CD3, CD8, CD4, and LIVE/DEAD cell stain (Invitrogen, UK). Subsequently, the cells were washed, treated with Cytofix and Perm Wash (BD biosciences) according to the manufacturer's instructions, and stained with IFN-γ-PE (BD biosciences) intracellularly.

In vivo Cytotoxicity Assay

Groups of homozygous AAD mice were intravenously injected with nanoparticles encapsulating all three peptides with or without IMM60 and nanoparticles only encapsulating IMM60 and peptide-3. All groups were dosed based on 6 ug peptide-3 content. Injections were repeated 28 days later or the experiment proceeded to the next step after the first injections. Six days after the injection, naive AAD mice splenocytes were loaded either with peptide-3, or HPV (irrelevant) peptide and stained with 5 uM celltrace violet, and celltrace CFSE, respectively. Antigen-loaded splenocytes were transferred as target cells to mice vaccinated with nanoparticles. One day later, all mice were euthanized, and cytotoxicity in spleens was measured by flow cytometry using the following formula:

Ratio = Irrelevant Percentage: Relevant Percentage

Percent Specific killing = [1–(non-vaccinated control ratio/Experimental ratio)] × 100

In vivo Tumor Challenge

A group of homozygous AAD mice was vaccinated intravenously with 1 mg NP (peptide mix+IMM60) containing 11.4 ug peptide-1, 13.4 ug peptide-2, and 11.5 ug peptide-3, and 1.39 ug IMM60. Seven months later groups of vaccinated and non-vaccinated mice were inoculated with 2.5 × 10^5 1C12 sarcoma cells expressing full-length NY-ESO-1. 1C12, a Methyl Colanthrene (MCA)-induced murine tumor cell line, was transduced with a NY-ESO-1 expressing lentiviral vector and cloned by limiting dilution. The parental MCA-induced cell line was isolated from a tumor that emerged in MCA injected (intramuscular) HHD mice. Nine days after tumor inoculation, the vaccinated group received a booster dose and tumor growths were recorded. Mice that rejected the first tumors were re-challenged with 5 × 10^5 1C12 sarcoma cells on day 74. On day 109, all mice were euthanized, spleens and blood were isolated. Splenocytes were *ex-vivo* restimulated with different peptides, and supernatants were collected 72 h later for IFN-γ analysis.

In vivo Toxicology

A single-species preclinical toxicology study was performed by Charles River Laboratories (Edinburg, UK) to determine the potential toxicity of a single intravenous (bolus) injection of PLGA nanoparticles containing 8.8 ug Peptide-1, 5.9 ug Peptide-2, and 12 ug Peptide-3 with 1.2 ug IMM60 per mg NP or 6.1 ug Peptide-1, 4.3 ug Peptide-2 and 11 ug Peptide-3 per mg NP without IMM60 in mice. One control group received only formulation buffer, one control group received 50 mg/kg PLGA particles containing NY-ESO-1 peptides (SRLLEFYLAMPFATPMEAELARRSLAQ, PVPGVLLKEFTVSG NILTIRLTAADHR, SLLMWITQC), and three groups received three dose levels (0.5, 5, and 50 mg/kg) of PLGA particles containing IMM60 and NY-ESO-1 peptides (SRLLEFYLAMPF ATPMEAELARRSLAQ, PVPGVLLKEFTVSGNILTIRLTAADH R, SLLMWITQC). Fifty mice were assigned to terminal necropsy 1 day after injection to monitor toxicological parameters at the peak level. Thirty mice were subjected to necropsy 7 days later to monitor intercurrent mortality and recovery of initial findings. Blood was collected, transferred into tubes containing lithium heparin, and processed for plasma, which was analyzed for Alanine aminotransferase (ALT), Aspartate aminotransferase (AST), and Alkaline phosphatase (ALP). Essential organs such as the liver, spleen, lungs, kidneys, heart, bone marrow, and thymus were stored in fixative. Tissues were processed at Charles River Edinburgh Ltd. PROPATH. Microscopic evaluation was conducted by a senior veterinary pathologist on all tissues.

ELISA

Human and mouse IFN gamma uncoated ELISA Kits (Invitrogen) were used to determine levels of IFN-γ in serum or culture media according to product protocols. Serum samples were diluted 1/8 −1/10 in blocking buffer before adding to ELISA plates.

For NY-ESO-1 specific antibody detection, ELISA plates were coated by overnight incubation with 10 μg/ml NY-ESO-1 protein or 30 μg/ml NY-ESO-1 protein and 30 μg/ml of each peptide in 100 ul PBS, separately. After washing with wash buffer (PBS, 0.5% Tween-20) plates were incubated with Solution B - Blocking Buffer (Mouse Anti-OVA IgG1 Antibody ELISA Kit 30,105, Chondrex) for 1 h. Sera were diluted 1/100 or 1/500, added into wells, and incubated for 2 h. The plates were incubated for 1 h with horseradish peroxidase-conjugated anti-mouse IgG1

(30133) or IgG2c (30293) (Chondrex) followed by the addition of tetramethylbenzidine substrate solution (Chondrex). The reaction was stopped by the addition of 2N H_2SO_4, and the absorbance was read at 450 nm.

Statistical Analysis

Levene's test was used to assess the homogeneity of group variances. An unpaired *t*-test was used to compare the means of two groups. For comparing more than two groups, one-way ANOVA or Kruskal-Wallis test was used with Tukey's or Dunn's *post-hoc* tests. GraphPad Prism version 9.0.0 for Windows was used for all statistical analysis and figures. $^{*}P < 0.05$; $^{**}P < 0.01$; $^{***}P < 0.001$; and $^{****}P < 0.0001$. ns, not significant. Mice were randomly assigned to all experimental groups based on online randomization software.

RESULTS

Peptides Derived From NY-ESO-1 Are Functional in PLGA Nanoparticles

The long NY-ESO-1 peptides that were used in this study contain known NY-ESO-1-derived peptide epitopes in the context of their respective HLA alleles (peptides-1 and−2 in **Table 1**) and are therefore, suitable candidates for the final

TABLE 1 | Epitopes, their binding HLA allele types, and positions in the NY-ESO-1 protein sequence.

Immunogenic epitopes of NY-ESO-1				
HLA	**Peptide sequence**	**Position**	**Peptide position**	**Long peptide sequence**
DR15	AGATGGRGPRGAGA	37–50		
A*31:01	ASGPGGGAPR	53–62		
B*07:02	APRGPHGGAASGL	60–72		
Cw*06:02	ARGPESRLL	80–88		
DRB5*02:02	SRLLEFYLAMPFATP	85–99		
DR2	RLLEFYLAMPFA	86–97		
DRB1*0901	LLEFYLAMPFATPM	87–100		
DPB1*0401/0402	LLEFYLAMPFATPMEAELARRSLAQ	87–111		
DRB1*0101	LLEFYLAMPFATPMEAELARRSLAQ	87–111		
DRB1*04:01	LLEFYLAMPFATPMEAELARRSLAQ	87–111		
DRB1*07:01	LLEFYLAMPFATPMEAELARRSLAQ	87–111		
DR1	EFYLAMPFATPM	89–100		
A*24:02	YLAMPFATPME	91–101	85–111 27 a.a	Peptide-1SRLLEFYLAMPFATPMEAELARRSLAQ
C*03:03/03:04	LAMPFATPM	92–100		
B*35:08:01	LAMPFATPM	92–100		
A*68:01:01	AMPFATPMEAELARR	93–107		
B*51:01	MPFATPMEA	94–102		
B*35:01	MPFATPMEAEL	94–104		
DQB1*0401	PFATPMEAELARR	95–107		
B*52 01	FATPMEAEL	96–104		
C*12:02	FATPMEAELAR	96–106		
B*07:02:01	ATPMEAELARRSLAQ	97–111		
DRB1*04:01/11:01/16:01	PVPGVLLKEFTVSGNILTIRLTA	117–139	117–143 27 a.a	Peptide-2PVPGVLLKEFTVSGNILTIRLTAADHR
DRB1*0401	PGVLLKEFTVSGNILTIRLT	119–138		
DRB1*0101	PGVLLKEFTVSGNILTIRLTAADHR	119–143		
DR7	PGVLLKEFTVSGNILTIRLTAADHR	119–143		
DRB1*04:01	VLLKEFTVSG	121–130		
DR52bDRB1*04:01	LKEFTVSGNILTIRL	123–137		
DRB1*0803	KEFTVSGNILT	124–134		
B*49:01	KEFTVSGNILTI	124–135		
A*68:01	TVSGNILTIR	127–136		
DR4	AADHRQLQLSISSCLQQL	139–156		
A*02:01	SLLMWITQC	157–165	157–165 9 a.a	Peptide-3SLLMWITQC
DPB1*04:01/04:02	SLLMWITQCFLPVF	157–170		

HLA class-I binding epitopes are in black and HLA class II-binding epitopes are in blue. The long peptide sequences present in nanoparticles are designated as peptide-1, 2, and 3. HLA, human leukocyte antigen; NY-ESO-1, New York esophageal squamous cell carcinoma 1.

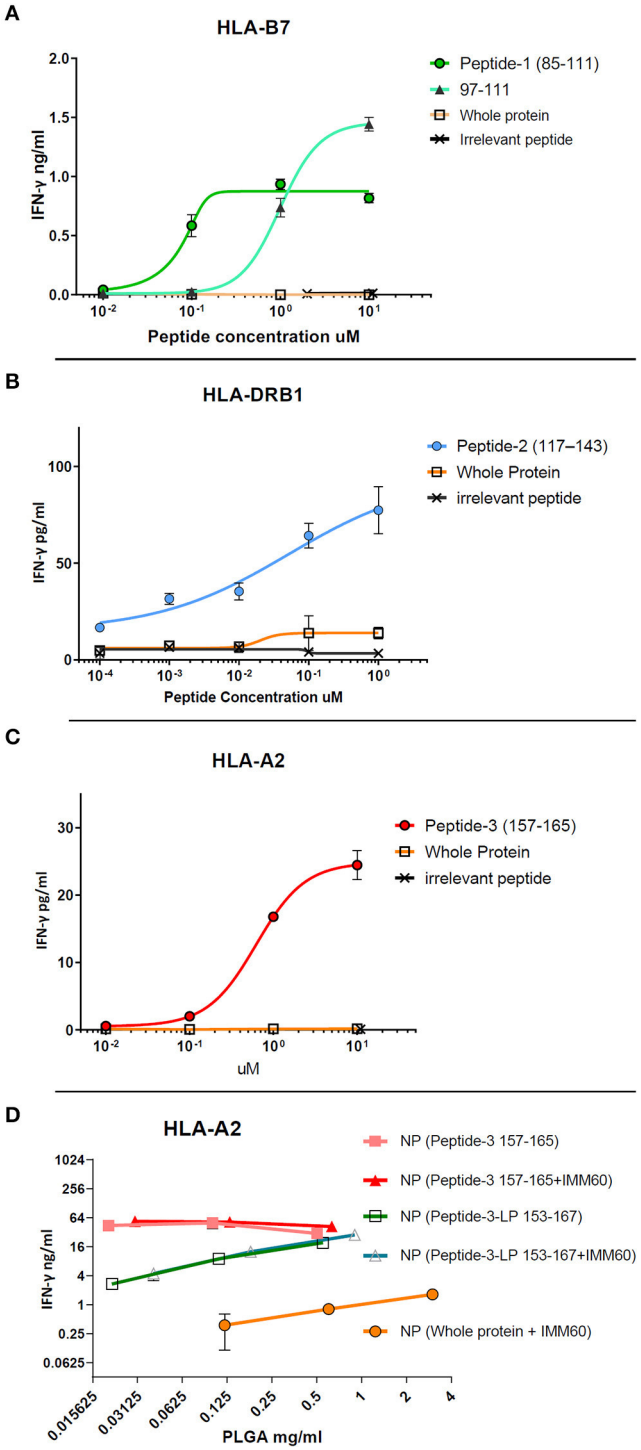

FIGURE 1 | Dose-response curves of selected peptides (dissolved in DMSO) obtained by TCR transfected T cell cultures *in vitro*. **(A)** CD8+ T cell response against free peptide-1 (circle) presented by HLA-B7 is compared with the minimal epitope 97–111 (triangle), the free form whole NY-ESO-1 protein (square), and an irrelevant peptide (cross). **(B)** CD4+ T cell response against peptide-2 (circle) presented by HLA-DRB1 is compared with the free form whole NY-ESO-1 protein (square) and an irrelevant peptide (cross). **(C)** CD8+ T *(Continued)*

FIGURE 1 | cell response against peptide-3 (circle) presented by HLA-A2 is compared with the free form whole NY-ESO-1 protein (square) and an irrelevant peptide (cross). **(D)** CD8+ T cell response against 157–165 epitope presented by HLA-A2. Nanoparticles containing peptide-3 (157–165) (filled square and triangle) or peptide-3-LP (153–167) (empty square and triangle) with/without IMM60 are compared with nanoparticles containing the whole NY-ESO-1 protein and IMM60 (filled circle) by total PLGA nanoparticle concentration due to the inability to calculate encapsulation of whole NY-ESO-1 protein. Each assay is repeated at least twice with similar results, response curves are fitted by four or five parameter non-linear regression analyses. Mean values are shown with SD.

nanoparticle formulation (20, 22, 23). To increase the coverage and immunogenicity of the final product, the short peptide 157–165 (peptide-3 in **Table 1**) was also included. This third peptide was preferred at minimal length to avoid the generation of an adjoining cryptic epitope present in the long peptide 153–167 (peptide-3-LP) with more dominant immunogenicity (24). Together, the selected peptides cover more than 80% of the European population for both class-I and class-II HLA alleles and are therefore, suitable candidates for inclusion into a nanoparticle cancer vaccine (**Supplementary Table 1**) (25).

The free peptides (dissolved in DMSO) were tested for processing and presentation by monocyte-derived DCs (moDCs) of healthy donors to autologous T cells transfected with TCRs derived from NY-ESO-1 specific T cells (26, 27). For peptide-1 (85–111), CD8 T cells were transfected with TCR mRNA (NY#12) recognizing 97–111 peptide of NY-ESO-1 presented by HLA-B*0702 (**Table 1**, **Supplementary Table 2A**) (27). IFN-γ production was observed after stimulation with peptide-1 (85–111) albeit lower than after stimulation with minimal epitope 97–111 at the highest dose (**Figure 1A**). To test peptide-2 (117–143), CD4 T cells were transfected with TCR mRNA (NY#3) recognizing 117–139 sequence presented by HLA-DRB1*0101 (**Table 1**, **Supplementary Table 2A**) (27). IFN-γ production was observed by CD4 T cells in a dose-dependent manner (**Figure 1B**). To test peptide-3, TCR transfected CD8 T cells of HLA-A*0201 donors were used, and dose-dependent production of IFN-γ was also observed with this peptide (**Figure 1C**). We could not observe any considerable IFN-γ response with whole NY-ESO-1 protein in any of the TCRs and corresponding HLA types tested (**Figures 1A–C**).

To test the capacity of the manufactured nanoparticles to elicit an immune response, nanoparticles containing whole NY-ESO-1 protein or NY-ESO-1 derived peptides were loaded onto moDCs and cultured with TCR transfected T cells. T cells stimulated with moDCs loaded with nanoparticles containing whole NY-ESO-1 protein produced low levels of IFN-γ even when high nanoparticle concentrations were used, and independent of the TCRs (**Figure 1D**, **Supplementary Figure 1A**). In contrast, when moDCs were loaded with nanoparticles containing either HLA-A2.1 binding short peptide-3 (157–165) or long peptide-3-LP (153–167) or HLA-DRB1 binding peptide-2 (117–143), high amounts (20–160-fold for the NY-ESO-$1_{157-165}$ epitope) of IFN-γ were observed (**Figure 1D**). These results demonstrate

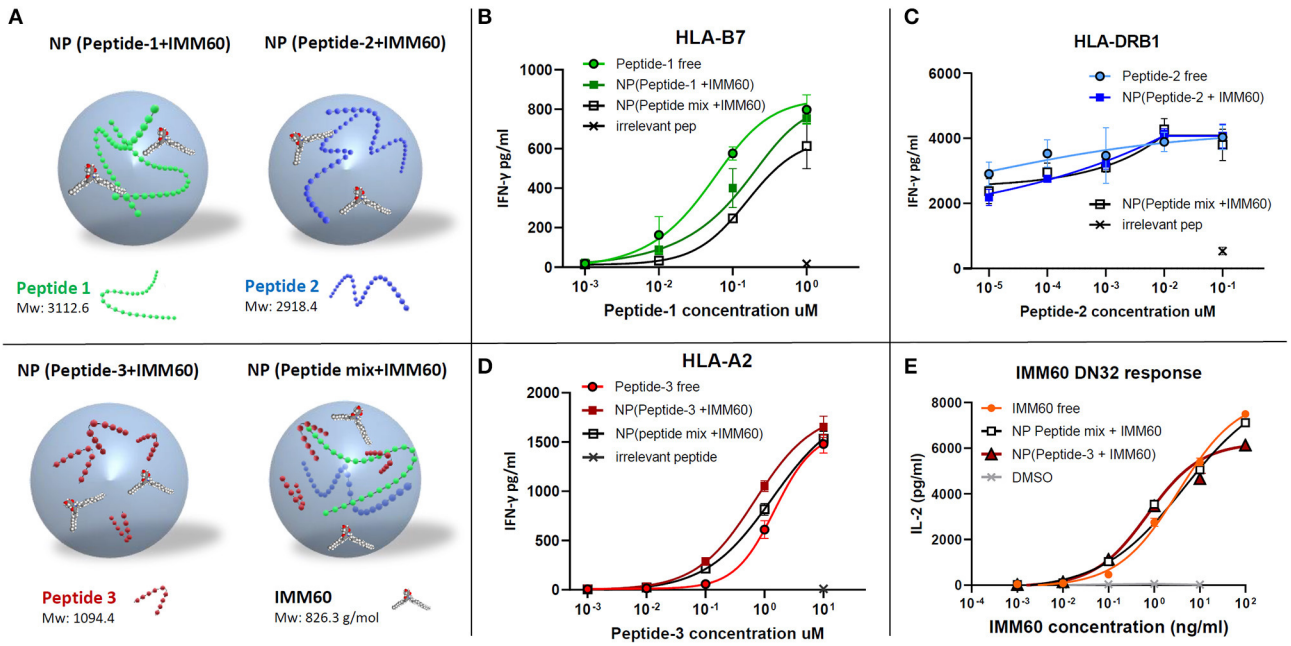

FIGURE 2 | (A) Schematic demonstration of nanoparticles produced with different components. **(B–D)** Dose/IFN-γ response curves of free (dissolved in DMSO) or nanoparticle (NP) encapsulated peptides obtained by TCR transfected T cell cultures *in vitro*. **(B)** CD8+ T cell response against peptide-1 presented by HLA-B7, **(C)** CD4+ T cell response against peptide-2 presented by HLA-DRB1, and **(D)** CD8+ T cell response against peptide-3 presented by HLA-A2. Free peptides in solution (circles), nanoparticles containing only one peptide (colored squares), a mixture of three peptides (empty squares), and an irrelevant peptide at the highest concentration (cross) were shown. **(E)** Dose-dependent IL-2 production by DN32 mouse NKT cell hybridoma activated by IMM60 *in vitro*. Free IMM60 in solution (circles), nanoparticles containing all three peptides and IMM60 (1.39 ug/mg) (empty squares), nanoparticles containing only peptide-3 and IMM60 (1.42 ug/mg) (colored triangles) and DMSO (cross) were shown. Each dot represents the mean value of triplicate wells. Assays are performed with three different nanoparticle batches and figures are representative of four experiments with similar results. Response curves are fitted by four or five parameter non-linear regression analyses. Mean values are shown with SD.

that peptides derived from NY-ESO-1 are functional and more preferable for encapsulation within PLGA nanoparticles than the complete recombinant NY-ESO-1 protein.

All Three NY-ESO-1 Peptides and IMM60 Are Functional Within Particles

PLGA nanoparticles produced with different amounts of peptides added per 1 mg PLGA were analyzed for peptide content. As expected, peptide content was higher in particles produced in the presence of high amounts of peptides. The amount of peptide that could be added during the production process was limited by its solubility in DMSO (**Supplementary Figure 2**, **Supplementary Table 3**).

Nanoparticles are primarily taken up by professional APCs such as DCs and macrophages and are useful carriers to deliver water-insoluble compounds or peptide/protein cargo which are prone to extracellular degradation (28, 29). Encapsulation of peptides may result in a poor release, degradation, or inability to escape to the cytosol once taken up by APCs, hampering cross-presentation. Therefore, antigen presentation of the nanoparticle-encapsulated peptides was compared to the free peptides (dissolved in DMSO). An overview of the different nanoparticles containing NY-ESO-1 peptides used in the study is given in **Figure 2A**. The IFN-γ production by TCR-transfected CD8 T cells was slightly less with the nanoparticle encapsulated peptide-1 (85–111) compared with free peptide-1 (**Figure 2B**). CD4 T cell response toward peptide-2 (117–143), already observed at a very low dose of the peptide, was not affected by the encapsulation procedure (**Figure 2C**). Further dilutions were performed with shorter incubation times or without LPS stimulation to reduce the response to this peptide. However, these changes also gave rise to higher inter and intra-assay variations in low doses with multiple nanoparticle batches and the encapsulated peptides performed at least equal when compared to soluble peptides (**Supplementary Figures 2C,D**). CD8 T cell response against peptide-3 (157–165) was also not affected (**Figure 2D**). Moreover, encapsulating all three peptides together neither affected the amount of each peptide within the nanoparticle (**Supplementary Table 3B**, **Supplementary Figure 2B**) nor their immunogenicity compared to the single encapsulated peptides (**Figures 2B–D**).

The functionality of the iNKT cell agonist, IMM60, in PLGA nanoparticles was analyzed by comparing the ability of free IMM60 or encapsulated IMM60 to induce IL-2 production by the mouse iNKT cell hybridoma DN32. Mouse JAWS-II DCs were loaded with IMM60-containing particles or free IMM60. No difference in IL-2 production by the mouse iNKT cells was

observed between the two forms of IMM60, indicating that the nanomanufacturing process did not influence the functionality of IMM60 (**Figure 2E**).

In summary, all three selected NY-ESO-1 peptides and IMM60 are processed and presented by DCs to T cells when delivered together in PLGA nanoparticles.

Patient-Derived T Cells Are Stimulated by Encapsulated Peptide-Loaded Autologous B Cells

To test a broader response, including other epitopes covered by the selected peptides, T cells within the PBMC of two patients (#6 and #7) that participated in a NY-ESO-1 vaccination trial were used (20). Autologous EBV-transformed B cells loaded with free peptides or peptide-containing PLGA nanoparticles were used as APCs. Encapsulated peptide-1 was recognized by CD8 T cells of patient #6 (**Figure 3A**). This patient has the HLA-B35 allele, which is known to present NY-ESO-1 epitopes 92–100 and 94–104 (**Table 1**, **Supplementary Tables 4A,B**). Indeed, CD8 T cell responses against soluble peptides 85–102, 89–103, and 93–107 covering the same epitopes were also observed (**Figure 3A**) (30). No CD8 T cell responses were detected in the PBMC of patient #7 which might be explained by the lack of MHC class I alleles known to present a NY-ESO-1 epitope (**Figure 3B**, **Supplementary Table 4B**). CD4 T cell responses were observed in both patients. Patient #6 had CD4 T cell responses against peptide-1 and peptide-2 (**Figure 3C**); the latter may correspond to a DRB1*0101 epitope covered by peptide-2 (**Table 1**). Furthermore, CD4 T cell responses against peptide-2 were also detected in patient #7, possibly presented by DRB1*0401 (**Figure 3D**, **Supplementary Tables 4A,B**). This experiment was repeated by directly introducing the antigens onto the PBMC cultures and without preloading onto autologous B cells. The trends in response to peptides were identical (**Supplementary Figure 3A**). CD8 T cell responses were heavily influenced by the lack of autologous B cells as antigen presenting cells which can be seen by the lower values of IFN-gamma producing cells in the latter setting (**Supplementary Figure 3A**). In comparison, CD4 T cell activation was less dependent on the B cell presentation.

Peptide-3 can only bind to HLA-A2.1; therefore, a broader response is not expected. The response to peptide-3 was tested with a patient-derived T-cell clone (4D8) cultured with EBV-transformed B cells as APCs. Similar stimulation of T cells was observed with a slightly higher activity of nanoparticle-encapsulated peptide-3 over its soluble counterpart in lower amounts (**Supplementary Figure 3B**).

Co-encapsulation of Peptides and IMM60 Enhances CD4 T Cell Responses *in vivo*

Endogenous CD4 T cell responses in wild type C57BL/6 mice are known to generate a CD4 T cell response against NY-ESO-1 86–99 epitope (31). This sequence is also present in peptide-1. To test the induction of T cell responses *in vivo*, wild type C57BL/6 mice were injected with nanoparticles containing the three selected peptides either with or without IMM60. One week after a single injection, splenocytes were restimulated with the individual peptides. As expected, IFN-γ production was only observed against peptide-1 (**Figure 4A**). Strikingly, IFN-γ production by CD4 T cells was predominantly observed in mice injected with particles containing IMM60, suggesting that iNKT cells can provide help for CD4 T cell responses (**Figure 4A**). In conclusion, IMM60 enhanced CD4 T cell responses against NY-ESO-1 in wild type mice vaccinated with PLGA nanoparticles containing the selected NY-ESO-1 peptides and IMM60.

Co-encapsulation of Peptides and IMM60 Enhances CD8 T Cell Responses *in vivo*

We could not observe any specific CD8 T cell response in wild type C57BL/6 mice (**Supplementary Figure 3C**). Therefore, we used both AAD and HHD mice which express a hybrid MHC class I molecule with α1 and α2 domains of the human HLA-A2.1 molecule fused to α3 domain of mouse H-2D^b molecule. In HHD mice, HLA-A2.1 heavy chain was covalently linked to the human β2 m light chain, denominated HHD molecule, and the H-2 Db and mouse β2-microglobulin genes have been disrupted preventing the expression of MHC class I K^b (as well as Class I like molecules such as CD1d) (32). In the F1 (HHD × C57BL/6J) generation of HHD mice, wild-type murine β2-microglobulin is expressed, allowing for the expression of CD1d, and thus the normal development of iNKT cells.

For experiments in HLA-A2 transgenic mice, we initially used the longer version of peptide-3 [peptide-3-LP (153–167)] presented by HLA-A2. This peptide induced lower IFN-γ responses than peptide-3 (157–165) in equimolar concentrations *in vitro* and both in free and nanoparticle encapsulated forms (**Supplementary Figure 4A**). To test the activity of the nanoparticles containing peptide-3-LP *in vivo*, adoptively transferred NY-ESO-1$_{157-165}$ specific mouse CD8 T cells (m1G4) were tested for their capacity to respond. CD8 T cells were fluorescently labeled and transferred to F1 (C57BL/6 × HHD) mice which were vaccinated with nanoparticles the next day. Nanoparticles containing peptide-3-LP were able to stimulate adoptively transferred CD8 T cells albeit with low sensitivity (2 nmol of the long peptide stimulated m1G4 T cell, 0.1 nmol failed to do so) (**Supplementary Figure 4B**).

For the induction of NY-ESO-1$_{157-165}$ specific T cells from the endogenous T cell repertoire, F1 (C57BL/6 × HHD) mice were injected intravenously with nanoparticles containing both peptide-3-LP as well as IMM60 or with soluble peptide-3-LP and soluble IMM60. After 28 days, a booster injection was given. Enhanced nanoparticle-mediated delivery of antigen was observed (**Figure 4B**). When nanoparticles containing peptide-3-LP and IMM60 were used, endogenous T cell responses could be detected even after a single dose up to 5.5 pmol 10 days after vaccination (**Figure 4C**). As a result, PLGA nanoparticles encapsulating NY-ESO-1 peptide-3-LP and IMM60 were able to expand endogenous antigen-specific CD8 T cells recognizing the HLA-A2 epitope.

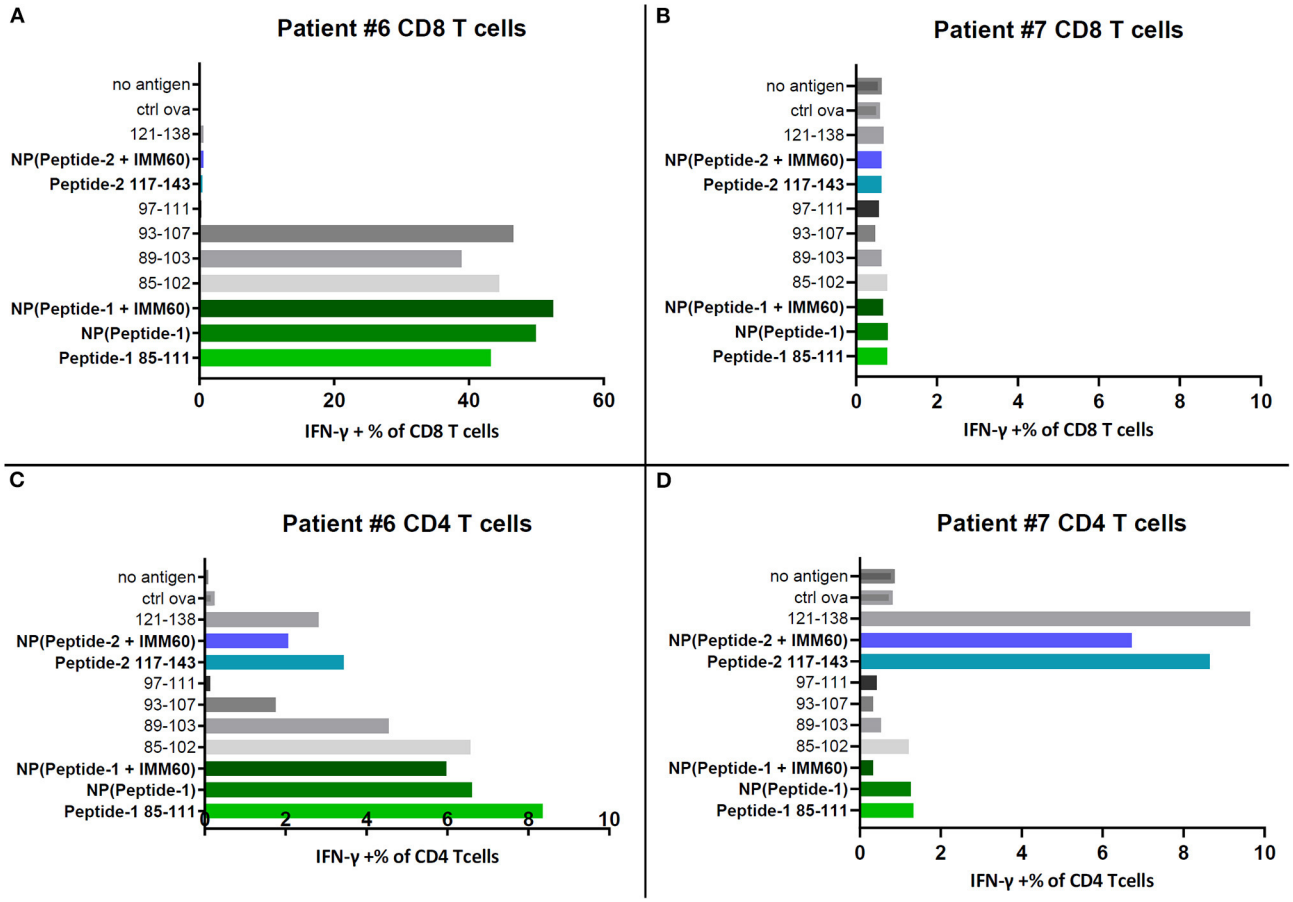

FIGURE 3 | IFN-γ production by PBMC samples of two patients restimulated with NY-ESO-1 derived overlapping peptides in solution or selected free peptides (dissolved in DMSO) or nanoparticles. **(A)** IFN-γ positive CD8 T cells in restimulated PBMCs of patient#6, **(B)** IFN-γ positive CD8 T cells in restimulated PBMCs of patient#7, **(C)** IFN-γ positive CD4 T cells in restimulated PBMCs of patient#6, **(D)** IFN-γ positive CD4 T cells in restimulated PBMCs of patient#7.

To further elucidate the role of IMM60 in CD8 T cell responses, homozygous AAD mice were used. In these mice, β2-microglobulin is intact; therefore, they have a similar expression of H2-Dd and HLA-A2.1 as well as other class I-like molecules such as CD1d (33) and have functional iNKT cells (**Supplementary Figures 5A,B**). AAD mice were vaccinated with nanoparticles containing all three peptides (peptide-1, peptide-2, peptide-3) with or without IMM60 or only peptide-3 with IMM60. After 2 monthly injections, target cells were loaded with peptide-3, transferred to immunized mice, and antigen-specific cytotoxicity was measured. The mice injected with nanoparticles containing IMM60 demonstrated higher peptide-3 specific CD8 T cell cytotoxicity than in mice injected with nanoparticles without IMM60 but a mixture of peptides (**Figure 5A**). When we repeated this experiment without a booster injection, the cytotoxic response against peptide-3 with nanoparticles containing a peptide mixture but not IMMM60 did not show a major change. However, cytotoxic responses against particles containing both the single and multiple peptides with IMM60 were reduced compared to the booster regime. Nevertheless, nanoparticles with peptide mix (containing a mouse CD4 T cell epitope) and IMM60 was superior to both the nanoparticles without IMM60 and nanoparticles with a single CD8 T cell-specific peptide and IMM60 (**Figure 5B**).

Together, these results demonstrate that PLGA encapsulated long peptides have higher CD8 T cell immunogenicity *in vivo* than freely administered formulations which can be further enhanced by co-delivery of IMM60.

PLGA Nanoparticles With Peptides and IMM60 Enhance Antibody Responses Against NY-ESO-1

AAD mice inoculated with full-length NY-ESO-1 expressing 1C12 sarcoma tumor cells rejected the tumors spontaneously, and T cell responses were observed in most mice (**Supplementary Figures 5C,D**). Sera of these mice were analyzed to test if the nanoparticles containing three NY-ESO-1 peptides and IMM60 can boost antibody responses against NY-ESO-1. Despite a similar tumor rejection in both groups, NY-ESO-1 specific antibodies in IgG1 and IgG2c isotypes were detected exclusively in the sera of mice injected with nanoparticles containing three peptides and IMM60

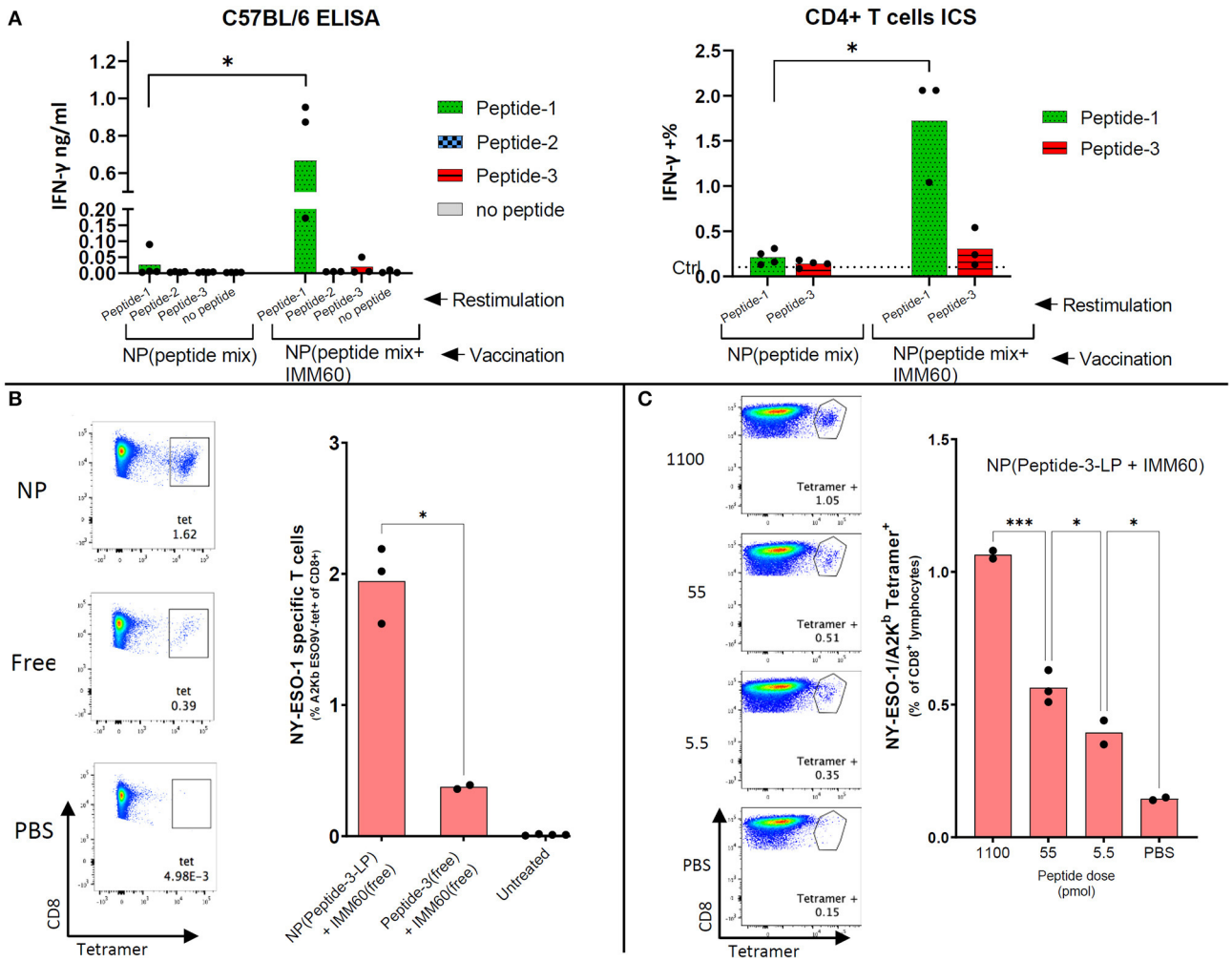

FIGURE 4 | Endogenous CD4 and CD8 responses obtained by nanoparticle vaccination of mice. **(A)** C57Bl/6 mice were intravenously injected with 1 mg nanoparticles (NP) containing all three peptides with or without IMM60. Left: 7 days later, splenocytes were isolated and restimulated separately with peptide-1, peptide-2, or peptide-3. IFN-γ amounts in culture supernatants were determined 48 h later. Right: Splenocytes were restimulated *ex-vivo* either with peptide-1 or peptide-3 and stained with CD3, CD4, and intracellularly IFN-γ. IFN-γ staining in non-vaccinated mouse cells is shown as a dashed line. Dots represent each mouse. **(B)** F1 (HHD × C57BL/6J) mice were intravenously injected with 1.1 ug (0.6 nmol) peptide-3-LP either in solution or encapsulated within nanoparticles mixed with 50 ng IMM60 in solution. Twenty eight days later all mice were boosted with 1.1 ug peptide-3-LP in a solution mixed with 50 ng IMM60 in solution. Eight days after boost splenocytes were isolated and stained with HLA-A2/K^b NY-ESO-$1_{157-165}$ tetramers. FACS plots show the NY-ESO-$1_{157-165}$ specific CD8 T cells (in the square). Unpaired *t*-test with Welch's correction was used to determine statistical significance. **(C)** F1 (HHD × B6SJLCD45.1) mice were injected with nanoparticles containing Peptide-3-LP and IMM60 intravenously with different doses [2 ug (1.1 nmol), 100 ng (55 pmol), or 10 ng (5.5 pmol)] and 10 days later, splenocytes were isolated and stained with HLA-A2/K^b NY-ESO-$1_{157-165}$ tetramers. Mean values are shown. Dots represent each mouse. One-way ANOVA with Tukey's correction was used to determine statistical significance.

(**Figure 5C**). When the sera of these mice were subjected to an ELISA with peptide coated wells, almost all reactivity against whole NY-ESO-1 protein could be reproduced with Peptide-1 (**Figure 5D**, **Supplementary Figure 6**). The B cell epitope was also preserved within the shorter 93–107 and 97–111 peptides (**Figure 5D**, **Supplementary Figure 6**). Since both groups were subjected to two challenges with NY-ESO-1 expressing tumors, injection of nanoparticles, containing both iNKT cell agonist and NY-ESO-1 peptides, are likely to have a critical contribution to antibody responses against NY-ESO-1.

PLGA Nanoparticles With Peptides and IMM60 Have Reversible Side Effects in Preclinical Toxicology Studies

The toxicity of PLGA nanoparticles containing the 3 selected NY-ESO-1 peptides and IMM60 was tested in a preclinical toxicology study. During the toxicology study, no unscheduled deaths were observed. One day after injection, an increase in the liver enzymes AST and ALT was observed, which normalized at day 7, indicating transient liver toxicity (**Figure 6**). Moreover, necropsy results showed IMM60-associated liver toxicity

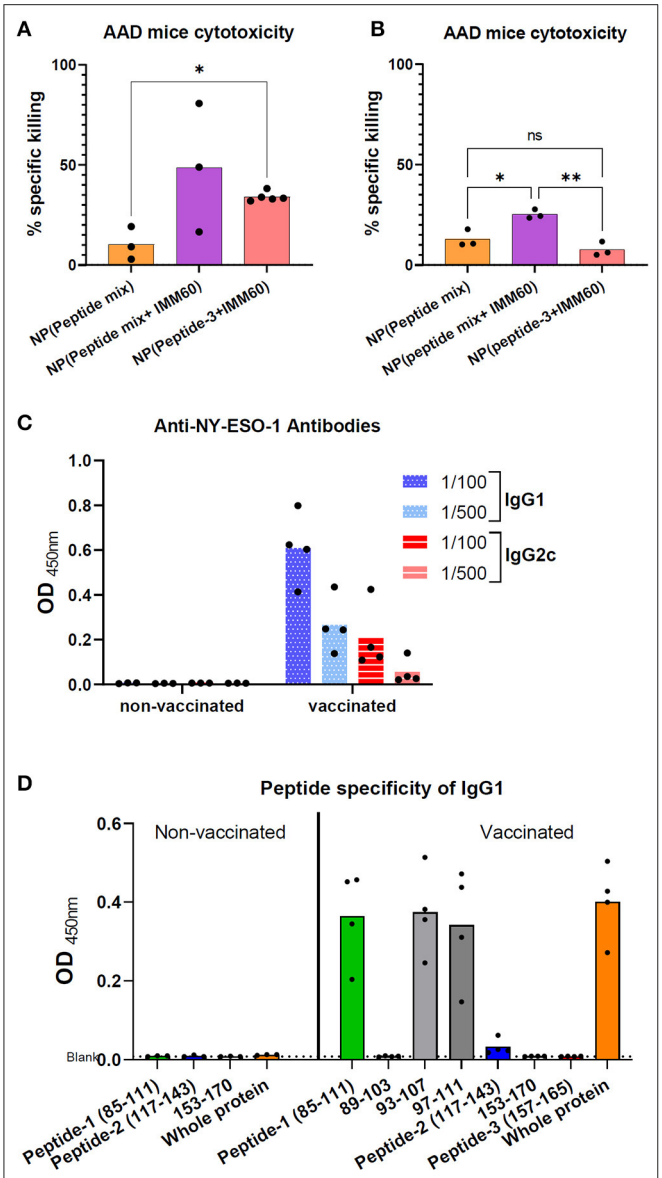

FIGURE 5 | (A) Homozygous AAD mice were intravenously injected with nanoparticles encapsulating 6 ug (5.5 nmol) peptide-3 either mixed with peptide-1 and 2 [NP (Peptide mix)], mixed with peptide-1,2 and IMM60 [NP (peptide mix+IMM60)], or only with IMM60. All mice were boosted with the same nanoparticles on day 28. Seven days after booster injections, specific *in vivo* cytotoxicity of peptide-3 loaded target cells was analyzed. Dots represent each mouse, 3–5 mice were used per group. **(B)** Experiment in A is repeated without any booster injections and peptide-3 loaded target cells were transferred 7 days after a single injection of nanoparticles with a dose of each containing 6 ug peptide-3. Dots represent each mouse, 3 mice were used per group. **(C)** Anti-NY-ESO-1 antibody levels in the sera of AAD mice vaccinated with NP (peptide mix+IMM60) or non-vaccinated and inoculated with 1C12 sarcoma cells expressing full-length NY-ESO-1. Serum samples were diluted 1/100 and 1/500, optical densities of duplicate wells are shown. Dots represent each mouse. **(D)** Peptide specificity of anti-NY-ESO-1 antibodies in the sera of the same AAD mice as shown in **(C)**. Optical density of ELISA wells indicating relative IgG1 antibody levels is shown. Bars show mean optical density values of all mice, dots represent each mouse.

[i.e., hepatocellular necrosis, (peri)vascular mononuclear cell infiltration, and thrombus formation] on day 1 without a dose-response relation (**Supplementary Table 5**). Also, minimal/mild pulmonary vascular mononuclear cell infiltration was observed.

On day 7, despite a low-grade granulomatous inflammation in one mouse and minimal (peri)vascular mononuclear cell infiltration in three mice, hepatocellular necrosis in the 50 mg/kg subgroup was no longer recorded (**Supplementary Table 6**), and thrombus formation was almost completely recovered. Similarly, the pulmonary findings observed in 3 out of 10 mice were recovered (**Supplementary Table 6**). In mice injected with nanoparticles encapsulating the 3 peptides only, hepatocellular apoptosis/necrosis was also observed. The lesions were, however, smaller and without thrombosis or mononuclear cell infiltration compared to the mice injected with nanoparticles containing IMM60.

In brief, the presence of minimal/mild thrombosis and necrosis in the liver 1 day after nanoparticle injection was considered to be adverse, while partial recovery of necrosis and almost complete recovery of thrombosis were noted within 7 days.

DISCUSSION

In our previous studies, iNKT cell agonists outperformed TLR ligands upon encapsulation in PLGA nanoparticles for the co-delivery of antigen and adjuvant to DCs (14). Effects were mediated by chemokines, CCL17, and CXCL9, induced by iNKT cells during the cross-priming of CD8 T cells (16). Besides, intravenous injection of nanoparticles was necessary for a robust anti-tumor immune response which can synergize with checkpoint modulation (15). However, so far, mostly ovalbumin protein was used in these studies as a model antigen. Here, we took the next step toward clinical application by moving to the widely expressed tumor-associated cancer germline antigen NY-ESO-1.

NY-ESO-1 can be qualified as the most suitable TAA for an "off the shelf" cancer vaccine due to its leading immunogenicity which has been reaffirmed by a recent mRNA vaccination trial incorporating various tumor-associated antigens (13). Although mRNAs encoding multiple full-length antigens can be easily encapsulated within liposomes, peptide/protein antigens within PLGA have the advantage of long-term stability and wide storage conditions. NY-ESO-1 whole protein is known to be poorly cross-presented when delivered to DCs in free form (19). The cross-presentation of NY-ESO-1 is enhanced by different formulations which were previously demonstrated to induce specific T cell responses in clinical trials (19, 20, 34). We also reported high T cell stimulation with nanoparticles made of the same full-length NY-ESO-1 and LPS coated with polyphenol (35). However, in this study, no considerable response with PLGA nanoparticles encapsulating NY-ESO-1 protein was observed. This could be due to the low solubility of the NY-ESO-1 protein in aqueous and organic solvents which hampers encapsulation

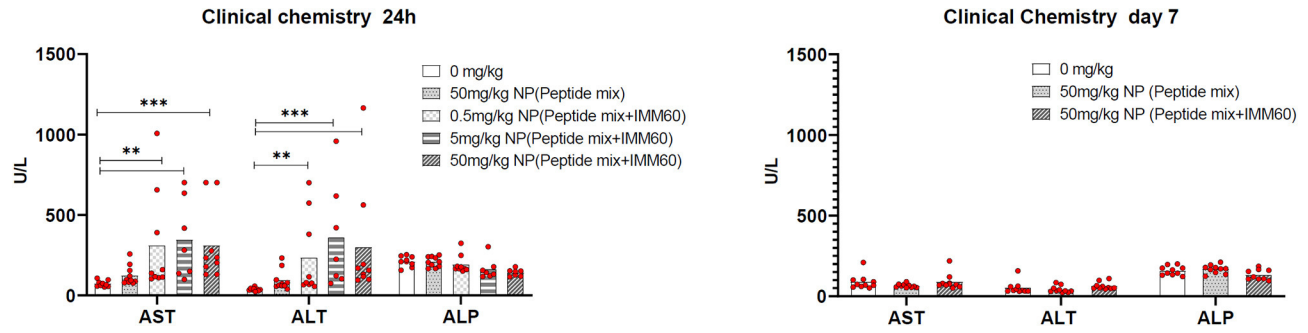

FIGURE 6 | Wild type C57BL/6 mice were intravenously injected either with PBS (0 mg/kg), nanoparticles containing NY-ESO-1 peptide mix (6.1 ug Peptide-1, 4.3 ug Peptide-2, and 11 ug Peptide-3 per mg NP) (50 mg/kg NP peptide mix) or increasing doses of nanoparticles containing NY-ESO-1 peptide mix and IMM60 (8.8 ug Peptide-1, 5.9 ug Peptide-2 and 12 ug Peptide-3 with 1.2 ug IMM60 per mg NP) 0.5, 5, 50 mg/kg NP (peptide mix+IMM60). Total IMM60 doses for a mouse weighing 20 g were 0.012, 0.12, and 1.2 ug, respectively. Twenty-four hour and 7 days after injections Alanine aminotransferase (ALT), Aspartate aminotransferase (AST), and Alkaline phosphatase (ALP) levels were measured in blood plasma. Five male and 5 female, 10 mice were used for each group, dots represent each mouse, Kruskal-Wallis and Dunn's pairwise comparisons were performed for statistical analysis. Only significant differences were shown.

and quantification. In contrast, peptides derived from NY-ESO-1 were shown to be effective for vaccination, and higher molar quantities of peptides could be encapsulated improving the immunogenicity of the PLGA nanoparticle vaccine (11, 36–38). Accordingly, we focused on immunogenic epitopes of NY-ESO-1 and determined two NY-ESO-1 long (85–111 and 117–143) peptides and one short (157–165) peptide which are presented in a range of MHC class-I and MHC class-II molecules covering more than 80% of the European population.

In a previous study, similar NY-ESO-1-derived peptides and α-GalCer loaded onto monocyte-derived DCs induced iNKT cell expansion and CD4 T cell responses in the majority, and CD8 T cell responses in some patients (38). Besides, we also added a third short peptide (peptide-3, 157–165) presented by the highly prevalent HLA-A2.1 molecule, which may improve CD8 T cell response rates. The same epitope was used previously in clinical trials but suffered from either a cryptic epitope emerging in longer forms due to extracellular cleavage or being presented by non-APCs in the short form (24, 39). Nanoparticle delivery can protect peptides from extracellular cleavage until professional APCs take them up, and spleen resident cDC1s can enhance priming of CD8 T cells by utilizing the CCL17 and CXCL9 networks (16, 40, 41). Indeed, we observed higher endogenous CD8 T cell responses against this epitope *in vivo* with PLGA nanoparticles, and short peptides could also induce cytotoxic T cell response in nanoparticle form. As expected, CD8 T cell cytotoxicity against NY-ESO-$1_{157-165}$ is further enhanced by the presence of IMM60 within the particles reaffirming our previous findings on CD8 T cell responses against ovalbumin protein and HPV-E7 peptide (14, 15). Moreover, we observed even higher cytotoxic T cell responses when a CD4 T cell epitope is also introduced within particles together with IMM60. This hints at a further enhancement of iNKT cell help by CD4 T cell help when multiple epitopes are covered within the particles. Therefore, nanoparticle-mediated peptide delivery is expected to enhance CD8 T cell responses against 157–165 epitope together with the extended activation of human iNKT cells by the novel iNKT cell agonist IMM60 (14, 18).

Harnessing the helper functions of iNKT cells is also known to enhance antigen-specific CD4 T cell responses (42, 43). This was also relevant in our vaccination strategy with nanoparticles containing NY-ESO-1 peptides in which the presence of IMM60 primed endogenous CD4 T cells that were otherwise almost absent with particles containing only peptides. Tumor cells could also present MHC class-II epitopes of NY-ESO-1 on their surface, and NY-ESO-1 specific CD4 T cells were previously demonstrated to induce tumor regression in melanoma patients (44, 45). CD4 T cells can play various critical roles in sustaining an anti-tumor microenvironment, helping NK and CD8 T cell survival and cytotoxicity as well as B cell responses.

IC12 sarcoma line was transduced with a lentiviral vector to express full-length NY-ESO-1 and was cloned based on the highest expression of NY-ESO-1. Unfortunately, this also increased the immunogenicity of the tumor to cause spontaneous rejections with a visible CD8 T cell response hampering the detection of vaccine-induced T cell immunity. On the other hand, we could demonstrate a *de novo* antibody response against NY-ESO-1 protein in the IC12 sarcoma inoculated mice which were also vaccinated with nanoparticles containing three peptides and IMM60. Even though all mice have been introduced with NY-ESO-1 *via* the sarcoma cell line twice, the full-length antigen may not be easily accessible to the B cells as well as the nanoparticle delivered peptides or IMM60 could be responsible for transactivating the B cells in the vaccination group. Considering the CD4 T cell responses which were dependent on co-encapsulation of IMM60 but not the peptides, IMM60 is likely to have a significant contribution also to the antibody responses. INKT cells are known to provide both cognate and non-cognate help to B cells leading to enhanced antibody responses. Through cognate help, marginal zone B cells can acquire the particles and present glycolipid to iNKT cells. By contrast, by non-cognate help, DCs licensed by iNKT cells activate the CD4 helper T cells, which facilitates B cell stimulation (46, 47). However, further research is required to fully decipher the mechanism of help toward B cells in the PLGA nanoparticle-mediated peptide and agonist co-delivery settings.

As a final step toward clinical application, the systemic toxicity of PLGA nanoparticles containing three NY-ESO-1 peptides and IMM60 was evaluated. Mild and mostly transient liver toxicity was observed in mice treated with IMM60 containing nanoparticles indicating that the toxicity is dependent on iNKT cell activation, which is known to reside in the liver of mice in high numbers. Considering the lower numbers of iNKT cells in humans compared with mice, and the safety of the iNKT cell agonist α-GalCer in previous clinical treatments, the PLGA nanoparticle vaccines containing iNKT cell agonists can be regarded as a safe and effective modality. We believe that the long-term stability and a full spectrum of immunity could also render these nanoparticles with potential use against viral infections.

In summary, we demonstrated the feasibility to encapsulate three NY-ESO-1-derived peptides together with IMM60 in PLGA nanoparticles. All peptides are efficiently processed and presented by multiple HLA types *in vitro* and *in vivo* while preserving the potency of IMM60. Furthermore, iNKT cell help was provided for multiple epitope-specific CD8 and CD4 T cell responses, and a *de novo* antibody response was observed in NY-ESO-1 positive tumor-bearing mice *via* PLGA nanoparticle-mediated co-delivery. Finally, no serious adverse events occurred in the toxicological evaluation warranting the clinical testing of these nanoparticles.

DATA AVAILABILITY STATEMENT

The raw data supporting the conclusions of this article will be made available by the authors, without undue reservation.

ETHICS STATEMENT

The animal study was reviewed and approved by Nijmegen Animal Experiments Committee (Project No: DEC2015-019 and DEC2019-020) and the Oxford Animal Welfare Ethics Review Board (Home Office under license number PBA43A2E4).

AUTHOR CONTRIBUTIONS

IdV, CF, and VC conceived the research question. YD, UG, and MV designed the peptides and experiments. EV produced all nanoparticles, analyzed peptide contents and physical characteristics, contributed to tissue processing, and ELISA's. JC assisted in designing the toxicology study and interpreting the results. NvR assisted in *in vivo* experiments. EJ and MH developed the method for the IMM60 quantification and performed IMM60 content analysis. MD supervised TCR transfection and antigen presentation assays and contributed to the interpretation of the results. YD, UG, and J-LC planned and performed the experiments, processed the experiment data, designed the figures, and interpreted results. VC and CF supervised the experiments. YD drafted. UG supplemented, reviewed, and edited. J-LC, MV, EJ, MH, MD, and JC edited. CF and IdV reviewed and edited. IdV revised the manuscript. All authors contributed to the article and approved the submitted version.

FUNDING

This work was supported by Horizon 2020 project PRECIOUS (H2020-NMP-2015-two-stage, grant #686089) and the U.K. Medical Research Council, the Oxford Biomedical Research Center, and Cancer Research UK (Programme Grant C399/A2291 to VC). CF is a recipient of the ERC Advanced grant ARTimmune (#834618) and the NWO Spinoza award. IdV received a NWO-Vici (Grant 918.14.655) and the H2020 EU Grant PROCROP (Grant 635122).

ACKNOWLEDGMENTS

We are grateful to Jonathan Skipper at Ludwig Institute for Cancer Research, for providing NY-ESO full-length proteins, Ian Walters at iOx Therapeutics for providing clinical-grade IMM60, Prof. Ton N.M. Schumacher at NKI for permission to use the TCR sequence specific for the HLA-A2 epitope and Prof. Ugur Sahin at BioNTech for permission to use the TCR sequence specific for the HLA-B7 and DRB1 epitope and for providing all three TCR mRNAs. We thank Bianca Sänger at BioNTech for the transfer of skills related to *in vitro* mRNA transfection and Fiona Born, Jo Bates, and the toxicology team at Charles River Edinburg for their intense assistance and work in toxicology evaluations. We are grateful for the efforts of Jeanette Pots at Tumor Immunology department of Radboudumc for her significant contribution to GMP nanoparticle production and for assessing the quality compliance of production batches as well as Kevin Bos, Tom van Oorschot, and TJitske Duiveman-de Boer for their assistance in particle production and quality control phases. We would like to dedicate this paper to the ones we lost during the Covid-19 pandemic.

SUPPLEMENTARY MATERIAL

The Supplementary Material for this article can be found online at: https://www.frontiersin.org/articles/10.3389/fimmu.2021.641703/full#supplementary-material

REFERENCES

1. Janelle V, Rulleau C, Del Testa S, Carli C, Delisle JS. T-Cell Immunotherapies targeting histocompatibility and tumor antigens in hematological malignancies. *Front Immunol*. (2020) 11:276. doi: 10.3389/fimmu.2020.00276
2. Akers SN, Odunsi K, Karpf AR. Regulation of cancer germline antigen gene expression: implications for cancer immunotherapy. *Future Oncol*. (2010) 6:717–32. doi: 10.2217/fon.10.36
3. Thomas R, Al-Khadairi G, Roelands J, Hendrickx W, Dermime S, Bedognetti D, et al. NY-ESO-1 based immunotherapy of cancer: current perspectives. *Front Immunol*. (2018) 9:947. doi: 10.3389/fimmu.2018.00947

4. Esfandiary A, Ghafouri-Fard S. New York esophageal squamous cell carcinoma-1 and cancer immunotherapy. *Immunotherapy*. (2015) 7:411–39. doi: 10.2217/imt.15.3
5. Bendelac A, Savage PB, Teyton L. The biology of NKT cells. *Annu Rev Immunol*. (2007) 25:297–336. doi: 10.1146/annurev.immunol.25.022106.141711
6. Brennan PJ, Brigl M, Brenner MB. Invariant natural killer T cells: an innate activation scheme linked to diverse effector functions. *Nat Rev Immunol*. (2013) 13:101–17. doi: 10.1038/nri3369
7. Cerundolo V, Silk JD, Masri SH, Salio M. Harnessing invariant NKT cells in vaccination strategies. *Nat Rev Immunol*. (2009) 9:28–38. doi: 10.1038/nri2451
8. Chen YT, Scanlan MJ, Sahin U, Tureci O, Gure AO, Tsang S, et al. A testicular antigen aberrantly expressed in human cancers detected by autologous antibody screening. *Proc Natl Acad Sci USA*. (1997) 94:1914–8. doi: 10.1073/pnas.94.5.1914
9. Jungbluth AA, Chen YT, Stockert E, Busam KJ, Kolb D, Iversen K, et al. Immunohistochemical analysis of NY-ESO-1 antigen expression in normal and malignant human tissues. *Int J Cancer*. (2001) 92:856–60. doi: 10.1002/ijc.1282
10. Gnjatic S, Nishikawa H, Jungbluth AA, Gure AO, Ritter G, Jager E, et al. NY-ESO-1: review of an immunogenic tumor antigen. *Adv Cancer Res*. (2006) 95:1–30. doi: 10.1016/S0065-230X(06)95001-5
11. Kakimi K, Isobe M, Uenaka A, Wada H, Sato E, Doki Y, et al. A phase I study of vaccination with NY-ESO-1f peptide mixed with Picibanil OK-432 and Montanide ISA-51 in patients with cancers expressing the NY-ESO-1 antigen. *Int J Cancer*. (2011) 129:2836–46. doi: 10.1002/ijc.25955
12. Odunsi K, Matsuzaki J, James SR, Mhawech-Fauceglia P, Tsuji T, Miller A, et al. Epigenetic potentiation of NY-ESO-1 vaccine therapy in human ovarian cancer. *Cancer Immunol Res*. (2014) 2:37–49. doi: 10.1158/2326-6066.CIR-13-0126
13. Sahin U, Oehm P, Derhovanessian E, Jabulowsky RA, Vormehr M, Gold M, et al. An RNA vaccine drives immunity in checkpoint-inhibitor-treated melanoma. *Nature*. (2020) 585:107–12. doi: 10.1038/s41586-020-2537-9
14. Dolen Y, Kreutz M, Gileadi U, Tel J, Vasaturo A, van Dinther EA, et al. Co-delivery of PLGA encapsulated invariant NKT cell agonist with antigenic protein induce strong T cell-mediated antitumor immune responses. *Oncoimmunology*. (2016) 5:e1068493. doi: 10.1080/2162402X.2015.1068493
15. Dölen Y, Valente M, Tagit O, Jäger E, Van Dinther EAW, van Riessen NK, et al. Nanovaccine administration route is critical to obtain pertinent iNKt cell help for robust anti-tumor T and B cell responses. *OncoImmunology*. (2020) 9:1738813. doi: 10.1080/2162402X.2020.1738813
16. Valente M, Dolen Y, van Dinther E, Vimeux L, Fallet M, Feuillet V, et al. Cross-talk between iNKT cells and CD8 T cells in the spleen requires the IL-4/CCL17 axis for the generation of short-lived effector cells. *Proc Natl Acad Sci USA*. (2019) 116:25816–27. doi: 10.1073/pnas.1913491116
17. Bartkowiak T, Singh S, Yang G, Galvan G, Haria D, Ai M, et al. Unique potential of 4-1BB agonist antibody to promote durable regression of HPV+ tumors when combined with an E6/E7 peptide vaccine. *Proc Natl Acad Sci USA*. (2015) 112:E5290–9. doi: 10.1073/pnas.1514418112
18. Jukes JP, Gileadi U, Ghadbane H, Yu TF, Shepherd D, Cox LR, et al. Non-glycosidic compounds can stimulate both human and mouse iNKT cells. *Eur J Immunol*. (2016) 46:1224–34. doi: 10.1002/eji.201546114
19. Robson NC, McAlpine T, Knights AJ, Schnurr M, Shin A, Chen W, et al. Processing and cross-presentation of individual HLA-A, -B, or -C epitopes from NY-ESO-1 or an HLA-A epitope for Melan-A differ according to the mode of antigen delivery. *Blood*. (2010) 116:218–25. doi: 10.1182/blood-2009-10-249458
20. Chen JL, Dawoodji A, Tarlton A, Gnjatic S, Tajar A, Karydis I, et al. NY-ESO-1 specific antibody and cellular responses in melanoma patients primed with NY-ESO-1 protein in ISCOMATRIX and boosted with recombinant NY-ESO-1 fowlpox virus. *Int J Cancer*. (2015) 136:E590–601. doi: 10.1002/ijc.29118
21. Choi EM, Palmowski M, Chen J, Cerundolo V. The use of chimeric A2K(b) tetramers to monitor HLA A2 immune responses in HLA A2 transgenic mice. *J Immunol Methods*. (2002) 268:35–41. doi: 10.1016/S0022-1759(02)00198-9
22. Jackson H, Dimopoulos N, Mifsud NA, Tai TY, Chen Q, Svobodova S, et al. Striking immunodominance hierarchy of naturally occurring CD8+ and CD4+ T cell responses to tumor antigen NY-ESO-1. *J Immunol*. (2006) 176:5908–17. doi: 10.4049/jimmunol.176.10.5908
23. Nguyen DT. *Cancer Antigenic Peptide Database*. (2019). Available online at: https://caped.icp.ucl.ac.be/Peptide/list (accessed January 21, 2019).
24. Gnjatic S, Jager E, Chen W, Altorki NK, Matsuo M, Lee SY, et al. CD8(+) T cell responses against a dominant cryptic HLA-A2 epitope after NY-ESO-1 peptide immunization of cancer patients. *Proc Natl Acad Sci USA*. (2002) 99:11813–8. doi: 10.1073/pnas.142417699
25. *IEDB Analysis Resource: National Institute of Allergy and Infectious Diseases*. (2019). Available online at: https://tools.iedb.org/population/ (accessed January 21, 2019).
26. Bidmon N, Attig S, Rae R, Schroder H, Omokoko TA, Simon P, et al. Generation of TCR-engineered T cells and their use to control the performance of T cell assays. *J Immunol*. (2015) 194:6177–89. doi: 10.4049/jimmunol.1400958
27. Simon P, Omokoko TA, Breitkreuz A, Hebich L, Kreiter S, Attig S, et al. Functional TCR retrieval from single antigen-specific human T cells reveals multiple novel epitopes. *Cancer Immunol Res*. (2014) 2:1230–44. doi: 10.1158/2326-6066.CIR-14-0108
28. Jia J, Zhang Y, Xin Y, Jiang C, Yan B, Zhai S. Interactions between nanoparticles and dendritic cells: from the perspective of cancer immunotherapy. *Front Oncol*. (2018) 8:404. doi: 10.3389/fonc.2018.00404
29. Chenthamara D, Subramaniam S, Ramakrishnan SG, Krishnaswamy S, Essa MM, Lin FH, et al. Therapeutic efficacy of nanoparticles and routes of administration. *Biomater Res*. (2019) 23:20. doi: 10.1186/s40824-019-0166-x
30. Benlalam H, Linard B, Guilloux Y, Moreau-Aubry A, Derre L, Diez E, et al. Identification of five new HLA-B*3501-restricted epitopes derived from common melanoma-associated antigens, spontaneously recognized by tumor-infiltrating lymphocytes. *J Immunol*. (2003) 171:6283–9. doi: 10.4049/jimmunol.171.11.6283
31. Lopes L, Dewannieux M, Gileadi U, Bailey R, Ikeda Y, Whittaker C, et al. Immunization with a lentivector that targets tumor antigen expression to dendritic cells induces potent CD8+ and CD4+ T-cell responses. *J Virol*. (2008) 82:86–95. doi: 10.1128/JVI.01289-07
32. Firat H, Garcia-Pons F, Tourdot S, Pascolo S, Scardino A, Garcia Z, et al. H-2 class I knockout, HLA-A2.1-transgenic mice: a versatile animal model for preclinical evaluation of antitumor immunotherapeutic strategies. *Eur J Immunol*. (1999) 29:3112–21.
33. Newberg MH, Smith DH, Haertel SB, Vining DR, Lacy E, Engelhard VH. Importance of MHC class 1 alpha2 and alpha3 domains in the recognition of self and non-self MHC molecules. *J Immunol*. (1996) 156:2473–80.
34. Kageyama S, Wada H, Muro K, Niwa Y, Ueda S, Miyata H, et al. Dose-dependent effects of NY-ESO-1 protein vaccine complexed with cholesteryl pullulan (CHP-NY-ESO-1) on immune responses and survival benefits of esophageal cancer patients. *J Transl Med*. (2013) 11:246. doi: 10.1186/1479-5876-11-246
35. Qiu L, Valente M, Dolen Y, Jager E, Beest MT, Zheng L, et al. Endolysosomal-escape nanovaccines through adjuvant-induced tumor antigen assembly for enhanced effector CD8(+) T cell activation. *Small*. (2018) 14:e1703539. doi: 10.1002/smll.201703539
36. Wada H, Isobe M, Kakimi K, Mizote Y, Eikawa S, Sato E, et al. Vaccination with NY-ESO-1 overlapping peptides mixed with Picibanil OK-432 and montanide ISA-51 in patients with cancers expressing the NY-ESO-1 antigen. *J Immunother*. (2014) 37:84–92. doi: 10.1097/CJI.0000000000000017
37. Baumgaertner P, Costa Nunes C, Cachot A, Maby-El Hajjami H, Cagnon L, Braun M, et al. Vaccination of stage III/IV melanoma patients with long NY-ESO-1 peptide and CpG-B elicits robust CD8(+) and CD4(+) T-cell responses with multiple specificities including a novel DR7-restricted epitope. *Oncoimmunology*. (2016) 5:e1216290. doi: 10.1080/2162402X.2016.1216290
38. Gasser O, Sharples KJ, Barrow C, Williams GM, Bauer E, Wood CE, et al. A phase I vaccination study with dendritic cells loaded with NY-ESO-1 and alpha-galactosylceramide: induction of polyfunctional T cells in high-risk melanoma patients. *Cancer Immunol Immunother*. (2018) 67:285–98. doi: 10.1007/s00262-017-2085-9

39. Dutoit V, Taub RN, Papadopoulos KP, Talbot S, Keohan ML, Brehm M, et al. Multiepitope CD8(+) T cell response to a NY-ESO-1 peptide vaccine results in imprecise tumor targeting. *J Clin Invest*. (2002) 110:1813–22. doi: 10.1172/JCI16428
40. Bijker MS, van den Eeden SJ, Franken KL, Melief CJ, van der Burg SH, Offringa R. Superior induction of anti-tumor CTL immunity by extended peptide vaccines involves prolonged, DC-focused antigen presentation. *Eur J Immunol*. (2008) 38:1033–42. doi: 10.1002/eji.200737995
41. Globisch T, Steiner N, Fulle L, Lukacs-Kornek V, Degrandi D, Dresing P, et al. Cytokine-dependent regulation of dendritic cell differentiation in the splenic microenvironment. *Eur J Immunol*. (2014) 44:500–10. doi: 10.1002/eji.201343820
42. Fujii S, Shimizu K, Smith C, Bonifaz L, Steinman RM. Activation of natural killer T cells by alpha-galactosylceramide rapidly induces the full maturation of dendritic cells *in vivo* and thereby acts as an adjuvant for combined CD4 and CD8 T cell immunity to a coadministered protein. *J Exp Med*. (2003) 198:267–79. doi: 10.1084/jem.20030324
43. Hermans IF, Silk JD, Gileadi U, Salio M, Mathew B, Ritter G, et al. NKT cells enhance CD4+ and CD8+ T cell responses to soluble antigen *in vivo* through direct interaction with dendritic cells. *J Immunol*. (2003) 171:5140–7. doi: 10.4049/jimmunol.171.10.5140
44. Hunder NN, Wallen H, Cao J, Hendricks DW, Reilly JZ, Rodmyre R, et al. Treatment of metastatic melanoma with autologous CD4+ T cells against NY-ESO-1. *N Engl J Med*. (2008) 358:2698–703. doi: 10.1056/NEJMoa0800251
45. Fonteneau JF, Brilot F, Munz C, Gannage M. The tumor antigen NY-ESO-1 mediates direct recognition of melanoma cells by CD4+ T cells after intercellular antigen transfer. *J Immunol*. (2016) 196:64–71. doi: 10.4049/jimmunol.1402664
46. Tonti E, Galli G, Malzone C, Abrignani S, Casorati G, Dellabona P. NKT-cell help to B lymphocytes can occur independently of cognate interaction. *Blood*. (2009) 113:370–6. doi: 10.1182/blood-2008-06-166249
47. Dellabona P, Abrignani S, Casorati G. iNKT-cell help to B cells: a cooperative job between innate and adaptive immune responses. *Eur J Immunol*. (2014) 44:2230–7. doi: 10.1002/eji.201344399

Conflict of Interest: The authors declare that the research was conducted in the absence of any commercial or financial relationships that could be construed as a potential conflict of interest.

frontiers in Immunology

ORIGINAL RESEARCH
published: 08 March 2021
doi: 10.3389/fimmu.2021.586220

Arrest in the Progression of Type 1 Diabetes at the Mid-Stage of Insulitic Autoimmunity Using an Autoantigen-Decorated All-*trans* Retinoic Acid and Transforming Growth Factor Beta-1 Single Microparticle Formulation

*Brett E. Phillips[1], Yesica Garciafigueroa[1], Carl Engman[1], Wen Liu[1,2], Yiwei Wang[2], Robert J. Lakomy[1], Wilson S. Meng[2,3], Massimo Trucco[1] and Nick Giannoukakis[1]**

[1] Institute of Cellular Therapeutics, Allegheny Health Network, Pittsburgh, PA, United States, [2] Graduate School of Pharmaceutical Sciences, Duquesne University, Pittsburgh, PA, United States, [3] McGowan Institute for Regenerative Medicine, University of Pittsburgh, Pittsburgh, PA, United States

OPEN ACCESS

Edited by:
Maud Plantinga,
University Medical Center
Utrecht, Netherlands

Reviewed by:
Tatjana Nikolic,
Leiden University, Netherlands
Jacques C. Mbongue,
Oakwood University, United States

***Correspondence:**
Nick Giannoukakis
nick.giannoukakis@ahn.org

Specialty section:
This article was submitted to Antigen Presenting Cell Biology, a section of the journal Frontiers in Immunology

Received: 22 July 2020
Accepted: 15 February 2021
Published: 08 March 2021

Citation:
Phillips BE, Garciafigueroa Y, Engman C, Liu W, Wang Y, Lakomy RJ, Meng WS, Trucco M and Giannoukakis N (2021) Arrest in the Progression of Type 1 Diabetes at the Mid-Stage of Insulitic Autoimmunity Using an Autoantigen-Decorated All-trans Retinoic Acid and Transforming Growth Factor Beta-1 Single Microparticle Formulation. Front. Immunol. 12:586220. doi: 10.3389/fimmu.2021.586220

Type 1 diabetes (T1D) is a disorder of impaired glucoregulation due to lymphocyte-driven pancreatic autoimmunity. Mobilizing dendritic cells (DC) *in vivo* to acquire tolerogenic activity is an attractive therapeutic approach as it results in multiple and overlapping immunosuppressive mechanisms. Delivery of agents that can achieve this, in the form of micro/nanoparticles, has successfully prevented a number of autoimmune conditions *in vivo*. Most of these formulations, however, do not establish multiple layers of immunoregulation. all-*trans* retinoic acid (RA) together with transforming growth factor beta 1 (TGFβ1), in contrast, has been shown to promote such mechanisms. When delivered in separate nanoparticle vehicles, they successfully prevent the progression of early-onset T1D autoimmunity *in vivo*. Herein, we show that the approach can be simplified into a single microparticle formulation of RA + TGFβ1 with surface decoration with the T1D-relevant insulin autoantigen. We show that the onset of hyperglycemia is prevented when administered into non-obese diabetic mice that are at the mid-stage of active islet-selective autoimmunity. Unexpectedly, the preventive effects do not seem to be mediated by increased numbers of regulatory T-lymphocytes inside the pancreatic lymph nodes, at least following acute administration of microparticles. Instead, we observed a mild increase in the frequency of regulatory B-lymphocytes inside the mesenteric lymph nodes. These data suggest additional and potentially-novel mechanisms that RA and TGFβ1 could be modulating to prevent progression of mid-stage autoimmunity to overt T1D. Our data further strengthen the rationale to develop RA+TGFβ1-based micro/nanoparticle "vaccines" as possible treatments of pre-symptomatic and new-onset T1D autoimmunity.

Keywords: type 1 diabetes, vaccine, tolerance, microparticles, immunoregulation, autoimmunity

INTRODUCTION

Type 1 diabetes (T1D) is widely-viewed as a disorder of impaired glucoregulation primarily due to a pancreatic beta (β) cell-selective, largely lymphocyte-driven autoimmunity (1–3). Significant knowledge about pathogenesis of T1D derives from the spontaneously diabetic nonobese diabetic (NOD) mouse strain, believed to share etiopathogenesis with human T1D (4). TH1 and TH17 T-lymphocytes (T-cells) lead this process resulting in β cell destruction (5–8). Dead and dying β cells are acquired by macrophages and DC in steady-state flux through islet structures which migrate into the pancreatic lymph nodes (PLN) where they amplify a vicious circle of T1D autoimmunity by triggering expansion of more β cell-autoreactive T-cells. Regulatory lymphocytes, especially T-cells that stably-express the Foxp3 transcription factor (Foxp3+ Tregs) prevent autoimmune diabetes in the NOD mouse (9) and there is strong evidence that they can regulate the pool of autoreactive effector CD4+ and CD8+ T-cells in humans (10–12). Indeed, autologous Tregs are now in different phases of clinical trials to preserve residual beta cell mass in new onset T1D patients (13–17). While *ex vivo* generation of Tregs has been realized, logistic hurdles stand in the way of expanding personalized Treg cell therapy at a population level (13–17). A simpler way to generate Tregs *in vivo*, and fortify other layers of immune tolerance using a "vaccine," would be decisive in preventing and treating new onset disease.

We have demonstrated that microsphere formulations of antisense DNA oligonucleotides targeting the primary transcripts of CD40, CD80, and CD86 prevent and reverse T1D (18). We observed an increased prevalence of Foxp3+ Tregs together with a decrease in TH1 cytokine levels in successfully-treated, diabetes-free mice, especially in PLN, when injected into the abdominal region overlying the expected location of the pancreas. The effect was β-cell specific since T-cells from successfully-treated mice proliferated vigorously to alloantigen, but not to β-cell antigens *in vitro*. Protection offered by the microspheres was adoptively-transferable to immunodeficient recipients even in the presence of diabetogenic immune cells (18). In parallel, we had examined the effects of the antisense DNA oligonucleotides on dendritic cells (DC) and we discovered that they stimulated the DC to produce retinoic acid (RA) (19, 20). These RA-producing DC were further shown to increase the frequency of IL-10+ regulatory B-lymphocytes (Bregs) as well as stimulate the proliferation of existing Bregs (19, 20). We surmised that a microsphere formulation of the antisense DNA oligonucleotides could also confer RA-producing ability to DC. In fact, we subsequently discovered that DC isolated from the injection site of microsphere-formulated antisense DNA oligonucleotides acquired the ability to produce retinoic acid (RA) as they took up the microsphere formulations and migrated from this injection site to PLN. These DC, accumulated inside PLN, continued to produce RA. These microspheres were subsequently shown to mobilize DC and Tregs inside the PLN of mice exhibiting an ongoing *ex vivo*-induced inflammation (21).

While a number of factors, and different *in vitro* and *in vivo* environments can support the differentiation of Foxp3+ Tregs from precursor T-cells (22–25), transforming growth factor beta (TGFβ) appears to be a common denominator (26–32). Evidence of the *in vivo* effect of TGFβ in Treg cell pool expansion is described in NOD mice treated with TGFβ. In these mice, TGFβ inhibits T1D development, and increases Treg frequency inside islets. Studies in human T-cells demonstrate TGFβ is necessary to induce Tregs. Treatment of human CD4+ cells with TGFβ increases the number of Tregs and expression of CD25 and intracellular CTLA-4. Expansion is due to increased proliferation and protection of cells from activation-induced apoptosis (33). TGFβ promotes induction of Tregs accompanied by an increase in Foxp3 expression. TGFβ converts CD4+ CD25– Foxp3– non-Tregs into CD4+ CD25+ Foxp3+ Tregs. On its own, however, TGFβ is unable to mediate Treg cell induction. RA appears to be an additional factor that licenses the induction process. In mucosal tissue, mature tolerogenic DC producing RA induce Foxp3+ Tregs via a TGFβ -dependent mechanism. RA enhances TGFβ signaling by increasing expression and phosphorylation of Smad3, and this results in increased Foxp3 expression, even in presence of proinflammatory IL-6 or IL-21 (34). Two studies addressed the role of retinoids in T1D using NOD mice. One examined the effect of high vitamin A concentrations on T1D development (35). RA was protective. The other demonstrated that RA inhibited disease development in multiple low dose streptozotocin and naturally-occurring T1D in NOD mice. Prevention was abrogated in Foxp3+ Treg-depleted mice. T1D hyperglycemia was reversible in new onset NOD mice so long as RA was available (36).

The conceptual feasibility of an RA-based immunoregulatory microparticle method to suppress inflammation has been demonstrated (37, 38). PLGA-based particle RA formulation suppressed IL-17 production and RORγ(t) expression in T-cells polarized toward TH17 phenotype *in vitro* with similar potency to that of free drug. RA nanoparticles enhanced TGFβ -dependent Foxp3 expression and IL-10 production in T-cells *in vitro* with similar potency to free RA. T-cells polarized toward TH17 phenotype in presence of free and nanoparticulate RA similarly suppress ability to induce IL-6 production by fibroblasts. DC isolated from cervical lymph nodes and pulsed with PLGA nanoparticles efficiently induces proliferation of Foxp3+ Tregs *in vitro*. Further data demonstrate that nanoparticle formulations that contain *either RA or* TGFβ in combination with another drug (39, 40), or in one instance administered together as *separate* particles (40) are effective in suppression of inflammation through regulatory cell networks.

Until now, no formulation that combined RA and TGFβ together with a T1D-relevant autoantigen, to induce antigen-specific immune hyporesponsiveness, was considered as a potential therapeutic vehicle. We present evidence, herein, that a novel and stable formulation of a RA and TGFβ-formulated single microparticle, decorated with a T1D-relevant autoantigen (Insulin B9-23 peptide) (41–44) can prevent the onset of hyperglycemia when administered into NOD mice that are at the mid-stage of active islet-selective autoimmunity. Acute treatment of late stage autoimmune pre-diabetic NOD mice with the combined RA/TGFβ/T1D-relevant autoantigen microparticle formulation resulted in a mild increase in the frequency of regulatory B-lymphocytes (Bregs) inside the mesenteric lymph

nodes (MLN), but not the PLN. These data suggest additional and potentially-novel mechanisms that RA and TGFβ could be modulating in the prevention of progression of mid-stage autoimmunity to hyperglycemic T1D.

MATERIALS AND METHODS

Experimental Animals

Female NOD/LtJ mice were purchased from the Jackson Laboratories (Bar Harbor, ME) at 6–8 weeks of age and housed up to 34 weeks. Prior to randomization into the treatment arms, NOD female mice between 9 and 11 weeks of age were pre-screened to insure absence of overt hyperglycemia. Blood glucose was assessed using the One Touch Ultra Blood Glucose Meter (Lifescan, Malvern, PA). Animals were maintained in a specific pathogen-free environment in the Animal Facility of the Allegheny Health Network Research Institute. All procedures utilized were in full compliance with and approved by the Institutional Animal Care and Use Research Committee of the Allegheny Health Network Research Institute.

Synthesis and Characterization of RA and TGFβ-Formulated Microparticles

We have previously described surface-functionalized poly lactic-co-glycolic acid (PLGA) particles as drug carriers (45–49). In particular, surface nickel (Ni)-formulated PLGA microparticles (PLGA-Ni) serves as the backbone of our formulations. PLGA-Ni particles were prepared by incorporating the metal chelating lipid 18:1 DOGS-NTA-Ni into the PLGA matrix using a double-emulsion solvent evaporation method. Briefly, 90 mg of PLGA (50:50) dissolved in 2.4 ml dichloromethane (DCM) was admixed with 0.6 ml of 10 mg/ml DOGS-NTA-Ni dissolved in the same solvent. The organic mixture was slowly added to 20 ml 1% polyvinyl alcohol aqueous solution and homogenized at 25,000 rpm for 5 min on ice. These microparticles are designated as PLGA-Ni. Additional PLGA-Ni formulations include all-*trans* retinoic acid (RA) (Sigma-Aldrich, St. Louis, MO) or Nile Red dye (Thermo Fisher Scientific, Waltham, MA). 5.0 mg of RA or Nile red dye were loaded in the organic phase (DCM) with PLGA and the lipid. Using a solvent extraction method, loading of RA was determined to be 4.8 μg per mg of dry powder, with the efficiency determined to be 61% by BCA protein assay (data not shown). Microparticles containing Nile Red dye are designated as PLGA-Red in this manuscript. Particles were precipitated by evaporating DCM and collected by centrifugation, before lyophilization in 2% trehalose for long-term storage at 4°C in a desiccator until use. His-tagged proteins were attached after washing and resuspension in low protein binding microcentrifuge tubes (Thermo Fisher Scientific). Five microgram of the following His-tagged proteins were incubated per 10 mg of microparticles for 1 h: G protein (pG), GFP (Thermo Fisher Scientific), TGFβ1 (Prospec, Rehovot, Israel), or human insulin B9-23 peptide (8 μg) (R&D Biosystems, Minneapoplis, MN). Using the BCA assay, 45.5% of the His-tagged TGF β1protein was associated with the microparticles (data not shown). RA-formulated, TGFβ1 and insulin B9-23 peptide-modified microparticles (all three components constituting the microparticle) were designated Ins-RT-NP.

Microparticle Microscopy and Size Determination

Fluorescence microscopy was performed with a IX53 inverted microscope (Olympus, Shinjuku, Japan) with a 20x objective. His-tagged GFP was admixed with particle suspensions, fixed on slide cover and mounted with Slowfade Diamond solution. Scanning electron microscopy (SEM) of the microparticle formulations was conducted after placing the sample solution (200 μL) directly onto sample stubs. Stubs were then covered in foil and left in a desiccator overnight before testing. Samples were examined using a S-3400N Scanning Electron Microscope 14 (Hitatchi, Tokyo, Japan) equipped with an AXS XFlash Detector 5010 (Bruker, Billerica, MA) and a BrukerNano e-Flash 1000+ (Bruker, Billerica, MA). Hydrodynamic size of the microparticle formulations was measured using a Zetasizer Nano-S; particles were washed to remove trehalose and resuspended in ultrapure water (pH 7.4); measurements were made with dilutions at 5, 2.5, 0.25, 0.0125, 0.00025, and 0.0000025 mg per ml to obtain consensus.

Formulation Release Kinetics

His-tagged GFP was used as a TGFβ1 surrogate to determine release kinetics *in vitro*. Briefly, 5 mg of the PLGA-Ni microparticles were washed and resuspend in 100 μl of pH 8 Tris buffer with 0.1% BSA and loaded with 200 μl of 0.025 mg/ml His-GFP to 0.2 ml pH 8 Tris buffer (0.5 ml Tris buffer in total) and incubated for 1 h at room temperature. Particles were then washed to remove unbound proteins before re-suspended in 1 ml of release medium (1% BSA) and transferred into a 1 ml syringe fitted with a 0.22 μm syringe. Samples (100 μl) were dispensed from the syringe kept at 37°C at the specific time points. Equal volume of the release medium was replaced in the syringe after each sampling. The concentration of His-GFP collected at each time point was determined by measuring the fluorescence intensity ($\lambda = 508$ nm) using a Tecan M1000 spectrophotometer (Tecan, Mannedorf, Switzerland) with an established standard curve. Similarly PLGA-Ni microparticles bound with TGFβ1 were placed in a complete elution buffer. A small sample (5 μl) of the elution was loaded into individual wells of a 6–12% polyacrylamide gradient gel, together with molecular weight marker proteins (Thermo Fisher Scientific) and separated by SDS-PAGE in single dimension. The separated proteins were visualized in the gel *in situ* using silver staining. RA was found to release gradually from the particles at 37°C in PBS. In a preparation of 10 mg of PLGA-Ni RA containing microparticles was dissolved in 1 ml of PBS, and the rate of release was monitored over 18 days *in vitro* by UV absorbance.

Ex vivo Microparticle Uptake

Spleens were harvested from NOD female mice euthanized at 10 weeks of age. A single cells suspension was made by first physically dissociating the spleen followed by a 10 min incubation in RBC lysis buffer (eBioscience) to remove red blood cells.

The cell suspension was then strained through a 100 μm filter and plated at 1×10^6 cells/well in complete RPMI cell culture media (Sigma Aldrich) *plus* 10% fetal bovine serum (Gibco). Cells were plated in a 96-well tissue culture plate in a final volume of 200 μl and allowed to settle prior to addition of microparticles. PLGA-Red microparticles were resuspended in tissue culture media. 0.25 mg of reconstituted particles were then added to the cell wells and incubated together at 37°C for 18 h. Cells were then collected and washed three times to remove extra-cellular particles. The uptake of particles by cells was measured by flow cytometry (BD Influx) and the data were analyzed by FlowJo software version 10.7.1.

In vivo Microparticle Administration

Microparticles were prepared at a concentration of 10 mg per 200 μL vehicle volume for administration to mice. PLGA-Ni and PLGA-Red microparticles were resuspended in sterile saline in low protein binding microcentrifuge tubes. PLGA (RA)-Ni were incubated with His-tagged recombinant human TGFβ1 at a concentration of 25 μg/mL, or 5 μg total weight and His-tagged human insulin B9-23 peptide (3-letter amino acid sequence: H-Ser-His-Leu-Val-Glu-Ala-Leu-Tyr-Leu-Val-Cys-Gly-Glu-Arg-Gly-OH) was added at a concentration of 40 μg/mL, or 8 μg total weight. The microparticle suspension was maintained dispersed by pipet mixing and incubated at room temperature for 30 min. After incubation, the suspension was again mixed by pipetting and loaded into 1 ml syringes with 27 gauge needles. Eleven week-old female NODLtJ/Shi mice were administered the microparticle formulations by subcutaneous (s.c.) injection into the abdomen. None of the mice were hyperglycemic or exhibited dysglycemia at the time of microparticle administration.

Tissue Single Cell Collection and Processing

PLN, MLN and skin (a 1×1 cm^2 patch at the injection site) were resected from randomly-selected diabetes-free mice from all the treatment arms. Lymph nodes were physically dissociated and the tissue was strained through 100 μm filters (Fisher Scientific) to produce single cell suspensions. Viability of cells was assessed by Trypan Blue staining and counted in a Countess II FL device (Thermo Fisher). Skin was isolated and processed into single cells as described previously (50). Briefly, hair around the injection site on the mouse abdomen was removed with hair trimmers. After euthanasia a 1×1 cm^2 patch of skin was resected. Excess fat and connective tissue were scraped off the sample. Skin was incubated in a HBSS solution containing 5 mM EDTA, 10 mM HEPES, and 10% FBS for 30 min at 37°C. Skin was then placed in HBSS media supplemented with 0.7 mg/mL collagenase (Sigma Aldrich) and cut into small pieces with surgical scissors. The tissue was incubated for 30 min at 37°C, vigorously vortexed, and single cells were isolated through a 70 μm filter (Thermo Fisher Scientific). Isolated cells were further purified by density gradient centrifugation on Ficoll (GE Healthcare) prior to further processing.

Flow Cytometry

Single cells from lymph nodes, spleen and skin from mice randomly-selected for euthanasia in all treatment groups were treated with Mouse BD Fc block (BD Pharmigen) for 5 min to reduce nonspecific antibody binding. Cells were incubated with fluorochrome-labeled antibodies at the manufacturer's recommended dilutions for 30 min. Cells were then permeabilized for internal staining with FoxP3/Transcription Factor Staining Buffer Set (eBioscience) for nuclear proteins according to manufacturer's protocols. All antibodies were obtained from BD Pharmigen unless specified otherwise. DC were characterized as CD11c+ (clone REA754; Miltenyi Biotech) and CD45+ (clone 30-F11). Tregs were characterized as CD4+ (clone RM4-5), CD25+ (clone PC61), and FoxP3+ (Internal nuclear, clone FJK-16s) (eBioscience). Bregs were characterized as B220+ (clone RA3-6B2), CD19+ (clone 1D3), CD1d+ (clone 1B1), and CD5+ (clone 53-7.3). Elsewhere, we (20) and others (51–56) have shown that the precursor B-cells to IL-10-producing Bregs as well as >50% of IL-10 actively-producing Bregs lie inside this CD1d+ CD5+ B-cell population. Appropriate fluorochrome and antibody type matched isotypes were used, as well as single stain controls for cytometer compensation. Cytometry was conducted in the BD Influx cell sorter with 50,000 events recorded per sample. The data were analyzed with FlowJo software version 10.7.1. Data presented exclude cellular debris and are displayed as a percentage of target cells within the total intact cell population.

Incidence of Hyperglycemia in Mice *in vivo* and Insulitis Scoring

Female NOD mice were randomly distributed into saline, PLGA-Ni, or Ins-RT-NP treatment groups with an $n = 12$ animals per group. Microparticles or vehicle were administered on Day 0, 3, 7, 14, and 21. Blood glucose was monitored twice a week. An animal was considered diabetic if two consecutive readings, spaced 2 days apart were ≥300 mg/dL. Animals were euthanized within 4 days of diabetes confirmation. Tissues collected from euthanized mice included PLN, MLN, pancreas, and spleen. To assess the grade of insulitis in randomly-selected sections of pancreata from diabetic mice as well as RT-NP recipients who were diabetes-free at 33 weeks of age, we visualized hematoxylin/eosin-stained sections by light microscopy at 10X magnification and assigned scores as follows: 1 = up to 25% of the islet mass infiltrated; 2 = between 25 and 50% of the islet infiltrated; 3 = between 50 and 75% of the islet infiltrated; and 4 = Between 75 and 100% of the islet infiltrated. Scoring was conducted in a blinded manner (i.e., pathologist was not aware of the treatment assigned to the mouse from which the sections of the pancreas were derived).

Statistical Analyses of the Data

Statistical analysis was performed with GraphPad Prism software version 7.0c. Student's *t*-tests, ANOVA, and Kruskal-Wallis tests were performed as appropriate to compare the statistical relevance of differences in outcomes between and among treatment groups. A *p*-value of ≤0.05 was considered significant. Survival curves (Log-Rank test, Mantel-Cox) were analyzed for significance between two treatments at a time, where a $p < 0.0167$

was deemed significant (Bonferroni correction for three groups). Graphs are displayed as mean and standard deviation. A Dixon q test was performed to remove any data point outliers.

RESULTS

TGFβ1 and Human Insulin B9-23 Peptide Bind Efficiently to PLGA-Ni Microparticles

The ability of PGLA-Ni microparticles to adsorb His-tagged proteins was confirmed by fluorescent microscopy. **Figure 1A** shows His-tagged GFP conjugated PLGA-Ni microparticles. PLGA-Ni microparticles were also imaged in scanning electron microscopy where they exhibited spherical morphology (**Figure 1B**), and self-association when formulated as His-tagged TGFβ1 microparticles (**Figure 1C**). In the absence of TGFβ1, the particles are found in the micron size range with a hydrodynamic diameter (D_h) of 867.5 ± 41.6 nm (PDI = 0.18; **Figure 1D**). Adding TGFβ1 to the particles increased the D_h to 1,088.6 ± 15.6 nm (PDI = 0.15). The kinetics of RA release was subsequently characterized *in vitro*. RA was found to release gradually from PLGA-Ni microparticles at 37°C in PBS with an average release rate of 1 μg/day from 10 mg of microparticles over 10 days *in vitro,* resulting in a total release of approximately 15 μg by day 18 at 37°C. This represents 31% of the total RA contained in 10 mg of microparticles (**Figure 2A**). PLGA-Ni microparticles incubated with His-tagged GFP (as a protein surrogate for TGFβ1) showed a more rapid and complete release of GFP (**Figure 2B**). This is indicative of the His-tag more readily detaching from the Ni ion compared to RA released from the intact or deformulating particle. GFP concentration was maintained at 150 ng/mL, yielding a concentration above the anticipated physiologically-active concentration of TGFβ1 (57). Additional preparations of PLGA-Ni microparticles were incubated with His-tagged TGFβ1 (a 17.3 kDa non-glycosylated fragment fused to a 4.5 kDa amino terminal hexa-histidine tag) and subsequently eluted. **Figure 2C** shows a representative result following SDS-PAGE of eluates *in vitro* from the TGFβ1-formulated microparticles indicating that upon elution, the TGFβ1 protein exists predominately as dimers and monomers, with some higher order oligomers.

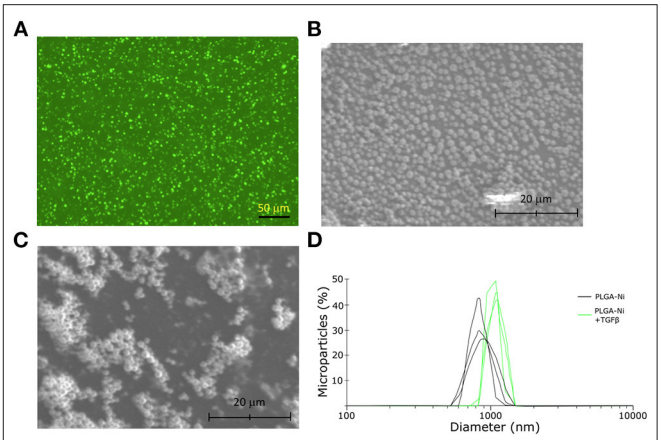

FIGURE 1 | Physical characteristics of the PLGA-Ni microparticles. **(A)** Fluorescence microscopy image of His-tagged GFP admixed with PLGA-Ni microparticle suspensions. Autofluorescence has been subtracted from the image. Scanning electron microscopy images of PLGA-Ni without **(B)** and with **(C)** adsorbed TGFβ1. **(D)** A histogram of hydrodynamic microparticle size of PLGA-Ni alone or with His-tagged TGFβ1, reveals hydrodynamic diameters (D_h) of 867.5 ± 41.6 nm (PDI = 0.18) and 1,088.6 ± 15.6 nm (PDI = 0.15), respectively.

DC Take up PLGA-Ni Particles *in vitro* as Well as *in vivo*, Following Subcutaneous Administration

We first sought to confirm that the PLGA-Ni backbone would be taken up by DC *in vitro*. CD45+ CD11c+ DC were identified by flow cytometry (**Supplementary Figure 1**) in freshly-obtained splenocytes after a 18 h exposure to PLGA-Ni or PLGA-Red microparticles. In **Figures 3A–C** we show that Nile Red dye was detected in up to 85% of CD45+ CD11c+ DC incubated with PLGA-Red microparticles, with little detection in cell unexposed to the PLGA-Red microparticles or cells incubated with PLGA-Ni microparticles that were not formulated with Nile Red. We then sought to determine the uptake of PLGA-Red by DC in the skin following subcutaneous (s.c.) injection into 8–10 week-old female NOD mice. In **Figure 3D**, we show substantial accumulation (>88%) of PLGA-Red microparticles in CD45+ CD11c+ DC recovered from a 1 × 1 cm^2 of abdominal skin (that contains the dermal and subdermal tissue; anatomic site known to facilitate the accumulation of exogenously-administered DC and microparticles inside the PLN (20, 21, 58–61) 18 h following the injection of PLGA-Red. Any fluorescence detected in CD45+ CD11c+ cells from vehicle-treated animals represents the expected autofluorescence of DC.

Insulin B9-23 Peptide-Decorated RT-NP Treatment Prevents the Onset of Diabetes When Administered Into Early Mid-stage Insulitic NOD Mice

Having confirmed that PLGA-Ni delivery resulted in substantial accumulation inside DC, with the expectation that these DC would be converted into tolerogenic cells using RA and TGFβ1-formulated microparticles, we then sought to determine if a PLGA-Ni formulation of RA and TGFβ1 additionally-engineered with adsorbed insulin peptide B9-23 (Ins-RT-NP) could alter the progression of the underlying autoimmunity in NOD female mice toward overt diabetic hyperglycemia. In **Figure 4A**, we show the timeline of microparticle injections, where each of the mice were administered five s.c. injections of either vehicle saline, PLGA-Ni, or Ins-RT-NP starting at 11 weeks of age. This is an age where insulitis is evident inside the pancreas of NOD mice. Prior to randomization into the treatment arms, NOD female mice between 9 and 11 weeks of age were pre-screened to insure absence of hyperglycemia. Fasting blood glucose, immediately prior to treatment, did not exceed 131 mg/dL (**Figure 4B**). In **Figure 4C**, we show that Ins-RT-NP administration beginning at 11 weeks of age when substantial insulitis is known to exist, prevented the onset of hyperglycemia

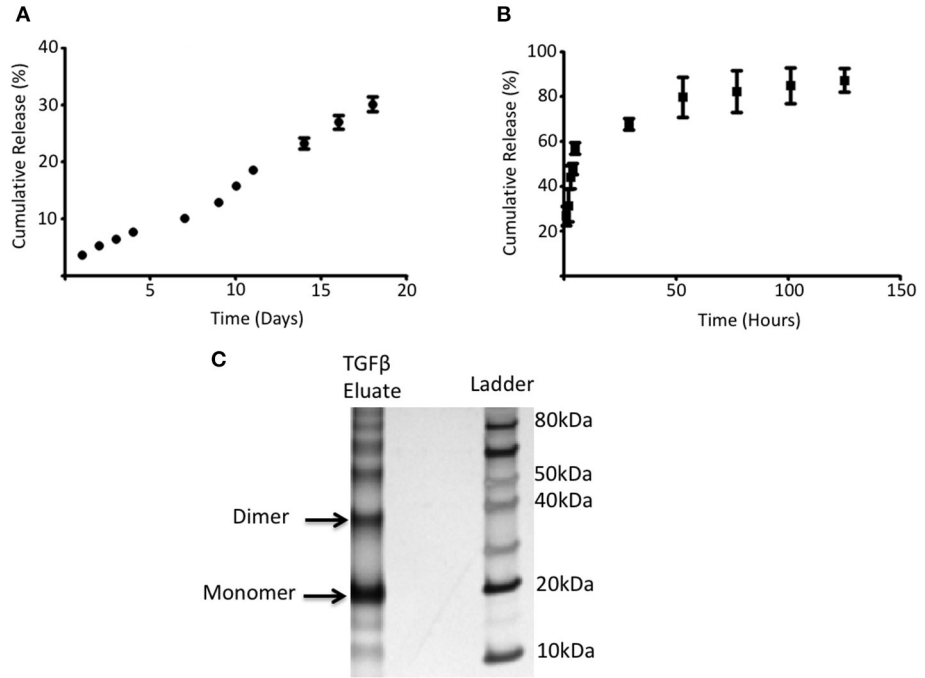

FIGURE 2 | RA and adsorbed protein release from PLGA-Ni microparticles. **(A)** The rate of RA release was determined by UV absorption and shown as cumulative release (% of starting amount) over time. **(B)** 5 mg of PLGA-Ni particles with adsorbed His-tagged GFP was incubated in pH 8 Tris buffer at 37°C for 5 days. Free His-tagged GFP was measured with a fluorescent spectrometer ($\lambda = 508$ nm) at the indicated time points and the amount of free protein is shown as cumulative release (% of starting amount) over time. **(C)** Eluate from TGFβ1-adsorbed PLGA-Ni microparticles contains monomers, dimers, and higher order multimers of TGFβ1.

in a significant proportion of recipients compared to mice treated with microparticles that were devoid of RA, TGFβ1 and insulin B9-23 peptide, or mice treated with vehicle alone. It is noteworthy that the diabetes-free state was maintained for a substantial amount of time (33 week-old mice; 22 weeks diabetes-free following treatment) without additional injections of the microparticles. Insulitis grade was significantly-lower in pancreas sections of 33 week-old diabetes-free RT-NP recipients compared to all the diabetic mice in the control arms (**Figures 4D,E**).

Increased Frequency of Bregs but Not Foxp3+ Tregs in Ins-RT-NP-Treated NOD Mice

Data by others indicate that nanoparticle formulations of RA and TGFβ can convert T-cells into Tregs (37), and when administered (nanoparticles or hydrogels) into NOD female mice, they foster an increase in the number of Foxp3+ Tregs inside the PLN and/or the pancreata of diabetes-free mice (58, 59, 62, 63). Since there were no surviving mice in the control treatment arms at 22 weeks following test article administration, it proved challenging for us to interpret the differences in Tregs in PLN and MLN obtained from vehicle or PLGA-Ni-treated mice to those in the diabetes-free Ins-RT-NP recipients. Therefore, to ensure matched populations and matched times at which PLN and MLN were collected in order to obtain interpretable data, we used an acute model of test article administration. For this, 11 week-old NOD mice in all treatment arms ($n = 7$–9) were euthanized 1 or 3 days following microparticle or vehicle administration. We then measured regulatory immune cell population numbers by flow cytometry (**Supplementary Figures 2**, **3**) in PLN and MLN from these mice. Much to our surprise, and in contrast to our expectations, the frequency of Foxp3+ Tregs inside the PLN among all treatment groups was not different (**Figure 5**). There was a surprising lower, albeit statistically-not significant, Treg content in the MLN of mice treated with Ins-RT-NP compared to the controls (**Figure 6**). Considering the possibility that the viability of the cells inside the pancreatic and/or mesenteric lymph nodes could be affected by microparticles drained into the tissue (PLN and/or MLN), we measured the viability of single cells from dispersed lymph node tissue. We did not see any significant differences in viability of single cells from PLN and MLN of diabetes-free mice (**Supplementary Figure 4**). We then looked for possible differences in Breg frequency. Although we could not discern any differences inside the PLN of mice among the three treatment arms (**Figure 5**), we confirmed a small but statistically-relevant difference inside the MLN of mice treated with the Ins-RT-NP (**Figure 6**) at 3 days following administration. The ratio of Tregs to Bregs in PLN at 1 or 3 days following test article administration was statistically-indistinguishable among the treatment arms (**Figure 5**). In the MLN, however, the ratio was statistically-different in the Ins-RT-NP-treatment arm at 3 days post-administration compared to the other treatments (**Figure 6**).

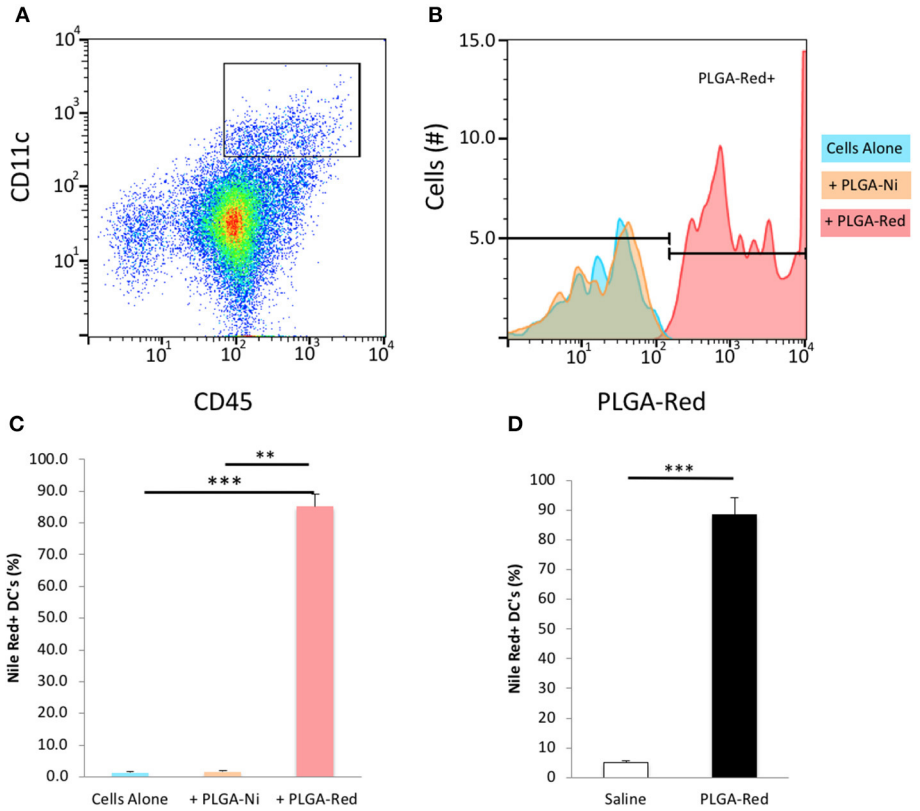

FIGURE 3 | Microparticle uptake by DC *in vitro* and *in vivo*. Single cell suspensions of freshly isolated splenocytes were incubated with PLGA-Ni, PLGA-Red, or saline vehicle *in vitro* for 18 h. **(A)** Flow cytometry-identified CD45+ CD11c+ splenic DC were evaluated **(B)** for PLGA-Red microparticle uptake with PE fluorochrome settings. Saline (blue) and PLGA-Ni (orange) treatment populations showed similar PE signal indicating PLGA-Ni alone had low-to-no autofluorescence. PLGA-Red (red) treated DC showed PE signal which when quantified **(C)** displayed a 85% uptake of microparticles ($n = 10$ wells). PLGA-Red uptake was significant compared to the other treatment groups (Kruskal-Wallis test) with p-values of 0.0001 (saline vs. PLGA-Red) and 0.0026 (PLGA-Ni vs. PLGA-Red). PLGA-Red particles alone did not exhibit signal in DC marker fluorochrome channels (data not shown). **(D)** PLGA-Red microparticles were administered subcutaneously in mice and DC were isolated from a 1 cm^2 patch of skin 18 h later. DC from the skin patch of PLGA-Red treated animals exhibited a 88.5% uptake of microparticles ($n = 5$ mice, Student t-test $p = 0.0001$). Experiments were performed twice in mice from separate NOD cohorts. Statistical significance is designated with ** if $p < 0.01$ and *** if $p = 0.0001$.

DISCUSSION

Although insulin therapy can adequately manage the day-to-day glucose control in T1D, the lifestyle changes, the considerable risk of insulin-induced hypoglycemia, and the progression of many T1D patients to cardiovascular, renal, neural, and ophthalmic complications, indicate that pharamcologic insulin is not a cure. The once widely-held dogma that insulin-requiring patients were devoid of a substantial mass of beta cells inside the pancreas due to autoimmune destruction, has now yielded to a more balanced view. Based on accumulating evidence, a respectable mass of beta cells remains in T1D patients whose disease duration can be long-standing (64–69) that is functionally-impaired, although potentially "re-activatable" if the underlying autoimmunity as well as non-autoimmune pancreas-selective innate inflammation can be attenuated. A number of approaches have been implemented over the past decade to depress the underlying autoimmunity including single or combination agents from the categories of pharmacologic immunosuppressives, cytokine neutralizing antibodies, lymphocyte depletion, and T1D autoantigens (70–80). Where animal studies demonstrated sufficient efficacy, when implemented as clinical trials, each of the referenced approaches could not achieve long-term insulin independence (70–72). In fact, systemic as well as parenteral administration of most of these agents resulted in significant toxicity and adverse effects.

Micro/nanoparticle-based delivery of immunomodulatory agents, with or without autoantigen co-delivery to treat autoimmune disease, offers many attractive advantages over systemic immunomodulators. Site-specific delivery minimizes off-target effects, licenses leukocytes that can be "reprogrammed" to build regulatory leukocyte networks that can become antigen-specific, even in the absence of exogenous supply of autoantigen(s). We have demonstrated the latter using a specific abdominal site in mice and non-human primates, whose epidermal space is served by lymphatic drainage that accumulates or transits, in part, inside the PLN (18, 21). Taking advantage of this intriguing anatomical feature, we demonstrated that autoantigen-free microsphere formulations of antisense DNA targeting the primary transcripts of CD40, CD80, and CD86,

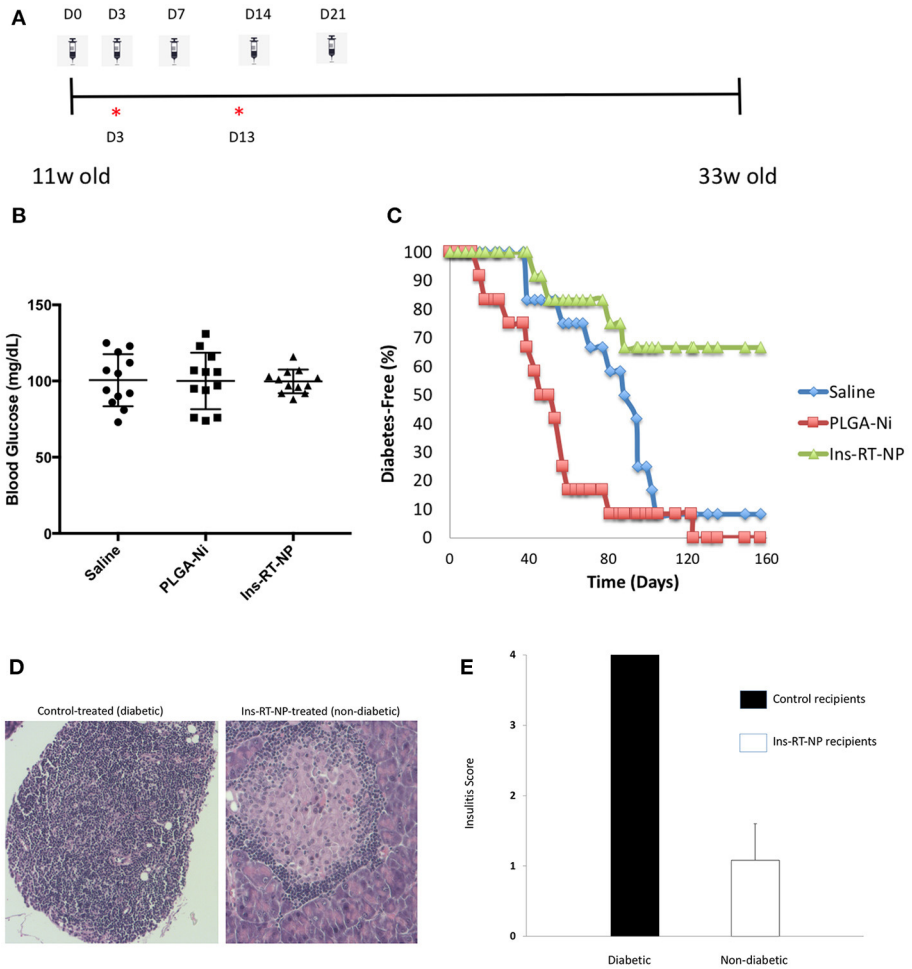

FIGURE 4 | Prevention of diabetes onset following Ins-RT-NP administration. Non-diabetic female NOD mice at 11 weeks of age were randomly assigned to three treatment groups ($n = 12$ per group). Each mouse received five subcutaneous abdominal injections of saline vehicle, 10 mg of PLGA-Ni in solution, or 10 mg of Ins-RT-NP in solution as shown in the dosing schedule timeline **(A)**. The timeline also shows the tissue harvest time points ("*") from an additional cohort of animals ("*acute study cohort*"; **Figure 5**). **(B)** No significant difference was observed in the starting blood glucose values (prior to microparticle injection; $p = 0.981$, Kruskal-Wallis test). **(C)** Mice were assessed for diabetes status by measuring tail vein blood glucose, where two consecutive readings over 300 mg/dL indicated diabetes onset. Shown in the graph are the survival curves representing diabetes-free mice. Diabetes incidence in Ins-RT-NP-treated mice was significantly lower when compared to saline ($p = 0.0119$) and PLGA-Ni ($p = 0.0001$) treatment. A log-rank test (Mantel-Cox) confirms significance in the differences among the treatment groups ($p < 0.0167$; $p < 0.05$ Bonferonni-corrected for three groups). **(D)** Insulitis grade was significantly-lower in pancreas sections of 33 week-old diabetes-free RT-NP recipients compared to all the diabetic mice in the control arms. Shown are images at 10X magnification representative of >5 islets/field visualized per treatment arm. **(E)** Summary of insulitis scores between all diabetic mice and the Ins-RT-NP recipients who were diabetes-free at 33 weeks of age.

preferentially accumulated inside PLN, generated Foxp3+ Tregs therein, and in NOD mice, prevented the progression of late-stage dysglycemia to overt clinical diabetes and also achieved reversal of new-onset hyperglycemia and long-term stability of a normoglycemic state (18, 21).

Our technology (18, 21) was developed to exploit the phagocytic nature of epidermis-residing as well as migratory DC to take up exogenously-administered particles loaded with molecules that are able to direct them toward a functionally-tolerogenic state *in vivo*. Since then, other groups have developed conceptually similar architecture with different approaches to stabilize functional tolerance in DC (40, 58, 59, 81–92). These approaches have resulted in successful treatment of autoimmune disease in animal models of T1D (58, 59) and multiple sclerosis (81–83, 85). As we continue to decipher the mechanisms that our earlier-reported microspheres use to confer tolerogenic functional properties to DC beyond the knockdown of the primary transcripts of CD40, CD80, and CD86, we have uncovered the involvement of RA (19). The combination of the DNA antisense oligonucleotides stimulates the production of RA by DC in a manner that involves cell-intrinsic retinaldehyde dehydrogenase 1 (RALDH1) (19).

The combination of RA and TGFβ1 is critical in peripheral generation of immunosuppressive T-cells characterized by the expression of the Foxp3 transcription factor (Foxp3+ Tregs) (93–98). Tregs prevent emergence of autoimmune disease (99,

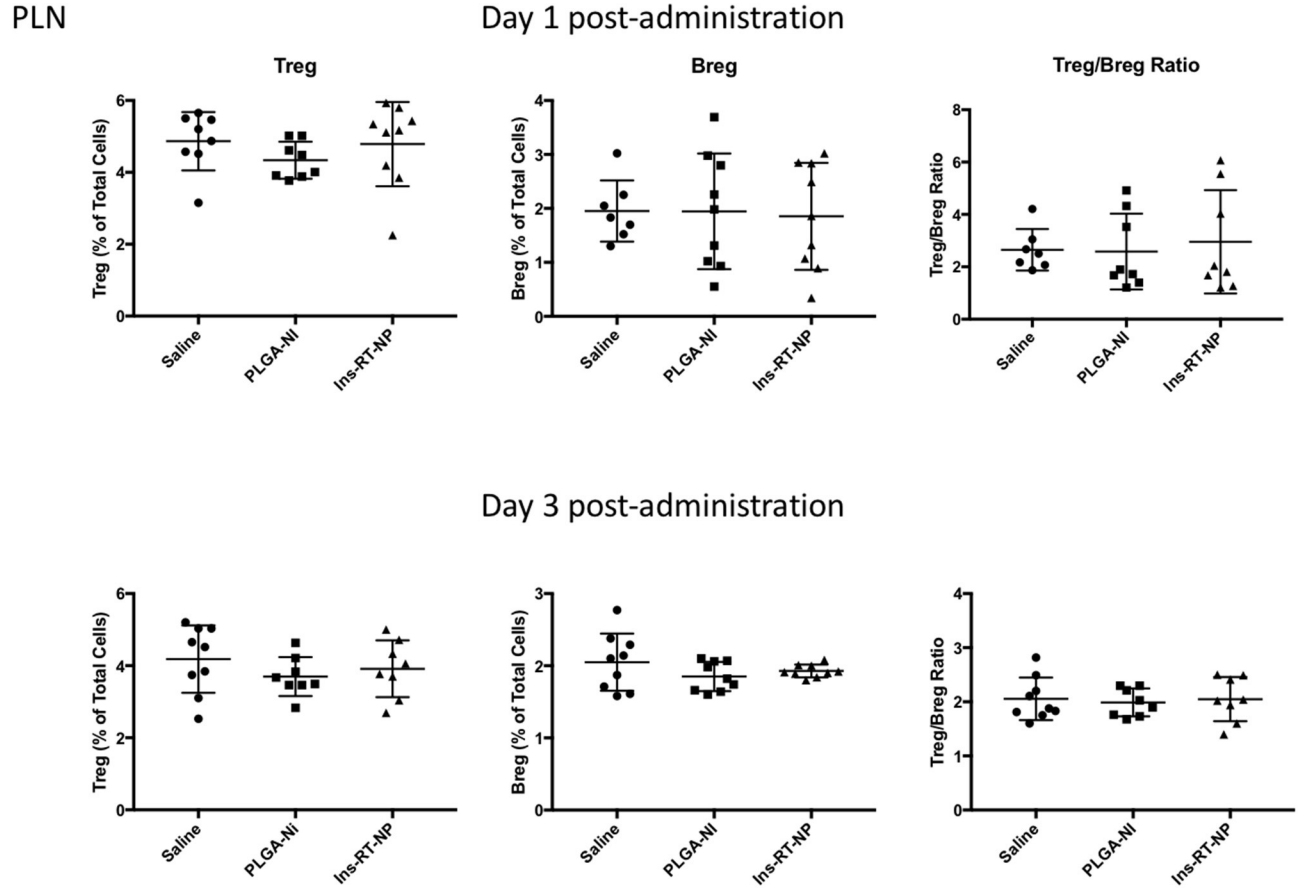

FIGURE 5 | Changes in the frequency of regulatory lymphocyte cell populations inside the PLN of NOD mice following acute microparticle administration. Animals from the acute study cohort (See timeline in **Figure 4A**) were euthanized at 1 or 3 days following test article administration. Single cell suspensions from resected PLN were then assessed by flow cytometry for Treg and Breg frequency. There were no discernible differences in the Treg or Breg frequency in the PLN among the mice of the three treatment arms at 1 or 3 days following microparticle administration. Similarly the ratios between Treg and Breg cells were unaltered. Data are combined from the outcomes in two independent animal cohorts examined at different times in the study ($n = 7$–9 per arm).

100). Subsets of Foxp3+ Tregs are found in mice and humans: natural Treg and induced Treg (iTreg) (101, 102). In the periphery, iTreg differentiate from naive T-cells under sub-immunogenic conditions of antigen presentation and in the presence of RA and TGFβ (103). That RA is a cofactor in the generation of iTregs stems from *in vitro* findings that mesenteric lymph node and lamina propria DC potently induced iTreg differentiation in the presence of TGFβ (98, 104, 105). Addition of RA to co-cultures with splenic DC and TGFβ enhances iTreg induction (94, 98, 105). Exogenous RA sustains iTreg generation in conditions that typically oppose it, such as presence of inflammatory cytokines (IL-6, IL-21) and high co-stimulatory environments (34, 94, 98). These observations made for a very compelling case to combine RA with TGFβ1 with a T1D-relevant autoantigen in a microparticle formulation. One could argue that non-formulated RA and TGFβ1 co-administered could achieve similar if not identical outcomes thereby questioning the need to engineer micro-/nanoparticle formulations of the agents. To our knowledge, and also in our experience, administration of RA or TGFβ1 alone or together as an injectable suspension cannot prevent T1D (unpublished observations) even though iTreg frequency is increased inside the site of the injection in the skin but not the draining lymph nodes. Also, the iTregs are not functionally-stable in suppression assays (unpublished observations). As the studies reported herein were underway, a number of supportive findings were published using particle designs different from ours. Keselowsky et al., using a mixture of two separate microparticle populations (population 1 consisting of TGFβ or IL-10 and population 2 consisting of either rapamaycin or RA), conferred a tolerogenic-reminiscent phenotype in DC *in vitro* (40). They also developed a more complex variation where one of the microparticle populations contained either GM-CSF or TGFβ and the other contained vitamin D3 and denatured insulin, to prevent progression of early-stage autoimmunity to diabetic hyperglycemia and to reverse, to some degree, new-onset hyperglycemia (59). This approach resulted in protective outcomes similar to those achieved by Miller et al. in mouse models of multiple sclerosis (81, 83, 85). Mechanistically, the involvement of DC as mediators of a tolerogenic state, mainly via the increase in Treg

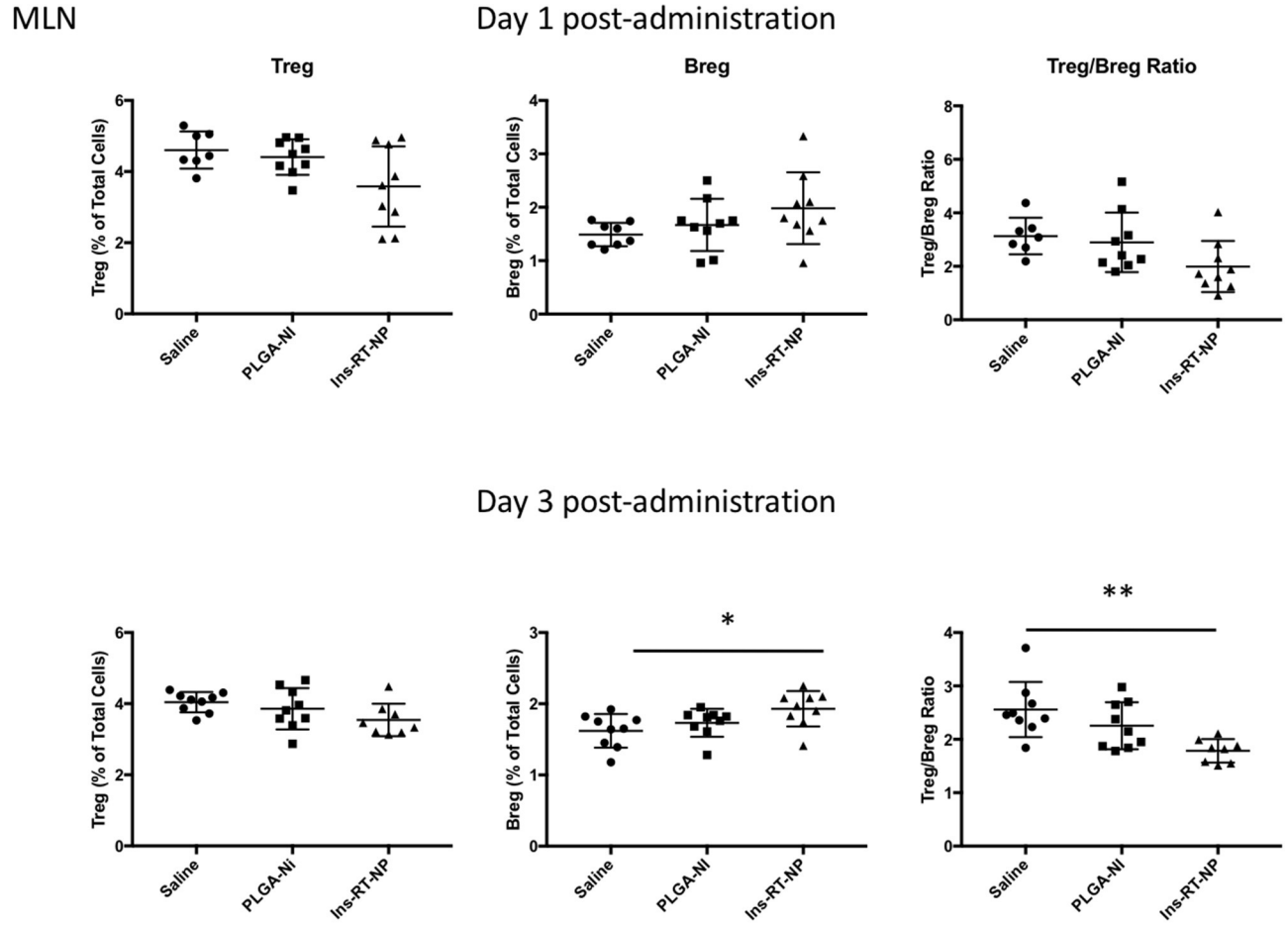

FIGURE 6 | Changes in the frequency of regulatory lymphocyte cell populations inside the MLN of NOD mice following acute microparticle administration. Animals from the acute study cohort (See timeline in **Figure 4A**) were euthanized at 1 or 3 days following test article administration. Single cell suspensions from resected MLN were then assessed by flow cytometry for Treg and Breg frequency. A non-significant downward trend is seen in Treg frequency in MLN of mice treated with Ins-RT-NP vs. saline. Breg frequency exhibited an upward trend in mice treated with Ins-RT-NP, becoming statistically-significant significant compared to control test articles by the time of the third injection ($n = 9$, ANOVA $p = 0.0262$). Tukey's multiple comparisons determined $p = 0.0215$ between the saline and Ins-RT-NP treatment group. The Treg/Breg ratio was similarly significantly-different with the three-injection treatment (ANOVA $p = 0.0035$, post test $p = 0.0025$ for saline vs. Ins-RT-NP). Statistical significance is displayed as * for $p < 0.05$ and ** for $p < 0.01$ as assessed by ANOVA. Data are combined from the outcomes in two independent animal cohorts examined at different times in the study.

numbers, was a shared feature of these approaches (59, 81, 83, 85).

In addition to the increase in the frequency of Tregs, we have shown that one mechanism by which RA participates in the induction of immune hyporesponsiveness is through the differentiation of B-lymphocytes into IL-10+ Bregs as well as the proliferation of existing Bregs (19, 20). Although initial studies indicated that suppression ability was specific for IL-10+ CD1d+ CD5+ B-cells, it was later discovered that the progenitors of as well as the majority of IL-10-producing Bregs resided inside CD1d+ CD5+ population and that additionally, IL-10 expression was not a condition sine qua non for CD1d+ CD5+ B-cell suppressive ability (51–56). To date, none of the previous studies in the delivery of potentially-tolerogenic micro/nanoparticles into animal models of autoimmunity have studied their effects on Bregs as possible unique or Treg-overlapping cellular mediators of the action of the micro/nanoparticles. Our report here is the first to demonstrate the possible involvement of Bregs in the absence of increases in Treg frequency in NOD mice acutely-treated with single microparticle-formulated RA, TGFβ1 and insulin autoantigen peptide. What is, at the moment, unclear, is why Bregs are elevated inside the MLN when compared to the PLN (**Figures 5**, **6**). Although NOD mice treated with Ins-RT-NP exhibit Foxp3 positivity at 22 weeks from the time of the last microparticle injection (data not shown), in the absence of age-matched diabetes-free and age-matched new-onset diabetic mice treated with the control test articles, it is currently not known if the frequency of Tregs or Bregs changes longitudinally resulting in a greater population of these cells inside the PLN and/or the MLN of Ins-RT-NP-treated mice. If so, the observations we present following acute administration

will not reflect a mechanistically-interpretable outcome, when measured longitudinally. These studies are currently underway with large animal cohorts to capture age-matched diabetic and non-diabetic control microparticle recipients. Nevertheless, the microparticle formulation, when delivered into NOD mice is protective against the progression of mid-stage autoimmunity to overt clinical hyperglycemia.

Our Ins-RT-NP delivery system has several advantages over the other reported approaches, referenced above. First is in the design complexity. Our system consists of a *single* formulation that brings together only two bioactive agents (RA and TGFβ1) with the addition of a unique T1D-relevant autoantigen. Second, from a biologic aspect, DC need acquire only one population of particles without the potential of competition for uptake and/or selectivity in action imposed by a second population. Third, from a potential future regulatory aspect, a single population of easily-characterizable particles that are manufactured to predictable physicochemical properties facilitates a target product profile that would be human-specific compared to more complex microparticle chemistry and the requirement for more than one particle population. Finally, only a short course of microsphere treatment (five injections) was required to achieve a long-term diabetes-free state (**Figure 4**). It is possible that even fewer injections could achieve comparable outcomes, something that is under investigation currently. This suggests that, even if the induced Bregs are the only layer of autoimmunity regulation, their effect is potentially long lasting (e.g., due to a longitudinal expansion and/or a long half-life of these Bregs *in vivo*). Although this does not rule out the possibility that other regulatory cell changes occur in different organs or time points of the treatment progression.

Recently, an orally-delivered formulation of TGFβ and RA was reported to result in decreased potentially-autoreactive effector T-cells inside the pancreas of mice rendered diabetic by multiple low-dose streptozotocin (MLDS) (106). The reported data suggest suppressed insulitis and a statistically-greater proportion of diabetes-free mice in the RA/TGFβ microparticle treatment arm compared to controls. The conceptual novelty and achievement of an orally-available microparticle formulation is very noteworthy and certainly commendable, however, the findings raise some important questions that need to be addressed. First is the model. All studies, including ours, using micro/nanoparticle approaches to treat T1D, use the NOD/LtJ strain mouse strain, widely regarded as the best *in vivo* test system for T1D immunotherapeutics, so long as one is aware of the model's limitations (72, 107–110). The authors, instead used a model (MLDS in C57BL/6 mice) that does not reflect the genetic component as well as the chronic development of an underlying autoimmune state. Second, diabetes incidence was only monitored up to 28 days following the MLDS treatment. In our view, this time frame is insufficient to draw any conclusions about the stability of any efficacy. Third, most of the measured differences in the frequency of leukocyte populations recovered from mice in the different treatment arms in that report are not readily discernible. The differences appear to be quite small. Nevertheless, that report can be considered a first in terms of demonstrating proof-in-concept, at least in terms of oral delivery of a potentially-tolerogenic microparticle system that has a broad impact on treating autoimmunity.

Our findings support the ongoing trajectory to develop TGFβ/RA-based tolerogenic micro/nanoparticle "vaccines" for the treatment of T1D (38–40, 58, 81). The strengths of our system and approach include a simple one-population microparticle with the efficacy to prevent the progression of mid-stage autoimmunity characterized by fulminant insulitis to overt diabetic hyperglycemia achieved by only five s.c. injections of an amount of particles that would translate to a well-tolerated human-relevant target product profile. Furthermore, we have achieved long term stability of the normoglycemic state (33 weeks) that may in part be due to the regulation of the progressive autoimmunty via Bregs, at least in the MLN, even though the increase in Bregs we present herein (**Figure 6**) was an acute response specifically to the Ins-RT-NP. It remains to be determined if Breg frequency in diabetes-free mice remains increased in Ins-RT-NP compared to age-matched diabetic control mice (untreated and control test article-treated recipients). The differences in the Treg:Breg ratio we observe in the MLN among the treatment arms at 3 days post-administration of the Ins-RT-NP are intriguing and remain to be mechanistically-understood. It is possible that our particles act by modifying the biology of other T-cells by a number of overlapping and complementary mechanisms of action. For example, DC that take up these particles could modify the numbers and/or action of Tr1 regulatory T-cells and not Foxp3+ Tregs. Or, the surface-bound TGFβ1 on our particles could bind to TGF receptors on DC and /or other regulatory leukocytes to license their suppressive abilities that are expressed only inside secondary lymphoid organs. These possibilities, among a number of others, are currently under investigation so that we can better understand the mechanism of action of our particle system.

Whether provision of other, or additional T1D autoantigens to the TGFβ/RA-based formulation can improve the prophylactic outcomes or could reverse new-onset hyperglycemia is currently unknown, although many other particle formulations tested appear to require at least one autoantigen peptide or intact protein to induce some form of disease-specific immune hyporesponsiveness (40, 58, 59, 81–92).

DATA AVAILABILITY STATEMENT

The original contributions presented in the study are included in the article/**Supplementary Material**, further inquiries can be directed to the corresponding author/s.

ETHICS STATEMENT

The animal study was reviewed and approved by AHN IACUC; Allegheny Health Network IACUC.

AUTHOR CONTRIBUTIONS

BP, CE, and YG administered the microparticles into the mice, collected the tissues and organs, conducted the

immunophenotyping, conducted the statistical analyses, and wrote the initial version of the manuscript. WM, YW, and WL manufactured the microparticle formulations and characterized those formulations, wrote the sections in the materials and methods part of the manuscript that describe the manufacture and characterization of the particles, and verified the statistical analyses. RL and BP conducted the flow cytometry and analysis of the outcomes and participated in the statistical analysis of those data. MT and NG edited the manuscript from the first draft onwards, discussed the findings and the significance with the co-authors, and verified the statistical outcomes. NG as principal investigator of the study was responsible for the oversight of the study at all levels and ensured that the outcomes were reproducible, that the experiments were rigorously conducted, and that the data presented in this manuscript reflect the raw data obtained faithfully.

FUNDING

This work was partially funded by research support in the form of a peer-reviewed research grant provided by the JDRF (SRA-2016-318-S-B).

SUPPLEMENTARY MATERIAL

The Supplementary Material for this article can be found online at: https://www.frontiersin.org/articles/10.3389/fimmu.2021.586220/full#supplementary-material

Supplementary Figure 1 | Dendritic cell antibody isotypes and controls used in flow cytometry. Single cell suspensions of splenocytes were isolated and grown *in vitro*. Splenocytes were analyzed by flow cytometry to identify dendritic cells using the CD45 and CD11c cell surface markers 18 h later. Fluorescence histograms of unstained cells are shown in red and cells stained with matched fluorochrome-conjugated isotypes are shown in blue. Cells with antibody against **(A)** CD45 or **(B)** CD11c are shown in orange. A signal intensity cut off is shown which displays positively stained cells to the right. **(C)** Signal intensity is shown in both CD45 and CD11c channels, with CD45+ CD11c+ cells located inside the box.

Supplementary Figure 2 | Antibody controls and gating method in Treg flow cytometry. Single cell suspensions of lymph nodes were analyzed by flow cytometry to identify Tregs by cell surface markers CD4, CD25, and nuclear marker FoxP3. Histograms of control unstained cells are shown in red and cells stained with matched fluorochrome-conjugated isotypes are shown in blue. Cells with antibody against **(A)** CD4, **(B)** CD25, **(C)** FoxP3 are shown in orange. A signal intensity cut off is shown which displays positively stained cells to the right. **(D)** The gating method for identifying Foxp3+ Tregs is shown. First, cells are selected for low granularity based on low side scatter. Within this population, CD4+ cells are selected as a general T-cell population. Finally, within the CD4+ cell population, cells that are CD25+ FoxP3+ are selected for further analysis and quantitation.

Supplementary Figure 3 | Breg antibody controls and gating method in Breg flow cytometry. Single cell suspensions of lymph nodes were analyzed by flow cytometry to identify Bregs by cell surface markers CD19, B220, CD1d, and CD5. Histograms of control unstained cells are shown in red and cells stained with matched fluorochrome-conjugated isotypes are shown in blue. Cells with antibody against **(A)** CD19, **(B)** B220, **(C)** CD1d, and **(D)** CD5 are shown in orange. A signal intensity cut off is shown which displays positively stained cells to the right. **(E)** The gating method for identifying Bregs is shown. First, cells are selected for low granularity as indicated by low side scatter. Within this population, the prevalent CD19+ B220+ double positive B-cells are selected. Finally, within this B cell population, cells that are CD1d+ CD5+ are selected as shown for further analysis.

Supplementary Figure 4 | Lymph node (LN) cell viability. Animals received a single injection of saline, 10 mg PLGA-Ni, or 10 mg Ins-RT-NP. Single cell suspensions were made from MLN and PLN. Cell viability was assessed after LN dissociation by Trypan Blue staining. The percentage of viable cells is displayed and no significant differences in viability were detected (individual one-way ANOVA per LN type). Experiments include two separate animal cohorts combined ($n = 9$).

REFERENCES

1. Insel RA, Dunne JL, Atkinson MA, Chiang JL, Dabelea D, Gottlieb PA, et al. Staging presymptomatic type 1 diabetes: a scientific statement of JDRF, the Endocrine Society, and the American Diabetes Association. *Diabetes Care.* (2015) 38:1964–74. doi: 10.2337/dc15-1419
2. Atkinson MA, Eisenbarth GS, Michels AW. Type 1 diabetes. *Lancet.* (2014) 383:69–82. doi: 10.1016/S0140-6736(13)60591-7
3. Atkinson MA. The pathogenesis and natural history of type 1 diabetes. *Cold Spring Harb Perspect Med.* (2012) 2. doi: 10.1101/cshperspect.a007641
4. Roep BO, Atkinson M, von Herrath M. Satisfaction (not) guaranteed: re-evaluating the use of animal models of type 1 diabetes. *Nat Rev Immunol.* (2004) 4:989–97. doi: 10.1038/nri1502
5. Emamaullee JA, Davis J, Merani S, Toso C, Elliott JF, Thiesen A, et al. Inhibition of Th17 cells regulates autoimmune diabetes in NOD mice. *Diabetes.* (2009) 58:1302–11. doi: 10.2337/db08-1113
6. Ferraro A, Socci C, Stabilini A, Valle A, Monti P, Piemonti L, et al. Expansion of Th17 cells and functional defects in T regulatory cells are key features of the pancreatic lymph nodes in patients with type 1 diabetes. *Diabetes.* (2011) 60:2903–13. doi: 10.2337/db11-0090
7. Jain R, Tartar DM, Gregg RK, Divekar RD, Bell JJ, Lee HH, et al. Innocuous IFNgamma induced by adjuvant-free antigen restores normoglycemia in NOD mice through inhibition of IL-17 production. *J Exp Med.* (2008) 205:207–18. doi: 10.1084/jem.20071878
8. Wang B, Andre I, Gonzalez A, Katz JD, Aguet M, Benoist C, et al. Interferon-gamma impacts at multiple points during the progression of autoimmune diabetes. *Proc Natl Acad Sci USA.* (1997) 94:13844–9. doi: 10.1073/pnas.94.25.13844
9. Sakaguchi S, Ono M, Setoguchi R, Yagi H, Hori S, Fehervari Z, et al. Foxp3+ CD25+ CD4+ natural regulatory T cells in dominant self-tolerance and autoimmune disease. *Immunol Rev.* (2006) 212:8–27. doi: 10.1111/j.0105-2896.2006.00427.x
10. Miska J, Abdulreda MH, Devarajan P, Lui JB, Suzuki J, Pileggi A, et al. Real-time immune cell interactions in target tissue during autoimmune-induced damage and graft tolerance. *J Exp Med.* (2014) 211:441–56. doi: 10.1084/jem.20130785
11. Salvany-Celades M, van der Zwan A, Benner M, Setrajcic-Dragos V, Bougleux Gomes HA, Iyer V, et al. Three types of functional regulatory T cells control T cell responses at the human maternal-fetal interface. *Cell Rep.* (2019) 27:2537–47 e5. doi: 10.1016/j.celrep.2019.04.109
12. Wu J, Ma S, Hotz-Wagenblatt A, Angel P, Mohr K, Schlimbach T, et al. Regulatory T cells sense effector T-cell activation through synchronized JunB expression. *FEBS Lett.* (2019) 593:1020–9. doi: 10.1002/1873-3468.13393
13. Golab K, Krzystyniak A, Marek-Trzonkowska N, Misawa R, Wang LJ, Wang X, et al. Impact of culture medium on CD4(+) CD25(high)CD127(lo/neg) Treg expansion for the purpose of clinical application. *Int Immunopharmacol.* (2013) 16:358–63. doi: 10.1016/j.intimp.2013.02.016
14. Marek-Trzonkowska N, Mysliwec M, Siebert J, Trzonkowski P. Clinical application of regulatory T cells in type 1 diabetes. *Pediatr Diabetes.* (2013) 15:322–32. doi: 10.1111/pedi.12029
15. Thompson JA, Perry D, Brusko TM. Autologous regulatory T cells for the treatment of type 1 diabetes. *Curr Diab Rep.* (2012) 12:623–32. doi: 10.1007/s11892-012-0304-5

16. Bluestone JA, Buckner JH, Fitch M, Gitelman SE, Gupta S, Hellerstein MK, et al. Type 1 diabetes immunotherapy using polyclonal regulatory T cells. *Sci Transl Med.* (2015) 7:315ra189. doi: 10.1126/scitranslmed.aad4134
17. Marek-Trzonkowska N, Mysliwiec M, Dobyszuk A, Grabowska M, Derkowska I, Juscinska J, et al. Therapy of type 1 diabetes with CD4(+)CD25(high)CD127-regulatory T cells prolongs survival of pancreatic islets - results of one year follow-up. *Clin Immunol.* (2014) 153:23–30. doi: 10.1016/j.clim.2014.03.016
18. Phillips B, Nylander K, Harnaha J, Machen J, Lakomy R, Styche A, et al. A microsphere-based vaccine prevents and reverses new-onset autoimmune diabetes. *Diabetes.* (2008) 57:1544–55. doi: 10.2337/db07-0507
19. Di Caro V, Phillips B, Engman C, Harnaha J, Trucco M, Giannoukakis N. Retinoic acid-producing, ex-vivo-generated human tolerogenic dendritic cells induce the proliferation of immunosuppressive B lymphocytes. *Clin Exp Immunol.* (2013) 174:302–17. doi: 10.1111/cei.12177
20. Di Caro V, Phillips B, Engman C, Harnaha J, Trucco M, Giannoukakis N. Involvement of suppressive B-lymphocytes in the mechanism of tolerogenic dendritic cell reversal of type 1 diabetes in NOD mice. *PLoS ONE.* (2014) 9:e83575. doi: 10.1371/journal.pone.0083575
21. Engman C, Wen Y, Meng WS, Bottino R, Trucco M, Giannoukakis N. Generation of antigen-specific Foxp3+ regulatory T-cells *in vivo* following administration of diabetes-reversing tolerogenic microspheres does not require provision of antigen in the formulation. *Clin Immunol.* (2015) 160:103–23. doi: 10.1016/j.clim.2015.03.004
22. Barbi J, Pardoll D, Pan F. Treg functional stability and its responsiveness to the microenvironment. *Immunol Rev.* (2014) 259:115–39. doi: 10.1111/imr.12172
23. Chaudhry A, Rudensky AY. Control of inflammation by integration of environmental cues by regulatory T cells. *J Clin Invest.* (2013) 123:939–44. doi: 10.1172/JCI57175
24. Hoeppli RE, Wu D, Cook L, Levings MK. The environment of regulatory T cell biology: cytokines, metabolites, the microbiome. *Front Immunol.* (2015) 6:61. doi: 10.3389/fimmu.2015.00061
25. Pesenacker AM, Broady R, Levings MK. Control of tissue-localized immune responses by human regulatory T cells. *Eur J Immunol.* (2015) 45:333–43. doi: 10.1002/eji.201344205
26. Konkel JE, Zhang D, Zanvit P, Chia C, Zangarle-Murray T, Jin W, et al. Transforming growth factor-beta signaling in regulatory T cells controls T helper-17 cells and tissue-specific immune responses. *Immunity.* (2017) 46:660–74. doi: 10.1016/j.immuni.2017.03.015
27. Oh SA, Liu M, Nixon BG, Kang D, Toure A, Bivona M, et al. Foxp3-independent mechanism by which TGF-beta controls peripheral T cell tolerance. *Proc Natl Acad Sci USA.* (2017) 114:E7536–44. doi: 10.1073/pnas.1706356114
28. Tran DQ. TGF-beta: the sword, the wand, and the shield of FOXP3(+) regulatory T cells. *J Mol Cell Biol.* (2012) 4:29–37. doi: 10.1093/jmcb/mjr033
29. Wan YY, Flavell RA. 'Yin-Yang' functions of transforming growth factor-beta and T regulatory cells in immune regulation. *Immunol Rev.* (2007) 220:199–213. doi: 10.1111/j.1600-065X.2007.00565.x
30. Wan YY, Flavell RA. Regulatory T cells, transforming growth factor-beta, immune suppression. *Proc Am Thorac Soc.* (2007) 4:271–6. doi: 10.1513/pats.200701-020AW
31. Wrzesinski SH, Wan YY, Flavell RA. Transforming growth factor-beta and the immune response: implications for anticancer therapy. *Clin Cancer Res.* (2007) 13(18 Pt 1):5262–70. doi: 10.1158/1078-0432.CCR-07-1157
32. Xu A, Liu Y, Chen W, Wang J, Xue Y, Huang F, et al. TGF-beta-induced regulatory T cells directly suppress B cell responses through a noncytotoxic mechanism. *J Immunol.* (2016) 196:3631–41. doi: 10.4049/jimmunol.1501740
33. Zheng SG, Gray JD, Ohtsuka K, Yamagiwa S, Horwitz DA. Generation ex vivo of TGF-beta-producing regulatory T cells from CD4+CD25- precursors. *J Immunol.* (2002) 169:4183–9. doi: 10.4049/jimmunol.169.8.4183
34. Xiao S, Jin H, Korn T, Liu SM, Oukka M, Lim B, et al. Retinoic acid increases Foxp3+ regulatory T cells and inhibits development of Th17 cells by enhancing TGF-beta-driven Smad3 signaling and inhibiting IL-6 and IL-23 receptor expression. *J Immunol.* (2008) 181:2277–84. doi: 10.4049/jimmunol.181.4.2277
35. Zunino SJ, Storms DH, Stephensen CB. Diets rich in polyphenols and vitamin A inhibit the development of type I autoimmune diabetes in nonobese diabetic mice. *J Nutr.* (2007) 137:1216–21. doi: 10.1093/jn/137.5.1216
36. Stosic-Grujicic S, Cvjeticanin T, Stojanovic I. Retinoids differentially regulate the progression of autoimmune diabetes in three preclinical models in mice. *Mol Immunol.* (2009) 47:79–86. doi: 10.1016/j.molimm.2008.12.028
37. Capurso NA, Look M, Jeanbart L, Nowyhed H, Abraham C, Craft J, et al. Development of a nanoparticulate formulation of retinoic acid that suppresses Th17 cells and upregulates regulatory T cells. *Self Nonself.* (2010) 1:335–40. doi: 10.4161/self.1.4.13946
38. Keijzer C, Spiering R, Silva AL, van Eden W, Jiskoot W, Vervelde L, et al. PLGA nanoparticles enhance the expression of retinaldehyde dehydrogenase enzymes in dendritic cells and induce FoxP3(+) T-cells *in vitro*. *J Control Release.* (2013) 168:35–40. doi: 10.1016/j.jconrel.2013.02.027
39. McHugh MD, Park J, Uhrich R, Gao W, Horwitz DA, Fahmy TM. Paracrine co-delivery of TGF-beta and IL-2 using CD4-targeted nanoparticles for induction and maintenance of regulatory T cells. *Biomaterials.* (2015) 59:172–81. doi: 10.1016/j.biomaterials.2015.04.003
40. Lewis JS, Roche C, Zhang Y, Brusko TM, Wasserfall CH, Atkinson M, et al. Combinatorial delivery of immunosuppressive factors to dendritic cells using dual-sized microspheres. *J Mater Chem B Mater Biol Med.* (2014) 2:2562–74. doi: 10.1039/C3TB21460E
41. Abiru N, Maniatis AK, Yu L, Miao D, Moriyama H, Wegmann D, et al. Peptide and major histocompatibility complex-specific breaking of humoral tolerance to native insulin with the B9-23 peptide in diabetes-prone and normal mice. *Diabetes.* (2001) 50:1274–81. doi: 10.2337/diabetes.50.6.1274
42. Eckenrode SE, Ruan QG, Collins CD, Yang P, McIndoe RA, Muir A, et al. Molecular pathways altered by insulin b9-23 immunization. *Ann N Y Acad Sci.* (2004) 1037:175–85. doi: 10.1196/annals.1337.029
43. Harrison LC, Solly NR, Martinez NR. (Pro)insulin-specific regulatory T cells. *Novartis Found Symp.* (2003) 252:132–41; discussion 141—5, 203–10.
44. Nakayama M, Babaya N, Miao D, Gianani R, Liu E, Elliott JF, et al. Long-term prevention of diabetes and marked suppression of insulin autoantibodies and insulitis in mice lacking native insulin B9-23 sequence. *Ann N Y Acad Sci.* (2006) 1079:122–9. doi: 10.1196/annals.1375.018
45. Jia L, Kovacs JR, Zheng Y, Gawalt ES, Shen H, Meng WS. Attenuated alloreactivity of dendritic cells engineered with surface-modified microspheres carrying a plasmid encoding interleukin-10. *Biomaterials.* (2006) 27:2076–82. doi: 10.1016/j.biomaterials.2005.09.032
46. Jia L, Kovacs JR, Zheng Y, Shen H, Gawalt ES, Meng WS. Expansion of Foxp3-expressing regulatory T cells *in vitro* by dendritic cells modified with polymeric particles carrying a plasmid encoding interleukin-10. *Biomaterials.* (2008) 29:1250–61. doi: 10.1016/j.biomaterials.2007.11.015
47. Kovacs JR, Tidball J, Ross A, Jia L, Zheng Y, Gawalt ES, et al. Characterization of nickel-decorated PLGA particles anchored with a his-tagged polycation. *J Biomater Sci Polym Ed.* (2009) 20:1307–20. doi: 10.1163/156856209X453015
48. Zheng Y, Kovacs JR, Gawalt ES, Shen H, Meng WS. Characterization of particles fabricated with poly(D, L-lactic-co-glycolic acid) and an ornithine-histidine peptide as carriers of oligodeoxynucleotide for delivery into primary dendritic cells. *J Biomater Sci Polym Ed.* (2006) 17:1389–403. doi: 10.1163/156856206778937217
49. Zheng Y, Wen Y, George AM, Steinbach AM, Phillips BE, Giannoukakis N, et al. A peptide-based material platform for displaying antibodies to engage T cells. *Biomaterials.* (2011) 32:249–57. doi: 10.1016/j.biomaterials.2010.08.083
50. Broggi A, Cigni C, Zanoni I, Granucci F. Preparation of single-cell suspensions for cytofluorimetric analysis from different mouse skin regions. *J Vis Exp.* (2016) 110:e52589. doi: 10.3791/52589
51. Bouaziz JD, Yanaba K, Tedder TF. Regulatory B cells as inhibitors of immune responses and inflammation. *Immunol Rev.* (2008) 224:201–14. doi: 10.1111/j.1600-065X.2008.00661.x
52. Hong C, Gao XM. Purification and immunophenotypic characterization of murine B10 B cells. *Methods Mol Biol.* (2014) 1190:35–44. doi: 10.1007/978-1-4939-1161-5_3
53. Karim MR, Wang YF. Phenotypic identification of CD19(+)CD5(+)CD1d(+) regulatory B cells that produce interleukin

10 and transforming growth factor beta1 in human peripheral blood. *Arch Med Sci.* (2019) 15:1176–83. doi: 10.5114/aoms.2018.77772
54. Matsushita T, Tedder TF. Identifying regulatory B cells (B10 cells) that produce IL-10 in mice. *Methods Mol Biol.* (2011) 677:99–111. doi: 10.1007/978-1-60761-869-0_7
55. Yanaba K, Bouaziz JD, Haas KM, Poe JC, Fujimoto M, Tedder TF. A regulatory B cell subset with a unique CD1dhiCD5+ phenotype controls T cell-dependent inflammatory responses. *Immunity.* (2008) 28:639–50. doi: 10.1016/j.immuni.2008.03.017
56. Yanaba K, Bouaziz JD, Matsushita T, Tsubata T, Tedder TF. The development and function of regulatory B cells expressing IL-10 (B10 cells) requires antigen receptor diversity and TLR signals. *J Immunol.* (2009) 182:7459–72. doi: 10.4049/jimmunol.0900270
57. Tsang ML, Zhou L, Zheng BL, Wenker J, Fransen G, Humphrey J, et al. Characterization of recombinant soluble human transforming growth factor-beta receptor type II (rhTGF-beta sRII). *Cytokine.* (1995) 7:389–97. doi: 10.1006/cyto.1995.0054
58. Lewis JS, Dolgova NV, Zhang Y, Xia CQ, Wasserfall CH, Atkinson MA, et al. A combination dual-sized microparticle system modulates dendritic cells and prevents type 1 diabetes in prediabetic NOD mice. *Clin Immunol.* (2015) 160:90–102. doi: 10.1016/j.clim.2015.03.023
59. Lewis JS, Stewart JM, Marshall GP, Carstens MR, Zhang Y, Dolgova NV, et al. Dual-sized microparticle system for generating suppressive dendritic cells prevents and reverses type 1 diabetes in the nonobese diabetic mouse model. *ACS Biomater Sci Eng.* (2019) 5:2631–46. doi: 10.1021/acsbiomaterials.9b00332
60. Suwandi JS, Toes RE, Nikolic T, Roep BO. Inducing tissue specific tolerance in autoimmune disease with tolerogenic dendritic cells. *Clin Exp Rheumatol.* (2015) 33(4 Suppl. 92):S97–103.
61. Creusot RJ, Chang P, Healey DG, Tcherepanova IY, Nicolette CA, Fathman CG. A short pulse of IL-4 delivered by DCs electroporated with modified mRNA can both prevent and treat autoimmune diabetes in NOD mice. *Mol Ther.* (2010) 18:2112–20. doi: 10.1038/mt.2010.146
62. Yoon YM, Lewis JS, Carstens MR, Campbell-Thompson M, Wasserfall CH, Atkinson MA, et al. A combination hydrogel microparticle-based vaccine prevents type 1 diabetes in non-obese diabetic mice. *Sci Rep.* (2015) 5:13155. doi: 10.1038/srep13155
63. Keselowsky BG, Xia CQ, Clare-Salzler M. Multifunctional dendritic cell-targeting polymeric microparticles: engineering new vaccines for type 1 diabetes. *Hum Vaccin.* (2011) 7:37–44. doi: 10.4161/hv.7.1.12916
64. Battaglia M, Ahmed S, Anderson MS, Atkinson MA, Becker D, Bingley PJ, et al. Introducing the endotype concept to address the challenge of disease heterogeneity in type 1 diabetes. *Diabetes Care.* (2019) 43:5–12. doi: 10.2337/dc19-0880
65. Battaglia M, Atkinson MA. The streetlight effect in type 1 diabetes. *Diabetes.* (2015) 64:1081–90. doi: 10.2337/db14-1208
66. Battaglia M, Petrelli A, Vecchio F. Neutrophils and type 1 diabetes: current knowledge and suggested future directions. *Curr Opin Endocrinol Diabetes Obes.* (2019) 26:201–6. doi: 10.1097/MED.0000000000000485
67. Campbell-Thompson M, Rodriguez-Calvo T, Battaglia M. Abnormalities of the exocrine pancreas in type 1 diabetes. *Curr Diab Rep.* (2015) 15:79. doi: 10.1007/s11892-015-0653-y
68. Valle A, Giamporcaro GM, Scavini M, Stabilini A, Grogan P, Bianconi E, et al. Reduction of circulating neutrophils precedes and accompanies type 1 diabetes. *Diabetes.* (2013) 62:2072–7. doi: 10.2337/db12-1345
69. Vecchio F, Lo Buono N, Stabilini A, Nigi L, Dufort MJ, Geyer S, et al. Type 1 diabetes trialnet study, Battaglia M. Abnormal neutrophil signature in the blood and pancreas of presymptomatic and symptomatic type 1 diabetes. *JCI Insight.* (2018) 3. doi: 10.1172/jci.insight.122146
70. Kolb H, von Herrath M. Immunotherapy for type 1 diabetes: why do current protocols not halt the underlying disease process? *Cell Metab.* (2017) 25:233–41. doi: 10.1016/j.cmet.2016.10.009
71. Kroger CJ, Clark M, Ke Q, Tisch RM. Therapies to suppress beta cell autoimmunity in type 1 diabetes. *Front Immunol.* (2018) 9:1891. doi: 10.3389/fimmu.2018.01891
72. Roep BO. Are insights gained from NOD mice sufficient to guide clinical translation? Another inconvenient truth. *Ann N Y Acad Sci.* (2007) 1103:1–10. doi: 10.1196/annals.1394.018
73. Couri CE, Oliveira MC, Stracieri AB, Moraes DA, Pieroni F, Barros GM, et al. C-peptide levels and insulin independence following autologous nonmyeloablative hematopoietic stem cell transplantation in newly diagnosed type 1 diabetes mellitus. *JAMA.* (2009) 301:1573–9. doi: 10.1001/jama.2009.470
74. Haller MJ, Gitelman SE, Gottlieb PA, Michels AW, Perry DJ, Schultz AR, et al. Antithymocyte globulin plus G-CSF combination therapy leads to sustained immunomodulatory and metabolic effects in a subset of responders with established type 1 diabetes. *Diabetes.* (2016) 65:3765–75. doi: 10.2337/db16-0823
75. Haller MJ, Gitelman SE, Gottlieb PA, Michels AW, Rosenthal SM, Shuster JJ, et al. Anti-thymocyte globulin/G-CSF treatment preserves beta cell function in patients with established type 1 diabetes. *J Clin Invest.* (2015) 125:448–55. doi: 10.1172/JCI78492
76. Herold KC, Hagopian W, Auger JA, Poumian-Ruiz E, Taylor L, Donaldson D, et al. Anti-CD3 monoclonal antibody in new-onset type 1 diabetes mellitus. *N Engl J Med.* (2002) 346:1692–8. doi: 10.1056/NEJMoa012864
77. Pescovitz MD, Greenbaum CJ, Krause-Steinrauf H, Becker DJ, Gitelman SE, Goland R, et al. Type 1 diabetes trialnet anti: rituximab, B-lymphocyte depletion, and preservation of beta-cell function. *N Engl J Med.* (2009) 361:2143–52. doi: 10.1056/NEJMoa0904452
78. Ryan EA, Paty BW, Senior PA, Bigam D, Alfadhli E, Kneteman NM, et al. Five-year follow-up after clinical islet transplantation. *Diabetes.* (2005) 54:2060–9. doi: 10.2337/diabetes.54.7.2060
79. Sherry N, Hagopian W, Ludvigsson J, Jain SM, Wahlen J, Ferry RJ, et al. Protege Trial, Teplizumab for treatment of type 1 diabetes (Protege study): 1-year results from a randomised, placebo-controlled trial. *Lancet.* (2011) 378:487–97. doi: 10.1016/S0140-6736(11)60931-8
80. Voltarelli JC, Couri CE, Stracieri AB, Oliveira MC, Moraes DA, Pieroni F, et al. Autologous nonmyeloablative hematopoietic stem cell transplantation in newly diagnosed type 1 diabetes mellitus. *JAMA.* (2007) 297:1568–76. doi: 10.1001/jama.297.14.1568
81. Casey LM, Pearson RM, Hughes KR, Liu JMH, Rose JA, North MG, et al. Conjugation of transforming growth factor beta to antigen-loaded poly(lactide- co-glycolide) nanoparticles enhances efficiency of antigen-specific tolerance. *Bioconjug Chem.* (2018) 29:813–23. doi: 10.1021/acs.bioconjchem.7b00624
82. Cho JJ, Stewart JM, Drashansky TT, Brusko MA, Zuniga AN, Lorentsen KJ, et al. An antigen-specific semi-therapeutic treatment with local delivery of tolerogenic factors through a dual-sized microparticle system blocks experimental autoimmune encephalomyelitis. *Biomaterials.* (2017) 143:79–92. doi: 10.1016/j.biomaterials.2017.07.029
83. Getts DR, Martin AJ, McCarthy DP, Terry RL, Hunter ZN, Yap WT, et al. Microparticles bearing encephalitogenic peptides induce T-cell tolerance and ameliorate experimental autoimmune encephalomyelitis. *Nat Biotechnol.* (2012) 30:1217–24. doi: 10.1038/nbt.2434
84. Hlavaty KA, Luo X, Shea LD, Miller SD. Cellular and molecular targeting for nanotherapeutics in transplantation tolerance. *Clin Immunol.* (2015) 160:14–23. doi: 10.1016/j.clim.2015.03.013
85. Hunter Z, McCarthy DP, Yap WT, Harp CT, Getts DR, Shea LD, et al. A biodegradable nanoparticle platform for the induction of antigen-specific immune tolerance for treatment of autoimmune disease. *ACS Nano.* (2014) 8:2148–60. doi: 10.1021/nn405033r
86. Kuo R, Saito E, Miller SD, Shea LD. Peptide-conjugated nanoparticles reduce positive co-stimulatory expression and T cell activity to induce tolerance. *Mol Ther.* (2017) 25:1676–85. doi: 10.1016/j.ymthe.2017.03.032
87. Luo X, Miller SD, Shea LD. Immune tolerance for autoimmune disease and cell transplantation. *Annu Rev Biomed Eng.* (2016) 18:181–205. doi: 10.1146/annurev-bioeng-110315-020137
88. McCarthy DP, Yap JW, Harp CT, Song WK, Chen J, Pearson RM, et al. An antigen-encapsulating nanoparticle platform for TH1/17 immune tolerance therapy. *Nanomedicine.* (2017) 13:191–200. doi: 10.1016/j.nano.2016.09.007
89. Pearson RM, Casey LM, Hughes KR, Miller SD, Shea LD. In vivo reprogramming of immune cells: technologies for induction of antigen-specific tolerance. *Adv Drug Deliv Rev.* (2017) 114:240–55. doi: 10.1016/j.addr.2017.04.005
90. Mukherjee G, Geliebter A, Babad J, Santamaria P, Serreze DV, Freeman GJ, et al. DEC-205-mediated antigen targeting to steady-state dendritic cells

induces deletion of diabetogenic CD8(+) T cells independently of PD-1 and PD-L1. *Int Immunol.* (2013) 25:651–60. doi: 10.1093/intimm/dxt031
91. Mukhopadhaya A, Hanafusa T, Jarchum I, Chen YG, Iwai Y, Serreze DV, et al. Selective delivery of beta cell antigen to dendritic cells in vivo leads to deletion and tolerance of autoreactive CD8+ T cells in NOD mice. *Proc Natl Acad Sci USA.* (2008) 105:6374–9. doi: 10.1073/pnas.0802644105
92. Jamison BL, Neef T, Goodspeed A, Bradley B, Baker RL, Miller SD, et al. Nanoparticles containing an insulin-ChgA hybrid peptide protect from transfer of autoimmune diabetes by shifting the balance between effector T cells and regulatory T cells. *J Immunol.* (2019) 203:48–57. doi: 10.4049/jimmunol.1900127
93. Bai A, Lu N, Guo Y, Liu Z, Chen J, Peng Z. All-trans retinoic acid down-regulates inflammatory responses by shifting the Treg/Th17 profile in human ulcerative and murine colitis. *J Leukoc Biol.* (2009) 86:959–69. doi: 10.1189/jlb.0109006
94. Benson MJ, Pino-Lagos K, Rosemblatt M, Noelle RJ. All-trans retinoic acid mediates enhanced T reg cell growth, differentiation, and gut homing in the face of high levels of co-stimulation. *J Exp Med.* (2007) 204:1765–74. doi: 10.1084/jem.20070719
95. Hall JA, Grainger JR, Spencer SP, Belkaid Y. The role of retinoic acid in tolerance and immunity. *Immunity.* (2011) 35:13–22. doi: 10.1016/j.immuni.2011.07.002
96. Iwata M, Yokota A. Retinoic acid production by intestinal dendritic cells. *Vitam Horm.* (2011) 86:127–52. doi: 10.1016/B978-0-12-386960-9.00006-X
97. Lu L, Ma J, Li Z, Lan Q, Chen M, Liu Y, et al. All-trans retinoic acid promotes TGF-beta-induced Tregs via histone modification but not DNA demethylation on Foxp3 gene locus. *PLoS ONE.* (2011) 6:e24590. doi: 10.1371/journal.pone.0024590
98. Mucida D, Park Y, Kim G, Turovskaya O, Scott I, Kronenberg M, et al. Reciprocal TH17 and regulatory T cell differentiation mediated by retinoic acid. *Science.* (2007) 317:256–60. doi: 10.1126/science.1145697
99. Sakaguchi S, Miyara M, Costantino CM, Hafler DA. FOXP3+ regulatory T cells in the human immune system. *Nat Rev Immunol.* (2010) 10:490–500. doi: 10.1038/nri2785
100. Wing K, Sakaguchi S. Regulatory T cells exert checks and balances on self tolerance and autoimmunity. *Nat Immunol.* (2010) 11:7–13. doi: 10.1038/ni.1818
101. Jordan MS, Boesteanu A, Reed AJ, Petrone AL, Holenbeck AE, Lerman MA, et al. Thymic selection of CD4+CD25+ regulatory T cells induced by an agonist self-peptide. *Nat Immunol.* (2001) 2:301–6. doi: 10.1038/86302
102. Kawahata K, Misaki Y, Yamauchi M, Tsunekawa S, Setoguchi K, Miyazaki J, et al. Generation of CD4(+)CD25(+) regulatory T cells from autoreactive T cells simultaneously with their negative selection in the thymus and from nonautoreactive T cells by endogenous TCR expression. *J Immunol.* (2002) 168:4399–405. doi: 10.4049/jimmunol.168.9.4399
103. Curotto de Lafaille MA, Lafaille JJ. Natural and adaptive foxp3+ regulatory T cells: more of the same or a division of labor? *Immunity.* (2009) 30:626–35. doi: 10.1016/j.immuni.2009.05.002
104. Coombes JL, Maloy KJ. Control of intestinal homeostasis by regulatory T cells and dendritic cells. *Semin Immunol.* (2007) 19:116–26. doi: 10.1016/j.smim.2007.01.001
105. Sun CM, Hall JA, Blank RB, Bouladoux N, Oukka M, Mora JR, et al. Small intestine lamina propria dendritic cells promote de novo generation of Foxp3 T reg cells via retinoic acid. *J Exp Med.* (2007) 204:1775–85. doi: 10.1084/jem.20070602
106. Koprivica I, Gajic D, Saksida T, Cavalli E, Auci D, Despotovic S, et al. Orally delivered all-trans-retinoic acid- and transforming growth factor-beta-loaded microparticles ameliorate type 1 diabetes in mice. *Eur J Pharmacol.* (2019) 864:172721. doi: 10.1016/j.ejphar.2019.172721
107. Atkinson MA, Leiter EH. The NOD mouse model of type 1 diabetes: as good as it gets? *Nat Med.* (1999) 5:601–4. doi: 10.1038/9442
108. Chen YG, Mathews CE, Driver JP. The role of NOD mice in type 1 diabetes research: lessons from the past and recommendations for the future. *Front Endocrinol.* (2018) 9:51. doi: 10.3389/fendo.2018.00051
109. Pearson JA, Wong FS, Wen L. The importance of the Non Obese Diabetic (NOD) mouse model in autoimmune diabetes. *J Autoimmun.* (2016) 66:76–88. doi: 10.1016/j.jaut.2015.08.019
110. Reed JC, Herold KC. Thinking bedside at the bench: the NOD mouse model of T1DM. *Nat Rev Endocrinol.* (2015) 11:308–14. doi: 10.1038/nrendo.2014.236

Conflict of Interest: The authors declare that the research was conducted in the absence of any commercial or financial relationships that could be construed as a potential conflict of interest.

frontiers in Immunology

ORIGINAL RESEARCH
published: 26 March 2021
doi: 10.3389/fimmu.2021.609029

Pre-Existing Humoral Immunity Enhances Epicutaneously-Administered Allergen Capture by Skin DC and Their Migration to Local Lymph Nodes

Pierre-Louis Hervé[1]*, *Camille Plaquet*[1], *Noémie Assoun*[1], *Nathalie Oreal*[1], *Laetitia Gaulme*[1], *Audrey Perrin*[1], *Adeline Bouzereau*[1], *Véronique Dhelft*[1], *Jean-Louis Labernardière*[1], *Lucie Mondoulet*[1] and *Hugh A. Sampson*[2]

[1] Research and Innovation, DBV Technologies, Montrouge, France, [2] Research and Innovation, DBV Technologies, New York, NY, United States

Due to its richness in antigen presenting cells, e.g., dendritic cells (DC), the skin has been identified as a promising route for immunotherapy and vaccination. Several years ago, a skin delivery system was developed based on epicutaneous patches allowing the administration of antigen through intact skin. Using mouse models, we have shown that epicutaneous allergen application leads to a rapid uptake and transport of allergen-positive cells to skin-draining lymph nodes (LN). This occurred primarily in animals previously sensitized to the same allergen. In that context, we sought to better understand the role of the specific preexisting immunity in allergen capture by skin DC and their subsequent migration to LN. Specifically, we investigated the role of humoral immunity induced by sensitization and the involvement of IgG Fc receptors (FcγR). Epicutaneous patches containing fluorescently-labeled ovalbumin (OVA) were applied to naïve mice that had previously received either sera or purified IgG isolated from OVA-sensitized mice. To investigate the involvement of FcγR, animals received 2.4G2 (anti-FcγRII/RIII) blocking antibody, 24 hours before patch application. Mice that received sera or purified IgG originating from OVA-sensitized mice showed an increase in the quantity of OVA-positive DC in skin and LN. Moreover, the blockade of FcγR reduced the number of OVA-positive DC in LN to a level similar to that observed in naïve animals. Overall, these results demonstrate that preexisting specific-IgG antibodies are involved in allergen capture by skin DC following EPIT through the involvement of antigen-specific IgG-FcγR.

Keywords: skin dendritic cells, epicutaneous delivery, allergen capture, Fc receptors (FcR), preexisting immunity

OPEN ACCESS

Edited by:
Irina Caminschi, Monash University, Australia

Reviewed by:
Diana Dudziak, Universitatsklinikum Erlangen, Germany
Tatyana Chtanova, Garvan Institute of Medical Research, Australia

***Correspondence:**
Pierre-Louis Hervé
pierre-louis.herve@dbv-technologies.com

Specialty section:
This article was submitted to Antigen Presenting Cell Biology, a section of the journal Frontiers in Immunology

Received: *22 September 2020*
Accepted: *10 March 2021*
Published: *26 March 2021*

Citation:
Hervé P-L, Plaquet C, Assoun N, Oreal N, Gaulme L, Perrin A, Bouzereau A, Dhelft V, Labernardière J-L, Mondoulet L and Sampson HA (2021) Pre-Existing Humoral Immunity Enhances Epicutaneously-Administered Allergen Capture by Skin DC and Their Migration to Local Lymph Nodes. Front. Immunol. 12:609029. doi: 10.3389/fimmu.2021.609029

INTRODUCTION

The skin barrier is comprised of a dense network of antigen presenting cells (APC), including dendritic cells (DC), such as Langerhans cells (LC), that reside in the epidermal layer (1). These DC provide immune-surveillance by "sensing" pathogens passing into the stratum corneum and play a central role in activating adaptive immunity. Due to this feature, skin has been clearly identified as a promising route for vaccination and immunotherapy. Several years ago a novel epicutaneous delivery system was designed for epicutaneous immunotherapy (EPIT) for the treatment of food allergy (2). This system utilized a patch (Viaskin™) that forms an occlusive condensation chamber where allergen is solubilized by skin humidity and delivered across the stratum corneum to skin DC (2–6). Previous studies demonstrated that allergens applied on intact skin *via* epicutaneous patches efficiently promote down-modulation of allergen-specific immune response in sensitized animal models in association with the induction of Tregs (2, 5, 6). This distinctive response could be related to the unique targeting of LC, which are mainly oriented to promote tolerance (4, 7, 8). It appeared that this tolerogenic immune-modulation could be obtained only when the antigen was administered on intact, uninflamed skin (9). Previous results also suggested that the preexisting immunological status of patch-treated mice had a significant impact on the antigen uptake by skin DC and their migration to the draining lymph nodes (4). Indeed, the capture of patch-administered ovalbumin (OVA) by skin DC was more efficient and occurred more rapidly in OVA-sensitized mice than in naïve animals. Remarkably, the migration of these OVA-positive DC to lymph nodes was observed only in OVA-sensitized mice. In that context, the aim of the present study was to better understand the impact of preexisting specific immunity on allergen capture by skin DC and their migration to draining lymph nodes, with a focus on humoral immunity. To that end, we first measured the expression of different antibody Fc receptors on the surface of skin DCs. Then, using a passive transfer model, we evaluated the capacity of the specific humoral response induced in sensitized animals to promote allergen capture by skin DC and their migration to draining lymph nodes. Finally, using a blocking antibody, we further investigated the specific role of IgG and IgG Fc receptors (FcγR). Our results showed that the humoral response elicited by OVA sensitization increased the capacity of skin DC to capture epicutaneously-administered OVA, leading to the migration of a higher number of OVA-positive DC to local draining lymph nodes. Moreover, our results demonstrated that IgG is the main class of antibody in mice involved in this effect.

MATERIALS AND METHODS

Animals and Ethics

BALB/c mice were purchased from Charles River (Lyon, France) and housed under conventional conditions (DBV Technologies, Montrouge, France, agreement number #A92-049-02). Experiments have been performed according to the European Community rules of animal care, and with permission of the French government (authorization #13305).

Sensitization of Mice

Mice were sensitized subcutaneously on days 0 and 7 with 10 mg of OVA grade V (Sigma) and 1.6 mg aluminum hydroxide (Sigma Aldrich) in 200 µl of PBS 1X. Two weeks after the end of sensitization phase, blood samples were collected by submandibular puncture into microtubes containing EDTA (Greiner Bio-One) and centrifuged at 3000 x g for 10 minutes to collect plasma. Plasma samples were then pooled. The quality of the sensitization has been controlled for each individual mouse and for each pool by measuring OVA-specific IgE, IgG1 and IgG2a using a quantitative ELISA as previously described (2).

Purification of Antibodies and Passive Transfer of Serum

IgG antibodies were purified from pooled sera using Nab Protein G Spin Kit (Thermo Scientific). The flow-through, corresponding to IgG-depleted serum was collected separately. This flow- through contained similar levels of IgE compared to the pooled sera, but no detectable IgG. Purified IgG were dialyzed against PBS 1X and concentrated to an appropriate volume using Vivaspin column (Merck Millipore). Purified IgG or pooled sera were sterile-filtered on a 0.22 µm filter and injected intraperitoneally into recipient mice (500 µL per mice). For each experiment, the quantities of OVA-specific IgG1 and IgE to be injected were determined using a quantitative ELISA. Of note, the injection of 500 µL of pooled sera (the maximum intraperitoneal volume authorized by our ethical guidelines) led to slightly lower titers of specific IgG1 in naïve recipient mice than in sensitized donor mice (see **Figure S1** for representative data). Specific IgE and IgG2a titers remained low or just above the level of detection in recipient mice (data not shown).

Preparation of OVA-AF488 Patches and Application to Mice

Epicutaneous patches were loaded dropwise with 100 µg of Alexa-Fluor®-488 (AF-488) conjugated ovalbumin (Life Technologies). Patches were dried at 30°C for 1 hour in a ventilated oven and stored at 4°C. Before patch application, mice were anaesthetized with ketamine and xylazine (50 and 10 mg/kg, respectively) and hair on the back was removed using electric clippers and depilatory cream (Reckitt Benckiser). Patches containing OVA-AF-488 were applied the following day and secured using an Urgoderm® bandage (Urgo Laboratories). Patches were maintained for 6 or 48 hours based on optimal timepoints previously defined (4).

Injection of IgG Receptor Blocking Antibodies

Mice received 500 µg of anti-FcγRII/RIII (clone 2.4G2, Bio X Cell) or rat IgG2b as isotype control (clone LTF-2, Bio X Cell) by intraperitoneal injection. To avoid any non-specific anaphylactic

reactions, all mice (including isotype control) received 200 μg of the anti-histamine triprolidine hydrochloride (Sigma) by intraperitoneal injection 30 minutes before injecting the monoclonal antibodies. Mice received patches 24 hours later.

Collection of Brachial Lymph Nodes (BLNs) for Flow Cytometric Analysis

BLNs were harvested in 2 mL of RPMI containing 0.26 U/mL Liberase TL and 25 μg/mL DNase I (Sigma Aldrich). Each BLN was flushed using a syringe and incubated for 20 min at 37°C. The enzymatic reaction was then stopped with 250 μL of EDTA (100 mM). Cells were homogenized with a 100 μm cell strainer in magnetic-activated cell sorting (MACS) buffer (Miltenyi Biotec) and counted.

Collection of Skin Samples for Flow Cytometric Analysis

A skin sample corresponding to the patch application area was harvested using an 8-mm disposal biopsy punch (KAI medical) and transferred into 1 mL of Liberase TM (Roche) prepared in basic medium (RPMI + PS + 55 μM BME + 20 mM HEPES), then incubated 2 hours at 37°C. The enzymatic reaction was then stopped with 75 μL of EDTA (100 mM). Cells were homogenized using the Medimachine tissue homogenizer (BD Bioscience) for 8 min and counted using an automated cell counter (BioRad).

Flow Cytometry Analysis

Cell suspensions were incubated for 15 min at 4°C with Fc Block (BD Biosciences) and then stained for 25 min at 4°C with the following fluorochrome-conjugated antibodies: anti-CD11c-APC-Cy7 (clone: HL3, BD Biosciences) or anti-CD11c-PE (clone REA754, Miltenyi Biotec), anti-MHC-II-VioBlue (clone: M5/114.15.2, Miltenyi Biotec), anti-CD11b-PerCP-Vio700 (clone: REA592, Miltenyi Biotec), anti-EpCAM-PE (clone: caa7-9G8, Miltenyi Biotec) or anti-EpCAM-PE-Vio770 (clone caa7-9G8, Miltenyi Biotec), anti-XCR1-APC-Vio700 (clone REA707, Miltenyi Biotec), anti-PD-L2-PE (clone MIH37, Miltenyi Biotec), CD86-APC (clone PO3.3, Miltenyi Biotec). Dead cells were excluded using Zombie Aqua Fixable Viability Kit (Biolegend). For the analysis of Fc receptor expression, cells were permeabilized using an intracellular fixation & permeabilization kit (eBioscience) and incubated for 25 min at 4°C with anti-CD16(FcγRIII)/CD32(FcγRII)-PE-Vio770 (instead of Fc Block, clone: 93, Miltenyi Biotec), anti-FcεRIα-APC (clone: MAR-1, Miltenyi Biotec), anti-CD23-APC (clone: B3B4, Miltenyi Biotec), anti-CD64-PE-Vio770 (clone: REA286, Miltenyi Biotec). Cells were acquired on a MACSquant 10 or a MACSquant 16 flow cytometer (Miltenyi Biotec) and data were analyzed using FlowJo software using the gating strategies described in **Figures S2** and **S3** (10).

Confocal Microscopy Analysis

Skin cell suspensions were obtained by Liberase digestion as mentioned above. Cell suspensions were diluted in RPMI and deposited in microplates containing poly-L-lysine-coated coverslips (Corning). Cells were incubated overnight at 4°C and fixed with 4% paraformaldehyde. Cells were then incubated with rat anti-mouse MHC-II (clone 2G9, BD Bioscience) and rabbit anti-clathrin heavy chain (Abcam), followed by AF647 goat anti-rabbit IgG (Invitrogen) and AF-555 goat anti-rat IgG (Invitrogen). Finally, coverslips were mounted on microscope slides using ProLong Gold with DAPI (Life Technologies). Cells were visualized with a LMS 700 confocal microscope (Zeiss) and pictures were edited using Zen software (Zeiss).

Statistical Data Analysis

Data are presented as median with interquartile ranges. The non-parametric Mann-Whitney test was used to compare unpaired values (GraphPad Prism®). Values of $p<0.05$ were considered significant. The level of significance is indicated with asterisks: *, $p<0.05$; **, $p<0.01$; ***, $p<0.001$; ****, $p<0.0001$ and n.s., non-significant.

RESULTS

Allergen Capture by Skin Dendritic Cells Is Increased in Sensitized Mice, Likely Through the Involvement of Fc Receptors (FcR)

OVA-sensitized and naïve mice received epicutaneous patches containing fluorescently labeled ovalbumin (OVA-AF488) for 6 hours. Skin cells were then collected and analyzed by flow cytometry (**Figure 1A**). As observed in previous studies, significant increases in the percentage of OVA-positive cDC1 and cDC2 were observed in OVA-sensitized mice compared to naïve animals. There was no significant difference in the percentage of OVA-positive LC observed in OVA-sensitized mice compared to naïve animals. Additionally, a significant increase of the OVA median of fluorescence (MFI) was observed for OVA-positive LC and cDC1 isolated from sensitized mice compared to naïve animals (**Figure 1B**). This suggests that the net amount of OVA antigen captured by these two subsets was greater in sensitized animals. The relative expression of FcR was evaluated by Flow Cytometry in skin DC isolated from naïve mice, naive mice that received an OVA-AF488 patch, OVA-sensitized mice or OVA-sensitized mice that received an OVA-AF488 patch (**Figure 1C**). The analysis was performed on permeabilized cells to allow for the quantification of FcRs that were internalized. In sensitized animals, a significant decrease in the relative expression of FcγRII/RIII (in all DC subsets), FcγRI (in cDC2), and FcεRI (cDC1) was observed in sensitized mice following patch application. In naïve animals, a slight decrease in the relative expression of FcγRII/RIII was also observed following patch application. However, this decrease was less than that observed in sensitized animals. Note that a similar trend was observed in non-permeabilized cells, although the relative expression of FcεRI, FcγRI and FcγRII/RIII were slightly lower, likely due to the sole detection of surface receptors (**Figure S4**). Graphs showing individual data points and error

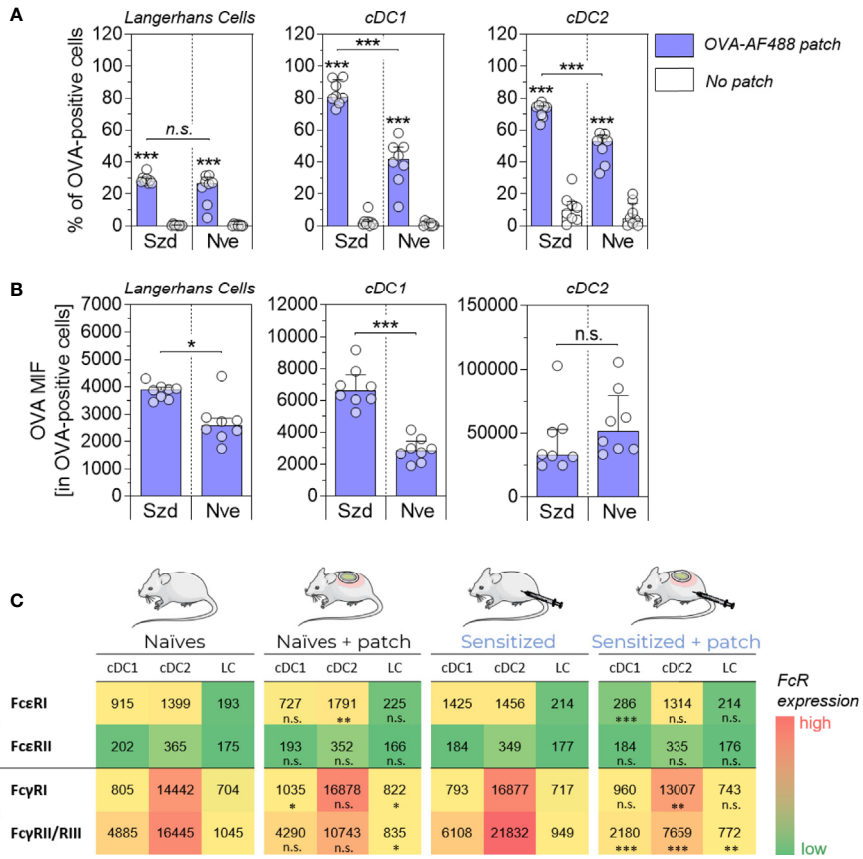

FIGURE 1 | Allergen uptake by skin DC is enhanced in sensitized animals and involves Fc receptors. OVA-sensitized (Szd) or naïve (Nve) mice received a patch containing OVA-AF488 on hair-free skin (depilated) on the back (in blue). As negative controls, mice received no patches (in white). Six hours after patch application, a skin sample corresponding to the patch application area was collected and cells were analyzed by Flow Cytometry. **(A)** The percentage of OVA-positive cells was measured among Langerhans cells, cDC1 and cDC2, as indicated. **(B)** The median of OVA fluorescence intensity (OVA MFI) was measured from OVA-positive DCs. Data are median and interquartile ranges of individual values (N = 8 per group). Data are representative of several independent experiments. **(C)** The relative expression of Fc receptors was evaluated by measuring MFI. Data are median of individual MFI (N = 8 per group). FcεRI, FcεRII and FcγRII/RIII expression data are representatives of two independent experiments. The level of significance indicated for sensitized + patch mice was derived from the comparison to sensitized mice. P values were determined using the Mann-Whitney test (*P < 0.05; **P < 0.01; ***P < 0.001; n.s., non-significant).

bars are available in **Figure S5**. From these results, we hypothesized that FcR, and especially FcγRII/RIII may be involved in the binding of immune complexes formed with OVA and specific antibodies, that then blocked access to immunolabeling antibodies by steric hindrance.

Specific Humoral Response Is Involved in the Enhancement of Allergen Capture by Skin DC, Leading to an Increase of the Number of OVA-Positive DCs in Local Lymph Nodes

Naïve mice received pooled sera originating from sensitized or naïve mice by intraperitoneal injection (**Figure 2A**). Twenty-four hours after the passive transfer, recipient mice received OVA-AF488 patches. Following 6 hours of patch application, skin cells were collected and analyzed by Flow Cytometry. A significant increase in the percentages of OVA-positive LC, cDC1 and cDC2 were observed in mice that received sera from OVA-sensitized animals compared to mice that received sera from naïve animals (**Figure 2B**). Additionally, an increase of OVA MFI was observed for OVA-positive DCs in mice that received sera from OVA-sensitized animals compared to mice that received sera from naïve animals (significant for cDC1 and cDC2) (**Figure 2C**). Surprisingly, no increase in the absolute number of OVA-positive DCs was found in mice that received sera from OVA-sensitized animals despite the increase in percentages of OVA-positive cells seen (**Figure 2D**). This may reflect a reduction in the total number of DCs in that group, which may result from an earlier migration to local lymph nodes. Following 48 hours of patch application, cells were isolated from BLN and analyzed by flow cytometry (**Figure 3**). A significant increase in the numbers of OVA-positive migratory LC, cDC1 and cDC2 was observed in mice that received sera from OVA-sensitized animals compared to mice that received sera from naïve animals. Overall, these results suggest that the humoral

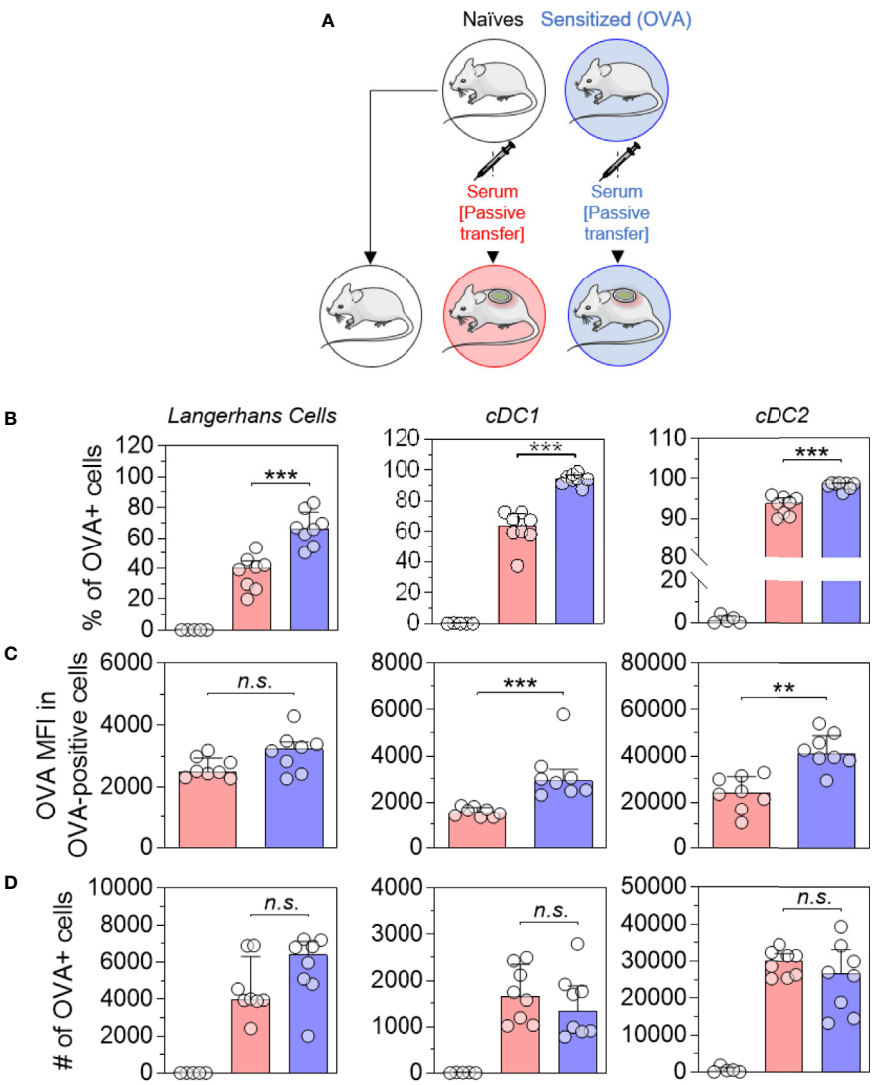

FIGURE 2 | Allergen-specific humoral immunity increases the local uptake of allergen by skin DCs. **(A)** Mice received pooled sera obtained from OVA-sensitized mice (in blue) or naive mice (in red), as indicated. The next day, recipient mice received a patch containing OVA-AF-488 on depilated areas of the back. As a negative control for Flow Cytometric analysis, a group of naïve mice was kept untreated (in white). Six hours after patch application, a skin sample corresponding to the patch application area was collected and cells were analyzed by Flow Cytometry. **(B)** The percentage of OVA positive cells was measured among Langerhans cells, cDC1 and cDC2, as indicated. **(C)** The median of OVA fluorescence intensity (OVA MFI) was measured from OVA-positive cells. **(D)** The absolute number of OVA-positive DC was calculated based on the percentages of OVA-positive cells and the total number of cells in each DC subset. Data are median and interquartile ranges of individual values (N = 8 per experimental group). Data are representative of several independent experiments. P values were determined using the Mann-Whitney test (**P < 0.01; ***P < 0.001; n.s., non-significant).

component is the main factor responsible for the increase of allergen capture observed in sensitized animals.

IgG Is Involved in the Increase of Allergen Capture by Skin DC and Their Migration to Local Lymph Nodes.

Figure 1 suggests that IgG receptors are mainly involved in allergen capture by skin DC. To assess the role of OVA-specific IgG in the increased number of OVA-positive migratory DC in local lymph nodes, IgG antibodies were purified from a pool of sera originating from OVA-sensitized mice and injected into naïve recipient mice. Twenty-four hours after passive transfer, recipient mice received OVA-AF488 patches (**Figure 4**). Following 48 hours of patch application, cells were isolated from BLN and analyzed by Flow Cytometry. A significant increase in the numbers of OVA-positive migratory LC, cDC1 and cDC2 were observed in mice that received purified IgG compared to untreated mice. Conversely, mice that received IgG-depleted sera originating from OVA-sensitized mice (flow through of IgG purification step containing high amount of

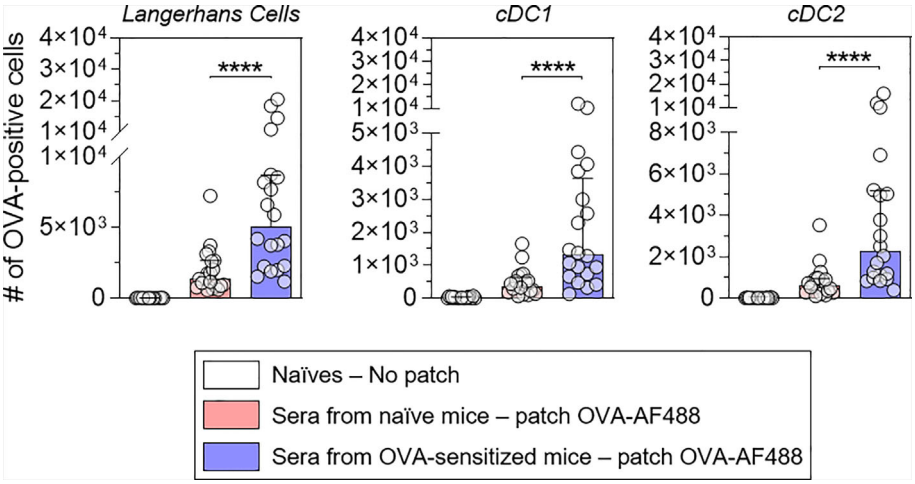

FIGURE 3 | Allergen-specific humoral immunity promotes the increase of the number of OVA-positive migratory DCs in local lymph nodes. Mice were treated as described in **Figure 2**. Forty-eight hours after patch application, brachial draining lymph nodes were collected, and cells were analyzed by Flow Cytometry. The number of OVA positive cells was quantified among migratory Langerhans cells, cDC1 and cDC2, as indicated (pool of two independent experiments, N = 10 per group for each of the two experiments). Data are median and interquartile ranges of individual values. P values were determined using the Mann-Whitney test (****P < 0.0001).

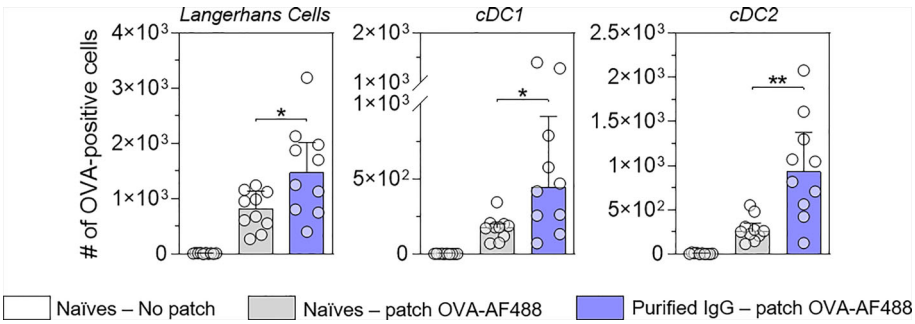

FIGURE 4 | IgG increases the number of allergen-positive DC in local lymph nodes. Mice received purified IgG (in blue) obtained from OVA-sensitized mice. As negative control, mice were kept untreated (in grey). The next day, recipient mice received a patch containing OVA-AF-488 on depilated areas of the back or remained untreated as a negative control (in white). Forty-eight hours after patch application, brachial draining lymph nodes were collected, and cells were analyzed by flow cytometry. The number of OVA positive cells was measured among migratory Langerhans cells, cDC1 and cDC2, as indicated (N = 10 per group, single experiment). Data are median and interquartile ranges of individual values. P values were determined using the Mann-Whitney test (*P < 0.05; **P < 0.01; n.s., non-significant).

IgE) did not show any increase of OVA-positive migratory DCs as compared to mice that received sera originating from naïve mice (**Figure S6**). These results suggest that IgG is the main class of immunoglobulin involved in the increase of OVA uptake by skin DC and the greater number of OVA-positive migratory DCs in lymph nodes following OVA-AF488 patch application.

Blockade of FcγRII/RIII Decreases the Number of OVA-Positive DC at Skin and BLN Levels

To further confirm the role of IgG and the involvement of FcγR, OVA-sensitized or naïve mice received anti-FcγRII/RIII blocking antibody or a relevant isotype control. Twenty-four hours after blocking antibody injection, mice received OVA-AF488 patches (**Figure 5A**). Following 6 hours of patch application, skin cells were collected and analyzed by Flow Cytometry (**Figure 5B**). A significant decrease in the percentages of OVA-positive LC and cDC1 were observed in sensitized mice that received blocking antibody compared to mice that received isotype control. Conversely, injection of the blocking antibody did not modify the proportion of OVA-positive LC and cDC1 in naïve animals. Of note, blocking antibody had no or even an inverse effect on cDC2, especially in naïve animals. This suggests that another mechanism may compensate for FcγR blockade in that subset, especially at the

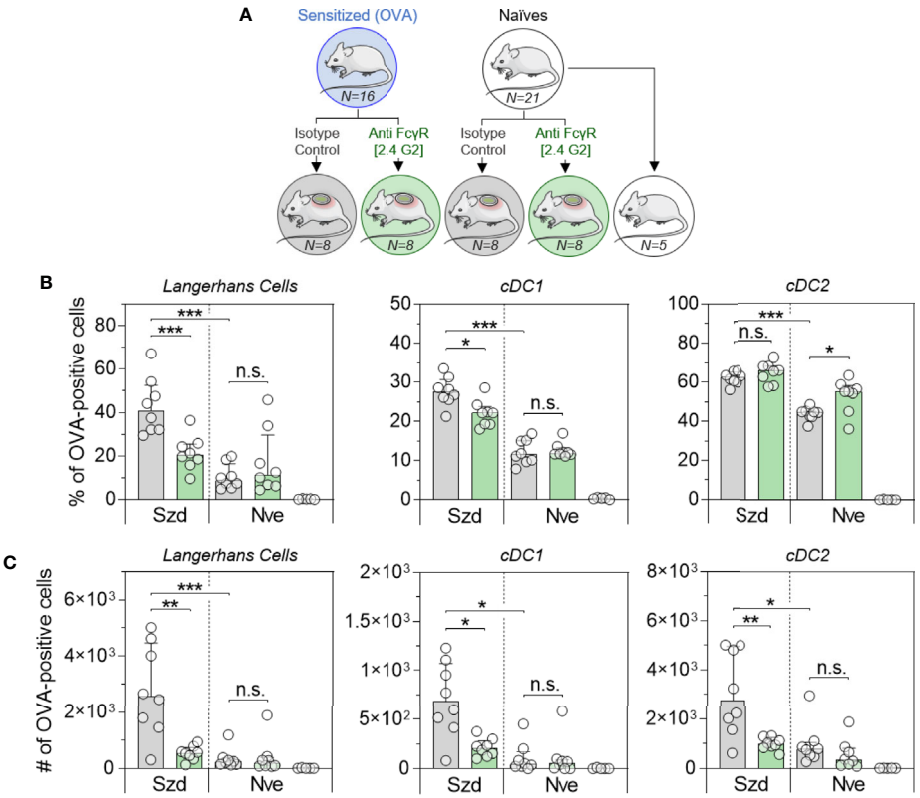

FIGURE 5 | Allergen uptake by skin DC is enhanced in sensitized animals and involves Fc receptors. **(A)** OVA-sensitized (Szd) or naïve (Nve) mice received anti-FcγRII/RIII antibodies (in green) or relevant isotype control (in grey). Twenty-four hours after blocking antibody injection, mice received a patch containing OVA-AF488 on depilated areas of the back (in blue). As a negative control a group of naive mice was kept untreated (in white). **(B)** Six hours after patch application, a skin sample corresponding to the patch application area was collected and cells were analyzed by Flow Cytometry. The percentage of OVA positive cells was measured among Langerhans cells, cDC1 and cDC2, as indicated. **(C)** Forty-eight hours after patch application, brachial draining lymph nodes were collected, and cells were analyzed by Flow Cytometry. The number of OVA positive cells was measured among migratory Langerhans cells, cDC1 and cDC2, as indicated. Data are Median and interquartile ranges of individual values (N = 8 per group, single experiment). P values were determined according to the Mann-Whitney test (*P < 0.05; **P < 0.01; ***P < 0.001; n.s., non-significant).

skin level. Following 48 hours of patch application, cells were isolated from BLN and analyzed by Flow Cytometry (**Figure 5C**). A significant decrease in the numbers of OVA-positive migratory LC, cDC1 and cDC2 were observed in sensitized mice that received the blocking antibody compared to mice that received an isotype control. Again, the injection of blocking antibodies had no effect in naïve animals. These data suggest that IgG, through the involvement of FcγRII/RIII, is mainly involved in the increase of OVA uptake observed in OVA-sensitized animals following the epicutaneous application of OVA-AF488.

DISCUSSION

In the present work, we aimed to better understand the role of the preexisting immunologic status in the capture of epicutaneously-administered allergen by skin APC and the subsequent migration of allergen-positive cells to local draining lymph nodes. This study was based on previous observations, showing an increase in the number of OVA-positive DC in the draining lymph nodes of OVA-sensitized mice compared to naïve mice, when OVA is administered epicutaneously (4). Our data strongly suggest that specific antibodies, especially IgG, are mainly involved in this effect through the involvement of FcγR. Of note, although all our data went in the same direction, some of our experiments have been performed once and additional tests would be required to confirm and elaborate on our findings. The increase in the number of OVA-positive migratory DCs observed in the draining lymph nodes of mice that received sera originating from sensitized mice is likely due to an enhancement of migration efficacy but may also be reflective of the higher proportion of OVA-positive DCs in the skin. Previous data demonstrated that the interaction of FcγR with immune complexes can stimulate the migration of DCs from peripheral tissues to draining lymph nodes *via* an increase of CCR7 expression (11). Therefore, in future investigations, it would be worthwhile evaluating whether the passive transfer of sera and/or IgG isolated from sensitized mice would modify the kinetics of skin DC migration to local lymph nodes and modulate the expression of

CCR7. In this study, we chose to focus on the three main skin DC subsets (LC, cDC1 and cDC2). However, it may be important to look at other skin APC populations that have been described previously (1, 12, 13).

In previous work, Campana *et al.* demonstrated that epicutaneous allergen application using atopy patch tests was able to boost an allergen-specific cellular response in allergic patients. However, no effect was shown in non-allergic individuals (14). Therefore, the authors suggested that allergen-specific IgE could facilitate allergen uptake by skin DC in humans as it has been previously shown with peripheral blood DC (15). Our data agree with this hypothesis but rather suggest a predominant role for IgG in mice, instead of IgE. This apparent mismatch could be explained by the difference between the two experimental systems that have been used (i.e., Human *versus* mouse). Indeed, our results show that FcεR are poorly expressed by LC and moderately expressed by dermal DC in mice. This is consistent with previous data suggesting that FcεR is not expressed in murine LC (16, 17). Overall, our data strongly suggest that IgG antibodies induced by OVA-sensitization form complexes with OVA administered epicutaneously that will be more efficiently captured by FcγR-expressing DC than free OVA. Additional experiments are warranted to confirm and illustrate that assumption. Additionally, it would be interesting to evaluate how these preclinical results are translated to the clinic, especially in patients undergoing EPIT for whom a progressive increase of allergen-specific IgG4 (human equivalent of mouse IgG1) has been observed (18). Our previous data generated in sensitized mice showed that the application of allergen-loaded patches on intact skin leads to an increase of PD-L2 expression and a concomitant decrease of CD86 expression in allergen-positive skin DC (19). Interestingly, this tolerogenic profile is not observed when patches are applied on naïve animals. In line with these observations, our recent preliminary data showed that injection of 2.4G2 blocking antibody prior to patch application had no impact on the subsequent modulation of PD-L2 and CD86 expression in OVA-positive DCs (**Figure S7A**). Of note, in mouse, 2.4G2 blocking antibodies bind to both FcγRIIB, which is an inhibitory receptor, and FcγRIII, which is an activating receptor. Therefore, it would be interesting in future experiments to explore the respective role of FcγRIIB and FcγRIII, as well as the role of other FcRs such as FcγRI, FcγRIV and FcεRs, in the modulation of skin DC activation between naïve and sensitized individuals. Interestingly, the differential expression of CD86 and PD-L2 observed between sensitized and naïve mice was not seen in OVA-negative DCs, except for CD86 in LC and cDC2 (**Figure S7B**). Of note, the relevance of the results obtained for cDC2 is unclear due to the low proportion of OVA-negative cells measured in that subset. For LCs, however, we cannot exclude an indirect impact of keratinocytes that are known to express several FcγRs (20–23). Future studies should explore the specific role of keratinocytes in LC activation, and how they may be modulated by specific humoral responses. In these future experiments, it would also be relevant to include additional groups of control mice that receive "blank" epicutaneous patches (containing excipient without OVA) to avoid any potential bias linked to patch application and/or excipient (PBS). In addition, it would also be worthwhile addressing whether antigen internalization pathways in skin DCs are different between sensitized and naïve mice and how FcRs may be involved in this internalization. In previous flow cytometry studies performed on permeabilized and non-permeabilized cells, we originally showed that permeabilization leads to a loss of OVA-positive DC subpopulations isolated from naïve mice, while it had no impact on DCs isolated from sensitized animals (**Figure S8**). Therefore, we hypothesized that antigen uptake by skin DCs in sensitized animals followed a pathway involving permeabilization-resistant vesicles. In a preliminary experiment, we evaluated by confocal microscopy whether clathrin vesicles were involved in OVA uptake by skin cells (**Figure S9**). In sensitized animals, we clearly showed intra-cytoplasmic vesicles containing OVA in MHC-II-high cells that might correspond to DCs. By contrast, OVA-positive DCs were very rare in the samples isolated from naïve animals. Although these data confirmed that OVA antigen was internalized by OVA-positive DCs following 6 hours of patch application, we did not show any clear co-localization between clathrin and OVA, suggesting that other pathways are involved.

Our previous data generated in murine and porcine models demonstrated that epicutaneous patches can also be used as a vaccine delivery platform, which is especially efficacious at boosting specific pre-existing immunity (24–26). However, several studies have highlighted the fact that pre-existing immunity, especially antibodies directed against a specific antigen, may interfere with the induction of immune response to an homologous antigen administered as a vaccine (27–31). Interestingly, this interference could be partially overcome by using mucosal routes of immunization such as intranasal administration (32–34). This antibody-mediated interference could result from multiple mechanisms including local antigen destruction by macrophages (35). Our results strongly suggest that pre-existing antibodies did not interfere with the uptake of an epicutaneously-delivered antigen by skin DC, suggesting that the epicutaneous route, similar to the mucosal route of immunization, may alleviate the loss of vaccine efficacy in seropositive individuals. However, in view of these preliminary results, further studies are needed to evaluate the benefit of the epicutaneous route of immunization over the "classical" parenteral route for boosting immune responses by bypassing the interfering effect of preexisting antibodies. If confirmed, this could give a solid advantage to epicutaneous delivery for boosting vaccine responses, and also suggest a role for this delivery route in priming of vaccine responses in seropositive individuals, such as young infants who have maternal antibodies.

DATA AVAILABILITY STATEMENT

The original contributions presented in the study are included in the article/**Supplementary Material**. Further inquiries can be directed to the corresponding author.

ETHICS STATEMENT

The animal study was reviewed and approved by CEEA127 - DBV Technologies.

AUTHOR CONTRIBUTIONS

P-LH, LM, and HS designed experiments. P-LH, CP, NA, NO, LG, AP, AB, VD and J-LL managed and performed experiments. P-LH, LM and HS analyzed data and wrote the manuscript. All authors contributed to the article and approved the submitted version.

ACKNOWLEDGMENTS

The authors wish to acknowledge Fred Finkelman for his advice on blocking antibody use, Marie Jessel and Justine Marathé for their continuous support in the animal facility, and Dianne Campbell, Katharine Bee, and Katie Matthews for proofreading the manuscript. The authors also thank Meriem Garfa-Traore and Louison Lallement (SFR Necker, UMS 24) for their help on confocal microscope acquisition.

SUPPLEMENTARY MATERIAL

The Supplementary Material for this article can be found online at: https://www.frontiersin.org/articles/10.3389/fimmu.2021.609029/full#supplementary-material

Supplementary Figure 1 | Measurement of IgG1 titers from sensitized donor mice and naïve recipient mice. Blood samples were collected from OVA-sensitized mice and pooled (Szd, donor mice, in blue). This serum pool was injected to naïve recipient mice (Sera Szd, Recipient mice, in blue). As negative controls, mice received pooled sera from naïve mice (Sera Nve, Recipient mice, in red) or were kept untreated (No transfer, in white). OVA-specific IgG1 titers were measured by quantitative ELISA from the pool of sera collected in sensitized donor mice or from blood samples collected in recipient mice, 24 hours after passive transfer. Data are median and interquartile ranges of individual values (N = 6 per group or recipient mice). P values were determined using the Mann-Whitney test (**, P<0.01).

Supplementary Figure 2 | Gating strategy used for the analysis of skin cells by FACS. Skin samples were collected 6 hours after patch application and incubated 2 hours at 37°C in 1 mL of Liberase TM prepared in basic medium (RPMI + PS + 55 µM BME + 20 mM HEPES). Then 500 µl of basic medium containing 500 µg/mL of DNase I and 15 mM of EDTA were added to stop the enzymatic reaction and skin samples were homogenized using a Medimachine tissue homogenizer for 8 min. Cells were filtered on 50 µm Filcon and labeled as follow: Cells were incubated 15 min at 4°C with 50 µl of FcBlock in microplates. Cells were washed with MACS buffer and incubated 25 min at 4°C with 50 µl of anti-Epcam-PE-Vio770, anti-CD11b-PerCP-Vio700, anti-MHCII-VioBlue and anti-XCR1-Vio770. Cells were then washed with PBS and incubated 15 min at room temperature with Zombie aqua viability marker. Cells were finally acquired on a MACSquant and gated as described using FlowJo software.

Supplementary Figure 3 | Gating strategy used for the analysis of lymph node cells by FACS. The two brachial lymph nodes of each mouse were harvested in 1 mL of FACS buffer in individual petri dishes. One mL of Liberase (0.52U/mL)/DNase I (50µg/mL) in MACS buffer was added in each Petri Dish. Each LN was flushed with a 1 mL syringe, incubated for 20 min at 37°C, and then 250 µl of EDTA 100 mM was added to each Petri Dish to stop the reaction. LN cell suspensions were obtained by dissociation and filtration on a cell strainer (100 µm). Cells were counted, labeled and analyzed as follow: Cells were incubated 15 min at 4°C with 50 µl of FcBlock in microplates. Cells were washed with MACS buffer and incubated 25 min at 4°C with 50 µl of anti-Epcam-PE-Vio770, anti-CD11b-PerCP-Vio700, anti-MHCII-VioBlue, anti-CD11c-PE and anti-XCR1-Vio770. Cells were then washed with PBS and incubated 15 min at room temperature with Zombie aqua viability marker. Cells were finally acquired on a MACSquant and gated as described using FlowJo software.

Supplementary Figure 4 | Analysis of Fc receptor expression in non-permeabilized skin DCs. Mice were treated as described in **Figure 1**. The relative expression of Fc receptors was evaluated from non-permeabilized cells by measuring MFI. Data are median of individual MFI (N = 8 per group). The level of significance indicated for patched mice results from the comparison to non-patched mice. P values were determined according to the Mann-Whitney test (*, P<0,05; **, P<0.01; ***, P<0.001; n.s., non-significant).

Supplementary Figure 5 | Graphical representation of FcR expression data. Mice were treated as described in **Figure 1**. The relative expression of Fc receptors was evaluated from permeabilized and non-permeabilized cells by measuring MFI, as indicated. Data are median and interquartile range of individual MFI (N = 8 per group). P values were determined according to the Mann-Whitney test (*, P<0,05; **, P<0.01; ***, P<0.001; n.s., non-significant).

Supplementary Figure 6 | Passive transfer of IgG-depleted sera does not modify the number of allergen-positive DCs in local lymph nodes. Mice received IgG-depleted sera (in green) originated from OVA-sensitized mice. As negative control, mice received sera originated from naïve mice. The day after, recipient mice received a patch containing OVA-AF488 on depilated back or remained untreated as a negative control (in white). Forty-eight hours after patch application, brachial draining lymph nodes were collected, and cells were analyzed by FACS. The number of OVA positive cells was measured among migratory Langerhans cells, cDC1 and cDC2, as indicated (N = 10 per group). Data are median and interquartile ranges of individual values. P values were determined according to the Mann-Whitney test (n.s., non-significant).

Supplementary Figure 7 | Involvement of FcγR has no impact on the tolerogenic profile of skin DC induced by allergen uptake. Mice were treated as described in **Figure 4**. Six hours after patch application, a skin sample corresponding to the patch application area was collected and cells were analyzed by Flow Cytometry. PD-L2 (top panels) and CD86 (bottom panels) expression was evaluated in OVA-positive DCs **(A)** or OVA-negative DCs **(B)** by measuring the median of fluorescence intensity (MFI). PD-L2-PE (clone MIH37, Miltenyi Biotec) and CD86-APC (clone PO3.3, Miltenyi Biotec) were used for cell surface immunolabeling. Data are Median and interquartile ranges of individual values (N = 8 per group, single experiment). P values were determined according to the Mann-Whitney test (*, P<0.05; **, P<0.01; ***, P<0.001; n.s., non-significant).

Supplementary Figure 8 | Cell permeabilization leads to the loss of OVA by skin DC isolated from naïve mice. Mice were treated as described in **Figure 1**. Six hours after patch application, a skin sample corresponding to the patch application area was collected and cells were analyzed by flow cytometry. The percentage of OVA-positive Langerhans cells, cDC1 and cDC2 was measured from permeabilized or non-permeabilized cells, as indicated. Data are median and interquartile ranges of individual values (N = 9-10 per experimental group, single experiment). P values were determined according to the Mann-Whitney test (****, P<0.0001).

Supplementary Figure 9 | Allergen delivery using epicutaneous patch leads to clathrin-independent allergen uptake by skin DCs. OVA-sensitized or naïve mice received a patch containing OVA-AF488 on depilated back. Six hours after patch application, a skin sample corresponding to the patch application area was collected and homogenized. Cells were deposited on a poly-L-lysine-coated coverslip and labeled with rat anti-mouse MHC-II and rabbit anti-clathrin heavy chain associated to relevant fluorochrome-conjugated secondary antibodies. Cells were acquired on a LMS 700 confocal microscope. A representative photograph of cells isolated from sensitized mice is shown.

REFERENCES

1. Malissen B, Tamoutounour S, Henri S. The origins and functions of dendritic cells and macrophages in the skin. *Nat Rev Immunol* (2014) 14:417–28. doi: 10.1038/nri3683
2. Mondoulet L, Dioszeghy V, Ligouis M, Dhelft V, Dupont C, Benhamou P-H. Epicutaneous immunotherapy on intact skin using a new delivery system in a murine model of allergy. *Clin Exp Allergy* (2010) 40:659–67. doi: 10.1111/j.1365-2222.2009.03430.x
3. Mondoulet L, Dioszeghy V, Ligouis M, Dhelft V, Puteaux E, Dupont C, et al. Epicutaneous Immunotherapy Compared with Sublingual Immunotherapy in Mice Sensitized to Pollen (Phleum pratense). *ISRN Allergy* (2012) 2012:375735. doi: 10.5402/2012/375735
4. Dioszeghy V, Mondoulet L, Dhelft V, Ligouis M, Puteaux E, Benhamou P-H, et al. Epicutaneous immunotherapy results in rapid allergen uptake by dendritic cells through intact skin and downregulates the allergen-specific response in sensitized mice. *J Immunol* (2011) 186:5629–37. doi: 10.4049/jimmunol.1003134
5. Dioszeghy V, Mondoulet L, Dhelft V, Ligouis M, Puteaux E, Dupont C, et al. The regulatory T cells induction by epicutaneous immunotherapy is sustained and mediates long-term protection from eosinophilic disorders in peanut-sensitized mice. *Clin Exp Allergy* (2014) 44:867–81. doi: 10.1111/cea.12312
6. Mondoulet L, Dioszeghy V, Puteaux E, Ligouis M, Dhelft V, Plaquet C, et al. Specific epicutaneous immunotherapy prevents sensitization to new allergens in a murine model. *J Allergy Clin Immunol* (2015) 135:1546–57. doi: 10.1016/j.jaci.2014.11.028
7. Gomez de Agüero M, Vocanson M, Hacini-Rachinel F, Taillardet M, Sparwasser T, Kissenpfennig A, et al. Langerhans cells protect from allergic contact dermatitis in mice by tolerizing CD8(+) T cells and activating Foxp3 (+) regulatory T cells. *J Clin Invest* (2012) 122:1700–11. doi: 10.1172/JCI59725
8. Seneschal J, Clark RA, Gehad A, Baecher-Allan CM, Kupper TS. Human epidermal Langerhans cells maintain immune homeostasis in skin by activating skin resident regulatory T cells. *Immunity* (2012) 36:873–84. doi: 10.1016/j.immuni.2012.03.018
9. Mondoulet L, Dioszeghy V, Puteaux E, Ligouis M, Dhelft V, Letourneur F, et al. Intact skin and not stripped skin is crucial for the safety and efficacy of peanut epicutaneous immunotherapy (EPIT) in mice. *Clin Transl Allergy* (2012) 2:22. doi: 10.1186/2045-7022-2-22
10. Dioszeghy V, Mondoulet L, Laoubi L, Dhelft V, Plaquet C, Bouzereau A, et al. Antigen uptake by Langerhans cells is required for the induction of regulatory T cells and the acquisition of tolerance during epicutaneous immunotherapy in OVA-sensitized mice. *Front Immunol* (2018) 9:1951. doi: 10.3389/fimmu.2018.01951
11. Clatworthy MR, Aronin CEP, Mathews RJ, Morgan NY, Smith KGC, Germain RN. Immune complexes stimulate CCR7-dependent dendritic cell migration to lymph nodes. *Nat Med* (2014) 20:1458–63. doi: 10.1038/nm.3709
12. Guilliams M, Dutertre CA, Scott CL, McGovern N, Sichien D, Chakarov S, et al. Unsupervised High-Dimensional Analysis Aligns Dendritic Cells across Tissues and Species. *Immunity* (2016) 45:669–84. doi: 10.1016/j.immuni.2016.08.015
13. Henri S, Guilliams M, Poulin LF, Tamoutounour S, Ardouin L, Dalod M, et al. Disentangling the complexity of the skin dendritic cell network. *Immunol Cell Biol* (2010) 88:366–75. doi: 10.1038/icb.2010.34
14. Campana R, Moritz K, Neubauer A, Huber H, Henning R, Brodie TM, et al. Epicutaneous allergen application preferentially boosts specific T cell responses in sensitized patients. *Sci Rep* (2017) 7:1–11. doi: 10.1038/s41598-017-10278-1
15. Sharquie IK, Al-Ghouleh A, Fitton P, Clark MR, Armour KL, Sewell HF, et al. An investigation into IgE-facilitated allergen recognition and presentation by human dendritic cells. *BMC Immunol* (2013) 14:54. doi: 10.1186/1471-2172-14-54
16. Hayashi S, Matsuda H, Okumura K, Ra C. Mouse Langerhans cells do not express the high-affinity receptor for IgE. *Arch Dermatol Res* (1999) 291:241–3. doi: 10.1007/s004030050401
17. Hertl M, Asada H, Katz SI. Murine epidermal Langerhans cells do not express the low-affinity receptor for immunoglobulin E, FcεRII (CD23). *J Invest Dermatol* (1996) 106:221–4. doi: 10.1111/1523-1747.ep12340546
18. Sampson HA, Shreffler WG, Yang WH, Sussman GL, Brown-Whitehorn TF, Nadeau KC, et al. Effect of varying doses of epicutaneous immunotherapy vs placebo on reaction to peanut protein exposure among patients with peanut sensitivity: A randomized clinical trial. *JAMA - J Am Med Assoc* (2017) 318:1798–809. doi: 10.1001/jama.2017.16591
19. Laoubi L, Sampson HA, Mondoulet L, Nicolas J, Dioszeghy V, Vocanson M. Skin Dendritic Cells Progressively Subvert The Activation Of Pathogenic Type-2 Immunity Upon Epicutaneous Allergen Immunotherapy. *J Allergy Clin Immunol* (2019) 143:AB242. doi: 10.1016/j.jaci.2018.12.739
20. Bjerke JR, Tigalonova M, Matre R. IgG-Fc receptors in stratum granulosum: An immunological defence in human skin? *Acta Derm Venereol* (1994) 74:429–32. doi: 10.2340/0001555574429432
21. Tigalonowa M, Bjerke JR, Livden JK, Matre R. The distribution of FcγR I, FcγR II and FcγR III on Langerhans' cells and keratinocytes in normal skin. *Acta Derm Venereol* (1990) 70:385–90. doi: 102340/0001555570385390
22. Cauza K, Grassauer A, Hinterhuber G, Horvat R, Rappersberger K, Wolff K, et al. FcγRIII expression on cultured human keratinocytes and upregulation by interferon-γ. *J Invest Dermatol* (2002) 119:1074–9. doi: 10.1046/j.1523-1747.2002.19527.x
23. Tigalonowa M, Bjerke JR, Matre R. Fcγ-receptors of Langerhans' cells and keratinocytes in suspension from normal skin characterized using soluble immune complexes and monoclonal antibodies. *Acta Derm Venereol* (1991) 71:99–103. doi: 10.2340/000155557199103
24. Gavillet BM, Mondoulet L, Dhelft V, Eberhardt CS, Auderset F, Pham HT, et al. Needle-free and adjuvant-free epicutaneous boosting of pertussis immunity: Preclinical proof of concept. *Vaccine* (2015) 33:3450–5. doi: 10.1016/j.vaccine.2015.05.089
25. Hervé P-L, Descamps D, Deloizy C, Dhelft V, Laubreton D, Bouguyon E, et al. Non-invasive epicutaneous vaccine against Respiratory Syncytial Virus: Preclinical proof of concept. *J Control Release* (2016) 243:146–59. doi: 10.1016/j.jconrel.2016.10.003
26. Hervé P-L, Dhelft V, Plaquet C, Rousseaux A, Bouzereau A, Gaulme L, et al. Epidermal micro-perforation potentiates the efficacy of epicutaneous vaccination. *J Control Release* (2019) 298:12–26. doi: 10.1016/j.jconrel.2019.02.004
27. Saxena M, Van TTH, Baird FJ, Coloe PJ, Smooker PM. Pre-existing immunity against vaccine vectors - friend or foe? *Microbiology* (2013) 159:1–11. doi: 10.1099/mic.0.049601-0
28. Pichla-gollon SL, Lin S, Hensley SE, Lasaro MO, Herkenhoff-haut L, Drinker M, et al. Effect of Preexisting Immunity on an Adenovirus Vaccine Vector: In Vitro Neutralization Assays Fail To Predict Inhibition by Antiviral Antibody In Vivo. *J Virol* (2009) 83:5567–73. doi: 10.1128/JVI.00405-09
29. Haut LH, Ratcliffe S, Pinto AR, Ertl H. Effect of preexisting immunity to adenovirus on transgene product-specific genital T cell responses on vaccination of mice with a homologous vector. *J Infect Dis* (2011) 203:1073–81. doi: 10.1093/infdis/jiq161
30. Edwards KM. Maternal antibodies and infant immune responses to vaccines. *Vaccine* (2015) 33:6469–72. doi: 10.1016/j.vaccine.2015.07.085
31. Gellin B, Modlin JF, Crowe JE. Influence of maternal antibodies on neonatal immunization against respiratory viruses. *Clin Infect Dis* (2001) 33:1720–7. doi: 10.1086/322971
32. Pandey A, Singh N, Vemula SV, Couëtil L, Katz JM, Donis R, et al. Impact of preexisting adenovirus vector immunity on immunogenicity and protection conferred with an adenovirus-based H5N1 influenza vaccine. *PloS One* (2012) 7:1–9. doi: 10.1371/journal.pone.0033428
33. Herve P-L, Raliou M, Bourdieu C, Dubuquoy C, Petit-Camurdan A, Bertho N, et al. A Novel Subnucleocapsid Nanoplatform for Mucosal Vaccination against Influenza Virus That Targets the Ectodomain of Matrix Protein 2. *J Virol* (2014) 88:325–38. doi: 10.1128/jvi.01141-13
34. Zhang F, Peng B, Chang H, Zhang R, Lu F, Wang F. Intranasal Immunization of Mice to Avoid Interference of Maternal Antibody against H5N1 Infection. *PloS One* (2016) 11:e0157041. doi: 10.1371/journal.pone.0157041
35. Kim D, Huey D, Oglesbee M, Niewiesk S. Insights into the regulatory mechanism controlling the inhibition of vaccine-induced seroconversion by maternal antibodies. *Blood* (2011) 117:6143–52. doi: 10.1182/blood-2010-11-320317

Conflict of Interest: All authors were employed by DBV Technologies at the time of completion of this work. P-LH, CP, J-LL, LM, and HS hold shares in the company.

frontiers in Immunology

REVIEW
published: 29 March 2021
doi: 10.3389/fimmu.2021.641307

Moving on From Sipuleucel-T: New Dendritic Cell Vaccine Strategies for Prostate Cancer

Sarah I. M. Sutherland[1,2,3,4], *Xinsheng Ju*[1,2], *L. G. Horvath*[2,4,5] *and Georgina J. Clark*[1,2*]

[1] *Dendritic Cell Research, ANZAC Research Institute, Concord, NSW, Australia,* [2] *Faculty of Medicine and Health, University of Sydney, Sydney, NSW, Australia,* [3] *Department of Medical Oncology, Concord Repatriation General Hospital, Concord, NSW, Australia,* [4] *Department of Medical Oncology, Chris O'Brien Lifehouse, Camperdown, NSW, Australia,* [5] *Garvan Institute of Medical Research, Darlinghurst, NSW, Australia*

Tumors evade the immune system though a myriad of mechanisms. Using checkpoint inhibitors to help reprime T cells to recognize tumor has had great success in malignancies including melanoma, lung, and renal cell carcinoma. Many tumors including prostate cancer are resistant to such treatment. However, Sipuleucel-T, a dendritic cell (DC) based immunotherapy, improved overall survival (OS) in prostate cancer. Despite this initial success, further DC vaccines have failed to progress and there has been limited uptake of Sipuleucel-T in the clinic. We know in prostate cancer (PCa) that both the adaptive and the innate arms of the immune system contribute to the immunosuppressive environment. This is at least in part due to dysfunction of DC that play a crucial role in the initiation of an immune response. We also know that there is a paucity of DC in PCa, and that those there are immature, creating a tolerogenic environment. These attributes make PCa a good candidate for a DC based immunotherapy. Ultimately, the knowledge gained by much research into antigen processing and presentation needs to translate from bench to bedside. In this review we will analyze why newer vaccine strategies using monocyte derived DC (MoDC) have failed to deliver clinical benefit, particularly in PCa, and highlight the emerging antigen loading and presentation technologies such as nanoparticles, antibody-antigen conjugates and virus co-delivery systems that can be used to improve efficacy. Lastly, we will assess combination strategies that can help overcome the immunosuppressive microenvironment of PCa.

Keywords: dendritic cell, vaccine, prostate cancer, tumor, immune system, immunotherapy

OPEN ACCESS

Edited by:
Irina Caminschi,
Monash University, Australia

Reviewed by:
Yifan Zhan,
Walter and Eliza Hall Institute of Medical Research, Australia
Richard A. Kroczek,
Robert Koch Institute (RKI), Germany

****Correspondence:***
Georgina J. Clark
georgina.clark@sydney.edu.au

Specialty section:
This article was submitted to Antigen Presenting Cell Biology, a section of the journal Frontiers in Immunology

Received: *14 December 2020*
Accepted: *12 February 2021*
Published: *29 March 2021*

Citation:
Sutherland SIM, Ju X, Horvath LG and Clark GJ (2021) Moving on From Sipuleucel-T: New Dendritic Cell Vaccine Strategies for Prostate Cancer. Front. Immunol. 12:641307. doi: 10.3389/fimmu.2021.641307

INTRODUCTION

Immune evasion has long been recognized as a problem in prostate cancer (PCa). To date checkpoint inhibitors that aim to release the "brakes" on T cell expansion have proved disappointing (1–3). Dendritic cells (DC) bridge the gap between the innate and adaptive immune response, playing a crucial role in tipping the direction toward inflammation or tolerance. Manipulating this balance through DC vaccine therapy has therapeutic potential. This is not a novel concept (4); in 2010, Sipuleucel-T was the first DC therapy approved by the FDA for the treatment of metastatic castrate resistant prostate cancer (mCRPCa) (5). Our understanding of DC biology has vastly increased over the last decade, yet no further DC therapy has been FDA approved.

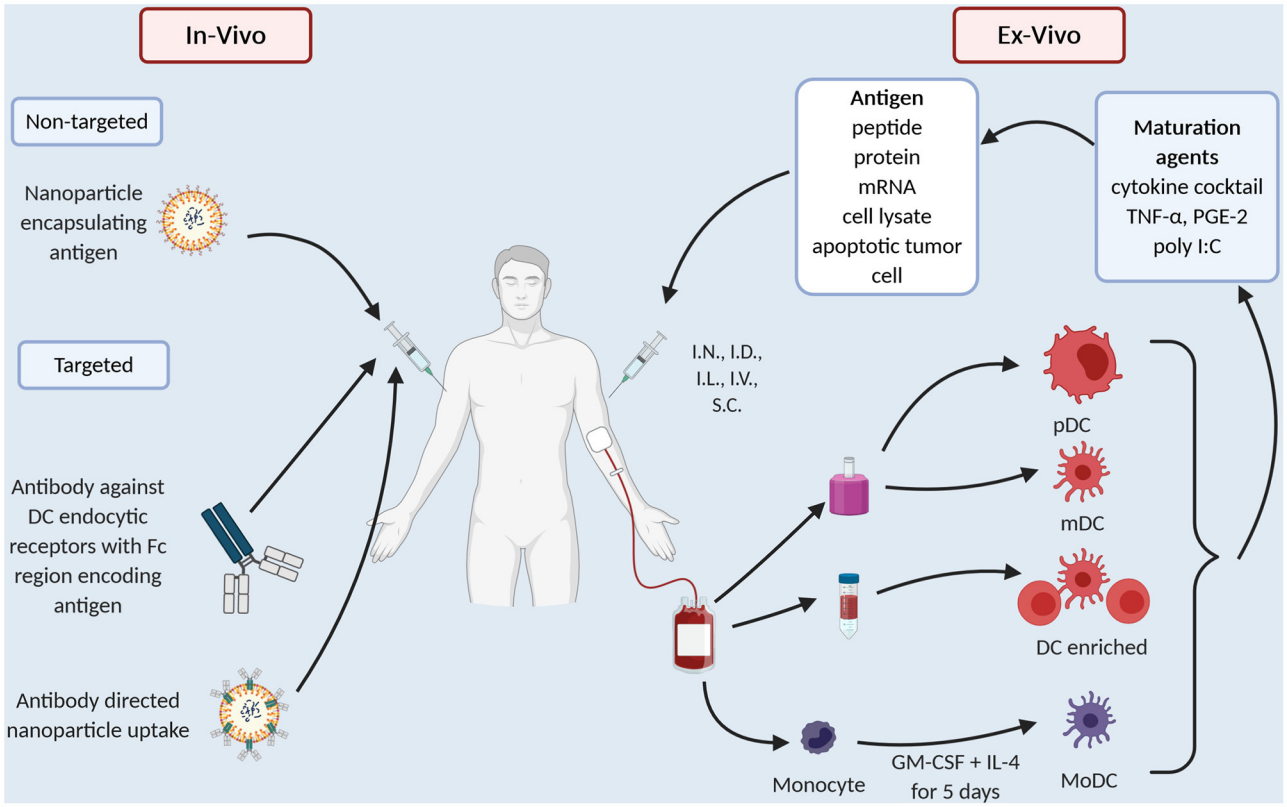

FIGURE 1 | Current dendritic cell vaccination technologies.

In this review we will assess the strengths and weaknesses of prior approaches and then look at the potential of new technologies to drive improvements. Here we review how these technologies apply to PCa and suggest combination therapies that might overcome the immunosuppressive microenvironment leading to better clinical outcomes.

DENDRITIC CELL VACCINATION IN PCA

In PCa DC are dysfunctional and key orchestrators of its immunosuppressive microenvironment (6–11). Sipuleucel-T demonstrates that taking antigen presenting cells (APC) from PCa patients, pulsing them with tumor peptide and inducing their maturation prior to returning them back to patients, primes T cells that track to the tumor itself (12). In a pooled analysis of two, phase III, randomized control trials (RCT) in minimally or asymptomatic mCRPCa, Sipuleucel-T, improved overall survival (OS) to 23 months from 19 months [Hazard Ratio (HR) 1.50, 95% CI: 1.10–2.05, $p = 0.01$] (13). This OS benefit was corroborated by a third trial where OS was similarly increased by 4.1 months (5). Despite such promise the use of Sipuleucel-T in the clinic remains low.

One reason is skepticism over the trial results. It has been proposed that the control arm did worse than anticipated and that the benefit seen was in fact due to the harm of apheresis, where fewer PBMC were returned to patients in the control arm than the treatment arm (14). This has not been helped by a plethora of further DC-based therapy trials performed with monocyte-derived DC (MoDC) that despite showing immunological responses, have failed to show real clinical benefit.

MoDC Vaccination

The common technical issue in any DC preparation is the low prevalence of DC in the peripheral blood, ranging 0.1–1% of peripheral blood mononuclear cells (PBMC) (15). Thus, early DC preparations such as Sipuleucel-T use a density gradient to prepare an APC enriched preparation (**Figure 1**). "Second generation" DC vaccines use strategies that differentiate monocytes into dendritic like cells called MoDC (**Figure 1**), creating a more readily available source of APC as monocytes make up ∼10% of PBMC compared to 1% for DC. MoDC are prepared by separating $CD14^+$ cells from PBMC either by their ability to adhere to plastic overnight culture or by anti-CD14 microbeads and magnetic separation. $CD14^+$ cells are then cultured with cytokines, typically GM-CSF and IL-4 for 4–5 days, after which they display an immature DC like phenotype (16). When cultured with tumor antigen in the form of peptide or protein these cells cross-present and induce T cell proliferation (16). In melanoma patients, whilst only a small proportion i.e.,

TABLE 1 | Published DC vaccination trials in prostate cancer.

Cell Type and Maturation	Antigen	Trials	Population	Phase	Pt #	Intervention:	Route ± adjuvant	Outcome
Immature MoDC						**Peptide (HLA-A2)**		
	PSMA-P1 and PSMA-P2	Murphy et al. (18)	CRPCa	1	51	Arm 1 + 2: Peptide ($n = 20$) Arm 3: DC ($n = 12$) Arm 4 + 5: DC Vaccine ($n = 19$) Arm 1 + 4: PSMA-1 Arm 2 + 5: PSMA-2	I.V.	**Primary:** *Safety:* (hypotension 24/51, fatigue 3/51 **Secondary:** *Immunological:* T cell proliferation in response to peptide (↑ in HLA-A2+ DC vac pts) *Clinical:* Peptide (PR 2/19, SD 2/19) DC (PR 0/12, SD 2/12) DC Vaccine (PR 5/20, SD 3/20)
	PSMA-P1 and PSMA-P2	Murphy et al. (19)	CRPCa	II	33		I.V.	*Clinical:* CR 2/25, PR 6/25, 1/25 SD
	PSMA-P1 and PSMA-P2	Murphy et al. (20)	Recurrent CSPCa	II	41		I.V.	*Clinical:* CR 1/37, PR 10/37
	PSMA-P1 and P2 + KLH	Murphy et al. (21)	CRPCA	II	17		I.V.	*Safety:* fever, fatigue, muscle cramps *Clinical:* CR 1/17, PR 3/17
	$PSMA_{4-12}$	Knight et al. (22)	CRPCa—HLA-A2 positive	I	12	Cells irradiated prior to infusion	S.C.	*Safety:* Fatigue 4/12, fever 4/12, pain 4/12 *Immunological:* ELISPOT 0/12
	$PSA_{146-154}$	Perambakam et al. (23)	CSPCa	I	28	Cohort 1: high risk locally advanced disease Cohort 2: metastatic disease Arm A: Peptide + GM-CSF (I.D.) Arm B: MoDC	I.L.	*Immunological:* DTH Arm A 9/14 Arm B: 5/14
						Protein		
	PSA	Barrou et al. (24)	bcrCSPCa	II	26	Used GM-CSF and IL-13 rather than IL-14	I.V., S.C., I.D.	*Safety:* 3/24 macular rash, 2/24 G2 increase in bilirubin, 1/24 asthenia, 1/24 halitosis *Clinical:* Circulating tumor cells 6/6. PSA response 0/24. *Immunological:* ELISPOT response to PSA 4/24 developed a response on treatment No antibody response.

(Continued)

TABLE 1 | Continued

Cell Type and Maturation	Antigen	Trials	Population	Phase	Pt #	Intervention:	Route ± adjuvant	Outcome
						Cell-lysate		
	LNCaP, DU145	Pandha et al. (25)	CRPCa	I/II	11		I.D.	**Primary:** *Feasibility:* Vaccine produced in 11/11 pts *Safety:* nil significant local or systemic toxicity **Secondary:** *Clinical:* PSA response 0/11, ↑PSADT in 3/11 *Radiological:* CR 0/11, PR 0/11, SD 4/11 *Immunological:* DTH response 0/11, ELISPOT response 6/11
						mRNA		
	PSA	Heiser et al. (26)	mPrCa	I	16		I.V., I.D.	*Feasibility:* assigned cell dose given 12/13 patients *Safety:* fever and flu-like sx 4/13, injection site reaction 4/13 *Immunological Response:* ELISPOT 9/9
Mature MoDC						**Peptide (HLA-A2)**		
TNF-α, PGE-2	$PSCA_{14-22}$ $PSA1_{141-150}$ $PSA2_{146-154}$ $PSA3_{154-163}$	Thomas-Kaskel et al. (27)	CRPCa HLA-A2+	I/II	12	Arm 1: PSCA peptide + PSA peptides Arm 2: cell penetrating peptide (CPP)-PSCA + PSA peptides	S.C.	**Primary:** *Feasibility:* 10/12 pts received at least 3 vaccinations *Safety:* no reported toxicity **Secondary:** *Immunological:* DTH to tumor peptide 5/10, Tetramer 1/10 *Clinical:* SD 4/10
	$PSA1_{141-150}$ $PSA2_{146-154}$ $PSA3_{154-163}$	Hildenbrand et al. (28)	CRPCa	I	15		I.D.	**Primary:** *Clinical Response:* PR 1/12, SD 4/12 *Biochemical Response:* 1/12, ↑PSADT **Secondary:** *QOL:* no change *Immunological:* DTH response: 9/12 *Feasibility:* 12/15 enrolled evaluable *Safety:* fever 11/12, local erythema 11/12, 6/12 bone pain, 3/12 slight articular pain, 1/12 insomnia

(Continued)

TABLE 1 | Continued

Cell Type and Maturation	Antigen	Trials	Population	Phase	Pt #	Intervention:	Route ± adjuvant	Outcome
	$PSA_{146-154}$ $PSMA_{4-12}$ $PAP_{299-307}$	Zhuang et al. (29)	CRPCa	I	16		S.C.	*Immunological:* DTH response 4/12 *Clinical:* PR 3/16, 7/16 SD
Poly I:C	$PSMA_{154-163}$ $Survivin_{95-104}$	Xi et al. (30)	Non-mCRPCa	II	21	Arm 1: DC vaccine ($n = 11$) Arm 2: Docetaxel and prednisone ($n = 11$)	S.C.	*Safety:* local reaction 4/11, *Immunological:* DTH response 11/11, ELISPOT increased compared to docetaxel arm ($p = 0.048$) *Clinical:* DC arm vs. docetaxel *PR:* 3/11 vs. 0/11, SD 6/11 vs. 5/11
Cytokine cocktail	$PSA3_{154-163}$ $PSMA_{4-12}$ $Prostein_{31-39}$ $Survivin_{950104}$ $Trp\text{-}p8_{187-195}$	Fuessel et al. (31)	CRPCa	I	8		I.V., I.D.	*Safety:* local reaction *Clinical:* PSA response 1/8 *Immunological:* ELISPOT 4/8
	$PSCA_{14-22}$ $PAP_{299-307}$ $PSMA_{4-12}$ $PSA_{154-163}$	Waeckerle-Men et al. (32)	mCRPCa	I	6		I.D.	*Safety:* local reaction 5/6 *Clinical:* ↑PSADT 3/6 *Immunological:* ELISPOT 3/6, DTH 3/6
						Protein		
Cytokine cocktail	Tn-MUC1 + KLH	Scheid et al. (33) NCT00852007	Non-mCRPCa	I/II	17	Tn-MUC1+	I.N., I.D.	*Safety:* local reaction 16/17, G1 fatigue 1/, G1 insomnia *Clinical Response:* biochemical 0/16, PSADT increased in 11/16. *Immunological:* Intracellular response in $CD4^+$ CD8 T cells in 2/16, CD4 in 1/16, CD8 in 2/16.
						mRNA		
Cytokine cocktail	mRNA from DU145, LNCaP, PC3	Mu et al. (34)	CRPCa	I/II	20	Arm A: I.N. ($n = 10$) Arm B: I.D. ($n = 9$)	I.N. or I.D.	*Safety:* injection site reactions *Immune response:* ELISPOT 10.19 *Clinical:* Reduced PSA slope 13/19
						Cell lysate		
Cytokine cocktail	DU145 LNCaP PC3	Reyes et al. (35)	CRPCa	I	20		S.C.	*Safety:* 8/20 local erythema and pain, 1/20 hypertension *Feasibility:* 14/20 completed study protocol *QOL:* no change *Immunological:* ELISPOT 7/14, DTH 9/14. *Clinical:* PSA response 6/14

(Continued)

TABLE 1 | Continued

Cell Type and Maturation	Antigen	Trials	Population	Phase	Pt #	Intervention:	Route ± adjuvant	Outcome
						Apoptotic cell line		
TNF-α, PGE-2	LNCaP	Frank et al. (36) NCT00289341	bcrCSPCa or CRPCa	1	24	Arm1 : Vaccine weeks 1–7 ($n = 12$) Arm 2: Placebo weeks 1–7, vaccine weeks 8–14 ($n = 12$)	S.C	*Safety:* injection site reactions in the first 7 weeks, 11/12 in arm 1 vs. 2/12 arm 2 *Immunological:* DTH response 16/24, T cell proliferation response *Clinical:* ↑PSADT prevaccine vs. post vaccine ($P = 0.003$)
						Transfected DC		
	PSMA protein	Sonpavde et al. (37)	mCRPCa	I	18	MoDC transfected with adenoviral vector Ad5f35 encoding inducible human CD40 injected I.D. then given rimiducid IV 24 h later to induce CD40 expression on DC	I.D.	*Safety*: 18/18 local reaction, fatigue 6/18, myalgias 5/18, anemia 4/18, diarrhea 4/18, respiratory tract infection 4/18, hypocalcaemia 4/18, arthralgia 4/18 *Clinical*: PSA response 1/18, Radiological: 2/18
Enriched DC prep						**Protein**		
	PA2024 (GM-CSF and PAP)	Burch et al. (38)	CRPCa	I	13	Two infusions of DC with PAP alone and then three infusions of PA2024	I.V.	*Safety:* G1-2 fever 5/13, G1-2 myalgia 5/13, G1-2 fatigue 6/13, G3 fatigue 1/13, local reactions 4/13 *Immunological:* T cell proliferation 9/9, *Clinical:* PSA response 3/12
	PA2024 (GM-CSF and PAP)	Small et al. (39)	CRPCa	I/II	31	Arm 1: Sipuleucel-T Arm 2: Sipuleucel-T as well KLH loaded DC ($n = 5$)	I.V.	*Safety:* febrile reactions 15/102, G3 febrile reactions 2/102, myalgias 2/31, fatigue 1/31, urinary symptoms 5/31 *Immunological:* T cell proliferation 10/26, 16/31 Antibody response 16/31 *Clinical:* PSA response 3/31
	Mouse PAP	Fong et al. (40, 41)	PrCa	I	21	Arm 1: I.V. ($n = 9$) Arm 2: I.D. ($n = 6$) Arm 3: I.L. ($n = 6$)	I.V., I.L., I.D.	*Safety:* Transfusion reactions in 2/18 I.V. injections *Immunological:* T cell proliferation against mPAP 21/21 pts. Ag specific IFN-γ response 0/9 I.V., 4/6 I.D., 3/6 I.L.

(Continued)

TABLE 1 | Continued

Cell Type and Maturation	Antigen	Trials	Population	Phase	Pt #	Intervention:	Route ± adjuvant	Outcome
	PA2024 (GM-CSF and PAP)	Fong et al. (12) NCT00715104	Localized PrCa	II	42	Three doses Neoadjuvant treated prior to planned RP Arm 1: 4th injection 12 weeks post RP Arm 2: NO boost		*Safety:* fatigue, oral paresthesia *Immunological:* 57% pts had a 3-fold increase in tumor interface T cells
	PA2024 (GM-CSF and PAP)	Higano et al. (13)	Asymptomatic CRPCA	III	147	Arm 1: Placebo Arm 2: Sipuleucel-T	I.V.	*Clinical:* OS 19 vs. 23.2 months (HR 1.5, CI 1.1–2.05, $p = 0.011$) TTP 10 vs. 11 months (HR 1.26 0.95–1.58, $p = 0.111$)
	PA2024 (GM-CSF and PAP)	Kantoff et al. (5)	Asymptomatic CRPCA	III	512	Arm 1: Sipuleucel-T Arm 2: Placebo	I.V.	*Clinical:* OS 25.8 vs. 21.7 months (HR 0.78 CI 0.61–0.98, $p = 0.03$)
	PA2024 (GM-CSF and PAP)	Beer et al. (42)	bcrCSPCa	III	176	Pts with biochemical recurrence after RP were given 3–4 months of ADT and then randomized to: Arm 1: Sipuleucel-T Arm 2: Placebo	I.V.	**Primary:** *Biochemical Failure PSA > 3.0:* 18 vs. 15.4 months HR 0.93, $p = 0.73$) **Secondary:** *PSADT:* ↑PSADT 48% ($p = 0.038$) OS
DC						**Peptide (HLA-A2)**		
CD1c	$PSA_{174-183}$ $PSMA_{711-719}$ $PAP_{299-311}$ Control peptides: FMP GILGFVFTL KLH	Prue et al. (43)	Asymptomatic mCRPCa (HLA-A2)	I	14	All 3 injections of CD1c: Arm 1: I.D. 1×10^6 Arm 2: I.D. $1–5 \times 10^6$ Arm 3: I.V. 1×10^6 Arm 4: I.V. $1–5 \times 10^6$	I.V. or I.D.	**Primary:** *Safety:* fever and pain *Feasibility:* 12/12 underwent leukapheresis and vaccination, 11/12 received 2nd vaccination **Secondary:** *Immunological:* DTH response 0/12, ELISPOT response 0/12, Pentamer positive $CD8^+$ T cells 0/12 *Clinical:* PSA response 0/12

(Continued)

TABLE 1 | Continued

Cell Type and Maturation	Antigen	Trials	Population	Phase	Pt #	Intervention:	Route ± adjuvant	Outcome
CD1c pDC (protamine and mRNA)	NY-ESO-$1_{157-165}$ NY-ESO-1 (peptivator) MAGE-$C2_{336-34}$ MUC1 (peptivator) KLH (control)	Westdorp et al. (44) NCT02692976	Chemo naive CRPCa (HLA-A2)	II	21	Arm 1: mDC vaccination Arm 2: pDC vaccination Arm 3: mDC and pDC vaccinations	I.N.	*Safety:* anemia 15/21, flu like symptoms 10/21, fatigue 8/21 *Immune Response:* Dextramer positive T cells to NY-ESO-1 5/21, MAGE-C2 4/21, MUC-1 2/21 Antigen Specific $CD8^+$ T cells in DTH Response: 15/21 pts—no difference between arms *Clinical Response:* PSA response 2/21, Radiological 1/21
						Combination therapy		
Mature MoDC (poly I:C)	Cell lysate (LNCaP)	Podrazil et al. (45)	CRPCa	I/II	25	7 days of metronomic cyclophosphamide then 2 doses of vaccine and then 3 weekly docetaxel and vaccine	S.C. with Imiquimod	*Safety:* fatigue 17/350 *Immunological:* Intracellular cytokine response to PSA 11/23, MAGE-A1 6/23, MAGE-A2 3/23 *Antibody Response:* PSA 6/23, Mage A3 8/23 *Clinical:* PSA response 9/23
Mature MoDC (cytokine cocktail)	mRNA PAP and PSA	Kongsted et al. (46) NCT01446731	CRPCa	II	43	Arm 1: Docetaxel 75 mg/m^2 every 3 weeks Arm 2: Docetaxel 75 mg/m^2 every 3 weeks DCvac twice every 3 weeks for cycles 1–4 then once cycles 5–10	I.D.	**Primary:** Development of measurable peripheral immune *Response:* ELISPOT: 9/18, DTH: 3/18 **Secondary:** *Safety and Toxicity:* local reactions and rash, *Discontinuation of Treatment:* 21.1 vs. 57% *PSA Response:* 58 vs. 38%, $p = 0.21$ *PFS:* 5.5 vs. 5.7 months ($p = 0.62$) *DSS:* 21.9 vs. 25.1 months ($p = 0.60$)
DC enriched	PA2024 (GM-CSF and PAP)	Twardowski et al. (47)	mCRPCa	II	51	Arm A: sipuleucel-T alone ($n = 24$) Arm B: RT to single metastatic site followed by sipuleucel-T ($n = 25$)	I.V.	**Primary:** *Safety:* G2 fatigue 1/24 vs. 3/25 **Secondary:** ELISPOT IFNy ↑in Arm A compared to B ($p = 0.028$). PFS 2.46 vs. 3.65 months ($p = 0.06$)
DC enriched	PA2024 (GM-CSF and PAP)	Antonarkis et al. (48) NCT01431391	bcrCSPCa	II		Arm A: Sipuleucel-T followed by ADT 2 weeks after Arm B: ADT for 12 weeks then Sipuleucel-T	I.V.	**Primary:** ELISPOT—approx. 2-fold higher for Arm A than Arm B ($p = 0.001$) **Secondary:** Time to PSA progression 21.8 vs. 22.6 ($p = 0.357$)

(Continued)

TABLE 1 | Continued

Cell Type and Maturation	Antigen	Trials	Population	Phase	Pt #	Intervention:	Route ± adjuvant	Outcome
DC enriched	PA2024 (GM-CSF and PAP)	Scholz et al. (49)	mCRPCa NCT01832870	I	9	Ipilimumab and Sipuleucel-T	I.V.	*Safety:* well tolerated only 1 G1 rash *Immunological:* increase in humeral immunity against PA2024 and PAP
Poly I:C	Cell lysate (LNCaP)	Fucikova et al. (50) EudraCT 2009-017259-91	bcrCSPCa	I/II	27	1 week of metronomic cyclophosphamide then DC vaccine every 2–6 weeks for approx. up to all manufactured doses on average 12	S.C. with Imiquimod	*Immunological:* IFN-γ specific T cells to PSA 12/27, MAGE 6/27 *Antibody Response to:* PSA 9/27, MAGE 9/27 *Clinical:* increase in PSADT 22/25
DC enriched	PA2024 (GM-CSF and PAP)	Small et al. (51) NCT01487863	mCRPCA	II	69	Arm A: concurrent Sipuleucel-T and abiraterone Arm B: Sipuleucel-T for 10 weeks then abiraterone	I.V.	No difference in immune response
DC enriched	PA2024 (GM-CSF and PAP)	Rini et al. (52) NCT00027599	bcrCSPCa	I	22	Sipuleucel-T and bevacizumab	I.V.	*Clinical:* ↑PSADT 6.9 vs. 12.7 months post treatment ($p = 0.01$)
DC enriched	PA2024 (GM-CSF and PAP)	Jha et al. (53)	mCRPCa	II	46	Arm A: Sipuleucel-T + indoximod Arm B: Sipuleucel-T	I.V.	*Clinical:* PSA progression no diff PFS 10.3 vs. 4.1 months ($p = 0.011$)

Cytokine cocktail (TNF-α, IL-1β, IL-6, PGE2), mCRPCa, metastatic castrate resistant prostate cancer; bcrCSPCa, biochemical recurrence of castrate sensitive prostate cancer; DTH, delayed hypersensitivity, antigen specific response reported; PSADT, PSA doubling time; I.V., intravenous; I.N., intranodal; I.D., intradermal; S.C., subcutaneous.

4% of I.D., injected DC, migrate to local lymph nodes but those that do activate $CD8^+$ T cells in a melanoma model, thus overcoming microenvironment of melanoma (17). There have been several clinic trials in PCa with MoDC (**Table 1**). They vary in their mode of antigen delivery (protein, peptide, apoptotic tumor cells, cell lysate from tumor cell lines or mRNA) (**Table 1**, **Figure 1**), whether the MoDC are immature or mature and if matured what activation agent was used (**Table 1**, **Figure 1**). All these nuances have a profound impact on efficacy and applicability thus it is worth exploring these differences in more detail.

Mature vs. Immature DC

Firstly, early trials used immature MoDC and as one would expect, immature MoDC have reduced expression of activation markers, reduced ability to stimulate T cells (54, 55) and reduced ability to migrate (55). A meta-analysis that extracted individual patient data from 10 clinical trials of DC vaccines in PCa confirmed that immature MoDC preparations had less clinical benefit than mature MoDC (56). In melanoma patients immature and mature MoDC preps were compared head-to-head, again immature MoDC were less effective (57).

Different maturation agents have been used (**Table 1**, **Figure 1**) and at least *in vitro* they activate different gene expression profiles in the MoDC which in turn causes differing T cell responses (58). Broadly, maturation agents haven been chosen that are GMP grade, induce activation markers and produce MoDC that stimulate T cells toward a type 1 helper T cell response. Human cytokine cocktail, consisting of TNF-α, IL-1β, IL-6, PGE2, has been most frequently used in MoDC trials (**Table 1**). This mix produces mature MoDC with a superior ability to stimulate T cells than immature MoDC (59) and improved migratory capacity to mobilize DC to lymph nodes where they can prime T cells (60). However, there is data that these MoDC preferentially recruit T-regs, thus, potentially dampening any immune response initiated (61, 62).

Polyinosinic-polycytidylic acid [poly(I:C)] is a synthetic analog of dsRNA and is a clinical grade TLR3 agonist that matures DC (63). These DC, unlike those produced by the cytokine cocktail, produced high levels IL-12 (64) which directs a Th1 type T cell response. *In vitro* experiments suggest better antigen specific T cell proliferation and less T reg development (60, 62). In clinical trials Poly I:C matured MoDC vaccines are reportedly well-tolerated producing immunological and clinical responses (50). However, there are no clinical trials that compare Poly (I:C) matured MoDC with cytokine cocktail matured MoDC directly.

A third combination of CD40L with IFN-γ has shown promise, similarly increasing IL-12 cytokine production (65). Whilst this combination has not been used in PCa, CD40L has been used in other cancer vaccines. In resected metastatic colorectal cancer, a small, randomized phase I DC vaccine trial randomized tumor lysate pulsed MoDC cultured with or without recombinant CD40L. CD40L induced CD86 and CD83 expression on DC but in this small study of only 26 patients, CD40L did not improve anti-tumor specific T cell proliferation, IFNγ ELISPOT response, DTH response or relapse free survival (66). Similarly, in melanoma patients where CD40L was compared to cytokine cocktail, no difference was found in immunological response (67).

There are numerous reasons why we do not see clinical effect of different DC maturation strategies despite promising preclinical data. One is that small gains in maturation state *in vitro* maybe overpowered by the immune environment *in vivo*. One strategy that aims to control this is the use of viral vectors to genetically modify DC. In PCa Sonpavde et al. (37) showed feasibility, safety, and the development of a peripheral immune response when DC were transfected with inducible human CD40 (37). In this trial an adenovirus vector was used to transfect DC with human CD40 that had its cytoplasmic domain fused to ligand-binding domains and a membrane-targeting sequence to allow CD40 to be regulated by lipid-permeable dimerizing drugs, in this case rimiducid (68). This allows control over the timing of CD40 expression. DC vaccine was given and 24 h after injection, when DC have migrated to the lymph node and are in close contact with T cells, rimiducid is given to activate CD40. In this phase 1 study, 86% of patients had stable disease, with just 10% with a partial response (37). In PCa PSA kinetics reported as PSA doubling time (PSADT) are an indicator of prognosis with a shorter PSADT indicating a worse prognosis (69). In this study, 53% of patients had an increase in their PSADT, a surrogate marker for improved clinical outcome. This proof of concept shows that we can co-ordinate both timing and activation state of DCs to improve clinical outcomes.

Form of Antigen

Another variable amongst the different DC vaccination strategy is the type and form of antigen loaded onto DC.

Peptide or Protein

The most common source of antigen is protein. Early DC vaccines use short peptide sequences unique to tumor associated antigens that are known to bind to specific HLA subtypes, mainly HLA-A2. Short peptides are easy to make and are quickly presented on MHC class I by DC when added to culture media. However, they have several disadvantages. They must be suitable for that patient's HLA subtype or else, as they will not be presented, and immune responses will be limited (18). Whilst several vaccines have been trialed selecting patients of HLA-A2 subtype this excludes at least half of eligible patients and represents a higher percentage of the Caucasian population than other ethnics backgrounds (70). Additionally, short peptides that target a $CD8^+$ T cell response won't harness $CD4^+$ T cell help limiting T cell expansion, cytotoxicity, and memory (71). MHC Class II molecules are more variable than MHC class I and thus designing short peptides to target them as well as MHC class I to cover large proportions of the populations becomes complicated and difficult to standardize.

The limitations of peptide loading can be overcome by administering whole protein for DC to uptake and process. Recombinant protein is easy to obtain and can be added directly to culture media. The advantage of administering whole protein is that after DC processing, multiple peptides are available that bind both MHC class I and II and multiple HLA types.

The disadvantages are that these proteins may not cover the potentially more immunogenic mutations found in the tumor and reagents to monitor peptide specific responses may not be available. Also, by focusing on one to four proteins, this leaves open the possibility of immune escape as tumors down regulate expression of these proteins. In the case of PCa, most proteins used in clinical trial including PSA, PSMA, and PAP are overexpressed self-antigen and thus have issue with self-tolerance.

Tumor Cells

Cell lysate has the benefit of presenting a multitude of tumor protein both known and unknown, as well as mutated protein found in the tumor. These mutated proteins give rise to neo-antigens that overcome the problem of self-tolerance and thus are more immunogenic. A common way to produce cell lysate is to freeze/thaw cells for several cycles producing necrotic cell death. This process leaves cell membrane fragments, RNA and DNA in the lysate which provide danger signals promoting DC maturation (72). Once produced cell lysate is added to culture media at ratios of 5:1 (45) and up to 1:1. This requires access to a large amount of tumor material, which, particularly in the setting of CRPCa, is difficult. This has led to the use of allogeneic cell lines as surrogate tumor tissue in four clinical trials in PCa (25, 35, 45, 50) (**Table 1**). Two of these trials combine treatment with metronomic cyclophosphamide for 7 days prior to DC vaccination (45, 50). These trials show that the use of tumor lysate is safe and produces a tumor-specific immunological response as well as increasing PSADT (36, 50).

Allogeneic apoptotic tumor cells (36) have similar capacity as cell lysate to mature DC and prime T cells to produce an antigen specific immune response (73). Apoptotic tumor cells are effectively phagocytosed by immature DC (74–76) and their tumor antigens are preferentially cross-presented to $CD8^+$ T cells. A melanoma mouse models suggest that apoptotic tumor cells induces more IL-12 secretion by DC than cell lysate (73). In patients with CLL *in vivo* studies support this finding show that apoptotic tumor cell loaded MoDC produce better T cell proliferation, higher frequency of IFNγ producing T cells *via* ELISPOT and by PCR less mRNA for the Th2 cytokines IL-4 and IL-10 than cell lysate and mRNA pulsed MoDC (77).

Other forms of presenting tumor antigen to DC include producing hybrids of DC and tumor cells fused using polyethylene glycol (PEG). These made *in vitro* using PCa cell lines ONYCAP23, P4E6, and LNCaP and MoDC, can produce a tumor cell-specific immune response (78). Conceptually, by fusing the cells, endogenous tumor antigens have better access to MHC class I molecules. Several early phase I/II clinical trials in melanoma, glioma, renal cell carcinoma, breast cancer demonstrate that this is feasible, safe, and produces clinical responses (79).

Exomes provide an acellular source of tumor antigen. Exomes are nano-sized particles originating from multivesicular bodies. They can be isolated from the blood and urine of PCa patients (80) providing a source of current antigenic material that is often difficult to obtain in mCRPCa and facilitating a mechanism for a personalized vaccine. Exomes have long been known to have immunosuppressive properties (81), suppressing T cell and NK cell function in the tumor microenvironment. In direct contrast to this, when exosomes activate DC which activate tumor specific T cells as effectively as cell lysate (81, 82). This creates a promising pathway for future autologous prostate cancer tumor loaded DC vaccines.

Messenger RNA

Finally, mRNA provides another source of antigen (74), which DC can take up and translate into protein for presentation on MHC class I. mRNA has the advantage that it can be prepared in sufficient quantity from a small tumor sample and thus it also allows for the ability to produce personalized vaccines. There are four ways of administering mRNA to the DC (a) passive, (b) liposome mediated, (c) electroporation, and (d) viral vector mediated. By far the most common way is electroporation. This has been done in a phase II trial in PCa that compares mRNA loaded MoDC in combination with docetaxel to docetaxel alone (46) (**Table 1**). Whilst it was deemed to be safe with the only toxicity identified as related to vaccine local reactions and rash, there was a much higher discontinuation of treatment in the vaccine arm-−57 vs. 21%. The vaccine arm required much more frequent visits, however, as reasons for discontinuation where not reported, additionally toxicity cannot be excluded.

Route of Administration

MoDC vaccines have been administered in multiple different routes including intravenous (I.V.), intranodal (I.N.), intralymphatic (I.L), intradermal (I.D.), and subcutaneous (S.C). In a meta-analysis that pooled individual data from 84 patients, routes that allow migration to local lymph nodes i.e., I.D./I.L./I.N./S.C lead to better clinical response compared to the I.V. route (OR 3.2, 95% CI 1.1–9.0) (56). Fong et al. (41) showed similar findings using density enriched DC with a better cytokine profile seen with I.D. and I.L. route compared to I.V. with a trend to more transfusion reactions in the I.V. group.

Despite the variability in preparation as a whole these trials (**Table 1**) show that MoDC vaccinations in PCa are safe, produce a cellular immune response and a clinical response with a fall in PSA seen in up 27% (9/33) (18, 50, 83). However, it is important to note that an immunological response does not necessarily correlate with outcome (45, 46, 50) and often peripheral immune responses when detected are not sustained (46). Thus, the outcomes measured may not be clinically significant. Surrogate endpoints of reduction in PSA and difference in PFS may also not correlated with OS, as seen with Sipuleucel-T (5). Thus, despite a multitude of early trials we really need a Phase III trial of MoDC that looks at OS to determine clinical significance. The results of NCT02111577, a double blinded Phase III trial of MoDC loaded with apoptotic LNCaP cells added to standard chemotherapy for men with mCRPCa which has completed recruitment with 1,182 patients, should provide us with some clearer answers.

However, even without the results of this trial there are a number of reasons why MoDC preparations may not be the optimal approach. Monocytes are known to be dysfunctional in advanced cancer including in PCa. Most preclinical information on MoDC has been collected using healthy donor PBMC.

However, when we compare MoDC prepared from healthy donors to those from patients with advanced cancer, patient MoDC are less efficient at phagocytosis, produce less IL-12 and express lower levels of the activation marker CD80 (84). In study of 24 patients with localized PCa, MoDC failed to upregulate CD80, CD83, and CCR7 after maturation with human cytokine cocktail, although for most patients, but not all, this was restored after surgery (85). In contrast two studies of only five patients each did show that MoDC from PCa patients were as good as healthy donors (32, 86).

The biggest issue with MoDC is that even from healthy donor PBMC, they do not perform as well as blood-derived DC; they do not stimulate T cells as well (54, 87), migrate as well (88) or have as much clinical efficacy (56). Thus, despite ease of production, MoDC vaccinations are unlikely to improve on the effectiveness of Sipuleucel-T.

Blood Derived DC Vaccines

Advances in efficiency of isolation protocols allow the use of blood DC as an alternative to MoDC or DC enriched preparations (**Figure 1**). Prue et al. (43) in a phase I trial showed that it was feasible to isolate $CD1c^+$ DC from CRPCa patients *via* magnetic separation and vaccination, was well-tolerated with fever and pain the most common toxicity (43). More recently, in a phase II RCT Westdorp compared the efficacy of matured myeloid (m)DC vs. plasmacytoid (p)DC vs. combination of mDC and pDC (44). Again, this showed that blood derived DC were safe and induced an immune response, with a trend to a better response with mDC alone. These technical advances in isolating DC as a pure population and, as demonstrated by Westdorp et al. (44) isolating specific DC subsets and utilize the underlying specialization of human DC to take up antigen allows us to direct the immune response in a particular direction.

Targeting DC Subsets

Blood DC can initially be divided into two main populations: pDC and mDC. Human pDC are identified by their surface expression of $CD304^+$. They are characterized by their ability to produce large amounts of Type 1 interferon in response to foreign nucleic acids i.e., in response to viral infections (89). In humans, they orchestrate antigen specific $CD4^+$ T cell responses as well as cross present antigen to create $CD8^+$ T cell responses (90, 91). mDC, divided based on phenotype and function into five subsets, the main being cDC1 and cDC2 (92). cDC1, characterized by CD141 expression, have the ability to cross present exogenous antigen to prime $CD8^+$ T cell response, direct a type 1 helper T cell responses and through the production of IL-12, and direct an NK response (93). cDC2, are characterized by $CD1c^+$ expression, have a more diverse function and are able to simulate Th1, Th2, Th17, and $CD8^+$ T cell responses (93). As suggested by Westdorp et al. (44) the mix of DC we use for a vaccine will affect efficacy (44). Whether we use a mixed preparation of mononuclear cells, DC, T cells, B cells, and NK cells such as in Sipuleucel-T (94), MoDC or a pure DC subset will change the direction of the T cell response. Traditionally we have looked at mDC particularly cDC1, as key to orchestrating a cytotoxic immune response. They are most adept at priming $CD8^+$ T cells because they have adapted their intracellular machinery to be extremely efficient at cross presentation of antigen (95). Whilst they have been the focus of much vaccine development, as we learn more about the need for T helper support to create effective $CD8^+$ T cell response (96, 97) an approach that utilizes both cDC1 to activate $CD8^+$ T cells and cDC2 to activate $CD4^+$ T cells would give a more robust anti-tumor immune response (98). A novel way of targeting these naturally occurring DC is to target DC *in situ*. Emerging technologies such as antibody-antigen conjugates and virus co-delivery systems not only provide a DC therapy that improve delivery they also improve efficacy.

IN SITU DC TARGETING

Antibody Directed Antigen-Uptake

One way to target DC is to couple antigen to antibodies that bind endocytic cell surface molecules unique to DC. Preclinical data in mouse models show that delivering antigen in this way increases the efficiency of antigen presentation. Coupling OVA to the rat anti-mouse DEC-205 antibody (clone: NLDC-145) lead to a >100-fold increase in efficiency of DC antigen presented to mouse $CD4^+$ and $CD8^+$ T cells (99). Thus, targeting antigen directly to DC with antibody increases antigen presentation and in both *in vivo* mouse models and *in vitro* human models this leads to improved T cell response (100–102). However, in the absence of a maturation signal to the DC or indeed as a consequence of the function of the molecule targeted, this T cell response did not persist and in fact peripheral tolerance was induced (99). In contrast, in the presence of adjuvant such as anti-CD40 a strong memory response is formed after injection with OVA conjugated DEC-205, with CTL responses detectable up to 90 days after a single immunization (100). This need for a second "danger" signal to direct the immune system to form an inflammatory rather than tolerogenic response to the targeted antigen is not unique to DEC-205 antibodies but common to many surface antibody targets studied to date (99, 100, 103, 104). However, the selection of adjuvant in a clinical setting will need careful consideration to minimize side effects.

Despite the need for adjuvant, the safety and ease of delivery of *in vivo* DC targeting has been demonstrated in a phase I clinical trial of CDX-1401, a fully human anti-DEC-205 (CD205) mAb (3G9) genetically fused to the full-length NY-ESO-1 protein. The vaccine was used in combination with resiquimod (TLR7/8 agonists) and poly-(I:C) as adjuvants. It was well-tolerated in the 45 patients who entered the study and, induced a cellular immune response in 56% and humoral immune response in 79% of cases. Thirteen patients developed stable disease and 2 a partial response (105). This demonstrates that using antibody to target antigen to DC is safe and feasible and can induce an immune response in humans.

While safety has been demonstrated, reports on trials in ovarian cancer and acute myeloid leukemia (AML) are awaited. There remains the question of choice of molecule to target as targeting DEC-205 which naturally trends toward tolerance

may be superceeded. Clec9a (CD370) is another endocytic surface marker with a much narrower expression profile. Whilst DEC-205 is highly expressed on cDC1 it is also expressed on monocytes, B lymphocytes and low levels on T cells and NK cells. In contrast, Clec-9A expression is limited to cDC1, which is the DC subset known for their ability to cross present antigen and elicit a $CD8^+$ cytotoxic T cell response, ideal for a tumor vaccine. The other interesting ability of Clec9a is its ability to drive a memory immune response without adjuvant, however, in mice tumor models, adjuvant is still required (106). Whilst this looks like a promising target, it has been demonstrated that the cDC1 population, which is targeted by Clec9a is reduced in PCa (107) and is less responsive to activation with poly (I:C). This suggests underlying functional impairment and testing these treatments in a PCa tumor model is awaited.

Antibody-directed antigen uptake demonstrates that DC can be loaded "*in vivo*" (105), is safe and produces an immune response. However, antibodies are limited by the amount of antigen that they can deliver through coupling protein to antibody before the latter's ability to bind and be endocytosed is impaired. This has led to the development of co-delivery systems.

Co-delivery Systems

Co-delivery systems have two advantages, they allow the co-administration of adjuvant with antigen and can deliver multiple antigens. Some co-delivery systems are easy to adapt to different antigen make ups thus allowing personalized vaccine with "neoantigens' matched to each patient. There are two main vehicles studied: modified viral vectors and nanoparticles. Viral vectors include the filamentous bacteriophage antigen display system and modified adenovirus. The filamentous bacteriophage system is based on a non-pathogenic prokaryotic virus which can be engineered to express exogenous peptides as fusions to viral capsid proteins (108, 109). The bacteriophage is the adjuvant and in a mouse model it has been manipulated to express both mouse DEC-205 and OVA. In this system it produces an enhanced T cell response compared to injection with OVA: DEC-205 antibody conjugate (108). Similarly, a model where attenuated adenovirus was manipulated to express OVA and anti-mouse DEC-205 (110), produced a memory CD8 T cell response. Whilst this shows promise in pre-clinical models, translation to humans is yet to come.

Nanoparticles

Nanoparticles perhaps are closer to translation, in particular Poly(DL-lactide-co-glycolide (PLGA), a biodegradable slow-release polymer that is FDA approved to encapsulate drugs, can be adapted to encapsulate antigen and adjuvant (111). Due to their size nanoparticles readily taken up by DC (112) and *in vitro* studies show human DC take up peptide more efficiently if it is delivered inside a PLGA nanoparticle rather than soluble form (113). Nanoparticles not only direct peptide to the DC but also protect peptide from degradation, thus increasing the length of time to which DC are exposed to peptide. PLGA delivery of peptide induced T cells with a much greater CTL response than peptide loaded DC both *in vitro* (113) and *in vivo* (113, 114). Nanoparticle delivery has been tested in a mouse models of prostate cancer with the mouse prostate tumor antigen, six-transmembrane epithelial antigen of the prostate (mSTEAP). In this model, a single dose of mSTEAP on PLGA nanoparticles was compared to mSTEAP peptide plus adjuvant. The nanoparticle bound mSTEAP reduced both growth of TRAMP-C2 tumor cells in C57BL/6 mice and increased OS of the mice compared to peptide combined with adjuvant (114). Thus, in a PCa model, nanoparticles were more effective than a peptide vaccine. It is important to note though that comparison to DC vaccination strategies, antibody directed antigen uptake or other novel vaccination strategies remains to be assessed.

Nanoparticles have been used as a co-delivery system for antibody directed antigen uptake. Nanoparticles coated in anti-DEC-205, anti-CD40, and anti-CD11c antibodies to deliver antigen and adjuvant direct to DC all lead to increased CD8 and CD4 T cell proliferation and cytotoxicity *in vitro* and *in vivo* above non-targeted nanoparticles. CD40 targeted nanoparticles improved antigen specific T cell proliferation in the draining LN above other target receptors, and also cytotoxicity against target cells (115). In a mouse tumor model, CD40 nanoparticles containing OVA improved OS of B16-OVA inoculated mice compared to isotype control (116).

Whilst these emerging technology show promise in improving deliverability and efficacy of a DC based vaccine, they are yet to be translated into clinical trials in prostate cancer.

Overcoming Tumor Escape

If we are to successfully translate *in situ* targeting of DC, clinical benefit will not occur without understanding what drives the immunosuppressive microenvironment of PCa.

Improving Antigen Processing Within Tumor Cells

PCa evades detection of the immune system by failing to display tumor peptide in MHC class I complexes on their cell surface. This is crucial to consider in the setting of DC vaccine as cytotoxic T cells primed by a DC vaccine will not be able to kill tumor cells without the presence of MHC Class I complex on tumor cells. In primary castrate sensitive prostate cancer (CSPCa) MHC class I was downregulated in 74% (311/419) and β2M 25% (117). In another study of 58 primary CSPC, defects in MHC class I were less common with loss of staining only in 5% of cases but heterogenous staining in 62% (117). This study also looked at the components of the antigen processing machinery within the tumor cells and demonstrated that loss or downregulation was frequent (118). Thus, treatment strategies that increase MHC Class I expression on tumor cells are candidates for combination therapies that may improve efficacy of DC vaccines. Histone deacetylase inhibitors have been assessed to reverse histone acetylation of the TAP1 promotor and, Trichostatin A, has been shown to upregulated MHC-class 1 and β2-microglobulin in LNCaP cells. Traditional anti-PCa therapies such as docetaxel and radiation also increase all components of antigen-processing machinery in the PC cell line, LNCaP (119, 120) and therefore are beneficial combination strategies for DC vaccines. A phase II trial that combined MoDC vaccine with

docetaxel showed a trend toward improvement in disease specific survival (DSS) (46), and results of the first phase III trial, NCT NCT02111577 that combines docetaxel and DC vaccine therapy are eagerly awaited.

Improving T Cell Function

A robust T cell response is essential for any effective DC vaccine. Thus, it is essential to understand any underlying dysfunction of the T cell repertoire in PCa. We know there are a paucity of T cells (121) in PCa and those present are less proliferative (122), more immunosuppressive (123) with a high proportion of T-regs (122, 123). Data from the NCT00715014 trial of neoadjuvant Sipuleucel-T shows that DC vaccination does lead to increased recruitment of T cells including $CD4^+$, $CD8^+$, and T-regs into the tumor (12). Comparing pre vaccination biopsies to post vaccination resection specimens, T cells had increased TCR sequence diversity in the resected prostate suggesting that Sipuleucel-T recruits T cells to the prostate (124) rather than reactivating those already *in situ*. Gene expression profiling showed an increase in Th1 associated genes and upregulation of immune checkpoint inhibitors including CTLA-4 and TIGIT (125). This raises the question of how long does the immune response last and whether combining with check point inhibitors will improve outcomes.

While monotherapy with both ipilimumab (anti-CTLA4) and PD-1 inhibitors have proved disappointing (2, 3, 126), recent long term follow of ipilimumab shows that despite low response rates those that do respond have enduring responses (127). The key will be to improve response rates and early data suggests that adding DC vaccination to immunotherapy may do just that. In a small study of nine men with mCRPCa treated with Sipuleucel-T and escalating doses of ipilimumab showed that IgG and IgM levels against PA2024 and PAP increased significantly after ipilipumab (49). A subsequent trial to look at immediate vs. delayed CTLA4 blockade (NCT01804465) has recruited and is in the follow up stage. PD-1 inhibitors have less severe immune toxicity than anti-CTLA4 antibodies, and thus are a more tolerable combination strategy. Pembrolizumab has been used in combination with a DNA vaccine in PCa and it was found that concurrent rather than sequential treatment improved PSA response (128). We look to the results of NCT03024216 to determine whether atezolizumab (anti-PD-L1) improves the efficacy of Sipuleucel-T.

Another strategy is to focus on depleting T-regs. In mouse models of PCa low dose cyclophosphamide caused transient depletion of T-regs and increased DC maturation markers and augmented anti-tumor immune response (129). In humans, metronomic oral cyclophosphamide was used in combination with a MoDC vaccine (50), and also prior to MoDC vaccine used in combination with docetaxel chemotherapy (45). In both instances it was well-tolerated. Another mechanism to reduce T-regs is to use IDO inhibitors to block the production of IDO-expressing DCs that drive T cells to T-regs and activate existing T regs. Indoximod, an IDO inhibitor administered after Sipuelucel-T therapy was found to be well-tolerated and improved PFS from 4.1 to 10.3 ($p = 0.011$) (53).

Over-coming Myeloid Derived Suppressor Cells

Myeloid cells play a large role in creating the tumor microenvironment of PCa. The presence of M2 macrophages in the tumor microenvironment is an indicator of poor prognosis (130–133). PCa cells recruit monocytes and polarize them to an M2 macrophage phenotype which then helps increase PCa cells migratory capacity, proliferation, survival and invasion (130, 134, 135) creating a symbiotic relationship. Interestingly, a reduction in MDSC predicts response (46) to mRNA loaded MoDC vaccination and tumor cell vaccine in combination with ipilimumab (136). In mice models of lung cancer MDSC reduce the activity of NK cells and T cells, thus, they will dampen any immune response developed by a DC vaccine. Novel combination strategies that further reduce MDSC may improve vaccination responses. Interestingly in a breast cancer tumor model docetaxel repolarized MDSC toward an M1-like phenotype further supporting the use of docetaxel as a combination for vaccination (137).

Timing and Interactions of Other Therapies

It has long been proposed that the best time to treat with a DC vaccine is when tumor burden is low either at diagnosis or remission. This hypothesis is supported by trials that low burden of disease predicts for good response (138). Another issue is the effect of treatment on the immune system's ability to create an immune response. In the instance of PCa, androgen deprivation therapy (ADT) is given throughout the entire treatment course. ADT enhances T cell responses. In a mouse model, after androgen withdrawal the biggest difference in $CD4^+$ T cells was in IFNγ signaling pathway and CD4 T helper differentiation (139). In patients in CSPCa this was also the case (140). However, we also know that these responses diminish with time, perhaps due to a disproportionate increase in T-regs (141). In a mouse model depleting T-regs with a CTLA-4 depleting antibody significantly improved OS when combined with ADT (142). The phase II STAND study assesses this in patients and showed that better immune responses were stimulated when a DC vaccine was given before initiation of ADT rather than after (48). Thus, the best timing for a DC vaccine maybe at biochemical recurrence when tumor burden is low and ADT has not been given.

CONCLUSION

DC vaccination strategies have been shown to be safe and improve OS. Yet they are still rarely used in clinical practice. Our understanding of antigen loading DC, antigen presentation, induction of T cell responses, extrinsic driving of cytotoxic responses provides multiple opportunities to improve vaccine strategy design. Here we show that emerging technologies present options for targeting DC *in situ* thus improving deliverability. Secondly, novel combination strategies prove promising to help improve on duration of T cell response.

That DC vaccines reach their potential in stimulating effective clinical responses relies on assessing what we have learned, how we adapt trials and looking for long term, durable (or sustainable) outcomes.

AUTHOR CONTRIBUTIONS

SS: writing and figures. XJ, LH and GC: reviewed. SS and GC: concept. All authors contributed to the article and approved the submitted version.

FUNDING

This work was funded by a Cancer Institute New South Wales Translational Program Grant (11/TPG/3-02). SS was funded by an Australian Postgraduate Award, a Sydney Catalyst Top-up Scholarship.

REFERENCES

1. Antonarakis ES, Piulats JM, Gross-Goupil M, Goh J, Ojamaa K, Hoimes CJ, et al. Pembrolizumab for treatment-refractory metastatic castration-resistant prostate cancer: multicohort, open-label phase II KEYNOTE-199 study. *J Clin Oncol.* (2020) 38:395–405. doi: 10.1200/JCO.19.01638
2. Beer TM, Kwon ED, Drake CG, Fizazi K, Logothetis C, Gravis G, et al. Double-blind, phase III trial of ipilimumab versus placebo in asymptomatic or minimally symptomatic patients with metastatic chemotherapy-naive castration-resistant prostate cancer. *J Clin Oncol.* (2017) 35:40–7. doi: 10.1200/JCO.2016.69.1584
3. Kwon ED, Drake CG, Scher HI, Fizazi K, Bossi A, van den Eertwegh AJ, et al. Ipilimumab versus placebo after radiotherapy in patients with metastatic castration-resistant prostate cancer that had progressed after docetaxel chemotherapy (CA184-043): a multicentre, randomised, double-blind, phase 3 trial. *Lancet Oncol.* (2014) 15:700–12. doi: 10.1016/S1470-2045(14)70189-5
4. Hart D. The delivery of effective therapeutic cancer vaccination. *Asian J Androl.* (2011) 13:183–4. doi: 10.1038/aja.2010.146
5. Kantoff PW, Higano CS, Shore ND, Berger ER, Small EJ, Penson DF, et al. Sipuleucel-T immunotherapy for castration-resistant prostate cancer. *N Engl J Med.* (2010) 363:411–22. doi: 10.1056/NEJMoa1001294
6. Troy A, Davidson P, Atkinson C, Hart D. Phenotypic characterisation of the dendritic cell infiltrate in prostate cancer. *J Urol.* (1998) 160:214–9. doi: 10.1016/S0022-5347(01)63093-3
7. Mihalyo MA, Hagymasi AT, Slaiby AM, Nevius EE, Adler AJ. Dendritic cells program non-immunogenic prostate-specific T cell responses beginning at early stages of prostate tumorigenesis. *Prostate.* (2007) 67:536–46. doi: 10.1002/pros.20549
8. Higham EM, Shen CH, Wittrup KD, Chen J. Cutting edge: delay and reversal of T cell tolerance by intratumoral injection of antigen-loaded dendritic cells in an autochthonous tumor model. *J Immunol.* (2010) 184:5954–8. doi: 10.4049/jimmunol.1000265
9. Drake CG, Doody AD, Mihalyo MA, Huang CT, Kelleher E, Ravi S, et al. Androgen ablation mitigates tolerance to a prostate/prostate cancer-restricted antigen. *Cancer Cell.* (2005) 7:239–49. doi: 10.1016/j.ccr.2005.01.027
10. Bak SP, Barnkob MS, Bai A, Higham EM, Wittrup KD, Chen J. Differential requirement for CD70 and CD80/CD86 in dendritic cell-mediated activation of tumor-tolerized CD8 T cells. *J Immunol.* (2012) 189:1708–16. doi: 10.4049/jimmunol.1201271
11. Aalamian-Matheis M, Chatta GS, Shurin MR, Huland E, Huland H, Shurin GV. Inhibition of dendritic cell generation and function by serum from prostate cancer patients: correlation with serum-free PSA. *Adv Exp Med Biol.* (2007) 601:173–82. doi: 10.1007/978-0-387-72005-0_18
12. Fong L, Carroll P, Weinberg V, Chan S, Lewis J, Corman J, et al. Activated lymphocyte recruitment into the tumor microenvironment following preoperative sipuleucel-T for localized prostate cancer. *J Natl Cancer Inst.* (2014) 106:dju268. doi: 10.1093/jnci/dju268
13. Higano CS, Schellhammer PF, Small EJ, Burch PA, Nemunaitis J, Yuh L, et al. Integrated data from 2 randomized, double-blind, placebo-controlled, phase 3 trials of active cellular immunotherapy with sipuleucel-T in advanced prostate cancer. *Cancer.* (2009) 115:3670–9. doi: 10.1002/cncr.24429
14. Huber ML, Haynes L, Parker C, Iversen P. Interdisciplinary critique of sipuleucel-T as immunotherapy in castration-resistant prostate cancer. *J Natl Cancer Inst.* (2012) 104:273–9. doi: 10.1093/jnci/djr514
15. Fearnley DB, Whyte LF, Carnoutsos SA, Cook AH, Hart DN. Monitoring human blood dendritic cell numbers in normal individuals and in stem cell transplantation. *Blood.* (1999) 93:728–36. doi: 10.1182/blood.V93.2.728
16. Sallusto F, Lanzavecchia A. Efficient presentation of soluble antigen by cultured human dendritic cells is maintained by granulocyte/macrophage colony-stimulating factor plus interleukin 4 and downregulated by tumor necrosis factor alpha. *J Exp Med.* (1994) 179:1109–18. doi: 10.1084/jem.179.4.1109
17. Verdijk P, Aarntzen EHJG, Lesterhuis WJ, Boullart ACI, Kok E, van Rossum MM, et al. Limited amounts of dendritic cells migrate into the T-cell area of lymph nodes but have high immune activating potential in melanoma patients. *Clin Cancer Res.* (2009) 15:2531–40. doi: 10.1158/1078-0432.CCR-08-2729
18. Murphy G, Tjoa B, Ragde H, Kenny G, Boynton A. Phase I clinical trial: T-cell therapy for prostate cancer using autologous dendritic cells pulsed with HLA-A0201-specific peptides from prostate-specific membrane antigen. *Prostate.* (1996) 29:371–80. doi: 10.1002/(SICI)1097-0045(199612)29:6<371::AID-PROS5>3.0.CO;2-B
19. Murphy GP, Tjoa BA, Simmons SJ, Jarisch J, Bowes VA, Ragde H, et al. Infusion of dendritic cells pulsed with HLA-A2-specific prostate-specific membrane antigen peptides: a phase II prostate cancer vaccine trial involving patients with hormone-refractory metastatic disease. *Prostate.* (1999) 38:73–8. doi: 10.1002/(SICI)1097-0045(19990101)38:1<73::AID-PROS9>3.0.CO;2-V
20. Murphy GP, Tjoa BA, Simmons SJ, Ragde H, Rogers M, Elgamal A, et al. Phase II prostate cancer vaccine trial: report of a study involving 37 patients with disease recurrence following primary treatment. *Prostate.* (1999) 39:54–9. doi: 10.1002/(SICI)1097-0045(19990401)39:1<54::AID-PROS9>3.0.CO;2-U
21. Murphy GP, Tjoa BA, Simmons SJ, Rogers MK, Kenny GM, Jarisch J. Higher-dose and less frequent dendritic cell infusions with PSMA peptides in hormone-refractory metastatic prostate cancer patients. *Prostate.* (2000) 43:59–62. doi: 10.1002/(SICI)1097-0045(20000401)43:1<59::AID-PROS8>3.0.CO;2-D
22. Knight D, Peterson AC, Rini BI, Harlin H, Gajewski TF, Stadler WM. The HLA-A2-restricted PSMA peptide LLHETDSAV is poorly immunogenic in patients with metastatic prostate cancer. *Prostate.* (2009) 69:142–8. doi: 10.1002/pros.20864
23. Perambakam S, Hallmeyer S, Reddy S, Mahmud N, Bressler L, DeChristopher P, et al. Induction of specific T cell immunity in patients with prostate cancer by vaccination with PSA146-154 peptide. *Cancer Immunol Immunother.* (2006) 55:1033–42. doi: 10.1007/s00262-005-0090-x
24. Barrou B, Benoit G, Ouldkaci M, Cussenot O, Salcedo M, Agrawal S, et al. Vaccination of prostatectomized prostate cancer patients in biochemical relapse, with autologous dendritic cells pulsed with recombinant human PSA. *Cancer Immunol Immunother.* (2004) 53:453–60. doi: 10.1007/s00262-003-0451-2
25. Pandha HS, John RJ, Hutchinson J, James N, Whelan M, Corbishley C, et al. Dendritic cell immunotherapy for urological cancers using cryopreserved allogeneic tumour lysate-pulsed cells: a phase I/II study. *BJU Int.* (2004) 94:412–8. doi: 10.1111/j.1464-410X.2004.04922.x

26. Heiser A, Coleman D, Dannull J, Yancey D, Maurice MA, Lallas CD, et al. Autologous dendritic cells transfected with prostate-specific antigen RNA stimulate CTL responses against metastatic prostate tumors. *J Clin Investig.* (2002) 109:409–17. doi: 10.1172/JCI0214364
27. Thomas-Kaskel AK, Zeiser R, Jochim R, Robbel C, Schultze-Seemann W, Waller CF, et al. Vaccination of advanced prostate cancer patients with PSCA and PSA peptide-loaded dendritic cells induces DTH responses that correlate with superior overall survival. *Int J Cancer.* (2006) 119:2428–34. doi: 10.1002/ijc.22097
28. Hildenbrand B, Sauer B, Kalis O, Stoll C, Freudenberg MA, Niedermann G, et al. Immunotherapy of patients with hormone-refractory prostate carcinoma pre-treated with interferon-gamma and vaccinated with autologous PSA-peptide loaded dendritic cells–a pilot study. *Prostate.* (2007) 67:500–8. doi: 10.1002/pros.20539
29. Zhuang ZX, Shen LQ, Shi Y, Lu X, Shi HZ. Auto-dendritic cell vaccines pulsed with PSA, PSMA and PAP peptides for hormone-refractory prostate cancer. *Zhonghua Nan Ke Xue.* (2010) 16:698–704.
30. Xi HB, Wang GX, Fu B, Liu WP, Li Y. Survivin and PSMA loaded dendritic cell vaccine for the treatment of prostate cancer. *Biol Pharm Bull.* (2015) 38:827–35. doi: 10.1248/bpb.b14-00518
31. Fuessel S, Meye A, Schmitz M, Zastrow S, Linne C, Richter K, et al. Vaccination of hormone-refractory prostate cancer patients with peptide cocktail-loaded dendritic cells: results of a phase I clinical trial. *Prostate.* (2006) 66:811–21. doi: 10.1002/pros.20404
32. Waeckerle-Men Y, Allmen EU, von Moos R, Classon BJ, Scandella E, Schmid HP, et al. Dendritic cells generated from patients with androgen-independent prostate cancer are not impaired in migration and T-cell stimulation. *Prostate.* (2005) 64:323–31. doi: 10.1002/pros.20231
33. Scheid E, Major P, Bergeron A, Finn OJ, Salter RD, Eady R, et al. Tn-MUC1 DC vaccination of rhesus macaques and a phase I/II trial in patients with nonmetastatic castrate-resistant prostate cancer. *Cancer Immunol Res.* (2016) 4:881–92. doi: 10.1158/2326-6066.CIR-15-0189
34. Mu LJ, Kyte JA, Kvalheim G, Aamdal S, Dueland S, Hauser M, et al. Immunotherapy with allotumour mRNA-transfected dendritic cells in androgen-resistant prostate cancer patients. *Br J Cancer.* (2005) 93:749–56. doi: 10.1038/sj.bjc.6602761
35. Reyes D, Salazar L, Espinoza E, Pereda C, Castellon E, Valdevenito R, et al. Tumour cell lysate-loaded dendritic cell vaccine induces biochemical and memory immune response in castration-resistant prostate cancer patients. *Br J Cancer.* (2013) 109:1488–97. doi: 10.1038/bjc.2013.494
36. Frank MO, Kaufman J, Tian S, Suarez-Farinas M, Parveen S, Blachere NE, et al. Harnessing naturally occurring tumor immunity: a clinical vaccine trial in prostate cancer. *PLoS ONE.* (2010) 5:e12367. doi: 10.1371/journal.pone.0012367
37. Sonpavde G, McMannis JD, Bai Y, Seethammagari MR, Bull JMC, Hawkins V, et al. Phase I trial of antigen-targeted autologous dendritic cell-based vaccine with *in vivo* activation of inducible CD40 for advanced prostate cancer. *Cancer Immunol Immunother.* (2017) 66:1345–57. doi: 10.1007/s00262-017-2027-6
38. Burch PA, Breen JK, Buckner JC, Gastineau DA, Kaur JA, Laus RL, et al. Priming tissue-specific cellular immunity in a phase I trial of autologous dendritic cells for prostate cancer. *Clin Cancer Res.* (2000) 6:2175–82.
39. Small EJ, Fratesi P, Reese DM, Strang G, Laus R, Peshwa MV, et al. Immunotherapy of hormone-refractory prostate cancer with antigen-loaded dendritic cells. *J Clin Oncol.* (2000) 18:3894–903. doi: 10.1200/JCO.2000.18.23.3894
40. Fong L, Brockstedt D, Benike C, Breen JK, Strang G, Ruegg CL, et al. Dendritic cell-based xenoantigen vaccination for prostate cancer immunotherapy. *J Immunol.* (2001) 167:7150–6. doi: 10.4049/jimmunol.167.12.7150
41. Fong L, Brockstedt D, Benike C, Wu L, Engleman EG. Dendritic cells injected via different routes induce immunity in cancer patients. *J Immunol.* (2001) 166:4254–9. doi: 10.4049/jimmunol.166.6.4254
42. Beer TM, Bernstein GT, Corman JM, Glode LM, Hall SJ, Poll WL, et al. Randomized trial of autologous cellular immunotherapy with sipuleucel-T in androgen-dependent prostate cancer. *Clin Cancer Res.* (2011) 17:4558–67. doi: 10.1158/1078-0432.CCR-10-3223
43. Prue RL, Vari F, Radford KJ, Tong H, Hardy MY, D'Rozario R, et al. A phase I clinical trial of CD1c (BDCA-1)+ dendritic cells pulsed with HLA-A*0201 peptides for immunotherapy of metastatic hormone refractory prostate cancer. *J Immunother.* (2015) 38:71–6. doi: 10.1097/CJI.0000000000000063
44. Westdorp H, Creemers JHA, van Oort IM, Schreibelt G, Gorris MAJ, Mehra N, et al. Blood-derived dendritic cell vaccinations induce immune responses that correlate with clinical outcome in patients with chemo-naive castration-resistant prostate cancer. *J Immunother Cancer.* (2019) 7:302. doi: 10.1186/s40425-019-0787-6
45. Podrazil M, Horvath R, Becht E, Rozkova D, Bilkova P, Sochorova K, et al. Phase I/II clinical trial of dendritic-cell based immunotherapy (DCVAC/PCa) combined with chemotherapy in patients with metastatic, castration-resistant prostate cancer. *Oncotarget.* (2015) 6:18192–205. doi: 10.18632/oncotarget.4145
46. Kongsted P, Borch TH, Ellebaek E, Iversen TZ, Andersen R, Met O, et al. Dendritic cell vaccination in combination with docetaxel for patients with metastatic castration-resistant prostate cancer: a randomized phase II study. *Cytotherapy.* (2017) 19:500–13. doi: 10.1016/j.jcyt.2017.01.007
47. Twardowski P, Wong JYC, Pal SK, Frankel PH, Franklin K, Junqueira M. Randomized phase II trial of sipuleucel-T immunotherapy preceded by sensitizing radiation therapy and sipuleucel-T alone in patients with metastatic castrate resistant prostate cancer. *J Clin Oncol.* (2017) 35:222. doi: 10.1200/JCO.2017.35.6_suppl.222
48. Antonarakis ES, Kibel AS, Yu EY, Karsh LI, Elfiky A, Shore ND, et al. Sequencing of sipuleucel-T and androgen deprivation therapy in men with hormone-sensitive biochemically recurrent prostate cancer: a phase II randomized trial. *Clin Cancer Res.* (2017) 23:2451–9. doi: 10.1158/1078-0432.CCR-16-1780
49. Scholz M, Yep S, Chancey M, Kelly C, Chau K, Turner J, et al. Phase I clinical trial of sipuleucel-T combined with escalating doses of ipilimumab in progressive metastatic castrate-resistant prostate cancer. *Immunotargets Ther.* (2017) 6:11–6. doi: 10.2147/ITT.S122497
50. Fucikova J, Podrazil M, Jarolim L, Bilkova P, Hensler M, Becht E, et al. Phase I/II trial of dendritic cell-based active cellular immunotherapy with DCVAC/PCa in patients with rising PSA after primary prostatectomy or salvage radiotherapy for the treatment of prostate cancer. *Cancer Immunol Immunother.* (2018) 67:89–100. doi: 10.1007/s00262-017-2068-x
51. Small EJ, Lance RS, Gardner TA, Karsh LI, Fong L, McCoy C, et al. A randomized phase II trial of sipuleucel-T with concurrent versus sequential abiraterone acetate plus prednisone in metastatic castration-resistant prostate cancer. *Clin Cancer Res.* (2015) 21:3862–9. doi: 10.1158/1078-0432.CCR-15-0079
52. Rini BI, Weinberg V, Fong L, Conry S, Hershberg RM, Small EJ. Combination immunotherapy with prostatic acid phosphatase pulsed antigen-presenting cells (provenge) plus bevacizumab in patients with serologic progression of prostate cancer after definitive local therapy. *Cancer.* (2006) 107:67–74. doi: 10.1002/cncr.21956
53. Jha GG, Gupta S, Tagawa ST, Koopmeiners JS, Vivek S, Dudek AZ, et al. A phase II randomized, double-blind study of sipuleucel-T followed by IDO pathway inhibitor, indoximod, or placebo in the treatment of patients with metastatic castration resistant prostate cancer (mCRPC). *J Clin Oncol.* (2017) 35:3066. doi: 10.1200/JCO.2017.35.15_suppl.3066
54. Sim WJ, Malinarich F, Fairhurst AM, Connolly JE. Generation of immature, mature and tolerogenic dendritic cells with differing metabolic phenotypes. *J Vis Exp.* (2016) 112:54128. doi: 10.3791/54128
55. De Vries IJ, Krooshoop DJ, Scharenborg NM, Lesterhuis WJ, Diepstra JH, Van Muijen GN, et al. Effective migration of antigen-pulsed dendritic cells to lymph nodes in melanoma patients is determined by their maturation state. *Cancer Res.* (2003) 63:12–7.
56. Draube A, Klein-Gonzalez N, Mattheus S, Brillant C, Hellmich M, Engert A, et al. Dendritic cell based tumor vaccination in prostate and renal cell cancer: a systematic review and meta-analysis. *PLoS ONE.* (2011) 6:e18801. doi: 10.1371/journal.pone.0018801
57. de Vries IJ, Lesterhuis WJ, Scharenborg NM, Engelen LP, Ruiter DJ, Gerritsen MJ, et al. Maturation of dendritic cells is a prerequisite for inducing immune responses in advanced melanoma patients. *Clin Cancer Res.* (2003) 9:5091–100.

58. Castiello L, Sabatino M, Jin P, Clayberger C, Marincola FM, Krensky AM, et al. Monocyte-derived DC maturation strategies and related pathways: a transcriptional view. *Cancer Immunol Immunother.* (2011) 60:457–66. doi: 10.1007/s00262-010-0954-6
59. Spisek R, Bretaudeau L, Barbieux I, Meflah K, Gregoire M. Standardized generation of fully mature p70 IL-12 secreting monocyte-derived dendritic cells for clinical use. *Cancer Immunol Immunother.* (2001) 50:417–27. doi: 10.1007/s002620100215
60. Moller I, Michel K, Frech N, Burger M, Pfeifer D, Frommolt P, et al. Dendritic cell maturation with poly(I:C)-based versus PGE2-based cytokine combinations results in differential functional characteristics relevant to clinical application. *J Immunother.* (2008) 31:506–19. doi: 10.1097/CJI.0b013e318177d9e5
61. Muthuswamy R, Urban J, Lee JJ, Reinhart TA, Bartlett D, Kalinski P. Ability of mature dendritic cells to interact with regulatory T cells is imprinted during maturation. *Cancer Res.* (2008) 68:5972–8. doi: 10.1158/0008-5472.CAN-07-6818
62. Jongmans W, Tiemessen DM, van Vlodrop IJ, Mulders PF, Oosterwijk E. Th1-polarizing capacity of clinical-grade dendritic cells is triggered by Ribomunyl but is compromised by PGE2: the importance of maturation cocktails. *J Immunother.* (2005) 28:480–7. doi: 10.1097/01.cji.0000171290.78495.66
63. Verdijk RM, Mutis T, Esendam B, Kamp J, Melief CJ, Brand A, et al. Polyriboinosinic polyribocytidylic acid (poly(I:C)) induces stable maturation of functionally active human dendritic cells. *J Immunol.* (1999) 163:57–61.
64. Rouas R, Lewalle P, El Ouriaghli F, Nowak B, Duvillier H, Martiat P. Poly(I:C) used for human dendritic cell maturation preserves their ability to secondarily secrete bioactive IL-12. *Int Immunol.* (2004) 16:767–73. doi: 10.1093/intimm/dxh077
65. Hoffmann TK, Meidenbauer N, Muller-Berghaus J, Storkus WJ, Whiteside TL. Proinflammatory cytokines and CD40 ligand enhance cross-presentation and cross-priming capability of human dendritic cells internalizing apoptotic cancer cells. *J Immunother.* (2001) 24:162–71. doi: 10.1097/00002371-200103000-00011
66. Barth RJ Jr, Fisher DA, Wallace PK, Channon JY, Noelle RJ, Gui J, et al. A randomized trial of *ex vivo* CD40L activation of a dendritic cell vaccine in colorectal cancer patients: tumor-specific immune responses are associated with improved survival. *Clin Cancer Res.* (2010) 16:5548–56. doi: 10.1158/1078-0432.CCR-10-2138
67. Gross S, Erdmann M, Haendle I, Voland S, Berger T, Schultz E, et al. Twelve-year survival and immune correlates in dendritic cell-vaccinated melanoma patients. *JCI Insight*. (2017) 2:e91438. doi: 10.1172/jci.insight.91438
68. Hanks BA, Jiang J, Singh RA, Song W, Barry M, Huls MH, et al. Re-engineered CD40 receptor enables potent pharmacological activation of dendritic-cell cancer vaccines *in vivo*. *Nat Med.* (2005) 11:130–7. doi: 10.1038/nm1183
69. Vickers AJ, Brewster SF. PSA velocity and doubling time in diagnosis and prognosis of prostate cancer. *Br J Med Surg Urol.* (2012) 5:162–8. doi: 10.1016/j.bjmsu.2011.08.006
70. Ellis JM, Henson V, Slack R, Ng J, Hartzman RJ, Katovich Hurley C. Frequencies of HLA-A2 alleles in five U.S. population groups. Predominance Of A*02011 and identification of HLA-A*0231. *Hum Immunol.* (2000) 61:334–40. doi: 10.1016/S0198-8859(99)00155-X
71. Janssen EM, Lemmens EE, Wolfe T, Christen U, von Herrath MG, Schoenberger SP. CD4+ T cells are required for secondary expansion and memory in CD8+ T lymphocytes. *Nature.* (2003) 421:852–6. doi: 10.1038/nature01441
72. Sauter B, Albert ML, Francisco L, Larsson M, Somersan S, Bhardwaj N. Consequences of cell death: exposure to necrotic tumor cells, but not primary tissue cells or apoptotic cells, induces the maturation of immunostimulatory dendritic cells. *J Exp Med.* (2000) 191:423–34. doi: 10.1084/jem.191.3.423
73. Kotera Y, Shimizu K, Mule JJ. Comparative analysis of necrotic and apoptotic tumor cells as a source of antigen(s) in dendritic cell-based immunization. *Cancer Res.* (2001) 61:8105–9.
74. Hoffmann TK, Meidenbauer N, Dworacki G, Kanaya H, Whiteside TL. Generation of tumor-specific T-lymphocytes by cross-priming with human dendritic cells ingesting apoptotic tumor cells. *Cancer Res.* (2000) 60:3542–9.
75. Brusa D, Garetto S, Chiorino G, Scatolini M, Migliore E, Camussi G, et al. Post-apoptotic tumors are more palatable to dendritic cells and enhance their antigen cross-presentation activity. *Vaccine.* (2008) 26:6422–32. doi: 10.1016/j.vaccine.2008.08.063
76. Di Nicola M, Napoli S, Anichini A, Mortarini R, Romagnoli L, Magni M, et al. Dendritic cell viability is decreased after phagocytosis of apoptotic tumor cells induced by staurosporine or vaccinia virus infection. *Haematologica.* (2003) 88:1396–404.
77. Kokhaei P, Choudhury A, Mahdian R, Lundin J, Moshfegh A, Osterborg A, et al. Apoptotic tumor cells are superior to tumor cell lysate, and tumor cell RNA in induction of autologous T cell response in B-CLL. *Leukemia.* (2004) 18:1810–5. doi: 10.1038/sj.leu.2403517
78. Lundqvist A, Palmborg A, Bidla G, Whelan M, Pandha H, Pisa P. Allogeneic tumor-dendritic cell fusion vaccines for generation of broad prostate cancer T-cell responses. *Med Oncol.* (2004) 21:155–65. doi: 10.1385/MO:21:2:155
79. Koido S, Homma S, Hara E, Namiki Y, Takahara A, Komita H, et al. Regulation of tumor immunity by tumor/dendritic cell fusions. *Clin Dev Immunol.* (2010) 2010:516768. doi: 10.1155/2010/516768
80. Lorenc T, Klimczyk K, Michalczewska I, Slomka M, Kubiak-Tomaszewska G, Olejarz W. Exosomes in prostate cancer diagnosis, prognosis and therapy. *Int J Mol Sci*. (2020) 21:2118. doi: 10.3390/ijms21062118
81. Zhang H, Tang K, Zhang Y, Ma R, Ma J, Li Y, et al. Cell-free tumor microparticle vaccines stimulate dendritic cells via cGAS/STING signaling. *Cancer Immunol Res.* (2015) 3:196–205. doi: 10.1158/2326-6066.CIR-14-0177
82. Bu N, Wu H, Sun B, Zhang G, Zhan S, Zhang R, et al. Exosome-loaded dendritic cells elicit tumor-specific CD8+ cytotoxic T cells in patients with glioma. *J Neurooncol.* (2011) 104:659–67. doi: 10.1007/s11060-011-0537-1
83. Tjoa BA, Simmons SJ, Bowes VA, Ragde H, Rogers M, Elgamal A, et al. Evaluation of phase I/II clinical trials in prostate cancer with dendritic cells and PSMA peptides. *Prostate.* (1998) 36:39–44. doi: 10.1002/(SICI)1097-0045(19980615)36:1<39::AID-PROS6>3.0.CO;2-6
84. Onishi H, Morisaki T, Baba E, Kuga H, Kuroki H, Matsumoto K, et al. Dysfunctional and short-lived subsets in monocyte-derived dendritic cells from patients with advanced cancer. *Clin Immunol.* (2002) 105:286–95. doi: 10.1006/clim.2002.5293
85. Brusa D, Carletto S, Cucchiarale G, Gontero P, Greco A, Simone M, et al. Prostatectomy restores the maturation competence of blood dendritic cell precursors and reverses the abnormal expansion of regulatory T lymphocytes. *Prostate.* (2011) 71:344–52. doi: 10.1002/pros.21248
86. Orange DE, Jegathesan M, Blachere NE, Frank MO, Scher HI, Albert ML, et al. Effective antigen cross-presentation by prostate cancer patients' dendritic cells: implications for prostate cancer immunotherapy. *Prostate Cancer Prostatic Dis.* (2004) 7:63–72. doi: 10.1038/sj.pcan.4500694
87. Osugi Y, Vuckovic S, Hart DN. Myeloid blood CD11c(+) dendritic cells and monocyte-derived dendritic cells differ in their ability to stimulate T lymphocytes. *Blood.* (2002) 100:2858–66. doi: 10.1182/blood.V100.8.2858
88. Fromm PD, Papadimitrious MS, Hsu JL, Van Kooten Losio N, Verma ND, Lo TH, et al. CMRF-56(+) blood dendritic cells loaded with mRNA induce effective antigen-specific cytotoxic T-lymphocyte responses. *Oncoimmunology.* (2016) 5:e1168555. doi: 10.1080/2162402X.2016.1168555
89. Reizis B, Bunin A, Ghosh HS, Lewis KL, Sisirak V. Plasmacytoid dendritic cells: recent progress and open questions. *Annu Rev Immunol.* (2011) 29:163–83. doi: 10.1146/annurev-immunol-031210-101345
90. Tel J, Schreibelt G, Sittig SP, Mathan TS, Buschow SI, Cruz LJ, et al. Human plasmacytoid dendritic cells efficiently cross-present exogenous Ags to CD8+ T cells despite lower Ag uptake than myeloid dendritic cell subsets. *Blood.* (2013) 121:459–67. doi: 10.1182/blood-2012-06-435644
91. Nierkens S, Tel J, Janssen E, Adema GJ. Antigen cross-presentation by dendritic cell subsets: one general or all sergeants? *Trends Immunol.* (2013) 34:361–70. doi: 10.1016/j.it.2013.02.007
92. Villani AC, Satija R, Reynolds G, Sarkizova S, Shekhar K, Fletcher J, et al. Single-cell RNA-seq reveals new types of human blood

dendritic cells, monocytes, and progenitors. *Science.* (2017) 356:eaah4573. doi: 10.1126/science.aah4573
93. Collin M, Bigley V. Human dendritic cell subsets: an update. *Immunology.* (2018) 154:3–20. doi: 10.1111/imm.12888
94. Sheikh NA, Petrylak D, Kantoff PW, Dela Rosa C, Stewart FP, Kuan LY, et al. Sipuleucel-T immune parameters correlate with survival: an analysis of the randomized phase 3 clinical trials in men with castration-resistant prostate cancer. *Cancer Immunol Immunother.* (2013) 62:137–47. doi: 10.1007/s00262-012-1317-2
95. Bachem A, Guttler S, Hartung E, Ebstein F, Schaefer M, Tannert A, et al. Superior antigen cross-presentation and XCR1 expression define human CD11c+CD141+ cells as homologues of mouse CD8+ dendritic cells. *J Exp Med.* (2010) 207:1273–81. doi: 10.1084/jem.20100348
96. Gerner MY, Casey KA, Mescher MF. Defective MHC class II presentation by dendritic cells limits CD4 T cell help for antitumor CD8 T cell responses. *J Immunol.* (2008) 181:155–64. doi: 10.4049/jimmunol.181.1.155
97. Zhu Z, Cuss SM, Singh V, Gurusamy D, Shoe JL, Leighty R, et al. CD4+ T cell help selectively enhances high-avidity tumor antigen-specific CD8+ T cells. *J Immunol.* (2015) 195:3482–9. doi: 10.4049/jimmunol.1401571
98. Srivastava MK, Dubinett S, Sharma S. Targeting MDSCs enhance therapeutic vaccination responses against lung cancer. *Oncoimmunology.* (2012) 1:1650–51. doi: 10.4161/onci.21970
99. Bonifaz L, Bonnyay D, Mahnke K, Rivera M, Nussenzweig MC, Steinman RM. Efficient targeting of protein antigen to the dendritic cell receptor DEC-205 in the steady state leads to antigen presentation on major histocompatibility complex class I products and peripheral CD8+ T cell tolerance. *J Exp Med.* (2002) 196:1627–38. doi: 10.1084/jem.20021598
100. Bonifaz LC, Bonnyay DP, Charalambous A, Darguste DI, Fujii S, Soares H, et al. *In vivo* targeting of antigens to maturing dendritic cells via the DEC-205 receptor improves T cell vaccination. *J Exp Med.* (2004) 199:815–24. doi: 10.1084/jem.20032220
101. Bozzacco L, Trumpfheller C, Huang Y, Longhi MP, Shimeliovich I, Schauer JD, et al. HIV gag protein is efficiently cross-presented when targeted with an antibody towards the DEC-205 receptor in Flt3 ligand-mobilized murine DC. *Eur J Immunol.* (2010) 40:36–46. doi: 10.1002/eji.200939748
102. Gurer C, Strowig T, Brilot F, Pack M, Trumpfheller C, Arrey F, et al. Targeting the nuclear antigen 1 of Epstein-Barr virus to the human endocytic receptor DEC-205 stimulates protective T-cell responses. *Blood.* (2008) 112:1231–9. doi: 10.1182/blood-2008-03-148072
103. Hawiger D, Inaba K, Dorsett Y, Guo M, Mahnke K, Rivera M, et al. Dendritic cells induce peripheral T cell unresponsiveness under steady state conditions *in vivo*. *J Exp Med.* (2001) 194:769–79. doi: 10.1084/jem.194.6.769
104. Idoyaga J, Lubkin A, Fiorese C, Lahoud MH, Caminschi I, Huang YX, et al. Comparable T helper 1 (Th1) and CD8 T-cell immunity by targeting HIV gag p24 to CD8 dendritic cells within antibodies to Langerin, DEC205, and Clec9A. *Proc Natl Acad Sci USA.* (2011) 108:2384–89. doi: 10.1073/pnas.1019547108
105. Dhodapkar MV, Sznol M, Zhao B, Wang D, Carvajal RD, Keohan ML, et al. Induction of antigen-specific immunity with a vaccine targeting NY-ESO-1 to the dendritic cell receptor DEC-205. *Sci Transl Med.* (2014) 6:232ra51. doi: 10.1126/scitranslmed.3008068
106. Sancho D, Mourao-Sa D, Joffre OP, Schulz O, Rogers NC, Pennington DJ, et al. Tumor therapy in mice via antigen targeting to a novel, DC-restricted C-type lectin. *J Clin Invest.* (2008) 118:2098–110. doi: 10.1172/JCI34584
107. Mastelic-Gavillet B, Sarivalasis A, Lozano LE, Wyss T, Inoges S, de Vries IJM, et al. Quantitative and qualitative impairments in dendritic cell subsets of patients with ovarian or prostate cancer. *Eur J Cancer.* (2020) 135:173–82. doi: 10.1016/j.ejca.2020.04.036
108. D'Apice L, Costa V, Sartorius R, Trovato M, Aprile M, De Berardinis P. Stimulation of innate and adaptive immunity by using filamentous bacteriophage FD targeted to DEC-205. *J Immunol Res.* (2015) 2015:585078. doi: 10.1155/2015/585078
109. Sartorius R, Bettua C, D'Apice L, Caivano A, Trovato M, Russo D, et al. Vaccination with filamentous bacteriophages targeting DEC-205 induces DC maturation and potent anti-tumor T-cell responses in the absence of adjuvants. *Eur J Immunol.* (2011) 41:2573–84. doi: 10.1002/eji.201141526
110. Tenbusch M, Nchinda G, Storcksdieck genannt Bonsmann M, Temchura V, Uberla K. Targeting the antigen encoded by adenoviral vectors to the DEC205 receptor modulates the cellular and humoral immune response. *Int Immunol.* (2013) 25:247–58. doi: 10.1093/intimm/dxs112
111. Cruz LJ, Tacken PJ, Fokkink R, Joosten B, Stuart MC, Albericio F, et al. Targeted PLGA nano- but not microparticles specifically deliver antigen to human dendritic cells via DC-SIGN *in vitro*. *J Control Release.* (2010) 144:118–26. doi: 10.1016/j.jconrel.2010.02.013
112. Manolova V, Flace A, Bauer M, Schwarz K, Saudan P, Bachmann MF. Nanoparticles target distinct dendritic cell populations according to their size. *Eur J Immunol.* (2008) 38:1404–13. doi: 10.1002/eji.200737984
113. Ma W, Chen M, Kaushal S, McElroy M, Zhang Y, Ozkan C, et al. PLGA nanoparticle-mediated delivery of tumor antigenic peptides elicits effective immune responses. *Int J Nanomedicine.* (2012) 7:1475–87. doi: 10.2147/IJN.S29506
114. Chen Q, Bao Y, Burner D, Kaushal S, Zhang Y, Mendoza T, et al. Tumor growth inhibition by mSTEAP peptide nanovaccine inducing augmented CD8(+) T cell immune responses. *Drug Deliv Transl Res.* (2019) 9:1095–105. doi: 10.1007/s13346-019-00652-z
115. Cruz LJ, Rosalia RA, Kleinovink JW, Rueda F, Lowik CW, Ossendorp F. Targeting nanoparticles to CD40, DEC-205 or CD11c molecules on dendritic cells for efficient CD8(+) T cell response: a comparative study. *J Control Release.* (2014) 192:209–18. doi: 10.1016/j.jconrel.2014.07.040
116. Rosalia RA, Cruz LJ, van Duikeren S, Tromp AT, Silva AL, Jiskoot W, et al. CD40-targeted dendritic cell delivery of PLGA-nanoparticle vaccines induce potent anti-tumor responses. *Biomaterials.* (2015) 40:88–97. doi: 10.1016/j.biomaterials.2014.10.053
117. Kitamura H, Torigoe T, Asanuma H, Honma I, Sato N, Tsukamoto T. Down-regulation of HLA class I antigens in prostate cancer tissues and up-regulation by histone deacetylase inhibition. *J Urol.* (2007) 178:692–6. doi: 10.1016/j.juro.2007.03.109
118. Seliger B, Stoehr R, Handke D, Mueller A, Ferrone S, Wullich B, et al. Association of HLA class I antigen abnormalities with disease progression and early recurrence in prostate cancer. *Cancer Immunol Immunother.* (2010) 59:529–40. doi: 10.1007/s00262-009-0769-5
119. Ahmed MM, Hodge JW, Guha C, Bernhard EJ, Vikram B, Coleman CN. Harnessing the potential of radiation-induced immune modulation for cancer therapy. *Cancer Immunol Res.* (2013) 1:280–4. doi: 10.1158/2326-6066.CIR-13-0141
120. Hodge JW, Garnett CT, Farsaci B, Palena C, Tsang KY, Ferrone S, et al. Chemotherapy-induced immunogenic modulation of tumor cells enhances killing by cytotoxic T lymphocytes and is distinct from immunogenic cell death. *Int J Cancer.* (2013) 133:624–36. doi: 10.1002/ijc.28070
121. Leclerc BG, Charlebois R, Chouinard G, Allard B, Pommey S, Saad F, et al. CD73 expression is an independent prognostic factor in prostate cancer. *Clin Cancer Res.* (2016) 22:158–66. doi: 10.1158/1078-0432.CCR-15-1181
122. Yunger S, Bar El A, Zeltzer LA, Fridman E, Raviv G, Laufer M, et al. Tumor-infiltrating lymphocytes from human prostate tumors reveal anti-tumor reactivity and potential for adoptive cell therapy. *Oncoimmunology.* (2019) 8:e1672494. doi: 10.1080/2162402X.2019.1672494
123. Kiniwa Y, Miyahara Y, Wang HY, Peng W, Peng G, Wheeler TM, et al. CD8+ Foxp3+ regulatory T cells mediate immunosuppression in prostate cancer. *Clin Cancer Res.* (2007) 13:6947–58. doi: 10.1158/1078-0432.CCR-07-0842
124. Sheikh N, Cham J, Zhang L, DeVries T, Letarte S, Pufnock J, et al. Clonotypic diversification of intratumoral T cells following sipuleucel-T treatment in prostate cancer subjects. *Cancer Res.* (2016) 76:3711–8. doi: 10.1158/0008-5472.CAN-15-3173
125. Hagihara K, Chan S, Zhang L, Oh DY, Wei XX, Simko J, et al. Neoadjuvant sipuleucel-T induces both Th1 activation and immune regulation in localized prostate cancer. *Oncoimmunology.* (2019) 8:e1486953. doi: 10.1080/2162402X.2018.1486953
126. Hansen AR, Massard C, Ott PA, Haas NB, Lopez JS, Ejadi S, et al. Pembrolizumab for advanced prostate adenocarcinoma: findings of the KEYNOTE-028 study. *Ann Oncol.* (2018) 29:1807–13. doi: 10.1093/annonc/mdy232
127. Fizazi K, Drake CG, Beer TM, Kwon ED, Scher HI, Gerritsen WR, et al. Final analysis of the ipilimumab versus placebo following radiotherapy phase III trial in postdocetaxel metastatic castration-resistant prostate cancer

identifies an excess of long-term survivors. *Eur Urol.* (2020) 78:822–30. doi: 10.1016/j.eururo.2020.07.032
128. McNeel DG, Eickhoff JC, Wargowski E, Zahm C, Staab MJ, Straus J, et al. Concurrent, but not sequential, PD-1 blockade with a DNA vaccine elicits anti-tumor responses in patients with metastatic, castration-resistant prostate cancer. *Oncotarget.* (2018) 9:25586–96. doi: 10.18632/oncotarget.25387
129. Wada S, Yoshimura K, Hipkiss EL, Harris TJ, Yen HR, Goldberg MV, et al. Cyclophosphamide augments antitumor immunity: studies in an autochthonous prostate cancer model. *Cancer Res.* (2009) 69:4309–18. doi: 10.1158/0008-5472.CAN-08-4102
130. Comito G, Giannoni E, Segura CP, Barcellos-de-Souza P, Raspollini MR, Baroni G, et al. Cancer-associated fibroblasts and M2-polarized macrophages synergize during prostate carcinoma progression. *Oncogene.* (2014) 33:2423–31. doi: 10.1038/onc.2013.191
131. Gannon PO, Poisson AO, Delvoye N, Lapointe R, Mes-Masson AM, Saad F. Characterization of the intra-prostatic immune cell infiltration in androgen-deprived prostate cancer patients. *J Immunol Methods.* (2009) 348:9–17. doi: 10.1016/j.jim.2009.06.004
132. Erlandsson A, Carlsson J, Lundholm M, Falt A, Andersson SO, Andren O, et al. M2 macrophages and regulatory T cells in lethal prostate cancer. *Prostate.* (2019) 79:363–369. doi: 10.1002/pros.23742
133. Cortesi F, Delfanti G, Grilli A, Calcinotto A, Gorini F, Pucci F, et al. Bimodal CD40/Fas-dependent crosstalk between iNKT cells and tumor-associated macrophages impairs prostate cancer progression. *Cell Rep.* (2018) 22:3006–20. doi: 10.1016/j.celrep.2018.02.058
134. Zheng T, Ma G, Tang M, Li Z, Xu R. IL-8 Secreted from M2 macrophages promoted prostate tumorigenesis via STAT3/MALAT1 pathway. *Int J Mol Sci.* (2018) 20:27. doi: 10.3390/ijms20010098
135. Wang C, Peng G, Huang H, Liu F, Kong DP, Dong KQ, et al. Blocking the feedback loop between neuroendocrine differentiation and macrophages improves the therapeutic effects of enzalutamide (MDV3100) on prostate cancer. *Clinical Cancer Research.* (2018) 24:708–23. doi: 10.1158/1078-0432.CCR-17-2446
136. Santegoets SJ, Stam AG, Lougheed SM, Gall H, Jooss K, Sacks N, et al. Myeloid derived suppressor and dendritic cell subsets are related to clinical outcome in prostate cancer patients treated with prostate GVAX and ipilimumab. *J Immunother Cancer.* (2014) 2:31. doi: 10.1186/s40425-014-0031-3
137. Kodumudi KN, Woan K, Gilvary DL, Sahakian E, Wei S, Djeu JY. A novel chemoimmunomodulating property of docetaxel: suppression of myeloid-derived suppressor cells in tumor bearers. *Clin Cancer Res.* (2010) 16:4583–94. doi: 10.1158/1078-0432.CCR-10-0733
138. Schellhammer PF, Chodak G, Whitmore JB, Sims R, Frohlich MW, Kantoff PW. Lower baseline prostate-specific antigen is associated with a greater overall survival benefit from sipuleucel-T in the immunotherapy for prostate adenocarcinoma treatment (IMPACT) trial. *Urology.* (2013) 81:1297–302. doi: 10.1016/j.urology.2013.01.061
139. Kissick HT, Sanda MG, Dunn LK, Pellegrini KL, On ST, Noel JK, et al. Androgens alter T-cell immunity by inhibiting T-helper 1 differentiation. *Proc Natl Acad Sci USA.* (2014) 111:9887–92. doi: 10.1073/pnas.1402468111
140. Dallos M, Obradovic A, Chowdhury N, Bujanda ZL, Aggen DH, Hawley J, et al. Human prostate cancer immune phenotypes after androgen deprivation therapy. *J Clin Oncol.* (2019) 37:5083. doi: 10.1200/JCO.2019.37.15_suppl.5083
141. Flammiger A, Weisbach L, Huland H, Tennstedt P, Simon R, Minner S, et al. High tissue density of FOXP3+ T cells is associated with clinical outcome in prostate cancer. *Eur J Cancer.* (2013) 49:1273–9. doi: 10.1016/j.ejca.2012.11.035
142. Shen YC, Ghasemzadeh A, Kochel CM, Nirschl TR, Francica BJ, Lopez-Bujanda ZA, et al. Combining intratumoral Treg depletion with androgen deprivation therapy (ADT): preclinical activity in the Myc-CaP model. *Prostate Cancer Prostatic Dis.* (2018) 21:113–25. doi: 10.1038/s41391-017-0013-x

Conflict of Interest: The authors declare that the research was conducted in the absence of any commercial or financial relationships that could be construed as a potential conflict of interest.

frontiers in Immunology

ORIGINAL RESEARCH
published: 22 April 2021
doi: 10.3389/fimmu.2021.673454

Quantitative Phosphoproteomic Analysis Reveals Dendritic Cell-Specific STAT Signaling After α2-3–Linked Sialic Acid Ligand Binding

*Rui-Jún Eveline Li[1], Aram de Haas[1], Ernesto Rodríguez[1], Hakan Kalay[1], Anouk Zaal[1], Connie R. Jimenez[2], Sander R. Piersma[2], Thang V. Pham[2], Alex A. Henneman[2], Richard R. de Goeij-de Haas[2], Sandra J. van Vliet[1] and Yvette van Kooyk[1]**

[1] Department of Molecular Cell Biology and Immunology, Cancer Center Amsterdam, Amsterdam Infection and Immunity Institute, Amsterdam UMC, Vrije Universiteit Amsterdam, Amsterdam, Netherlands, [2] Department of Medical Oncology, Cancer Center Amsterdam, Amsterdam UMC, Vrije Universiteit Amsterdam, Amsterdam, Netherlands

OPEN ACCESS

Edited by:
Maud Plantinga, University Medical Center Utrecht, Netherlands

Reviewed by:
Bernd Lepenies, University of Veterinary Medicine Hannover, Germany
Joseph T. Y. Lau, University at Buffalo, United States

***Correspondence:**
Yvette van Kooyk
y.vankooyk@amsterdamumc.nl

Specialty section:
This article was submitted to Antigen Presenting Cell Biology, a section of the journal Frontiers in Immunology

Received: *27 February 2021*
Accepted: *06 April 2021*
Published: *22 April 2021*

Citation:
Li R-JE, de Haas A, Rodríguez E, Kalay H, Zaal A, Jimenez CR, Piersma SR, Pham TV, Henneman AA, de Goeij-de Haas RR, van Vliet SJ and van Kooyk Y (2021) Quantitative Phosphoproteomic Analysis Reveals Dendritic Cell- Specific STAT Signaling After α2-3–Linked Sialic Acid Ligand Binding. Front. Immunol. 12:673454. doi: 10.3389/fimmu.2021.673454

Dendritic cells (DCs) are key initiators of the adaptive immunity, and upon recognition of pathogens are able to skew T cell differentiation to elicit appropriate responses. DCs possess this extraordinary capacity to discern external signals using receptors that recognize pathogen-associated molecular patterns. These can be glycan-binding receptors that recognize carbohydrate structures on pathogens or pathogen-associated patterns that additionally bind receptors, such as Toll-like receptors (TLRs). This study explores the early signaling events in DCs upon binding of α2-3 sialic acid (α2-3sia) that are recognized by Immune inhibitory Sialic acid binding immunoglobulin type lectins. α2-3sias are commonly found on bacteria, e.g. Group B *Streptococcus*, but can also be expressed by tumor cells. We investigated whether α2-3sia conjugated to a dendrimeric core alters DC signaling properties. Through phosphoproteomic analysis, we found differential signaling profiles in DCs after α2-3sia binding alone or in combination with LPS/TLR4 co-stimulation. α2-3sia was able to modulate the TLR4 signaling cascade, resulting in 109 altered phosphoproteins. These phosphoproteins were annotated to seven biological processes, including the regulation of the IL-12 cytokine pathway. Secretion of IL-10, the inhibitory regulator of IL-12 production, by DCs was found upregulated after overnight stimulation with the α2-3sia dendrimer. Analysis of kinase activity revealed altered signatures in the JAK-STAT signaling pathway. PhosphoSTAT3 (Ser727) and phosphoSTAT5A (Ser780), involved in the regulation of the IL-12 pathway, were both downregulated. Flow cytometric quantification indeed revealed de-phosphorylation over time upon stimulation with α2-3sia, but no α2-6sia. Inhibition of both STAT3 and -5A in moDCs resulted in a similar cytokine secretion profile as α-3sia triggered DCs. Conclusively, this study revealed a specific alteration of the JAK-STAT pathway in DCs upon simultaneous α2-3sia and LPS stimulation, altering the IL10:IL-12 cytokine secretion profile associated with reduction of inflammation. Targeted control of

the STAT phosphorylation status is therefore an interesting lead for the abrogation of immune escape that bacteria or tumors impose on the host.

Keywords: dendritic cell, sialic acid, α2-3sia, STAT3, STAT5, Phosphoproteomics, Siglec, tolerance

INTRODUCTION

Dendritic cells (DCs) are antigen presenting cells that continuously sense the intrinsic host environment. DCs possess the extraordinary capacity to recognize internal and external danger signals and respond appropriately using pattern recognition receptors (PPRs) (1). Upon encounter of pathogen-associated molecular patterns (PAMPs) or danger-associated molecular patterns (DAMPs), DCs can leave the periphery and migrate to the lymphoid tissues to activate an appropriate adaptive immune response (2). In contrast, recognition of self-associated molecular patterns (SAMPs), such as self-antigens, leads to the induction of a tolerogenic response (3).

Glycans form cellular immune recognition elements and are considered key modulators of the immunological outcome (4, 5). Glycosylation is a common post-translational modification in eukaryotes, and glycan patterns can be recognized as PAMPs or SAMPs by DC PRRs, such as C-type lectin receptors (CLRs) and Sialic acid binding immunoglobulin type lectins (Siglecs) (6). SAMP-associated glycan patterns predominantly refer to sialic acids (3). This negatively charged monosaccharide decorates the terminal positions of larger polysaccharide molecules on cell surfaces. Positioned at the outer rim of the glycocalyx in an α2-3-, α2-6-, or α2-8-linkage, sialic acids portray a dominant role in cell-cell interactions and maintenance of intrinsic homeostasis (7). Due to its presence on all cells, the inherent sialic acid signature is an effective marker to promote tolerance upon encounter of self-antigens (3). Synthetic antigens modified with a sialic acid can alter the immunogenicity of the antigen by imposing a regulatory program on DCs. The DC can subsequently skew the differentiation of naïve T cells to regulatory T cells *via* e.g. an altered cytokine secretion profile, and reduce inflammatory T effector cell responses (8). The impact of sialic acids on altering T cell differentiation is therefore highly appealing as a target in DC-based immunotherapeutic strategies (9, 10).

Furthermore, sialic acids are increasingly acknowledged for their role in the immune regulation of cancer. During cancer progression, tumor cells often highly increase their sialic acid expression to create an immunosuppressive tumor microenvironment (11). Tumor hypersialylation furthermore alters myeloid cells and hamper immunotherapy efficacy, as the T cell and NK cell responses are dampened by the tolerogenic immune signals emanating from the tumor cell surfaces (11). Novel approaches to combat quenching of immune cell activity using targeted delivery of sialyltransferase inhibitors are currently being explored to improve immunotherapeutic strategies (12, 13).

Sialic acids are also taken advantage of by pathogens to benefit their own survival. Bacteria obtain sialic acids by *de novo* synthesis or from an environmental source (14). By doing so pathogens can hide and escape from immune surveillance. Group B *Streptococcus* (GBS) uses sialic acids to mimic the host cell surface. The capsular polysaccharides of all serotypes are decorated with terminal α2-3-linked sialic acids, causing suppression of the host immune response, promoting bacterial survival (15, 16). This exploitation of sialic acid by GBS eventually results in the devastatingly high incidence of sepsis and meningitis in infants (16).

To gain insight into the self and foreign discrimination by DCs, and the *in vivo* induction of an immune suppressive T cell response (8), we explored human DC immune signaling upon sialic acid binding. We conjugated α2-3-linked sialic acids to a dendrimeric core for multivalent ligand presentation. By proteomic and phosphoproteomic analysis we studied the induced signaling pathways. With concomitant TLR4 stimulation to trigger DC maturation and cytokine secretion, we mimicked bacterial pathogen recognition by DCs. We report specific signaling profiles upon stimulation with α2-3 sialic acid in presence of LPS, affecting kinases within the MAPK/ERK and JAK-STAT pathway and subsequent anti-inflammatory cytokine responses. These results demonstrate the dynamic signaling networks and specific pathways underlying DC immune suppressive signaling upon recognition of sialic acid linkages.

Targeted control of STAT phosphorylation provides an interesting lead for the revocation of tolerance in bacterial and tumoral immune surveillance escape. Continued investigations on the DC signaling cascade from the JAK-STAT pathway to the control of the IL-12 transcripts and the ensuing suppression of effector T cells could be an appropriate continuation of this study. Moreover, this study also provided insight in the alterations in the MAPK signaling pathways and other kinome signatures, which were not pursued here. Further efforts to analyze these pathways and profiles will yield information on the role of DCs in the polarization of naïve T cells towards effector or regulatory T cells. The upstream signaling from the α2-3sia binding Siglec towards the immunosuppressive DC phenotype has important practical implications for the use of the sialic acid-Siglec axis as a therapeutic strategy in immunotherapy. The homology of the Siglec receptors and their affinity towards multiple sialic acids complicates their therapeutic application. Moreover, it must also be taken into account that the use of Siglec receptor-specific antibodies as blocking agent may also trigger Siglec-dependent signaling pathways. Nonetheless, these challenges are manageable with the rapid developments currently in the field of Siglec research.

MATERIALS AND METHODS

Synthesis of the Glycodendrimers

Three glycodendrimers were synthesized for this study, the control, α2-3 sialic acids and α2-6 sialic acids. To generate 2.0

PAMAM dendrimers with a cystamine core (Sigma-Aldrich) the glycans 3'-Sialyl-N-acetyllactosamine (Dextra Laboratories; α2-3sia dendrimer) and 6'-Sialyl-N-acetyllactosamine (Dextra Laboratories; α2-6sia dendrimer), and D-(+)-galactose (Sigma-Aldrich; control dendrimer), were conjugated *via* reductive animation using the free reducing ends. Approximately 32 equivalents of the glycan were added per dendrimer in dimethylsulphoxide (DMSO, Sigma-Aldrich) and acetic acid (8:2 ratio, Sigma-Aldrich). To the cocktail 160 equivalents of 2-Methylpyridine borane complex (Sigma-Aldrich) was added up to a desired total volume of 200 µL, and incubated at 65°C for 2 hours with repeated vortexing. The reaction products were purified over disposable PD10 desalting columns (GE Healthcare) using 50 mM NH_4HCO_3 pH 4.4, and submitted to multiple cycles of lyophilization and redisolving in H_2O. The products were validated using LC-MS and plant lectin binding.

Primary Cell Isolation and Culture

Monocytes were obtained from buffy coats obtained from healthy donors (Sanquin Amsterdam, reference: S03.0023-XT) using Ficoll (Stemcell Technologies) and Percoll (Sigma-Aldrich) gradient centrifugation. The monocytes were cultured for four days in RPMI 1640 (Invitrogen), supplemented with 10% FCS (Biowittaker), 1.000 U/mL penicillin (Lonza), 1 U/mL streptomycin (Lonza), 262.5 U/mL IL-4 (Biosource) and 112.5 U/mL GM-CSF (Biosource) to obtain immature monocyte-derived DCs (moDCs). Expression of CD1a and CD14 (both BioLegend) was monitored *via* flow cytometric analysis as markers of moDC differentiation, and CD83 and CD86 (both Becton Dickinson) as markers of maturation.

Cytokine Analysis

1 µM dendrimer was added to approximately $50{\cdot}10^3$ day 4 moDCs, with or without 10 ng/mL LPS derived from E. coli 0111:B4 (Sigma-Aldrich). For the inhibition studies, 0.25 µM of the STAT5 inhibitor CAS 285986-31-4 (Calbiochem) or the STAT3 inhibitor JSI-124 (Sigma Aldrich) were used. After overnight stimulation, the supernatants were harvested and the cytokines IL-10 and IL-12p70 (both Biosource) were measured by sandwich ELISA according to the manufacturer's protocol. Briefly, NUNC MaxiSorp plates were coated with the capture antibody in 0.05 M $NaHCO_3$ buffer overnight at 4°C. The plates were washed and blocked using PBS + 1% BSA (EMD Millipore). The supernatants were incubated on the coated plates for 2 hours at room temperature, washed, and binding of the cytokine was detected with a peroxidease-conjugated detection antibody. Binding was visualized with 3,3',5,5'-tetramethylbenzidine (Sigma-Aldrich) and quantified on the iMarkTM Microplate Absorbance Reader (Bio-RAD) at 450 nm.

Primary Cell Stimulation, Lysis and Protein Extraction

Approximately $2.5{\cdot}10^7$ day 4 moDCs were stimulated at 37°C with 1 µM of the dendrimer with or without LPS (Sigma-Aldrich). After 30 minutes, the cells were immediately cooled to 4°C by placement on ice and washed using pre-cooled 4°C PBS. Lysis buffer (20 mM HEPES pH 8.0, 9 M CH_4N_2O, 1 mM Na_3VO_4, 2.5 mM $Na_4P_2O_7$, and 1 mM $Na_2C_3H_7PO_6$) was freshly prepared and added to the cells. After vortexing the cells were snap frozen in liquid nitrogen. The protein concentration was measured by BCA assay (Thermo Fisher Scientific) according to manufacturer's protocol. 45 mM DDT was added to 10 mg protein, incubated for 30 minutes at 55°C, followed by reduction of the lysate. Subsequent addition of 110 mM iodoacetamide solution alkylated the protein lysate. The urea concentration was then diluted to 2 M with 20 mM HEPES buffer pH 8.0 for digestion with sequencing grade modified trypsin (enzyme: protein 1:100 w/w). The tryptic lysate digests were acidified with 1% TFA and checked for the pH (<3). The tryptic peptides were then captured through solid-phase extraction with the OASIS HLB-based cartridges (Waters Corporation). After washing with 0.1% TFA, the peptides were eluted with 0.1% TFA and 80% acetonitrile.

TiOx Phosphopeptide Enrichment

Titanium dioxide (TiOx) chromatography was applied to capture the phosphopeptides. 500 µg desalted tryptic digests were diluted 1:1 with lactic acid solution (0.3 g/mL lactic acid, 0.07% TFA/53% acetonitrile). 200 µL pipette tips were fitted with a 16G-needle punch of a C8 disk EMPORE, on which 2.5 mg TiO_2 was added. The TiOx bed was preconditioned with 0.1% TFA and 80% acetonitrile before equilibration with 0.3 g/mL lactic acid in 0.07% TFA/54% acetonitrile, allowing capture of phosphorylated serine and threonine peptides of the tryptic digest. After sequential washing of the bedding with lactic acid, and 0.1% TFA + 80% acetonitrile, the phosphopeptides were eluted with 0.5% and 5% (v/v) piperidine in 20% (v/v) phosphoric acid to quench the basic solution. Pipette tips (200 µL) were again fitted with a 16G-needle punch of an EMPORE disk of poly(StyreneDivinylBenzene) material, preconditioned with 0.1% TFA and 80% acetonitrile, and equilibrated with 0.1% TFA. After loading the enriched phosphopeptide mixture, the bedding was washed with 0.1% TFA. Through centrifugal filtration, the phosphopeptides were desalted in 0.1% TFA and 80% acetonitrile and lyophilized.

NanoLC-MS/MS Acquisition and Data Processing

The peptides were redissolved in loading solvent (0.5% TFA/4% acetonitrile) prior to separation on an Ultimate 3000 nanoLC (Dionex LC-Packings) equipped with a 20 cm x 75 µmID fused silica column, custom packed with 3 µm 120 Å ReproSil Pur C18 aqua (Dr Maisch GMBH) on-line coupled to a MS/MS platform (QExactive, ThermoFisher). The MS/MS spectra were matched to the Uniprot human reference proteome FASTA file (release February 2013, 70136 entries) in MaxQuant v1.4.1.2. The measured phosphopeptides intensities were normalized to the median intensity of all identified peptides ('normalized intensity' from the MaxQuant Evidence table) and quantified by their extracted ion chromatograms ('Intensity' in MaxQuant).

The fold change was calculated in R, as well as the p values from the replicates using a limma test (17), which were considered significantly altered at $p < 0.05$. Phosphopeptide quantification by the OncoProteomics Laboratory, VUmc has been previously described thoroughly (18, 19). The significant peptides were functionally correlated using the online STRING tool v11.0 (https://string-db.org/), and mapped in Cytoscape v3.5.1 (https://cytoscape.org/) (20, 21). Gene Ontology (GO) term enrichment analysis was performed with the Cytoscape plugin ClueGO v2.5.5 (http://apps.cytoscape.org/apps/cluego) (21). The significantly altered phosphoproteins were integrated and visualized in pathways using Pathview under default settings (https://pathview.uncc.edu/) (22). Phosphoproteomic alterations were analyzed and visualized using Integrative Inferred Kinase Activity (InKA) analysis v1.2.2 (https://inkascore.org/) and PTMsigDB analysis v2.0 (https://github.com/broadinstitute/ssGSEA2.0) (23, 24).

Flowcytometric Quantification of Phosphoproteins

Approximately $5{\cdot}10^4$ day 4 moDCs were stimulated at 37°C with 1 μM the dendrimer with or without LPS (Sigma-Aldrich). After the indicated time points, cells were immediately cooled to 4°C by placement on ice and washed using pre-cooled 4°C PBS. The cells were gently fixed in PBS + 4% PFA, for 15 minutes at room temperature, followed by washing in PBS. Permeabilization of the cells was performed by adding 90% pre-cooled 4°C methanol for 30 minutes. After washing, STAT3 (1:1000, clone 124H6, Cell Signaling), STAT5A (1:500, clone 4H1, Cell Signalling), pSTAT3 (1:1000, clone E121-31, Abcam), or pSTAT5A (1:500, ab30649, Abcam) antibodies were added and incubated for 60 minutes at room temperature. After extensive washing, the secondary antibodies Alexa-488 goat anti-mouse IgG2a and Alexa-647 donkey anti-rabbit IgG (both 1:1000, from Invitrogen) were added for 30 minutes before flow cytometric analysis by CyAn™ ADP (Beckman Coulter), and analyzed using FlowJo v10.

Statistics

The plotted data is represented as mean ± SD of at least three healthy donors or independent experiments. The statistical analyses were performed in GraphPad Prism v7.04. Independent samples were evaluated by the Students t-test, groups with a non-normal distribution were compared by the Kruskal-Wallis test, with the overall statistical significance set at $P < 0.05$.

RESULTS AND DISCUSSION

Quantitative Analysis of the DC Phosphoproteome After α2-3 Sialic Acid Stimulation

To obtain a global overview of the α2-3 sialic acid-induced signaling in DCs, we performed LC-MS/MS-based phosphoproteomic analysis of human DCs stimulated with sialic acid-coated dendrimers. From peripheral blood of three human donors, we isolated the monocytes and differentiated these to monocyte-derived DCs (moDCs) using an IL-4/GM-CSF cocktail for four days of culture. We introduced α2-3-linked sialic acids (α2-3sia) to a dendrimer through reductive animation (25). The small second generation dendrimeric core was selected as carrier system, as the spherical platform allows compact packing of the glycans and multivalent presentation on the polymeric arms. We selected 3'-sialyl-N-acetyllactosamine for coupling, as the saccharide ring is opened at the carbon atom during conjugation (**Figure 1A**). By using this trisaccharide, the α2-3sia–galactose linkage is maintained, mimicking the sialic acid decorated bacterial capsule of GBS (26). We also conjugated a galactose in a similar fashion, which served as a $C_6H_{12}O_5$ (open galactose)-dendrimer control. The dendrimers were validated using plant lectins (**Sl. Figure 1**) and incubated after overnight with moDCs to study alterations in cytokine secretion profiles. IL-12 secreted by DCs is a key inducer of the pro-inflammatory immune response, while IL-10 regulates IL-12 production and plays a significant role the induction of regulatory T cells (27). The antagonistic relation of the two cytokines is therefore an effective indicator of the DC immune status. We determined the optimal dendrimer concentration at 1 μM (data not shown) measured an increased IL-10:IL-12 secretion profile when the α2-3sia dendrimer was given to DCs in the presence of LPS, which was not observed with the control dendrimer (**Figure 1B**). No cytokines were measured in the medium controls, without the TLR4 stimulus.

To decipher the signaling events occurring upon α2-3 sialic acid recognition by dendritic cells, we added 1 μM of the glycodendrimer to approximately $2.5{\cdot}10^7$ moDCs with or without LPS for 30 minutes at 37°C (**Figure 1C**). To maintain the phosphorylation signatures, the cells were immediately chilled, lysed in a buffer with protease and phosphatase inhibitors, and snap-frozen in liquid nitrogen until the solid-phase extraction of the peptides before titanium dioxide (TiOx) chromatography and nanoLC-MS/MS quantification. A total of 9,566 phosphopeptides and 12,851 proteins were quantified with a false discovery rate of < 1% (**Figure 1D**). The majority of the phosphopeptides found were phosphorylated at the serine, while only approximately 10% was phosphorylated at the threonine (**Figure 1E**). TiOx chromatography also captured the much less prevalent phosphorylated tyrosine residues, resulting in a total presence of <1%. The amount of (phospho)peptides and sites identified was not altered upon stimulation with either of the glycodendrimers.

Alterations in the moDC Phosphoproteome After α2-3 Sialic Acid Binding

To reveal the most significantly altered phosphoproteins, we used a pairwise comparison for each donor. Furthermore, the sialic acid stimulated conditions were compared to the ctrl-dendrimer stimulations (Ctrl *vs* α2-3sia; Ctrl+LPS *vs* α2-3sia +LPS). A total of 68 significantly altered phosphorylation sites were found upon α2-3 sialic acid triggering, while, compared to the control dendrimer, simultaneous α2-3sia and LPS

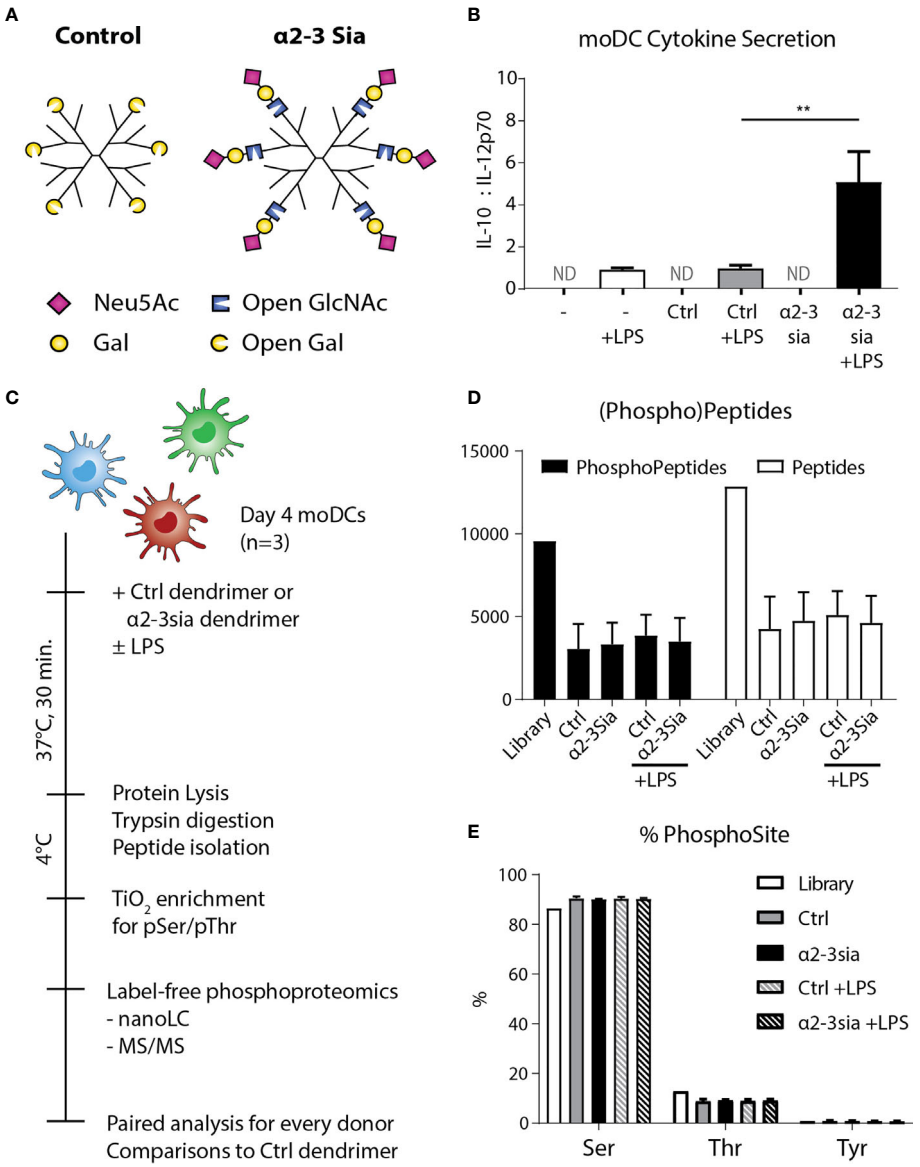

FIGURE 1 | Experimental setup and quality control of the phosphoproteomics. **(A)** A schematic model of the two glycodendrimers synthesized, the control and α2-3 sialic acid dendrimer. Through reductive animation an excess of the glycans is introduced and conjugated to the dendrimer, by opening the saccharide ring at the reducing end. **p < 0.01 **(B)** After overnight stimulation of the moDCs with the dendrimers, IL-10 and IL-12 were quantified in the supernatant through an ELISA assay. Only in the conditions with LPS stimulation cytokines were measured. Stimulation with LPS plus the α2-3 sialic acid dendrimer resulted in a significant decrease of IL-10. One donor is depicted as a representative of 8 individuals, ND, Not Determined; range IL-10 319-6072 pg/mL; IL-12 48-1175 pg/mL. **(C)** Day 4 human moDCs from three independent donors were stimulated with the control or the α2-3 sialic acid dendrimers with or without LPS stimulation for 30 minutes at 37°C. The cells were immediately cooled to 4°C to maintain the phosphoprotein signature, and lysed. The lysate was digested with trypsin, and subsequently prepped and subjected for peptide isolation. Using TiOx chromatography, the lysate was enriched for phospho-serine and –threonine, before label-free phosphoproteomic analysis using LC-MS/MS. **(D)** 9,566 phosphopeptides and 12,851 proteins were quantified with a false discovery rate of < 1% (n=3). **(E)** Approximately 90% of the phosphopeptides identified were phosphorylated at the serine, 10% at the threonine, and <1% at the tyrosine (n=3).

stimulation resulted in 109 altered phosphosites (**Figures 2A–C** and **Sl. Tables 1, 2**). Only 4 altered phosphorylation sites were shared between the conditions (AHNAK Thr4100, Ser5749, Ser5393 and STK10 Ser448). The presence of LPS resulted in a different signaling profile, indicating modulation of the TLR4 signaling pathway by α2-3sia. The additional 41 altered phosphorylation sites found in the simultaneous α2-3sia and LPS-stimulated condition could therefore be involved in crosstalk between the α2-3sia dendrimers binding receptors and TLR4 signaling. The 86% decrease in phosphorylated

proteins in the LPS stimulated condition is furthermore notable, while 84% of the phosphoproteins in the α2-3sia-dendrimer-only condition had a higher phosphorylation status (**Figure 2C** and **Sl. Tables 1, 2**). To determine whether the identified phosphoproteins are functionally cooperative after α2-3sia stimulation, sequential STRING and cytoscape analysis was employed on the significantly altered phosphoproteins (28). Due to the relatively low number of phosphoproteins, we excluded a cutoff in fold change and explored all 109 significantly altered phosphorylation sites. This resulted in a network of 58 significant phosphoproteins functionally interconnected after α2-3sia stimulation in presence of LPS (**Figure 2D** and **Sl. Table 2**). Only 7 of these phosphoproteins in the network were increased in phosphorylation. Remarkable were SRRM2 with the highest increase (9.19-fold) in phosphorylation, and HNRNPA2B1 with the strongest decrease in phosphorylation of 10.2-fold. SRMM2 is involved in pre-mRNA splicing, and HNRNPA2B1 is associated with packaging of pre-mRNAs into exosomes (28, 29). The two proteins are known to interact, suggesting a role for sialic acids in the processing of pre-mRNA (30). Furthermore, two STAT proteins had a lower phosphorylation status (4.08-fold decrease for STAT3, and 2.53-fold decrease for STAT5A). Both proteins have dual roles as signal transducers and transcription factors, and are key regulators of DC activity and DC skewing of specific T cell responses (31, 32). Notable is the phosphoprotein JUN with the most interactions with 9 other linked nodes. The 1.75-fold de-phosphosphorylated protein JUN is a transcription factor and interconnects with other DNA/RNA binding proteins, indicating activation of genetic reprogramming after α2-3sia stimulation. Analysis of altered phosphoproteins in the α2-3sia only conditions showed a small cluster of 13 interconnected nodes, and separate connections between 13 phosphoproteins (**Sl. Figure 2**). Notable is the connectivity between the SRRM2 protein with ACIN1. The mRNA splicing involved protein was upregulated in phosphorylation upon α2-3sia, while the presence of LPS downregulated phosphorylation on this protein. Furthermore, the phosphorylation of the transcriptional repressor BCLAF1 was remarkable. Stimulation with α2-3sia increased phosphorylation 2-folds at Ser285, while α2-3sia and LPS co-stimulation resulted in 2-fold downregulation at the same site (**Sl. Tables 1, 2**). In conclusion, upon α2-3sia stimulation phosphorylation was enhanced upon α2-3sia stimulation, while simultaneous α2-3sia and LPS stimulation resulted in less phosphorylation, indicating that recognition of a2-3 sialic acid by DC alters TLR 4 triggering and DC signaling. Differential signaling is therefore identified after α2-3sia stimulation in presence or absence of LPS, which leads, amongst others, to an altered cytokine secretion profile.

To further investigate the specificity of the α2-3-linked sialic acid altered phosphorylation, we additionally synthesized dendrimers with α2-6-linked sialic acids (α2-6sia, **Sl. Figure 1**). Although both structures contain a terminal sialic acid, the linkage to the underlying galactose is structurally different. The α2-6sia binding to moDCs was studied in presence of LPS, as more biological processes were affected, similarly to the α2-3sia binding with LPS (**Figure 2E** and **Sl Figure 3A**). Only 8 of the 72 significantly altered phosphoproteins were shared between the two glycans in presence of LPS and phosphorylated at the at the same phosphorylation site (**Figures 2E, F** and **Table 1**). The directionality of the protein phosphorylation status additionally overlapped, except for RGS14 phosphorylation (-2.06 with α2-3sia; 2.27 with α2-6sia). Other studies have found a relationship between this G protein-coupled receptor and TLR4 signaling, where stimulation of DCs with LPS markedly decreased RGS14 phosphorylation, which negatively impacted DC IL-12 production (33, 34). To reveal whether the 8 overlapping phosphoproteins were correlated in function, we performed STRING analysis. However, no interactions were found (data not shown). Therefore, we concluded that the stimulation with α2-3sia leads to a very distinct signaling profile compared to α2-6sia in presence of LPS. The distinction between the two patterns might be explained by might be explained by the presence of multiple Siglec receptors and their individual binding preferences for specific sialic acid linkages (35). Siglec-7, and -9 are expressed by moDCs and bind α2-3sia, while α2-6sia is recognized by more Siglecs (36). Siglec-10 binds α2-6sia and is also able to recognize α2-3sia to a lesser extent (36). Nonetheless, the Siglec-10 receptor is expressed on moDCs only at very low levels compared to Siglec-7 and -9 (36). This would indicate binding of the α2-3sia dendrimer to both Siglec-7 and -9, while the α2-6sia dendrimer likely triggers other Siglec receptors. The observed signaling patterns are therefore the result of the collective Siglec receptors expressed by moDCs that recognize the particular sialic acid. Further elucidation of the Siglec-specific pathways upon α2-3sia and LPS co-stimulation would therefore be an intriguing area for future investigations. Analysis of altered biological processes after α2-3 sialic acid and LPS encounter.

Despite the large amount of functionally connected nodes, the biological processes affected were difficult to predict. Therefore, we applied gene ontology analysis using the Cytoscape plug-in tool ClueGO to classify in which biological processes the 109 phosphoproteins play a role (37). We continued only with the α2-3sia plus LPS stimulated condition, as the higher number of significantly altered proteins generated a more interconnected GO network compared to the α2-3sia only, α2-6sia only, or α2-6sia with LPS stimulations (**Sl. Figure 2B, 3**). The proteins were annotated to 36 different GO terms and organized in groups. Seven groups were found, including regulation of proliferation, growth hormone response, RNA regulation, growth factor response, organelle and podosome assembly, and SMAD protein signaling (**Figures 3A, B**). The proteins involved with each GO term and groups can be found in **Sl. Table 5**. A smaller cluster was found involving the regulation of IL-12 (**Figure 3A**), which could result in the alterations on the IL-10:IL-12 axis (**Figure 1B**). STAT3 was annotated to each of the GO terms within the IL-12 group. Pathview analysis of the JAK-STAT signaling pathway revealed that other proteins in this specific pathway were affected by α2-3sia and LPS stimulation, including the STAT proteins themselves, SOS, mTOR, CBP, and PIAS (**Figure 3C**) (38). Furthermore, HNRNPA2B1 within the purple IL-12 regulatory group (**Figure 3A** and **Sl. Table 5**) has been

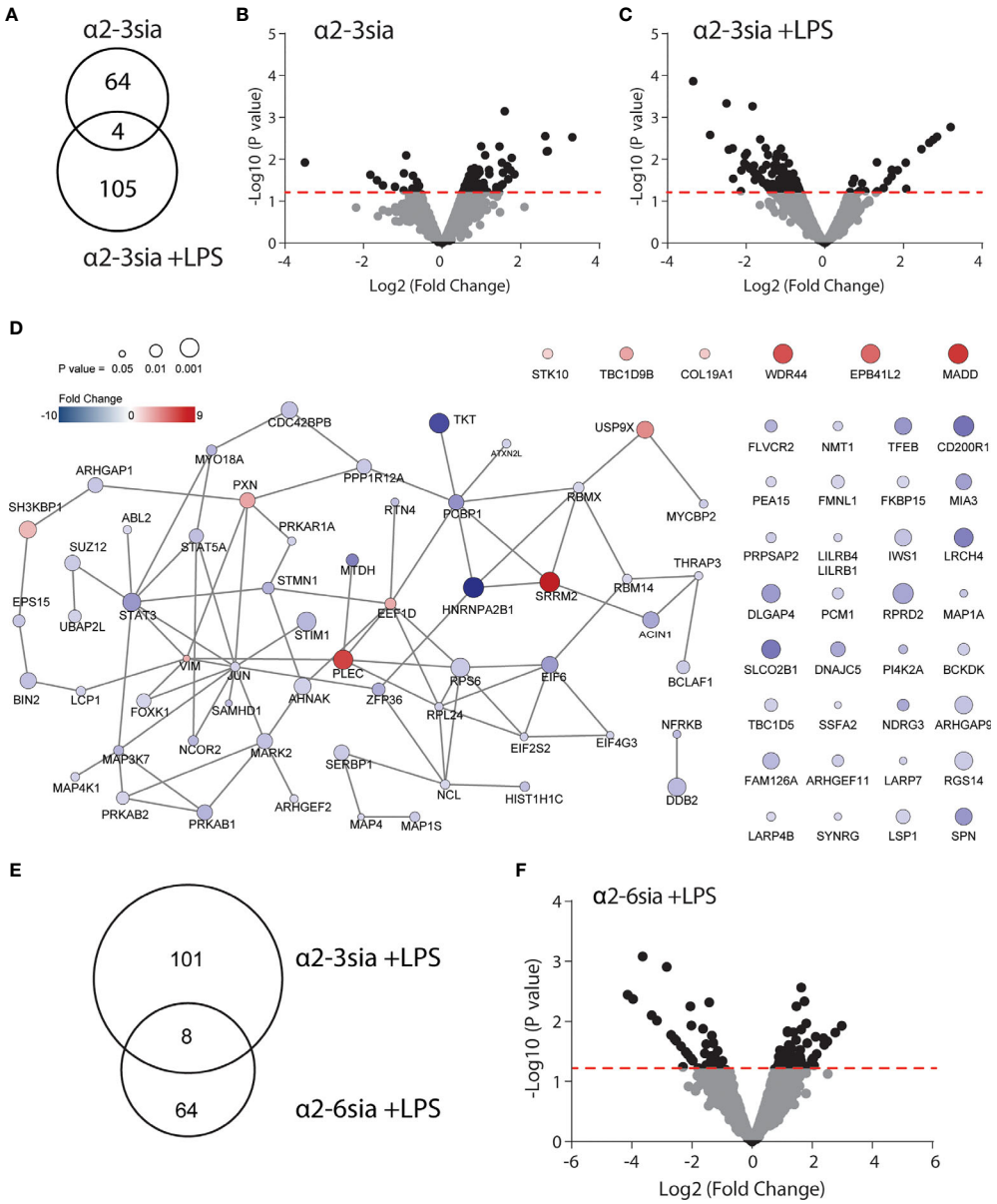

FIGURE 2 | Alterations in the phosphoproteomic landscape after sialic acid stimulation. **(A)** A total of 68 phosphorylation sites were significantly altered by α2-3sia stimulation, while 109 were altered by α2-3sia and LPS. Only 4 phosphorylation sites were identical between the two conditions. **(B)** The Volcano plot demonstrates the directionality of the phosphorylation status on proteins after stimulation with the α2-3sia dendrimer. The data above de red dotted line represent all the significantly altered phosphoproteins in three donors. The –Log10 of the average p values, calculated with a limma test, is presented against the Log2 in fold change. **(C)** The Volcano plot demonstrates modified phosphoprotein expression after stimulation with the α2-3 sialic acid dendrimer. The data above de red dotted line represent all the significantly altered phosphoproteins in three donors. The –Log10 of the average p values, calculated with a limma test, is presented against the Log2 in fold change. **(D)** STRING analysis reveals a network of 88 phosphoprotein significantly affected by α2-3 sialic acid binding in the presence of LPS. **(E)** Phosphoproteomic analysis after α2-6sia stimulation in presence of LPS revealed 72 significantly altered phosphoproteins, of which 8 overlapped with α2-3sia stimulation with LPS. **(F)** The Volcano plot demonstrates the directionality of phosphorylation status on proteins after stimulation with the α2-6sia dendrimer and LPS. The data above de red dotted line represent all the significantly altered phosphoproteins in three donors. The –Log10 of the average p values, calculated with a limma test, is presented against the Log2 fold change.

associated with the JAK-STAT signaling pathway in T cells, where stimulation with IL-12 resulted in decreased expression of HNRNPA2B1 through STAT signaling (39). The JAK-STAT signaling pathway is therefore an interesting lead to study the mechanism behind the downregulation of IL-12 secretion in DCs upon encounter of α2-3sia and LPS.

TABLE 1 | The 8 shared phosphoproteins in the α2-3sia and α2-6sia stimulation with LPS.

Protein Name	UniProt ID	PhosphoSite	α2-3sia		α2-6sia	
			Fold Change	P value	Fold Change	P value
RGS14	O43566	Ser288	-2.06	0.0087	2.27	0.0146
EEF1D	P29692	Ser133	3.03	0.0330	4.34	0.0180
SH3KBP1	Q96B97	Ser587	2.51	0.0119	2.68	0.0493
EPS15	P42566	Ser796	-2.23	0.0302	-2.44	0.0231
SERBP1	Q8NC51	Ser203	-2.12	0.0182	-2.68	0.0048
CD200R1	Q8TD46	Ser297	-5.65	0.0005	-2.58	0.0447
PXN	P49023	Ser126	3.25	0.0179	3.04	0.0390
DDB2	Q92466	Ser24	-2.72	0.0078	-3.09	0.0133

The overlapping proteins are presented with their protein ID and phosphorylation status upon stimulation. Apart from RGS14, the phosphorylation was similarly affected by the different stimulation conditions. No functional connectivity between these proteins was found.

Altered Kinase Signatures After α2-3 Sialic Acid Binding in the Presence of LPS

Kinases are essential to signal transduction. Their phosphorylation activity on proteins directs the protein function and localization (40). Integrative Inferred Kinase Activity (INKA) analysis was applied on the phosphoproteomic data to assess the kinase activity after moDC binding to α2-3sia in presence of LPS. This method integrates four phosphoproteomic analyses of one sample to a scoring system, allowing ranking of the kinase activity and visualization of the kinase-substrate networks (23). Multiple kinases were affected by α2-3sia and LPS stimulation (**Figure 4A** and **Sl. Figure 4**). Particularly the scoring of kinases ERK and AKT1 was lower after stimulation, while an overall decreased trend was seen with the affected kinase signature. Additionally, we performed a phosphoproteomic analysis to validate kinase signature found with the INKA scoring. This allowed evaluation of the kinase signatures after α2-3sia and LPS stimulation through Gene Set Enrichment Analysis using a post-translational modification database (PTMsigDB) with site-specific signature information of perturbations, kinase activities and signaling pathways (**Figure 4B** and **Sl. Figure 5**) (24). The red signature scores indicate a significant positive correlation between the signature and data set, while an anti-correlation is reflected by the blue negative scores. The arrows indicate a shared affected signature with the INKA scoring. A significant positive correlation was found of the signature involving U0126, a highly selective inhibitor of the MEK kinase, implying inhibition of the MAPK/ERK signaling pathway after α2-3sia binding to DCs in presence of LPS (41, 42). Furthermore, a negative correlation of the thymic stromal lymphopoietin (TSLP) signature was found. Activation of DCs by TSLP has been linked to the initiation of T_H2 responses, and to promote triggering of the JAK-STAT pathway (43, 44). A negative correlation was additionally observed with the Leptin and Insulin pathways, although it was not found by INKA scoring. Interestingly, both signatures are involved in promoting DC maturation and migration (45, 46). The negative correlation would therefore indicate that the maturation process of DCs are negatively affected by α2-3sia stimulation. The phosphoproteomic analysis therefore indicates that DC triggering with α2-3sia and LPS is negatively correlated to DC maturation and the induction of inflammatory T cell responses. The kinases that emerged from the INKA and PTMsigDB analyses were mapped to the chemokine signaling pathway (**Figure 4C**). The kinase activity within the pathway is associated with various processes, such as genetic reprogramming and regulation of the actin cytoskeleton. DC binding of α2-3sia in presence of LPS was able to affect this signaling pathway through several kinases. Furthermore, kinase activity within the MAPK signaling pathway was additionally affected, which could lead to altered dendritic cell proliferation and differentiation (**Sl. Figure 6**). These results therefore imply that α2-3sia binding to moDCs enables a kinase activity pattern through similar pathways as DC triggering with chemokines. Alterations in the MAPK/ERK, and JAK-STAT signaling pathway could therefore contribute to skewing of the DC toward a tolerogenic immune status, by means of the altered IL-10:IL-12 secretion axis.

JAK-STAT Signaling Pathway Is Affected After α2-3 Sialic Acid Binding in the Presence of LPS

Stimulation with α2-3sia in presence of LPS altered multiple proteins within the JAK-STAT signaling pathway (**Figure 3C**). The STAT proteins have been described as important regulators of DC activity and are involved in DC-mediated T cell skewing (31, 32). In the phosphoproteomic quantification, both the phosphorylation of STAT3 and STAT5A was significantly downregulated (**Figures 5A, B**). The STAT3 phosphorylation on serine-727 was 4.08-fold lower. Hypersialylation of cancer cells and secretion of sialic acids in the tumor microenvironment is a common step in cancer cell progression to facilitate immune escape. In NSCLC, α2-3 sialylation was elevated in total serum and phosphorylation of STAT3 Ser727 (and Tyr705) was also reduced in moDCs upon stimulation with sera of multiple non-small cell lung cancer (NSCLC) patients (47), validating the decrease in STAT3 phosphorylation measured here (48).

Phosphorylation of STAT5A on the Ser780 residue was 2.5-fold lower after 30 minutes of α2-3sia stimulation in the presence of LPS (**Figure 5B**). In contrast to STAT3, an immune suppressive role for STAT5A in dendritic cell signaling has not been described yet. Nevertheless, a critical role is reserved for STAT5 in DCs in the skewing of T_H2, but not T_H1-type immune responses (32). Phosphorylation of the Ser780 residue is

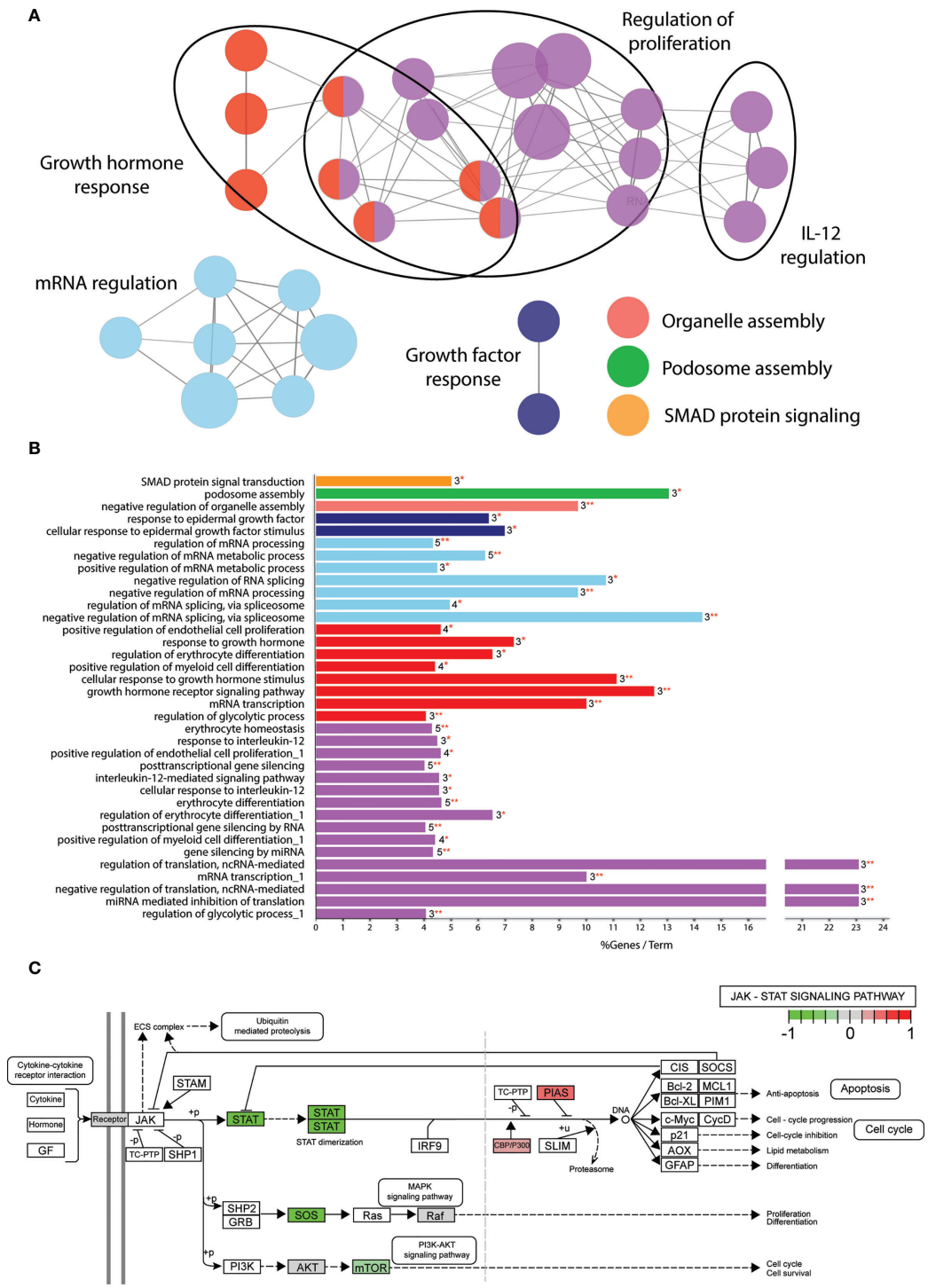

FIGURE 3 | Significantly altered phosphoproteins are involved in multiple biological processes. **(A)** GO term enrichment analysis through ClueGO of the α2-3sia altered proteins in presence of LPS mapped to multiple networks. The node color groups multiple GO terms. The node size represents the number of genes annotated to each term, and de edges between the nodes indicate an overlap in proteins. The differentially affected proteins are clustered into multiple networks and processes. **(B)** GO analysis results are classified in functionally grouped network of terms/pathways and color coded to the GO groups. The bars represent the % genes per term, followed by the absolute number of proteins annotated to the term and with what significance (*$p < 0.05$, **$p < 0.01$). Terms with multiple occurrences in functional groups are marked with "_1" in the name. The differentially affected proteins are categorized into 7 groups total. **(C)** Visualization of the significantly altered proteins of α2-3sia stimulated moDCs in presence of LPS within the JAK-STAT signaling pathway.

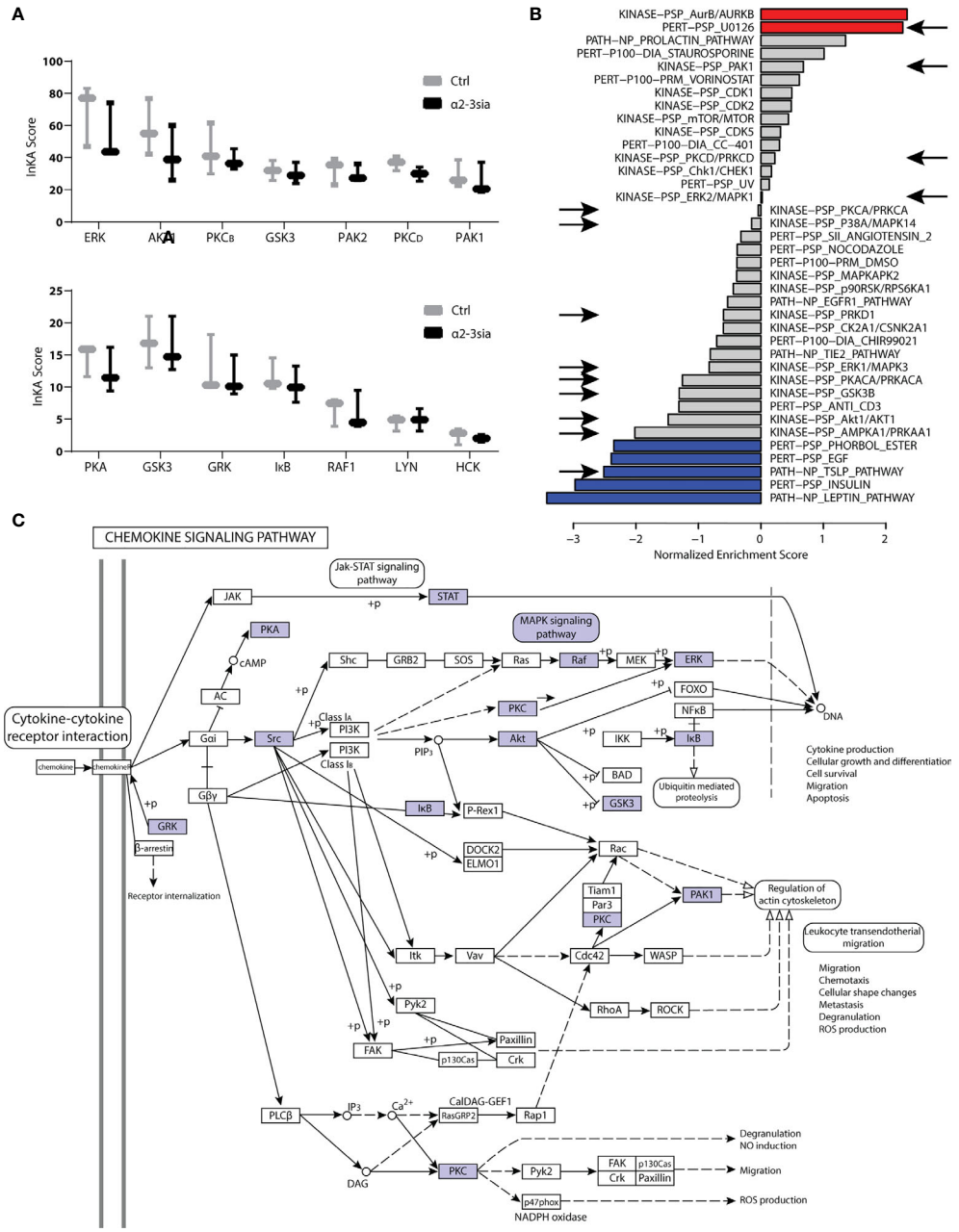

FIGURE 4 | Kinase activity in α2-3sia and LPS stimulation conditions. **(A)** INKA analysis of α2-3sia stimulated moDCs compared to control stimulation all in presence of LPS shows decreased scoring of kinases ERK, AKT1, PKCB, GSK3, PKCD, PAK1, PKA, GSK3, GRK, IκB, and RAF1. **(B)** PTMsigDB signature scoring after stimulation with α2-3sia and LPS is divided into three categories (perturbations, kinases and signatures of molecular pathways). Particularly the red and blue signatures are significantly altered after the stimulation. The signatures appointed by the arrows were also affected in the INKA analysis. **(C)** The affected kinase signatures were involved in the chemokine signaling pathway, indicated by the blue colored kinases.

necessary for translocation of the protein to the nucleus to affect genetic reprogramming of DCs during maturation (49). Analysis of the phosphorylation status through flow cytometric measurement showed only little de-phosphorylation of both the STAT proteins over time compared to control (**Figures 5C, D** and **Sl. Figure 7A**). While both the STAT protein quantities remained relatively similar over time, only a small decrease in fluorescent signal was seen at 30 minutes. Quantification of four donors however, demonstrated decreased phosphorylation of STAT3 at 30 minutes, while the phosphorylation status of STAT5A is variable over time between donors. De-phosphorylation was at its lowest already at 20

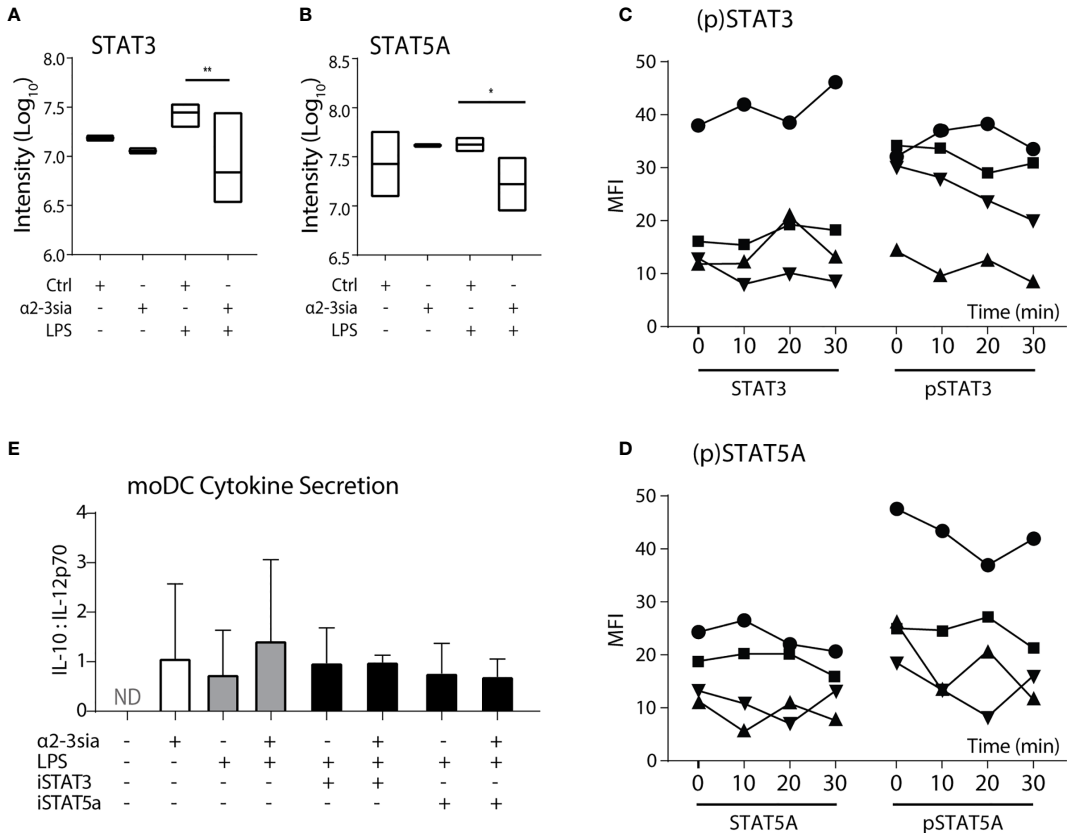

FIGURE 5 | STAT5A phosphorylation is decreased after α2-3 sialic acid binding. **(A)** The phosphoproteomic results (Log10 normalized intensity) of STAT3 phosphorylation after stimulation with the glycodendrimers with or without LPS stimulation. A significant decrease was seen after stimulation with α2-3sia in presence of LPS. **p < 0.01, n=3. **(B)** The phosphoproteomic results (Log10 normalized counts) of STAT5A phosphorylation after stimulation with the glycodendrimers with or without LPS stimulation. A significant decrease was seen after stimulation with α2-3sia stimulation in presence of LPS. *p < 0.05, n=3. **(C)** Flow cytometric quantification of (phosphorylated) STAT3 proteins. A trend towards decreased STAT3 phosphorylation is seen over time. **(D)** Flow cytometric quantification of (phosphorylated) STAT5A proteins of four different individuals. A trend towards decreased STAT5A phosphorylation is seen over time. **(E)** The IL10:IL-12 ratio after overnight stimulation with either of the STAT inhibitors resulted in a similar level as the α2-3sia dendrimer stimulation. Dual stimulation with the inhibitor and dendrimer demonstrated similar results. Range IL-10 22-1061 pg/mL; IL-12 7-1921 pg/mL.

minutes for two donors, while the other two donors exhibited the decrease at 30 minutes. Overnight moDCs co-stimulation with LPS and either STAT inhibitor demonstrated an increase of IL-10 secretion (**Sl. Figure 7B**). Nonetheless, inhibition of both STAT proteins minimally affected IL-12 secretion (data not shown), resulting in an unaltered IL10:IL-12 ratio compared to α2-3sia stimulation (**Figure 5E**).

α2-3sia stimulation was able to affect the JAK-STAT signaling within LPS-treated DCs by lowering the phosphorylation status of STAT3 and STAT5A after approximately 30 minutes. STAT3 in DCs has already been proposed as a potential therapeutic target for induction of tolerance (50). Inhibition of this protein attenuates immune responses through IL-10 biased skewing of the IL-10:IL-12 axis and thus less effector T cell development. It is therefore tempting to speculate that moDC binding to α2-3sia also results the increase of IL-10 secretion through de-phosphorylation of STAT3 Ser727. Continued investigation of the DC STAT3 phosphorylation and the effect on the cytokine secretion profiles would therefore be highly relevant for insight regarding the induction of DC-mediated immune suppression. For STAT5 the therapeutic outcome is less straightforward. De-phosphorylation of STAT5A after α2-3sia and LPS stimulation suggests decreased nuclear translocation and inhibition of its transcriptional function. Translocation studies could elucidate STAT5A activity and localization within DCs after α2-3sia engagement. Furthermore, the transcriptional role of STAT5 in naïve T cell skewing is highly relevant for the suppression of the effector T cell response induced by α2-3sia and LPS-treated moDCs. Analysis of the T_H1/T_H2 skewing after blocking of both STAT proteins in DCs could additionally establish the validity of the JAK-STAT signaling by α2-3sia and LPS stimulation. The importance of the JAK-STAT signaling in the induction of tolerance could furthermore be elucidated *via* co-stimulation with the α2-3sia dendrimer and other TLR stimuli, such as DAMPs. Triggering of JAK-STAT signaling would indicate a central role of this pathway after α2-3sia recognition. Lastly,

underlying glycan moieties to the sialic acid can contribute to alterations in Siglec recognition and the induced signaling (51). Larger sialic acid-harboring saccharides that are present *in situ* are therefore very appealing for further exploration. The use of these glycans could additionally contribute to defining the upstream proteins and receptor of the JAK-STAT pathway to provide insight of the induction of tolerance *via* the sialic acid-Siglec axis *in situ* such as in the case of tumor immune evasion (52).

CONCLUSION

DCs possess the extraordinary capacity to elicit an appropriate tailored immune response after recognizing internal or external danger signals. This study set out to explore the early events of dendritic cell immune signaling induced upon α2-3 sialic acid dendrimer binding in presence of LPS. Through analysis of phosphoproteomic and kinase activity we found that α2-3 sialic acid modulates LPS stimulation of DCs. The differences in the phosphoproteome induced were not observed in LPS alone nor α2-3sia alone, implying specific modulation of the TLR4 signaling pathway by α2-3sia. Gene ontology revealed that some of these altered proteins were involved in the regulation of IL-12. The IL-10:IL-12 ratio was indeed increased upon α2-3sia stimulation, implying a significant role for the annotated phosphoproteins. Kinome analysis demonstrated a negative correlation with the TSLP signature, which promotes triggering of the JAK-STAT signaling pathway and initiation of T_H2 responses. The analysis of the DC kinase activity therefore indicates that α2-3sia and LPS triggering results in a kinome that negatively correlates to the induction of inflammatory T cell responses. We additionally identified a decreased phosphorylation of the STAT3 and STAT5A proteins, and the HNRNPA2B1 protein within 30 minutes after addition of α2-3sia to LPS matured DC, again indicating the involvement of the JAK-STAT pathways. Especially the critical role of DC STAT5 in the naïve T cell skewing away from T_H1-type immune responses is highly relevant in the α2-3sia-mediated DC suppression of the T effector response. The decrease in STAT phosphorylation was furthermore α2-3sia-specific and could not be observed upon α2-6sia binding.

DATA AVAILABILITY STATEMENT

All relevant data is contained within the article: The original contributions presented in the study are included in the supplementary files. The mass spectrometry proteomics data have been deposited to the ProteomeXchange Consortium via the PRIDE partner repository with the dataset identifier PXD024443 (http://proteomecentral.proteomexchange.org/cgi/GetDataset).

AUTHOR CONTRIBUTIONS

R-JL and AH were involved in all experiments and wrote the manuscript. The dendrimers were synthesized by R-JL and HK. Under the supervision of CJ, R-JL and RG-H executed the phosphoproteomic enrichment and isolation, SP executed the LC-Ms/Ms measurements, and TP and AAH performed the statistical analyses. ER and AZ aided R-JL in the visualization of the data, all supervised by SV and YK. All authors contributed to the article and approved the submitted version.

FUNDING

This work was funded by the NWO gravitation program 2013 granted to the Institute for Chemical Immunology (ICI-024.002.009) and the LSH-TKI project DC4Balance (LSHM18056-SGF). Cancer Center Amsterdam is acknowledged for support of the proteomics infrastructure.

ACKNOWLEDGMENTS

The authors would like to thank the Biochemistry GlycO2Peptide Unit and the Microscopy and Cytometry Core Facility for their support.

SUPPLEMENTARY MATERIAL

The Supplementary Material for this article can be found online at: https://www.frontiersin.org/articles/10.3389/fimmu.2021.673454/full#supplementary-material

REFERENCES

1. Novak N, Gros E, Bieber T, Allam J-P. Human Skin and Oral Mucosal Dendritic Cells as "Good Guys" and "Bad Guys" in Allergic Immune Responses. *Clin Exp Immunol* (2010) 161(1):28–33. doi: 10.1111/j.1365-2249.2010.04162.x
2. Tang D, Kang R, Coyne CB, Zeh HJ, Lotze MT. Pamps and DAMPs: Signal 0s That Spur Autophagy and Immunity. *Immunol Rev* (2012) 249(1):158–75. doi: 10.1111/j.1600-065X.2012.01146.x
3. Varki A. Letter to the Glyco-Forum: Since There are PAMPs and DAMPs, There Must be SAMPs? Glycan "Self-Associated Molecular Patterns" Dampen Innate Immunity, But Pathogens can Mimic Them. *Glycobiology* (2011) 21(9):1121–4. doi: 10.1093/glycob/cwr087
4. Pereira MS, Alves I, Vicente M, Campar A, Silva MC, Padrão NA, et al. Glycans as Key Checkpoints of T Cell Activity and Function. *Front Immunol Front Media SA* (2018). doi: 10.3389/fimmu.2018.02754
5. Johannssen T, Lepenies B. Glycan-Based Cell Targeting To Modulate Immune Responses. *Trends Biotechnol Elsevier Ltd* (2017) 334–46. doi: 10.1016/j.tibtech.2016.10.002
6. Macauley MS, Crocker PR, Paulson JC. Siglec-Mediated Regulation of Immune Cell Function in Disease. *Nat Rev Immunol* (2014) 14(10):653–66. doi: 10.1038/nri3737
7. Varki A. Sialic Acids in Human Health and Disease. *Trends Mol Med* (2008) 14(8):351–60. doi: 10.1016/j.molmed.2008.06.002
8. Perdicchio M, Ilarregui JM, Verstege MI, Cornelissen LAM, Schetters STT, Engels S, et al. Sialic Acid-Modified Antigens Impose Tolerance *Via*

Inhibition of T-Cell Proliferation and De Novo Induction of Regulatory T Cells. *Proc Natl Acad Sci USA* (2016) 113(12):3329–34. doi: 10.1073/pnas.1507706113
9. Bandala-Sanchez E, Zhang Y, Reinwald S, Dromey JA, Lee B-H, Qian J, et al. Cell Regulation Mediated by Interaction of Soluble CD52 With the Inhibitory Receptor Siglec-10. *Nat Immunol* (2013) 14(7):741–8. doi: 10.1038/ni.2610
10. O'Reilly MK, Paulson JC. Siglecs as Targets for Therapy in Immune-Cell-Mediated Disease. *Trends Pharmacol Sci* (2009) 30(5):240–8. doi: 10.1016/j.tips.2009.02.005
11. Rodrigues E, Macauley MS. Hypersialylation in Cancer: Modulation of Inflammation and Therapeutic Opportunities. *Cancers (Basel)* (2018) 10(6). doi: 10.3390/cancers10060207
12. Büll C, Boltje TJ, van Dinther EAW, Peters T, de Graaf AMA, Leusen JHW, et al. Targeted Delivery of a Sialic Acid-Blocking Glycomimetic to Cancer Cells Inhibits Metastatic Spread. *ACS Nano* (2015) 9(1):733–45. doi: 10.1021/nn5061964
13. Xiao H, Woods EC, Vukojicic P, Bertozzi CR. Precision Glycocalyx Editing as Strategy for Cancer Immunotherapy. *PNAS* (2016) 113(37):10304–9. doi: 10.1073/pnas.1608069113
14. Severi E, Hood DW, Thomas GH. Sialic Acid Utilization by Bacterial Pathogens. *Microbiology* (2007) 153(9):2817–22. doi: 10.1099/mic.0.2007/009480-0
15. Chang Y-C, Olson J, Beasley FC, Tung C, Zhang J, Crocker PR, et al. Group B Streptococcus Engages an Inhibitory Siglec Through Sialic Acid Mimicry to Blunt Innate Immune and Inflammatory Responses In Vivo. *PloS Pathog* (2014) 10(1):e1003846. doi: 10.1371/journal.ppat.1003846
16. Uchiyama S, Sun J, Fukahori K, Ando N, Wu M, Schwarz F, et al. Dual Actions of Group B Streptococcus Capsular Sialic Acid Provide Resistance to Platelet-Mediated Antimicrobial Killing. *Proc Natl Acad Sci USA* (2019) 116(15):7465–70. doi: 10.1073/pnas.1815572116
17. Ritchie ME, Phipson B, Wu D, Hu Y, Law CW, Shi W, et al. Limma Powers Differential Expression Analyses for RNA-sequencing and Microarray Studies. *Nucleic Acids Res* (2015) 43(47):e47. doi: 10.1093/nar/gkv007
18. Piersma SR, Knol JC, de Reus I, Labots M, Sampadi BK, Pham TV, et al. Feasibility of Label-Free Phosphoproteomics and Application to Base-Line Signaling of Colorectal Cancer Cell Lines. *J Proteomics* (2015) 127:247–58. doi: 10.1016/J.JPROT.2015.03.019
19. van der Mijn JC, Labots M, Piersma SR, Pham TV, Knol JC, Broxterman HJ, et al. Evaluation of Different Phospho-Tyrosine Antibodies for Label-Free Phosphoproteomics. *J Proteomics* (2015) 127(Pt B):259–63. doi: 10.1016/j.jprot.2015.04.006
20. Szklarczyk D, Gable AL, Lyon D, Junge A, Wyder S, Huerta-Cepas J, et al. String V11: Protein-Protein Association Networks With Increased Coverage, Supporting Functional Discovery in Genome-Wide Experimental Datasets. *Nucleic Acids Res* (2019) 47(D1):D607–13. doi: 10.1093/nar/gky1131
21. Shannon P, Markiel A, Ozier O, Baliga NS, Wang JT, Ramage D, et al. Cytoscape: A Software Environment for Integrated Models of Biomolecular Interaction Networks. *Genome Res* (2003) 13(11):2498–504. doi: 10.1101/gr.1239303
22. Luo W, Brouwer C. Pathview: An R/Bioconductor Package for Pathway-Based Data Integration and Visualization. *Bioinformatics* (2013) 29(14):1830–1. doi: 10.1093/bioinformatics/btt285
23. Beekhof R, Alphen C, Henneman AA, Knol JC, Pham TV, Rolfs F, et al. INKA, an Integrative Data Analysis Pipeline for Phosphoproteomic Inference of Active Kinases. *Mol Syst Biol* (2019) 15(5). doi: 10.15252/msb.20198981
24. Krug K, Mertins P, Zhang B, Hornbeck P, Raju R, Ahmad R, et al. A Curated Resource for Phosphosite-Specific Signature Analysis. *Mol Cell Proteomics* (2019) 18(3):576–93. doi: 10.1074/mcp.TIR118.000943
25. García-Vallejo JJ, Ambrosini M, Overbeek A, van Riel WE, Bloem K, Unger WWJ, et al. Multivalent Glycopeptide Dendrimers for the Targeted Delivery of Antigens to Dendritic Cells. *Mol Immunol* (2013) 53(4):387–97. doi: 10.1016/J.MOLIMM.2012.09.012
26. Chaffin DO, Mentele LM, Rubens CE. Sialylation of Group B Streptococcal Capsular Polysaccharide Is Mediated by CpsK and Is Required for Optimal Capsule Polymerization and Expression. *J Bacteriol* (2005) 187(13):4615–26. doi: 10.1128/JB.187.13.4615-4626.2005
27. Qi H, Denning TL, Soong L. Differential Induction of Interleukin-10 and Interleukin-12 in Dendritic Cells by Microbial Toll-Like Receptor Activators and Skweing of T-Cell Cytokine Profiles. *Infect Immun* (2003) 71(6):3337–42. doi: 10.1128/IAI.71.6.3337-3342.2003
28. Wojcechowskyj JA, Didigu CA, Lee JY, Parrish NF, Sinha R, Hahn BH, et al. Quantitative Phosphoproteomics Reveals Extensive Cellular Reprogramming During HIV-1 Entry. *Cell Host Microbe* (2013) 13(5):613–23. doi: 10.1016/j.chom.2013.04.011
29. Villarroya-Beltri C, Gutiérrez-Vázquez C, Sánchez-Cabo F, Pérez-Hernández D, Vázquez J, Martin-Cofreces N, et al. Sumoylated HnRNPA2B1 Controls the Sorting of MiRNAs Into Exosomes Through Binding to Specific Motifs. *Nat Commun* (2013) 4:2980. doi: 10.1038/ncomms3980
30. McCracken S, Longman D, Marcon E, Moens P, Downey M, Nickerson JA, et al. Proteomic Analysis of SRm160-Containing Complexes Reveals a Conserved Association With Cohesin. *J Biol Chem* (2005) 280(51):42227–36. doi: 10.1074/jbc.M507410200
31. Melillo JA, Song L, Bhagat G, Blazquez AB, Plumlee CR, Lee C, et al. Dendritic Cell (Dc)-Specific Targeting Reveals Stat3 as a Negative Regulator of DC Function. *J Immunol* (2010) 184(5):2638–45. doi: 10.4049/jimmunol.0902960
32. Bell BD, Kitajima M, Larson RP, Stoklasek TA, Dang K, Sakamoto K, et al. The Transcription Factor STAT5 is Critical in Dendritic Cells for the Development of TH2 But Not Th1 Responses. *Nat Immunol* (2013) 14(4):364–71. doi: 10.1038/ni.2541
33. Shi G-X, Harrison K, Han S-B, Moratz C, Kehrl JH, Piemonti L, et al. Toll-Like Receptor Signaling Alters the Expression of Regulator of G Protein Signaling Proteins in Dendritic Cells: Implications for G Protein-Coupled Receptor Signaling. *J Immunol* (2004) 172(9):5175–84. doi: 10.4049/jimmunol.172.9.5175
34. Braun MC, Kelsall BL. Regulation of Interleukin-12 Production ByG-Protein-Coupled Receptors. *Microbes Infect* (2001) 3(2):99–107. doi: 10.1016/S1286-4579(00)01357-5
35. Lock K, Zhang J, Lu J, Lee SH, Crocker PR. Expression of CD33-related Siglecs on Human Mononuclear Phagocytes, Monocyte-Derived Dendritic Cells and Plasmacytoid Dendritic Cells. *Immunobiology* (2004) 209(1-2):199–207. doi: 10.1016/j.imbio.2004.04.007
36. Crocker PR, Paulson JC, Varki A. Siglecs and Their Roles in the Immune System. *Nat Rev Immunol* (2007) 7(4):255–66. doi: 10.1038/nri2056
37. Bindea G, Mlecnik B, Hackl H, Charoentong P, Tosolini M, Kirilovsky A, et al. Cluego: A Cytoscape Plug-in to Decipher Functionally Grouped Gene Ontology and Pathway Annotation Networks. *Bioinformatics* (2009) 25(8):1091–3. doi: 10.1093/bioinformatics/btp101
38. Luo W, Pant G, Bhavnasi YK, Blanchard SG, Brouwer C. Pathview Web: User Friendly Pathway Visualization and Data Integration. *Nucleic Acids Res* (2017) 45(W1):W501–8. doi: 10.1093/nar/gkx372
39. Rosengren AT, Nyman TA, Lahesmaa R. Proteome Profiling of Interleukin-12 Treated Human T Helper Cells. *Proteomics* (2005) 5(12):3137–41. doi: 10.1002/pmic.200401151
40. Hardie DG. Roles of Protein Kinases and Phosphatases in Signal Transduction. *Symp Soc Exp Biol* (1990) 44:241–55.
41. Duan W, Chan JHP, Wong CH, Leung BP, Wong WSF. Anti-Inflammatory Effects of Mitogen-Activated Protein Kinase Kinase Inhibitor U0126 in an Asthma Mouse Model. *J Immunol* (2004) 172(11):7053–9. doi: 10.4049/jimmunol.172.11.7053
42. Marampon F, Bossi G, Ciccarelli C, Di Rocco A, Sacchi A, Pestell RG, et al. Mek/Erk Inhibitor U0126 Affects in Vitro and in Vivo Growth of Embryonal Rhabdomyosarcoma. *Mol Cancer Ther* (2009) 8(3):543–51. doi: 10.1158/1535-7163.MCT-08-0570
43. Ito T, Wang YH, Duramad O, Hori T, Delespesse GJ, Watanabe N, et al. Tslp-Activated Dendritic Cells Induce an Inflammatory T Helper Type 2 Cell Response Through OX40 Ligand. *J Exp Med* (2005) 202(9):1213–23. doi: 10.1084/jem.20051135
44. Shi Z, Jiang W, Wang M, Wang X, Li X, Chen X, et al. Inhibition of JAK/STAT Pathway Restrains Tslp-Activated Dendritic Cells Mediated Inflammatory T Helper Type 2 Cell Response in Allergic Rhinitis. *Mol Cell Biochem* (2017) 430(1–2):161–9. doi: 10.1007/s11010-017-2963-7
45. Al-Hassi HO, Bernardo D, Murugananthan AU, Mann ER, English NR, Jones A, et al. A Mechanistic Role for Leptin in Human Dendritic Cell Migration: Differences Between Ileum and Colon in Health and Crohn's Disease. *Mucosal Immunol* (2013) 6(4):751–61. doi: 10.1038/mi.2012.113

46. Lu H, Huang D, Yao K, Li C, Chang S, Dai Y, et al. Insulin Enhances Dendritic Cell Maturation and Scaventer Receptor-Mediated Uptake of Oxidised Low-Density Lipoprotein. *J Diabetes Complications* (2015) 29(4):465–71. doi: 10.1016/j.jdiacomp.2015.03.005
47. Li R, Fang F, Jiang M, Wang C, Ma J, Kang W, et al. STAT3 and NF-Kb Are Simultaneously Suppressed in Dendritic Cells in Lung Cancer. *Sci Rep* (2017) 7(1):45395. doi: 10.1038/srep45395
48. Ferens-Sieczkowska M, Kratz E, Kossowska B, Passowicz-Muszyńska E, Jankowska R. Comparison of Haptoglobin and Alpha1-Acid Glycoprotein Glycosylation in the Sera of Small Cell and Non-Small Cell Lung Cancer Patients. *Postepy Hig Med Dosw* (2013) 67:828–36. doi: 10.5604/17322693.1061788
49. Berger A, Hoelbl-Kovacic A, Bourgeais J, Hoefling L, Warsch W, Grundschober E, et al. Pak-Dependent STAT5 Serine Phosphorylation is Required for BCR-ABL-Induced Leukemogenesis. *Leukemia* (2014) 28 (3):629–41. doi: 10.1038/leu.2013.351
50. Barton BE. Stat3: A Potential Therapeutic Target in Dendritic Cells for the Induction of Transplant Tolerance. *Expert Opin Ther Targets* (2006) 10 (3):459–70. doi: 10.1517/14728222.10.3.459
51. Alphey MS, Attrill H, Crocker PR, van Aalten DM. High Resolution Crystal Structures of Siglec-7. Insights Into Ligand Specificity in the Siglec Family. *J Biol Chem* (2003) 31278(5):3372–7. doi: 10.1074/jbc.M210602200
52. Perdicchio M, Cornelissen LAM, Streng-Ouwehand I, Engels S, Verstege MI, Boon L, et al. Tumor Sialylation Impedes T Cell Mediated Anti-Tumor Responses While Promoting Tumor Associated-Regulatory T Cells. *Oncotarget* (2016) 7(8):8771–82. doi: 10.18632/oncotarget.6822

Conflict of Interest: The authors declare that the research was conducted in the absence of any commercial or financial relationships that could be construed as a potential conflict of interest.

frontiers in Immunology

REVIEW
published: 13 May 2021
doi: 10.3389/fimmu.2021.674048

Therapeutic Liposomal Vaccines for Dendritic Cell Activation or Tolerance

Noémi Anna Nagy[1†], Aram M. de Haas[2†], Teunis B. H. Geijtenbeek[1], Ronald van Ree[1,3], Sander W. Tas[1,4], Yvette van Kooyk[2‡] and Esther C. de Jong[1‡]*

[1] Department of Experimental Immunology, Amsterdam University Medical Center, Amsterdam Institute for Infection and Immunity, University of Amsterdam, Amsterdam, Netherlands, [2] Department of Molecular Cell Biology and Immunology, Amsterdam University Medical Center, Cancer Center Amsterdam, Amsterdam Institute for Infection and Immunity, Vrije Universiteit Amsterdam, Amsterdam, Netherlands, [3] Department of Otorhinolaryngology, Amsterdam University Medical Center, University of Amsterdam, Amsterdam, Netherlands, [4] Department of Rheumatology and Clinical Immunology, Amsterdam University Medical Center, Amsterdam Rheumatology and Immunology Center, University of Amsterdam, Amsterdam, Netherlands

OPEN ACCESS

Edited by:
Irina Caminschi, Monash University, Australia

Reviewed by:
Hiroaki Hemmi, Okayama University of Science, Japan
Roman Spörri, ETH Zürich, Switzerland

***Correspondence:**
Esther C. de Jong
e.c.dejong@amsterdamumc.nl

[†]These authors have contributed equally to this work and share first authorship

[‡]These authors have contributed equally to this work and share last authorship

Specialty section:
This article was submitted to Antigen Presenting Cell Biology, a section of the journal Frontiers in Immunology

Received: *28 February 2021*
Accepted: *26 April 2021*
Published: *13 May 2021*

Citation:
Nagy NA, de Haas AM, Geijtenbeek TBH, van Ree R, Tas SW, van Kooyk Y and de Jong EC (2021) Therapeutic Liposomal Vaccines for Dendritic Cell Activation or Tolerance. Front. Immunol. 12:674048. doi: 10.3389/fimmu.2021.674048

Dendritic cells (DCs) are paramount in initiating and guiding immunity towards a state of activation or tolerance. This bidirectional capacity of DCs sets them at the center stage for treatment of cancer and autoimmune or allergic conditions. Accordingly, many clinical studies use *ex vivo* DC vaccination as a strategy to boost anti-tumor immunity or to suppress immunity by including vitamin D3, NF-κB inhibitors or retinoic acid to create tolerogenic DCs. As harvesting DCs from patients and differentiating these cells *in vitro* is a costly and cumbersome process, *in vivo* targeting of DCs has huge potential as nanoparticulate platforms equipped with activating or tolerogenic adjuvants can modulate DCs in their natural environment. There is a rapid expansion of the choices of nanoparticles and activation- or tolerance-promoting adjuvants for a therapeutic vaccine platform. In this review we highlight the most recent nanomedical approaches aimed at inducing immune activation or tolerance *via* targeting DCs, together with novel fundamental insights into the mechanisms inherent to fostering anti-tumor or tolerogenic immunity.

Keywords: dendritic cell (DC), nanoparticle, liposomes, tolerance, activation, antigen, targeting, adjuvant

INTRODUCTION

The incidence and prevalence of cancer as well as several auto-immune, inflammatory and allergic conditions is on the rise (1, 2). While multiple treatment strategies exist for these conditions, the majority of them have side effects or other drawbacks. Chemotherapy is toxic to all dividing cells in the body, causing strong systemic side effects. Allergies are mostly treated by symptomatic drugs such as antihistamines and local and systemic corticosteroids. For some allergies, a disease-modifying treatment, allergen immunotherapy (AIT), is available but is not used very broadly (3). Although AIT is quite effective, it requires monthly injections or daily sublingual administration of allergen extract for at least 3-5 years. Moreover, it carries the risk for anaphylactic reactions. For autoimmune diseases so-called Disease Modifying Anti-Rheumatic Drugs (DMARDS) are often prescribed (4, 5). These therapies suppress a wider set of immune cells than the pathogenic players, increasing the risk for infections. Furthermore, treatment has to be continued throughout life,

yielding no perspective of a cure (6). There has been tremendous progress in our understanding and harnessing of the immune system to treat these diseases. Immunotherapy is already used in the clinic to treat cancer and inflammatory diseases, but the reprogramming of the immune system to attack and eliminate the tumor or suppress inflammatory responses is also very attractive.

Dendritic cells (DCs) are key in initiating a proper anti-tumor response, as well as dampening adaptive immunity when tolerance to innocuous antigens or auto-antigens is needed (7, 8). DCs initiate an anti-tumor cascade by the uptake of particles derived from tumor cells and cross-presenting the tumor antigens on MHC-I for efficient activation of CD8+ T cell responses (9). Initiation of T_H1 type CD4+ T cell responses *via* DC-derived cytokines such as IL-12 is a crucial component in the anti-tumor response, reinforcing the expansion of CD8+ T cells and licensing CTLs for (tumor) killing (10).

To foster central tolerance in cooperation with thymic epithelial cells, DCs contribute to the deletion of effector T cells in the thymus (11). Lack of co-stimulation by DCs in the periphery leads to anergy or apoptosis of effector T cells. A long reigning dogma proposed that DCs rather passively mediate tolerance *via* an immature or semi-mature state. Opposing this dogma, recent insights challenge the notion that immature DCs effectively promote steady-state tolerance *in vivo*, suggesting that both immunogenic and tolerogenic migratory DCs are 'mature' or activated, and clearly distinguishable by differential expression of quantitative and qualitative markers (12). Supporting this statement, DCs are known to actively induce tolerance *via* co-inhibitory signaling and tolerogenic cytokine production. Active engagement of co-inhibitory signals, such as programmed cell death-1 (PD-1), cytotoxic T-lymphocyte-associated antigen 4 (CTLA-4), and others by their respective receptors on DCs leads not only to anergy and effector T cell deletion, but also to the development of regulatory T cells (Tregs) and reverse signaling in DCs that reinforces their tolerogenic capacity (13). Similarly, distinct surface molecules, immunoregulatory enzymes and cytokines, such as indoleamine-2,3-dioxygenase (IDO), IL-10 and TGF-β produced by DCs can dampen effector T cells, and potently induce several subtypes of Tregs (14). With these strategies at hand tolerogenic DCs can contribute both to deletion of autoreactive T cells in autoimmunity and deletion of T_H2 cells supporting allergic inflammation (15, 16). Moreover, DCs facilitate the development of regulatory B cells which produce more IL-10 for ameliorating autoimmune conditions as well as IgG4, essential for dampening pro-allergic responses (16–18). The versatile skills of DCs coordinating both tolerogenic and inflammatory immune responses make them an excellent target for novel therapies against cancer, autoimmune disease and allergies.

Unsurprisingly, DC-based therapies are now in clinical trial phases for the treatment of various forms of cancer and autoimmune disease (8, 15). A popular DC-based approach is *ex vivo* DC vaccination, a therapy in which patient monocytes or CD34+ progenitors are cultured together with DC activating adjuvants, or DC dampening anti-inflammatory adjuvants, and disease relevant antigen, for subsequent reinfusion in the patient (8, 15). Unfortunately, even though these therapies appear to be safe and well-tolerated, much needs to be done to increase therapeutic efficacy. One putative explanation for this observation is that *ex vivo* cultured DCs are largely monocyte-derived that differ from the naturally occurring DCs *in vivo* (19). In addition, *ex vivo* DC therapy is costly and cumbersome, as cells have to be processed in a controlled, sterile lab environment.

A radically different, promising approach is the targeting of DCs *in vivo*, *via* a therapeutic vaccination-like strategy (**Figure 1**). This approach has the advantage of bypassing costly *ex vivo* isolation and preparation of DCs and potentially provides opportunities of tissue-site targeting of multiple DC subsets in their natural environment (8). Furthermore, *in vivo* targeting platforms can be made available to a broad range of patients, as they are not donor dependent.

One type of treatment focusses on the targeting of DCs *via* antibody-antigen or glycan-antigen conjugates for routing to various surface receptors predominantly expressed on these antigen presenting cells (APCs), as recently reviewed in the context of cancer or immune tolerance elsewhere (20, 21).

A second strategy employs nanoparticles as vehicles for loading disease relevant antigen, adjuvant and targeting molecules to reach DCs *in vivo* (**Figure 1**). Nanoparticle platforms provide the pharmacological advantages of sequestering potentially toxic contents from undesired targets, and release of contents in a controlled fashion to increase bioavailability of compounds (22, 23). Besides these general advantages, a large body of literature states that various nanoparticles have *bona fide* adjuvant effects as they preferentially are engulfed by APCs (22). Although a wide variety of different nanoparticles for various purposes have been developed, we mainly focus on liposomes, nanoparticles composed of a lipid bilayer. Liposomes are not only already FDA approved, but are also highly flexible in that several of their characteristics, such as lipid composition, size, shape, electrical charge and rigidity can be modified (24). Furthermore, due to their chemical structure consisting of a lipophilic bi-layer and a hydrophilic core, liposomes also provide an ideal platform for uniting all desired components of an immune modulatory vaccine (disease relevant antigens, DC-targeting moieties and adjuvants) in one spatial compartment.

DC SUBSETS FOR ANTI-CANCER AND TOLEROGENIC IMMUNOMODULATION

For *in vivo* targeting of DCs one needs to consider that *in-situ* DCs are comprised of a heterogenous mix of subpopulations, with indications of functional differences between the subsets. In humans, current nomenclature describes three major subtypes of DCs based on surface markers: conventional type 1 DCs (cDC1s or CD141+ DCs), conventional type 2 DCs (cDC2s or CD1c+DCs) and plasmacytoid DCs (pDCs) (25). One feature supporting an intrinsic inclination of these subsets to respond in a pro-or anti-inflammatory fashion to different pathogens is their differential

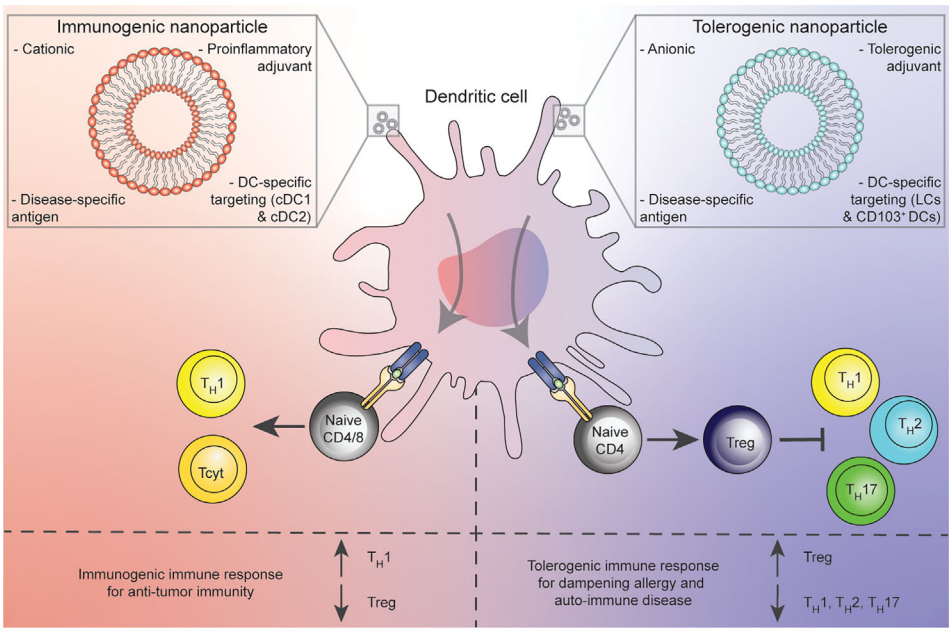

FIGURE 1 | Concept of *in vivo* treatment of DCs with immunogenic (red) or tolerogenic (blue) nanoparticle platforms resulting in pro-inflammatory DCs that prime for T_H1 or Tcyt polarization against cancer (left) or Tregs for the dampening of allergic and auto-immune conditions (right).

expression of various pattern recognition receptors (PRRs) (26). cDC1s highly express toll-like receptors (TLRs) 3, 9 and 10 enabling recognition of intracellular dsRNA or DNA leading to production of type-I interferons and IL-12 (27). cDC2s express the full range of TLR1-9 and a wide range of C-type lectins (CLRs) equipping them with a broad toolkit to respond to various pathogens. pDCs highly express TLRs 7 and 9, leading to a swift type I and III interferon response *via* IRF7 and an efficient anti-viral reaction. cDC1s are classically described to be more apt at cross-presenting antigen to CD8+ T cells, yet can also potently silence these cells for tolerance, and cDC2s seem to effectively advance CD4+ T cell proliferation (26). Also, under inflammatory conditions monocytes can differentiate into monocyte-derived DCs (moDCs) (28). Recent research further subdivides and expands on the current populations of DCs, for example the cDC2-A (DC2), cDC2-B (DC3), and Axl+DCs (27, 29). It is however beyond the scope of this review to go into detail about all the classes and subdivision within the DCs, and we will therefore mainly discuss cDC1, cDC2 and moDC.

Arguably, cDC1s are an important subset in antitumor immunity, as they are very proficient in antigen uptake and cross-presentation to CD8+ T cells, which leads to the induction of cytotoxic effector T cells and a T_H1 response (30). cDC2s, although possibly less apt at cross-presentation and priming of CD8+ T cells, are excellent inducers of CD4+ T cells (31). A recent paper by Bosteels et al. showed that inflammatory cDC2s share important characteristics with cDC1s, including potent induction of CD4+ and CD8+ T cell-immunity to viral infections (32). MoDCs are capable in sampling the environment, but are less efficient in migrating to the lymph nodes for activation of CD8+ T cells (31, 33). However, under the right conditions moDCs can activate the antitumor immunity *via* CD8+ T cells (34). Therefore, although moDCs lack clear *de novo* anti-tumor activity, they are also important to consider in anti-tumor therapies.

It is less clear whether any of the circulating DC subsets have a clear-cut tolerogenic function. cDC2s have been described to produce less TNF-α, IL-6, and IL-12 compared to other subsets, together with more IL-10 (35). However, as discussed above, they are also considered potent activators of CD4+ T cell responses. Both mature and immature cDC1s have recently been described as more apt at producing IDO compared to cDC2s (36, 37). However, as stated before, cDC1s are also regarded as important in activating T cells against tumors *via* cross-presentation.

For emphasizing the role of DC subsets in tolerogenic immune modulation it may be more straightforward to look at DC behavior in steady-state tissue. In peripheral tissue, DCs constantly encounter harmless antigens to which an adaptive response has to be dampened (38). Thus, the tissue niche in which DCs reside is an important environmental determinant that shapes the phenotype of DCs further. The skin, for example, harbors epidermal Langerhans cells (LCs), and several dermal DC subsets (DDCs) that seed the skin from cDC2 blood DC progenitors (39). We demonstrated that in contrast to DDCs residing in the deeper dermis layer of skin, epidermal LCs have intrinsically low expression of TLR2, 4 and 5, and accomplish unresponsiveness to innocuous bacteria by limited uptake and presentation of bacterial antigens (38, 40). Similarly, it has been established that under non-inflammatory conditions, CD103+ DC of the gut promote tolerance to harmless commensal bacteria (41, 42). Thus, for the induction of immune tolerance

in skin or gut, it may be of therapeutic benefit to target LCs or CD103+ DCs.

It must be emphasized that a clear-cut distinction in pro- or anti-inflammatory specialization of DC subsets in general is difficult. Function of DCs is controlled mainly by stimuli and environmental context, and we can harness this to induce activating or tolerogenic immune responses (17). Therefore, when DCs are targeted with vaccines for either immunity or tolerance, it may be important to filter out beneficial subsets, but it is equally important to provide the right combination of triggers for DCs in order to shape a T cell activating or tolerizing phenotype (43–45).

DESIGN OF A DC-MODULATING LIPOSOMAL VACCINE AGAINST CANCER, AUTO-IMMUNITY OR ALLERGIES

For successful DC-based immune modulation with *in vivo* liposome-based vaccines, there are four key components to be considered: a) physicochemical properties of the liposomes, b) disease-specific antigens, c) DC targeting moieties, d) potent adjuvants, with functional properties to induce either immunity or tolerance (**Figure 2**).

Physicochemical properties of nanoparticles are not only important for the stability of the vaccine formulation, but there are also indications in literature that this versatility in design provides DC-modulating and ultimately, general immune modulating opportunities (22).

Disease relevant antigens should be considered in a nano-vaccine platform in order to reprogram antigen-specific adaptive cells against cancer, autoimmunity or allergies, focusing therapies towards modulation of pathogenic immune responses, while leaving the rest of the immune system intact.

Although having the correct antigen is essential in achieving the desired antigen-specific immune response, the quality and magnitude of the immune response also depends on antigen dose. Thus, it is imperative to get sufficient levels of antigens to DCs (46, 47). Targeting nanoparticles to specific surface receptors also induces receptor-specific immune-modulatory effects. Hence, targeting the antigen-carrying nanoparticles to DCs is beneficial for improving specificity of immunotherapy, but also for obtaining durable immune responses *via* receptor-induced immune modulation.

For DC-specific targeting, various surface receptors can be considered. DCs sense pathogen-associated molecular patterns (PAMPs) or danger associated molecular patterns (DAMPS), the 'flavor' of a pathogen or the 'flavor' of inflammation, *via* PRRs including TLRs, CLRs, NOD-like receptors, Siglecs, and others. The sensing determines the type of polarizing signal expressed by migrant DCs in the lymph node, which may consist of cytokines, membrane-bound or small molecules. In turn, the polarizing signal determines T cell polarization and subset differentiation (48, 49). When triggered, these receptors not only induce or alter various types of (immune) signaling, but in case of CLRs also enhance internalization and (cross-) presentation of the bound molecule (50).

Finally, beyond intrinsic functions of DC subsets and the antigen DCs encounter, the niche, or microenvironment in which this encounter happens seems to be a strong overriding factor for the final outcome of immune modulation (51). Potent adjuvants are therefore needed, that can either revert immune suppression of DCs in the tumor microenvironment or suppress activated DCs in pathogenic inflammation. Loading such potent adjuvants in liposomes may avoid systemic side effects and in

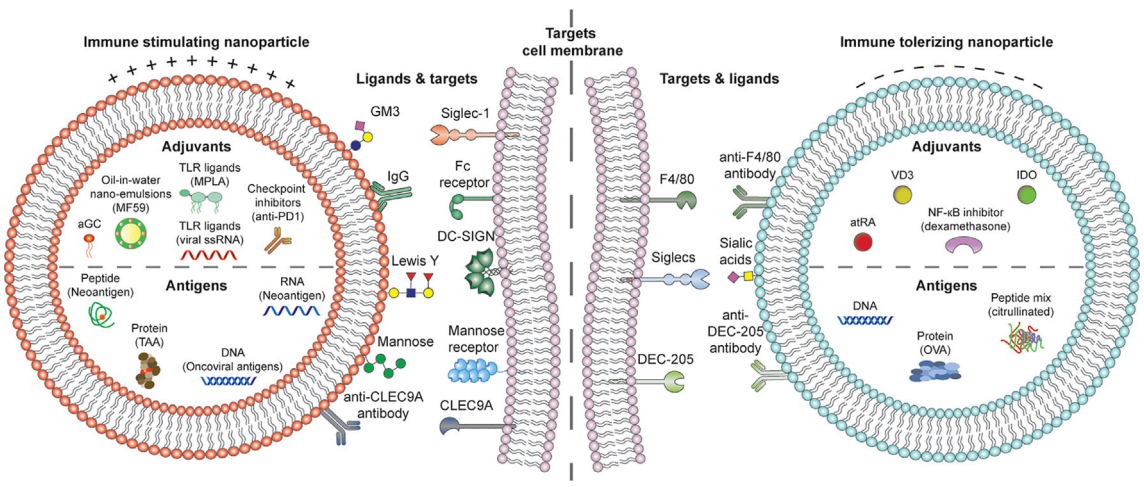

FIGURE 2 | Putative DC-activating cationic (left) or DC tolerizing anionic (right) liposome platforms incorporating disease-specific RNA, DNA, peptide or protein antigens, DC targeting molecules for activation or tolerance, and adjuvants for shaping pro-or anti-inflammatory DCs. αGC, α-galactosylceramide; TLR, toll-like receptor; IgG, Immunoglobulin G; DC-SIGN, Dendritic Cell-Specific Intercellular adhesion molecule-3-Grabbing Non-integrin; atRA, all-trans retinoic acid; VD3, vitamin D3; IDO, indoleamine-2,3-dioxygenase.

conjunction with targeting, focus therapies to the specific disease niche. In the next sections, we will discuss these four key elements of DC-liposome vaccines in context of cancer, allergies and autoimmune disease (**Figure 2**).

IMMUNE MODULATING PROPERTIES OF EMPTY LIPOSOMES

Lipid Composition, Charge, and Rigidity

Various lipids of neutral, positive (cationic) or negative (anionic) electrical charges can be assembled into liposomes with consequences for how they interact with APCs. Positively charged formulations containing lipids, such as 1,2-dioleoyl-3-trimethylammonium-propane (DOTAP), or 3ß-[N-(N',N'-dimethylaminoethane)-carbamoyl]cholesterol (DC-Chol) have been associated with DC-activating effects. Here, both the net positive electric charge, supporting a favorable interaction with the negatively charged cell membrane, as well as APC interaction with the lipid head groups appear to be important factors for inducing DC activation (52). Several mouse and *in vitro* human studies found an upregulating effect on DC maturation markers and on production of pro-inflammatory cytokines by cationic liposomes (53–55). Due to this assumed adjuvant quality, cationic liposomes are popular candidates for the development of new tumor targeting particulate therapies. Moreover, cationic liposomes appear to be toxic to cells, although a disadvantage when targeting DCs, toxicity is a feature which could be exploited for enhanced tumor cell lysis, thereby also enhancing immunogenicity of cancerous cells (56). Intriguingly, DC-Chol and DOTAP liposomes were found superior in stimulating cross-presentation of OVA to OT-I transgenic CD8+ T cells compared to anionic formulations containing Egg L-α-phosphatidylcholine (EggPC) (57). The authors of that study propose an alkalizing effect of the positively charged formulations on BMDC lysosomes, which leaves OVA more intact for cross-presentation (57). If confirmed by further studies, this would yield another argument for the use of cationic liposomes in anti-tumor targeting. Interestingly, several studies in the context of allergy also employ cationic liposomes, since these formulations proved to be superior in preventing mast cell degranulation and lead to a more efficient reduction in airway eosinophilia and OVA-IgE in allergic mouse models compared to neutrally charged formulations or empty antigen (58, 59).

In the tolerogenic field, liposomes containing the negatively charged lipid, phosphatidylserine (PS) gained considerable attention (22, 60, 61). The most prominent theory for a tolerogenic adjuvant effect of PS containing particles puts forth the notion that such particles resemble apoptotic bodies, thereby silencing DC maturation upon their encounter. Utilizing PS liposomes added to mouse DCs *in vitro*, Shi and colleagues demonstrated that the DCs were resistant to maturation, produced less pro-inflammatory cytokines, acquired the capacity to suppress CD4+ T cell proliferation, as well as to induce PD-1 surface expression on T cells (61). Similar effects were confirmed in a human *in vitro* study, in the context of Type-I diabetes, where patient DCs pulsed with PS-liposomes retained a tolerogenic profile, and suppressed autologous T cell proliferation (62). Interestingly, in a recent study by Benne and colleagues it was not PS containing liposomes, but liposomes incorporating the anionic lipid 1,2-distearoyl-*sn*-glycero-3-phosphoglycerol (DSPG) that induced antigen specific Foxp3+ T cells upon *in vivo* injection in mice (55), the mechanisms of which are yet elusive.

A characteristic that is often altered when changing lipid composition of a formulation is rigidity (22). APCs envelope rigid particles easier than flexible ones leading to more efficient uptake (63–65). In line with these observations Benne *et al.* confirmed enhanced uptake of more rigid variants of the DSPG containing tolerogenic liposomes mentioned above, where injection of more rigid formulations in mice also correlated with stronger Treg responses (66). Similarly, more solid gel-phase pegylated 1,2-distearoyl-sn-glycero-3-phosphocholine (DSPC-PEG) or 1,2-dio- leoyl-sn-glycero-3-phosphocholine (DOPC-PEG) liposomes were taken up better by bone marrow-derived DCs (MDCs) and activated these cells more than their fluid-phase counterparts. Of note, this study used Cholera toxin antigen loaded formulations, and empty formulations did not have an adjuvant effect on BMDCs (67).

Liposome Size and Shape

Multiple studies emphasize the effect of particle size on uptake mechanisms by APCs, which in turn may influence how liposomal cargo is processed and presented to T cells (22, 68, 69). Similar to how viruses enter cells, particles smaller than 100nm are taken up efficiently by clathrin mediated endocytosis, whereas particles larger than 200nm are phagocytosed or internalized by macropinocytosis (68). This may influence intracellular routing of the liposomal cargo. Cargo escaping the lysosomal route can be more available for cross-presentation on MHC-I, a desirable outcome for DC-mediated cancer therapies but also for tolerizing CD8+ memory T cells employing liposomes with self-antigen (70). Cargo following phagocytosis and the endo-lysosomal route will be preferentially processed towards MHC-II presentation, priming for interaction with CD4+ T cells. Moreover, some studies suggest that particle size has a specific influence on T cell polarization. Nanobeads smaller than 100nm were shown to elicit stronger IFN-γ responses in mice leading to superior T_H1 immunity compared to beads larger than 100nm (71). As already mentioned small particles may be taken up by DCs similarly to viruses mimicking anti-viral immunity (71). Biodegradable polymer particles in a size range of 1-5µm, on the other hand, were shown to adhere to the DC membrane and offload their cargo there, leading to a T_H2 response (72, 73). However, conclusions about liposomes seem to point in the opposite direction: liposomes smaller than 200nm were reported to induce T_H2 immunity whereas larger ones primed towards T_H1 (74, 75). These observed differences may be explained by uptake and intracellular processing differences between solid particles (such as nanobeads and various polymers) and semi-solid or fluid liposomes. In contrast to solid particles which are taken up by active processes, liposomes can also fuse with the cell

membrane and offload cargo directly into the cytoplasm (76). This difference in interaction with DCs can lead to different intracellular processing and presentation of cargo to T cells.

In addition to differences in cellular uptake and processing, size of particles influences bioavailability and biodistribution upon *in vivo* injection. Only particles smaller than 200nm seem to drain to lymph nodes where they can be directly processed by lymph node resident DCs for early T cell activation (22). Larger particles, in contrast, remain at the injection site until phagocytosed by DCs that can migrate to the lymph node, possibly leading to a less vigorous T cell response.

Although less studied, particle shape seems to have an immune modulating effect on APCs as well, where rod-shaped structures (nanorods) were reported as more pro-inflammatory compared to spherical particles (22, 77). However, this feature is less relevant for liposomes as they do not belong to the group of solid nanoparticles.

Despite demonstrated evidence on adjuvant characteristics of certain nanoparticles, a large body of evidence with human cells is lacking. Often several characteristics of a particle are altered at once, making it difficult to discern which characteristic is responsible for observed differences in immunogenicity (22). As visible from the studies discussed in this section, there is also a great need for standardization of different particles or liposomal formulations in order to facilitate a valid comparison between studies. Finally, the therapeutic content loaded in a particle, such as tolerogenic or immune activating adjuvants together with any targeting molecules, may overrule the immune modulatory effect of empty particles (78).

BATTLING CANCER WITH DC TARGETED LIPOSOME VACCINES

Role of Cancer Antigens

Tumors display a wide variety of (abnormally expressed) tumor-associated antigens (TAA), and TAAs such as MART-1, MUC1, WT1, gp100 and the MAGE-A antigens, have been tested in various vaccines in clinical trials (79–82). Using TAA-loaded nanoparticles in different clinical trials have, so far, resulted in mixed responses (83, 84). Since TAA are expressed on both healthy and transformed cells, it is possible that T cells specific for these antigens are deleted during the negative selection in the thymus, which therefore leads to the observed suboptimal anti-tumor responses in many TAA (85, 86). The potential off-target effects induced by targeting TAA make tumor-specific antigens (TSA) an interesting alternative. These antigens are not expressed on healthy cells, and therefore also have limited tolerance related complications.

TSA include mutated neoantigens, but also antigens from endogenous origin. In particular, because ~12% of human cancers are caused by viruses, the foreign (viral) antigens expressed on the transformed cells are highly immunogenic (87, 88). The VGX-3100 vaccine, targeting the HPV proteins E6 and E7, the main oncoviral antigens of the cancer caused by the virus, is based on a DNA vaccine of the mentioned antigen, and is currently tested in a phase III clinical trial (NCT03185013) (89). Parallel to this non-liposomal vaccine liposomal (archaesomes) delivery systems for DNA encoding the HPV antigens are being tested, and show the induction of a potent anti-tumor immune response in an *in vivo* cancer model (90). Another class of TSA arise from non-synonymous DNA mutations, and are therefore called neoantigens (91). These antigens are highly immunogenic and therefore highly sought after targets for therapeutic vaccines (92). Since the neoantigens are personal to the patient, they will need to be identified per patient through genomic comparison of tumor and normal tissue (93). Recent personalized clinical trials with vaccines targeting neoantigens feature high immune activation and overall promising results (94, 95). Nanoparticles are already used to deliver the neoantigens (e.g. RNA, DNA or peptides) to DCs *in vitro, in vivo* and in clinical trials (85, 96, 97). Especially for (m)RNA vaccines, nanoparticles such as liposomes are greatly beneficial since they protect the payload against degradation (98). Accordingly, a recent phase I clinical trial with patient personalized tumor mRNA-loaded nanoparticles showed high tolerability, and the interim results from another recent phase I clinical trial showed encouraging clinical responses (NCT03897881) (99). Exploiting the same pharmacological advantage, the recently successful mRNA based SARS-CoV-2 vaccines have a nanoparticle delivery system (100, 101).

Targeting DCs *In Vivo* for Immune Activation

PRRs researched for targeting of DCs in context of cancer therapy include CLRs, the Siglec receptor Siglec-1, and Fc receptors (FcR). CLRs recognize carbohydrate ligands, which makes them important sensors of differently glycosylated PAMPS (102). Some of these receptors are expressed on a broad class of APCs, whereas others are DC or even DC-subset specific. Thus, targeting of these receptors by adding glycan moieties or CLR antibodies to liposomes can be used for reaching APCs with a varying spectrum of cell specificity. DC-SIGN is a CLR expressed on different subsets of APCs, including moDCs, CD14+ dermal DCs, subsets of macrophages and DCs at mucosal sites (103). Targeting liposomes to DC-SIGN *via* its natural glycan ligand Lewis Y showed increased CD8+ T cell responses *in vitro* and *ex-vivo (*104). Also, targeting the DC-SIGN receptor with antibodies conjugated to nanostructures, leads to increased immune responses (105). Unfortunately, a clinical trial with a DC-SIGN targeting nanoparticle vaccine Lipovaxin-MM has not resulted in immunogenic anti-tumor responses (106). The vaccine's antigens (e.g. gp100 and MART-1) were derived from plasma membrane vesicles from a human melanoma cell line, and modified with a liposomal mixture, also containing IFN-γ. A DC-SIGN targeting antibody was also incorporated in the membrane, allowing for targeting to various APCs. While the vaccine was well tolerated, significant immunogenicity of the vaccine was not detected. Similarly to DC-SIGN, the mannose receptor (MR) is also expressed on

various APCs, such as macrophages and moDCs. Targeting of MR has already been evaluated in a clinical trial, proving that the administration of the MR-targeting vaccine together with local application of TLR agonists, induces significant humoral and cellular immune responses (107). When mannosylated nanoparticles were used to target the MR, it led to high effector T cell responses and reduced tumor growth *in vivo* (108). Immunization of mice with liposomes made of mannose-mimicking ligands loaded with DNA encoding for MART-1 allowed for efficient transfection of CD11c+ DCs, inducing long lasting melanoma specific prophylactic CTL responses (109). Therapeutic vaccination with these liposomes resulted in delayed tumor growth in mice. In contrast to the previously discussed CLRS, DEC-205 appears more DC-specific with expression demonstrated on cDC1s, cDC2s and moDCs. When DCs were targeted with PLGA nanoparticles coupled to monoclonal anti-DEC205 antibodies, the treatment lead to enhanced internalization, cross-presentation and CD8+ T cell activation (110). Similar results were observed by another group, showing that targeting of nanoparticles to DEC-205, CD40 or CD11c improved priming of cytotoxic CD8+ T cells over untargeted nanoparticles (111). Targeting CLEC9A, a CLR with advantageously restricted expression on cDC1 DCs, also elicited anti-tumor responses in multiple studies, coherent with the potent (cross-)presenting function of these DCs (112, 113). In an additional study, targeting PLGA nanoparticles loaded with the TAA Trp2 and gp100 to CLEC9A expressing DCs *via* antibodies resulted in strong therapeutic anti-tumor responses *in vivo*, but also induced *in vitro* expansion of NKT and CD8+ T cells specific for melanoma in PBMCs from both healthy donors and melanoma patients (114).

Other groups of receptors that have been used for targeting APC in the context of cancer are Siglecs and FcR. While most Siglecs confer tolerogenic responses, the Siglec-1 (or CD169) receptor, expressed on splenic macrophages is of special interest for anti-tumor responses. These cells transferred antigen to cross-presenting cDC1s when targeted with liposomes coated with the Siglec-1 ligand GM3, conferring beneficial anti-tumor CD8+ T cell responses (115). FcR, which bind to the constant domains of antibodies can be targeted by coating liposomes with antibodies. Indeed, IgG coated liposomes bearing the OVA antigen prevented development of OVA-expressing lymphoma, in contrast to the liposomes without IgG coating (116). Also, specifically the Fc fragment of an antibody can be used on the outside of a nanoparticle for targeting purposes, which induced increased cellular and humoral immune responses in mice when a cancer peptide was included in the nanoparticle (117).

Targeting one receptor may in several cases induce either immunity or tolerance, depending on the vaccine formulation and microenvironment. For instance, targeting DC-SIGN can display T_H2 polarizing effects, combined with inhibition of T_H1/T_H17, when targeted with natural ligands (118). Accordingly, depending on the adjuvants used, DEC-205 targeting is used for both tolerogenic and immunogenic purposes (119). Therefore, when targeting DCs *via* specific receptors, it is not only important to target the appropriate receptor, but also to provide efficient co-stimulatory adjuvants to properly skew the immune response (51).

Vaccine Adjuvants for Immune Activation

TLRs are a well-known class of PRRs, and some of these are targeted for induction of antitumor responses (120). Molecules targeting TLR4 are LPS structures derived from bacteria, but as adjuvant the less toxic variant of LPS, monophosphoryl lipid A (MPLA) is used. The incorporation of MPLA in PLGA nanoparticles increases T_H1 and pro-inflammatory responses in comparison to the non-encapsulated administration of MPLA (121). Agonists for TLR7/8 are viral ssRNA and synthetic compounds like R848. Triggering TLR7 for cancer therapy with Imiquimod has already been approved by the FDA, and clinical trials with the TLR7/8 stimulating adjuvant R848 have been conducted (120, 122). The prophylactic and therapeutic effect of OVA mRNA-loaded nanoparticles as vaccine against OVA expressing lymphoma in an *in vivo* mouse model is increased when R848 is added, and results in increased TAA presentation and antigen specific CD8+ T cell populations (123). The TLR9 stimulating ligand CpG has also been evaluated in clinical trials, with positive outcomes (124). When CpG is incorporated into a nanoparticle, its efficacy in terms of (delayed) tumor growth was superior in comparison to the soluble form of CpG, again highlighting the potential of nanoparticles for antigen and adjuvant delivery (125). TLR3, recognizing dsRNA, is another PRR receptor that is targeted for pro-inflammatory responses (126). The synthetic analogue of TLR3, Poly (I:C), is being evaluated as adjuvant in (pre-) clinical trials, and elicits favorable effects (94). Thereby, encapsulation of the TLR3 adjuvant in a nanoparticle further potentiates the inflammatory immune responses (127). Especially when Poly (I:C) is combined with the TLR9 stimulant CpG in a nanoparticle, it induces protective and therapeutic immune responses in *in vivo* models (128, 129). Other combinations of TLR ligands in nanoparticles are also used, with established synergistic effects (120, 130). Hence, it is becoming clear that incorporating multiple TLR stimuli in liposomes will be a promising adjuvant strategy for immunogenic vaccines.

An adjuvant that works directly *via* presentation on DCs is α-galactosylceramide (αGC), a potent immune activating glycolipid which when presented on DCs, initially activates iNKTs (131). In turn, these iNKTs activate other NK-, CD8+-T, B-cells and DCs, *via* increased cytokine production (132). Since αGC is a glycolipid, it also allows for easy incorporation in- for example- liposomal nanoparticles. Incorporated in liposomes, αGC leads to the increase in CD8+ T cell responses *in vitro* (104). Accordingly, αGC incorporated in liposomes is able to reduce the outgrowth of lung melanoma metastasis *in vivo* (133).

Another way to increase vaccine efficiency is by increasing the numbers, and immunological state, of immune cells in the site of vaccination. The adjuvant (MF59) used in the seasonal influenza vaccine, based on an oil-in-water nano-emulsion, increases the number of APCs and creates an immunogenic microenvironment (134). Enhancement of APC numbers also improves trafficking of antigens to the draining lymph nodes *via* leukocytes, favoring a

stronger immunogenic response. Oil-in-water nano-emulsions are able to encapsulate both antigens and antibodies, for specific targeting to for instance the CLEC9A receptor, thereby becoming self-adjuvating delivery systems for DC vaccination (135).

FOSTERING IMMUNE TOLERANCE WITH DC-TARGETED LIPOSOME VACCINES

Role of Disease Specific Antigens in Immune Tolerance

Repeated exposure to antigen has shown tolerance inducing effects. AIT exploits this very concept with curative success demonstrated for various pollen and venom allergies (3). However, treatment efficacy for other allergies, such as food allergies, could be increased, together with reduction of risk of anaphylaxis by incorporating allergens in nanoparticles. A clinical study with subcutaneous injection of liposomes incorporating house-dust mite extract was already carried out as early as 2002 (136). Unfortunately, this study did not compare treatment with soluble allergen and no clear line of clinical studies followed. Even though the validity of allergic mouse models is somewhat questionable, several recent studies demonstrate therapeutic proof-of concept. In a mouse model of pollen allergy to the weedy plant *Chenopodium album*, subcutaneous injection of allergen incorporating protamine-DNA liposomes shifted a predominant T_H2 response to the allergen in a T_H1 direction, with decrease of IgE, increase in IgG2a and IFN-γ production specific to allergen (137). Chaisri et al. tested effects of intranasal vaccination with liposomes incorporating Derp1 and Derp2 separately, or in combination (138). Interestingly, even though all formulations reduced T_H2 immune reactions, only the liposomes incorporating single allergens lead to expression of tolerogenic cytokine genes TGF-β, IL-35 and IL-10 in mouse lung cells. In an OVA mouse model of allergy, sublingual treatment with OVA incorporating liposomes preceding allergen challenge was superior to treatment with free OVA (59). Unfortunately, none of the above studies examined airway hyperresponsiveness as a read-out, which could make the conclusions about treatment efficacy stronger.

In contrast to allergies where the antigen is known and clearly defined, autoimmune conditions pose the difficult challenge of unknown causative auto-antigens or foreign antigens that may trigger disease. In rheumatoid arthritis (RA), anti-citrulline antibodies (ACPA) appear in blood before disease onset and can be very specifically linked to RA pathogenesis (139). This knowledge stimulated a quest for putative, citrullinated antigens on cartilaginous surfaces capable of stimulating auto-reactive T cells. Indeed, using a panel of HLA-DRB1*04:01 tetramers, James and colleagues confirmed an increased presence of citrullinated antigen specific T cells in peripheral blood of RA patients compared to healthy subjects (140). Of note, Benham and colleagues performed immunotherapy using *ex vivo* RA patient-derived moDCs with an NF-κB inhibitor and a mix of citrullinated antigens (141). This (uncontrolled) treatment strategy proved safe and showed some signs of efficacy such as a decrease in effector T cells and improvement in clinical RA scores. As early as 2009, the same research group established that citrullinated antigens loaded in EggPC liposomes can efficiently be used to induce antigen-specific Foxp3+ Tregs in mice, an effect that was specifically mediated by DCs (142).

Targeting DCs *In Vivo* for Tolerogenic Immune Modulation

Several CLRs and Siglecs are under scrutiny for targeting, as an attempt to specify tolerogenic *in vivo* DC therapies. For an extensive review on this subject we refer the reader to a very recent piece published by our colleagues (21). The CLR DEC-205 is highly expressed on the cross-presenting cDC1 DC subset (as well as on cDC2s and moDCs) and is therefore a widely studied receptor for nanoparticle DC targeting, for example *via* antibodies (143). Targeting the DEC-205 receptor *via* antibodies without providing maturation stimuli can lead to specific induction of T-cell anergy as well as increased T cells suppression (119). OVA-loaded PLGA nanoparticles that were conjugated with antibodies to DEC-205 induced IL-10 production in DCs and subsequently T cells, of which the levels were dependent on the amount of antibodies on the nanoparticles (144). However, the T_H1 priming of DCs targeted with these nanoparticles was not impeded.

The F4/80 receptor, expressed on macrophages and DCs, shows promise in inducing tolerance in a nonobese diabetic mouse model. The progression of diabetes in the *in vivo* model was prevented by vaccinating mice with liposomes coated with anti-F4/80 antibodies and a disease specific short peptide joined with a TLR-2 ligand (145).

Modification of antigens with the carbohydrate ligands (sialic acid) of Siglecs expressed by DCs results in the induction of antigen specific Tregs and alleviation of allergic symptoms in mice (146, 147). Other studies focus on nanoparticles targeting Siglecs to induce tolerance in B-cells or other immune cells, but to date, no studies have been reported using nanoparticles that target to Siglecs on DCs (148, 149).

Similarly to allergies, there is pre-clinical precedent for the use of nanoparticles for developing new treatment modalities against RA and other autoimmune diseases. However, studies with a targeting component towards DCs are not abundant in literature, highlighting a knowledge gap that needs to be addressed.

Vaccine Adjuvants for Immune Tolerance

In order to prevent adverse reactions to allergens or a worsening of autoimmunity it is highly likely that co-delivery of tolerance inducing compounds together with disease relevant antigen will be a necessary element of successful *in vivo* targeting therapies. Indeed, multiple studies observed immunogenic reactions to nanoparticles delivering antigen only (69, 150–152). This may also apply to AIT utilizing nanocarriers. For example, in a mouse study of cockroach allergy, only allergen encapsulated in liposomes together with a tolerogenic adjuvant induced increased transcription of IL-10, TGF-β and IL-35 as well as IDO1 (153).

The choice of adjuvants with the strongest immune dampening effect may be critical for successful DC-mediated

tolerance *in vivo*. The vitamins D and A have been extensively studied in the tolerogenic context. 1,25alfa-dehydroxycalciferol, or vitamin D3 (VD3) appears to be the most potent immunosuppressant of all forms of vitamin D (154, 155). Both mouse and human studies have demonstrated that VD3 priming of immature and mature DCs results in a tolerogenic phenotype with induction of co-inhibitory receptors, reduced IL-12 production and induced IL-10 secretion (156–160). The tolerogenic effects of VD3 have also been shown in several skin-derived DC subsets where priming of *in vitro* cultured LCs, CD1a+ DDCs or skin-derived DCs with VD3 resulted in the outgrowth of distinct Treg phenotypes (161, 162). Most importantly, VD3-raised DCs show tolerogenic stability in face of repeated rechallenge with pro-inflammatory stimuli, making VD3 a robust DC-tolerizing candidate in an already inflamed environment (163). In line with that, several recent studies in mice demonstrated that nanoparticles loaded with VD3 and OVA induced tolerogenic DCs with *in vitro* and *in vivo* suppressive capacity of OVA-specific T cells (164, 165). Additionally, subcutaneous injection of VD3-loaded particles resulted in effective targeting of PD-L1 high draining lymph node DCs, resulting in amelioration of a RA disease model (165).

In contrast to the well-established tolerogenic role of VD3, there is still considerable debate on whether the active form of Vitamin A, all-trans retinoic acid (atRA) has pro- or anti-inflammatory effects (166). Similarly to murine mucosal CD103+ DCs (167), human moDCs raised with atRA, induce the development of IL-10 producing Tr1 in co-culture (41). Building on the anti-inflammatory potential of atRA, the compound was recently incorporated in PLGA particles together with atherosclerosis autoantigen and improved atherosclerotic lesions *in vivo (*168). In a further recent study, atRA was encapsulated together with another anti-inflammatory adjuvant, triptolide, in galactose-containing nanoparticles (78). *In vivo* effects in mice consisted of reduced infiltration of these sites by T cells and pro-inflammatory macrophages, together with reduced expression of T_H1-T_H17 polarizing cytokines in inflamed tissue extracts. However, atRA also supports induction of T_H1 and T_H2 responses upon inflammatory stimulation, serving as one explanation of contradictory pro- and anti-inflammatory effects observed (169, 170). Thus, loading of atRA in nanoparticle platforms for tolerogenic purposes may be an interesting option, but with a sidenote of caution.

A central transcription factor downstream of activating signals delivered to DCs is NF-κB, which makes it one of the key targets for immune modulation. Corticosteroids and glucocorticoids are well-known to exert their immunosuppressive effects *via* NF-κB inhibition (171, 172). Treatment of moDCs with the corticosteroid dexamethasone leads to an immature phenotype with loss of IL-12 secretion and high IL-10 secretion. Similarly to VD3 treated DCs, dexamethasone DCs seem robustly maturation resistant and capable of inducing IL-10 producing Tregs, although these Tregs exert suppression in a non-antigen specific manner (173). To prevent systemic immune suppression, loading of corticosteroids into nanoparticles and targeting the particles only to cells relevant for inflammation is a treatment approach considered in RA and other autoimmune conditions, showing promising treatment efficacy in several mouse studies (174). In addition to these rather a specific inhibitors of NF-κB signaling, also several highly specific inhibitors of (non)canonical signaling have been investigated in human moDCs and demonstrated to potently reduce T cell responses (175). Recently, also VD3 was confirmed to downmodulate NF-κB signaling in human moDCs matured with LPS, providing an elegant bridge between VD3 and NF-κB inhibition as adjuvants (176).

Indoleamine 2,3-dioxygenase (IDO), the enzyme responsible for breaking down the essential amino acid tryptophan into kynurenine can be produced by DCs, which leads to decreased T cell proliferation, induction of Tregs and an anergic T cell phenotype in co-culture experiments (177–179). IDO production in the gut is intricately intertwined with the gut microbiota, and exerts tolerogenic effects on CD103+ DCs as well as dampening tissue T_H1/T_H17 responses (180–182). Several molecules may induce IDO production by DCs, however, some of these, such as type I interferons or IFN-γ are also pro-inflammatory cytokines, hindering their use in tolerance inducing therapies (183). Induction of IDO has been described upon CD40 ligation of moDCs, where the enzyme was induced by non-canonical NF-κB signaling (36). After treating mouse pDCs with TGF-β, IDO was activated as a downstream signaling molecule, leading to inhibitory signaling and the activation of the non-canonical NF-κB pathway, further strengthening IDO expression in a self-feeding loop (184). Further compounds that were demonstrated to induce IDO are soluble CTLA-4, the TLR-agonists LPS and CpG, together with DNA agonists of stimulator of interferon genes (STING) (183). As treatment with TLR-agonists carries pro-inflammatory risks, soluble CTLA-4 and STING agonists seem better suited candidates for DC-treatment. Indeed, nanoparticles constituted of CpG free pDNA were demonstrated to induce IDO *via* the STING pathway, leading to amelioration in experimental autoimmune encephalomyelitis (183). Moreover, this therapeutic effect could be strengthened when blocking downstream metabolites of IDO additionally to DNA nanoparticle treatment.

In addition to the above compounds discussed in detail, several other materials are tested for their tolerogenic potential, such as various parasite-derived antigens, plant-derived adjuvants or compounds already well-known in the clinic, like the m-TOR inhibitor rapamycin (185). In fact, just like VD3 and dexamethasone, rapamycin was demonstrated to induce robustly tolerogenic, clinical grade DCs (186). Although rapamycin loading into several forms of nanoparticles is actively tested for better delivery to cancer cells or as an inflammation dampening adjuvant, targeting to DCs has not been in the focus of research thus far (187).

OUTLOOK

Based on the discussion presented in this review an ideal immune modulating nanoparticle DC-vaccine should harbor

the following properties: a) physicochemical characteristics promoting tolerance or activation, b) antigen relevant for the given disease condition to create disease specificity c) specific targeting molecules aimed at tolerogenic or pro-inflammatory DCs, and d) tolerogenic or immune activating adjuvants (**Figure 2**). For unravelling exact immune modulatory properties of all vaccine components, further fundamental studies will be needed, featuring a careful comparison of nanoparticle characteristics, with a stepwise selective approach towards the most optimal particle-targeting-adjuvant and antigen combination for DC-therapy. It is clear that the field of nanomedicine is in need for standardized research, carried out with similar methodology, using similar nanoparticles.

Apart from immune modulating elements, the advantage of nanoparticles lies in the ability to synergistically combine multiple characteristics and compounds to achieve a desired DC-tolerizing or activating outcome. Indeed, ongoing clinical trials conducted with DC-targeting nanoparticles, combining targeting, antigen and adjuvants in the context of cancer and several mouse studies in autoimmune or allergic disease leave cause for optimism. However, beyond advantages, several key aspects need more consideration during development of novel nanomedical treatments. Cationic liposomes have cytotoxic effects as they disrupt cell membranes, a possible advantage when targeting cancer cells directly but not when targeting APCs (76). While solid polymer particles are generally stable, semi-solid liposomes can be unstable depending on their surface chemistry. Neutral lipids or cationic formulations, for example, are known to aggregate quickly due to lack of electrostatic repulsion or rapid attraction of negatively charged proteins to their surface (188). In fundamental studies, liposomal formulations are often used within two weeks of manufacturing and opinions on their stability differ (55). Clearly, studies need to monitor stability more strictly and for a longer period of time. Furthermore, hydrophilic cargo such as peptide or protein antigens, as well as other chemical components, such as fluorescent lipid dyes loaded onto the surface of liposomes tend to dissociate (189). Dependent on the nature of the cargo this could lead to undesired bystander effects, deleterious side effects such as anaphylaxis in case of allergen loading, and misinterpretation of molecular results, such as of cellular uptake and intracellular processing (189). The potential disadvantages carefully need to be assessed in the context of each specific disease setting.

As highlighted earlier, for the induction of a potent anti-tumor response, it is crucial to use DC targeted vaccines that will provide enough antigen and co-stimulation for the DC to mount an inflammatory response (190). Since nano-formulations can provide all four components, a plethora of research is focused on these platforms. So far, pre-clinical data has shown promising results in favor of using DC-targeting nanoparticle formulations for the induction of potent anti-tumor responses. While nanotechnology for directly targeting DCs for anti-cancer immunotherapy is mainly applied in *in vivo* and *ex-vivo* models, some clinical trials are conducted with this platform (106, 191). Unfortunately, liposomes targeting the DC-SIGN receptor in patients with metastatic melanoma did not yield desired clinical results (106). The authors note that it is not the lack of anti-melanoma immunity that may cause absence of treatment efficacy, but rather the suppression of (pre-existing) anti-melanoma immunity. This notion can be extrapolated to other immunogenic tumors as well, suggesting the use of additional components in the vaccine platform in order to boost pre-existing anti-tumor immunity (192). The promising research into checkpoint inhibitors (CI) could provide another combinational treatment option for cancer, since CI effectiveness is in large part dependent on the pre-existing anti-cancer immunity (193, 194). Of note, the combination of checkpoint inhibitors, and nanoparticles incorporating TLR agonists and peptides, showed strong synergistic effects in *in vivo* mouse models for the treatment of cancer (195, 196). Therefore, combining CI with a (nanoparticle based) therapy aimed to initiate/reinvigorate the anti-tumor response, should be strongly considered (197, 198).

Similarly to the cancer field, the stage is set for clinical trials of *in vivo* targeting of DCs to treat inflammatory diseases. In a much awaited clinical study in RA research, the previously mentioned EPC liposomes incorporating the NF-κB inhibitor BAY11-7082 and citrullinated peptides are injected in RA patients for antigen-specific inhibition of pro-arthritic immune responses (142). For a successful therapeutic outcome in tolerogenic applications essential factors will be co-delivery of disease relevant antigens with an immune-dampening adjuvant in order to avoid adverse pro-inflammatory effects (69). In the same line, adjuvant cargo will have to be carefully chosen based on pre-existing studies demonstrating ability to induce robustly tolerogenic DCs that withstand the immunogenic temptations of highly inflammatory environments (163). Route of administration should also be studied further as it can potentially play a role in tolerogenic effects. For example, only when applied as an intranasal vaccine and not intra-muscularly, did OVA-loaded PLGA particles promote transcription of FoxP3 in cervical lymph nodes (199).

To date, no *in vivo* DC-targeting nanoparticle vaccine is available in the clinic, but the promising mRNA-based nanoparticle vaccines for SARS-CoV-2 and new results from ongoing nanoparticle-based cancer clinical trials, as well as preclinical studies in autoimmune diseases are expected to accelerate research into the platform (200).

Based on existing evidence presented in this review, it is certain that collaborations, synchronization of nanomedical experimental practices as well as the accumulation of data in human cells and clinical studies will bring a new wave of promising research strengthening the potential of DC-based treatments for cancer, allergies and autoimmunity.

AUTHOR CONTRIBUTIONS

NN and AH performed the literature search, wrote the manuscript, and created all figures. EJ and YK critically read

and carefully revised all versions of the manuscript providing valuable guidance and insight. TG, RR, and ST critically read the manuscript and provided valuable additions. All authors contributed to the article and approved the submitted version.

FUNDING

This work was supported by LSH-TKI project DC4Balance LSHM18056-SGF.

REFERENCES

1. Tang MLK, Mullins RJ. Food Allergy: Is Prevalence Increasing? *Intern Med J* (2017) 47(3):256–61. doi: 10.1111/imj.13362
2. Mukherjee S. *The Emperor of All Maladies. 1st ed.* New York: Scribner (2010).
3. Berings M, Karaaslan C, Altunbulakli C, Gevaert P, Akdis M, Bachert C, et al. Advances and Highlights in Allergen Immunotherapy: On the Way to Sustained Clinical and Immunologic Tolerance. *J Allergy Clin Immunol* (2017) 140(5):1250–67. doi: 10.1016/j.jaci.2017.08.025
4. Caspi RR. Immunotherapy of Autoimmunity and Cancer: The Penalty for Success. *Nat Rev Immunol* (2008) 8:970–6. doi: 10.1038/nri2438
5. Boardman DA, Levings MK. Cancer Immunotherapies Repurposed for Use in Autoimmunity. *Nat Biomed Eng* (2019) 3:259–63. doi: 10.1038/s41551-019-0359-6
6. Stanway JA, Isaacs JD. Tolerance-Inducing Medicines in Autoimmunity: Rheumatology and Beyond. *Lancet Rheumatol* (2020) 2(9):e565–75. doi: 10.1016/S2665-9913(20)30100-4
7. Fucikova J, Palova-Jelinkova L, Bartunkova J, Spisek R. Induction of Tolerance and Immunity by Dendritic Cells: Mechanisms and Clinical Applications. *Front Immunol* (2019) 10:2393. doi: 10.3389/fimmu.2019.02393
8. Baldin AV, Savvateeva LV, Bazhin AV, Zamyatnin AA. Dendritic Cells in Anticancer Vaccination: Rationale for Ex Vivo Loading or In Vivo Targeting. *Cancers* (2020) 12. doi: 10.3390/cancers12030590
9. Kamphorst AO, Guermonprez P, Dudziak D, Nussenzweig MC. Route of Antigen Uptake Differentially Impacts Presentation by Dendritic Cells and Activated Monocytes. *J Immunol* (2010) 185(6):3426–35. doi: 10.4049/jimmunol.1001205
10. Gardner A, Ruffell B. Dendritic Cells and Cancer Immunity. *Trends Immunol* (2016) 37:855–65. doi: 10.1016/j.it.2016.09.006
11. Anderson MS, Venanzi ES, Klein L, Chen Z, Berzins SP, Turley SJ, et al. Projection of an Immunological Self Shadow Within the Thymus by the Aire Protein. *Sci (80-)* (2002) 298(5597):1395–401. doi: 10.1126/science.1075958
12. Lutz MB, Backer RA, Clausen BE. Revisiting Current Concepts on the Tolerogenicity of Steady-State Dendritic Cell Subsets and Their Maturation Stages. *J Immunol* (2021) 206(8):1681–9. doi: 10.4049/jimmunol.2001315
13. Munn DH, Sharma MD, Mellor AL. Ligation of B7-1/B7-2 by Human Cd4 + T Cells Triggers Indoleamine 2,3-Dioxygenase Activity in Dendritic Cells. *J Immunol* (2004) 172(7):4100–10. doi: 10.4049/jimmunol.172.7.4100
14. Grohmann U, Fallarino F, Puccetti P. Tolerance, DCs and Tryptophan: Much Ado About IDO. *Trends Immunol* (2003) 24:242–8. doi: 10.1016/S1471-4906(03)00072-3
15. Mosanya CH, Isaacs JD. Tolerising Cellular Therapies: What is Their Promise for Autoimmune Disease? *Ann Rheum Dis* (2018) 78:297–310. doi: 10.1136/annrheumdis-2018-214024
16. Shamji MH, Durham SR, London F. Mechanisms of Allergen Immunotherapy for Inhaled Allergens and Predictive Biomarkers. *J Allergy Clin Immunol* (2017) 140:1485–98. doi: 10.1016/j.jaci.2017.10.010
17. Obregon C, Kumar R, Pascual MA, Vassalli G, Golshayan D. Update on Dendritic Cell-Induced Immunological and Clinical Tolerance. *Front Immunol* (2017) 8:1514. doi: 10.3389/fimmu.2017.01514
18. Boldison J, Da Rosa LC, Davies J, Wen L, Wong FS. Dendritic Cells License Regulatory B Cells to Produce IL-10 and Mediate Suppression of Antigen-Specific CD8 T Cells. *Cell Mol Immunol* (2020) 17(8):843–55. doi: 10.1038/s41423-019-0324-z
19. Cauwels A, Tavernier J. Tolerizing Strategies for the Treatment of Autoimmune Diseases: From Ex Vivo to In Vivo Strategies. *Front Immunol* (2020) 11:674. doi: 10.3389/fimmu.2020.00674
20. Hossain MK, Wall KA. Use of Dendritic Cell Receptors as Targets for Enhancing Anti-Cancer Immune Responses. *Cancers (Basel)* (2019) 11(3). doi: 10.3390/cancers11030418
21. Castenmiller C, Keumatio-Doungtsop BC, van Ree R, de Jong EC, van Kooyk Y. Tolerogenic Immunotherapy: Targeting DC Surface Receptors to Induce Antigen-Specific Tolerance. *Front Immunol* (2021) 12:643240. doi: 10.3389/fimmu.2021.643240
22. Benne N, van Duijn J, Kuiper J, Jiskoot W, Slütter B. Orchestrating Immune Responses: How Size, Shape and Rigidity Affect the Immunogenicity of Particulate Vaccines. *J Control Release* (2016) 234:124–34. doi: 10.1016/j.jconrel.2016.05.033
23. Pearson RM, Casey LM, Hughes KR, Miller SD, Shea LD. In Vivo Reprogramming of Immune Cells: Technologies for Induction of Antigen-Specific Tolerance. *Adv Drug Deliv Rev* (2017) 114:240–55. doi: 10.1016/j.addr.2017.04.005
24. Zarghami N, Davaran S, Nejati-Koshki K, Rezaei-Sadabady R, Kouhi M, Joo SW, et al. Liposome: Classification, Preparation, and Applications. *Nanoscale Res Lett* (2013) 8(1):1. doi: 10.1186/1556-276X-8-102
25. Guilliams M, Dutertre CA, Scott CL, McGovern N, Sichien D, Chakarov S, et al. Unsupervised High-Dimensional Analysis Aligns Dendritic Cells Across Tissues and Species. *Immunity* (2016) 45(3):669–84. doi: 10.1016/j.immuni.2016.08.015
26. Collin M, Bigley V. Human Dendritic Cell Subsets: An Update. *Immunology* (2018) 154:3–20. doi: 10.1111/imm.12888
27. Rhodes JW, Tong O, Harman AN, Turville SG. Human Dendritic Cell Subsets, Ontogeny, and Impact on HIV Infection. *Front Immunol* (2019) 10:1088. doi: 10.3389/fimmu.2019.01088
28. Wculek SK, Cueto FJ, Mujal AM, Melero I, Krummel MF, Sancho D. Dendritic Cells in Cancer Immunology and Immunotherapy. *Nat Rev Immunol* (2020) 20p:7–24. doi: 10.1038/s41577-019-0210-z
29. Villani AC, Satija R, Reynolds G, Sarkizova S, Shekhar K, Fletcher J, et al. Single-Cell RNA-seq Reveals New Types of Human Blood Dendritic Cells, Monocytes, and Progenitors. *Sci (80-)* (2017) 356(6335):eaah4573. doi: 10.1126/science.aah4573
30. Roberts EW, Broz ML, Binnewies M, Headley MB, Nelson AE, Wolf DM, et al. Critical Role for CD103+/CD141+ Dendritic Cells Bearing CCR7 for Tumor Antigen Trafficking and Priming of T Cell Immunity in Melanoma. *Cancer Cell* (2016) 30(2):324–36. doi: 10.1016/j.ccell.2016.06.003
31. Laoui D, Keirsse J, Morias Y, Van Overmeire E, Geeraerts X, Elkrim Y, et al. The Tumour Microenvironment Harbours Ontogenically Distinct Dendritic Cell Populations With Opposing Effects on Tumour Immunity. *Nat Commun* (2016) 7(1):1–17. doi: 10.1038/ncomms13720
32. Bosteels C, Neyt K, Vanheerswynghels M, van Helden MJ, Sichien D, Debeuf N, et al. Inflammatory Type 2 Cdcs Acquire Features of cDC1s and Macrophages to Orchestrate Immunity to Respiratory Virus Infection. *Immunity* (2020) 52(6):1039–1056.e9. doi: 10.1016/j.immuni.2020.04.005
33. Tamoutounour S, Guilliams M, MontananaSanchis F, Liu H, Terhorst D, Malosse C, et al. Origins and Functional Specialization of Macrophages and of Conventional and Monocyte-Derived Dendritic Cells in Mouse Skin. *Immunity* (2013) 39(5):925–38. doi: 10.1016/j.immuni.2013.10.004
34. Kuhn S, Yang J, Ronchese F. Monocyte-Derived Dendritic Cells are Essential for CD8+ T Cell Activation and Antitumor Responses After Local Immunotherapy. *Front Immunol* (2015) 6(NOV):23. doi: 10.3389/fimmu.2015.00584
35. Solano-Gálvez S, Tovar-Torres S, Tron-Gómez M, Weiser-Smeke A, Álvarez-Hernández D, Franyuti-Kelly G, et al. Human Dendritic Cells: Ontogeny and Their Subsets in Health and Disease. *Med Sci* (2018) 6(4):88. doi: 10.3390/medsci6040088
36. Tas SW, Vervoordeldonk MJ, Hajji N, Schuitemaker JHN, Van Der Sluijs KF, May MJ, et al. Noncanonical NF-κb Signaling in Dendritic Cells is Required for Indoleamine 2,3-Dioxygenase (IDO) Induction and Immune Regulation. *Blood* (2007) 110(5):1540–9. doi: 10.1182/blood-2006-11-056010
37. Sittig SP, van Beek JJP, Flórez-Grau G, Weiden J, Buschow SI, van der Net MC, et al. Human Type 1 and Type 2 Conventional Dendritic Cells Express

Indoleamine 2,3-Dioxygenase 1 With Functional Effects on T Cell Priming. *Eur J Immunol* (2021) 2021. doi: 10.1002/eji.202048580
38. Van Der Aar AMG, Picavet DI, Muller FJ, De Boer L, Van Capel TMM, Zaat SAJ, et al. Langerhans Cells Favor Skin Flora Tolerance Through Limited Presentation of Bacterial Antigens and Induction of Regulatory T Cells. *J Invest Dermatol* (2013) 133(5):1240–9. doi: 10.1038/jid.2012.500
39. Hasegawa H, Matsumoto T. Mechanisms of Tolerance Induction by Dendritic Cells In Vivo. *Front Immunol* (2018) 9:1. doi: 10.3389/fimmu.2018.00350
40. van der Aar AMG, Sylva-Steenland RMR, Bos JD, Kapsenberg ML, de Jong EC, Teunissen MBM. Cutting Edge: Loss of TLR2, TLR4, and TLR5 on Langerhans Cells Abolishes Bacterial Recognition. *J Immunol* (2007) 178(4):1986–90. doi: 10.4049/jimmunol.178.4.1986
41. Bakdash G, Vogelpoel LTC, Van Capel TMM, Kapsenberg ML, De Jong EC. Retinoic Acid Primes Human Dendritic Cells to Induce Gut-Homing, IL-10-producing Regulatory T Cells. *Mucosal Immunol* (2015) 8(2):265–78. doi: 10.1038/mi.2014.64
42. Scott CL, Aumeunier AM, Mowat AMI. Intestinal CD103 + Dendritic Cells: Master Regulators of Tolerance? *Trends Immunol* (2011) 32:412–9. doi: 10.1016/j.it.2011.06.003
43. Jongbloed SL, Lebre MC, Fraser AR, Gracie JA, Sturrock RD, Tak PP, et al. Enumeration and Phenotypical Analysis of Distinct Dendritic Cell Subsets in Psoriatic Arthritis and Rheumatoid Arthritis. *Arthritis Res Ther* (2005) 8(1):R15. doi: 10.1186/ar1864
44. Lebre MC, Jongbloed SL, Tas SW, Smeets TJM, McInnes IB, Tak PP. Rheumatoid Arthritis Synovium Contains Two Subsets of CD83 -DC-LAMP- Dendritic Cells With Distinct Cytokine Profiles. *Am J Pathol* (2008) 172(4):940–50. doi: 10.2353/ajpath.2008.070703
45. Bangert C, Rindler K, Krausgruber T, Alkon N, Thaler FM, Kurz H, et al. Persistence of Mature Dendritic Cells, TH2A, and Tc2 Cells Characterize Clinically Resolved Atopic Dermatitis Under IL-4Rα Blockade. *Sci Immunol* (2021) 6(55):1–17. doi: 10.1126/sciimmunol.abe2749
46. Seder RA, Darrah PA, Roederer M. T-Cell Quality in Memory and Protection: Implications for Vaccine Design. *Nat Rev Immunol* (2008) 8:247–58. doi: 10.1038/nri2274
47. Zinkernagel RM. Localization Dose and Time of Antigens Determine Immune Reactivity. *Semin Immunol* (2000) 12(3):163–71. doi: 10.1006/smim.2000.0253
48. Nicoli F, Paul S, Appay V. Harnessing the Induction of CD8+ T-Cell Responses Through Metabolic Regulation by pathogen-Recognition-receptor Triggering in Antigen Presenting Cells. *Front Immunol* (2018) 9p:2372. doi: 10.3389/fimmu.2018.02372
49. De Jong EC, Smits HH, Kapsenberg ML. Dendritic Cell-Mediated T Cell Polarization. *Springer Semin Immunopathol* (2005) 26:289–307. doi: 10.1007/s00281-004-0167-1
50. Geijtenbeek TBH, Gringhuis SI. Signalling Through C-type Lectin Receptors: Shaping Immune Responses. *Nat Rev Immunol* (2009) 9:465–79. doi: 10.1038/nri2569
51. Pérez O, Romeu B, Cabrera O, González E, Batista-Duharte A, Labrada A, et al. Adjuvants are Key Factors for the Development of Future Vaccines: Lessons From the Finlay Adjuvant Platform. *Front Immunol* (2013) 4(DEC):407. doi: 10.3389/fimmu.2013.00407
52. Vangasseri DP, Cui Z, Chen W, Hokey DA, Falo LD, Huang L. Immunostimulation of Dendritic Cells by Cationic Liposomes. *Mol Membr Biol* (2006) 23(5):385–95. doi: 10.1080/09687860600790537
53. Ma Y, Zhuang Y, Xie X, Wang C, Wang F, Zhou D, et al. The role of surface charge density in cationic liposome-promoted dendritic cell maturation and vaccine-induced immune responses. *Nanoscale* (2011) 3(5):2307–14. doi: 10.1039/c1nr10166h
54. Soema PC, Willems GJ, Jiskoot W, Amorij JP, Kersten GF. Predicting the Influence of Liposomal Lipid Composition on Liposome Size, Zeta Potential and Liposome-Induced Dendritic Cell Maturation Using a Design of Experiments Approach. *Eur J Pharm Biopharm* (2015) 94:427–35. doi: 10.1016/j.ejpb.2015.06.026
55. Benne N, van Duijn J, Lozano Vigario F, Leboux RJT, van Veelen P, Kuiper J, et al. Anionic 1,2-distearoyl-sn-glycero-3-phosphoglycerol (DSPG) Liposomes Induce Antigen-Specific Regulatory T Cells and Prevent Atherosclerosis in Mice. *J Control Release* (2018) 291(May):135–46. doi: 10.1016/j.jconrel.2018.10.028
56. Cong X, Tian H, Liu S, Mao K, Chen H, Xin Y, et al. Cationic Liposome/DNA Complexes Mediate Antitumor Immunotherapy by Promoting Immunogenic Tumor Cell Death and Dendritic Cell Activation. *ACS Appl Mater Interfaces* (2020) 12(25):28047–56. doi: 10.1021/acsami.0c08112
57. Gao J, Ochyl LJ, Yang E, Moon JJ. Cationic Liposomes Promote Antigen Cross-Presentation in Dendritic Cells by Alkalizing the Lysosomal Ph and Limiting the Degradation of Antigens. *Int J Nanomed* (2017) 12:1251–64. doi: 10.2147/IJN.S125866
58. Inoh Y, Tadokoro S, Tanabe H, Inoue M, Hirashima N, Nakanishi M, et al. Inhibitory Effects of a Cationic Liposome on Allergic Reaction Mediated by Mast Cell Activation. *Biochem Pharmacol* (2013) 86(12):1731–8. doi: 10.1016/j.bcp.2013.09.023
59. Aliu H, Rask C, Brimnes J, Andresen TL. Enhanced Efficacy of Sublingual Immunotherapy by Liposome-Mediated Delivery of Allergen. *Int J Nanomed* (2017) 12:8377–88. doi: 10.2147/IJN.S137033
60. Mori M, Nishida M, Maekawa N, Yamamura H, Tanaka Y, Kasai M, et al. An Increased Adjuvanticity of Liposomes by the Inclusion of Phosphatidylserine in Immunization With Surface-Coupled Liposomal Antigen. *Int Arch Allergy Immunol* (2005) 136(1):83–9. doi: 10.1159/000082588
61. Shi D, Fu M, Fan P, Li W, Chen X, Li C, et al. Artificial Phosphatidylserine Liposome Mimics Apoptotic Cells in Inhibiting Maturation and Immunostimulatory Function of Murine Myeloid Dendritic Cells in Response to 1-chloro-2,4-dinitrobenze In Vitro. *Arch Dermatol Res* (2007) 299(7):327–36. doi: 10.1007/s00403-007-0770-9
62. Rodriguez-Fernandez S, Pujol-Autonell I, Brianso F, Perna-Barrull D, Cano-Sarabia M, Garcia-Jimeno S, et al. Phosphatidylserine-Liposomes Promote Tolerogenic Features on Dendritic Cells in Human Type 1 Diabetes by Apoptotic Mimicry. *Front Immunol* (2018) 9(FEB):14. doi: 10.3389/fimmu.2018.00253
63. Yi X, Shi X, Gao H. Cellular Uptake of Elastic Nanoparticles. *Phys Rev Lett* (2011) 107(9):098101. doi: 10.1103/PhysRevLett.107.098101
64. Sun J, Zhang L, Wang J, Feng Q, Liu D, Yin Q, et al. Tunable Rigidity of (Polymeric Core)-(Lipid Shell) Nanoparticles for Regulated Cellular Uptake. *Adv Mater* (2015) 27(8):1402–7. doi: 10.1002/adma.201404788
65. Hartmann R, Weidenbach M, Neubauer M, Fery A, Parak WJ. Stiffness-Dependent In Vitro Uptake and Lysosomal Acidification of Colloidal Particles. *Angew Chemie - Int Ed* (2015) 54(4):1365–8. doi: 10.1002/anie.201409693
66. Benne N, Leboux RJT, Glandrup M, van Duijn J, Lozano Vigario F, Neustrup MA, et al. Atomic Force Microscopy Measurements of Anionic Liposomes Reveal the Effect of Liposomal Rigidity on Antigen-Specific Regulatory T Cell Responses. *J Control Release* (2020) 318(October 2019):246–55. doi: 10.1016/j.jconrel.2019.12.003
67. Norling K, Bernasconi V, Agmo Hernández V, Parveen N, Edwards K, Lycke NY, et al. Gel Phase 1,2-distearoyl-sn-glycero-3-phosphocholine-based Liposomes are Superior to Fluid Phase Liposomes At Augmenting Both Antigen Presentation on Major Histocompatibility Complex Class II and Costimulatory Molecule Display by Dendritic Cells In Vitro. *ACS Infect Dis* (2019) 5(11):1867–78. doi: 10.1021/acsinfecdis.9b00189
68. Getts DR, Shea LD, Miller SD, King NJC. Harnessing Nanoparticles for Immune Modulation. *Trends Immunol* (2015) 36:419–27. doi: 10.1016/j.it.2015.05.007
69. Cifuentes-Rius A, Desai A, Yuen D, Johnston APR, Voelcker NH. Inducing Immune Tolerance With Dendritic Cell-Targeting Nanomedicin. *Nat Nanotechnol* (2021) 16p:37–46. doi: 10.1038/s41565-020-00810-2
70. Tran KK, Shen H. The Role of Phagosomal Ph on the Size-Dependent Efficiency of Cross-Presentation by Dendritic Cells. *Biomaterials* (2009) 30(7):1356–62. doi: 10.1016/j.biomaterials.2008.11.034
71. Mottram PL, Leong D, Crimeen-Irwin B, Gloster S, Xiang SD, Meanger J, et al. Type 1 and 2 Immunity Following Vaccination is Influenced by Nanoparticle Size: Formulation of a Model Vaccine for Respiratory Syncytial Virus. *Mol Pharm* (2007) 4(1):73–84. doi: 10.1021/mp060096p
72. Kanchan V, Panda AK. Interactions of Antigen-Loaded Polylactide Particles With Macrophages and Their Correlation With the Immune Response. *Biomaterials* (2007) 28(35):5344–57. doi: 10.1016/j.biomaterials.2007.08.015
73. Joshi VB, Geary SM, Salem AK. Biodegradable Particles as Vaccine Delivery Systems: Size Matters. *AAPS J* (2013) 15(1):85–94. doi: 10.1208/s12248-012-9418-6

74. Mann JFS, Shakir E, Carter KC, Mullen AB, Alexander J, Ferro VA. Lipid Vesicle Size of an Oral Influenza Vaccine Delivery Vehicle Influences the Th1/Th2 Bias in the Immune Response and Protection Against Infection. *Vaccine* (2009) 27(27):3643–9. doi: 10.1016/j.vaccine.2009.03.040
75. Henriksen-Lacey M, Devitt A, Perrie Y. The Vesicle Size of DDA:TDB Liposomal Adjuvants Plays a Role in the Cell-Mediated Immune Response But has No Significant Effect on Antibody Production. *J Control Release* (2011) 154(2):131–7. doi: 10.1016/j.jconrel.2011.05.019
76. Verma A, Uzun O, Hu Y, Hu Y, Han HS, Watson N, et al. Surface-Structure-Regulated Cell-Membrane Penetration by Monolayer-Protected Nanoparticles. *Nat Mater* (2008) 7(7):588–95. doi: 10.1038/nmat2202
77. Patra JK, Das G, Fraceto LF, Campos EVR, Rodriguez-Torres MDP, Acosta-Torres LS, et al. Nano Based Drug Delivery Systems: Recent Developments and Future Prospects 10 Technology 1007 Nanotechnology 03 Chemical Sciences 0306 Physical Chemistry (Incl. Structural) 03 Chemical Sciences 0303 Macromolecular and Materials Chemistry 11 Medical and He. *J Nanobiotechnol* (2018) 16:71. doi: 10.1186/s12951-018-0392-8
78. Li P, Yang X, Yang Y, He H, Chou CK, Chen F, et al. Synergistic Effect of All-Trans-Retinal and Triptolide Encapsulated in an Inflammation-Targeted Nanoparticle on Collagen-Induced Arthritis in Mice. *J Control Release* (2020) 319:87–103. doi: 10.1016/j.jconrel.2019.12.025
79. Zhang W, Lu X, Cui P, Piao C, Xiao M, Liu X, et al. Phase I/II Clinical Trial of a Wilms' Tumor 1-Targeted Dendritic Cell Vaccination-Based Immunotherapy in Patients With Advanced Cancer. *Cancer Immunol Immunother* (2019) 68(1):121–30. doi: 10.1007/s00262-018-2257-2
80. Patel PM, Ottensmeier CH, Mulatero C, Lorigan P, Plummer R, Pandha H, et al. Targeting gp100 and TRP-2 With a DNA Vaccine: Incorporating T Cell Epitopes With a Human IgG1 Antibody Induces Potent T Cell Responses That are Associated With Favourable Clinical Outcome in a Phase I/II Trial. *Oncoimmunology* (2018) 7(6):e1433516. doi: 10.1080/2162402X.2018.1433516
81. Taylor-Papadimitriou J, Burchell JM, Graham R, Beatson R. Latest Developments in MUC1 Immunotherapy. *Biochem Soc Trans* (2018) 46:659–68. doi: 10.1042/BST20170400
82. Zajac P, Schultz-Thater E, Tornillo L, Sadowski C, Trella E, Mengus C, et al. MAGE-a Antigens and Cancer Immunotherapy. *Front Med* (2017) 4 (MAR):18. doi: 10.3389/fmed.2017.00018
83. Sahin U, Oehm P, Derhovanessian E, Jabulowsky RA, Vormehr M, Gold M, et al. An RNA Vaccine Drives Immunity in Checkpoint-Inhibitor-Treated Melanoma. *Nature* (2020) 585(7823):107–12. doi: 10.1038/s41586-020-2537-9
84. Butts C, Socinski MA, Mitchell PL, Thatcher N, Havel L, Krzakowski M, et al. Tecemotide (L-BLP25) Versus Placebo After Chemoradiotherapy for Stage III non-Small-Cell Lung Cancer (START): A Randomised, Double-Blind, Phase 3 Trial. *Lancet Oncol* (2014) 15(1):59–68. doi: 10.1016/S1470-2045(13)70510-2
85. Hollingsworth RE, Jansen K. Turning the Corner on Therapeutic Cancer Vaccines. *NPJ Vaccines* (2019) 4:1–10. doi: 10.1038/s41541-019-0103-y
86. Buonaguro L, Tagliamonte M. Selecting Target Antigens for Cancer Vaccine Development. *Vaccines* (2020) 8(4):615. doi: 10.3390/vaccines8040615
87. De Martel C, Georges D, Bray F, Ferlay J, Clifford GM. Global Burden of Cancer Attributable to Infections in 2018: A Worldwide Incidence Analysis. *Lancet Glob Heal* (2019) 8:e180–90. doi: 10.1016/S2214-109X(19)30488-7
88. White MK, Pagano JS, Khalili K. Viruses and Human Cancers: A Long Road of Discovery of Molecular Paradigms. *Clin Microbiol Rev* (2014) 27(3):463–81. doi: 10.1128/CMR.00124-13
89. Trimble CL, Morrow MP, Kraynyak KA, Shen X, Dallas M, Yan J, et al. Safety, Efficacy, and Immunogenicity of VGX-3100, a Therapeutic Synthetic DNA Vaccine Targeting Human Papillomavirus 16 and 18 E6 and E7 Proteins for Cervical Intraepithelial Neoplasia 2/3: A Randomised, Double-Blind, Placebo-Controlled Phase 2b Trial. *Lancet* (2015) 386(10008):2078–88. doi: 10.1016/S0140-6736(15)00239-1
90. Karimi H, Soleimanjahi H, Abdoli A, Banijamali RS. Combination Therapy Using Human Papillomavirus L1/E6/E7 Genes and Archaeosome: A Nanovaccine Confer Immuneadjuvanting Effects to Fight Cervical Cancer. *Sci Rep* (2020) 10(1):5787. doi: 10.1038/s41598-020-62448-3
91. Srivastava PK. Neoepitopes of Cancers: Looking Back, Looking Ahead. *Cancer Immunol Res* (2015) 3(9):969–77. doi: 10.1158/2326-6066.CIR-15-0134
92. Peng M, Mo Y, Wang Y, Wu P, Zhang Y, Xiong F, et al. Neoantigen Vaccine: An Emerging Tumor Immunotherapy. *Mol Cancer* (2019) 18:1–14. doi: 10.1186/s12943-019-1055-6
93. Van Buuren MM, Calis JJA, Schumacher TNM. High Sensitivity of Cancer Exome-Based CD8 T Cell Neo-Antigen Identification. *Oncoimmunology* (2014) 3(5):5. doi: 10.4161/onci.28836
94. Ott PA, Hu Z, Keskin DB, Shukla SA, Sun J, Bozym DJ, et al. An Immunogenic Personal Neoantigen Vaccine for Patients With Melanoma. *Nature* (2017) 547(7662):217–21. doi: 10.1038/nature22991
95. Sahin U, Derhovanessian E, Miller M, Kloke BP, Simon P, Löwer M, et al. Personalized RNA Mutanome Vaccines Mobilize Poly-Specific Therapeutic Immunity Against Cancer. *Nature* (2017) 547(7662):222–6. doi: 10.1038/nature23003
96. Kranz LM, Diken M, Haas H, Kreiter S, Loquai C, Reuter KC, et al. Systemic RNA Delivery to Dendritic Cells Exploits Antiviral Defence for Cancer Immunotherapy. *Nature* (2016) 534(7607):396–401. doi: 10.1038/nature18300
97. Esprit A, de Mey W, Bahadur Shahi R, Thielemans K, Franceschini L, Breckpot K. Neo-Antigen mRNA Vaccines. *Vaccines* (2020) 8(4):776. doi: 10.3390/vaccines8040776
98. Reichmuth AM, Oberli MA, Jeklenec A, Langer R, Blankschtein D. mRNA Vaccine Delivery Using Lipid Nanoparticles. *Ther Deliv* (2016) 7(5):319–34. doi: 10.4155/tde-2016-0006
99. Cafri G, Gartner JJ, Zaks T, Hopson K, Levin N, Paria BC, et al. mRNA Vaccine–Induced Neoantigen-Specific T Cell Immunity in Patients With Gastrointestinal Cancer. *J Clin Invest* (2020) 130(11):5976–88. doi: 10.1172/JCI134915
100. Mulligan MJ, Lyke KE, Kitchin N, Absalon J, Gurtman A, Lockhart S, et al. Phase I/II Study of COVID-19 RNA Vaccine BNT162b1 in Adults. *Nature* (2020) 586(7830):589–93. doi: 10.1038/s41586-020-2639-4
101. Jackson LA, Anderson EJ, Rouphael NG, Roberts PC, Makhene M, Coler RN, et al. An Mrna Vaccine Against SARS-CoV-2 — Preliminary Report. *N Engl J Med* (2020) 383(20):1920–31. doi: 10.1056/NEJMoa2022483
102. Busold S, Nagy NA, Tas SW, van Ree R, de Jong EC, Geijtenbeek TBH. Various Tastes of Sugar: The Potential of Glycosylation in Targeting and Modulating Human Immunity Via C-Type Lectin Receptors. *Front Immunol* (2020) 11:134. doi: 10.3389/fimmu.2020.00134
103. Fehres CM, Van Beelen AJ, Bruijns SCM, Ambrosini M, Kalay H, Van Bloois L, et al. In Situ Delivery of Antigen to DC-SIGN + CD14 + Dermal Dendritic Cells Results in Enhanced Cd8 + T-Cell Responses. *J Invest Dermatol* (2015) 135(9):2228–36. doi: 10.1038/jid.2015.152
104. Stolk DA, de Haas A, Vree J, Duinkerken S, Lübbers J, van de Ven R, et al. Lipo-Based Vaccines as an Approach to Target Dendritic Cells for Induction of T- and Inkt Cell Responses. *Front Immunol* (2020) 11:990. doi: 10.3389/fimmu.2020.00990
105. Cruz LJ, Tacken PJ, Fokkink R, Joosten B, Stuart MC, Albericio F, et al. Targeted PLGA Nano- But Not Microparticles Specifically Deliver Antigen to Human Dendritic Cells Via DC-SIGN In Vitro. *J Control Release* (2010) 144(2):118–26. doi: 10.1016/j.jconrel.2010.02.013
106. Gargett T, Abbas MN, Rolan P, Price JD, Gosling KM, Ferrante A, et al. Phase I Trial of Lipovaxin-MM, a Novel Dendritic Cell-Targeted Liposomal Vaccine for Malignant Melanoma. *Cancer Immunol Immunother* (2018) 67 (9):1461–72. doi: 10.1007/s00262-018-2207-z
107. Morse MA, Chapman R, Powderly J, Blackwell K, Keler T, Green J, et al. Phase I Study Utilizing a Novel Antigen-Presenting Cell-Targeted Vaccine With Toll-Like Receptor Stimulation to Induce Immunity to Self-Antigens in Cancer Patients. *Clin Cancer Res* (2011) 17(14):4844–53. doi: 10.1158/1078-0432.CCR-11-0891
108. Zhang C, Shi G, Zhang J, Song H, Niu J, Shi S, et al. Targeted Antigen Delivery to Dendritic Cell Via Functionalized Alginate Nanoparticles for Cancer Immunotherapy. *J Control Release* (2017) 256:170–81. doi: 10.1016/j.jconrel.2017.04.020
109. Moku G, Vangala S, Gulla SK, Yakati V. In Vivo Targeting of DNA Vaccines to Dendritic Cells Via the Mannose Receptor Induces Long-Lasting Immunity Against Melanoma. *ChemBioChem* (2020) 22:523–31. doi: 10.1002/cbic.202000364
110. Saluja SS, Hanlon DJ, Sharp FA, Hong E, Khalil D, Robinson E, et al. Targeting Human Dendritic Cells Via DEC-205 Using PLGA Nanoparticles

Leads to Enhanced Cross-Presentation of a Melanoma-Associated Antigen. *Int J Nanomed* (2014) 9:5231–46. doi: 10.2147/IJN.S66639
111. Cruz LJ, Rosalia RA, Kleinovink JW, Rueda F, Löwik CWGM, Ossendorp F. Targeting Nanoparticles to CD40, Dec-205 or CD11c Molecules on Dendritic Cells for Efficient CD8+ T Cell Response: A Comparative Study. *J Control Release* (2014) 192:209–18. doi: 10.1016/j.jconrel.2014.07.040
112. Tullett KM, Leal Rojas IM, Minoda Y, Tan PS, Zhang J-G, Smith C, et al. Targeting CLEC9A Delivers Antigen to Human CD141+ DC for CD4+ and CD8+T Cell Recognition. *JCI Insight* (2016) 1(7):1–12. doi: 10.1172/jci.insight.87102
113. Schreibelt G, Klinkenberg LJJ, Cruz LJ, Tacken PJ, Tel J, Kreutz M, et al. The C-type Lectin Receptor CLEC9A Mediates Antigen Uptake and (Cross-) Presentation by Human Blood BDCA3+ Myeloid Dendritic Cells. *Blood* (2012) 119(10):2284–92. doi: 10.1182/blood-2011-08-373944
114. Ghinnagow R, De Meester J, Cruz LJ, Aspord C, Corgnac S, Macho-Fernandez E, et al. Co-Delivery of the NKT Agonist α-Galactosylceramide and Tumor Antigens to Cross-Priming Dendritic Cells Breaks Tolerance to Self-Antigens and Promotes Antitumor Responses. *Oncoimmunology* (2017) 6(9):e1339855. doi: 10.1080/2162402X.2017.1339855
115. Affandi AJ, Grabowska J, Olesek K, Lopez Venegas M, Barbaria A, Rodríguez E, et al. Selective Tumor Antigen Vaccine Delivery to Human CD169 + Antigen-Presenting Cells Using Ganglioside-Liposomes. *Proc Natl Acad Sci* (2020) 117(44):202006186. doi: 10.1073/pnas.2006186117
116. Suzuki R, Utoguchi N, Kawamura K, Kadowaki N, Okada N, Takizawa T, et al. Development of Effective Antigen Delivery Carrier to Dendritic Cells Via Fc Receptor in Cancer Immunotherapy. *Yakugaku Zasshi Yakugaku Zasshi* (2007) 127:301–6. doi: 10.1248/yakushi.127.301
117. Hossain MK, Vartak A, Sucheck SJ, Wall KA. Liposomal Fc Domain Conjugated to a Cancer Vaccine Enhances Both Humoral and Cellular Immunity. *ACS Omega* (2019) 4(3):5204–8. doi: 10.1021/acsomega.9b00029
118. Marciani DJ. Effects of Immunomodulators on the Response Induced by Vaccines Against Autoimmune Diseases. *Autoimmunity* (2017) 50(7):393–402. doi: 10.1080/08916934.2017.1373766
119. Stern JNH, Keskin DB, Kato Z, Waldner H, Schallenberg S, Anderson A, et al. Promoting Tolerance to Proteolipid Protein-Induced Experimental Autoimmune Encephalomyelitis Through Targeting Dendritic Cells. *Proc Natl Acad Sci USA* (2010) 107(40):17280–5. doi: 10.1073/pnas.1010263107
120. Shi M, Chen X, Ye K, Yao Y, Li Y. Application Potential of Toll-Like Receptors in Cancer Immunotherapy. *Med (United States)* (2016) 95:e3951. doi: 10.1097/MD.0000000000003951
121. Elamanchili P, Lutsiak CME, Hamdy S, Diwan M, Samuel J. "Pathogen-Mimicking" Nanoparticles for Vaccine Delivery to Dendritic Cells. *J Immunother* (2007) 30(4):378–95. doi: 10.1097/CJI.0b013e31802cf3e3
122. Frega G, Wu Q, Le Naour J, Vacchelli E, Galluzzi L, Kroemer G, et al. Trial Watch: Experimental TLR7/TLR8 Agonists for Oncological Indications. *OncoImmunology* (2020) 9:1796002. doi: 10.1080/2162402X.2020.1796002
123. Islam MA, Rice J, Reesor E, Zope H, Tao W, Lim M, et al. Adjuvant-Pulsed mRNA Vaccine Nanoparticle for Immunoprophylactic and Therapeutic Tumor Suppression in Mice. *Biomaterials* (2021) 266:120431. doi: 10.1016/j.biomaterials.2020.120431
124. Kayraklioglu N, Horuluoglu B, Klinman DM. Cpg Oligonucleotides as Vaccine Adjuvants. In: *Methods Mol Biol* Humana Press Inc. (2021). 2197 p. 51–85.
125. Jeanbart L, Ballester M, De Titta A, Corthésy P, Romero P, Hubbell JA, et al. Enhancing Efficacy of Anticancer Vaccines by Targeted Delivery to Tumor-Draining Lymph Nodes. *Cancer Immunol Res* (2014) 2(5):436–47. doi: 10.1158/2326-6066.CIR-14-0019-T
126. Liu C, Chu X, Sun P, Feng X, Huang W, Liu H, et al. Synergy Effects of Polyinosinic-polycytidylic Acid, CpG Oligodeoxynucleotide, and Cationic Peptides to Adjuvant HPV E7 Epitope Vaccine Through Preventive and Therapeutic Immunization in a TC-1 Grafted Mouse Model. *Hum Vaccin Immunother* (2018) 14(4):931–40. doi: 10.1080/21645515.2017.1420446
127. Speth MT, Repnik U, Müller E, Spanier J, Kalinke U, Corthay A, et al. Poly(I:C)-Encapsulating Nanoparticles Enhance Innate Immune Responses to the Tuberculosis Vaccine Bacille Calmette-Guérin (BCG) Via Synergistic Activation of Innate Immune Receptors. *Mol Pharm* (2017) 14(11):4098–112. doi: 10.1021/acs.molpharmaceut.7b00795
128. Liu C, Chu X, Yan M, Qi J, Liu H, Gao F, et al. Encapsulation of Poly I:C and the Natural Phosphodiester CpG ODN Enhanced the Efficacy of a Hyaluronic Acid-Modified Cationic lipid-PLGA Hybrid Nanoparticle Vaccine in TC-1-grafted Tumors. *Int J Pharm* (2018) 553(1–2):327–37. doi: 10.1016/j.ijpharm.2018.10.054
129. Bayyurt B, Tincer G, Almacioglu K, Alpdundar E, Gursel M, Gursel I. Encapsulation of Two Different TLR Ligands Into Liposomes Confer Protective Immunity and Prevent Tumor Development. *J Control Release* (2017) 247:134–44. doi: 10.1016/j.jconrel.2017.01.004
130. Ni Q, Zhang F, Liu Y, Wang Z, Yu G, Liang B, et al. A Bi-Adjuvant Nanovaccine That Potentiates Immunogenicity of Neoantigen for Combination Immunotherapy of Colorectal Cancer. *Sci Adv* (2020) 6 (12):6071–89. doi: 10.1126/sciadv.aaw6071
131. Fujii SI, Shimizu K, Smith C, Bonifaz L, Steinman RM. Activation of Natural Killer T Cells by α-Galactosylceramide Rapidly Induces the Full Maturation of Dendritic Cells In Vivo and Thereby Acts as an Adjuvant for Combined CD4 and CD8 T Cell Immunity to a Coadministered Protein. *J Exp Med* (2003) 198(2):267–79. doi: 10.1084/jem.20030324
132. Hermans IF, Silk JD, Gileadi U, Salio M, Mathew B, Ritter G, et al. Nkt Cells Enhance CD4 + and CD8 + T Cell Responses to Soluble Antigen In Vivo Through Direct Interaction With Dendritic Cells. *J Immunol* (2003) 171 (10):5140–7. doi: 10.4049/jimmunol.171.10.5140
133. Nakamura T, Yamazaki D, Yamauchi J, Harashima H. The Nanoparticulation by Octaarginine-Modified Liposome Improves α-Galactosylceramide-Mediated Antitumor Therapy Via Systemic Administration. *J Control Release* (2013) 171(2):216–24. doi: 10.1016/j.jconrel.2013.07.004
134. Cioncada R, Maddaluno M, Vo HTM, Woodruff M, Tavarini S, Sammicheli C, et al. Vaccine adjuvant MF59 promotes the intranodal differentiation of antigen-loaded and activated monocyte-derived dendritic cells. Bayry J, Editor. *PloS One* (2017) 12(10):e0185843. doi: 10.1371/journal.pone.0185843
135. Zeng B, Middelberg APJ, Gemiarto A, MacDonald K, Baxter AG, Talekar M, et al. Self-Adjuvanting Nanoemulsion Targeting Dendritic Cell Receptor Clec9A Enables Antigen-Specific Immunotherapy. *J Clin Invest* (2018) 128 (5):1971–84. doi: 10.1172/JCI96791
136. Basomba A, Tabar AI, De Rojas DHF, García BE, Alamar R, Olaguíbel JM, et al. Allergen Vaccination With a Liposome-Encapsulated Extract of Dermatophagoides Pteronyssinus: A Randomized, Double-Blind, Placebo-Controlled Trial in Asthmatic Patients. *J Allergy Clin Immunol* (2002) 109 (6):943–8. doi: 10.1067/mai.2002.124465
137. Nouri HR, Varasteh A, Jaafari MR, Davies JM, Sankian M. Induction of a Th1 Immune Response and Suppression of IgE Via Immunotherapy With a Recombinant Hybrid Molecule Encapsulated in Liposome–Protamine–DNA Nanoparticles in a Model of Experimental Allergy. *Immunol Res* (2015) 62 (3):280–91. doi: 10.1007/s12026-015-8659-8
138. Chaisri U, Tungtrongchitr A, Indrawattana N, Meechan P, Phurttikul W, Tasaniyananda N, et al. Immunotherapeutic Efficacy of Liposome-Encapsulated Refined Allergen Vaccines Against Dermatophagoides Pteronyssinus Allergy. *PloS One* (2017) 12(11):e0188627. doi: 10.1371/journal.pone.0188627
139. Nielen MMJ, Van Schaardenburg D, Reesink HW, Van De Stadt RJ, Van Der Horst-Bruinsma IE, De Koning MHMT, et al. Specific Autoantibodies Precede the Symptoms of Rheumatoid Arthritis: A Study of Serial Measurements in Blood Donors. *Arthritis Rheumatol* (2004) 50(2):380–6. doi: 10.1002/art.20018
140. James E, Rieck M, Pieper J, Gebe JA, Yue BB, Tatum M, et al. Citrulline Specific Th1 Cells are Increased in Rheumatoid Arthritis and Their Frequency is Influenced by Disease Duration and Therapy. *Arthritis Rheumatol* (2014) 66(7):1712–22. doi: 10.1002/art.38637
141. Benham H, Nel HJ, Law SC, Mehdi AM, Street S, Ramnoruth N, et al. Citrullinated Peptide Dendritic Cell Immunotherapy in HLA Risk Genotype-Positive Rheumatoid Arthritis Patients. *Sci Transl Med* (2015) 7 (290):1–12. doi: 10.1126/scitranslmed.aaa9301
142. Capini C, Jaturanpinyo M, Chang H-I, Mutalik S, McNally A, Street S, et al. Antigen-Specific Suppression of Inflammatory Arthritis Using Liposomes. *J Immunol* (2009) 182(6):3556–65. doi: 10.4049/jimmunol.0802972
143. Katakowski JA, Mukherjee G, Wilner SE, Maier KE, Harrison MT, Di Lorenzo TP, et al. Delivery of siRNAs to Dendritic Cells Using DEC205-targeted Lipid Nanoparticles to Inhibit Immune Responses. *Mol Ther* (2016) 24(1):146–55. doi: 10.1038/mt.2015.175

144. Bandyopadhyay A, Fine RL, Demento S, Bockenstedt LK, Fahmy TM. The impact of nanoparticle ligand density on dendritic-cell targeted vaccines. *Biomaterials* (2011) 32(11):3094–105. doi: 10.1016/j.biomaterials.2010.12.054
145. Nandedkar-Kulkarni N, Vartak AR, Sucheck SJ, Wall KA, Quinn A, Morran MP, et al. Development of a Bioconjugate Platform for Modifying the Immune Response of Autoreactive Cytotoxic T Lymphocytes Involved in Type 1 Diabetes. *Bioconjug Chem* (2019) 30(7):2049–59. doi: 10.1021/acs.bioconjchem.9b00332
146. Perdicchio M, Ilarregui JM, Verstege MI, Cornelissen LAM, Schetters STT, Engels S, et al. Sialic acid-modified antigens impose tolerance via inhibition of T-cell proliferation and de novo induction of regulatory T cells. *Proc Natl Acad Sci USA* (2016) 113(12):3329–34. doi: 10.1073/pnas.1507706113
147. Hesse L, Feenstra R, Ambrosini M, de Jager WA, Petersen A, Vietor H, et al. Subcutaneous Immunotherapy Using Modified Phl p5a-derived Peptides Efficiently Alleviates Allergic Asthma in Mice. *Allergy: Eur J Allergy Clin Immunol* (2019) 74:2495–8. doi: 10.1111/all.13918
148. Pang L, Macauley MS, Arlian BM, Nycholat CM, Paulson JC. Encapsulating an Immunosuppressant Enhances Tolerance Induction by Siglec-Engaging Tolerogenic Liposomes. *ChemBioChem* (2017) 18(13):1226–33. doi: 10.1002/cbic.201600702
149. Spence S, Greene MK, Fay F, Hams E, Saunders SP, Hamid U, et al. Targeting Siglecs With a Sialic Acid-Decorated Nanoparticle Abrogates Inflammation. *Sci Transl Med* (2015) 7(303):303ra140. doi: 10.1126/scitranslmed.aab3459
150. Kishimoto TK, Maldonado RA. Nanoparticles for the Induction of Antigen-Specific Immunological Tolerance. *Front Immunol* (2018) 9:230. doi: 10.3389/fimmu.2018.00230
151. Kim SH, Moon JH, Jeong SU, Jung HH, Park CS, Hwang BY, et al. Induction of Antigen-Specific Immune Tolerance Using Biodegradable Nanoparticles Containing Antigen and Dexamethasone. *Int J Nanomed* (2019) 14:5229–42. doi: 10.2147/IJN.S210546
152. Yeste A, Nadeau M, Burns EJ, Weiner HL, Quintana FJ. Nanoparticle-Mediated Codelivery of Myelin Antigen and a Tolerogenic Small Molecule Suppresses Experimental Autoimmune Encephalomyelitis. *Proc Natl Acad Sci USA* (2012) 109(28):11270–5. doi: 10.1073/pnas.1120611109
153. Prangtaworn P, Chaisri U, Seesuay W, Mahasongkram K, Onlamoon N, Reamtong O, et al. Tregitope-Linked Refined Allergen Vaccines for Immunotherapy in Cockroach Allergy. *Sci Rep* (2018) 8(1):15480. doi: 10.1038/s41598-018-33680-9
154. Kreutz M, Andreesen R, Krause SW, Szabo A, Ritz E, Reichel H. 1,25-Dihydroxyvitamin D3 Production and Vitamin D3 Receptor Expression are Developmentally Regulated During Differentiation of Human Monocytes Into Macrophages. *Blood* (1993) 82(4):1300–7. doi: 10.1182/blood.V82.4.1300.bloodjournal8241300
155. Gottfried E, Rehli M, Hahn J, Holler E, Andreesen R, Kreutz M. Monocyte-Derived Cells Express CYP27A1 and Convert Vitamin D3 Into its Active Metabolite. *Biochem Biophys Res Commun* (2006) 349(1):209–13. doi: 10.1016/j.bbrc.2006.08.034
156. Penna G, Adorini L. 1α,25-Dihydroxyvitamin D 3 Inhibits Differentiation, Maturation, Activation, and Survival of Dendritic Cells Leading to Impaired Alloreactive T Cell Activation. *J Immunol* (2000) 164(5):2405–11. doi: 10.4049/jimmunol.164.5.2405
157. Penna G, Amuchastegui S, Giarratana N, Daniel KC, Vulcano M, Sozzani S, et al. 1,25-Dihydroxyvitamin D 3 Selectively Modulates Tolerogenic Properties in Myeloid But Not Plasmacytoid Dendritic Cells. *J Immunol* (2007) 178(1):145–53. doi: 10.4049/jimmunol.178.1.145
158. Wu J, Horuzsko A. Expression and Function of Immunoglobulin-Like Transcripts on Tolerogenic Dendritic Cells. *Hum Immunol* (2009) 70(5):353–6. doi: 10.1016/j.humimm.2009.01.024
159. Švajger U, Rožman Pj. Synergistic Effects of Interferon-γ and Vitamin D3 Signaling in Induction of ILT-3highPDL-1high Tolerogenic Dendritic Cells. *Front Immunol* (2019) 10(November):2627. doi: 10.3389/fimmu.2019.02627
160. Saul L, Mair I, Ivens A, Brown P, Samuel K, Campbell JDM, et al. 1,25-Dihydroxyvitamin D3 Restrains CD4+ T Cell Priming Ability of CD11c+ Dendritic Cells by Upregulating Expression of CD31. *Front Immunol* (2019) 10(MAR):600. doi: 10.3389/fimmu.2019.00600
161. Van Der Aar AMG, Sibiryak DS, Bakdash G, Van Capel TMM, Van Der Kleij HPM, Opstelten DJE, et al. Vitamin D3 Targets Epidermal and Dermal Dendritic Cells for Induction of Distinct Regulatory T Cells. *J Allergy Clin Immunol* (2011) 127(6):1532–40.e7. doi: 10.1016/j.jaci.2011.01.068
162. Bakdash G, Schneider LP, Van Capel TMM, Kapsenberg ML, Teunissen MBM, De Jong EC. Intradermal Application of Vitamin D3 Increases Migration of CD14+ Dermal Dendritic Cells and Promotes the Development of Foxp3+ Regulatory T Cells. *Hum Vaccines Immunother* (2013) 9(2):250–8. doi: 10.4161/hv.22918
163. Nikolic T, Roep BO. Regulatory Multitasking of Tolerogenic Dendritic Cells - Lessons Taken From Vitamin D3-treated Tolerogenic Dendritic Cells. *Front Immunol* (2013) 4:113. doi: 10.3389/fimmu.2013.00113
164. Jung HH, Kim SH, Moon JH, Jeong SU, Jang S, Park CS, et al. Polymeric Nanoparticles Containing Both Antigen and Vitamin d3induce Antigen-Specific Immune Suppression. *Immune Netw* (2019) 19(3):e19. doi: 10.4110/in.2019.19.e19
165. Galea R, Nel HJ, Talekar M, Liu X, Ooi JD, Huynh M, et al. Pd-L1– and Calcitriol-Dependent Liposomal Antigen-Specific Regulation of Systemic Inflammatory Autoimmune Disease. *JCI Insight* (2019) 4(18):e126025. doi: 10.1172/jci.insight.126025
166. Oliveira LDM, Teixeira FME, Sato MN. Impact of Retinoic Acid on Immune Cells and Inflammatory Diseases. *Mediators Inflammation* (2018) 2018:3067126. doi: 10.1155/2018/3067126
167. Agace WW, Persson EK. How Vitamin A Metabolizing Dendritic Cells are Generated in the Gut Mucosa. *Trends Immunol* (2012) 33p:42–8. doi: 10.1016/j.it.2011.10.001
168. Yi X, Wang Y, Jia Z, Hiller S, Nakamura J, Luft JC, et al. Retinoic Acid-Loaded Poly(Lactic-Co-Glycolic Acid) Nanoparticle Formulation of ApoB-100-Derived Peptide 210 Attenuates Atherosclerosis. *J BioMed Nanotechnol* (2020) 16(4):467–80. doi: 10.1166/jbn.2020.2905
169. Erkelens MN, Mebius RE. Retinoic Acid and Immune Homeostasis: A Balancing Act. *Trends Immunol* (2017) 38(3):168–80. doi: 10.1016/j.it.2016.12.006
170. Thangavelu G, Lee Y-C, Loschi M, Schaechter KM, Feser CJ, Koehn BH, et al. Dendritic Cell Expression of Retinal Aldehyde Dehydrogenase-2 Controls Graft-versus-Host Disease Lethality. *J Immunol* (2019) 202(9):2795–805. doi: 10.4049/jimmunol.1800899
171. Švajger U, Rožman Pj. Recent discoveries in dendritic cell tolerance-inducing pharmacological molecules. *Int Immunopharmacol* (2020) 81:106275. doi: 10.1016/j.intimp.2020.106275
172. Chambers ES, Nanzer AM, Pfeffer PE, Richards DF, Martineau AR, Griffiths CJ, et al. Dendritic Cell Phenotype in Severe Asthma Reflects Clinical Responsiveness to Glucocorticoids. *Clin Exp Allergy* (2018) 48(1):13–22. doi: 10.1111/cea.13061
173. Unger WWJ, Laban S, Kleijwegt FS, Van Der Slik AR, Roep BO. Induction of Treg by Monocyte-Derived DC Modulated by Vitamin D3 or Dexamethasone: Differential Role for PD-L1. *Eur J Immunol* (2009) 39(11):3147–59. doi: 10.1002/eji.200839103
174. Meka RR, Venkatesha SH, Acharya B, Moudgil KD. Peptide-Targeted Liposomal Delivery of Dexamethasone for Arthritis Therapy. *Nanomedicine* (2019) 14(11):1455–69. doi: 10.2217/nnm-2018-0501
175. Tas SW, de Jong EC, Hajji N, May MJ, Ghosh S, Vervoordeldonk MJ, et al. Selective Inhibition of NF-κb in Dendritic Cells by the NEMO-binding Domain Peptide Blocks Maturation and Prevents T Cell Proliferation and Polarization. *Eur J Immunol* (2005) 35(4):1164–74. doi: 10.1002/eji.200425956
176. Kundu R, Theodoraki A, Haas CT, Zhang Y, Chain B, Kriston-Vizi J, et al. Cell-Type-Specific Modulation of Innate Immune Signalling by Vitamin D in Human Mononuclear Phagocytes. *Immunology* (2017) 150(1):55–63. doi: 10.1111/imm.12669
177. Hippen KL, O'Connor RS, Lemire AM, Saha A, Hanse EA, Tennis NC, et al. In Vitro Induction of Human Regulatory T Cells Using Conditions of Low Tryptophan Plus Kynurenines. *Am J Transplant* (2017) 17(12):3098–113. doi: 10.1111/ajt.14338
178. Mbongue JC, Nicholas DA, Torrez TW, Kim NS, Firek AF, Langridge WHR. The Role of Indoleamine 2, 3-Dioxygenase in Immune Suppression and Autoimmunity. *Vaccines* (2015) 3:703–29. doi: 10.3390/vaccines3030703
179. Wu H, Gong J, Liu Y. Indoleamine 2, 3-Dioxygenase Regulation of Immune Response (Review). *Mol Med Rep* (2018) 17:4867–73. doi: 10.3892/mmr.2018.8537

180. Harrington L, Srikanth CV, Antony R, Rhee SJ, Mellor AL, Hai NS, et al. Deficiency of Indoleamine 2,3-Dioxygenase Enhances Commensal-Induced Antibody Responses and Protects Against Citrobacter Rodentium-Induced Colitis. *Infect Immun* (2008) 76(7):3045–53. doi: 10.1128/IAI.00193-08
181. Atarashi K, Tanoue T, Ando M, Kamada N, Nagano Y, Narushima S, et al. Th17 Cell Induction by Adhesion of Microbes to Intestinal Epithelial Cells. *Cell* (2015) 163(2):367–80. doi: 10.1016/j.cell.2015.08.058
182. Matteoli G, Mazzini E, Iliev ID, Mileti E, Fallarino F, Puccetti P, et al. Gut CD103+ Dendritic Cells Express Indoleamine 2,3-Dioxygenase Which Influences T Regulatory/T Effector Cell Balance and Oral Tolerance Induction. *Gut* (2010) 59(5):595–604. doi: 10.1136/gut.2009.185108
183. Mellor AL, Lemos H, Huang L. Indoleamine 2,3-Dioxygenase and Tolerance: Where Are We Now? *Front Immunol* (2017) 8(OCT):27. doi: 10.3389/fimmu.2017.01360
184. Pallotta MT, Orabona C, Volpi C, Vacca C, Belladonna ML, Bianchi R, et al. Indoleamine 2,3-Dioxygenase is a Signaling Protein in Long-Term Tolerance by Dendritic Cells. *Nat Immunol* (2011) 12(9):870–8. doi: 10.1038/ni.2077
185. Keijzer C, Van der Zee R, Van Eden W, Broere F. Treg Inducing Adjuvants for Therapeutic Vaccination Against Chronic Inflammatory Diseases. *Front Immunol* (2013) 4:1–10. doi: 10.3389/fimmu.2013.00245
186. Naranjo-Gómez M, Raïch-Regué D, Oñate C, Grau-López L, Ramo-Tello C, Pujol-Borrell R, et al. Comparative Study of Clinical Grade Human Tolerogenic Dendritic Cells. *J Transl Med* (2011) 9(1):89. doi: 10.1186/1479-5876-9-89
187. Haeri A, Osouli M, Bayat F, Alavi S, Dadashzadeh S. Nanomedicine Approaches for Sirolimus Delivery: A Review of Pharmaceutical Properties and Preclinical Studies. *Artif Cells Nanomed Biotechnol* (2018) 46(sup1):1–14. doi: 10.1080/21691401.2017.1408123
188. Qi X-R, Zhao W, Zhuang S. Comparative study of the in vitro and in vivo characteristics of cationic and neutral liposomes. *Int J Nanomed* (2011) 6:3087. doi: 10.2147/IJN.S25399
189. Cauzzo J, Nystad M, Holsæter AM, Basnet P, Škalko-Basnet N. Following the Fate of Dye-Containing Liposomes In Vitro. *Int J Mol Sci* (2020) 21(14):1–17. doi: 10.3390/ijms21144847
190. Joshi MD, Unger WJ, Storm G, Van Kooyk Y, Mastrobattista E. Targeting Tumor Antigens to Dendritic Cells Using Particulate Carriers. *J Controlled Release* (2012) 161:25–37. doi: 10.1016/j.jconrel.2012.05.010
191. Burris HAII, Patel MR, Cho DC, Clarke JM, Gutierrez M, Zaks TZ, et al. A Phase 1, Open-Label, Multicenter Study to Assess the Safety, Tolerability, and Immunogenicity of mRNA-4157 Alone in Subjects With Resected Solid Tumors and in Combination With Pembrolizumab in Subjects With Unresectable Solid Tumors (Keynote-603). *J Glob Oncol* (2019) 5 (suppl):93–3. doi: 10.1200/JGO.2019.5.suppl.93
192. Dolcetti R, López-Soto A, Dal Col J. Editorial: Dendritic Cell-Based Immunotherapy in Solid and Haematologic Tumors. *Front Immunol* (2020) 11:507. doi: 10.3389/fimmu.2020.00507
193. Spranger S, Spaapen RM, Zha Y, Williams J, Meng Y, Ha TT, et al. Up-Regulation of PD-L1, IDO, and Tregs in the Melanoma Tumor Microenvironment is Driven by CD8+ T Cells. *Sci Trans Med* (2013) 5:200ra116. doi: 10.1126/scitranslmed.3006504
194. Tumeh PC, Harview CL, Yearley JH, Shintaku IP, Taylor EJM, Robert L, et al. PD-1 Blockade Induces Responses by Inhibiting Adaptive Immune Resistance. *Nature* (2014) 515(7528):568–71. doi: 10.1038/nature13954
195. Buss CG, Bhatia SN. Nanoparticle Delivery of Immunostimulatory Oligonucleotides Enhances Response to Checkpoint Inhibitor Therapeutics. *Proc Natl Acad Sci USA* (2020) 117(24):13428–36. doi: 10.1073/pnas.2001569117
196. Kroll AV, Fang RH, Jiang Y, Zhou J, Wei X, Yu CL, et al. Nanoparticulate Delivery of Cancer Cell Membrane Elicits Multiantigenic Antitumor Immunity. *Adv Mater* (2017) 29(47). doi: 10.1002/adma.201703969
197. Bol KF, Schreibelt G, Gerritsen WR, De Vries IJM, Figdor CG. Dendritic Cell-Based Immunotherapy: State of the Art and Beyond. *Clin Cancer Res* (2016) 22(8):1897–906. doi: 10.1158/1078-0432.CCR-15-1399
198. Deng H, Zhang Z. The Application of Nanotechnology in Immune Checkpoint Blockade for Cancer Treatmen. *J Controlled Release* (2018) 290:28–45. doi: 10.1016/j.jconrel.2018.09.026
199. Keijzer C, Slütter B, van der Zee R, Jiskoot W, van Eden W, Broere F. PLGA. Plga-TMC and TMC-TPP Nanoparticles Differentially Modulate the Outcome of Nasal Vaccination by Inducing Tolerance or Enhancing Humoral Immunity. Fessler MB, editor. *PloS One* (2011) 6(11):e26684. doi: 10.1371/journal.pone.0026684
200. Krienke C, Kolb L, Diken E, Streuber M, Kirchhoff S, Bukur T, et al. A Noninflammatory mRNA Vaccine for Treatment of Experimental Autoimmune Encephalomyelitis. *Sci (80-)* (2021) 371(6525):145–53. doi: 10.1126/science.aay3638

Conflict of Interest: The authors declare that the research was conducted in the absence of any commercial or financial relationships that could be construed as a potential conflict of interest.

frontiers in Immunology

ORIGINAL RESEARCH
published: 28 July 2021
doi: 10.3389/fimmu.2021.697840

CD169 Defines Activated CD14$^+$ Monocytes With Enhanced CD8$^+$ T Cell Activation Capacity

*Alsya J. Affandi[1], Katarzyna Olesek[1], Joanna Grabowska[1], Maarten K. Nijen Twilhaar[1], Ernesto Rodríguez[1], Anno Saris[2,3], Eline S. Zwart[1,4], Esther J. Nossent[5,6], Hakan Kalay[1], Michael de Kok[1], Geert Kazemier[4], Johannes Stöckl[7], Alfons J. M. van den Eertwegh[8], Tanja D. de Gruijl[8], Juan J. Garcia-Vallejo[1], Gert Storm[9,10,11], Yvette van Kooyk[1] and Joke M. M. den Haan[1]**

[1] Department of Molecular Cell Biology and Immunology, Cancer Center Amsterdam, Amsterdam Institute for Infection and Immunity, Amsterdam UMC, Vrije Universiteit Amsterdam, Amsterdam, Netherlands, [2] Center for Experimental and Molecular Medicine, Amsterdam UMC, Academic Medical Center, University of Amsterdam, Amsterdam, Netherlands, [3] Department of Infectious Diseases, Leiden University Medical Center, Leiden, Netherlands, [4] Department of Surgery, Cancer Center Amsterdam, Amsterdam UMC, Vrije Universiteit Amsterdam, Amsterdam, Netherlands, [5] Department of Pulmonary Medicine, Amsterdam UMC, Vrije Universiteit Amsterdam, Amsterdam, Netherlands, [6] Amsterdam Cardiovascular Sciences Research Institute, Amsterdam UMC, Amsterdam, Netherlands, [7] Institute of Immunology, Centre for Pathophysiology, Infectiology and Immunology, Medical University of Vienna, Vienna, Austria, [8] Department of Medical Oncology, Cancer Center Amsterdam, Amsterdam UMC, Vrije Universiteit Amsterdam, Amsterdam, Netherlands, [9] Department of Pharmaceutics, Utrecht Institute for Pharmaceutical Sciences, Utrecht University, Utrecht, Netherlands, [10] Department of Biomaterials, Science and Technology, Faculty of Science and Technology, University of Twente, Enschede, Netherlands, [11] Department of Surgery, Yong Loo Lin School of Medicine, National University of Singapore, Singapore, Singapore

OPEN ACCESS

Edited by:
Peter M. Van Endert, Institut National de la Santé et de la Recherche Médicale (INSERM), France

Reviewed by:
Jianyun Liu, Indiana University Bloomington, United States
Diana Dudziak, Universitatsklinikum Erlangen, Germany

***Correspondence:**
Joke M. M. den Haan
j.denhaan@amsterdamumc.nl

Specialty section:
This article was submitted to Antigen Presenting Cell Biology, a section of the journal Frontiers in Immunology

Received: *20 April 2021*
Accepted: *13 July 2021*
Published: *28 July 2021*

Citation:
Affandi AJ, Olesek K, Grabowska J, Nijen Twilhaar MK, Rodríguez E, Saris A, Zwart ES, Nossent EJ, Kalay H, de Kok M, Kazemier G, Stöckl J, van den Eertwegh AJM, de Gruijl TD, Garcia-Vallejo JJ, Storm G, van Kooyk Y and den Haan JMM (2021) CD169 Defines Activated CD14$^+$ Monocytes With Enhanced CD8$^+$ T Cell Activation Capacity. Front. Immunol. 12:697840. doi: 10.3389/fimmu.2021.697840

Monocytes are antigen-presenting cells (APCs) that play diverse roles in promoting or regulating inflammatory responses, but their role in T cell stimulation is not well defined. In inflammatory conditions, monocytes frequently show increased expression of CD169/Siglec-1, a type-I interferon (IFN-I)-regulated protein. However, little is known about the phenotype and function of these CD169$^+$ monocytes. Here, we have investigated the phenotype of human CD169$^+$ monocytes in different diseases, their capacity to activate CD8$^+$ T cells, and the potential for a targeted-vaccination approach. Using spectral flow cytometry, we detected CD169 expression by CD14$^+$ CD16$^-$ classical and CD14$^+$ CD16$^+$ intermediate monocytes and unbiased analysis showed that they were distinct from dendritic cells, including the recently described CD14-expressing DC3. CD169$^+$ monocytes expressed higher levels of co-stimulatory and HLA molecules, suggesting an increased activation state. IFNα treatment highly upregulated CD169 expression on CD14$^+$ monocytes and boosted their capacity to cross-present antigen to CD8$^+$ T cells. Furthermore, we observed CD169$^+$ monocytes in virally-infected patients, including in the blood and bronchoalveolar lavage fluid of COVID-19 patients, as well as in the blood of patients with different types of cancers. Finally, we evaluated two CD169-targeting nanovaccine platforms, antibody-based and liposome-based, and we showed that

CD169$^+$ monocytes efficiently presented tumor-associated peptides gp100 and WT1 to antigen-specific CD8$^+$ T cells. In conclusion, our data indicate that CD169$^+$ monocytes are activated monocytes with enhanced CD8$^+$ T cell stimulatory capacity and that they emerge as an interesting target in nanovaccine strategies, because of their presence in health and different diseases.

Keywords: monocyte, CD169, antigen-presentation, CD8+ T cell, nanovaccine, cancer, COVID-19, Siglec-1

INTRODUCTION

Monocytes are members of the innate immune system circulating in the blood that are important in sensing danger signals such as pathogens. They comprise of about 10-15% of human peripheral blood mononuclear cells (PBMCs) and their many roles include phagocytosis of pathogens or foreign bodies, differentiation into tissue macrophages upon inflammation, and antigen presentation. Together with dendritic cells (DCs) they function as antigen-presenting cells (APCs) that activate the adaptive immune responses, including CD4$^+$ and CD8$^+$ T cells (1). Furthermore, their potency in the production of pro- and anti-inflammatory cytokines allows them to govern both local and systemic immunity.

Monocytes can be broadly categorized into classical (CD14$^+$ CD16$^-$), intermediate (CD14$^+$ CD16$^+$), and non-classical (CD14$^-$ CD16$^+$) populations (2). Monocytes originate in the bone marrow, then they enter the blood stream as classical monocytes, and further differentiate into intermediate monocytes and to non-classical monocytes in a linear fashion (3, 4). While non-classical monocytes have a 'patrolling function', crawling the endothelium and supporting blood vessels integrity, classical monocytes have the ability to enter tissue or lymphoid organs. Depending on the tissue microenvironmental cues, tissue-migrated monocytes have diverse differentiation potential, giving rise to tissue macrophages with inflammatory or resolving functions (5).

During inflammation, monocytes can also acquire DC-like properties; however, their precise characterization, definition, and functions are continuously evolving (1, 6). *In vitro*, monocytes exposed to GM-CSF and IL-4 (moDC) are able to prime and to stimulate T cell responses. Although they are distinct from naturally occurring DCs found in the circulation, *ex vivo* generated moDCs have been used during initial efforts in the development of cancer vaccination. However, moDC-based vaccination is laborious and costly, hence more research has focused on targeting of naturally occurring APCs *in situ* (7, 8).

The distribution and numbers of monocyte subsets can change dramatically under inflammatory conditions, such as during bacterial or virus infection. In COVID-19 patients, HLA-DR^{hi} inflammatory monocytes were reported to be increased in patients with mild symptoms, whereas HLA-DR^{lo} monocytes were more prominent in severely ill patients (9). While these monocytes also expressed high co-stimulatory molecules and pro-inflammatory cytokines (9, 10), their contribution towards activation of virus-specific T cell responses remains unclear.

In cancer, monocytes are thought to contribute to tumor progression as the major source of tumor-associated macrophages or myeloid-derived suppressor cells with high immune-suppressive activity (11). However, monocytes have also anti-tumoral roles; they can engulf tumor cells and process them for antigen presentation and they elicit direct tumoricidal activities (11–14). Moreover, high frequency of circulating classical monocytes have been described to be predictive of a successful anti-PD1 immunotherapy in melanoma (15), suggesting that monocytes can play an important role in activating anti-tumor T cell responses in cancer.

With the rise of single-cell approaches, recent studies have broadened the heterogeneity of DC and monocyte subsets. Until recently, DCs were categorized into the type-I interferon (IFN-I) producing CD123$^+$ plasmacytoid DCs (pDCs) and conventional DCs (cDCs) that include CD141$^+$ DC1 and CD1c$^+$ DC2, which both have high antigen-presentation and T cell-activating potential (16). Two single-cell RNA sequencing (scRNA-seq) studies have identified Axl$^+$ DC (pre-DC/AS-DC) that expresses Axl, Siglec-6, and CD169 (17, 18). Axl$^+$ DCs are unable to produce IFN-I, but they can present antigen and activate T cells and can further differentiate into DC1 or DC2 (17–20). Next to this, DC3 has also been identified as a new subset of DC that displays a monocyte/DC2 hybrid phenotype (21, 22). Since DC3 express classical monocytic markers such as CD14 and CD163, the inclusion of CD88 and FcεRIa as markers have been used to better discriminate between monocyte and DC3, respectively (23, 24). DC3s are proficient in activating T cells and they were expanded in patients with systemic lupus erythematosus, melanoma, and breast cancer (23–25).

CD169 (Siglec-1, sialoadhesin) is a sialic-acid binding transmembrane receptor that is expressed mainly by a subset of macrophages in the spleen and lymph nodes (CD169$^+$ macrophages). These macrophages function as gatekeeper of the immune system and the CD169 molecule is involved in pathogen capture and antigen transfer to DCs, leading to T cell activation (26). CD169 is also expressed by monocytes, moDC, and Axl$^+$ DC, and its expression is upregulated by type I interferon (IFN-I). In inflammatory conditions where IFN-I levels are high, such as in autoimmunity or viral infection, CD169 expression in monocytes is increased (27–30). Moreover, viruses such as HIV are able to exploit CD169-sialic acid interaction, by incorporating ganglioside GM3 in their membrane, to infect CD169$^+$ monocytes or DCs (31–33).

Based on the CD169-sialic acid interaction, we designed a lipid-based nanovaccine that can selectively target CD169$^+$

APCs, by incorporating GM3 or other gangliosides in the liposome membrane (20, 34, 35). Using human cells, we showed that ganglioside-liposomes could stimulate tumor-antigen specific $CD8^+$ T cell responses mediated by CD169 expression on Axl^+ DCs. Next to Axl^+ DCs, we also observed that $CD169^+$ monocytes could efficiently bind ganglioside-liposomes, however, whether they contribute to $CD8^+$ T cell activation is unknown.

In this study, we used spectral flow cytometry to perform immunophenotypical analyses of $CD169^+$ monocytes as compared to DC subsets in PBMCs of healthy individuals. By combining spectral flow cytometry and analysis of public single-cell RNA sequencing datasets, we examined the presence of $CD169^+$ monocytes in COVID-19 patients and patients with five different cancer types. We then determined the capacity of $CD169^+$ monocytes to cross-present tumor-associated gp100 peptides to $CD8^+$ T cells. Furthermore, we evaluated vaccination strategies that specifically target antigens to $CD169^+$ monocytes using anti-CD169 antibodies and ganglioside-liposomes. Here, we demonstrate that CD169 expression reflect a higher activation status of monocytes, with an enhanced $CD8^+$ T cells activating capacity. Importantly, delivery of tumor-antigen to $CD169^+$ monocytes using two forms of CD169-targeting nanovaccines leads to robust activation of antigen-specific $CD8^+$ T cell responses.

MATERIALS AND METHODS

Study Patients

Human peripheral blood mononuclear cells (PBMC) were collected from patients with gastrointestinal malignancies, metastatic melanoma, or COVID-19 in accordance with the Helsinki Declaration of 1975 and approved by the institutional ethical review board of the Amsterdam Universitair Medische Centra (UMC). All patients provided written consent for research purposes. Informed consent was deferred until discharge from the intensive care units (ICU). In case of death, informed consent was requested from the patient's relatives. COVID-19 patients were enrolled in the ArtDECO-1 study, a cohort study of COVID-19 patients with persistent acute respiratory distress syndrome (ARDS). Leftover biological samples were stored in the anonymized Amsterdam UMC COVID-19 biobank (#2020-182). This study procedure was approved by the Review Committee Biobank of the Amsterdam UMC (2020-065).

Pancreatic ductal adenocarcinoma (PDAC), hepatocellular carcinoma (HCC), and colorectal liver metastasis (CRLM) patients were enrolled in the Hepatobiliary (HPB) biobank at Amsterdam UMC, location VU University medical center (VUmc, Medical Ethical Committee approval 2016.510). Melanoma patients were enrolled in a clinical study of autologous whole-cell vaccination at the VUmc between 1987 and 1998 (36). Leftover human spleen tissue was obtained anonymously from the VUmc Biobank (BUP 2015-074), therefore approval by the Medical Ethical Committee was not required.

Isolation of Human Primary Cells

PBMCs from heparinized blood were isolated by density gradient centrifugation (Lymphoprep; Axis-Shield PoC AS). To isolate bronchoalveolar lavage fluid mononuclear cells (BALFMCs), during bronchoscopy lungs were instilled with 2 x 20 ml 0.9% NaCl for diagnostics and remaining 3-20 ml was centrifuged. Cell pellets were suspended in 2 mM dithiothreitol (Sigma), and BALFMCs were isolated using Ficoll isolation and cryopreserved. Human spleen was mechanically and enzymatically digested with Liberase and DNAse I (Roche) at 37°C for 30 min. Cells were then depleted of red blood cells using ammonium chloride lysing buffer. Following PBS washes, cells were further processed as described below.

Monocyte Isolation and Culture

$CD14^+$ monocytes were isolated using magnetic beads (Miltenyi) on LS column according to manufacturer's recommendation. Where indicated, monocytes were isolated using Percoll density gradient. Monocytes were cultured in RPMI 1640 complete medium (Thermo Fisher Scientific) containing 10% fetal calf serum (Biowest), 50 U/mL penicillin, 50 μg/mL streptomycin, and 2 mM glutamine (all from Thermo Fisher Scientific). Monocytes were then treated with recombinant human IFNα (Miltenyi Biotec) at indicated doses and time-points.

Antibody-Antigen (Ab-Ag) Conjugation

As described previously, gp100 [YLEPGPVTAC-6-ahx-lysine (biotin)] peptide was conjugated to purified anti-CD169 (clone 7-239, produced in house) or control mouse IgG, using sulfhydryl-based coupling (37). In short, purified antibodies (Abs) were functionalized with 2–8 equivalents of SMCC [succinimidyl 4-(N-maleimidomethyl) cyclohexane-1-carboxylate, Thermo Fisher Scientific]. After purification over PD-10 columns (GE Life Sciences) activated Abs were concentrated with centricon 30 (Merck Millipore) to 500 μL. 2–4 Equivalents of peptides in 50 μl was added to the Abs and after 1 h incubation at room temperature conjugates were purified over a Sephadex 75 10/30 column (GE Life Sciences) according to manufacturer's HPLC settings. Concentration was determined using BCA assay (Pierce, Thermo Fisher Scientific).

Liposome Preparation

Liposomes were prepared from a mixture of phospholipids and cholesterol utilizing the film extrusion method as described previously (38, 39). In brief, egg phosphatidylcholine (EPC)-35 (Lipoid GmbH): egg phosphatidylglycerol (EPG)-Na (Lipoid GmbH): Cholesterol (Sigma-Aldrich) were mixed at a molar ratio of 3.8:1:2.5. 3 mol% of ganglioside (GM3, Avanti Polar Lipids; GT1b, Matreya LLC), and 0.1 mol% of lipophilic fluorescent tracer DiD (1,1′-dioctadecyl-3,3,3′,3′-Tetra methylindodicarbocyanine, Thermo Fisher Scientific). TLR-ligand R848 (4 mol%, Invivogen) was included where specified. The solvent was evaporated under vacuum on a rotavapor to generate a lipid film and the residual organic solvent was removed by nitrogen flush. The lipid film was then hydrated in HEPES-buffered saline (10 mM HEPES buffer pH 7.4, 0.8% NaCl)

with mechanical agitation by rotary-mixing for 20 min until the lipid film was completely resuspended. For antigen presentation assay, the pancreatic cancer-associated antigen Wilms' Tumor 1 (WT1) short peptide (RMFPNAPYL, 3 mg/ml) was encapsulated into the liposomes during the hydration step. Peptides were produced by solid phase peptide synthesis using Fmoc-chemistry with a Symphony peptide synthesizer (Protein Technologies Inc). The liposomes were sized by sequential extrusion through two stacked polycarbonate filters (400 and 200 nm) with Lipex high-pressure extrusion device (Northern Lipids). Non-incorporated materials were removed in two consecutive steps by sedimentation of the liposomes by ultracentrifugation at 200,000 x g. The final resuspension of the liposomes was performed in HEPES buffer at pH 7.4. The mean particle size, polydispersity index, and zeta potential were measured using Malvern Zetasizer (Malvern Instruments). Physical properties of liposomes are shown in **Table S1**.

Liposome Uptake

Cells were incubated with ganglioside-liposomes (100 μM, unless indicated otherwise) for 45 min at 37°C to evaluate liposomes uptake. Specific uptake of ganglioside-liposomes mediated by CD169 was determined by pre-incubation of cells for at least 15 min at 4°C with 2 μg/ml neutralizing antibody against CD169, clone 7-239.

Flow Cytometry

Cells were incubated with Fc block (BD Biosciences, cat. #564219) and viability dye (Fixable viability dye eFluor 780 or 455UV, FVD, eBioscience), prior to cell surface staining with fluorescence-conjugated antibodies in 0.5% BSA/PBS for 20 min at 4°C. After thorough washes, cells were fixed with 2% paraformaldehyde for 10 min at RT. For intracellular staining, cells were additionally incubated with antibodies in 0.5% BSA/PBS with 0.5% saponin for 20 min at 4°C. Cells were acquired on Fortessa (BD Biosciences) or Aurora spectral flow cytometer (Cytek) and analyzed on FlowJo software (Tree Star) or OMIQ. High dimensionality reduction analysis opt-SNE was performed using FlowJo software. Antibody clones and dilutions used are listed in **Table S2**. Antibodies and reagents used for the ArtDECO cohort have been listed elsewhere (40). BALF samples were excluded when too few viable $CD45^+$ cells were measured (i.e., less than 2,000) or during active therapy with corticosteroids, as described previously (40). PBMC samples were only included if a paired BALF sample was available.

Monocyte Activation and Antigen Presentation

PBMCs were incubated with ganglioside-liposomes at 37°C for 45 min, washed, and cultured for 5 hours in RPMI complete medium, with the addition of Brefeldin A (BD GolgiPlug) for the final 3 hours. TNFα production was measured by intracellular flow cytometry. For antigen presentation, $CD14^+$ monocytes were incubated with gp100 synthetic peptides (short, YLEPGPVTA; long, VTHTYLEPGPVTANRQLYPEWTEAQRLD; 3h, 37°C), ganglioside-liposomes encapsulating WT1 short peptide (1h, 37°C), or antibody-gp100 conjugates (30 min, 4°C), followed by medium washes. R848 (2.5 μg/ml, Invitrogen) was added to the soluble peptides or Ab-Ag conjugates conditions during uptake. Antigen-loaded monocytes were then co-cultured overnight with $WT1_{126\text{-}134}$ or $gp100_{280–288}$ T-cell receptor (TCR) transduced HLA-A2.1 restricted T cell lines (0.5-1 × 10^5 cells per well), at a ratio of 1:1. After 24 h, production of IFNγ in the supernatants of the co-cultures was determined by ELISA (eBioscience).

Analysis of Single-Cell RNA Sequencing

We performed analysis of public datasets from patients with PDAC (GSE155698), lung cancer (GSE127465), as well as patients with severe influenza or COVID-19 (SARS-CoV-2) and healthy donors (GSE149689). We used Seurat package (version 3.2.2) and unsupervised UMAP high dimensionality reduction analysis, with R version 4.0.3. IFN-I score (GSEA GO:0034340) and TLR activation (KEGG hsa04620) score were calculated using AddModuleScore function. Codes are available upon request.

Statistics

Statistical analysis of Friedman test, corrected using a two-stage linear step-up procedure of Benjamini, Krieger and Yekutieli, or paired t-test, were performed using GraphPad Prism 8 (GraphPad Software), unless indicated otherwise.

RESULTS

CD169 Is Expressed by $CD14^+$ Monocytes With Increased Maturation Status in Healthy Donors

We previously showed CD169 expression within HLA-DR^+ $CD14^+$ Lin^- populations (20). However, CD14 expression is not restricted to monocytes and can also be observed in $CD1c^+$ DC3 (17, 23). We then sought a strategy to define monocytes and DC subsets unequivocally based on markers identified recently (23, 24), by including CD88 to identify *bona fide* monocytes, and FcεRIα to distinguish the DC lineage. We performed unsupervised spectral cytometry analysis of circulating HLA-DR^+ Lin^- cells from healthy donors using opt-SNE (**Figure 1A**) overlaid with conventional gating (**Figure S1A**). By using CD88 to classify total monocytes, we identified classical ($CD14^+$ $CD16^-$), intermediate ($CD14^+$ $CD16^+$), and non-classical ($CD14^-$ $CD16^+$) monocytes. The $CD88^-$ DC populations consisted of Axl^+ DC (Axl^+ Siglec-6^+), pDC ($CD123^+$), DC1 ($CD141^+$), DC2 ($CD1c^+$), and the CD14-expressing DC3 ($CD1c^+$ $CD163^+$). As we described previously, CD169 expression was found within $CD14^+$ monocytes and Axl^+ DCs (**Figures 1A-C**). A proportion of DC3 also expressed CD169, however they expressed FcεRIα^+ and lacked CD88, confirming their DC lineage (**Figure 1A** and **Figures S1B, C**). Thus, although both cell types share the expression of CD14 and other markers, $CD14^+$ $CD169^+$ monocytes are distinct from DC3.

Among monocytes, $CD169^+$ cells were present within classical and intermediate monocytes, and they were much less

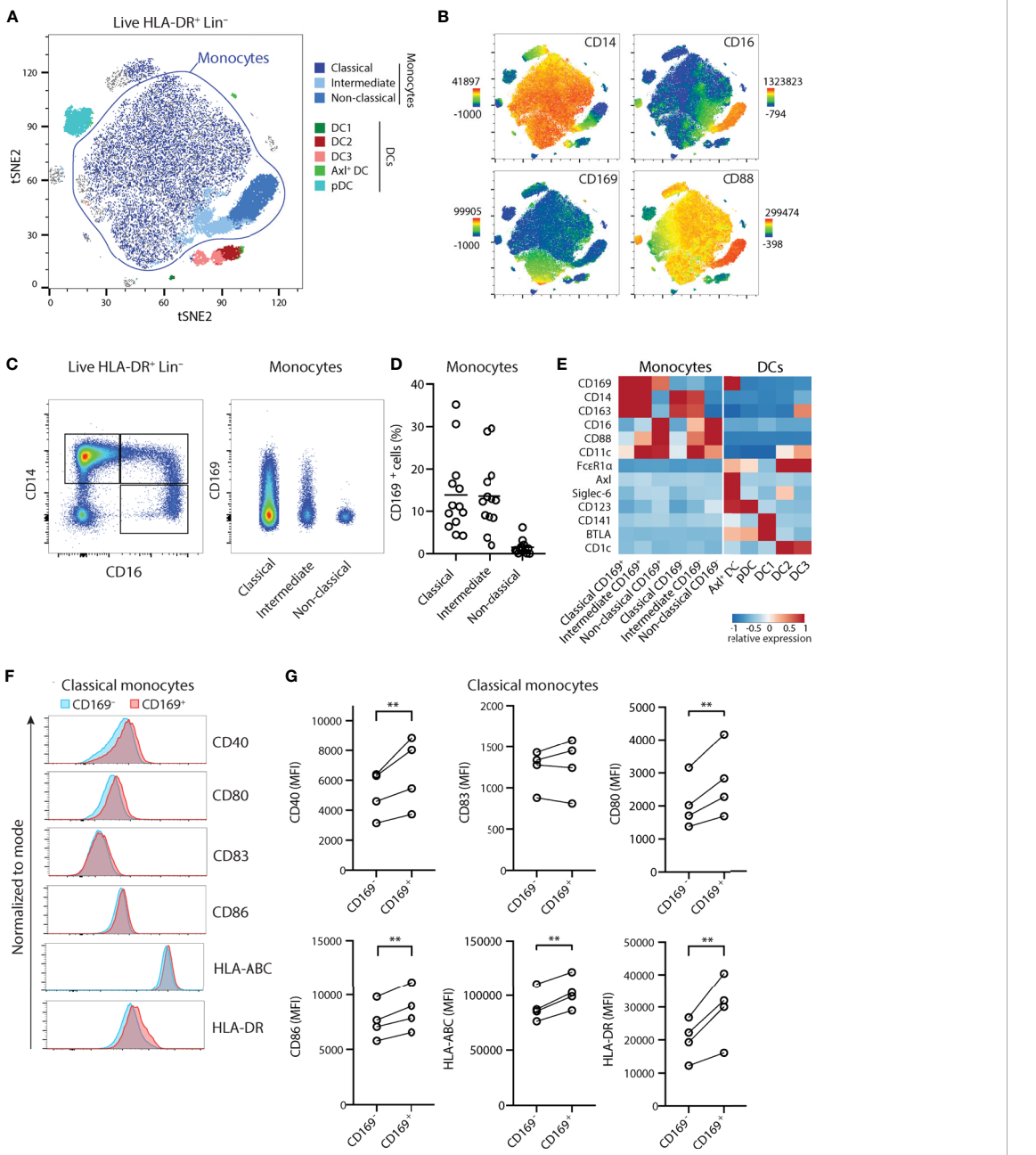

FIGURE 1 | $CD14^+$ $CD169^+$ monocytes display enhanced maturation status. **(A)** Unsupervised high dimensionality reduction analysis of circulating monocytes and dendritic cells ($HLA\text{-}DR^+$ CD3/CD19/$CD56^-$) using CD14, CD16, CD88, CD163, HLA-DR, FcεR1α, CD123, CD11c, CD1c, CD141, Axl, Siglec-6, BTLA, and CD169 using opt-SNE, and overlaid with conventional gating. **(B)** The expression of CD14, CD16, CD88, and CD169 on tSNE plots. **(C)** Gating strategy identifies classical ($CD14^+$ $CD16^-$), intermediate ($CD14^+$ $CD16^+$), or non-classical ($CD14^-$ $CD16^+$) monocytes, and $CD169^+$ cells. **(D)** Percentage of $CD169^+$ cells within monocytes subsets (n = 13) in healthy donors. **(E)** Heatmaps comparing the relative expression of markers defining monocytes and DC subsets. **(F, G)** Expression of co-stimulatory and HLA molecules are compared between $CD169^+$ and $CD169^-$ classical monocytes shown as **(F)** representative histograms and **(G)** quantification (n = 4). Paired t-tests were used. $^{**}P < 0.01$.

frequent in non-classical monocytes (**Figures 1C–E**). When stratified based on CD169 expression, $CD14^+$ $CD169^+$ monocytes expressed a similar level of CD169 to Axl^+ DCs (**Figure 1C** and **Figure S1C**). Since $CD14^+$ $CD169^+$ monocytes were frequently found in inflammatory conditions, we screened for expression of maturation markers. Interestingly, $CD169^+$ classical monocytes expressed higher levels of co-stimulatory molecules CD40, CD80, CD86, HLA-ABC, and HLA-DR, as

compared to CD169$^-$ classical monocytes (**Figures 1F–G**). A similar increase of maturation markers was found in CD169-expressing intermediate monocytes (**Figure S1D**). These suggest that CD14-expressing classical and intermediate CD169$^+$ monocytes represent monocytes with a higher activation status.

CD169-Expressing CD14$^+$ Monocytes in Viral Infection

CD169 expression in monocytes has been shown to be upregulated upon exposure to type I interferon (IFN-I) in many inflammatory conditions, including in autoimmune diseases and viral infections (27–30). To predict their developmental trajectories, we applied Wanderlust analysis using CD14$^+$ CD169$^-$ classical monocytes as a starting population and the inclusion of 9 phenotypic markers. CD14$^+$ CD169$^+$ monocytes were in close proximity to CD14$^+$ CD169$^-$ monocytes, whereas intermediate and non-classical monocytes were further away along the trajectory (**Figure 2A**). The expression of CD169 was also increased at an early stage (**Figures S2A, B**), suggesting that CD169-expressing monocytes arise immediately from CD14$^+$ CD169$^-$ classical monocytes. Next, we isolated CD14$^+$ monocytes and exposed them to IFNα. In line with previous findings, we observed an increased expression of CD169 in a time- and dose-dependent manner (**Figures 2B, C** and **Figure S2C**). IFNα treatment led to upregulation of HLA-DR, CD80, CD86, and CD16, in CD14$^+$ monocytes, although we noticed that CD16 expression was already high upon culture with medium alone (**Figures S2D–F**). CD169 expression was also increased in CD14$^-$ CD16$^+$ non-classical monocytes, albeit at a much lower extent (**Figures S2G, H**). Transcriptomic analyses of IFNβ-treated monocytes showed similar findings (**Figures S2I–P**). Thus, CD169 upregulation in circulating CD14$^+$ monocytes is likely to be driven by increased IFN-I levels during inflammation.

Since IFN-I is a crucial component of host defense against viruses, we then analyzed a recently published single-cell RNA sequencing (scRNA-seq) dataset of PBMCs of patients with COVID-19, severe influenza, and healthy controls (41). We applied Seurat pipeline and subjected them to Uniform Manifold Approximation and Projection (UMAP) dimensionality reduction analysis. UMAP visualization identified all major immune cell populations, including clusters of classical monocytes as identified by *CD14* and *VCAN* (cluster 0, 5, 9, 10, and 22), and cells expressing *FCGR3A* (encoding CD16) and *MS4A7*, evoking intermediate/non-classical monocytes (cluster 11) (**Figure 2D** and **Figure S3**). Two DC populations were also found: the *FCER1A*$^+$ *CD1C*$^+$ DC3 (cluster 20), which expressed low *CD14* but lacked *C5AR1* (encoding CD88), and *LILRA4*$^+$ *IL3RA*$^+$ pDCs (cluster 26) (**Figure S3**). *SIGLEC1* (encoding CD169) transcript was mainly detected within clusters of monocytes and appeared to be increased in a few COVID-19 patients (**Figures 2E, F**). Focusing on monocytes, we observed that *SIGLEC1* was highly increased in cluster 22, which was a cluster almost exclusively comprised of COVID-19 patients (**Figure 2F**). Remarkably, *SIGLEC1* was one of the most highly expressed genes in this cluster as compared to other monocytes (**Table S3**). Furthermore, cells in cluster 22 showed increased expression of genes involved in IFN-I pathway and TLR signaling (**Figure 2G**), and expressed high levels of *CD83* and *CD86*, indicating an increased activation state of monocytes. To confirm this on protein level, we examined CD169 expression in blood and BALF of COVID-19 patients of the ArtDECO cohort using spectral cytometry. Indeed, CD169$^+$ monocytes were present in both blood and BALF of these patients (**Figure 2H** and **Figure S3F**). CD169 was also expressed in alveolar macrophages, as we described previously (40). The expression of HLA-DR was also consistently higher in CD169$^+$ cells monocytes/macrophages (**Figure 2I**). These observations indicate that CD169$^+$ monocytes are activated monocytes associated with IFN-I signature upon viral infection, and are present in the circulation and lungs of COVID-19 patients.

CD14$^+$ CD169$^+$ Monocytes Are Present in Cancer Patients

Although the presence of CD169$^+$ macrophages in draining lymph nodes has been associated with anti-tumor responses (42–44), there is little known about circulating CD169$^+$ monocytes in cancer. We analyzed public scRNA-seq dataset of PBMCs from PDAC patients [GSE155698 (45)] and healthy controls. UMAP analysis showed that cells expressing *SIGLEC1* transcript were found primarily within clusters of *CD14*-expressing monocytes (**Figure 3A** and **Figure S4**), confirming our flow cytometry findings. Similar observations were made for the scRNA-seq dataset of PBMCs from lung cancer patients [GSE127465 (46), **Figure 3B**]. We further validated these findings in PBMCs of patients with PDAC, HCC, CRLM, and melanoma, using flow cytometry. Indeed, we were able to identify CD169$^+$ cells among classical and intermediate monocytes and they expressed higher HLA-DR than the CD169$^-$ counterparts (**Figures 3C, D**). Thus, CD169$^+$ monocytes are present in the circulation of cancer patients.

IFNα Treatment Gives Rise to CD14$^+$ CD169^{high} Monocytes With an Enhanced CD8$^+$ T Cell Activating Capacity

The increased expression of activation markers in CD169$^+$ monocytes propelled us to investigate their capacity to stimulate T cells. Since CD169 expression in monocytes is heterogenous, we used CD14$^+$ monocytes exposed to IFNα, which showed high homogenous levels of CD169 (CD169^{high} monocytes), for functional analysis (**Figure S2**). To assess their antigen-presentation capacity, we incubated monocytes with pre-processed melanoma-associated peptides gp100 (short peptide), followed by co-culture with gp100$_{280-288}$-specific CD8$^+$ T cells (**Figure 4A**). We observed an increased IFNγ secretion by CD8$^+$ T cells after co-culture with antigen-loaded CD169^{high} monocytes compared to untreated monocytes (**Figure 4B**). Subsequently, we assessed their antigen-processing and cross-presentation abilities using gp100 long peptide. Interestingly, CD169^{high} monocytes were able to stimulate a higher amount of IFNγ production by gp100-specific CD8$^+$ T cells in almost every donor (**Figure 4C**), indicating their cross-presentation potential. Next to the increased expression of activation markers, these data suggest

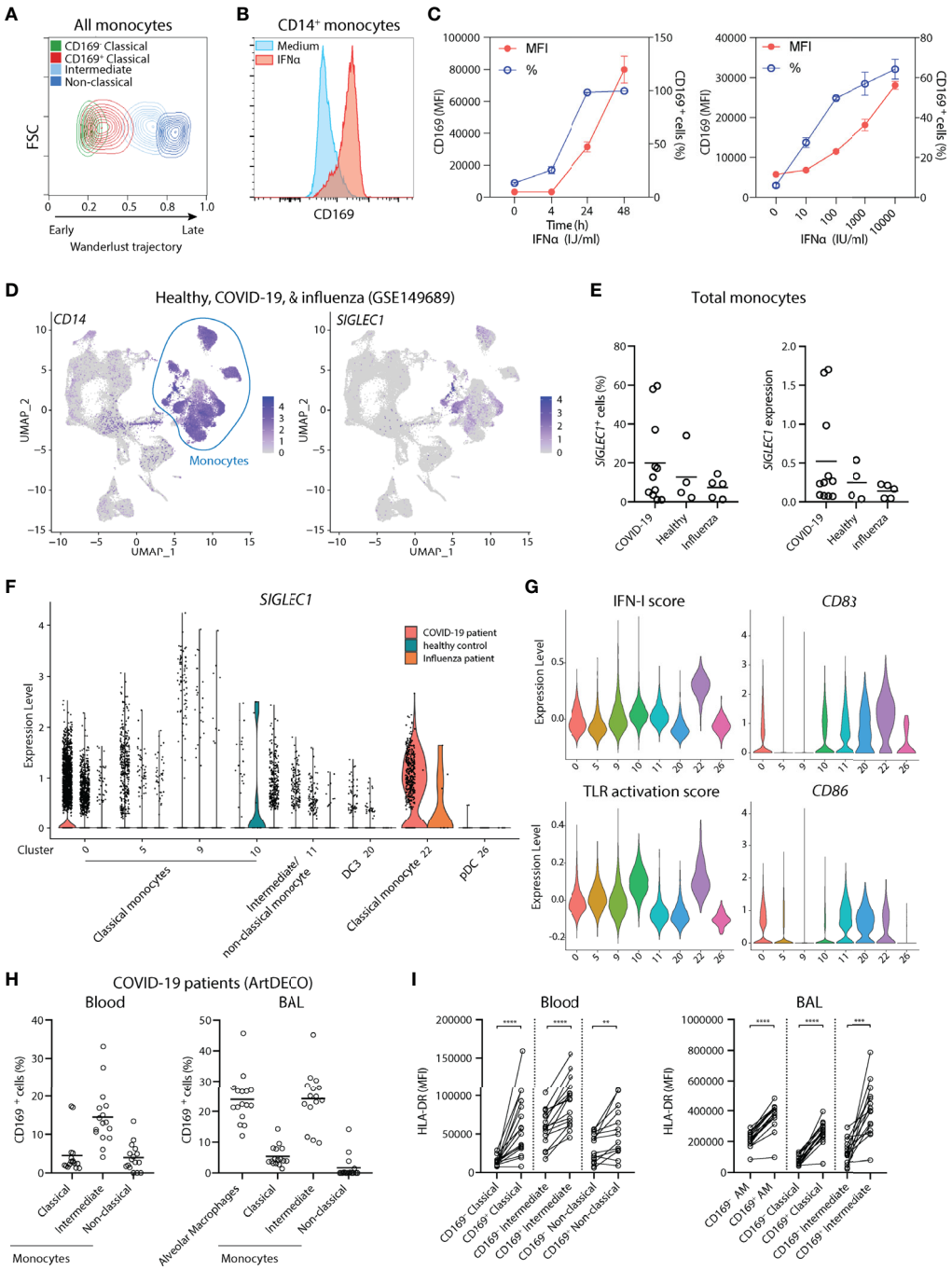

FIGURE 2 | CD169 expression in monocytes is driven by IFN-I and CD14$^+$ CD169$^+$ monocytes are present in COVID-19 patients. **(A)** Wanderlust trajectory analysis of monocyte population using CD14$^+$ CD169$^-$ monocytes as starting population overlaid by conventional gating of monocyte subsets. **(B, C)** CD14$^+$ monocytes were isolated and treated with 1,000 IU/ml IFNα for 24h unless indicated otherwise. Percentage of CD169$^+$ cells or CD169 median fluorescence intensity (MFI) of CD169$^+$ population are shown. (n = 4). **(D–G)** Analysis of public scRNA-seq dataset of PBMCs from patients with COVID-19 (n = 9), severe influenza (n = 5) and healthy controls (n = 4) using Seurat pipeline. **(D)** UMAP analysis showing the expression of *CD14* and *SIGLEC1*. **(E)** *SIGLEC1* expressing monocytes as shown as percentages or MFI in different groups. **(F)** Violin plot of *SIGLEC1* expression in clusters of monocytes and DC subsets from each patient group. **(G)** Violin plots of IFN-I score, TLR activation score, maturation markers *CD83* and *CD86*, in monocytes and DC clusters of all groups. **(H, I)** Spectral flow cytometry analysis of COVID-19 patients (ArtDECO cohort) of CD169-expressing monocytes/macrophages in circulation or bronchoalveolar space. **(H)** Percentage of CD169$^+$ cells within monocytes subsets or alveolar macrophages (AM) (n = 16) in the (left panel) blood or (right panel) BALF of COVID-19 patients. **(I)** Expression of HLA-DR compared between CD169$^+$ and CD169$^-$ subsets of monocytes or alveolar macrophages (AM). Paired t-tests were used. **P < 0.01, ***P < 0.001, ****P < 0.0001.

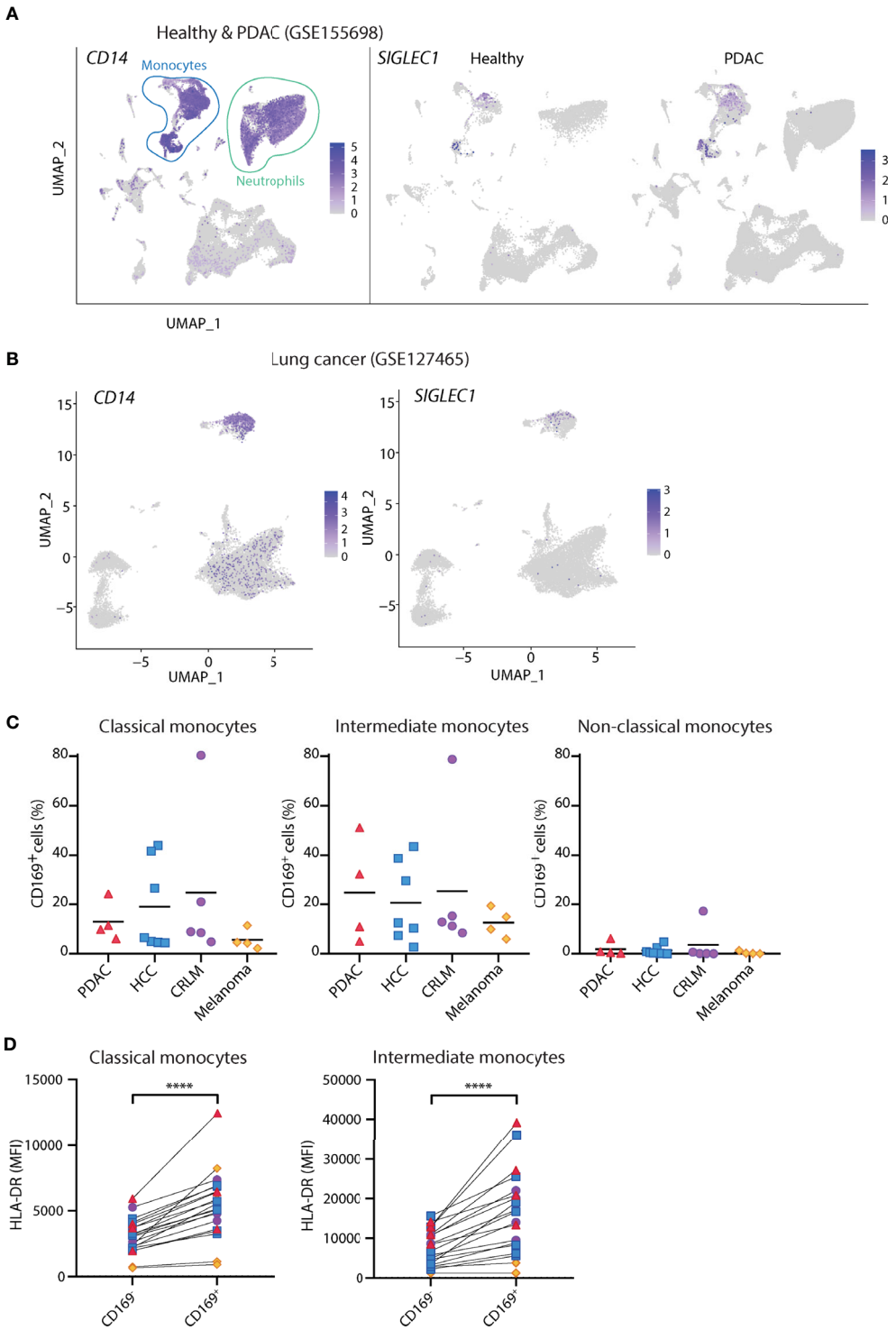

FIGURE 3 | CD14$^+$ CD169$^+$ monocytes are present in cancer patients. **(A)** Analysis of public scRNA-seq dataset of PBMCs from PDAC patients (n = 12) and healthy controls (n = 4) using Seurat algorithm and projected onto UMAP space where cell types are indicated. The expressions of *CD14* and *SIGLEC1* are visualized on UMAP. **(B)** Analysis of public scRNA-seq dataset of PBMCs from patients with lung cancer (n = 7) using Seurat and UMAP clustering. The expression of *SIGLEC1* and *CD14* are shown. **(C)** Percentage of CD169$^+$ cells within classical (CD14$^+$ CD16$^-$), intermediate (CD14$^+$ CD16$^+$), or non-classical (CD14$^-$ CD16$^+$) monocytes in patients with pancreatic ductal adenocarcinoma (PDAC, n = 4), hepatocellular carcinoma (HCC n = 7), colorectal liver metastasis (CRLM, n = 4), and melanoma (n = 4). Monocytes were gated on live, HLA-DR$^+$ Lin(CD3/CD19/CD56)$^-$ cells. **(D)** Expression of HLA-DR between CD169$^+$ and CD169$^-$ classical or intermediate monocytes in cancer patients. Paired t-tests were used. ****P < 0.0001.

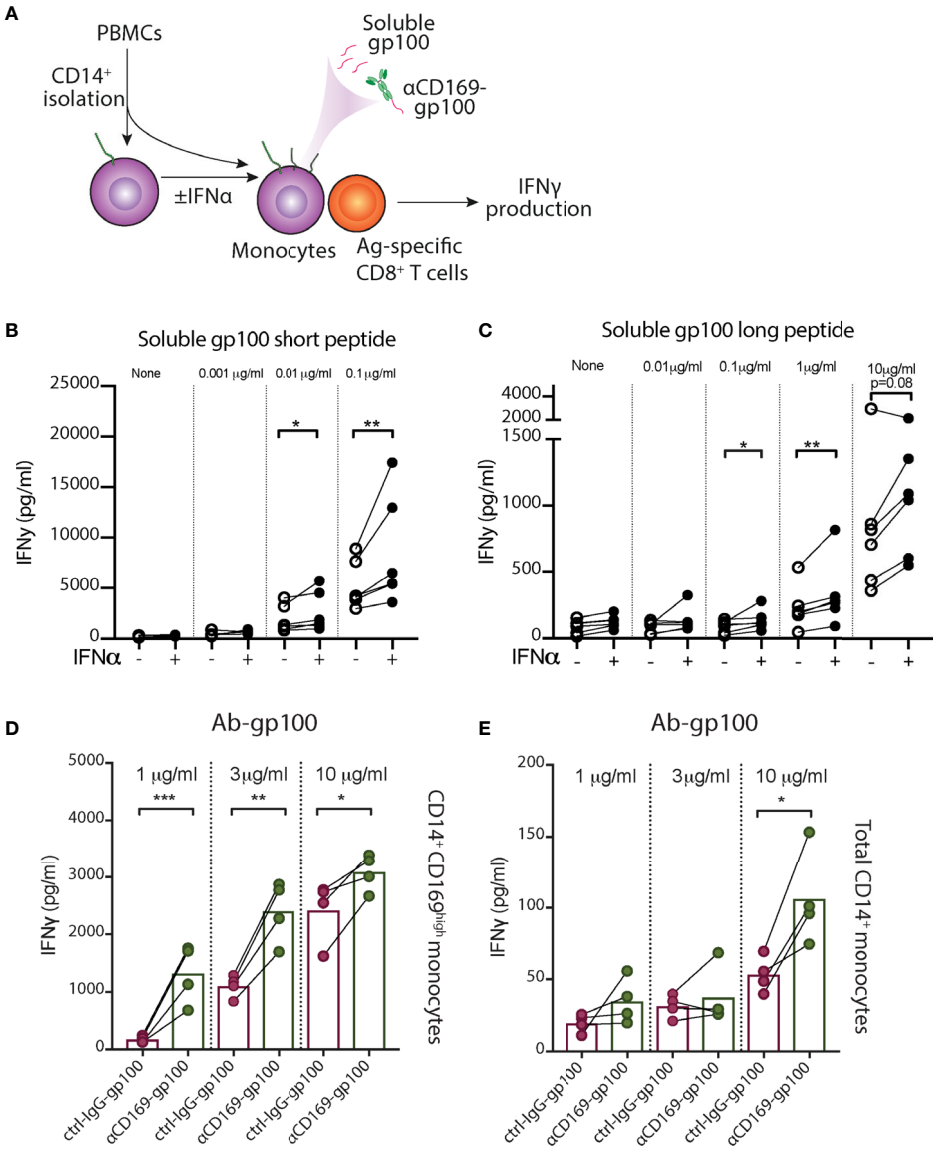

FIGURE 4 | IFN-α treated monocytes showed enhanced peptide presentation to CD8$^+$ T cells. **(A–C)** After CD14$^+$ isolation, monocytes were incubated with IFNα overnight, loaded with different concentrations of gp100, washed, and gp100-specific CD8$^+$ T cells were added. After 24h, IFNγ secretion by CD8$^+$ T cells after co-culture with monocyte loaded with **(B)** short peptide or **(C)** long peptide was measured by ELISA. **(D, E)** Targeted antigen delivery to CD14$^+$ CD169$^+$ monocytes using antibody conjugated with gp100 peptide. **(D)** IFNα-treated CD14$^+$ CD169^{high} monocytes or **(E)** freshly-isolated total CD14$^+$ monocytes were loaded with different doses of αCD169-gp100 or control IgG-gp100 antibody-conjugates, washed, and gp100-specific CD8$^+$ T cells were added. After 24h IFNγ secretion was measured by ELISA. Data are mean from four donors. Paired t-tests were used. *P < 0.05, **P < 0.01, ***P < 0.001.

that IFNα-induced CD14$^+$ CD169$^+$ monocytes have an enhanced capacity to cross-present antigen and to stimulate CD8$^+$ T cells.

Targeted Antigen Delivery to CD14$^+$ CD169$^+$ Monocytes Using Ab-Ag Stimulate CD8$^+$ T Cell Activation

To evaluate whether CD14$^+$ CD169$^+$ monocytes can be used for targeted vaccination, we conjugated gp100 peptide to αCD169 antibody. After incubation with αCD169-gp100 or control-IgG-gp100 conjugates, IFNα-treated CD169^{high} monocytes were washed and co-cultured with gp100$_{280-288}$-specific CD8$^+$ T cells. We found a significantly higher IFNγ secretion by CD8$^+$ T cells in αCD169-gp100-treated condition (**Figure 4D**). Similar result was seen when we used freshly-isolated CD14$^+$ monocytes, however, the level of IFNγ production was much lower due to a lower expression of CD169 on only a small percentage (5-15%) of total monocytes (**Figure 4E**). This suggests that CD14$^+$ CD169$^+$ monocytes can potentially be used for an effective targeted vaccination strategy.

Ganglioside-Liposomes Target CD14$^+$ CD169$^+$ Monocytes Leading to Antigen-Presentation to CD8$^+$ T Cells

We previously described a nanovaccine platform targeting CD169$^+$ cells using gangliosides, the endogenous ligands for CD169, and we showed that ganglioside-liposomes activated and delivered tumor antigens to Axl$^+$ CD169$^+$ DCs (20). These liposomes were 200 nm in size, negatively charged, and also contained antigen and adjuvant. We assessed their uptake in PBMCs and splenocytes using flow cytometry (**Table S1** and **Figure 5A**). Within circulating classical CD169$^+$ monocytes, we observed that inclusion of GM3 or GT1b as targeting moieties strongly increased the uptake of liposomes (**Figures 5B, C**). This uptake was significantly reduced when anti-CD169 antibody was used as blocking antibody prior to addition of liposomes, indicating that uptake was mediated primarily by ganglioside-CD169 interaction (**Figure 5C**). A similar uptake of ganglioside-liposomes was observed in splenic CD14$^+$ CD169$^+$ monocytes (**Figure 5D** and **Figure S5A**). Ganglioside-liposomes can thus be taken up by both, blood and splenic CD14$^+$ CD169$^+$ monocytes.

Furthermore, we performed reanalysis of our previous findings on ganglioside-liposome uptake by blood CD14$^+$ cells to reevaluate possible ganglioside-liposome uptake by CD14-expressing DC3 (20). Since CD88 was not included in this panel, here we defined classical monocytes as CD14^{high} CD1c$^-$ cells and CD14^{dim} CD1c$^+$ as DC3 (**Figure S5B**). While CD14^{high} CD1c$^-$ CD169$^+$ classical monocytes took up ganglioside-liposomes, we did not detect significant ganglioside-liposome uptake by CD14^{dim} CD1c$^+$ DC3 population (**Figure 5E**). However, upon DC3 repartition based on CD169 expression, we observed a similar trend on ganglioside-liposome uptake by CD169-expressing DC3s, albeit to a much lower extent than the CD169$^+$ monocytes (**Figure S5C**). This suggests that among CD14-expressing cells, ganglioside liposomes are largely taken up by CD169$^+$ classical monocytes rather than CD169$^+$ DC3.

We then assessed whether the ganglioside-liposomes could target CD169$^+$ monocytes in cancer patients. Similar to our findings in healthy individuals, both GM3- and GT1b-liposomes were taken up by CD169$^+$ classical monocytes of all cancer patients we tested (**Figures 5F, G**), further supporting the potential of targeting CD169$^+$ monocytes as a vaccination strategy.

Finally, we evaluated antigen/adjuvant delivery to CD169$^+$ monocytes by ganglioside-liposomes. To determine the capacity of ganglioside-liposome to activate monocytes, we incorporated TLR7/8 agonist R848 into the liposomes. We showed that GM3/R848 and GT1b/R848 liposomes induced TNFα expression in total CD14$^+$ monocytes, significantly higher than the non-targeting control/R848 liposome (**Figures 5H, I**). Next, we evaluated antigen presentation capacity of CD14$^+$ CD169$^+$ monocytes after antigen delivery by ganglioside-liposomes. We encapsulated pancreatic cancer-associated antigen WT1 short peptide into the liposomes, and incubated them with CD14$^+$ isolated monocytes. Following co-culture with WT1-specific CD8$^+$ T cell clone, we measured the amount of secreted IFNγ. Upon incubation with GM3/WT1/R848 liposome, CD14$^+$ monocytes were able to stimulate higher secretion of IFNγ by WT1 CD8$^+$ T cells as compared to control liposome (**Figures 5J, K**). Interestingly, although GT1b-liposome uptake was higher than GM3-liposome uptake, it did not lead to activation of WT1 CD8$^+$ T cells. This data indicates that GM3-liposomes are able to target and deliver tumor antigen to CD14$^+$ CD169$^+$ monocytes leading to a strong CD8$^+$ T cell stimulation.

DISCUSSION

CD169$^+$ monocytes are detected under homeostatic and inflammatory conditions, however, their phenotype and functional role in T cell activation is underexplored. Here, we show that CD14$^+$ CD169$^+$ monocytes exhibit a higher activation phenotype with enhanced capacity for antigen presentation and CD8$^+$ T cells activation. Our spectral cytometry data show that they are distinct from the recently defined CD14$^+$ DC3 population, and that they are present in the circulation of healthy donors, SARS-CoV-2-infected patients, as well as patients with five different types of cancer. Furthermore, we show that CD169-targeting nanovaccines can deliver antigen/adjuvant to CD169$^+$ monocytes that leads to robust antigen-specific T cell activation, indicating their potential for novel CD169 targeting vaccination strategies.

The increase of CD169 expression on monocytes was initially described in patients with increased IFN-I signature, such as systemic sclerosis (27). A high level of IFNα in the circulation of systemic lupus erythematosus patients was demonstrated to increase the capacity of monocytes to activate CD4$^+$ T cells and to contribute to the break of tolerance (47). Furthermore, exposure of IFNα to monocytes was shown to lead to upregulation of maturation markers, and an increased potency of monocytes to activate CD4$^+$ T cells in an allogeneic setting (48). This was confirmed in a more recent unbiased proteomic analysis, in which CD169 was among the highest upregulated membrane proteins by IFNα treatment, along with HLA-molecules and co-stimulatory markers (49). The enhanced capacity of T cell activation by IFN-treated monocytes is therefore attributed to the increased expression of HLA molecules and these activating ligands. In line with these findings, our data have demonstrated that IFNα-exposed monocytes showed increased HLA- and co-stimulatory molecules and had enhanced capacity to cross-present antigen to CD8$^+$ T cells.

Although DC1 has the highest proficiency in cross-presentation of cell-associated antigens (50–53), monocytes and monocyte-derived cells are also capable to uptake exogenous antigen and process them for CD8$^+$ T cell activation (48, 54–56). Here, we showed that IFNα-treated CD169^{high} monocytes were able to present both pre-processed and unprocessed gp100 peptides to antigen-specific CD8$^+$ T cells. Interestingly, monocytes loaded with MART1 long peptide were shown to retain this peptide and to present it to CD8$^+$ T cells after a full differentiation into moDC with GM-CSF/IL-4 (54). *Ex vivo* loading of monocytes with antigen followed by intravenous transfer of these loaded monocytes was shown to induce strong anti-tumor T cell responses in several mouse models (57). In this study, antigen transfer to DC1s by monocytes appeared to be involved. As we previously showed a

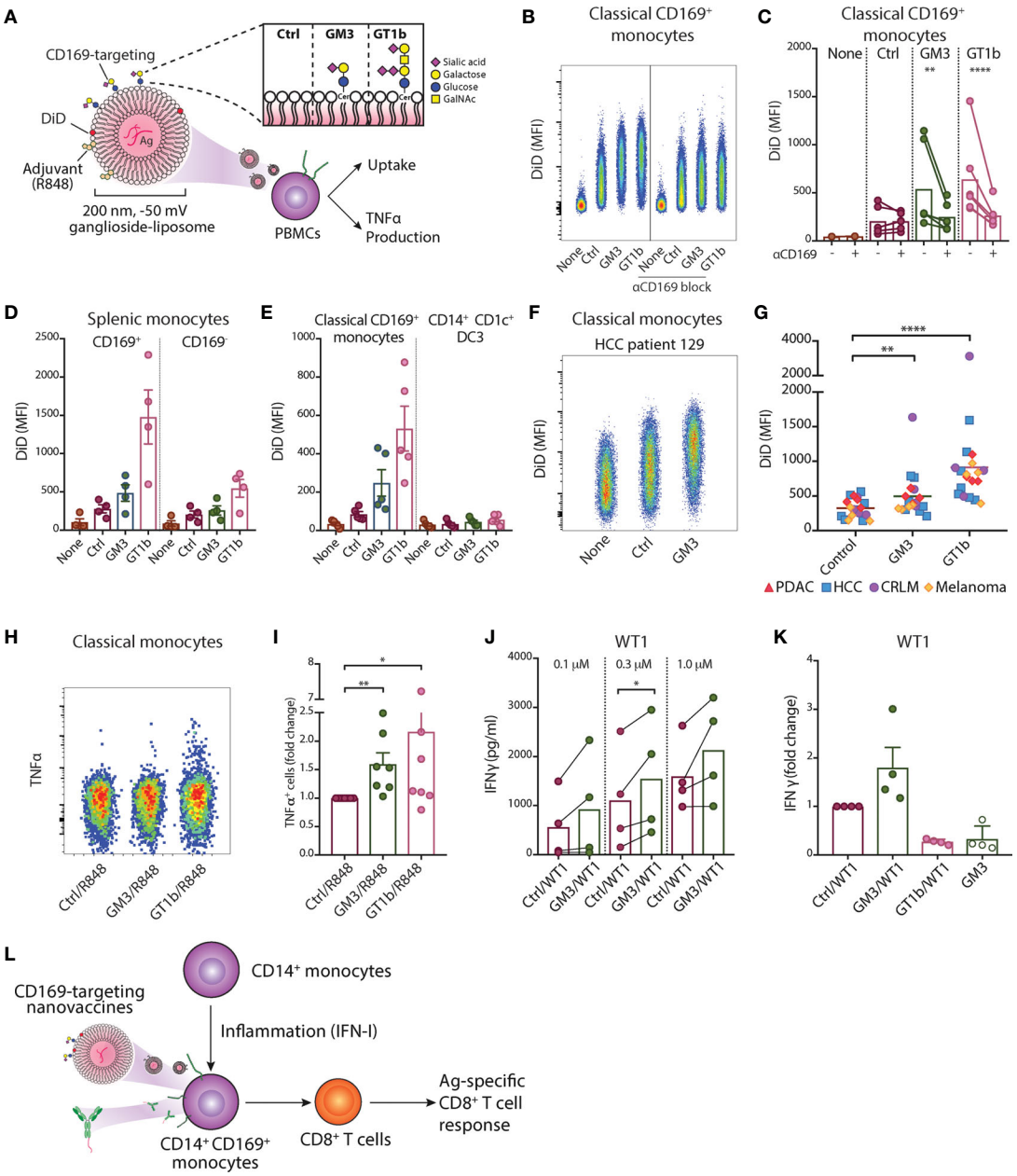

FIGURE 5 | Ganglioside-liposomes deliver antigen/adjuvant to CD14$^+$ CD169$^+$ monocytes for presentation to CD8$^+$ T cells. **(A)** Gangliosides GM3 and GT1b were incorporated into DiD-labeled liposomes and uptake was determined by flow cytometry. GalNAc, N-acetyl galactosamine; Cer, ceramide; Ctrl, control. Additionally, toll-like receptor 7/8 agonist R848 was incorporated and tumor-associated peptide was encapsulated. **(B, C)** Ganglioside liposome uptake by human CD14$^+$ CD169$^+$ monocytes as **(B)** representative plots and **(C)** quantification (n = 4) are shown. **(D)** Ganglioside-liposome uptake by human splenic autofluorescence (AF)$^-$ CD14$^+$ Lin(CD3/CD19/CD56)$^-$ monocytes, repartitioned as CD169$^+$ or CD169$^-$ cells. **(E)** Reanalysis of ganglioside-liposome uptake on circulating classical CD169$^+$ monocytes (HLA-DR$^+$ Lin$^-$ CD14^{high} CD1c$^-$) and DC3 (HLA-DR$^+$ Lin$^-$ CD14^{int} CD1c$^+$). **(F, G)** Ganglioside-liposome uptake by CD169$^+$ classical monocytes of cancer patients as **(F)** representative plot and **(G)** quantification are shown. Friedman test using a two-stage linear step-up procedure of Benjamini, Krieger and Yekutieli, with Q = 0.05, was used. **adjusted P < 0.01, ****adjusted P < 0.0001. **(H, I)** PBMCs were incubated with R848-containing ganglioside-liposomes at 37°C for 45 min, washed, and cultured for five hours in complete medium, with the addition of brefeldin-A for the final three hours. TNFα production by classical monocytes was measured by intracellular flow cytometry, gated on live CD14$^+$ CD16$^-$ HLA-DR$^+$ Lin(CD3/CD19/CD56)$^-$ cells. **(H)** Representative plot from one donor and **(I)** quantification as fold change over control are shown. Data are mean ± SEM from 6-7 donors. **(J, K)** After CD14$^+$ isolation, monocytes were incubated with different concentrations of Ganglioside/WT1/R848 liposome or control (Ctrl) liposome, washed, and WT1-specific CD8$^+$ T cells were added. **(J)** IFNγ secretion after 24h was determined by ELISA. **(K)** Fold change of IFNγ secretion over Ctrl liposome is shown for GM3/WT1, GT1b/WT1, or GM3 devoid of peptide, at 1.0 μM dose. Paired t-tests were used. *P < 0.05, **P < 0.01, ****P < 0.001. **(L)** Two nanovaccine platforms, antibody- and liposome-based, deliver antigen to CD169+ monocytes for antigen-specific CD8$^+$ T cell activation.

similar collaboration between CD169$^+$ macrophages and DC1 in mice (58), the potential interplay between CD169$^+$ monocytes, DC, and CD8$^+$ T cells in humans needs further investigation.

CD169$^+$ monocytes have been proposed to be a diagnostic biomarker for viral infections including in COVID-19 patients with high sensitivity (59–61). Several studies have also revealed CD169 alterations when comparing mild and severe COVID-19 cases. CD169-expressing monocytes were found to be more prominent in mild cases and the amount of CD169 expression correlated with plasma IFNα levels (60, 62). CD169 also identified early activated monocyte clusters in COVID-19 patients, that were absent in healthy controls (63), reminiscent to our scRNA-seq analysis. In this study, CD169 trajectory analysis predicted that CD169$^+$ monocytes could be derived from both, classical and intermediate monocytes, thus corroborating our analysis. Additionally, we observed a higher proportion of CD169$^+$ intermediate monocytes as compared to classical or non-classical subsets in COVID-19 patients. Intermediate monocytes are known to be increased during infection, including SARS-CoV-2 (64), and it is likely that these CD169$^+$ intermediate monocytes were transitioning from activated classical monocytes. Remarkably, the frequency of CD169$^+$ monocytes was also associated with high IFNγ levels (63). These data suggests that CD169$^+$ monocytes reflect high IFN levels and may potentially be involved in the activation of T cell responses required for virus clearance in COVID-19 patients.

In cancer, monocytes are known to play dual roles in promoting or suppressing tumor growth (11). CD169$^+$ monocytes were previously reported to be highly increased in the circulation of patients with colorectal carcinoma, to produce high amount of IL-10, and were associated with tumor-infiltrating CD169$^+$ monocytes/macrophages and poor prognosis (65). In breast cancer, CD169 also marked tumor-associated macrophages and *SIGLEC1* expression was associated with poor outcome (66). On the other hand, *SIGLEC1* expression was correlated with immune cell infiltration in endometrial cancer and survival (67). Along the same line, tumor-infiltrating CD169$^+$ monocytes/macrophages were shown to be a good prognostic marker in hepatocellular carcinoma (68). In hepatocellular carcinoma, tumor-infiltrating CD169$^+$ monocytes/macrophages presence was correlated with CD8$^+$ T cell frequency and both were found in close proximity. Moreover, hepatocellular carcinoma-associated CD169$^+$ monocytes/macrophages showed elevated expression of HLA-DR and CD86, similar to the pattern we observed in CD169$^+$ monocytes. Furthermore, several studies have reported that the presence of CD169$^+$ macrophages in the tumor draining lymph node is associated with better prognosis in multiple types of cancer (42–44). Thus, the role of CD169-expressing monocytes/macrophages is highly dependent on tumor types and tissues investigated.

Interestingly, CD169 molecule itself has been suggested to promote T cell activation. Addition of recombinant human CD169 to anti-CD3-stimulated PBMCs induced CD8$^+$ T cell proliferation and cytokine production in an autologous condition (68). In an allogeneic setting, blocking of CD169 expressed on IFN-α treated monocytes, led to a reduced proliferation and cytokine production by CD8$^+$ and CD4$^+$ T cells (69). However, also contradictory data exists, in which CD169 is involved in T cell suppression (70, 71). Further research into the interaction of CD169 with T cells and to elucidate the ligands involved will be necessary. These studies suggest that CD169 expression on monocytes could potentially act as an additional signal that can influence CD8$^+$ T cell activation.

Finally, to evaluate the potential of CD169$^+$ monocytes for a vaccination strategy, we used two forms of CD169-targeting nanovaccine platforms (**Figure 5L**). Our data showed that anti-CD169 Ab-Ag conjugate and ganglioside-liposomes were efficiently taken up by CD169$^+$ monocytes and delivered tumor-associated antigens which led to robust antigen-specific CD8$^+$ T cell responses. This is in line with our previous reports using CD169$^+$ moDC and Axl$^+$ DC (20, 37). Interestingly, only GM3-liposome, and not GT1b-liposome, that was able to deliver antigen for CD8$^+$ T cells activation by CD169$^+$ monocytes, similar to Axl$^+$ DCs. Future experiments investigating ganglioside-liposome intracellular trafficking, peptide processing and presentation on MHC are needed to determine the underlying mechanisms. Since CD169 is also expressed by Axl$^+$ DC, targeting the CD169 molecule would give additional benefits of targeting both Axl$^+$ DCs to prime naïve CD8$^+$ T cells and CD169$^+$ monocytes to stimulate antigen-experienced T cells. In addition, intravenous administration of CD169-targeting nanovaccines in mice specifically targets splenic CD169$^+$ macrophages, leading to strong T cell responses that depend on DC1 (34, 35, 37, 72). A similar type of macrophage is present in human spleen and are described as perifollicular macrophages (37), but have not been studied because of their scarcity. Together, this suggest that cancer vaccines targeting CD169 could potentially mediate T cell activation *via* the consorted action of targeting splenic CD169$^+$ perifollicular macrophages, Axl$^+$ DCs, and CD169$^+$ monocytes.

Taken together, our data show that CD169$^+$ monocytes are activated monocytes that are present in both, healthy and diseased conditions, including in viral infections and cancer. Increased expression of CD169 in monocytes is driven by IFN-I and it is accompanied by increased expression of co-stimulatory and HLA molecules. CD169$^+$ monocytes exhibit an enhanced antigen presentation and CD8$^+$ T cell activation capacity, and can be selectively targeted and activated by CD169-targeting nanovaccines. Thereby, CD169$^+$ monocytes are APCs with potential for an effective targeted nano-vaccination strategy.

DATA AVAILABILITY STATEMENT

The raw data supporting the conclusions of this article will be made available by the authors, without undue reservation.

ETHICS STATEMENT

The studies involving human participants were reviewed and approved by Medical Ethical Committee, Review Committee Biobank, Amsterdam UMC. The patients/participants provided their written informed consent to participate in this study.

AUTHOR CONTRIBUTIONS

AA and JH conceived and planned the experiments. AA wrote the first draft of the manuscript. AA, KO, JG, MN, ER, AS, EZ, EN, HK, and MK carried out the experiments, analyzed, and interpreted the data. EZ, GK, TG, AE, AS, EN, and JG-V provided clinical materials and information. JS, JG-V, TG, GS, YK, and JH supervised the study. All authors contributed to the article and approved the submitted version.

FUNDING

This work was supported by grants from the Dutch Cancer Society (VU2016-10449, VU2019-12802) to JH, YK, TG, and (VU2019-12802) to AE, from the Phospholipid Research Center to JH and YK (JDH-2020-082/1-1), from NWO ZonMW (TOP 91218024) to JH and GS, and de Bennink and Cancer Center Amsterdam Foundations to GK.

ACKNOWLEDGMENTS

We acknowledge the Microscopy and Cytometry Core Facility at the Amsterdam UMC, location VUmc for providing assistance in cytometry. We thank Daan J. Brinkman (Amsterdam UMC, Catharina Hospital) and Wouter J. de Jonge (Amsterdam UMC) for additional patient material, and the dedicated people at Amsterdam UMC Liquid Biopsy Center. We would like to thank ArtDECO study consortium for the collection and processing of samples. The authors greatly acknowledge the Amsterdam UMC – Cytek Spectral Cytometry Knowledge Center for their continuous support in panel design, experiment acquisition, and spectral unmixing of data.

SUPPLEMENTARY MATERIAL

The Supplementary Material for this article can be found online at: https://www.frontiersin.org/articles/10.3389/fimmu.2021.697840/full#supplementary-material

REFERENCES

1. Jakubzick CV, Randolph GJ, Henson PM. Monocyte Differentiation and Antigen-Presenting Functions. *Nat Rev Immunol* (2017) 17:349–62. doi: 10.1038/nri.2017.28
2. Wong KL, Yeap WH, Tai JJ, Ong SM, Dang TM, Wong SC. The Three Human Monocyte Subsets: Implications for Health and Disease. *Immunol Res* (2012) 53:41–57. doi: 10.1007/s12026-012-8297-3
3. Patel AA, Zhang Y, Fullerton JN, Boelen L, Rongvaux A, Maini AA, et al. The Fate and Lifespan of Human Monocyte Subsets in Steady State and Systemic Inflammation. *J Exp Med* (2017) 214:1913–23. doi: 10.1084/jem.20170355
4. Tak T, Drylewicz J, Conemans L, de Boer RJ, Koenderman L, Borghans JAM, et al. Circulatory and Maturation Kinetics of Human Monocyte Subsets in Vivo. *Blood* (2017) 130:1474–7. doi: 10.1182/blood-2017-03-771261
5. Guilliams M, Mildner A, Yona S. Developmental and Functional Heterogeneity of Monocytes. *Immunity* (2018) 49:595–613. doi: 10.1016/j.immuni.2018.10.005
6. Guilliams M, Ginhoux F, Jakubzick C, Naik SH, Onai N, Schraml BU, et al. Dendritic Cells, Monocytes and Macrophages: A Unified Nomenclature Based on Ontogeny. *Nat Rev Immunol* (2014) 14:571–8. doi: 10.1038/nri3712
7. Bol KF, Schreibelt G, Gerritsen WR, de Vries IJ, Figdor CG. Dendritic Cell-Based Immunotherapy: State of the Art and Beyond. *Clin Cancer Res* (2016) 22:1897–906. doi: 10.1158/1078-0432.CCR-15-1399
8. Lehmann CH, Heger L, Heidkamp GF, Baranska A, Luhr JJ, Hoffmann A, et al. Direct Delivery of Antigens to Dendritic Cells via Antibodies Specific for Endocytic Receptors as a Promising Strategy for Future Therapies. *Vaccines (Basel)* (2016) 4:1–32. doi: 10.3390/vaccines4020008
9. Schulte-Schrepping J, Reusch N, Paclik D, Bassler K, Schlickeiser S, Zhang B, et al. Severe COVID-19 is Marked by a Dysregulated Myeloid Cell Compartment. *Cell* (2020) 182:19–40.e23. doi: 10.1016/j.cell.2020.08.001
10. Zhang D, Guo R, Lei L, Liu H, Wang Y, Wang Y, et al. Frontline Science: COVID-19 Infection Induces Readily Detectable Morphologic and Inflammation-Related Phenotypic Changes in Peripheral Blood Monocytes. *J Leukoc Biol* (2021) 109:13–22. doi: 10.1002/JLB.4HI0720-470R
11. Olingy CE, Dinh HQ, Hedrick CC. Monocyte Heterogeneity and Functions in Cancer. *J Leukoc Biol* (2019) 106:309–22. doi: 10.1002/JLB.4RI0818-311R
12. Griffith TS, Wiley SR, Kubin MZ, Sedger LM, Maliszewski CR, Fanger NA. Monocyte-Mediated Tumoricidal Activity *via* the Tumor Necrosis Factor-Related Cytokine, TRAIL. *J Exp Med* (1999) 189:1343–54. doi: 10.1084/jem.189.8.1343
13. Nakayama M, Kayagaki N, Yamaguchi N, Okumura K, Yagita H. Involvement of TWEAK in Interferon Gamma-Stimulated Monocyte Cytotoxicity. *J Exp Med* (2000) 192:1373–80. doi: 10.1084/jem.192.9.1373
14. Tel J, Anguille S, Waterborg CE, Smits EL, Figdor CG, de Vries IJ. Tumoricidal Activity of Human Dendritic Cells. *Trends Immunol* (2014) 35:38–46. doi: 10.1016/j.it.2013.10.007
15. Krieg C, Nowicka M, Guglietta S, Schindler S, Hartmann FJ, Weber LM, et al. High-Dimensional Single-Cell Analysis Predicts Response to Anti-PD-1 Immunotherapy. *Nat Med* (2018) 24:144–53. doi: 10.1038/nm.4466
16. Collin M, Bigley V. Human Dendritic Cell Subsets: An Update. *Immunology* (2018) 154:3–20. doi: 10.1111/imm.12888
17. Villani AC, Satija R, Reynolds G, Sarkizova S, Shekhar K, Fletcher J, et al. Single-Cell RNA-Seq Reveals New Types of Human Blood Dendritic Cells, Monocytes, and Progenitors. *Science* (2017) 356(6335):eaah4573. doi: 10.1126/science.aah4573
18. See P, Dutertre CA, Chen J, Gunther P, McGovern N, Irac SE, et al. Mapping the Human DC Lineage Through the Integration of High-Dimensional Techniques. *Science* (2017) 356(6342):eaag3009. doi: 10.1126/science.aag3009
19. Alcantara-Hernandez M, Leylek R, Wagar LE, Engleman EG, Keler T, Marinkovich MP, et al. High-Dimensional Phenotypic Mapping of Human Dendritic Cells Reveals Interindividual Variation and Tissue Specialization. *Immunity* (2017) 47:1037–1050 e6. doi: 10.1016/j.immuni.2017.11.001
20. Affandi AJ, Grabowska J, Olesek K, Lopez Venegas M, Barbaria A, Rodriguez E, et al. Selective Tumor Antigen Vaccine Delivery to Human CD169(+) Antigen-Presenting Cells Using Ganglioside-Liposomes. *Proc Natl Acad Sci USA* (2020) 117:27528–39. doi: 10.1073/pnas.2006186117
21. Villar J, Segura E. Decoding the Heterogeneity of Human Dendritic Cell Subsets. *Trends Immunol* (2020) 41:1062–71. doi: 10.1016/j.it.2020.10.002
22. Heger L, Hofer TP, Bigley V, de Vries IJM, Dalod M, Dudziak D, et al. Subsets of CD1c(+) Dcs: Dendritic Cell Versus Monocyte Lineage. *Front Immunol* (2020) 11:559166. doi: 10.3389/fimmu.2020.559166
23. Dutertre CA, Becht E, Irac SE, Khalilnezhad A, Narang V, Khalilnezhad S, et al. Single-Cell Analysis of Human Mononuclear Phagocytes Reveals Subset-Defining Markers and Identifies Circulating Inflammatory Dendritic Cells. *Immunity* (2019) 51:573–589 e8. doi: 10.1016/j.immuni.2019.08.008
24. Bourdely P, Anselmi G, Vaivode K, Ramos RN, Missolo-Koussou Y, Hidalgo S, et al. Transcriptional and Functional Analysis of CD1c(+) Human Dendritic Cells Identifies a CD163(+) Subset Priming CD8(+)CD103(+) T Cells. *Immunity* (2020) 53:335–352 e8. doi: 10.1016/j.immuni.2020.06.002
25. Bakdash G, Buschow SI, Gorris MA, Halilovic A, Hato SV, Skold AE, et al. Expansion of a BDCA1+CD14+ Myeloid Cell Population in Melanoma Patients may Attenuate the Efficacy of Dendritic Cell Vaccines. *Cancer Res* (2016) 76:4332–46. doi: 10.1158/0008-5472.CAN-15-1695
26. Grabowska J, Lopez-Venegas MA, Affandi AJ, den Haan JMM. CD169(+) Macrophages Capture and Dendritic Cells Instruct: The Interplay of the Gatekeeper and the General of the Immune System. *Front Immunol* (2018) 9:2472. doi: 10.3389/fimmu.2018.02472

27. York MR, Nagai T, Mangini AJ, Lemaire R, van Seventer JM, Lafyatis R. A Macrophage Marker, Siglec-1, is Increased on Circulating Monocytes in Patients With Systemic Sclerosis and Induced by Type I Interferons and Toll-Like Receptor Agonists. *Arthritis Rheum* (2007) 56:1010–20. doi: 10.1002/art.22382
28. Xiong YS, Cheng Y, Lin QS, Wu AL, Yu J, Li C, et al. Increased Expression of Siglec-1 on Peripheral Blood Monocytes and its Role in Mononuclear Cell Reactivity to Autoantigen in Rheumatoid Arthritis. *Rheumatol (Oxford)* (2014) 53:250–9. doi: 10.1093/rheumatology/ket342
29. Pino M, Erkizia I, Benet S, Erikson E, Fernandez-Figueras MT, Guerrero D, et al. HIV-1 Immune Activation Induces Siglec-1 Expression and Enhances Viral Trans-Infection in Blood and Tissue Myeloid Cells. *Retrovirology* (2015) 12:37. doi: 10.1186/s12977-015-0160-x
30. Rempel H, Calosing C, Sun B, Pulliam L. Sialoadhesin Expressed on IFN-Induced Monocytes Binds HIV-1 and Enhances Infectivity. *PloS One* (2008) 3: e1967. doi: 10.1371/journal.pone.0001967
31. Akiyama H, Miller C, Patel HV, Hatch SC, Archer J, Ramirez NG, et al. Virus Particle Release From Glycosphingolipid-Enriched Microdomains is Essential for Dendritic Cell-Mediated Capture and Transfer of HIV-1 and Henipavirus. *J Virol* (2014) 88:8813–25. doi: 10.1128/JVI.00992-14
32. Puryear WB, Yu X, Ramirez NP, Reinhard BM, Gummuluru S. HIV-1 Incorporation of Host-Cell-Derived Glycosphingolipid GM3 Allows for Capture by Mature Dendritic Cells. *Proc Natl Acad Sci USA* (2012) 109:7475–80. doi: 10.1073/pnas.1201104109
33. Izquierdo-Useros N, Lorizate M, Puertas MC, Rodriguez-Plata MT, Zangger N, Erikson E, et al. Siglec-1 is a Novel Dendritic Cell Receptor That Mediates HIV-1 Trans-Infection Through Recognition of Viral Membrane Gangliosides. *PloS Biol* (2012) 10:e1001448. doi: 10.1371/journal.pbio.1001448
34. Grabowska J, Affandi AJ, van Dinther D, Nijen Twilhaar MK, Olesek K, Hoogterp L, et al. Liposome Induction of CD8(+) T Cell Responses Depends on CD169(+) Macrophages and Batf3-Dependent Dendritic Cells and is Enhanced by GM3 Inclusion. *J Control Release* (2021) 331:309–20. doi: 10.1016/j.jconrel.2021.01.029
35. Nijen Twilhaar MK, Czentner L, Grabowska J, Affandi AJ, Lau CYJ, Olesek K, et al. Optimization of Liposomes for Antigen Targeting to Splenic CD169(+) Macrophages. *Pharmaceutics* (2020) 12:1–12. doi: 10.3390/pharmaceutics12121138
36. Baars A, Claessen AM, van den Eertwegh AJ, Gall HE, Stam AG, Meijer S, et al. Skin Tests Predict Survival After Autologous Tumor Cell Vaccination in Metastatic Melanoma: Experience in 81 Patients. *Ann Oncol* (2000) 11:965–70. doi: 10.1023/A:1008363601515
37. van Dinther D, Lopez Venegas M, Veninga H, Olesek K, Hoogterp L, Revet M, et al. Activation of CD8(+) T Cell Responses After Melanoma Antigen Targeting to CD169(+) Antigen Presenting Cells in Mice and Humans. *Cancers (Basel)* (2019) 11:1–17. doi: 10.3390/cancers11020183
38. Unger WW, van Beelen AJ, Bruijns SC, Joshi M, Fehres CM, van Bloois L, et al. Glycan-Modified Liposomes Boost CD4+ and CD8+ T-Cell Responses by Targeting DC-SIGN on Dendritic Cells. *J Control Release* (2012) 160:88–95. doi: 10.1016/j.jconrel.2012.02.007
39. Boks MA, Ambrosini M, Bruijns SC, Kalay H, van Bloois L, Storm G, et al. MPLA Incorporation Into DC-Targeting Glycoliposomes Favours Anti-Tumour T Cell Responses. *J Control Release* (2015) 216:37–46. doi: 10.1016/j.jconrel.2015.06.033
40. Saris A, Reijnders TDY, Nossent EJ, Schuurman AR, Verhoeff J, Asten SV, et al. Distinct Cellular Immune Profiles in the Airways and Blood of Critically Ill Patients With COVID-19. *Thorax* (2021) 1–10. doi: 10.1136/thoraxjnl-2020-216256
41. Lee JS, Park S, Jeong HW, Ahn JY, Choi SJ, Lee H, et al. Immunophenotyping of COVID-19 and Influenza Highlights the Role of Type I Interferons in Development of Severe COVID-19. *Sci Immunol* (2020) 5(49):eabd1554. doi: 10.1126/sciimmunol.abd1554
42. Ohnishi K, Komohara Y, Saito Y, Miyamoto Y, Watanabe M, Baba H, et al. CD169-Positive Macrophages in Regional Lymph Nodes are Associated With a Favorable Prognosis in Patients With Colorectal Carcinoma. *Cancer Sci* (2013) 104:1237–44. doi: 10.1111/cas.12212
43. Saito Y, Ohnishi K, Miyashita A, Nakahara S, Fujiwara Y, Horlad H, et al. Prognostic Significance of CD169+ Lymph Node Sinus Macrophages in Patients With Malignant Melanoma. *Cancer Immunol Res* (2015) 3:1356–63. doi: 10.1158/2326-6066.CIR-14-0180
44. Asano T, Ohnishi K, Shiota T, Motoshima T, Sugiyama Y, Yatsuda J, et al. CD169-Positive Sinus Macrophages in the Lymph Nodes Determine Bladder Cancer Prognosis. *Cancer Sci* (2018) 109:1723–30. doi: 10.1111/cas.13565
45. Steele NG, Carpenter ES, Kemp SB, Sirihorachai VR, The S, Delrosario L, et al. Multimodal Mapping of the Tumor and Peripheral Blood Immune Landscape in Human Pancreatic Cancer. *Nat Cancer* (2020) 1:1097–112. doi: 10.1038/s43018-020-00121-4
46. Zilionis R, Engblom C, Pfirschke C, Savova V, Zemmour D, Saatcioglu HD, et al. Single-Cell Transcriptomics of Human and Mouse Lung Cancers Reveals Conserved Myeloid Populations Across Individuals and Species. *Immunity* (2019) 50:1317–1334 e10. doi: 10.1016/j.immuni.2019.03.009
47. Blanco P, Palucka AK, Gill M, Pascual V, Banchereau J. Induction of Dendritic Cell Differentiation by IFN-Alpha in Systemic Lupus Erythematosus. *Science* (2001) 294:1540–3. doi: 10.1126/science.1064890
48. Gerlini G, Mariotti G, Chiarugi A, Di Gennaro P, Caporale R, Parenti A, et al. Induction of CD83+CD14+ Nondendritic Antigen-Presenting Cells by Exposure of Monocytes to IFN-Alpha. *J Immunol* (2008) 181:2999–3008. doi: 10.4049/jimmunol.181.5.2999
49. Soday L, Potts M, Hunter LM, Ravenhill BJ, Houghton JW, Williamson JC, et al. Comparative Cell Surface Proteomic Analysis of the Primary Human T Cell and Monocyte Responses to Type I Interferon. *Front Immunol* (2021) 12:600056. doi: 10.3389/fimmu.2021.600056
50. Poulin LF, Salio M, Griessinger E, Anjos-Afonso F, Craciun L, Chen JL, et al. Characterization of Human DNGR-1+ BDCA3+ Leukocytes as Putative Equivalents of Mouse CD8alpha+ Dendritic Cells. *J Exp Med* (2010) 207:1261–71. doi: 10.1084/jem.20092618
51. Jongbloed SL, Kassianos AJ, McDonald KJ, Clark GJ, Ju X, Angel CE, et al. Human CD141+ (BDCA-3)+ Dendritic Cells (DCs) Represent a Unique Myeloid DC Subset That Cross-Presents Necrotic Cell Antigens. *J Exp Med* (2010) 207:1247–60. doi: 10.1084/jem.20092140
52. Crozat K, Guiton R, Contreras V, Feuillet V, Dutertre CA, Ventre E, et al. The XC Chemokine Receptor 1 is a Conserved Selective Marker of Mammalian Cells Homologous to Mouse CD8alpha+ Dendritic Cells. *J Exp Med* (2010) 207:1283–92. doi: 10.1084/jem.20100223
53. Bachem A, Guttler S, Hartung E, Ebstein F, Schaefer M, Tannert A, et al. Superior Antigen Cross-Presentation and XCR1 Expression Define Human CD11c+CD141+ Cells as Homologues of Mouse CD8+ Dendritic Cells. *J Exp Med* (2010) 207:1273–81. doi: 10.1084/jem.20100348
54. Faure F, Jouve M, Lebhar-Peguillet I, Sadaka C, Sepulveda F, Lantz O, et al. Blood Monocytes Sample Melana/MART1 Antigen for Long-Lasting Cross-Presentation to CD8(+) T Cells After Differentiation Into Dendritic Cells. *Int J Cancer* (2018) 142:133–44. doi: 10.1002/ijc.31037
55. Tang-Huau TL, Gueguen P, Goudot C, Durand M, Bohec M, Baulande S, et al. Human *in Vivo*-Generated Monocyte-Derived Dendritic Cells and Macrophages Cross-Present Antigens Through a Vacuolar Pathway. *Nat Commun* (2018) 9:2570. doi: 10.1038/s41467-018-04985-0
56. Coillard A, Segura E. In Vivo Differentiation of Human Monocytes. *Front Immunol* (2019) 10:1907. doi: 10.3389/fimmu.2019.01907
57. Huang MN, Nicholson LT, Batich KA, Swartz AM, Kopin D, Wellford S, et al. Antigen-Loaded Monocyte Administration Induces Potent Therapeutic Antitumor T Cell Responses. *J Clin Invest* (2020) 130:774–88. doi: 10.1172/JCI128267
58. van Dinther D, Veninga H, Iborra S, Borg EGF, Hoogterp L, Olesek K, et al. Functional CD169 on Macrophages Mediates Interaction With Dendritic Cells for CD8(+) T Cell Cross-Priming. *Cell Rep* (2018) 22:1484–95. doi: 10.1016/j.celrep.2018.01.021
59. Ortillon M, Coudereau R, Cour M, Rimmele T, Godignon M, Gossez M, et al. Monocyte CD169 Expression in COVID-19 Patients Upon Intensive Care Unit Admission. *Cytometry A* (2021) 99(5):466–71. doi: 10.1002/cyto.a.24315
60. Doehn JM, Tabeling C, Biesen R, Saccomanno J, Madlung E, Pappe E, et al. CD169/SIGLEC1 is Expressed on Circulating Monocytes in COVID-19 and Expression Levels are Associated With Disease Severity. *Infection* (2021) 1–6. doi: 10.1007/s15010-021-01606-9
61. Bedin AS, Makinson A, Picot MC, Mennechet F, Malergue F, Pisoni A, et al. Monocyte CD169 Expression as a Biomarker in the Early Diagnosis of Coronavirus Disease 2019. *J Infect Dis* (2021) 223:562–7. doi: 10.1093/infdis/jiaa724

62. Silvin A, Chapuis N, Dunsmore G, Goubet AG, Dubuisson A, Derosa L, et al. Elevated Calprotectin and Abnormal Myeloid Cell Subsets Discriminate Severe From Mild COVID-19. *Cell* (2020) 182:1401–18.e18. doi: 10.1016/j.cell.2020.08.002
63. Chevrier S, Zurbuchen Y, Cervia C, Adamo S, Raeber ME, de Souza N, et al. A Distinct Innate Immune Signature Marks Progression From Mild to Severe COVID-19. *Cell Rep Med* (2021) 2:100166. doi: 10.1016/j.xcrm.2020.100166
64. Kvedaraite E, Hertwig L, Sinha I, Ponzetta A, Hed Myrberg I, Lourda M, et al. Major Alterations in the Mononuclear Phagocyte Landscape Associated With COVID-19 Severity. *Proc Natl Acad Sci USA* (2021) 118:e2018587118. doi: 10.1073/pnas.2018587118
65. Li C, Luo X, Lin Y, Tang X, Ling L, Wang L, et al. A Higher Frequency of CD14+ CD169+ Monocytes/Macrophages in Patients With Colorectal Cancer. *PloS One* (2015) 10:e0141817. doi: 10.1371/journal.pone.0141817
66. Cassetta L, Fragkogianni S, Sims AH, Swierczak A, Forrester LM, Zhang H, et al. Human Tumor-Associated Macrophage and Monocyte Transcriptional Landscapes Reveal Cancer-Specific Reprogramming, Biomarkers, and Therapeutic Targets. *Cancer Cell* (2019) 35:588–602.e10. doi: 10.1016/j.ccell.2019.02.009
67. Chen P, Yang Y, Zhang Y, Jiang S, Li X, Wan J. Identification of Prognostic Immune-Related Genes in the Tumor Microenvironment of Endometrial Cancer. *Aging (Albany NY)* (2020) 12:3371–87. doi: 10.18632/aging.102817
68. Zhang Y, Li JQ, Jiang ZZ, Li L, Wu Y, Zheng L. CD169 Identifies an Anti-Tumour Macrophage Subpopulation in Human Hepatocellular Carcinoma. *J Pathol* (2016) 239:231–41. doi: 10.1002/path.4720
69. Xiong YS, Wu AL, Lin QS, Yu J, Li C, Zhu L, et al. Contribution of Monocytes Siglec-1 in Stimulating T Cells Proliferation and Activation in Atherosclerosis. *Atherosclerosis* (2012) 224:58–65. doi: 10.1016/j.atherosclerosis.2012.06.063
70. Kirchberger S, Majdic O, Steinberger P, Bluml S, Pfistershammer K, Zlabinger G, et al. Human Rhinoviruses Inhibit the Accessory Function of Dendritic Cells by Inducing Sialoadhesin and B7-H1 Expression. *J Immunol* (2005) 175:1145–52. doi: 10.4049/jimmunol.175.2.1145
71. Kidder D, Richards HE, Ziltener HJ, Garden OA, Crocker PR. Sialoadhesin Ligand Expression Identifies a Subset of CD4+Foxp3- T Cells With a Distinct Activation and Glycosylation Profile. *J Immunol* (2013) 190:2593–602. doi: 10.4049/jimmunol.1201172
72. Edgar LJ, Kawasaki N, Nycholat CM, Paulson JC. Targeted Delivery of Antigen to Activated CD169(+) Macrophages Induces Bias for Expansion of CD8(+) T Cells. *Cell Chem Biol* (2019) 26:131–6.e4. doi: 10.1016/j.chembiol.2018.10.006

Conflict of Interest: The authors declare that the research was conducted in the absence of any commercial or financial relationships that could be construed as a potential conflict of interest.

Publisher's Note: All claims expressed in this article are solely those of the authors and do not necessarily represent those of their affiliated organizations, or those of the publisher, the editors and the reviewers. Any product that may be evaluated in this article, or claim that may be made by its manufacturer, is not guaranteed or endorsed by the publisher.

frontiers in Immunology

ORIGINAL RESEARCH
published: 28 February 2022
doi: 10.3389/fimmu.2022.752714

Targeting Xcr1 on Dendritic Cells Rapidly Induce Th1-Associated Immune Responses That Contribute to Protection Against Influenza Infection

Demo Yemane Tesfaye[1,2†], Sonja Bobic[1,2†], Anna Lysén[1,2], Peter Csaba Huszthy[1,3], Arnar Gudjonsson[1,2], Ranveig Braathen[1,2], Bjarne Bogen[1,2,3] and Even Fossum[1,2]*

[1] Department of Immunology, Division of Laboratory Medicine, Oslo University Hospital, Oslo, Norway, [2] Kristian Gerhard Jebsen Center for Research on Influenza Vaccines, University of Oslo and Oslo University Hospital, Oslo, Norway, [3] Center for Immune Regulation, Institute of Immunology, University of Oslo and Oslo University Hospital Rikshospitalet, Oslo, Norway

Targeting antigen to conventional dendritic cells (cDCs) can improve antigen-specific immune responses and additionally be used to influence the polarization of the immune responses. However, the mechanisms by which this is achieved are less clear. To improve our understanding, we here evaluate molecular and cellular requirements for $CD4^+$ T cell and antibody polarization after immunization with Xcl1-fusion vaccines that specifically target cDC1s. Xcl1-fusion vaccines induced an IgG2a/IgG2b-dominated antibody response and rapid polarization of Th1 cells both *in vitro* and *in vivo*. For comparison, we included fliC-fusion vaccines that almost exclusively induced IgG1, despite inducing a more mixed polarization of T cells. Th1 polarization and IgG2a induction with Xcl1-fusion vaccines required IL-12 secretion but were nevertheless maintained in $BATF3^{-/-}$ mice which lack IL-12-secreting migratory DCs. Interestingly, induction of IgG2a-dominated responses was highly dependent on the early kinetics of Th1 induction and was important for optimal protection in an influenza infection model. Early Th1 induction was dominant, since a combined Xcl1- and fliC-fusion vaccine induced IgG2a/IgG2b polarized antibody responses similar to Xcl1-fusion vaccines alone. In summary, our results demonstrate that targeting antigen to $Xcr1^+$ cDC1s is an efficient strategy for enhancing IgG2a antibody responses through rapid Th1 induction, which can be utilized for improved vaccine design.

Keywords: dendritic cells, XCR1, Th1, IgG2a, targeting

OPEN ACCESS

Edited by:
Maud Plantinga, University Medical Center Utrecht, Netherlands

Reviewed by:
Tsuneyasu Kaisho, Wakayama Medical University, Japan
Kohtaro Fujihashi, The University of Tokyo, Japan

***Correspondence:**
Even Fossum
even.fossum@rr-research.no

†These authors have contributed equally to this work

Specialty section:
This article was submitted to Antigen Presenting Cell Biology, a section of the journal Frontiers in Immunology

Received: *03 August 2021*
Accepted: *02 February 2022*
Published: *28 February 2022*

Citation:
Tesfaye DY, Bobic S, Lysén A, Huszthy PC, Gudjonsson A, Braathen R, Bogen B and Fossum E (2022) Targeting Xcr1 on Dendritic Cells Rapidly Induce Th1-Associated Immune Responses That Contribute to Protection Against Influenza Infection. Front. Immunol. 13:752714. doi: 10.3389/fimmu.2022.752714

INTRODUCTION

Conventional dendritic cells (cDCs) capture and process foreign antigens for presentation of antigen-specific T cells. Through this function, cDCs have a central role in the initiation phase of the cellular immune response and can as a consequence influence the polarization of the ensuing immune responses (1).

cDCs can be identified as MHC-II$^+$CD11c$^+$ cells and can be further divided into two subpopulations on the basis of functional and ontogenic differences (2). cDC1s are able to cross-present antigen to CD8$^+$ T cells (3, 4) and selectively express the surface receptor Xcr1 (5, 6), while cDC2s can be identified based on express CD11b and SIRP1α expression (7, 8). Previous studies have indicated that cDC1s preferentially polarize the CD4$^+$ T cell response toward Th1, while cDC2 polarize toward Th2 (9, 10), suggesting that targeting antigens toward specific DC subsets can be a valid strategy for influencing the polarization of the vaccine-induced immune responses. Antigens can be targeted directly to cDCs by fusion to antibodies, chemokines, or other ligands that bind surface receptors expressed on the cDCs [reviewed in (1, 11, 12)]. Such approaches have been shown to enhance antigen-specific immune responses in mice as well as in larger animals (13–17).

In this study, we deliver antigen to cDC1s by genetic fusion to the chemokine Xcl1, the ligand of the Xcr1 receptor. Xcl1-fusion vaccines have been demonstrated to enhance CD8$^+$ T cell response (13, 14, 18) and to induce a preferential IgG2a/IgG2b antibody response, associated with Th1 polarization (13, 19). While Xcl1 has previously been identified as a Th1-associated chemokine (20), it is unclear if the chemokine directly influences Th1 polarization when used for targeting antigens to cDC1s. As a second targeting strategy, we included antigens fused to flagellin (fliC) from *Salmonella typhimurium* that has been reported to induce a Th2-polarized response (21, 22) and which we have previously seen to induce an IgG1-dominated antibody response (22). FliC acts as a ligand for TLR5, which has been reported to be expressed on cDC2s (23) but also on pDCs and a specific subset of CD8$^+$Xcr1$^-$ DCs in skin-draining lymph nodes (LN) (24, 25). In addition, fliC is a ligand for the intracellular NLRC4–NAIP5 inflammasome activating complex (26, 27).

Through a series of *in vitro* and *in vivo* experiments, we evaluate the molecular and cellular requirements for Xcl1- and fliC-fusion vaccines to influence antibody and CD4$^+$ T cell polarization. The results demonstrate that Xcl1- and fliC-fusion vaccines both induce IFNγ-secreting CD4$^+$ Th1 cells, although with different kinetics. Our observations indicate that the kinetics of T cell polarization play a crucial role in determining the polarization of antibody responses.

MATERIAL AND METHODS

Cell Lines, Virus, and Antibodies

Human embryonic kidney (HEK) 293E cells (from ATCC) were used for the expression of HA and ovalbumin (OVA) fusion proteins. The HEK293E cells were cultured in complete RPMI media. Complete RPMI medium contains RPMI 164 (Invitrogen, Waltham, MA) supplemented with 40 mg/ml gensumycin (Sanofi-Aventis Norge AS, Lysaker, Norway), 50 μM monothioglycerol (Sigma, St. Louis, MO, USA), 1 mM sodium pyruvate, and 0.1 mM non-essential amino acids (Lonza, Walkersville, MD, USA). For serum ELISAs, ALP-conjugated anti-mouse IgG (Fc-specific) from Sigma (St. Louis, MO, USA) and anti-mouse IgG1-bio (clone 10.9), anti-mouse IgG2a-bio (clone 8.3), and anti-mouse IgG2b-bio (clone R12-3) from BD Pharmingen (San Diego, CA, USA) were used. For flow cytometric analysis, anti-CD3e (145-2C11, Tonbo Biosciences, San Diego, CA, USA), anti-CD19 (1D3, Tonbo Biosciences), anti-CD49b (DX5, eBioscience, San Diego, CA, USA), anti-Ly6G (1A8, Tonbo Biosciences), CD45R/B220 (RA3-6B2, Tonbo Biosciences), anti-MHCII (M5/114.15.2, BioLegend, San Diego, CA, USA), anti-CD11c (N418, Tonbo Biosciences), anti-CD11b (M1/70, Tonbo Biosciences), anti-CD24 (M1/69, BioLegend), anti-CD8α (53-6.7, BioLegend), anti-CD4 (GK1.5, BioLegend), anti-DO11.10 (KJ1-26, BioLegend), anti-CD14 (rmC5-3), anti-IFNγ (XMG1.2), anti-T-bet (eBio4B10, eBioscience), anti-GATA3 (TWAJ, Invitrogen, Carlsbad, CA, USA), and anti-RORγt (AFKJS-9, eBioscience) and were used.

Mice

All animal experiments were approved by the Norwegian Food Safety Authority (NFSA). BALB/c mice aged 6–8 weeks were purchased from Janvier, France. BATF3$^{-/-}$ mice bred on a BALB/c background were purchased from The Jackson Laboratory (Stock No.: 013755) and bred in-house. Mice were euthanized if they lose 80% of their original weight after influenza virus challenge as a human endpoint according to the guidelines of NFSA.

Generation and Purification of Targeted Vaccines

Construction of fusion vaccines that contain targeting, dimerization, and antigenic domains has been described before (28). The targeting units used in this study were the chemokine ligand Xcl1 specific for Xcr1, the TLR5 ligand fliC, or a scFV specific for the hapten 4-hydroxy-3-iodo-5-nitrophenylacetic acid (NIP) as negative control. As antigens, aa 18-541 of HA from influenza A/PR/8/34 or full-length ovalbumin (OVA) was used.

Purification of fusion vaccine proteins was done as described in Gudjonsson et al. (29) with some modifications. In brief, HEK293E cells were seeded in 5-layer tissue culture flasks (Falcon Multi-Flasks) and transfected using polyethylenimine (PEI, 1 mg/ml stock) at a ratio of 500 μg PEI to 250 μg DNA. The supernatant was harvested after 4–5 days and applied on a CaptureSelect FcXL Affinity Matrix column (Life Technologies, Carlsbad, CA, USA) connected to an ÄKTAprime plus (GE Healthcare, Chicago, IL, USA). Bound fusion vaccines were washed with PBS, eluted in 0.1 M glycin–HCl pH 2.7, and immediately dialyzed twice against PBS. Purified fusion vaccines were concentrated using 10-Kd cutoff Vivaspin columns (Sartorius Stedim Biotech, Göttingen, Germany), aliquoted, and stored at -80°C until use.

Intradermal DNA Vaccination of Mice

BALB/c mice were anesthetized by intraperitoneal injection of 150 µl ZRF mixture containing 250 mg/ml Zoletil Forte (Virbac, Carros, France), 20 mg/ml Rompun (Bayer Animal Health), and 50 µg/ml fentanyl (Actavis, Parsippany-Troy Hills, NJ, USA). After shaving the lower back, 25 µl of DNA vaccine (0.5 µg/µl in 0.9% NaCl) was injected intradermally (i.d.) on the left and right flanks. Immediately after injection, the skin was electroporated using the Derma Vax (Cyto Pulse Sciences, Inc., Glen Burnie, MD, USA) system with two pulses of 450 V/cm × 2.5 µs and eight pulses of 110 V/cm × 8.1 ms.

Isolation of $CD4^+$ T Cells From Spleen

Splenocytes from BALB/c, $BATF3^{-/-}$, and DO11.10 mice were prepared using the GentleMACS dissociator (Miltenyi Biotec, Bergisch Gladbach, Germany) according to the manufacturer's protocol. Briefly, spleens were dissociated in GentleMACS C tubes in complete RPMI media. Erythrocytes were lysed by incubation with ACT buffer for 5 min on ice. Finally, cells were filtered through a 70-µm nylon cell strainer. $CD4^+$ T cells from DO11.10 mice spleens were isolated using a $CD4^+$ isolation kit (Miltenyi Biotec), according to the manufacturer's protocol.

In Vitro Generation of Bone Marrow-Derived DCs

Bone marrow cells were harvested by flushing tibiae and femur with medium. The cell suspension was filtered through a 70-µm nylon cell strainer, and 1×10^7 single-cell suspension in 5 ml total volume was seeded in a 6-well plate. Flt3L (PeproTech, Rocky Hill, NJ, USA) (0.1 µg/ml) was added, and the cells were incubated for 9 days at 37°C, 5% CO_2 (30). Semi-adherent cells were subsequently harvested and analyzed by flow cytometry after staining with anti-CD45/B220, anti-CD11c, anti-CD11b, and anti-CD24 for 20 min on ice.

Serum ELISA

High binding 96-well ELISA plates (Coster) were coated with inactivated PR8 virus (Charles River Laboratories, Wilmington, MA, USA) (1:1,600 in PBS) overnight (ON) at 4°C and blocked with 1% w/v BSA in PBS with 0.02% w/v Na azide for 1 h at room temperature (RT). Blood samples were collected from the saphenous vein of mice and sera isolated by two successive centrifugations for 5 min at 13,000 rpm. Serum samples were titrated down 3-fold starting from 1:50 in ELISA buffer (0.1% w/v BSA, 0.2% Tween, and 0.02% w/v in PBS) into the coated 96-well plate and incubated ON at 4°C. Next, the plates were washed (3×) and 50 µl of 1 µg/ml biotinylated anti-mouse IgG1[a], IgG2a[a], or IgG2b diluted in ELISA buffer was added and incubated for 1.5 h at RT. After washing (3×), the plates were incubated with 1:3,000 diluted streptavidin-ALP (GE Healthcare (RPN1234V)) for 45 min at RT. The plates were then washed (3×) and developed using 100 µl/well of substrate buffer (1 mg/ml phosphate substrate (Sigma, P4744)). After 30 min, OD_{405} was measured on a Tecan Sunrise spectrophotometer. The cutoff value for the Ab titer was determined by calculating the mean OD (+ 3 SD) of sera from NaCl-vaccinated control groups. The reciprocal of the highest serum dilution of a sample giving more OD than the cutoff is reported. If an OD value of a sample did not exceed that of the cutoff value, the sample was given an endpoint titer of 1.

IFNγ ELISPOT

A single-cell suspension from spleen was prepared as described above. To detect IFNγ and IL4 secreted by splenocytes, ELISpotPLUS for mouse IFNγ and IL4 kit with precoated anti-IFNγ and anti IL4 plates, respectively, was used in accordance with the manufacturer's protocol (Mabtech AB, Nacka Strand, Sweden). In short, spleens were dissociated, treated with Tris-buffered ammonium chloride (ACT) lysis buffer, and filtered through a 70-µm nylon strainer to prepare single-cell suspensions. Cells were added to the plates at a concentration of 0.5×10^6 and restimulated with the HA-derived peptide HNTNGVTAACSHEG (MHC-II, $I\text{-}E^d$-restricted) or a negative control peptide at a concentration of 2 µg/ml for 18 h at 37°C 5% CO_2. The plates were automatically counted and analyzed using a CTL ELISPOT reader (CTL Europe GmbH, Bonn, Germany). The values obtained from the negative control peptide wells were subtracted from the values obtained from stimulation with specific peptides for each sample.

In Vitro Th Polarization

OVA-specific $CD4^+$ T cells were isolated from DO11.10 TCR transgenic mice by harvesting spleens and generating single-cell suspensions as described for isolation CD4+ T cells from spleen. DO11.10 $CD4^+$ T cells were then purified using a CD4 T cell isolation kit (Miltenyi Biotec), according to the manufacturer's protocol. Purified DO11.10 cells were seeded at a concentration of 5×10^4 cells in 48-well plates together with 2.5×10^5 BM DCs and 0.5 µg αNIP-, Xcl1-, or fliC-OVA in RPMI with 10% FCS. The plates were incubated for 72 h at 37°C with 5% CO_2 before cells were harvested and analyzed by flow cytometry after staining for anti-CD4, anti-DO11.10, anti-T-bet, ant-GATA3, and anti-RORγt. Data were acquired on a Fortessa (BD) flow cytometer and analyzed using FlowJo software (FlowJo, LLC, Ashland, OR, USA).

In Vitro Proliferation on Sorted Bone Marrow-Derived DCs

Bone marrow-derived cDC1s and cDC2s were defined as $CD45R^-$ $CD11c^+CD11b^-CD24^+$ and $CD45R^-CD11c^+CD11b^+CD24^-$ cells, respectively, and sorted on a BD FACSMelody (BD Biosciences, Franklin Lakes, NJ, USA). Post-sorting evaluation confirmed a purity >99% for two bone marrow-derived DC (BMDC) populations. OVA-specific $CD4^+$ DO11.10 cells were isolated as described above and stained with 5 µM CellTrace CTV before incubation with sorted DCs at a ratio of (3:1) and 1 µg/ml Xcl1-OVA, fliC-OVA, or αNIP-OVA for 4 days. As a positive control, cells were incubated with 0.5 µg/ml of the $OVA_{323\text{-}339}$ peptide. Proliferation of DO11.10 cells were determined by flow cytometry on an Attune NxT (Thermo Fisher Scientific, Waltham, MA, USA).

In Vivo Th Polarization

OVA-specific DO11.10 cells were isolated as for *in vitro* Th polarization, and 1×10^6 cells transferred to naïve mice one day before intradermal immunization with 25 μg DNA encoding αNIP-, Xcl1-, or fliC-OVA. Inguinal and axillary LNs were harvested on specified days after immunization and single-cell suspensions generated using GentleMACS dissociator (Miltenyi Biotec). In short, LNs were placed in C MACS tubes containing complete RPMI medium dissociated by running program B on the GentleMACS dissociator. After filtration, the single-cell suspensions from LNs were filtered through a 70-μm nylon cell strainer washed in PBS and analyzed by flow cytometry after staining for anti-CD19, anti-CD14, anti-CD3, anti-CD4, anti-DO11.10, anti-T-bet, ant-GATA3, and anti-RORγt. Data were acquired on a Fortessa (BD) flow cytometer and analyzed using FlowJo software (FlowJo, LLC).

IL-12 Blocking

In vitro cocultures of BMDC and DO11.10+ CD4+ T cells in the presence of Xcl1, fliC-, or αNIP-Ova were treated with 10 μg/ml of anti-IL12 (AF-419-SP, R&D Systems, Minneapolis, MN, USA) or an unspecific isotype antibody control for 72 h. DO11.10$^+$CD4$^+$ T cells were then evaluated for the expression of transcription factors and supernatants harvested for cytokine ELISA as described above.

In vivo: mice were vaccinated as described in the intradermal DNA vaccination. For the early time-point blockade, 500 μg of anti-IL12 antibody (clone R2-9A5) (Bio X Cell, Lebanon, NH, USA) was injected i.p 1 and 2 days after vaccination, while for the later time inhibition the anti-IL12 antibody was injected on days 6 and 7. Controls at each time point received an unspecific isotype control antibody.

In Vivo Cytotoxicity

Cytotoxicity was performed as previously described (31). In short, splenocytes from BALB/c mice were incubated with the HA-derived MHC-I restricted peptide (IYSTVASSL) or an unspecific control peptide at a concentration of 1 μg/ml in 5×10^7 cells/ml for 1 h at 4°C. Peptide-loaded cells were stained with 1.25 μM (negative control) or 12.5 μM (IYSTVASSL) CellTrace™ Violet (Thermo Fisher) for 30 min at 37°C, before they were washed 2× in PBS, resuspended in PBS at a concentration of 5×10^7 cells/ml, and mixed 1:1. A total of 1×10^7 cells were injected *i.v.* into BALB/c or BATF3$^{-/-}$ mice that had been DNA immunized with 25 μg Xcl1-HA, fliC-HA, or NaCl 9 days prior. After 18 h, spleens were harvested and the ratio of CTV^{low} to CTV^{high} determined by flow cytometry. Cytotoxicity was calculated as % specific lysis = [1 - (Avg NaCl ratio/ experimental ratio)] × 100.

Statistics

All statistical analyses were performed using the GraphPad Prism 8 software. Significant differences in antibody responses, cytokine ELISA, or T-cell responses were calculated using the parametric t-test or non-parametric t-test (Mann–Whitney) when comparing two treatment groups and one-way ANOVA with multiple-comparison correction when comparing >2 groups (*$p < 0.05$, **$p < 0.01$, ***$p < 0.001$). Differences in antibody responses over time and weight curves after infection were calculated using two-way ANOVA (*$p < 0.05$, **$p < 0.01$, ***$p < 0.001$). Differences in survival were calculated by Mantel–Cox (*$p < 0.05$, **$p < 0.01$, ***< 0.001). Data and error bars are presented as mean ± SEM.

RESULTS

Xcl1-Fusion Vaccines Induce Rapid Th1 Responses After DNA Vaccination

To better understand the mechanism of how targeting cDCs can influence the polarization of the immune response, we compared Xcl1- and fliC-fusion vaccine molecules, as these have previously been seen to induce differently polarized antibody responses (**Supplementary Figure 1A**) (28, 32). While Xcl1-fusion vaccines target the Xcr1 receptor which is specifically expressed on cDC1s (5, 6, 29), the surface receptor for fliC, TLR5, has been reported to be expressed on CD11b$^+$ cDC2s (**Supplementary Figure 1B**) (23). However, when staining for TLR5 in spleen we only observed a small percentage of TLR5$^+$ DC, although the percentage was higher on cDC2 than cDC1s (**Supplementary Figure 1C**). In addition, fliC has also been reported to activate the intracellular NLRC4–NAIP5 inflammasome activating complex, suggesting that fliC-fusion vaccines may enhance immune responses though several mechanisms. Intradermal (i.d.) DNA vaccination using Xcl1- or fliC-fusion vaccines containing hemagglutinin (HA) from influenza A/Puerto Rico/8/34 (PR8) as an antigen demonstrated that fliC-HA induced almost exclusively antibodies of the IgG1 subclass, while Xcl1-HA induced higher titers of IgG2a and IgG2b (**Figures 1A, B** and **Supplementary Figure 1D**) (22). Both vaccines did, however, induce protection against a lethal dose (50xLD$_{50}$) of influenza A (PR8) (**Supplementary Figures 1E, F**).

The IgG subclass data suggest that Xcl1- and fliC-HA differentially influence Th polarization. To test this, IFNγ and IL4 ELISPOT assays were performed on splenocytes from BALB/C mice vaccinated by i.d. DNA immunization (**Supplementary Figures 2A, B**). Spleens were harvested 1 or 2 weeks after vaccination, and single-cell suspensions were stimulated with the MHC-II restricted HA peptide HNTNGVTAACSHEG. Already after 1 week, immunization with Xcl1-HA induced INFγ–secreting splenocytes (**Supplementary Figure 2A**). Neither of the vaccines induced IL4-secreting splenocytes above background at this time point (data not shown). Somewhat surprisingly, fliC-HA induced significantly higher numbers of IFNγ–secreting cells compared to Xcl1-HA immunized mice after 2 weeks, while there was no difference in IL4-secreting splenocytes (**Supplementary Figure 2B**).

The ELISPOT results suggest that Xcl1-fusion vaccines rapidly induce IFNγ–secreting splenocytes when delivered by i.d. DNA vaccination. To obtain a better understanding of the kinetics, we utilized DO11.10 transgenic mice that have CD4$^+$ T cells with a TCR specific for the peptide OVA$_{323\text{-}339}$ presented on

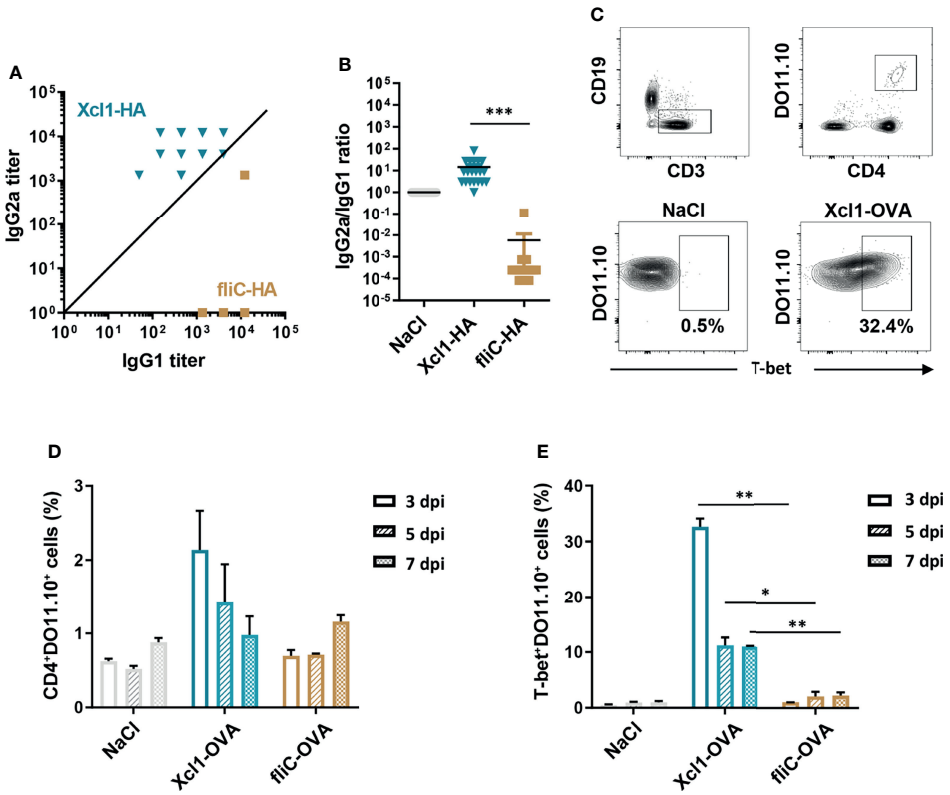

FIGURE 1 | DNA immunization with Xcl1-HA induces rapid Th1-associated immune responses. **(A)** IgG1 and IgG2a anti-HA antibodies in sera from BALB/C mice obtained 2 weeks after a single i.d. DNA immunization/electroporation with 25 µg plasmid encoding Xcl1-HA or fliC-HA. **(B)** IgG2a/IgG1 ratios in single mice presented in **(A)**. **(C–E)** 1×10^6 naïve DO11.10 cells were transferred to BALB/c mice that were subsequently immunized with 25 µg plasmid encoding Xcl1-OVA or fliC-OVA. Inguinal LNs were harvested 3, 5, or 7 days after vaccination. **(C)** Gating strategy for identification of $CD4^+DO11.10^+$ and expression of the transcription factor T-bet. **(D)** Percentage of $CD4^+DO11.10^+$ cells and **(E)** $T\text{-bet}^+$ DO11.10 cells elicited by immunization. Data shown are either pooled from 2 independent experiments **(A, B)**, or representative of two independent experiments **(C–E)**, with 20 **(A, B)**, or 3 **(C–E)** mice per group. Statistical analysis was performed using the non-parametric t-test **(B)** or one-way ANOVA with Tukey's multiple-comparison test comparing Xcl1-OVA and fliC-OVA for the different timepoints **(D, E)**. *$p < 0.05$, **$p < 0.01$, ***$p < 0.001$.

the MHC-II molecule $I\text{-}A^d$ (33). 1×10^6 $CD4^+DO11.10$ cells were injected i.v. into naïve BALB/c mice that were immunized 1 day later by i.d. delivery of DNA encoding Xcl1-OVA, fliC-OVA, or NaCl followed by electroporation. Draining LNs were harvested 3, 5, or 7 days after immunization and evaluated for proliferation and polarization of DO11.10 cells (**Figures 1C–E**). DNA immunization with Xcl1-OVA induced the highest percentage of $CD4^+DO11.10^+$ cells on day 3 after vaccination (**Figure 1D**). $CD4^+DO11.10^+$ cells were then analyzed for expression of T-bet, GATA-3, or RORγt, indicative of Th1, Th2, or Th17 cells, respectively. Xcl1-OVA induced a high percentage of $T\text{-bet}^+DO11.10$ cells already at day 3 after immunization, which dropped off on days 5 and 7 after immunization, probably reflecting egress of T cells from the LN (**Figure 1E**). However, there were still ~10% $T\text{-bet}^+DO11.10$ cells remaining at days 5 and 7 after immunization (**Figure 1E**). While Xcl1-OVA also induced a higher percentage of $GATA3^+$ and $ROR\gamma t^+$ cells 3 days after immunization, the numbers declined at 5 and 7 days after immunization (**Supplementary Figures 2C, D**). Consequently, DNA immunization with Xcl1-OVA induces expansion of $T\text{-bet}^+$ cells with a clear Th1 phenotype within 1 week. In contrast, there was hardly any enhanced proliferation of DO11.10 cells after DNA immunization with fliC-OVA, although we did observe a slight increase on day 7 after immunization. To ensure that the OVA antigen did not adversely affect the antibody polarization, serum samples were analyzed for OVA-specific IgG1 and IgG2a antibody titers 2 weeks after i.d. DNA immunization with Xcl1- or fliC-OVA. As seen with fliC-HA, fliC-OVA induced an almost exclusive IgG1 response, while Xcl1 induced higher titers of IgG2a (**Supplementary Figure 2E**).

Xcl1-OVA Fusion Proteins Enhance Th1 Polarization *In Vitro* and *In Vivo*

The observation that i.d. DNA vaccination with fliC-OVA induced poor proliferation of $CD4^+$ T cells *in vivo* was surprising. To test if this observation was related to the use of DNA, bone marrow-derived DCs (BMDCs) were incubated with DO11.10 cells and purified Xcl1- or fliC-OVA proteins in various concentrations for 72 h. In addition, we also included anti-NIP-OVA (referred to as αNIP) to serve as non-targeted control.

Proliferation of the OVA-specific CD4$^+$ T cells was determined by evaluating incorporation of radioactive thymidine (**Figure 2A**). Interestingly, purified fliC-OVA induced strong proliferation of DO11.10 cells, which was significantly higher than the non-targeted αNIP-OVA at 2 and 0.2 μg/ml. In contrast, Xcl1-OVA induced significantly higher proliferation than αNIP-OVA at concentrations <2 μg/ml and higher than fliC-OVA at 0.02 μg/ml (**Figure 2A**).

To study CD4$^+$ T cell polarization mediated by Xcl1- or fliC-fusion vaccines, DO11.10 cells were incubated with BMDCs in the presence of 0.5 μg/ml Xcl1-OVA, fliC-OVA, or αNIP-OVA for 72 h. 0.5 μg/ml was chosen since this concentration induced similar proliferation with fliC- and Xcl1-OVA (**Figure 2A**). After 72 h, DO11.10 cells incubated with Xcl1-OVA displayed significantly higher expression levels of T-bet compared to αNIP-OVA- or fliC-OVA-incubated cells (**Figure 2B**). As seen

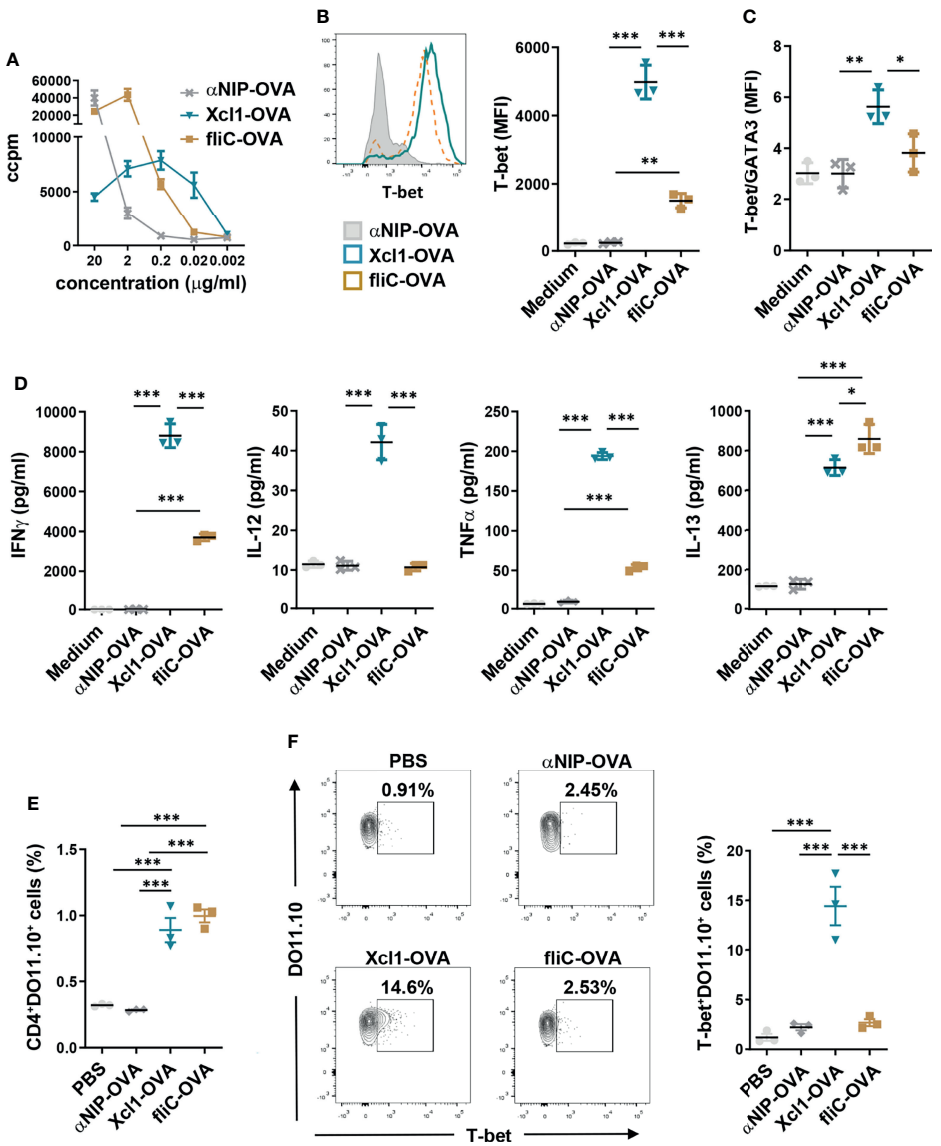

FIGURE 2 | Xcl1-OVA induces Th1 polarization of DO11.10 cells *in vitro* and *in vivo*. **(A)** CD4$^+$ cells were purified from spleen of DO11.10 TCR transgenic mice and incubated with BMDCs as APC in the presence of indicated amounts of Xcl1, fliC, or NIP-OVA protein for 72 h. Incorporation of radioactive thymidine was analyzed after 48 h. **(B–D)** CD4$^+$ from DO11.10 transgenic mice were incubated with BMDC in the presence of Xcl1-, fliC-, or NIP-OVA proteins (0.5 μg/ml) for 72 h. **(B)** CD4$^+$ DO11.10$^+$ cells were evaluated for expression of T-bet by flow cytometry. MFI for T-bet expression is summarized in the right graph. **(C)** Ratio of T-bet/GATA3 MFI for CD4$^+$DO11.10$^+$ cells in mice from **(B)** and **Supplementary Figure 3A**. **(D)** Concentrations of IFNγ, IL-12, TNFα, and IL-13 in supernatants. **(E, F)** 1 × 10^6 naïve DO11.10 cells were transferred to BALB/c mice that were subsequently injected i.v. with purified Xcl1-OVA, fliC-OVA, or αNIP-OVA proteins (5 μg). Spleens were harvested 72 h later and the percentage of **(E)** CD4$^+$DO11.10$^+$ and **(F)** T-bet$^+$DO11.10$^+$ cells determined by flow cytometry. Data are representative of one **(A)** or three **(B–D)** independent experiments with n = 3 samples per group. **(E, F)** Data from one experiment with n = 3 mice per group. Statistical analysis was performed by one-way ANOVA with Tukey's multiple-comparison corrections. *p < 0.05, **p < 0.01, ***p < 0.001.

after DNA vaccination *in vivo*, Xcl1-OVA also induced higher levels of GATA3 and RORγt compared to fliC-OVA, although the difference was lower than for T-bet (**Supplementary Figure 3A**). Indeed, when calculating the T-bet/GATA3 ratio, Xcl1-OVA clearly stood out as the strongest inducer of T-bet (**Figure 2C**). In accordance with the upregulation of T-bet, the supernatant from cells incubated with Xcl1-OVA contained significantly higher levels of the Th1-associated cytokines IFNγ, IL-12, and TNFα compared to supernatants from cells incubated with either fliC-OVA or αNIP-OVA (**Figure 2D**). DO11.10 cells incubated with fliC-OVA did not induce a clear polarization toward any Th subset based on the expression of T-bet, GATA-3, or RORγt (**Figures 2B, C** and **Supplementary Figure 3A**), although fliC-OVA induced slightly higher levels of IL-13 compared to Xcl1-OVA (**Figure 2D**). No difference was observed between Xcl1-OVA and fliC-OVA when determining secretion of the Th17-associated cytokine IL-17A, despite Xcl1-OVA inducing a higher expression of RORγt (**Supplementary Figures 3A, B**).

To obtain a better understanding on which DC subsets are presenting antigen to the DO11.10, sorted BM-derived cDC1s and cDC2s were incubated with CTV-labeled DO11.10 cells and 1 μg/ml Xcl1-OVA, fliC-OVA, or αNIP-OVA for 4 days. As expected, Xcl1-OVA predominantly induced proliferation of DO11.10 cells when incubated with cDC1s (**Supplementary Figures 3C, D**). While fliC-OVA induced significantly higher proliferation of DO11.10 cells on cDC2s compared to Xcl1-OVA, we were surprised to see that fliC-OVA also induced proliferation when incubated with cDC1s (**Supplementary Figures 3C, D**). Whether this is due to low-level TLR5 expression on BM cDC1s or activation of the NLRC4–NAIP5 inflammasome remains to be determined.

To test proliferation and polarization *in vivo*, 1×10^6 $CD4^+DO11.10$ cells were transferred to naïve BALB/c mice that were injected i.v. 1 day later with 5 μg purified Xcl1-, fliC-, or αNIP-OVA protein. After 3 days, spleens were harvested and single-cell suspensions analyzed by flow cytometry. Immunization with both Xcl1-OVA and fliC-OVA significantly enhanced the proliferation of DO11.10 cells, compared to αNIP-OVA- or PBS-immunized mice (**Figure 2E**). Correlating with our observations from DNA vaccination, immunization with Xc1-OVA protein induced a significantly higher percentage of $T\text{-}bet^+DO11.10$ cells, compared to fliC-OVA and αNIP-OVA (**Figure 2F**). No increase in $T\text{-}bet^+DO11.10$ cells was observed after immunization with fliC-OVA, although we did observe a slight but significant increase in the number of $GATA3^+DO11.10^+$ cells compared to αNIP-OVA (**Supplementary Figure 4A**). There was no difference in the percentage of $ROR\gamma t^+$ DO11.10 cells in mice immunized with Xcl1-OVA or fliC-OVA, although there was a slight increase for both compared to αNIP-OVA (**Supplementary Figure 4B**).

Xcl1-OVA-Induced Th1 Polarization Is Dependent on IL-12, but Independent of BATF3

Targeting antigens to the lectin receptor DEC-205 expressed on cDC1s has been reported to induce IL-12-independent Th1 responses through upregulation of CD70 (34). To evaluate the role of IL-12 in induction of Th1 responses when targeting cDC1s using Xcl1, DO11.10 cells were incubated with BMDCs and 0.5 μg/ml Xcl1-OVA, fliC-OVA, or αNIP-OVA protein in addition to the anti-IL-12 antibody. Blocking of IL-12 resulted in a significant reduction in T-bet expression in DO11.10 cells incubated with both Xcl1-OVA and fliC-OVA (**Figure 3A**). Correlating with reduced expression of T-bet, there was a significant reduction in the secretion of IFNγ (**Figure 3B**). Incubation with Xcl1-OVA in the presence of anti-IL-12 did not significantly influence the expression of GATA3 or the secretion of IL-4 (**Supplementary Figures 5A, B**).

To explore the IL-12 dependency of Xcr1-targeted Th1 responses *in vivo*, we transferred 1×10^6 DO11.10 cells to naïve BALB/c mice which were then immunized with 25 μg DNA encoding for Xcl1-OVA i.d 24 h later. The mice were subsequently injected i.p. with either 0.5 mg anti-IL-12 or isotype-matched control 24 and 48 h after vaccination. Skin-draining LNs and spleens were then harvested on day 7 after vaccination. Single-cell suspensions from the LNs were analyzed by flow cytometry, while splenocytes were restimulated with 2 μg/ml of the $OVA_{323\text{-}339}$ peptide for 48 h and secretion of IFNγ was analyzed by ELISA. Interestingly, there was a significant decline in the expansion of $T\text{-}bet^+$ DO11.10 cells in mice treated with anti-IL-12 (**Figure 3C**). The expression level of T-bet was however comparable between anti-IL-12-treated and control mice (**Figure 3D**). In accordance with fewer Th1 cells, there was a significant drop in the secretion of IFNγ from mice that were injected with anti-IL-12 antibodies compared with isotype control mice (**Figure 3E**). Taken together, our results suggest that the expansion of Th1 cells after i.d. DNA vaccination with Xcl1-OVA is IL-12 dependent.

BATF3 is a transcription factor that is essential for the development of $Xcr1^+$ cDC1s in spleen and $CD103^+Xcr1^+$ migratory cDC1s in skin-draining LN (35). Previous studies using different infectious models have suggested that the BATF3-dependent migratory $CD103^+$ cDC1s are the main producers of IL-12 that drive Th1 polarization (30). To test how the absence of BATF3 impacted the observed Th1 polarization seen with Xcl1-OVA, $BATF3^{-/-}$ were immunized with Xcl1-OVA, fliC-OVA, or αNIP-OVA by i.v. injection of purified protein and by i.d. DNA immunization. After i.v. injection of protein, fliC-OVA induced the proliferation of DO11.10 cells in spleen, potentially by targeting the BATF3-independent cDC2 population (**Supplementary Figure 5C**). In contrast, we observed no proliferation or induction of $T\text{-}bet^+$ DO11.10 cells with Xcl1-OVA after i.v. injection (**Figure 4A** and **Supplementary Figure 5C**). Surprisingly, DNA immunization with Xcl1-OVA induced a strong increase in the number of $CD4^+DO11.10^+$ and $T\text{-}bet^+$ DO11.10 cells in the $BATF3^{-/-}$ mice (**Figure 4B** and **Supplementary Figure 5D**). Indeed, the frequency of $T\text{-}bet^+$ DO11.10 cells was similar to those seen in BALB/c mice (**Figure 2F**), indicating that Th1 polarization after i.d. DNA vaccination with Xcl1-OVA is BATF3-independent. In support of this observation, i.d. DNA immunization with fliC-HA or Xcl1-HA in $BATF3^{-/-}$ mice induced a similar IgG1 to

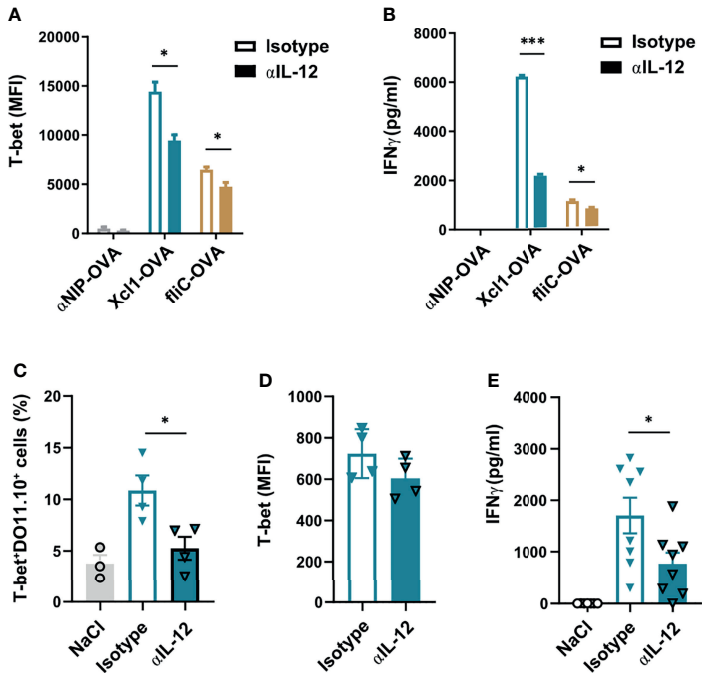

FIGURE 3 | Xcl1-OVA induced Th1 polarization is IL12 dependent. **(A, B)** $CD4^+$ cells from DO11.10 mice were incubated with BMDCs and Xcl1-OVA, fliC-OVA, or αNIP-OVA proteins (0.5 μg/ml), and either anti-IL-12 or isotype-matched mAbs (10 μg/ml) for 72 h. **(A)** DO11.10 cells were evaluated for expression of T-bet by flow cytometry, and **(B)** supernatants tested for secretion of IFNγ by ELISA. **(C–E)** 1×10^6 naïve DO11.10 cells were transferred i.v. to BALB/c mice that were subsequently immunized i.d. with 25 μg DNA encoding Xcl1-OVA. On days 1 and 2 after immunization, mice were injected i.p. with anti-IL12 or isotype-matched mAb (0.5 mg). Skin draining LNs and spleens were harvested after 1 week, and LN analyzed for **(C)** percentage of $T\text{-bet}^+DO11.10^+$ cells and **(D)** MFI of T-bet expression in $T\text{-bet}^+DO11.10^+$ cells. **(E)** Secretion of IFNγ from splenocytes stimulated for 24 h with the DO11.110 peptide. Data representative of two **(A–D)** or pooled from two **(E)** independent experiments with n = 3 samples per group **(A, B)**, n = 3–4 mice per group **(C, D)** or n = 7–8 mice per group **(E)**. Statistical analysis performed using the parametric t-test. *$p < 0.05$, ***$p < 0.001$.

IgG2a-polarized antibody response as in BALB/c mice (**Supplementary Figure 5E**).

To investigate the observed difference between i.v. protein and i.d. DNA vaccination with Xcl1-OVA, we analyzed Xcr1 expression on $MHC\text{-}II^+CD11c^+$ DCs from spleen and skin-draining LN after i.d. DNA immunization. In skin-draining LN, migratory DCs (migDCs) were defined as $CD11c^{int}MHC\text{-}II^{high}$, while resident DCs (resDCs) were defined as $CD11c^{high}MHC\text{-}II^{int}$. While $CD24^+Xcr1^+$ DCs were absent in the spleen of $BATF3^{-/-}$ mice, we observed a clear population of $CD24^+Xcr1^+$ resDCs in inguinal LNs from the same mice (**Figure 4C** and **Supplementary Figure 5F**). However, we did not observe any $CD24^+$ $Xcr1^+$ migDC in the LN from BATF3 KO mice, which is in accordance with previous observations (35). The presence of $Xcr1^+$ resident DCs in LN provides a possible explanation of why i.d. DNA immunization with Xcl1-OVA still induces $CD4^+$ T cell proliferation and Th1 polarization in the $BATF3^{-/-}$ mice.

To evaluate if the immune responses seen in $BATF3^{-/-}$ mice was sufficient to mediate protection against influenza infection, $BATF3^{-/-}$ mice were DNA immunized with Xcl1-HA or fliC-HA and challenged with 5xLD50 2 weeks later. Both Xcl1-HA- and fliC-HA-immunized mice were protected from challenge and only displayed moderate weight loss during the infection (**Figures 4D, E**). As $BATF3^{-/-}$ mice do not induce cytotox T cell responses after DNA vaccination (**Figure 4F**), this observation suggests that protection seen with Xcl1-HA is predominantly mediated by the antibody response.

Xcl1-Fusion Vaccines Maintain Th1/IgG2a Polarization When Combined With fliC-Fusion Vaccines *In Vitro* and *In Vivo*

Our results suggest that while Xcl1-fusion vaccines enhance Th1 polarization *in vitro* and *in vivo*, the fliC-fusion vaccines had a more modest Th2 polarization *in vitro*. The lack of a clear Th2 polarization with fliC-fusion vaccines is surprising given the highly IgG1-polarized antibody response seen after DNA vaccination with fliC-HA. fliC has previously been described to actively inhibit Th1 polarization (36), which could explain why fliC-OVA did not induce Th1 responses despite inducing proliferation of DO11.10 cells when incubated with cDC1s. To test if this was the case, DO11.10 cells were stimulated with BMDCs and a mixture of Xcl1-OVA and fliC-OVA. The Xcl1-OVA/fliC-OVA mix induced lower levels of T-bet compared to Xcl1-OVA alone, although the difference was not significant, and probably reflects the fact that half the concentration of Xcl1-OVA was present in the mix (**Supplementary Figure 6A**). There was also a slight reduction in GATA3 expression with the mix compared to Xcl1-OVA alone (**Supplementary Figure 6A**).

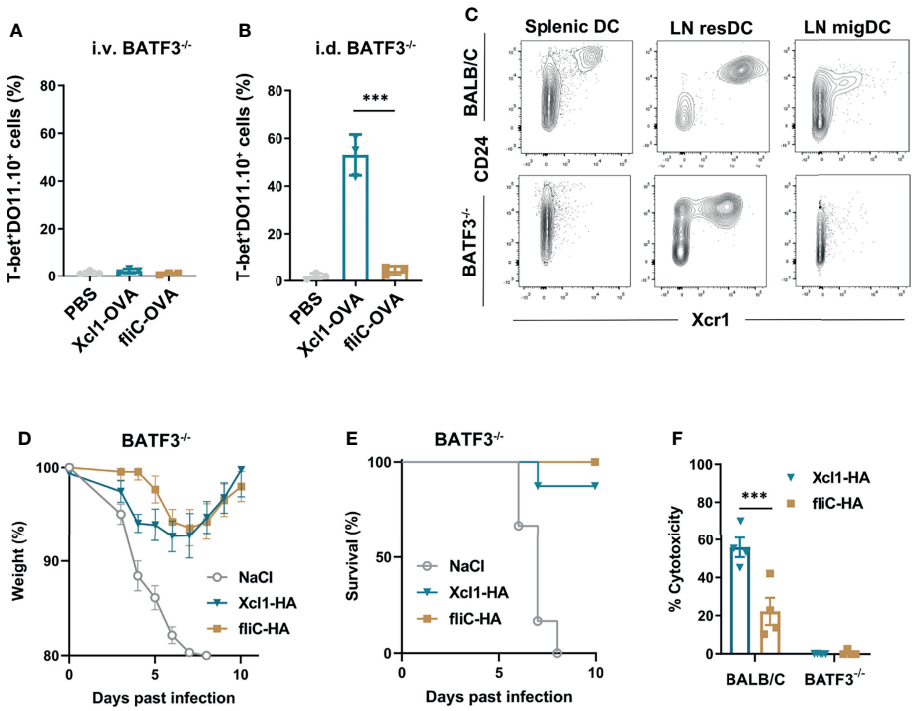

FIGURE 4 | Xcl1-OVA induced Th1 polarization is independent of BATF3. **(A, B)** BATF3$^{-/-}$ mice were injected i.v. with 1 × 10^6 naïve DO11.10 cells, and 24 h later **(A)** given an i.v. injection of either purified Xcl1- or fliC-OVA proteins (5 µg) or **(B)** DNA immunized i.d. with 25 µg plasmid encoding either Xcl1-OVA or fliC-OVA. The percentages of T-bet$^+$ DO11.10 cells evaluated in spleens **(A)** or in LNs **(B)** 3 days after immunization. **(C)** Spleens and inguinal LNs were harvested from BALB/c or BATF3$^{-/-}$ mice and analyzed for CD24$^+$Xcr1$^+$ cDC1s by flow cytometry after first gating on Lin$^-$MHC-II$^+$CD11c$^+$ cells. Migratory DCs were defined as CD11c^{int}MHC-II^{high} and resident DCs as CD11c^{high}MHC-II^{int} (**Supplementary Figure 5F**). **(D, E)** BATF3$^{-/-}$ mice were DNA immunized with 25 µg plasmid encoding either Xcl1-OVA or fliC-OVA and challenged 14 days later with 5xLD50 PR8 virus. **(D)** Weight and **(E)** survival was monitored for 10 days. **(F)** *In vivo* cytotoxicity after DNA immunization with 25 µg plasmid encoding either Xcl1-OVA or fliC-OVA in BALB/c or BATF3$^{-/-}$ mice. Data representative of two **(A–C)**, pooled from two **(D, E)** or from one **(F)** independent experiments with n = 3 samples per group **(A, B)**, n = 3–4 mice per group **(C, F)** or n = 6–8 mice per group **(D, E)**. Statistical analysis performed using parametric t-test. ***p < 0.001.

When evaluating cytokines expressed in supernatants, the Xcl1-OVA/fliC-OVA mix induced equal levels of IFNγ, and lower levels of IL-12 compared to Xcl1-OVA (**Supplementary Figure 6B**). Together, these results indicate that the Th1 polarization is largely maintained in the mix and not actively inhibited by the fliC-fusion protein.

Next, we tested if Xcl1-HA was able to skew the antibody response in the direction of IgG2a *in vivo* when combined with fliC-HA and delivered by i.d. DNA vaccination. As controls, BALB/c mice were immunized with Xcl1-HA and fliC-HA separately, or Xcl1-HA and fliC-HA delivered on opposite flanks of the mouse. Immunization on opposite flanks should predominantly result in draining and T cell priming in separate inguinal LNs. Serum samples were harvested after 2 weeks and evaluated for the presence of HA-specific antibodies of the IgG1, IgG2a, and IgG2b subclasses. As observed in **Figure 1**, immunization with Xcl1-HA or fliC-HA induced antibody responses dominated by IgG2a/IgG2b and IgG1, respectively (**Figure 5A**). Immunization with a mix of Xcl1-HA and fliC-HA induced similar levels of IgG1 as fliC-HA alone but significantly higher titers of IgG2a. Consequently, the IgG2a/IgG1 ratio seen with the mix was similar to that of Xcl1-HA alone (**Figure 5B**). In contrast, immunization with Xcl1-HA and fliC-HA on separate flanks induced similar titers of IgG1 and lower titers of IgG2a compared to the mix, resulting in a lower IgG2a/IgG1 ratio (**Figures 5A, B**). Together, these results suggest that the Xcl1-fusion vaccine exerts dominance in determining the polarization of the antibody response.

A Rapid Th1 Response Is Required for an IgG2a-Dominated Response and Contributes to Protective Responses

To further test how the kinetics of the Th1 response influence antibody polarization, we immunized mice with a mix of Xcl1-HA and fliC-HA and subsequently injected the anti-IL-12 or isotype antibody i.p. on days 1 and 2 or days 6 and 7 after immunization. The mix vaccine was chosen as it induced the strongest antibody responses with similar polarization to Xcl1-HA. Serum samples were harvested after 2, 5, 8, and 12 weeks after immunization and evaluated for HA-specific antibodies of the IgG1, IgG2a, and IgG2b subclasses. Early injection of anti-IL-12 resulted in a significant reduction in IgG2a and IgG2b titers at 5, 8, and 12 weeks after immunization (**Figure 5C**, **Supplementary Figure 6C**). In contrast, there was no difference in IgG2a when anti-IL-12 was injected on days 6 and 7 after immunization (**Figure 5C**). There was also no

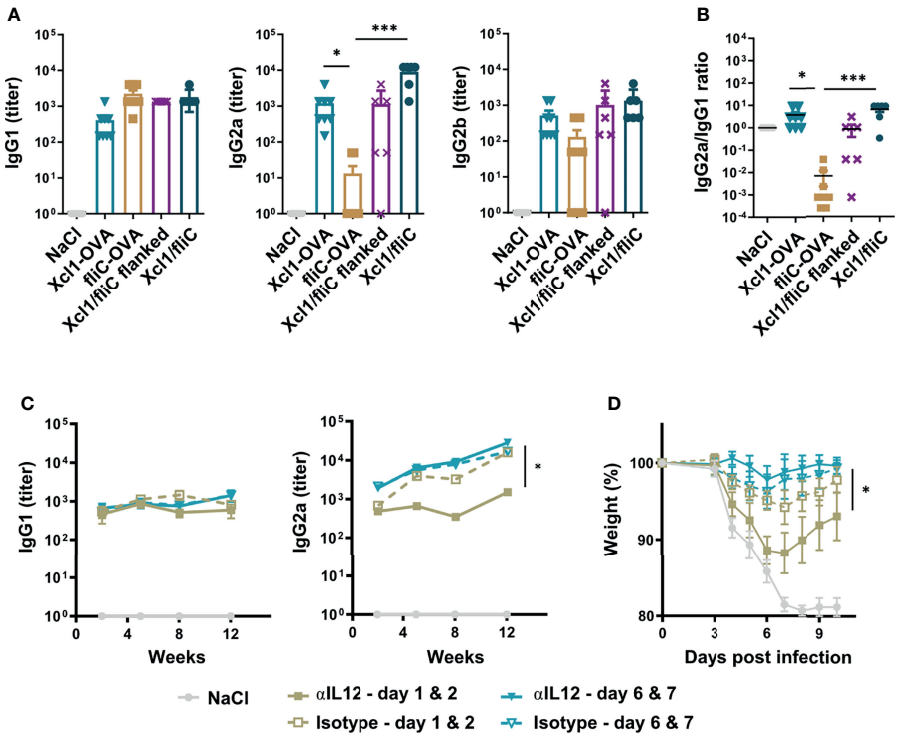

FIGURE 5 | Rapid Th1 induction is essential for induction of an IgG2a dominated response and improves protection induced by a mixed fliC-/Xcl1-HA vaccine. **(A, B)** DNA immunization of BALB/c mice with 25 µg DNA encoding Xcl1-HA, fliC-HA, a mixture of Xcl1-HA and fliC-HA, or Xcl1-HA and fliC-HA delivered on opposite flanks. **(A)** Serum titers of IgG1, IgG2a, and IgG2b were determined 2 weeks after vaccination. **(B)** IgG2a/IgG1 ratio of the serum samples presented in **(A)**. **(C, D)** Injection of either anti-IL-12 or isotype-matched mAbs on days 1 and 2 or 6 and 7 after DNA immunization with a mix of Xcl1-HA and fliC-HA plasmids. **(C)** Serum samples were harvested at the indicated time points and evaluated for the presence of HA-specific IgG1 or IgG2a. **(D)** Mice in **(C)** were challenged with 5xLD50 PR8 virus 12 weeks after immunization and weight loss monitored. Data representative of one experiment with n = 6–8 mice per group **(A, B)**, representative of two independent experiments with n = 4 mice per group **(C)** or pooled from two independent experiments with n = 8 mice per group **(D)**. Statistical analysis performed by non-parametric one-way ANOVA with Dunn's multiple-comparison corrections **(A, B)**, or two-way ANOVA with Tukey's multiple-comparison test **(C, D)**. *$p < 0.05$, ***$p < 0.001$.

difference in the HA-specific IgG1 titer after 5, 8, or 12 weeks, suggesting that injection of anti-IL-12 only affected Th1-associated IgG subclasses. Interestingly, early injection of anti-IL-12 resulted in more dramatic weight loss after influenza infection after 12 weeks, compared to injection of anti-IL-12 on days 6 and 7 after immunization (**Figure 5D**). There was also a reduction in the overall survival, although the difference was not significant (**Supplementary Figure 6D**). These results suggest that the early Th1 response is important for obtaining a strong IgG2a response and that Th1 cells contribute to the protection seen with the Xcl1/fliC vaccine.

In summary, our observations indicate that antibody polarization after DNA vaccination is determined very early after immunization and that Xcl1 fusion vaccines preferentially induce IgG2a and IgG2b due to a rapid induction of Th1 cells.

DISCUSSION

Here we compare Xcl1- and fliC-fusion vaccines in terms of the ability to differently influence the polarization of the resulting immune response. While Xcl1-fusion vaccines rapidly polarize $CD4^+$ T cells toward Th1 after immunization, fliC-fusion vaccines induced a more mixed Th1/Th2 polarization despite inducing almost exclusively antibodies of the IgG1 subclass. We further demonstrate that inhibiting Th1 polarization early after DNA immunization significantly reduced IgG2a and IgG2b responses, resulting in poorer protection against influenza infection. The results suggest that early induction of Th1 responses is a key determining factor in the polarization of the antibody response.

Previous studies have suggested that cDC1s and cDC2s preferentially polarize $CD4^+$ T cells toward Th1 and Th2, respectively (9, 10). Indeed, our observations that Xcl1-fusion proteins induce IgG2a-dominated antibody responses and Th1 polarization support these findings (13, 19, 29, 31). However, we have recently observed that the choice of target-receptor on cDC1s can influence the resulting immune response (19). It is therefore possible that the Xcl1–Xcr1 ligand interaction could lead to downstream signaling events in the cDC1s that enhance Th1 responses. Indeed, early studies have suggested that Xcl1 functions in concert with IFNγ, MIP1α, MIP1β, and RANTES in promoting Th1 responses after infection (20). Although fliC-OVA also induced the proliferation of DO11.10 cells when

incubated with cDC1s *in vitro*, it did not induce any significant Th1 polarization in the *in vitro* or the *in vivo* experiments. This indicate that additional stimulation of the cDC1s is needed to induce Th1 polarization, although it is currently not clear if fliC-fusion proteins target cDC1s *in vivo* to any significant degree.

Our experiments suggest that the early kinetics of the Th1 responses is crucial in obtaining an IgG2a-polarized antibody response. Class switch recombination (CSR) has been considered to occur within the germinal center (GC) reaction in combination with affinity maturation through somatic hyper mutation (SHM) (37). However, a recent study by Roco et al. observed that CSR predominantly takes place prior to GC formation and largely within 3–4 days of antigen challenge (38). Here we observe that injecting anti-IL-12 on days 1 and 2 after i.d. DNA vaccination with a Xcl1/fliC-HA mix significantly reduced the induction of IgG2a. In contrast, delaying anti-IL-12 injection until days 6 and 7 did not influence the IgG2a titers. Our experiments therefore correlate with a rapid CSR through induction of Th1 cells, which should be taken into consideration when developing vaccines aimed at inducing Th1-polarized immune responses.

These experiments also indicate that IL-12 played an important role in inducing efficient Th1 polarization and IgG2a responses after intradermal DNA immunization with Xcl1 fusion vaccines. These observations are contrary to previous studies by Soares and colleagues where targeting the LACK antigen from *Leishmania major* to DEC-205 (CD205) expressed on cDC1s resulted in an IL-12-independent induction of Th1 responses (34). However, it should be noted that these experiments were performed with addition of poly(I:C) as an adjuvant, which activates TLR3 expressed on cDC1s (25). Indeed, older studies have observed that viral infections with RNA viruses, which can trigger TLR3 activation, also induce an IL-12-independent induction of Th1 $CD4^+$ T cell and IgG2a responses (39).

Interestingly, i.d. DNA vaccination with Xcl1-OVA induced equal Th1 polarization and IgG2a induction in $BATF3^{-/-}$ mice. These mice have been reported to lack IL-12-producing $CD103^+$ cDC1s, disrupting their ability to induce Th1 responses in response to *Leishmania major* infection (30). In our study, flow cytometry analysis of skin-draining LN demonstrated the presence of $Xcr1^+$ resDCs in the $BATF3^{-/-}$ mice, while the $Xcr1^+$ migDC population was absent. These results are in accordance with observations by Bachem and colleagues (35) and may suggest that $Xcr1^+$ resDCs are responsible for inducing the rapid Th1 responses after intradermal DNA immunization with Xcl1-fusion vaccines. However, specific depletion of these cells would be required to confirm this hypothesis.

DNA immunization of $BATF3^{-/-}$ did not give any cytotoxic T cell responses, although the mice were still protected from a lethal challenge with influenza virus. Consequently, the antibodies induced after one immunization with Xcl1-HA or fliC-HA were sufficient to protect against infection. In addition, our results may indicate that the $Xcr1^+$ migDC population is needed for the induction of cytotoxic $CD8^+$ T cell responses after DNA vaccination (31). However, it is also possible that lack of BATF3 directly influences the cytotoxic function of the $CD8^+$ T cells, as recent studies have shown that BATF3 regulates the formation of $CD8^+$ memory T cells (40, 41).

We have previously observed that XCL1-fusion proteins can bind cDC1s from humans (42), macaques (42), and pigs (16, 43), as expression of the XCR1 receptor appear to be largely conserved on cDC1s in mammals (44). Consequently, Xcl1-fusion may be utilized in both clinical and veterinary medicine. However, it is currently unclear if our observations that Xcl1-fusion vaccines enhance Th1 polarization can be translated to other species. For instance, both human cDC1s and cDC2s can secrete IL12 and induce Th1 polarization (45, 46), raising the question whether there is any added effect of human XCR1–XCL1 ligation.

FliC-fusion vaccines only induced antibodies of the IgG1 subclass after i.d. DNA vaccination, despite limited proliferation and polarization of DO11.10 cells in iLNs. The lack of T cell proliferation after DNA vaccination *in vivo* was surprising given the observation that fliC-OVA could induce T cell proliferation when incubated with purified cDC1s and cDC2s. We did however observe increased the numbers of IFNγ-secreting $CD4^+$ T cells 2 weeks after immunization by ELISPOT analysis. *In vitro*, the purified fliC-OVA protein induced a more mixed Th1/Th2 polarization, although we did observe a modest upregulation of GATA3 *in vivo*. Consequently, our observations are in line with previous studies suggesting that fliC can induce a mixed Th1/Th2 responses (47, 48), instead of a pronounced Th2 polarization (21). It is possible that the responses obtained with fliC-fusion vaccines are dependent on other cell types than cDC2s, as TLR5 has also been reported to be expressed on pDCs and $CD8^+Xcr1^-$ DCs in skin-draining LN (24, 25). Indeed, when evaluating TLR5 expression on DCs in spleen, we observed a low-level expression on both cDC1s and cDC2s. It is however unlikely that fliC directly induces class switch recombination to IgG1, considering that TLR5 has been reported to be absent from murine B cells (49).

In conclusion, our results demonstrate that IgG2a/IgG2b polarization of the antibody responses is determined early after immunization, which should be taken into account when designing or evaluating immunization strategies aimed at inducing specific subclasses of IgG. For instance, non-neutralizing mAbs against influenza HA have been reported to provide protection when injected as IgG2a through Fc-mediated effector function, but not when injected as IgG1 (50).

DATA AVAILABILITY STATEMENT

The original contributions presented in the study are included in the article/**Supplementary Material**. Further inquiries can be directed to the corresponding author.

ETHICS STATEMENT

All animal studies were reviewed and approved by Norwegian Food Safety Authority.

AUTHOR CONTRIBUTIONS

DT, SB, AL, EF, and BB designed the experiments and conceptualized the study. DT, SB, AL, AG, PCH, and RB performed and analyzed the experiments. EF, DT, and BB wrote the first draft of the manuscript. All authors contributed to the article and approved the submitted version.

FUNDING

This study was funded by KG Jebsen Foundation (KG Jebsen Foundation, BB), EuroNanoMed (EU Grant 2012023, BB), Norway, Regional Health Authority (HSØ grant 2019118, EF) and The Research Council of Norway (NFR, Grant 250884, EF).

ACKNOWLEDGMENTS

We thank Peter Hofgaard for technical assistance with experiments and animal handling and the Center for Comparative Medicine at Oslo University Hospital for assistance with animal handling.

SUPPLEMENTARY MATERIAL

The Supplementary Material for this article can be found online at: https://www.frontiersin.org/articles/10.3389/fimmu.2022.752714/full#supplementary-material

REFERENCES

1. Tesfaye DY, Gudjonsson A, Bogen B, Fossum E. Targeting Conventional Dendritic Cells to Fine-Tune Antibody Responses. *Front Immunol* (2019) 10:1529. doi: 10.3389/fimmu.2019.01529
2. Guilliams M, Ginhoux M, Jakubzick M, Naik M, Onai M, Schraml M, et al. Dendritic Cells, Monocytes and Macrophages: A Unified Nomenclature Based on Ontogeny. *Nat Rev Immunol* (2014) 14(8):571–8. doi: 10.1038/nri3712
3. Pooley JL, Heath WR, Shortman K. Cutting Edge: Intravenous Soluble Antigen is Presented to CD4 T Cells by CD8- Dendritic Cells, But Cross-Presented to CD8 T Cells by CD8+ Dendritic Cells. *J Immunol* (2001) 166 (9):5327–30. doi: 10.4049/jimmunol.166.9.5327
4. Bedoui S, Whitney PG, Waithman J, Eidsmo L, Wakim L, Caminschi I, et al. Cross-Presentation of Viral and Self Antigens by Skin-Derived CD103+ Dendritic Cells. *Nat Immunol* (2009) 10(5):488–95. doi: 10.1038/ni.1724
5. Dorner BG, Dorner MB, Zhou X, Opitz C, Mora A, Guttler S, et al. Selective Expression of the Chemokine Receptor XCR1 on Cross-Presenting Dendritic Cells Determines Cooperation With CD8+ T Cells. *Immunity* (2009) 31 (5):823–33. doi: 10.1016/j.immuni.2009.08.027
6. Crozat K, Tamoutounour S, Vu Manh TP, Fossum E, Luche H, Ardouin L, et al. Cutting Edge: Expression of XCR1 Defines Mouse Lymphoid-Tissue Resident and Migratory Dendritic Cells of the CD8{alpha}+ Type. *J Immunol* (2011) 187(9):4411–5. doi: 10.4049/jimmunol.1101717
7. Becker M, Guttler S, Bachem A, Hartung E, Mora A, Jakel A, et al. Ontogenic, Phenotypic, and Functional Characterization of XCR1(+) Dendritic Cells Leads to a Consistent Classification of Intestinal Dendritic Cells Based on the Expression of XCR1 and SIRPalpha. *Front Immunol* (2014) 5:326. doi: 10.3389/fimmu.2014.00326
8. Guilliams M, Dutertre CA, Scott CL, McGovern N, Sichien D, Chakarov S, et al. Unsupervised High-Dimensional Analysis Aligns Dendritic Cells Across Tissues and Species. *Immunity* (2016) 45(3):669–84. doi: 10.1016/j.immuni.2016.08.015
9. Maldonado-Lopez R, De Smedt T, Michel P, Godfroid J, Pajak B, Heirman C, et al. CD8alpha+ and CD8alpha- Subclasses of Dendritic Cells Direct the Development of Distinct T Helper Cells *In Vivo*. *J Exp Med* (1999) 189 (3):587–92. doi: 10.1084/jem.189.3.587
10. Pulendran B, Smith JL, Caspary G, Brasel K, Pettit D, Maraskovsky E, et al. Distinct Dendritic Cell Subsets Differentially Regulate the Class of Immune Response *In Vivo*. *Proc Natl Acad Sci USA* (1999) 96(3):1036–41. doi: 10.1073/pnas.96.3.1036
11. Kastenmuller W, Kastenmuller K, Kurts C, Seder RA. Dendritic Cell-Targeted Vaccines–Hope or Hype? *Nat Rev Immunol* (2014) 14(10):705–11. doi: 10.1038/nri3727
12. Caminschi I, Shortman K. Boosting Antibody Responses by Targeting Antigens to Dendritic Cells. *Trends Immunol* (2012) 33(2):71–7. doi: 10.1016/j.it.2011.10.007
13. Fossum E, Grodeland G, Terhorst D, Tveita AA, Vikse E, Mjaaland S, et al. Vaccine Molecules Targeting Xcr1 on Cross-Presenting DCs Induce Protective CD8+ T-Cell Responses Against Influenza Virus. *Eur J Immunol* (2015) 45(2):624–35. doi: 10.1002/eji.201445080
14. Terhorst D, Fossum E, Baranska A, Tamoutounour S, Malosse C, Garbani M, et al. Laser-Assisted Intradermal Delivery of Adjuvant-Free Vaccines Targeting XCR1+ Dendritic Cells Induces Potent Antitumoral Responses. *J Immunol* (2015) 194 (12):5895–02. doi: 10.4049/jimmunol.1500564
15. Bonifaz LC, Bonnyay DP, Charalambous A, Darguste DI, Fujii S, Soares H, et al. *In Vivo* Targeting of Antigens to Maturing Dendritic Cells via the DEC-205 Receptor Improves T Cell Vaccination. *J Exp Med* (2004) 199(6):815–24. doi: 10.1084/jem.20032220
16. Deloizy C, Fossum E, Barnier-Quer C, Urien C, Chrun T, Duval A, et al. The Anti-Influenza M2e Antibody Response is Promoted by XCR1 Targeting in Pig Skin. *Sci Rep* (2017) 7(1):7639. doi: 10.1038/s41598-017-07372-9
17. Li J, Ahmet F, Sullivan LC, Brooks AG, Kent SJ, De Rose R, et al. Antibodies Targeting Clec9A Promote Strong Humoral Immunity Without Adjuvant in Mice and Non-Human Primates. *Eur J Immunol* (2015) 45(3):854–64. doi: 10.1002/eji.201445127
18. Hartung E, Becker M, Bachem A, Reeg N, Jakel A, Hutloff A, et al. Induction of Potent CD8 T Cell Cytotoxicity by Specific Targeting of Antigen to Cross-Presenting Dendritic Cells *In Vivo* via Murine or Human XCR1. *J Immunol* (2015) 194(3):1069–79. doi: 10.4049/jimmunol.1401903
19. Fossum E, Tesfaye DY, Bobic S, Gudjonsson A, Braathen R, Lahoud MH, et al. Targeting Antigens to Different Receptors on Conventional Type 1 Dendritic Cells Impacts the Immune Response. *J Immunol* (2020) 205(3):661–73. doi: 10.4049/jimmunol.1901119
20. Dorner BG, Scheffold A, Rolph MS, Huser MB, Kaufmann SH, Radbruch A, et al. MIP-1alpha, MIP-1beta, RANTES, and ATAC/lymphotactin Function Together With IFN-Gamma as Type 1 Cytokines. *Proc Natl Acad Sci USA* (2002) 99(9):6181–6. doi: 10.1073/pnas.092141999
21. Didierlaurent A, Ferrero I, Otten LA, Dubois B, Reinhardt M, Carlsen H, et al. Flagellin Promotes Myeloid Differentiation Factor 88-Dependent Development of Th2-Type Response. *J Immunol* (2004) 172(11):6922–30. doi: 10.4049/jimmunol.172.11.6922
22. Braathen R SH, Lindeberg MM, Fossum E, Grødeland G, Fredriksen AB, Bogen B. The Magnitude and IgG Subclass of Antibodies Elicited by Targeted DNA Vaccines Are Influenced by Specificity for APC Surface Molecules. *ImmunoHorizons* (2018) 2(1):38–53. doi: 10.4049/immunohorizons.1700038
23. Shibata T, Takemura N, Motoi Y, Goto Y, Karuppuchamy T, Izawa K, et al. PRAT4A-Dependent Expression of Cell Surface TLR5 on Neutrophils, Classical Monocytes and Dendritic Cells. *Int Immunol* (2012) 24(10):613–23. doi: 10.1093/intimm/dxs068
24. Wylie B, Read J, Buzzai AC, Wagner T, Troy N, Syn G, et al. CD8(+)XCR1 (neg) Dendritic Cells Express High Levels of Toll-Like Receptor 5 and a Unique Complement of Endocytic Receptors. *Front Immunol* (2018) 9:2990. doi: 10.3389/fimmu.2018.02990
25. Edwards AD, Diebold SS, Slack EM, Tomizawa H, Hemmi H, Kaisho T, et al. Toll-Like Receptor Expression in Murine DC Subsets: Lack of TLR7 Expression by CD8 Alpha+ DC Correlates With Unresponsiveness to

Imidazoquinolines. *Eur J Immunol* (2003) 33(4):827–33. doi: 10.1002/eji.200323797
26. Lin KH, Chang LS, Tian CY, Yeh YC, Chen YJ, Chuang TH, et al. Carboxyl-Terminal Fusion of E7 Into Flagellin Shifts TLR5 Activation to NLRC4/NAIP5 Activation and Induces TLR5-Independent Anti-Tumor Immunity. *Sci Rep* (2016) 6:24199. doi: 10.1038/srep24199
27. Hayashi F, Smith KD, Ozinsky A, Hawn TR, Yi EC, Goodlett DR, et al. The Innate Immune Response to Bacterial Flagellin Is Mediated by Toll-Like Receptor 5. *Nature* (2001) 410(6832):1099–103. doi: 10.1038/35074106
28. Fredriksen AB, Sandlie I, Bogen B. DNA Vaccines Increase Immunogenicity of Idiotypic Tumor Antigen by Targeting Novel Fusion Proteins to Antigen-Presenting Cells. *Mol Ther* (2006) 13(4):776–85. doi: 10.1016/j.ymthe.2005.10.019
29. Gudjonsson A, Lysen A, Balan S, Sundvold-Gjerstad V, Arnold-Schrauf C, Richter L, et al. Targeting Influenza Virus Hemagglutinin to Xcr1+ Dendritic Cells in the Absence of Receptor-Mediated Endocytosis Enhances Protective Antibody Responses. *J Immunol* (2017) 198(7):2785–95. doi: 10.4049/jimmunol.1601881
30. Martinez-Lopez M, Iborra S, Conde-Garrosa R, Sancho D. Batf3-Dependent CD103+ Dendritic Cells are Major Producers of IL-12 That Drive Local Th1 Immunity Against Leishmania Major Infection in Mice. *Eur J Immunol* (2015) 45(1):119–29. doi: 10.1002/eji.201444651
31. Lysen A, Braathen R, Gudjonsson A, Tesfaye DY, Bogen B, Fossum E, et al. Dendritic Cell Targeted Ccl3- and Xcl1-Fusion DNA Vaccines Differ in Induced Immune Responses and Optimal Delivery Site. *Sci Rep* (2019) 9 (1):1820. doi: 10.1038/s41598-018-38080-7
32. Fredriksen AB, Bogen B. Chemokine-Idiotype Fusion DNA Vaccines Are Potentiated by Bivalency and Xenogeneic Sequences. *Blood* (2007) 110 (6):1797–805. doi: 10.1182/blood-2006-06-032938
33. Shimonkevitz R, Colon S, Kappler JW, Marrack P, Grey HM. Antigen Recognition by H-2-Restricted T Cells. II. A Tryptic Ovalbumin Peptide That Substitutes for Processed Antigen. *J Immunol* (1984) 133(4):2067–74.
34. Soares H, Waechter H, Glaichenhaus N, Mougneau E, Yagita H, Mizenina O, et al. A Subset of Dendritic Cells Induces CD4+ T Cells to Produce IFN-Gamma by an IL-12-Independent But CD70-Dependent Mechanism *In Vivo*. *J Exp Med* (2007) 204(5):1095–106. doi: 10.1084/jem.20070176
35. Bachem A, Hartung E, Guttler S, Mora A, Zhou X, Hegemann A, et al. Expression of XCR1 Characterizes the Batf3-Dependent Lineage of Dendritic Cells Capable of Antigen Cross-Presentation. *Front Immunol* (2012) 3:214. doi: 10.3389/fimmu.2012.00214
36. Flores-Langarica A, Bobat S, Marshall JL, Yam-Puc JC, Cook CN, Serre K, et al. Soluble Flagellin Coimmunization Attenuates Th1 Priming to Salmonella and Clearance by Modulating Dendritic Cell Activation and Cytokine Production. *Eur J Immunol* (2015) 45(8):2299–311. doi: 10.1002/eji.201545564
37. Muramatsu M, Kinoshita K, Fagarasan S, Yamada S, Shinkai Y, Honjo T. Class Switch Recombination and Hypermutation Require Activation-Induced Cytidine Deaminase (AID), a Potential RNA Editing Enzyme. *Cell* (2000) 102(5):553–63. doi: 10.1016/S0092-8674(00)00078-7
38. Roco JA, Mesin L, Binder SC, Nefzger C, Gonzalez-Figueroa P, Canete PF, et al. Class-Switch Recombination Occurs Infrequently in Germinal Centers. *Immunity* (2019) 51(2):337–50.e337. doi: 10.1016/j.immuni.2019.07.001
39. Schijns VE, Haagmans BL, Wierda CM, Kruithof B, Heijnen IA, Alber G, et al. Mice Lacking IL-12 Develop Polarized Th1 Cells During Viral Infection. *J Immunol* (1998) 160(8):3958–64.
40. Ataide MA, Komander K, Knopper K, Peters AE, Wu H, Eickhoff S, et al. BATF3 Programs CD8(+) T Cell Memory. *Nat Immunol* (2020) 21(11):1397–407. doi: 10.1038/s41590-020-0786-2
41. Qiu Z, Khairallah C, Romanov G, Sheridan BS. Cutting Edge: Batf3 Expression by CD8 T Cells Critically Regulates the Development of Memory Populations. *J Immunol* (2020) 205(4):901–6. doi: 10.4049/jimmunol.2000228
42. Dutertre CA, Jourdain JP, Rancez M, Amraoui S, Fossum E, Bogen B, et al. TLR3-Responsive, XCR1+, CD141(BDCA-3)+/CD8alpha+-Equivalent Dendritic Cells Uncovered in Healthy and Simian Immunodeficiency Virus-Infected Rhesus Macaques. *J Immunol* (2014) 192(10):4697–708. doi: 10.4049/jimmunol.1302448
43. Deloizy C, Bouguyon E, Fossum E, Sebo P, Osicka R, Bole A, et al. Expanding the Tools for Identifying Mononuclear Phagocyte Subsets in Swine: Reagents to Porcine CD11c and XCR1. *Dev Comp Immunol* (2016) 65:31–40. doi: 10.1016/j.dci.2016.06.015
44. Crozat K, Guiton R, Contreras V, Feuillet V, Dutertre CA, Ventre E, et al. The XC Chemokine Receptor 1 is a Conserved Selective Marker of Mammalian Cells Homologous to Mouse CD8alpha+ Dendritic Cells. *J Exp Med* (2010) 207(6):1283–92. doi: 10.1084/jem.20100223
45. Sittig SP, Bakdash G, Weiden J, Skold AE, Tel J, Figdor CG, et al. A Comparative Study of the T Cell Stimulatory and Polarizing Capacity of Human Primary Blood Dendritic Cell Subsets. *Mediators Inflamm* (2016) 2016:3605643. doi: 10.1155/2016/3605643
46. Nizzoli G, Krietsch J, Weick A, Steinfelder S, Facciotti F, Gruarin P, et al. Human CD1c+ Dendritic Cells Secrete High Levels of IL-12 and Potently Prime Cytotoxic T-Cell Responses. *Blood* (2013) 122(6):932–42. doi: 10.1182/blood-2013-04-495424
47. Cunningham AF, Khan M, Ball J, Toellner KM, Serre K, Mohr E, et al. Responses to the Soluble Flagellar Protein FliC Are Th2, While Those to FliC on Salmonella are Th1. *Eur J Immunol* (2004) 34(11):2986–95. doi: 10.1002/eji.200425403
48. Bobat S, Flores-Langarica A, Hitchcock J, Marshall JL, Kingsley RA, Goodall M, et al. Soluble Flagellin, FliC, Induces an Ag-Specific Th2 Response, Yet Promotes T-Bet-Regulated Th1 Clearance of Salmonella Typhimurium Infection. *Eur J Immunol* (2011) 41(6):1606–18. doi: 10.1002/eji.201041089
49. Gururajan M, Jacob J, Pulendran B. Toll-Like Receptor Expression and Responsiveness of Distinct Murine Splenic and Mucosal B-Cell Subsets. *PloS One* (2007) 2(9):e863. doi: 10.1371/journal.pone.0000863
50. DiLillo DJ, Palese P, Wilson PC, Ravetch JV. Broadly Neutralizing Anti-Influenza Antibodies Require Fc Receptor Engagement for *In Vivo* Protection. *J Clin Invest* (2016) 126(2):605–10. doi: 10.1172/JCI84428

Conflict of Interest: BB is the inventor on patents on the vaccine molecules described herein (Vaccibodies). He is the leader of the scientific panel of Vaccibody AS and has shares in the company.

The remaining authors declare that the research was conducted in the absence of any commercial or financial relationships that could be construed as a potential conflict of interest.

Publisher's Note: All claims expressed in this article are solely those of the authors and do not necessarily represent those of their affiliated organizations, or those of the publisher, the editors and the reviewers. Any product that may be evaluated in this article, or claim that may be made by its manufacturer, is not guaranteed or endorsed by the publisher.

Advantages of publishing in Frontiers

OPEN ACCESS
Articles are free to read for greatest visibility and readership

FAST PUBLICATION
Around 90 days from submission to decision

HIGH QUALITY PEER-REVIEW
Rigorous, collaborative, and constructive peer-review

TRANSPARENT PEER-REVIEW
Editors and reviewers acknowledged by name on published articles

Frontiers
Avenue du Tribunal-Fédéral 34
1005 Lausanne | Switzerland

Visit us: www.frontiersin.org
Contact us: frontiersin.org/about/contact

REPRODUCIBILITY OF RESEARCH
Support open data and methods to enhance research reproducibility

DIGITAL PUBLISHING
Articles designed for optimal readership across devices

FOLLOW US
@frontiersin

IMPACT METRICS
Advanced article metrics track visibility across digital media

EXTENSIVE PROMOTION
Marketing and promotion of impactful research

LOOP RESEARCH NETWORK
Our network increases your article's readership